National Research
Council Canada

Conseil national
de recherches Canada

NRC · CNRC

Canadian Journal of Fisheries and Aquatic Sciences

Journal canadien des sciences halieutiques et aquatiques

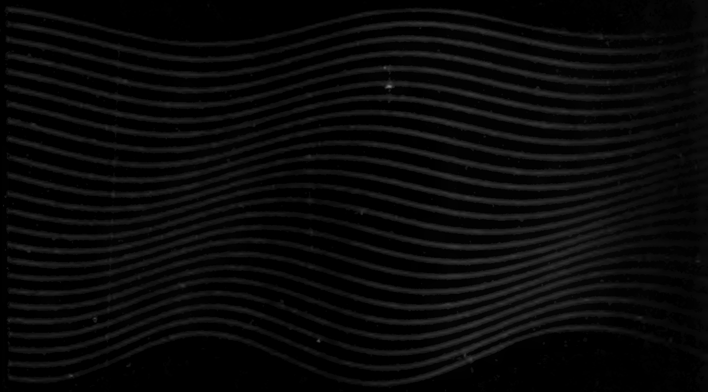

The *Canadian Journal of Fisheries and Aquatic Sciences* has been published continuously since 1901, previously as *Contributions to Canadian Biology* 1901–25, *Contributions to Canadian Biology and Fisheries* 1926–34, *Journal of the Biological Board of Canada* 1934–37, and *Journal of the Fisheries Research Board of Canada* 1938–79. The *Journal* is published by the National Research Council of Canada in cooperation with the Department of Fisheries and Oceans.

The *Journal* is issued monthly to form annual volumes of twelve numbers plus Supplements.

Editorial Policy

The *Journal* publishes original research articles, critical reviews, perspectives (essays of opinion or hypothesis), and comments. Papers may concern cells, organisms, populations, ecosystems, or processes that affect aquatic production systems, and they should lead to identifiable conclusions or syntheses, which variously may amplify, modify, question, or redirect accumulated knowledge embodied in contemporary perceptions of a particular state of fisheries and aquatic sciences. They should demonstrate clearly a contribution to knowledge beyond the confirmation state. Originality should relate to more than the particular (a certain year, place, taxon, or chemical compound) such that existing understanding is reformulated or extended.

It would assist the Editors if prospective authors identified briefly by covering letter (a) aspects of their papers that meet the foregoing objectives, (b) potential referees, and (c) other manuscripts contemplated or in press containing the same or similar information.

Submissions in English or French are acceptable. The information must be original, that is, not copyrighted, published, or submitted elsewhere except in abstract form or unless by written consent of the Editor. The National Research Council of Canada accepts no responsibility for statements or opinions expressed by a contributor. Acceptance of an advertisement, announcement, or other material does not imply endorsement by either the *Journal*'s Editors or the National Research Council. The use of proprietary names does not imply endorsement of the product or company.

Guides

A guide for authors appears in the first issue of each volume and is available free from the *Journal*.

Microfilm

Issues from 1934 through the current volume can be purchased on 16- or 35-mm microfilm. Photocopies of individual articles or issues can be purchased from University Microfilms International, 330 North Zeeb Road, Ann Arbor, MI 48106, USA.

©National Research Council of Canada 1994. World rights reserved.

The National Research Council of Canada grants permission* to individuals who wish to quote short excerpts and reproduce figures, tables, or photographs from articles in this journal, provided that the source of such material is fully acknowledged. As a courtesy the consent of authors of such material should be obtained.

Authorization to photocopy items for internal or personal use, or the internal or personal use of specific clients, is granted by the National Research Council of Canada for libraries and other users registered with the Copyright Clearance Center (CCC) Transactional Reporting Service, provided that the base fee of $3.00 per copy is paid directly to CCC, 21 Congress Street, Salem, MA 01970, USA. 0706-652X/94 $3.00 + 0.00.

*The above permission does not extend to other kinds of copying, such as copying for general distribution, for advertising, or promotional purposes, for creating new collective works, or for resale. For such copying, arrangements must be made with the National Research Council of Canada.

U.S. second-class postage paid at Champlain, N.Y., and at additional mailing offices. U.S. POSTMASTER: Send address changes to *Canadian Journal of Fisheries and Aquatic Sciences*, c/o USACAN Media Distribution Center, P.O. Box 2888, Plattsburg, NY 12901, USA.

Design: Ludvic Saleh & Associates, Ottawa
Conception graphique : Ludvic Saleh & Associates, Ottawa

Publié sans interruption depuis 1901, le *Journal canadien des sciences halieutiques et aquatiques* a paru sous plusieurs titres : *Contributions to Canadian Biology* 1901–1925, *Contributions to Canadian Biology and Fisheries* 1926–1934, *Journal of the Biological Board of Canada* 1934–1937 et *Journal de l'office des recherches sur les pêcheries du Canada* 1938–1979. Le *Journal* est publié par le Conseil national de recherches du Canada en collaboration avec le ministère des Pêches et des Océans.

Le *Journal* paraît tous les mois, formant ainsi un volume de douze numéros, et offre en plus jusqu'à deux suppléments par année.

Politique de rédaction

Le *Journal* publie des articles fondés sur une recherche originale, des critiques, des essais portant sur une opinion ou une hypothèse (perspectives) et des commentaires. Les textes peuvent avoir trait aux cellules, aux organismes, aux populations, aux écosystèmes ou aux processus qui influent sur les systèmes de production aquatique. Ils doivent aboutir à des conclusions ou synthèses précises qui, de diverses façons, peuvent accroître, modifier, remettre en question ou réorienter le bagage actuel des connaissances et perceptions dans une discipline donnée des sciences aquatiques. Ils doivent clairement démontrer qu'ils contribuent aux connaissances en faisant plus que corroborer des faits. L'originalité doit dépasser le caractère particulier (une année, un endroit, un taxon ou un composé chimique donné) et tenir à une épuration ou à une reformulation des connaissances actuelles.

Les auteurs éventuels aideraient les rédacteurs s'ils identifiaient brièvement, dans une lettre d'accompagnement a) les aspects de leurs textes qui répondent particulièrement aux objectifs indiqués ci-dessus, b) des arbitres possibles et c) d'autres manuscrits envisagés ou sous presse, dont la teneur est identique ou se rapproche de celui qui est soumis.

Les contributions peuvent être en anglais ou en français. Elles doivent être originales, c.-à.-d. qu'elles ne doivent pas avoir fait l'objet d'un copyright, avoir été publiées ou soumises ailleurs, sauf sous forme abrégée ou avec le consentement du rédacteur. Le Conseil national de recherches du Canada ne se tient en aucune façon responsable des opinions exprimées par un collaborateur ou des déclarations que pourrait faire ce dernier. La publication d'annonces publicitaires, d'avis et autres n'implique pas l'endossement de leur contenu par les directeurs du *Journal* ou du Conseil national de recherches du Canada. L'utilisation des noms de marques de commerce ne signifie aucunement une sanction du produit en question ou de la compagnie qui le fabrique.

Guides

Le guide des auteurs paraît dans la première livraison de chaque volume et est offert gratuitement par le *Journal*.

Microfilms

On peut acheter sur microfilms de 16 ou 35 mm tous les numéros publiés depuis 1934. Des photocopies d'articles ou de numéros individuels sont aussi en vente auprès de University Microfilms International, 330 North Zeeb Road, Ann Arbor, MI 48106, É.-U.

©Conseil national de recherches du Canada 1994. Tous droits réservés.

Le Conseil national de recherches du Canada accorde aux particuliers la permission* de citer de brefs extraits et de reproduire des figures, des tableaux ou des photos dans les articles du *Journal*, à la condition que la source soit indiquée explicitement. Dans ce cas, il convient, par courtoisie, d'obtenir le consentement des auteurs.

Le Conseil national de recherches du Canada autorise les bibliothèques et autres utilisateurs inscrits au Copyright Clearance Center (CCC) Transactional Reporting Service à photocopier les documents destinés à un usage interne ou personnel, ou à l'usage interne ou personnel de clients particuliers, à la condition que le tarif de base de 3 $ par copie soit payé directement au CCC, 21 Congress Street, Salem, MA 01970, USA. 0706-652X/94 3,00 $ + 0.00.

*La présente permission ne s'applique pas à d'autres genres de reproduction, notamment la reproduction en vue d'une distribution générale, à des fins de publicité ou de promotion, pour la création de nouveaux travaux collectifs, ou pour la revente. Dans ces cas, il faut prendre les dispositions qui s'imposent en communiquant avec le Conseil national de recherches du Canada.

Courrier de seconde classe des É.-U. payé à Champlain, N.Y., et d'autres centres de courrier. MAÎTRE DE POSTE des É.-U. : Faire parvenir les corrections d'adresse à *Journal canadien des sciences halieutiques et aquatiques*, a/s du Service de distribution médias USACAN Inc., C.P. 2888, Plattsburg, NY 12901, É.-U.

Canadian Journal of Fisheries and Aquatic Sciences

Journal canadien des sciences halieutiques et aquatiques

Volume 51, No. 3, March 1994

Volume 51, n° 3, mars 1994

D.G. Cook	*Editor/Rédacteur*
M.M. Milne	*Assistant to the Editor/Adjointe au rédacteur*
P.E.K. Symons	*Consulting Editor/Rédacteur-conseil (Victoria, B.C.)*
N. Moir	*Consulting Editor/Rédactrice-conseil (Nepean, Ont.)*

Editorial Board/Conseil de rédaction

L.M. Dickie	*DFO/MPO, Dartmouth (Advisor/Conseiller)*
G.S. Jamieson	*DFO/MPO, Nanaimo (Associate Editor/Rédacteur associé)*
J.R.M. Kelso	*DFO/MPO, Sault Ste. Marie (Associate Editor/Rédacteur associé)*
J.D. Neilson	*CFRAMP, St. Vincent (Associate Editor/Rédacteur associé)*
L.S. Parsons	*DFO/MPO, Ottawa (Advisor/Conseiller)*
R.M. Peterman	*Simon Fraser University (Advisor/Conseiller)*
J.C. Roff	*University of Guelph (Advisor/Conseiller)*
P. Schwinghamer	*DFO/MPO, St. John's (Deputy Editor/Rédacteur adjoint)*
C.J. Walters	*University of British Columbia (Advisor/Conseiller)*
W.G. Warren	*DFO/MPO, St. John's (Associate Editor/Rédacteur associé)*
N.H.F. Watson	*DFO/MPO, Halifax (Associate Editor/Rédacteur associé)*

Research Journals/Revues scientifiques

Bruce P. Dancik	*Editor-in-chief/Directeur général*
Iain E.P. Taylor	*Assistant Editor-in-chief/Directeur général adjoint*

Publishing Department/Service de publication

Aldyth Holmes	*Director/Directrice*
Joan E. Hill	*Operations Manager/Responsable des opérations*
Christine Shugar	*Head of Publications/Chef des publications*
Peter M. Burke	*Publication Officer/Agent de publication (613-993-0994)*
Ginette Fortier	*Publication Officer (French manuscripts)/Agente de publications (manuscrits français) (613-993-9117)*
Hoda Jabbour	*Advertising/Annonces publicitaires (613-993-9085)*
Eileen Fink	*Reprints/Tirés à part (613-993-0151)*

Editorial Office:

Research Journals
National Research Council of Canada
Ottawa, ON K1A 0R6
Canada
Telephone (613) 993-2209
FAX (613) 952-7656
E-mail: research.journals@nrc.ca

Bureau de rédaction:

Revues scientifiques
Conseil national de recherches du Canada
Ottawa ON K1A 0R6
Canada
Téléphone (613) 993-2209
Télécopieur (613) 952-7656
Courrier électronique : research.journals@nrc.ca

The *Journal* is abstracted or indexed in:/Le *Journal* est résumé ou signalé dans :

Aquatic Sciences and Fisheries Abstracts, Biological Abstracts, Biological & Agricultural Index, Chemical Abstracts, Current Awareness in Biological Sciences, Current Contents, FAO Freshwater and Aquaculture Contents Tables, FAO Marine Science Contents Tables, Meteorological and Geoastrophysical Abstracts, Oceanic Abstracts, and Science Citation Index

Seasonal Reproductive Patterns of Pumpkinseed (*Lepomis gibbosus*) Populations with Varying Body Size Characteristics

Andy J. Danylchuk and Michael G. Fox

Environmental and Resource Studies Program, Trent University, Peterborough, ON K9J 7B8, Canada

Danylchuk, A.J., and M.G. Fox. 1994. Seasonal reproductive patterns of pumpkinseed (*Lepomis gibbosus*) populations with varying body size characteristics. Can. J. Fish. Aquat. Sci. 51: 490–500.

To assess the implications of reproduction on body size and the potential physiological constraint imposed by small body size on reproductive patterns, we examined seasonal nesting patterns and gonad allocation in six pumpkinseed (*Lepomis gibbosus*) populations exhibiting a range of adult body size characteristics. We found that the two populations exhibiting stunted adult body size initiated nesting activity 1-wk later and had nesting periods 3–7 wk longer than the other four populations. Mean adult body size showed a significant negative correlation with both length of spawning season and gonadosomatic index in the six populations. Within populations, smaller females matured later in the season than larger females. Our results suggest that small adult body size is associated with high reproductive effort and that variation in the timing of reproduction is a consequence of differences in energy reserves between small and large individuals. The extended spawning season of some populations may result in a higher cost of reproduction than that which would be predicted from gonad size alone. Small individuals forced by energy limitations to spawn late in the season are likely to produce offspring with lower survival rates, and their reproductive fitness should be discounted accordingly.

Pour évaluer les liens entre la reproduction et la taille corporelle, et les contraintes physiologiques potentielles imposées par la faible taille du corps aux schèmes de reproduction, nous avons examiné les modes saisonniers de nidification et la distribution de la taille des gonades chez six populations de crapet soleil (*Lepomis gibbosus*) présentant des caractéristiques diverses de taille à l'âge adulte. Nous avons trouvé que les deux populations dont les adultes avaient une taille chétive commençaient leur nidification 1 sem plus tard et la poursuivaient pendant 3 à 7 sem de plus que les quatre autres populations. La taille moyenne des adultes montrait une corrélation négative significative avec la durée de la saison de ponte et l'index gonadosomatique dans les six populations. Au sein des populations, les femelles de plus petite taille atteignaient la maturité plus tard dans la saison que celles de grande taille. Nos résultats semblent indiquer que la faible taille des adultes est associée à un effort reproductif élevé, et que la variation dans la période de reproduction est une conséquence des différences dans les réserves énergétiques entre les individus de petite et de grande taille. L'allongement de la saison de ponte dans certaines populations peut avoir pour effet un coût de reproduction supérieur à celui qu'on aurait pu prédire à partir de la taille des gonades seulement. Les petits individus forcés par les limitations énergétiques à frayer tard dans la saison vont vraisemblablement produire des rejetons dont le taux de survie sera plus faible, et ont donc une faible valeur adaptative.

Received March 16, 1993
Accepted October 25, 1993
(JB848)

Reçu le 16 mars 1993
Accepté le 25 octobre 1993

Growth and reproduction are processes that compete for the same limited energetic resources (Roff 1984; Calow 1985). A central concept of life-history theory is that a trade-off exists between present and future reproduction, growth, and survival (Stearns 1977; Wootton 1990; Kozlowski 1992). Two critical factors concerning this trade-off are the amount of energy directed from somatic growth to reproductive processes and the size at which investment into reproduction should occur (reviewed in Calow 1985).

Fish have frequently been used to examine the trade-offs predicted by life-history theory because of the large variation in body size among breeding adults (Roff 1981; 1984; Ridgway et al. 1991). Since body size and fecundity are positively correlated in fish, decreased growth associated with increased reproductive investment can reduce future fecundity (Wootton 1979; Reznick 1983).

Studies with fish have shown that present reproduction is costly, as it occurs at the expense of postspawning growth, reproduction, and survivorship (Roff 1982; 1984; Reznick 1983; Wootton 1985; Stearns and Koella 1986; Hutchings 1993). Spawning fish have been shown to be in poorer somatic condition, making them more susceptible to predation, disease, or physiological stress than nonreproductive fish (Wootton 1977; Pressley 1981; Roff 1982). Reproduction can also place a heavy burden on energy reserves. For example, in American plaice (*Hippoglossoides platessoides*) the flesh becomes jellied as fish break down their body tissues to provide energy for gonadal development (Roff 1981).

The evidence relating reproductive effort to body size and survival suggests that stunting (small adult body size) may be a consequence of early maturation and high reproductive effort (Jennings 1991). However, the link between

TABLE 1. Body size and maturity characteristics of pumpkinseed in the six study lakes. Body size and maturity data were collected during 1988–1991.

Lake	Physical characteristics		Body size characteristics		
	Surface area (ha)	Mean depth (m)	Maximum length (mm)	Mean total length at age 5 (mm)	Mean length at maturity (males/females) (mm)
Little Round	8	11	97	96	55/64
Warrens	34	2.6	133	123	77/82
Black	40	7.8	152	132	82/91
Beloporine	7	2.6	154	141	102/92
Opinicon	787	2.5	170	128	116/108
Duncan	45	n/a	169	146	127/125

characteristics of stunted fish such as early maturation (reviewed in Murnyak et al. 1984) and slow growth (Alm 1946; Roff 1986) has not been demonstrated at the population level.

The energy available for reproduction can be restricted by body size. Several studies have shown that smaller fish have lower fat stores and higher rates of energy use than larger fish (reviewed by Shuter and Post 1990). Ridgway et al. (1991) showed that body size affected the timing of reproduction in smallmouth bass (*Micropterus dolomieu*, previously *M. dolomieui*). They found that large male bass nested earlier in the season than small males, and they hypothesized that these differences are linked to size-dependent energy deficits. Their results suggest that smaller fish require more time to rebuild overwinter energy deficits, resulting in a delay in the allocation of energy to reproduction. However, their study was within one population and the timing of female reproduction was not directly assessed.

The purpose of this study was to examine the nature of size-related energetic trade-offs in pumpkinseed (*Lepomis gibbosus*), a common centrarchid species in many north temperate lakes. Given that reproductive patterns are a product of available energy stores, and that smaller fish accumulate a higher overwinter energy deficit than larger fish (Shuter et al. 1980), we predicted that (1) pumpkinseed populations exhibiting small adult body size would initiate reproductive activity later in the spring than populations with comparatively larger adults, (2) smaller fish within populations should initiate reproductive activity later in the season than larger fish, and (3) smaller fish within populations should allocate energy to gonads later in the season than larger fish.

Given that there is a high cost to reproduction, we further predicted that body size at the population level would be negatively associated with reproductive effort and predicted that (4) pumpkinseed populations exhibiting small adult body size would have a protracted spawning season and (5) would allocate more energy to gonads than populations with normal adult body size characteristics.

Materials and Methods

Study Sites

Pumpkinseed populations used for this study were selected from a data base of 23 eastern and central Ontario populations used in an ongoing study (Fox 1994). Pumpkinseed from these waterbodies had been collected during the prereproductive periods from 1988 to 1991 to define the life-history characteristics of each population. To test the predictions of this study, six populations were selected encompassing a broad range of body size characteristics (Table 1). Little Round Lake (LR) and Warrens Lake (WA) populations exhibit stunted growth and small adult body size whereas populations in Lake Opinicon (OP) and Duncan Lake (DU) exhibit growth and adult body size characteristics typical of populations in eastern and central Ontario. Black Lake (BL) and Beloporine Lake (BP) populations exhibit intermediate adult body size characteristics.

The study lakes were geographically proximate (within 125 km and 20′ of latitude of each other) (Fig. 1). Lake area ranged from 7 to 787 ha, with mean depths ranging from 2.5 to 11 m (Table 1).

Assessment of Seasonal Nesting Patterns

Male pumpkinseed nest in diffuse colonies and aggregate in favoured habitat within the littoral zone (Breder 1936; Clark and Keenleyside 1967; Gross 1979). The location of nests constructed early in the season tends to define areas where the majority of nesting is to occur (Colgan and Ealey 1973; Gross 1979; Ridgway et al. 1991). Therefore, transects were established in suitable nesting habitat where parental males had initiated nest construction early in the spring. Two transects were used in each of Little Round, Warrens, Opinicon, and Beloporine lakes (Table 2). Three transects were established in Duncan and Black in order to increase the number of nests surveyed, since nest density early in the season was comparatively low in these two lakes. Transect dimensions varied within and between lakes and were dependent upon the location of nests early in the season and the morphological characteristics of the littoral zone.

Transects were examined for nesting activity on a biweekly basis from May to August 1992 and weekly at the initiation of the study to more precisely define when nesting was initiated in each lake. Nests within transects were marked and surveyed during each assessment period for parental occupation and the presence of eggs or larvae. Previously unmarked or "new" nests occupied by parental male pumpkinseed were marked and included in the assessment. Whole-lake inspections of other nesting areas conducted on each day of transect assessments confirmed that seasonal trends in parental occupation and nest content observed in transects were representative of the lake as a whole. All inspections were carried out by divers using mask and snorkel.

To compare reproductive activity to trends in water temperature, a minimum/maximum thermometer was placed in

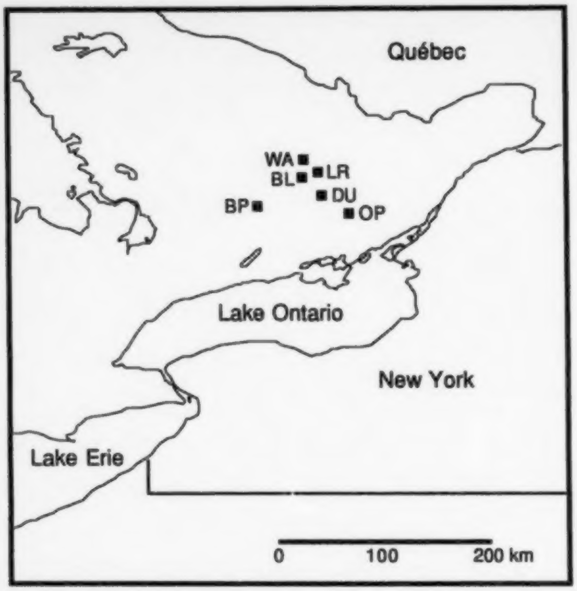

FIG. 1. Location of study lakes in eastern-central Ontario. LR = Little Round, WA = Warrens, BL = Black, BP = Beloporine, OP = Opinicon, and DU = Duncan.

approximately 1 m of water at or near one of the transects in each lake. Temperature data were read on the date that transects were surveyed, although some readings could not be made due to equipment damage and theft.

Assessment of Seasonal Allocation Patterns

Female pumpkinseed were collected from each waterbody on the day of transect assessments. Females were selected for this analysis, since the majority of seasonal reproductive energy in females is allocated to gonad development and not to secondary reproductive behaviour such as brood care (Miller 1963; Gross 1979; Vøllestad and L'Abée-Lund 1990). Collections were made in littoral zone areas with a bag seine and 1 m (length) × 40 cm (diameter) wire funnel traps set at a depth of approximately 1 m (Keast and Fox 1990). Collections were made away from transects to avoid disturbing survey nests.

Total length and wet weight were measured for each individual. Age was determined by reading acetate impressions of scales. Annuli were identified using the criteria outlined by Regier (1962). We validated our scale aging technique by comparing scale and otolith ages (Casselman 1987) in a subsample of 10 fish from each population. Ages determined from both methods were identical in all fish examined. Length at age was backcalculated on each fish using the Fraser–Lee method (Bagenal and Tesch 1978) and a standard body-scale length intercept (Carlander 1982) calculated as the mean of 23 populations surveyed (Fox 1994).

The proportion of gonad weight to total body weight (gonadosomatic index, GSI) was calculated for each mature fish. A fish was defined as mature if the ovaries contained yolked eggs. Spent females were also counted as mature. These females were identified by the presence of flaccid gonads containing a few yolked eggs and the protrusion of the gonadal papilla (Miller 1963). GSI was calculated for each population, collection period, and age-class.

TABLE 2. Number of transects and total transect area for the study lakes.

Lake	Number	Total area (m^2)
Little Round	2	392
Warrens	2	450
Black	3	1898
Beloporine	2	492
Opinicon	2	1185
Duncan	3	2624

Analysis of Seasonal Nesting Patterns

The number and density of occupied nests were calculated for each assessment period as an indicator of seasonal reproductive activity in each lake. Nest density was plotted according to assessment date to observe interpopulation trends in nesting activity, including initiation date, peak activity, and season duration. The number of occupied nests and those containing eggs and larvae were also plotted according to assessment date to observe interpopulation patterns in spawning and hatching.

Duration of the spawning season was defined as the number of weeks between the initiation of nesting activity and the complete abandonment of nests. The number of occupied nests with larvae and the accumulation of silt within those nests were also used to indicate the completion of the spawning season. Transects were surveyed 2 wk after total nest abandonment to ensure that a resurgence of reproductive activity did not occur.

Pearson correlations were used to test the prediction that seasonal duration is inversely related to female body size across populations. The 90th percentile length of all females was determined for each population and used as an indicator of maximum body size. The 90th percentile length was used instead of the length of the largest fish collected because the former is less subject to sampling error. Mean length of mature females was used as an indicator of average body size of reproductive fish. Both indicators were determined by backcalculating fish length to the beginning of the season (formation of the 1992 annulus) to standardize the length of mature fish collected at different times throughout the season.

Patterns of reproduction in centrarchids, including the time of initiation, duration, and proportion of energy allocated to gonads, can potentially be affected by water temperature (Kaya and Hasler 1972; Burns 1976; Ridgway et al. 1991). We therefore examined the water temperature regime within our study lakes to determine if interpopulation differences in reproductive activity were related to early season trends in water temperature. A Pearson correlation was used to examine the relationship between the time until peak nest density (in weeks) and thermal history, expressed as the number of degree-days greater than 16°C (Burns 1976) accumulated by that time. If temperature is the critical factor in determining interpopulation differences in the timing of reproductive activity, then peak nest density should occur in all of the waterbodies when a given number of degree-days is reached. We also examined the relationship between maximum body size and thermal history to determine if populations with comparatively smaller adults accumulated a

TABLE 3. Female body size and reproductive characteristics determined from samples taken during the 1992 spawning season.

	Body size characteristics[a]		Reproductive characteristics[b]	
Lake	90th percentile length (mm)	Mean length of matures (mm)	90th percentile GSI	Peak GSI[c]
Little Round	80 (333)	70 (287)	11.2	8.6
Warrens	95 (204)	78 (194)	10.4	7.9
Black	124 (172)	94 (110)	9.5	6.2
Beloporine	117 (223)	100 (160)	10.2	8.5
Opinicon	145 (145)	125 (102)	7.7	5.8
Duncan	155 (139)	128 (81)	6.4	4.3

[a] Standardized to the beginning of the season by backcalculation from scales (sample size in parentheses).

[b] Sample size of GSI characteristics is the same as that of mean length of mature fish.

[c] Highest mean GSI in any assessment period.

greater number of degree-days before the peak in nesting activity (Ridgway et al. 1991).

To examine growth trajectories of females in each population, mean length at age was calculated by averaging the backcalculated length of each age and the two successive older age-classes (for example, mean length at age 2 was calculated by averaging the backcalculated length for age-classes 2, 3, and 4). Older age-classes were not used in this calculation because several populations showed Lee's phenomenon, in which older fish appear to be slower growing as a result of selective mortality on faster growing individuals (Bagenal and Tesch 1978). Mean age at maturity was calculated according to the method of DeMaster (1978).

Analysis of Seasonal Allocation Patterns

Mean GSI and 90th percentile GSI for all mature females were determined and plotted according to assessment date to observe interpopulation trends in seasonal allocation of energy to gonads. Mean GSI was used as a value of average allocation whereas the 90th percentile GSI was an indicator of maximum allocation.

Pearson correlations were used to test the prediction that populations of small adult body size should allocate more energy to gonads. The 90th percentile GSI (maximum allocation) and the highest mean GSI during the assessment period (peak allocation) were used as two indicators of energy allocated to gonads. The latter indicator removed the confounding influence of date sampled and eliminated spent fish and those without fully developed gonads from the analysis. As an indicator of total seasonal reproductive allocation, we examined the combined effects of seasonal allocation and seasonal duration of reproductive activity by calculating the area under the mean GSI × date curve.

To test whether smaller fish within populations delay the allocation of energy to gonads and therefore initiate reproduction later in the season than larger fish, we determined the proportion of mature females for the first three age-classes that contained mature females for each population. To compare age-class trends in maturation, percent mature was plotted against assessment date until the youngest age-class reached peak maturity .

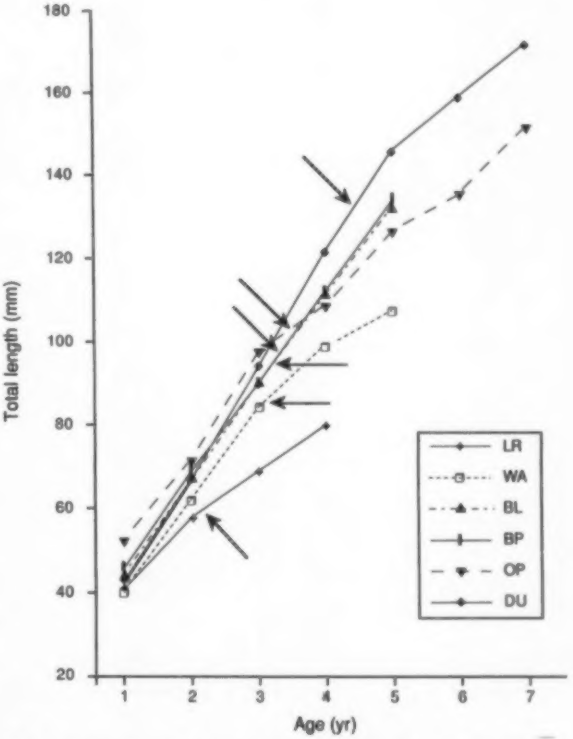

FIG. 2. Mean length at age for females from the six study populations. Mean age at maturity for each population is indicated by an arrow.

Bonferroni adjustments were used with multiple factor correlations to give guaranteed family-wise probability levels. We defined probability levels of <0.05 as signifi-

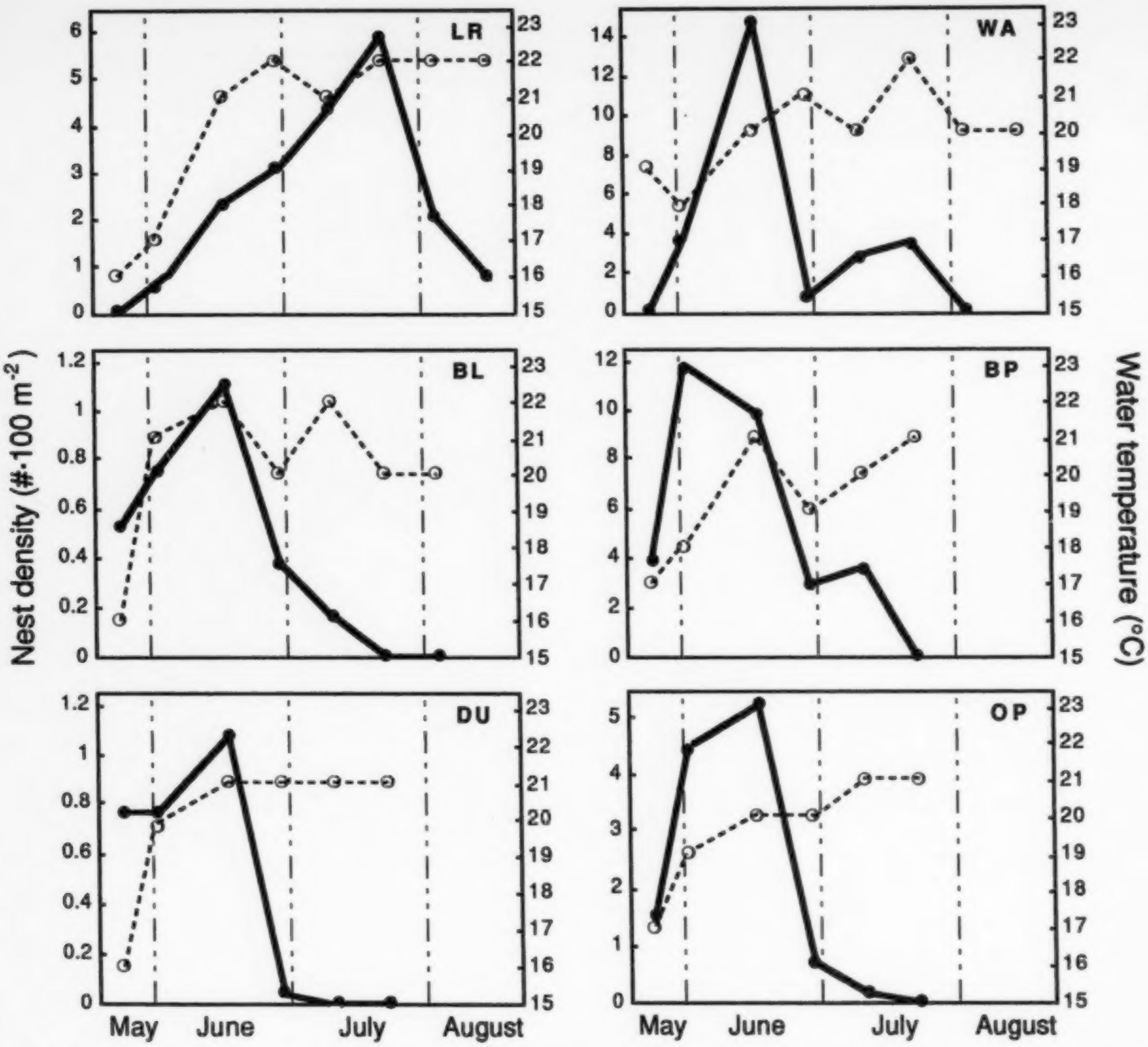

FIG. 3. Nest density and mean water temperature for the study lakes during the 1992 spawning season. Nest density is represented by solid circles/solid lines and mean water temperature by open circles/broken lines.

cant and denoted probability levels between 0.05 and 0.1 as marginally significant.

Results

Body Size, Growth, and Reproductive Allocation

Females from Little Round and Warrens exhibited the smallest body size and the greatest allocation to gonads (Table 3). The body size characteristics of Black and Beloporine females were intermediate to those of the other populations. GSI of Beloporine females was as high as those of the stunted populations.

A downward shift in the growth trajectory coincident with the mean age of maturation was evident in four of the six populations (Fig. 2). Females from Little Round and Warrens exhibited the earliest age at maturity and a major decline in the annual growth increment following the mean age at maturity (Fig. 2). Small adult body size in these two populations was coincident with small juvenile body size, but there was no correspondence between juvenile and adult body size in the other four populations.

Seasonal Nesting Patterns

Nesting activity began in late May or early June, with the stunted populations of Little Round and Warrens initiating nesting activity 1 wk later than other populations. Seasonal nest density ranged from 1 to 15 nests·100 m^{-2} (Fig. 3), and maximum seasonal nest density was not significantly correlated with either of the body size indicators (Table 4). Peak nest density occurred from early June to late June in all lakes except Little Round, which peaked in late July. Although nest density peaked latest in the most stunted pop-

TABLE 4. Correlation between female body size and reproductive characteristics in the six study populations.

	Body size characteristics			
	90th percentile length		Mean length of matures	
Reproductive characteristics	*r*	P^a	*r*	P^a
Seasonal duration	−0.94	0.005**	−0.89	0.01*
90th percentile GSI	−0.89	0.010*	−0.95	0.003**
Peak GSI	−0.96	0.003**	−0.83	0.04
Total seasonal allocation	−0.99	0.0001**	−0.97	0.001**
Maximum nest density	−0.55	0.27	−0.47	0.34

[a] Individual probability values are given. Asterisks denote Bonferroni-adjusted family-wise level of significance: $*P < 0.1$ and $**P < 0.05$.

ulation, the timing of this peak was not ordered by body size in the rest of the populations.

Water temperature at the initiation of nesting ranged from 16 to 18°C, and water temperature at peak nest density ranged from 20 to 22°C. The initiation of nesting did not occur in sequence with the warming of the lakes (see Fig. 3). In addition, peak nest density occurred in each lake after a different number of degree-days was accumulated (Fig. 4); thus, thermal regime does not explain the variation among lakes in the timing of nesting activity. There was a tendency for the number of thermal units until peak nesting occurs to decrease with increasing body size of the population (Fig. 4), but the relationship between these variables was not significant ($r = -0.58$, $P = 0.20$).

The nesting period of the stunted populations in Little Round and Warrens occurred for 12 and 10 wk, respectively, whereas Black, Beloporine, and Opinicon populations nested for 7 wk, and the Duncan Lake population nested for 5 wk. There was a significant negative correlation between seasonal duration of nesting and body size (Table 4). The underlying cause of this relationship was apparently not competition for mates or nesting sites because neither mean nor maximum nest density was significantly correlated with seasonal duration ($r = 0.39$, $P = 0.44$ and $r = 0.45$, $P = 0.37$ respectively).

Seasonal peaks in the number of occupied nests and the number of those nests that contained eggs were either synchronous or sequential for each lake (Fig. 5). The number of nests observed with larvae ranged in these lakes from 7 to 51% of the number of nests observed with eggs, and this proportion was unrelated to body size characteristics of the populations ($r = 0.59$, $P = 0.29$).

Seasonal Allocation and Maturity Patterns

Within-lake trends in mean GSI and 90th percentile GSI (Fig. 6) generally corresponded with seasonal nesting patterns for each lake (Fig. 3). Peak allocation occurred early in the season for each population except that of Little Round. Mean and 90th percentile GSI in Little Round Lake did not peak until mid-June and did not decrease until early July. Mean and 90th percentile GSI also remained near the seasonal peak for a longer period of time in the stunted populations.

Both measures of GSI as well as total seasonal allocation were highly correlated with adult body size (Table 4). Thus, populations exhibiting stunted body size characteristics allocated more energy to gonads on a seasonal basis and had higher seasonal peaks than populations with larger adult body size.

Within populations, a lower proportion of smaller/younger females were mature at the onset of nesting activity than larger/older females (Fig. 7). The proportion of the youngest age-class of females maturing increased over the reproductive season in each lake except Opinicon. In addition, age 2 females peaked in percent maturity 2–5 wk later than older fish in the four populations with age 2 mature fish.

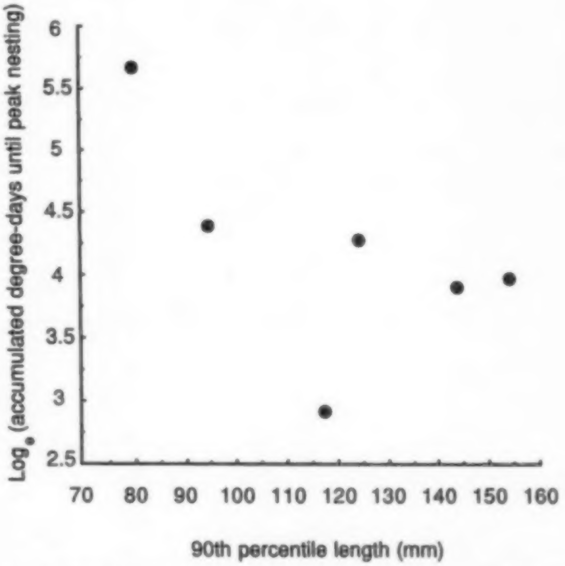

FIG. 4. Relationship between adult body size in the six study populations and accumulated degree-days prior to peak nest density.

Discussion

Our study showed that high reproductive effort is associated with small adult body size in pumpkinseed. We found that the populations exhibiting a longer spawning season, delayed seasonal reproductive activity, and greater gonad development were those with the smallest adult body size.

Size-specific differences in energy stores prior to reproduction could account for the delay in seasonal reproductive activity by stunted populations and by small maturing

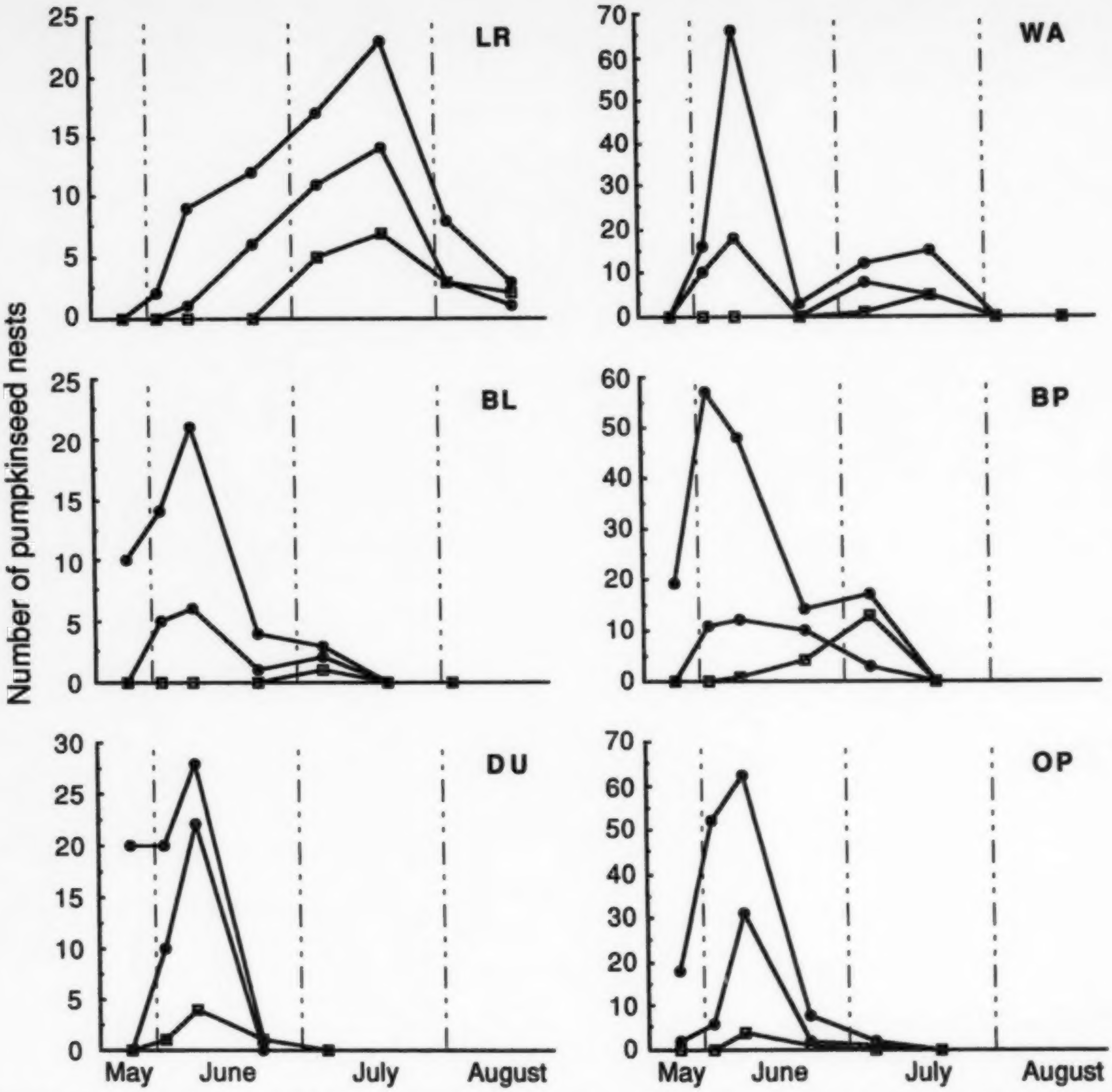

FIG. 5. Number of occupied nests (solid circles) and the number of those nests that contained eggs (open circles) or larvae (open squares) for the study lakes during the 1992 spawning season.

fish within populations. Trippel and Harvey (1989) showed that the onset of maturation in white sucker, (*Catostomus commersoni*) was energy dependent. Ridgway et al. (1991) postulated that more time should be required by smaller fish to replenish energy stores early in the spring, resulting in the delay of energy allocation to gonads. Our results are consistent with the hypothesis of Ridgway et al. (1991) and emphasize the importance of the overwinter period to the reproductive potential of small fish.

Burns (1976) showed that the seasonal timing of maturation in pumpkinseed is primarily a function of water temperature. Gonadal recrudescence in green sunfish (*Lepomis cyanellus*) was shown to be stimulated by a combination of elevated water temperature and extended photoperiod (Kaya and Hasler 1972). However, the initiation of nesting in our six lakes was not ordered by early season temperature; nor did nest density in these lakes peak at a set number of accumulated degree-days. While this does not mean that thermal regime is unimportant in regulating the timing of reproductive activity within a lake, it does show that thermal regime cannot account for the among-population differences in reproductive patterns demonstrated in our study.

Given that energy availability and energy stores are limited in the pumpkinseed populations we studied, it is reasonable to assume a cause–effect explanation for the negative relationship between reproductive effort and adult body size. Jennings (1991) had previously demonstrated such a relationship in two longear sunfish (*Lepomis megalotis*) sub-

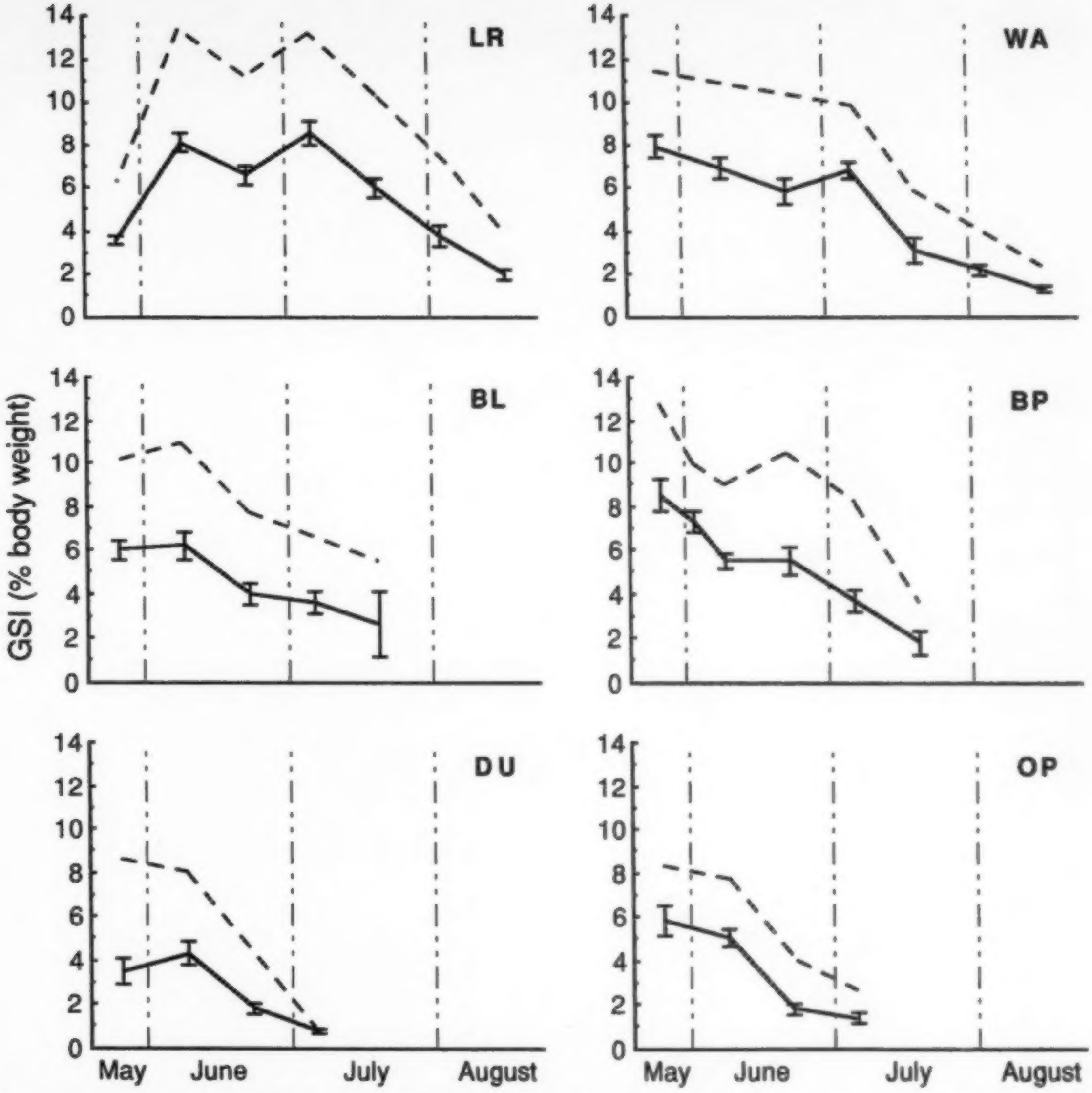

FIG. 6. Mean GSI (±1 SE) and 90th percentile GSI of females sampled from each study lake during the 1992 spawning season. Mean GSI is represented by solid lines and 90th percentile GSI by broken lines.

species; our work demonstrates that the relationship also applies at the population level. However, factors such as population density and resource availability can also influence adult body size in fish (Alm 1946; Murnyak et al. 1984; Deacon and Keast 1987; Fox and Keast 1990). Thus, although our data suggest that reproductive effort may account for much of the variation in adult body size among populations, its importance relative to other factors was not determined.

Values of energy allocated to reproduction are typically based on GSI (Vøllestad and L'Abée-Lund 1990), fecundity (Wootton 1979; Vøllestad and L'Abée-Lund 1990; Schultz and Warner 1991), and the energy content of gonads (Constantz 1979; Reznick 1983). Our study suggests that the traditional use of gonad data may actually underestimate the relative cost of reproduction in different populations. While conducting reciprocal transplants experiments with sculpin (*Cottus gobio*) between northern and southern streams, Mann et al. (1984) found that females that allocated more energy to reproduction also had longer spawning periods than females that allocated less energy to reproduction. On the other hand, gonad data may overestimate the absolute reproductive effort of some mature females, since it has been shown that mature individuals do not necessarily spawn in a given year (Raffetto et al. 1990; Ridgway et al. 1991; Danylchuk and Fox 1994).

An extended spawning season incurs a high energy cost, assuming that individuals are repeatedly spawning throughout the season. Repeat spawning throughout the season has been shown to occur in other centrarchids such as bluegill

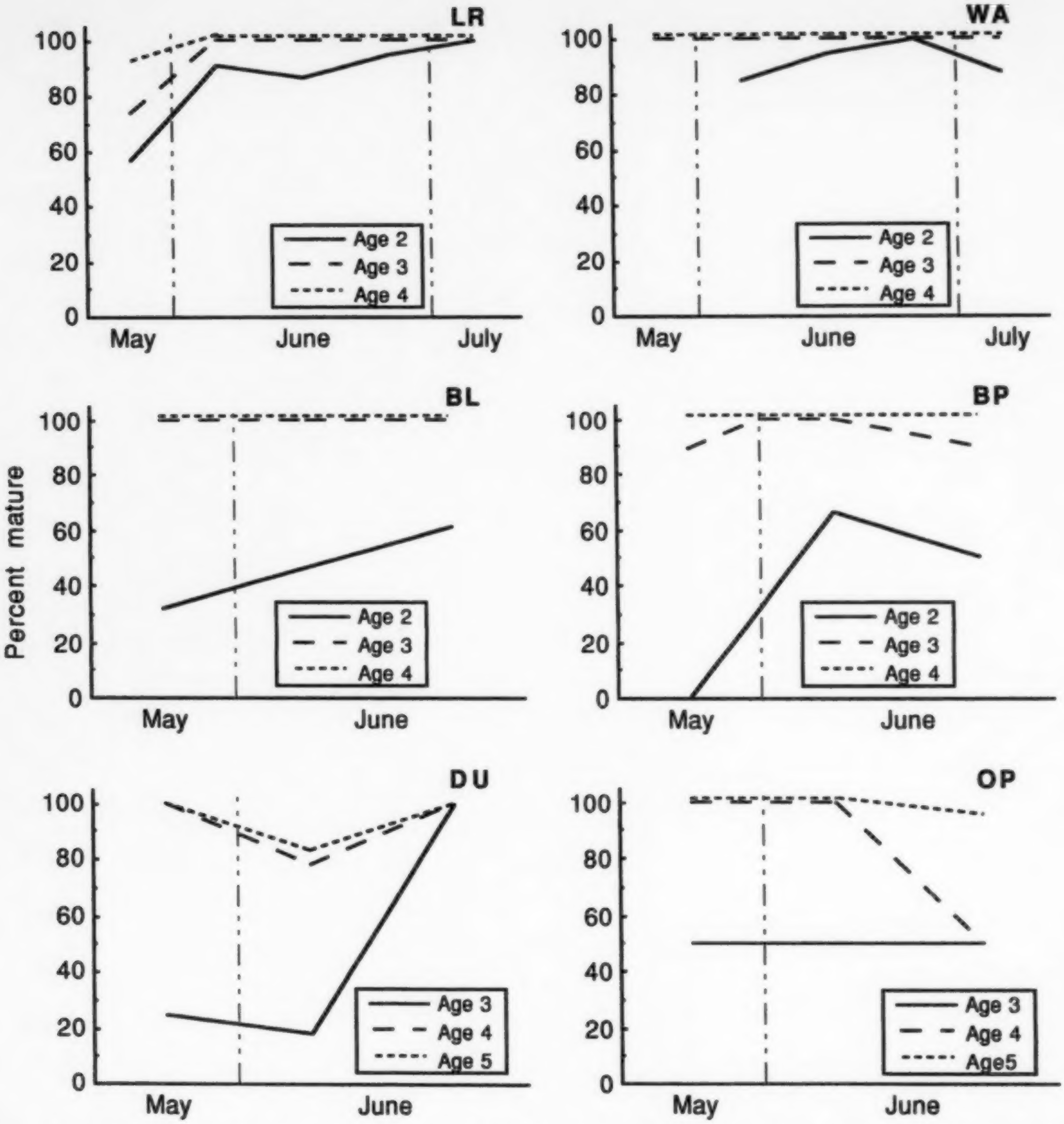

FIG. 7. Proportion of mature females collected from each study lake for the first three age-classes with mature fish. Proportions plotted until the youngest age class reached peak maturity.

(*Lepomis macrochirus*) (Gross 1982) and rock bass (*Ambloplites rupestris*) (Gross and Nowell 1980) and has been suggested for pumpkinseed (Miller 1963; Deacon and Keast 1987; Crivelli and Mestre 1988).

An issue raised by our study is whether size-dependent timing of reproduction may result in smaller individuals having lower reproductive fitness than larger individuals capable of spawning earlier in the season. Given that overwinter survival of young-of-the-year fish is highly size-dependent (Oliver et al. 1979; Post and Evans 1989), young born at the end of an extended spawning season may contribute minimally to the reproductive fitness of the parents. Thus, in trying to determine the fitness value of early maturity within a population, it would be necessary to discount the value of offspring production according to the time in the season when it occurs.

In summary, our study shows that the seasonal timing of reproductive activity is related to body size of the individual and that differences in adult body size among populations are linked to differences in reproductive allocation. Given that the energy available for growth and reproduction is limited, our results suggest that small adult body size can be a consequence of high reproductive effort. Our study provides support for the life-history assumptions relating energetic trade-offs between body size and reproduction. To further assess the consequences of reproductive effort on pumpkinseed populations, interpopulation differences in reproductive success and postreproductive survivorship should be addressed.

Acknowledgments

We thank Joseph Justus, Ian McDonald, and Kim Westcott for their assistance in the field and laboratory, Ed and Florence Warren for the use of their cabin in the field, and the staff of Sharbot Lake Provincial Park for the use of a campsite. We also thank David Philipp and Julie Claussen for their helpful advice during this study and Michael Berrill, Dave Lasenby, and two anonymous reviewers for their review of an earlier version of this manuscript. Financial support for this study was provided by a Natural Sciences and Engineering Research Council of Canada grant to M. Fox.

References

Alm, G. 1946. Reasons for the occurrence of stunted fish populations (with special regard to the perch). Inst. Freshwater Res. Drottningholm Rep. 25: 1–146.

Bagenal, T.B., and F.W. Tesch. 1978. Age and growth, p. 101–136. *In* T.B. Bagenal [ed.] Methods for the assessment of fish production in fresh waters. IBP Handbook No.3, Blackwell Scientific Publication, Oxford, U.K.

Breder, C. M. Jr. 1936. The reproductive habits of the North American sunfishes (family Centrarchidae). Zoologica 21: 1–47.

Burns, J.R. 1976. The reproductive cycle and its environmental control in the pumpkinseed, *Lepomis gibbosus* (Pisces: Centrarchidae). Copeia 3: 449–455.

Calow, P. 1985. Adaptive aspects of energy allocation, p. 13–31. *In* P. Tytler and P. Calow [ed.] Fish energetics: new perspectives. Johns Hopkins University Press, Baltimore, Md.

Carlander, K.D. 1982. Standard intercepts for calculating lengths from scale measurements of some centrarchid and percid fishes. Trans. Am. Fish. Soc. 111: 332–336.

Casselman, J.M. 1987. Determination of age and growth, p. 209–242. *In* A.H. Weatherly and H.S. Gill [ed.] The biology of fish growth. Academic Press, London, UK.

Clark, F.W., and M.H.A. Keenleyside. 1967. Reproductive isolation between the sunfish *Lepomis gibbosus* and *L. macrochirus*. J. Fish. Res. Board Can. 24: 495–514.

Colgan, P.W., and D. Ealey. 1973. Role of woody debris in nest site selection by pumpkinseed sunfish, *Lepomis gibbosus*. J. Fish. Res. Board Can. 30: 853–856.

Constantz, G.D. 1979. Life history patterns of a livebearing fish in contrasting environments. Oecologia 40: 189–201.

Crivelli, A.J., and D. Mestre. 1988. Life history patterns of pumpkinseed, *Lepomis gibbosus*, introduced into the Camargue, a mediterranean wetland. Arch. Hydrobiol. 111: 449–466.

Danylchuk, A.J., and M.G. Fox. 1994. Age and size-dependent variation in the seasonal timing and probability of reproduction among mature female pumpkinseed, *Lepomis gibbosus*. Environ. Biol. Fishes 39: 119–127.

Deacon, L.I., and J.A. Keast. 1987. Patterns of reproduction in two populations of pumpkinseed sunfish, *Lepomis gibbosus*, with differing food resources. Environ. Biol. Fishes 19: 281–296.

DeMaster, D.P. 1978. Calculation of the average age of sexual maturity in marine mammals. J. Fish. Res. Board Can. 35: 912–915.

Fox, M.G. 1994. Growth, density, and interspecific influences on pumpkinseed sunfish life histories. Ecology. (In press)

Fox, M.G., and A. Keast. 1990. Effects of winterkill on population structure, body size, and prey consumption patterns of pumpkinseed in isolated beaver ponds. Can. J. Zool. 68: 2489–2498.

Gross, M.R. 1979. Cuckoldry in sunfishes (*Lepomis* : Centrarchidae). Can. J. Zool. 57: 1507–1509.

Gross, M.R. 1982. Sneakers, satellites, and parentals: polymorphic mating strategies in North American sunfishes. Z. Tierpsychol. 60: 1–26.

Gross, M.R, and W.A. Nowell. 1980. The reproductive biology of rock bass, *Ambloplites rupestris* (Centrarchidae), in Lake Opinicon, Ontario. Copeia 1980: 482–494.

Hutchings, J.A. 1993. Adaptive life histories effected by age-specific survival and growth rate. Ecology 74: 673–684.

Jennings, M. 1991. Sexual selection, reproductive strategies, and genetic variation of the longear sunfish, *Lepomis megalotis*. Ph.D. thesis, University of Illinois, Champaign-Urbana, Ill. 171 p.

Kaya, C.M., and A.D. Hasler. 1972. Photoperiod and temperature effects on the gonads of green sunfish, *Lepomis cyanellus* (Rafinesque), during the quiesent, winter phase of its annual sexual cycle. Trans. Am. Fish. Soc. 101: 270–275.

Keast, A., and M.G. Fox. 1990. Fish community structure, spatial distribution and feeding ecology in a beaver pond. Environ. Biol. Fishes 27: 201–214.

Kozlowski, J. 1992. Optimal allocation of resources to growth and reproduction: implications for age and size at maturity. Trends Ecol. Evol. 7: 15–19.

Mann, R.H.K., C.D. Mills, and D.T. Crisp. 1984. Geographical variation in the life-history tactics of some species of freshwater fish, p. 171–186. *In* G.W. Potts and R.J. Wootton [ed.] Fish reproduction: strategies and tactics. Academic Press, London, U.K.

Miller, H.C. 1963. The behaviour of the pumpkinseed sunfish, *Lepomis gibbosus* (Linnaeus), with notes on the behaviour of other species of *Lepomis* and the pygmy sunfish, *Elassoma evergladei*. Behaviour 22: 88–151.

Murnyak, D.F., M.O. Murnyak, and L.J. Wolgast. 1984. Growth of stunted and nonstunted bluegill sunfish in ponds. Prog. Fish-Cult.46: 133–138.

Oliver, J.D., G.F. Holeton, and K.E. Chua. 1979. Overwinter mortality of fingerling smallmouth bass in relation to size, relative energy stores, and environmental temperature. Trans. Am. Fish. Soc. 108: 130–136.

Post, J.R., and D.O. Evans. 1989. Size-dependent overwinter mortality of young-of-the-year yellow perch (*Perca flavescens*): laboratory, in situ, and field experiments. Can. J. Fish. Aquat. Sci. 46: 1958–1968.

Pressley, P.H. 1981. Parental effort and the evolution of nest-guarding tactics in the threespine stickleback, *Gasterosteus aculeatus* L. Evolution 35: 282–295.

Raffetto, N.S., J.R. Baylis, and S.L. Serns. 1990. Complete estimates of reproductive success in a closed population of smallmouth bass (*Micropterus dolomieui*). Ecology 71: 1523–1535.

Regier, H.A. 1962. Validation of the scale method for estimating age and growth of bluegills. Trans. Am. Fish. Soc. 91: 362–374.

Reznick, D. 1983. The structure of guppy life histories: the tradeoff between growth and reproduction. Ecology 64: 862–873.

Ridgway, M.S., B.J. Shuter, and E.E. Post. 1991. The relative influence of body size and territorial behaviour on nesting asynchrony in male smallmouth bass, *Micropterus dolomieui* (Pisces: Centrarchidae). J. Anim. Ecol. 60: 665–681.

Roff, D.A. 1981. Reproductive uncertainty and the evolution of iteroparity: why don't flatfish put all their eggs in one basket? Can. J. Fish. Aquat. Sci. 38: 968–977.

Roff, D.A. 1982. Reproductive strategies in flatfish: a first synthesis. Can. J. Fish. Aquat. Sci. 39: 1686–1698.

Roff, D.A. 1984. The evolution of life history parameters in teleosts. Can. J. Fish. Aquat. Sci. 41: 989–1000.

Roff, D.A. 1986. Predicting body size with life history models. BioScience 36: 316–323.

Schultz, E.T., and R.R. Warner. 1991. Phenotypic plasticity in life-history traits of female *Thalassoma bifasciatum* (Pisces: Labridae): 2. Correlation of fecundity and growth rate in comparative studies. Environ. Biol. Fishes 30: 333–344.

Shuter, B.J., J.A. MacLean, F.E.J. Fry, and H.A. Regier. 1980. Stocastic simulation of temperature effects on first-year survival of smallmouth bass. Trans. Am. Fish. Soc. 109: 1–34.

Shuter, B.J, and J.R. Post. 1990. Climate, population variability, and the zoogeography of temperate fishes. Trans. Am. Fish. Soc. 119: 314–336.

Stearns, S.C. 1977. The evolution of life history traits: a critique of the theory and a review of the data. Annu. Rev. Ecol. Syst. 8: 145–171.

Stearns, S.C, and J.C. Koella. 1986. The evolution of phenotypic plasticity in life-history traits: predictions of reaction norms for age and size at maturity. Evolution 40: 893–913.

Trippel, E.A., and H.H. Harvey. 1989. Missing opportunities to reproduce: an energy dependent or fecundity gaining strategy in white sucker (*Catostomus commersoni*). Can. J. Zool. 67: 2180–2188.

Vøllestad, L.A., and J.H. L'Abée-Lund. 1990. Geographic variation in life-history strategy of female roach, Rutilus rutilus (L.). J. Fish Biol. 37: 853–864.

WOOTTON, R.J. 1977. Effects of food limitation during the breeding season on the size, body components, and egg production of female stickleback (*Gasterosteus aculeatus*). J. Anim. Ecol. 46: 823–834.

WOOTTON, R.J. 1979. Energy cost of egg production and environmental determinants of fecundity in teleost fishes. Symp. Zool. Soc. (Lond.) 44: 133–159.

WOOTTON, R.J. 1985. Energetics of reproduction, p. 231–254. *In* P. Tytler and P. Calow [ed.] Fish energetics: new perspectives. John Hopkins University Press, Baltimore, Md.

WOOTTON, R.J. 1990. Ecology of teleost fishes. Fish and fisheries series 1. Chapman and Hall, London, U.K. 404 p.

Change in the Known Ocean Distribution of Japanese Chum Salmon, *Oncorhynchus keta,* in Relation to the Progress of Stock Enhancement

Miki Ogura[1] and Soto-o Ito

National Research Institute of Far Seas Fisheries, Japan Fisheries Agency, 5-7-1, Orido, Shimizu, Japan 424

Ogura, M., and S. Ito. 1994. Change in the known ocean distribution of Japanese chum salmon, *Oncorhynchus keta*, in relation to the progress of stock enhancement. Can. J. Fish. Aquat. Sci. 51: 501–505.

New information on the ocean distribution of maturing Japanese chum salmon, *Oncorhynchus keta*, based on offshore tagging experiments conducted from 1956 to 1991 is summarized. Of 138 039 chum released in the North Pacific Ocean and its adjacent seas, 663 fish were recovered along the Japanese coast in the year of tagging and up to March of the next year. The distribution area of maturing Japanese chum indicated by these tag recoveries extended much further south and west than shown in previous studies. The central and western North Pacific Ocean now form important parts of the range. We conclude that extensive stock enhancement of chum in Japan is associated with enlargement of the known distribution area of maturing Japanese chum in the North Pacific Ocean.

Le présent article résume les nouvelles informations sur la répartition dans l'océan des saumons kéta japonais, *Oncorhynchus keta*, en phase de maturation, fondées sur des expériences de marquage en haute mer menées de 1956 à 1991. Sur les 138 039 saumons kéta relâchés dans le Pacifique nord et les mers contiguës, 663 poissons ont été récupérés le long de la côte japonaise l'année du marquage et jusqu'en mars de l'année suivante. L'aire de répartition du saumon kéta japonais en phase de maturation indiquée par les étiquettes récupérées s'étendait beaucoup plus au sud et à l'ouest que la répartition indiquée dans des études antérieures. Le centre et l'ouest du Pacifique nord constituent maintenant des parties importantes de l'aire. Nous en arrivons donc à la conclusion que la mise en valeur exhaustive du saumon kéta au Japon est associée à un agrandissement de l'aire de répartition connue du saumon kéta japonais en phase de maturation dans le Pacifique nord.

Received January 19, 1993
Accepted October 6, 1993
(JB758)

Reçu le 19 janvier 1993
Accepté le 6 octobre 1993

Chum salmon, *Oncorhynchus keta*, are the most widely distributed and the second most abundant species of all six species of Pacific salmon. During various portions of their life history, chum occupy most of the subarctic region of the North Pacific Ocean and adjacent seas (Shepard et al. 1968; Neave et al. 1976). Japan is the southernmost reproduction area along the western North Pacific coast (Salo 1991). Chum resources have undergone dramatic changes in the North Pacific Ocean since the 1970s. The annual catch of chum in Japanese coastal waters has increased exponentially from about 3 million individuals before 1970 to about 62 million in 1990 (Fig. 1). In Japan, enhancement of chum production began in the 1890s and since the 1970s has been very successful (Kaeriyama 1989). Concurrent with enhancement efforts, the high seas salmon fisheries began to decrease in 1977 and were finally terminated in 1991. The resulting increase in stock abundance has affected the growth of chum in the ocean (Kaeriyama 1989). The average body size of chum returning to Japanese and other areas has decreased (Ishida et al. 1993).

Since 1956, Japan, the United States, and Canada have conducted salmon tagging experiments under the auspices of the International North Pacific Fisheries Commission (INPFC) to determine the ocean distribution of Pacific salmon. Yonemori (1975) summarized the ocean distribution and migration routes of Japanese chum based on the data available up to 1971. Myers et al. (1990) have provided a summary of the ocean ranges of Pacific salmon based on more recent tag data.

The purpose of this paper is to use tag data from 1956 to 1991 to reassess the ocean distribution of Japanese chum and to clarify the changes that have occurred since enhancement of Japanese chum became pronounced in the 1970s.

Data Source

The tag release and recovery data of INPFC-related external tagging experiments conducted from 1956 to 1991 were used. Canada created a tag recovery computer database by coding recovery data collected during 1956–69 (Aro et al. 1971). Japan has independently maintained and updated that database to the present time. The release database for 1956–90 was provided by the United States and was updated to 1991 by Japan.

---

[1] Present address: Tohoku National Fisheries Research Institute, Japan Fisheries Agency, 3-27-5, Shinhama-cho, Shiogama, Miyagi, Japan 985.

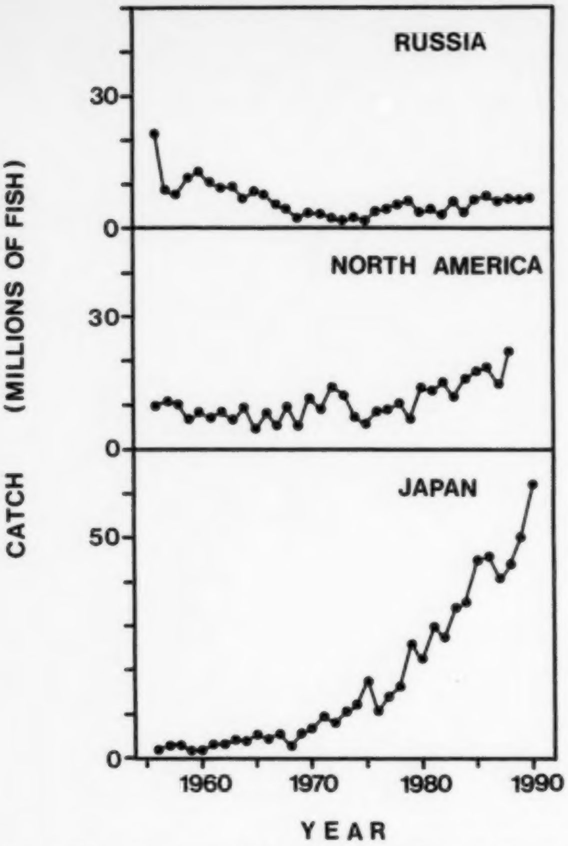

FIG. 1. Coastal commercial catch of chum salmon in Russia, North America, and Japan (Pacific Research Institute of Fisheries and Oceanography, Vladivostok, Russia, unpublished data; INPFC 1979, 1980–91; Fisheries Agency of Japan, Tokyo, Japan, unpublished data).

Floating long-lines were used to catch salmon for tagging experiments conducted by Japan and Canada, and purse seines were used for tagging experiments conducted by the United States and for cooperative work conducted by the United States and Russia (Neave et al. 1976). Most of the fish were tagged with disc tags, but a small number of Floy anchor-tags and spaghetti-tags were also used.

Results

In the North Pacific Ocean north of 38°N, including the Bering Sea, the Gulf of Alaska, and the Sea of Okhotsk, a total of 138 039 chum were tagged and released from 1956 to 1991 by Japan, Canada, the United States, and Russia. These tagging experiments were carried out mainly from April to August.

Based on the general life-history pattern of chum (e.g., Salo 1991), chum that were recovered in coastal waters during the same year they were tagged and up to March of the next year were considered to be sexually maturing at the time of tagging. A total of 1822 maturing tagged fish was recovered in coastal waters of the North Pacific Ocean up until May 1992, of which 663 were recovered in Japan (Hokkaido and Honshu coastal and inland waters). We assumed that these fish originated in Japan.

The general distribution pattern of maturing Japanese chum, based on the data from 1956 to 1991, is summarized as follows (Fig. 2). In April, maturing Japanese chum were distributed in the central North Pacific and the Gulf of Alaska from about 177°E longitude and 41°N latitude to as far north as 55°N latitude and as far east as 140°W longitude. In May, maturing chum were found widely in the North Pacific Ocean bounded by 166°E–141°W longitude and 43°N–52°N latitude. In June, the distribution area extended northward and some maturing chum had migrated into the central Bering Sea as far north as 58°N latitude. By July, chum had migrated northwestward and most were in the Bering Sea and the western North Pacific north of 46°N latitude. In August and later months, maturing chum were distributed from the western part of the Aleutian Islands to the area off the east coast of the Kamchatka Peninsula and along the Kuril Islands.

Tag release numbers for 1956–70 and 1971–91 (Table 1) were calculated for four tagging areas in the North Pacific Ocean (areas A, B, C, and D in Fig. 2), based on release data for grids 2° latitude × 5° longitude in size. The number of recoveries from releases in each of the four areas during 1956–70 and 1971–91 are listed by recovery area as follows: Japanese coast (Japan), Russian coast facing the Sea of Japan and the Sea of Okhotsk (Russian "I"), and Russian coast facing the North Pacific and the Bering Sea (Russian "II") (Table 1). In tagging area A, which includes the Bering Sea and the western and central North Pacific north of 48°N, more than 10 000 chum were released during each time period and notable recoveries in Japan were obtained. In tagging area B, which includes the western North Pacific (155°E–170°E) south of 48°N, there were several recoveries in Russia before 1970 and in Japan after 1971. In tagging area C, which includes the central North Pacific (170°E–165°W) south of 48°N, although there were more than 20 000 chum released from 1971 to 1991 with 64 subsequent recoveries in Japan and Russia, there was only one recovery from about 2000 chum released before 1970. In tagging area D, which includes the eastern North Pacific east of 165°W, the release number after 1971 was much smaller than before 1970 and only four recoveries in Japan were obtained from 1971 to 1991.

Tag recovery rates, calculated by dividing the number of tagged chum recovered by the number released, were compared between two time periods by each release and recovery area ($P < 0.05$; an approximate testing procedure (the normal approximation to the binomial distribution) for differences between two proportions (Zar 1984); in case of less than five recoveries, a randomization test for a difference between two proportions was used (Manly 1991)). Tag recovery rates along the Japanese coast, for releases from areas A–D, were consistently higher after 1971 than before 1970. In contrast, tag recovery rates in Russian "I", released from areas A and B, were lower after 1971 than before 1970 ($P < 0.05$).

Discussion

These latest tag recovery data reveal that the distribution area of maturing Japanese chum from April to July has became larger than shown in previous studies (Fig. 2 and 3)

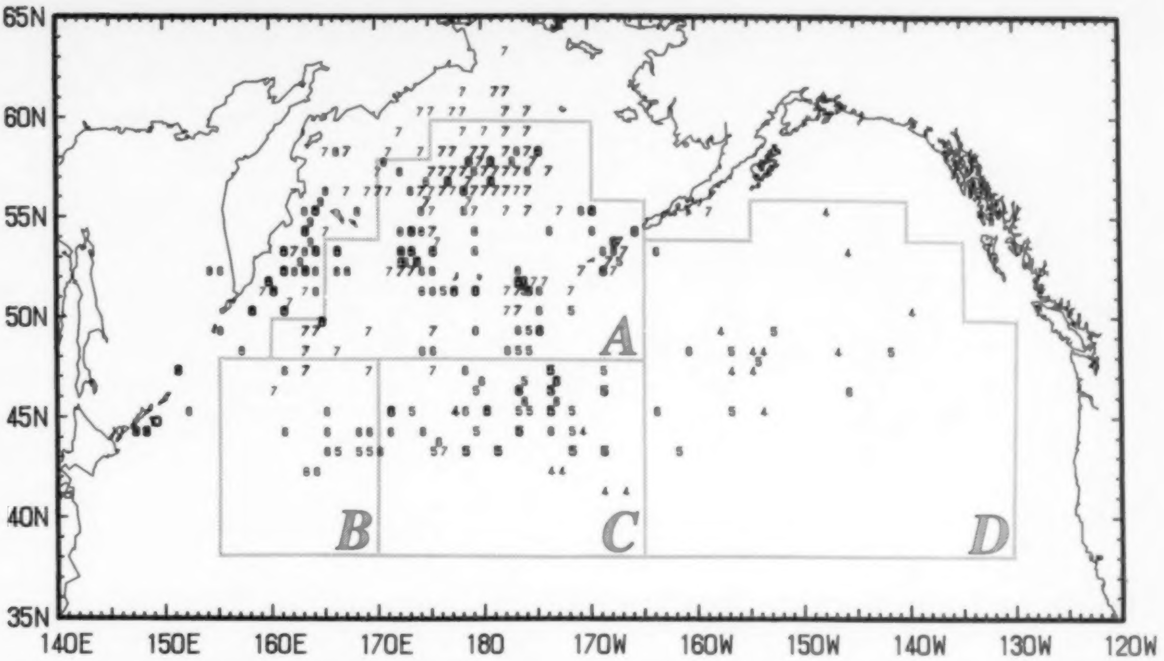

FIG. 2. Distribution of maturing Japanese chum salmon tagged in the North Pacific Ocean during 1956–91 and recovered along the Japanese coast in the year of tagging and up to March of the next year. The numerals show the month and location (in 1° latitude × 1° longitude areas) of tagging. Bold numerals indicate multiple recoveries. General release areas (A–D) used in Table 1 (shaded borders and letters).

TABLE 1. Number of chum salmon tagged and released during 1956–70 and 1971–91 in four oceanic rearing areas (see Fig. 2 and 3) and subsequently recovered in three coastal fishing areas. Russian "I" indicates a recovery area along the Russian coast facing the Sea of Okhotsk and the Sea of Japan. Russian "II" indicates a recovery area along the Russian coast facing the North Pacific Ocean and the Bering Sea. Numbers in parentheses indicate recovery rates (no. recovered/no. released; %).

			Number and rate of recoveries		
Area	Release period	Number	Japan	Russian "I"	Russian "II"
A	1956–70	52 074	202 (0.39)	68 (0.13)	64 (0.12)
	1971–91	13 580	251 (1.85)	4 (0.03)	11 (0.08)
B	1956–70	7 326	2 (0.03)	34 (0.46)	1 (0.14)
	1971–91	9 293	14 (0.15)	4 (0.04)	0 (0.00)
C	1956–70	2 117	0 (0.00)	1 (0.05)	0 (0.00)
	1971–91	21 645	56 (0.26)	5 (0.02)	3 (0.01)
D	1956–70	9 298	16 (0.17)	5 (0.05)	19 (0.20)
	1971–91	344	4 (0.86)	0 (0.00)	0 (0.00)

(Yonemori 1975; Neave et al. 1976). Some maturing Japanese chum were present in the central North Pacific Ocean (area C) in April and May and the data provide a substantial number of new records of distribution in the western North Pacific Ocean (area B) during May and June. Previously it was thought that chum present in the western North Pacific Ocean (area B) originated primarily from Russia (Neave et al. 1976). However, Myers et al. (1993) suggested that the majority of chum in the central and western North Pacific Ocean were of Asian, including Japanese, origin based on tagging data and tentative scale pattern analysis. These recent tag recoveries demonstrate that the central and western North Pacific Ocean are now also important parts of the distribution area for maturing Japanese chum.

Maturing Japanese chum may not actually have expanded their range southwestward, but rather have simply increased in number. One maturing chum released in the western North Pacific in 1959 (42°31′N, 163°54′E) was subsequently

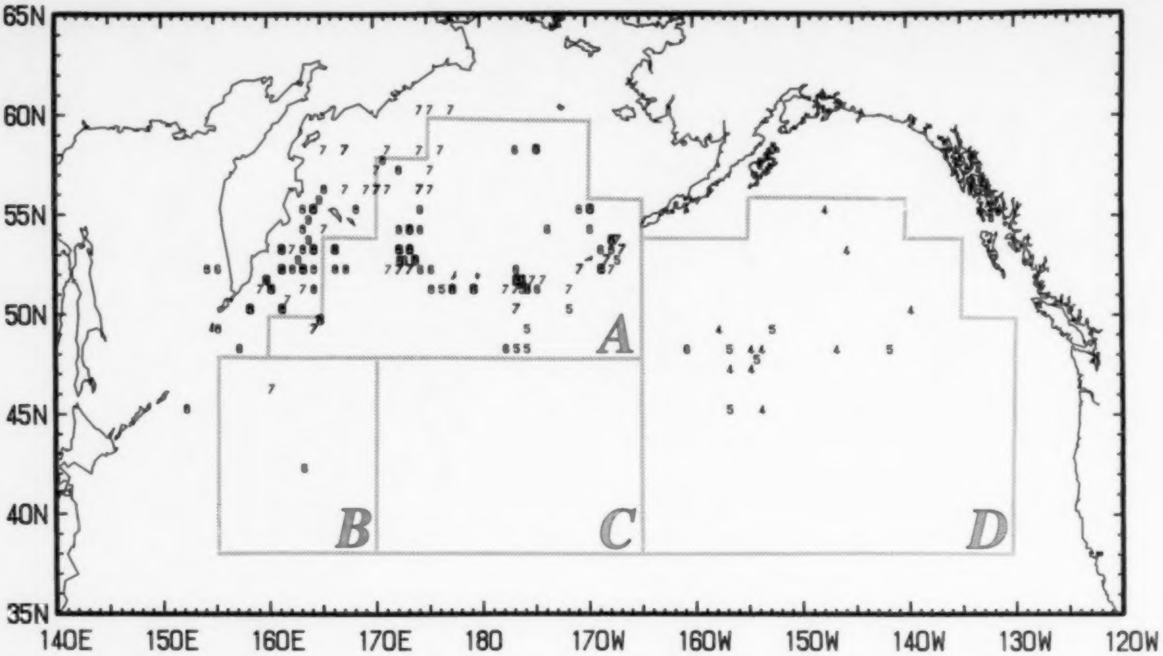

FIG. 3. Distribution of maturing Japanese chum salmon tagged in the North Pacific Ocean during 1956–70 and recovered along the Japanese coast in the year of tagging and up to March of the next year. The numerals show the month and location (in 1° latitude × 1° longitude areas) of tagging. Bold numerals indicate multiple recoveries. General release areas (A–D) used in Table 1 (shaded borders and letters).

recovered off Hokkaido, Japan (Fig. 3). Although this record has not been given much weight, the presence of this fish suggests that some maturing Japanese chum likely were distributed in the western North Pacific Ocean prior to the 1970s as well.

Although the enlargement of the known range of Japanese chum in the central North Pacific Ocean (area C) probably has resulted from the increase in release effort (Table 1), the apparent recent expansion in the western North Pacific Ocean (area B) is not due simply to the smaller numbers of chum tagged and released prior to the 1970s (Table 1). It may be due to the stock enhancement of chum in Japan. The number of adult chum returning to Japan has increased substantially in recent years (Fig. 1) (Kaeriyama 1989), while returns to North America have not increased much, and returns to Russia have decreased slightly over the same period (Fig. 1). As a result, Japanese chum currently comprise a higher proportion of the total chum population in the North Pacific Ocean than in the past. The increased recovery of tagged Japanese chum in recent years is more likely due to the higher proportion of Japanese chum now found in the North Pacific than to any other changes that could affect tag recovery rates.

The recent increase in recovery rates (i.e., proportion recovered) of tagged Japanese chum (Table 1), especially from area B, does not appear to have resulted from other possible changes. The tag recovery rate in this study is a function of the tagging mortality rate, the tag shedding rate, the exploitation rate of the stock in coastal areas, the reporting rate for tags found, and the proportion of maturing fish in the total stock that is distributed in each tag release area. Tagging mortality rate varies with the maturity of the fish; however, all chum tagged in this study were maturing fish. The rate may also vary somewhat with the size of the fish. The tag shedding rate varies among different tagging methods; however, the tagging method used to obtain the data in this study (largely the external disc tag) has remained basically the same from 1956 to 1991. It is likely therefore that these two factors have affected recovery rates of tagged Japanese and Russian chum equally.

Although absolute values of the exploitation and tag reporting rates were difficult to estimate, they were different among recovery areas and varied independently (Takei 1989). Both of these rates generally increased in response to the progress of the enhancement program for chum because of the increase in interest in chum returns and the proportion of fish caught in coastal and inland waters. Since the 1910s, Japanese chum populations have been maintained by artificial propagation, with most adult Japanese chum being caught in coastal waters by commercial fisheries and in river estuaries for artificial reproduction (Kaeriyama and Urawa 1992). Therefore, we assumed that for the fish recovered in Japanese waters the rates were high and did not change substantially during the study period. In Russia, although there apparently is no information on the size of the wild stock, these rates may have increased recently due to the gradual increase in the number of juvenile chum released there (McNeil 1977).

Although the four factors discussed above (other than the proportion of maturing fish in the total stock) may account for some of the change in the numbers of tagged chum recovered, they do not explain the concurrent recent increase in the numbers of recoveries in Japan from releases in all areas and the decrease in the numbers of recoveries in Russian "I" and Russian "II" (Table 1). Therefore the higher proportion of Japanese chum in the North Pacific is the most important factor related to the change in the number of tagged chum recovered.

Tagged chum were also intercepted by the Japanese high seas salmon fishery during their homing migration. Although effort and catch decreased greatly after the mid-1970s, this fishing mortality probably equally affected Japanese and Russian chum in the same tagging area.

The return migration pattern of chum from the western and central North Pacific illustrated by these new tag data cannot be explained simply on the basis of the ocean currents of the North Pacific Ocean as previously suggested (Yonemori 1975). Yonemori (1975) suggested that maturing Japanese chum begin their spawning migration in spring from an area in the Subarctic Current in the Gulf of Alaska and are later either transported or "assisted" into the Bering Sea by the Alaska Current. During their homing migration in the open sea, chum swim mainly in the upper 30 m of the water column (Ogura 1990), so surface currents should affect their migratory behavior to the same degree. For example, a recent computer simulation study has also suggested that the effects of surface currents in the Northeast Pacific must be included in the migration model of sockeye salmon (*Oncorhynchus nerka*) returning to the Fraser River (Thomson et al. 1992). However, chum from the central and western North Pacific must swim to the west against the Subarctic Current, and/or the West Wind Drift, and then across the Western Subarctic Gyre (see Favorite et al. 1976 for a detailed description of the current system in the North Pacific Ocean). Neave (1964) also suggested that Pacific salmon migrate across oceanic areas and major current features. Therefore, during their spawning migration, at least some maturing Japanese chum must migrate using some navigation cues instead of, or in addition to, the ocean currents.

In conclusion, the distribution area of maturing Japanese chum was wider than shown in previous studies, and the central and western North Pacific Ocean are now important parts of the range. The apparent expansion of the known range in the western North Pacific may be due to the stock enhancement of chum in Japan.

Acknowledgments

Many Japanese, American, and Canadian scientists have been involved in INPFC programs that have resulted in the creation and correction of the INPFC tag recovery and release databases. We would like to acknowledge their contributions and generosity in making the data available to us. We thank Mr. J. Ito of the National Research Institute of Far Seas Fisheries for his valuable comments on the manuscript. We are also grateful to Dr. N.B. Hargreaves of the Pacific Biological Station for reviewing the manuscript.

References

Aro, K.V., J. Thomson, and D. Giovando. 1971. Recoveries of salmon tagged offshore in the North Pacific Ocean by Canada, Japan, and the United States, 1956 to 1969. Fish. Res. Board Can. MS Rep. 1147: 493 p.

Favorite, F., A.J. Dodimead, and K. Nasu. 1976. Oceanography of the subarctic Pacific region. Int. N. Pac. Fish. Comm. Bull. 33: 187 p.

International North Pacific Fisheries Commission (INPFC). 1979. Historical catch statistics for salmon of the North Pacific Ocean. Int. N. Pac. Fish. Comm. Bull. 39: 166 p.

International North Pacific Fisheries Commission (INPFC). 1980–91. Statistical yearbook 1977–1988. INPFC, Vancouver, B.C.

Ishida, Y., S. Ito, M. Kaeriyama, S. McKinnell, and K. Nagasawa. Recent changes in age and size of chum salmon (*Oncorhynchus keta*) in the North Pacific Ocean and possible causes. Can. J. Fish. Aquat. Sci. 50: 290–295.

Kaeriyama, M. 1989. Aspects of salmon ranching in Japan. Physiol. Ecol. Jpn. Spec. Vol. 1: 625–638.

Kaeriyama, M., and S. Urawa. 1992. Future research by the Hokkaido Salmon Hatchery for the proper maintenance of Japanese salmonid stocks, p. 57–62. *In* Y. Ishida, K. Nagasawa, D.W. Welch, K.M. Myers, and A.P. Shershnev [ed.] Proceedings of the International Workshop on Future Salmon Research in the North Pacific Ocean. Spec. Publ. Natl. Res. Inst. Far Seas Fish. 20.

Manly, B.F.J. 1991. Romdomization and Monte Carlo methods in biology. Chapman and Hall, London. 281 p.

McNeil, W.J. 1977. Artificial recruitment of pink and chum salmon in Japan and eastern USSR. U.S. Department of Commerce Processed Rep., Northwest and Alaska Fisheries Center, Seattle, Wash. 13 p.

Myers, K.W., C.K. Harris, Y. Ishida, L. Margolis, and M. Ogura. 1993. Review of the Japanese landbased driftnet salmon fishery in the western North Pacific Ocean and the continent of origin of salmonids in this area. Int. N. Pac. Fish. Comm. Bull. 52: 86 p.

Myers, K.W., R.V. Walker, S. Fowler, and M.L. Dahlberg. 1990. Known ocean ranges of stocks of Pacific salmon and steelhead as shown by tagging experiments, 1956–1989. Int. N. Pac. Fish. Comm. Doc. FRI-UW-9009. Fisheries Research Institute, University of Washington, Seattle, Wash. 57 p.

Neave, F. 1964. Ocean migration of Pacific salmon. J. Fish. Res. Board Can. 21: 1227–1244.

Neave, F., T. Yonemori, and R.G. Bakkala. 1976. Distribution and origin of chum salmon in offshore waters of the North Pacific Ocean. Int. N. Pac. Fish. Comm. Bull. 35: 79 p.

Ogura, M. 1990. Outline of biotelemetry study of salmon by the *Shin-Riasu maru*, 1990. Int. N. Pac. Fish. Comm. Doc. National Research Institute of Far Seas Fisheries, Shimizu, Japan. 22 p.

Salo, E.O. 1991. Life history of chum salmon (*Oncorhynchus keta*), p. 231–297. *In* C. Groot and L. Margolis [ed.] Pacific salmon life histories. University of British Columbia Press, Vancouver, B.C.

Shepard, M.P., A.G. Hartt, and T. Yonemori. 1968. Salmon of the North Pacific Ocean — Part VIII. Chum salmon in offshore waters. Int. N. Pac. Fish. Comm. Bull. 25: 69 p.

Takei, A. 1989. Estimate of chum salmon (*Oncorhynchus keta*) of Japanese origin caught in the U.S. June fishery conducted in the Shumagin/Unimak waters. Int. N. Pac. Fish. Comm. Doc. Fishery Agency of Japan, Tokyo, Japan. 25 p.

Thomson, K.A., W.J. Ingraham, M.C. Healey, P.H. LeBlond, C. Groot, and C.G. Healey. 1992. The influence of ocean currents on latitude of landfall and migration speed of sockeye salmon returning to the Fraser River. Fish. Oceanogr. 1: 163–179.

Yonemori, T. 1975. A trial analysis of the results obtained from tagging on chum salmon originating from Hokkaido. Int. N. Pac. Fish. Comm. Bull. 32: 130–161.

Zar, J.H. 1984. Biostatistical analysis. Prentice Hall, Englewood Cliffs, N.J. 718 p.

Sources of Variation in Growth of the European Eel (*Anguilla anguilla*) Estimated from Otoliths

Jacques Panfili[1] and Marie-Claude Ximénès

CEMAGREF, Division Aquaculture et Pêche, B.P. 5095, 34033 Montpellier Cedex 1, France

and Alain J. Crivelli

Station Biologique de la Tour du Valat, Le Sambuc, 13200 Arles, France

Panfili, J., M.-C. Ximénès, and A.J. Crivelli. 1994. Sources of variation in growth of the European eel (*Anguilla anguilla*) estimated from otoliths. Can. J. Fish. Aquat. Sci. 51: 506–515.

Tetracycline labelling of otoliths was used for studying the growth of the European eel (*Anguilla anguilla*), which has strong individual variability. Two groups of eels were injected with tetracycline and released into a natural pond (Camargue, south of France) in spring 1989 and in autumn 1989. The marginal growth of otoliths between marking (tetracycline mark) and capture (otolith margin) was measured for all fish sampled until spring 1990. Comparisons of otolith growth rates were made according to fish size, age, sex, and growth period (ANCOVA). The results showed a great variability. After 15 mo of growth, the mean growth in length (back-calculated) was 6.6 cm. The three main factors tested, age, sex, and seasonal growth period, had a significant effect on otolith growth and therefore on somatic growth, since the relation between fish length and that of the otolith is highly significant ($r^2 = 0.802$). There was also a very significant effect of size at marking on otolith growth. It is difficult to rank qualitative importance of these various factors, even though there are no interactions among them. The best absolute growth in Mediterranean lagoons could be attained by 2-yr-old female fish growing in the summer months.

Le marquage à la tétracycline des otolithes a été utilisé pour étudier la croissance de l'anguille européenne (*Anguilla anguilla*) qui présente une forte variabilité individuelle. On a injecté de la tétracycline à deux groupes d'anguilles qui ont été relâchées dans un étant naturel (Camargue, sud de la France) au printemps de 1989 et à l'automne de 1989. La croissance marginale des otolithes entre le marquage (marque à la tétracycline) et la capture (bord de l'otolithe) a été mesurée chez tous les poissons échantillonnés jusqu'au printemps de 1990. On a comparé le taux de croissance des otolithes selon la taille du poisson, l'âge, le sexe et la période de croissance (ANCOVA). Les résultats étaient très variables. Après une croissance de 15 mo, la croissance moyenne en longueur (rétro-calcul) était de 6,6 cm. Les trois principaux facteurs vérifiés, l'âge, le sexe et la période de croissance saisonnière, avaient un effet important sur la croissance des otolithes, et donc sur la croissance somatique, puisque le rapport entre la longueur du poisson et celle de l'otolithe est très significative ($r^2 = 0{,}802$). Il y avait également un effet très important de la taille au moment du marquage sur la croissance des otolithes. Il est difficile de classer l'importance relative de ces différents facteurs même s'il n'y a pas d'interactions entre eux. C'est chez les femelles âgées de 2 ans en croissance pendant la période estivale que l'on pourrait observer la meilleure croissance absolue dans les bassins méditerranéens.

Received January 28, 1993
Accepted October 6, 1993
(JB773)

Reçu le 28 janvier 1993
Accepté le 6 octobre 1993

Exact estimates of the individual growth of fish in their natural environment can only be made by individual marking. This type of manipulation implies a minimum of four steps: capture of fish, marking, release into a given environment, and recapture. Marking can be external (tags, tattooing, etc.) or internal (magnetic rods, injection of fluorescent markers, various stress actions, etc.) or a combination of the two. Three main constraints are involved in marking experiments: (1) the marking must not affect subsequent growth, (2) the individual marks must remain visible for the entire length of the experiment, and (3) sufficient fish must be recaptured to obtain a good estimate of growth.

Internal markers of the fluoromarker type (e.g., tetracyclines) have been used for a long time to mark calcified tissues during their mineralisation (Van Coillie 1967; Weber and Rigway 1967; Meunier 1974; Meunier and Boivin 1974). These markers have often been used in experiments to validate the timing of deposition of growth marks on calcified tissues to determine the growth cycle (Beamish and McFarlane 1983, 1987), but they have seldom been used to study the variability in the growth of individual fish. If marking experiments can provide high rates of recapture, vital marking of calcified tissues, e.g., otoliths, can constitute a database for studying individual growth. Where growth is proportional to growth of the calcified piece (otolith), back-calculation can allow growth in length to be estimated. Results of back-calculation must, however, always be interpreted with care because the mathematical methods are

---

[1] Present address: ORSTOM, Centre de Brest, Laboratoire de Sclérochronologie des Animaux Aquatiques IFREMER-ORSTOM, B.P. 70, 29280 Plouzané, France.

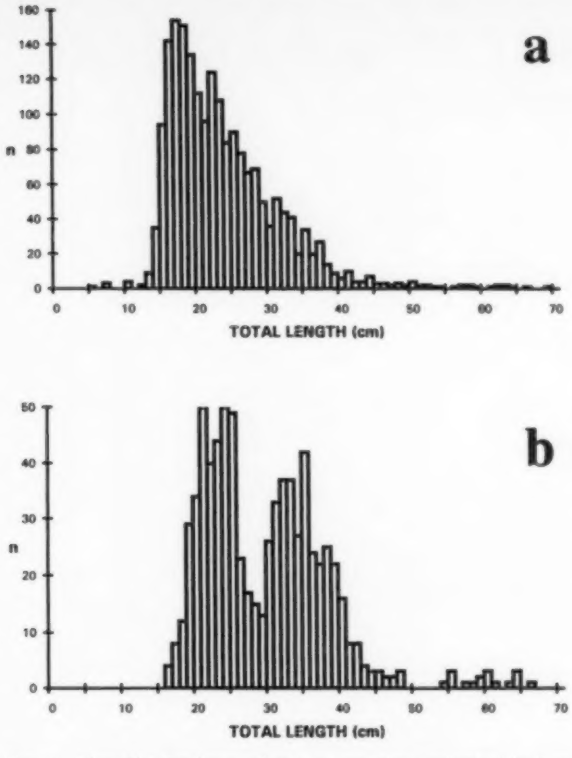

FIG. 1. Size distributions of eels at marking, released in Les Garcines pond. (a) Group 1 marked in March 1989; (b) group 2 marked in October 1989.

varied (Francis 1990) and the possibilities of bias due to the modelling are not insignificant (Small and Taylor 1987; Campana 1990; Ricker 1992).

Individual marking of European eels (*Anguilla anguilla*) during their continental life stage is especially difficult (see Nielsen 1988 for a review). Almost all marking techniques have deleterious effects on this fish, and marking is generally only carried out on groups (e.g., by tattooing). This is undoubtedly due to the morphology of this species and its benthic life style which prevent the use of external markers. In addition, these markers have a considerable effect on subsequent growth as has been shown by marking experiments in natural environments: e.g., Berg (1986) showed that jaw tags led to reduced individual growth, and Tulonen (1989) found that eels marked with Carlin-type tags practically ceased growing.

All the data in the literature on the growth of the European eel in various habitats show extreme qualitative and quantitative individual variability (Vøllestad 1989, 1992; Fontenelle 1991). This variability has been assessed to be great within any one population: in the estuarine environment (Fernández-Delgado et al. 1989), in freshwater habitats (Moriarty 1983; Vøllestad and Jonsson 1988; Poole 1991), in lake environments (Paulovits and Biró 1986; Nagiec and Bahnsawy 1990), and in fish farms (Egusa 1979; Kuhlmann 1979; Wickins 1985). Differences in growth among individuals are not restricted to the European species but have also been found in other species (*Anguilla rostrata*, Hansen and Eversole 1984; *Anguilla mossambica*, McEwan and Hecht 1984; *Anguilla australis*, Chisnall and Hayes 1991). Variability in the growth of the eel has usually been detected either directly in fish farms or indirectly by age studies within populations, but age is a variable that is difficult to assess from otoliths without ambiguity (Michaud et al. 1988; Vøllestad et al. 1988) because of problems of interpretation. Thus, observed variability in length at a given age could be due to errors introduced by the method used for age determination (Vøllestad 1985; Fontenelle 1991). A better understanding of the biotic and abiotic factors leading to this variability would undoubtedly enable more effective management of the exploited stages of this species throughout European inland waters and would also allow aquacultural constraints to be optimised. The sources of variation in eel growth in the natural environment are still to be explored. The main sources of individual variations certainly include age, sex, and seasonality in growth (a function of temperature). It is, however, essential to determine which of the various factors has the preponderant influence before defining the best management criteria.

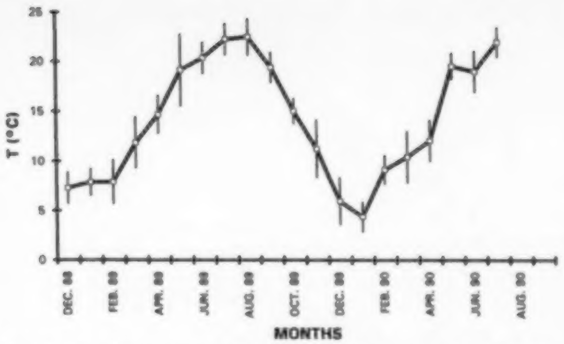

FIG. 2. Monthly means and standard deviations of the daily bottom temperatures in Les Garcines pond during the experiment.

For the European eel, a marking experiment was carried out with the aim of studying sources of variability in individual growth in a natural environment representative of a category of biotopes colonized by certain populations: the Mediterranean waterbodies of the south of France. Otoliths were marked with tetracycline, this internal mark being an indicator visible later upon recapture at various dates, for growth comparison. The effects of factors such as age, sex, and the growth period were tested.

Materials and Methods

Marking and Sampling

Two groups of eels originating from lagoons in the south of France were marked, in March 1989 (group 1) and in October 1989 (group 2), and then released into a natural freshwater pond (Les Garcines, Camargue), at densities of 30 $kg \cdot ha^{-1}$ (1973 individuals) and 20 $kg \cdot ha^{-1}$ (749 individuals), respectively. The eels in the two groups were of various sizes, ranging from 6 to 69 cm at the time of marking (Fig. 1). Marking consisted of (1) internal marking by intraperitoneal injection of tetracycline (75 $mg \cdot kg$ live $weight^{-1}$) and (2) external marking by ablation of part of the pectoral fin to distinguish between groups and by ventral

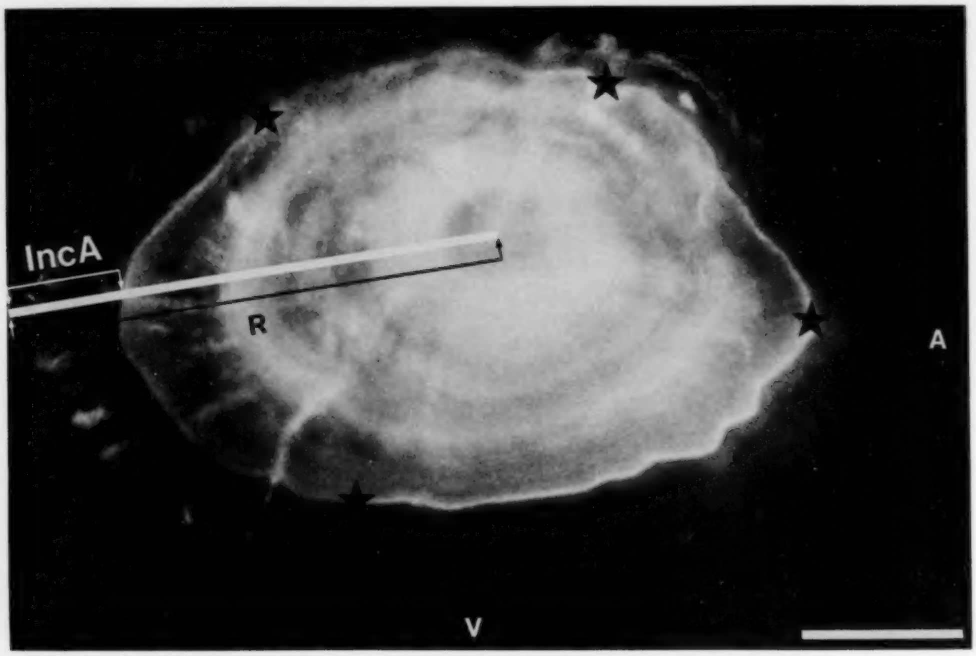

FIG. 3. Tetracycline-labelled otolith observed under reflected light, a dark background, and incident ultraviolet light. This view shows the measurements on the otolith: *R*, radius of maximum growth on the anteroposterior axis; IncA, absolute increment between the tetracycline mark (stars) and the margin. A = anterior; V = ventral. Scale bar = 0.3 mm.

TABLE 1. Number of individuals marked and recaptured at each date in Les Garcines pond.

	Group 1	Group 2
Marking in March 1989	1973 (G1)	
Intermediary captures (April to September 1989)	38	
Captures in October 1989	37 (G1O)	
Marking in October 1989		749 (G2)
Intermediary captures (September 1989 to May 1990)	51	12
Captures in June 1990	602 (G1J)	302 (G2J)

tattooing with alcian blue (subcutaneous injection). Les Garcines pond (2.1 ha) was a closed system throughout the experiment, with managed inputs and outputs of water and a known initial population of fish. Samples of fish were collected at monthly intervals from the first release and a more intensive fishing effort was made before the second release. At the end of the experiment in June 1990, the pond was drained and the remaining pool was treated with rotenone to capture all remaining fish. The numbers of fish marked and recaptured are given in Table 1. The water temperature in the pond was recorded daily throughout the experiment (Fig. 2).

Individual Examination

At each sampling date, the eels were measured (total length (TL), centimetres), weighed (grams), sexed macroscopically (undifferentiated: U, male: M, female: F), and their otoliths (sagitta) extracted. A total of 1004 individuals were recaptured, including 37 from group 1 in October 1989 and 602 from group 1 and 302 from group 2 in June 1990 (Table 1). All the otoliths were examined whole in reflected light against a black background (cleared in a bath of rosemary essential oil), with the distal face uppermost, under an epifluorescent microscope (Olympus BH, HBO 100-W lamp providing UVB at 490 nm). The tetracycline mark was located by its yellow–green fluorescence under the UVB excitation. Two measurements (millimetres) were made on the otolith (Fig. 3): *R*, the otolith radius along its anteroposterior axis measured from the nucleus centre to the posterior margin, and IncA, the absolute otolith increment between marking and capture, i.e., the distance between the inner margin of the tetracycline mark and the otolith margin along the radius defined above. The relative otolith increment, IncR, is the ratio of IncA over *R* (IncR = IncA/*R*). The age (*A*, years) of each individual in continental water was calculated by counting the number of opaque rings on the otolith from the nucleus outwards; it had previously been shown that a broad opaque zone and a broad hyaline were laid down each year in French Mediterranean lagoons (Panfili et al. 1992).

Analysis

Several variables are available for comparing individual growth: IncA, IncR, age (A), sex (U, M, F), and the various growth periods (G1O, G1J, G2J). G1O is the growth period for group 1 between March 89 and October 89, i.e., 7 mo including spring and summer. G1J is the growth period for group 1 between March 89 and June 90, i.e., 15 mo including an entire annual cycle. G2J is the growth period for group 2 between October 89 and June 90, i.e., 8 mo including autumn, winter, and the start of spring.

It would be preferable to compare the absolute otolith increments (IncA). However, it is essential beforehand to test whether age (A) or size (TLm) of the individual at the time of marking has an influence on this variable. If A or TLm does have a significant influence on IncA, which is probable in view of the deceleration of growth with age or size, relative individual increments (IncR) must be compared. To this end, TLm was back-calculated from the length at recapture (TL) and the otolith radius at the time of marking (R-IncA). The regression between the length of the fish and that of the otolith, necessary for back-calculation, was linear and highly significant ($p < 0.01$):

(1) $\mathrm{TL} = 1.163 + 26.336 \cdot R$ ($n = 908$ $r^2 = 0.802$).

The back-calculation formula used that of Francis (1990), based on the assumption that the length of fish and the growth of the otolith are proportional over time:

(2) $$\mathrm{TLm} = [(1.163 + 26.336 \cdot (R - \mathrm{IncA}))/(1.163 + 26.336 \cdot R)] \cdot \mathrm{TL}.$$

A one-way analysis of variance (ANOVA, Scheffe range test, Statgraphics®) was carried out on IncA to test the effects of age (A) and length at the time of marking (TLm). For this ANOVA, the TLm values were grouped into 5-cm size classes and the analysis was carried out for each time period (G1O, G1J, G2J). Initial tests showed significant differences in IncA between the various age ($F_{(5,573)} = 14.72$, $p < 0.01$, for G1J) and TLm classes ($F_{(8,578)} = 21.99$, $p < 0.01$, for G1J). Moreover, a two-way ANOVA (sex and period) conducted on the length of eels at recapture (TL) showed a very significant effect of sex on TL ($F_{(2,957)} = 478.1$, $p < 0.01$), but no influence of growth period ($F_{(2,957)} = 1.6$, $p > 0.05$). The size at marking therefore had a significant effect on absolute otolith increment. To make growth comparisons between the sexes, it is therefore necessary to examine the relative otolith increment (IncR). The analysis was then conducted on the IncR values.

An analysis of covariance (ANCOVA) (multifactor ANOVA, Scheffe range test, Statgraphics®) was carried out on IncR as a function of age (A, from 1 to 3 yr), sex (U, M, F), and period of growth (G1O, G1J, G2J), with TLm as covariate. Age classes older than 3 yr had to be eliminated from this analysis because they were not represented in all growth periods. The effect of individual maturation (change to the "silver eel" stage) could not be taken into account because of the very low number of silver eels recaptured (1% for G1J and 4% for G2J). Beforehand, a test for normality of distributions and homogeneity of variances was undertaken. This showed that the distributions were more similar to a Poisson type and that the variances were slightly heterogeneous for G2J, so the ANCOVA was performed on the transformed variable, log(IncR+1), for which the distributions were normal and the variances homogeneous. The relative importance of the various factors having a significant effect on IncR was assessed from an analysis of the centred residuals derived from the ANCOVA. To do this, the residual variances and the distributions of the residuals were examined.

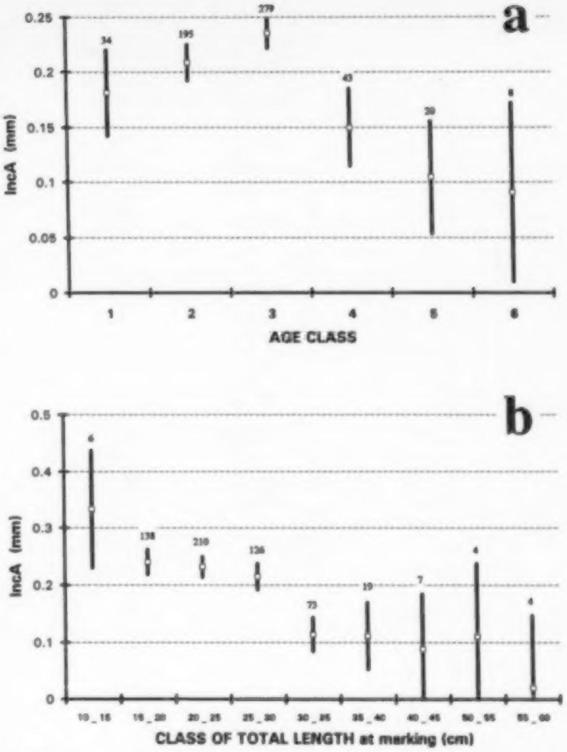

FIG. 4. Means and confidence intervals (95%) of the absolute otolith increment (IncA) for each class (G1J). Numbers above each class correspond to sample sizes. (a) Age classes; (b) total length at marking (TLm) classes.

Results

Absolute Growth

The absolute growth of otoliths in relation to age, sex, or growth period was extremely variable in Les Garcines pond, as shown by the high values for the coefficients of variation (CV) of IncA (Table 2). In October 89 (G1O), after 7 mo of growth, the length increment varied between 1.7 and 10.1 cm, with a mean of about 5 cm, sexually undifferentiated individuals and 2-yr-old fish having the greatest growth (Table 2). After 15 mo of growth (G1J), extreme values for length increments were from 0 to 18 cm, with a mean of 6.6 cm, and females and 3-yr-old fish had the best growth (Table 2). The growth of the otolith did slow with age (Fig. 4a) and there was a clear decrease in growth as a function of size at marking (Fig. 4b). For the G1J group, the percentage of individuals with zero growth was low: 0.4% of undifferentiated fish, 2.3% of males, and 6.5% of females, with no growth occurring particularly among the larger individuals (but not specially silver eels). Finally, the group that remained for 8 mo in the pond, over winter (G2J),

TABLE 2. Values of IncA (mm) for each class of the two factors age and sex and for each period. SD = standard deviation; CV = coefficient of variation; IncL = back-calculated length increment (cm) from mean of IncA.

	n	Mean	SD	CV (%)	IncL
G1O					
Age					
1	7	0.1486	0.0773	52.0	5.1
2	15	0.1587	0.0850	53.6	5.3
3	4	0.1300	0.0841	64.7	4.6
Sex					
U	14	0.1771	0.0811	45.8	5.8
M	5	0.1160	0.0792	68.3	4.2
F	17	0.1235	0.0864	69.9	4.4
G1J					
Age					
1	34	0.1815	0.0701	38.7	5.9
2	195	0.2087	0.0921	44.1	6.7
3	279	0.2355	0.0974	41.4	7.4
4	43	0.1498	0.1277	85.3	5.1
5	20	0.1050	0.1225	116.7	3.9
6	8	0.0912	0.0608	66.6	3.6
Sex					
U	251	0.2052	0.0842	41.0	6.6
M	211	0.1906	0.1038	54.5	6.2
F	134	0.2401	0.1287	53.6	7.5
G2J					
Age					
1	119	0.0610	0.0453	74.2	2.8
2	110	0.0453	0.0604	133.4	2.4
3	33	0.0673	0.1167	173.5	2.9
4	10	0.0250	0.0556	222.5	1.8
Sex					
U	151	0.0704	0.0613	86.9	3.0
M	97	0.0274	0.0373	136.1	1.9
F	43	0.0532	0.0923	173.4	2.6
Age, undifferentiated					
1	145	0.0929	0.0735	79.1	3.6
2	157	0.1827	0.0968	53.0	6.0
3	94	0.2151	0.0882	41.0	6.8
Age, male					
1	7	0.0314	0.0261	83.0	2.0
2	123	0.1129	0.1217	107.7	4.1
3	135	0.1894	0.1038	54.8	6.1
4	27	0.0807	0.0690	85.4	3.3
5	11	0.0473	0.0559	118.2	2.4
Age, female					
1	8	0.0975	0.0767	78.6	3.7
2	40	0.1362	0.1022	75.0	4.7
3	87	0.2605	0.1333	51.2	8.0
4	25	0.1772	0.1567	88.4	5.8
5	9	0.1467	0.1646	112.2	5.0
6	5	0.1040	0.0767	73.7	3.9

showed the lowest growth of 2.7 cm on average, with the greatest length increment among the undifferentiated and 3-yr-old fish (Table 2). Variability in growth was great for G2J, with a CV usually greater than 100% (Table 2).

Irrespective of the growth period, growth was always greater for individuals belonging to the younger age classes (1, 2, or 3 yr) and lower for males (Table 2). In general, variability (CV) was greater in older individuals, and undifferentiated individuals always had the lowest variability (Table 2). Variability in growth was greater for the short growth periods (G1O and G2J) than for the longer period (G1J). In the latter group, the CV was low for the first three age classes and for the different sex categories.

The ranking of the periods in terms of growth was the same for each sex category (Table 2): growth was lowest for G2J (8 mo, including winter), highest for G1J (15 mo), and intermediate for G1O (7 mo, including summer). In each sex category, age class 3 had the highest otolith incre-

TABLE 3. ANCOVA on the effect of age (1–3 yr), sex, and period on the relative increment of otoliths (IncR) after transformation (covariate = total length at marking, TLm). SS = sum of squares; df = degrees of freedom; *effect significant ($p < 0.01$).

Source of variation	SS	df	Mean square	F-ratio	Significance level
Covariate					
TLm	0.49943	1	0.49943	1000.000	0.001*
Main effects	0.40191	6	0.06698	165.300	0.001
Age	0.03156	2	0.01578	38.941	0.001*
Sex	0.05075	2	0.02537	62.613	0.001*
Period	0.05694	2	0.02847	70.259	0.001*
Two-factor interactions	0.00670	12	5.58×10^{-4}	1.379	0.170
Age vs. sex	0.00353	5	7.05×10^{-4}	1.740	0.123
Age vs. period	0.00233	5	4.66×10^{-4}	1.151	0.332
Sex vs. period	0.00063	4	1.58×10^{-4}	0.391	0.815
Residual	0.31122	768	4.05×10^{-4}		
Total	1.21926	787			

ment and the lowest variability (Table 2). Variability in growth was lowest for all sex categories in the longest growth period (Table 2).

Factor Effects on Growth

ANCOVA on IncR (transformed as log[IncR+1]) revealed a significant effect of age, sex, and growth period ($p < 0.01$; Table 3). The covariable TLm also had a highly significant effect ($p < 0.01$) on relative otolith growth (Table 3). In addition, there were no significant first-order interactions ($p > 0.05$) between the various factors taken as pairs (Table 3).

Otolith growth is therefore influenced by the age, body length, and sex of individuals. The age classes are clearly distinct for each of these factors (Table 4): for the first three age classes, growth increases with age. There is, however, a clear reduction in growth as from age class 3 in the G1J group, in which the number of age classes goes up to six (Fig. 4a). Undifferentiated fish and females form a homogeneous group in the factor sex and grow faster than males (Table 4). The period of growth also has an influence (Table 4): for the same time interval, growth is notably greater if the period includes the summer months than if it includes winter or even the start of spring. An entire annual growth cycle tends to reduce variability within age and sex classes (Table 2).

From the experiment conducted in this study, the growth periods can be summarized by the following equation:

G1O + G2J = G1J
(March 1989 to October 1989) + (October 1989 to June 1990) = (March 1989 to June 1990).

For each sex, the mean growth in G1J should therefore be equal to the sums of the mean growths in G1O and G2J. Taking the back-calculated absolute length increments (centimetres; Table 2), the values are as follows:

Undifferentiated: G1O + G2J (8.8 cm) > G1J (6.6 cm)
Males: G1O + G2J (6.1 cm) ≈ G1J (6.2 cm)
Females: G1O + G2J (7.0 cm) ≈ G1J (7.5 cm).

The equality of the growth periods is fairly well respected for males and females, but not for undifferentiated fish. These values were, however, calculated for all age classes.

TABLE 4. Homogeneity of the groups in terms of the various factors used in the ANCOVA on transformed IncR (Table 3). For each factor, similar letters indicate homogeneous groups.

Factor	n	Average	Homogeneous groups
Age			
1	158	0.04228	a
2	316	0.05976	b
3	314	0.07353	c
Sex			
Male	263	0.05215	a
Undifferentiated	393	0.06600	b
Female	132	0.06818	b
Period			
G2J	258	0.02423	a
G1O	26	0.05734	b
G1J	504	0.08117	c

Importance of Factors

Among the various factors having an influence on otolith growth, age, sex, and growth period seem to have qualitatively similar effects, on the basis of the ANCOVA residuals (Fig. 5) and the residual standard deviations (Table 5). Among the age classes, age class 2 has the preponderant effect on growth rate whereas females are preponderant for the factor "sex" and the longest growth period (Table 5). In order of relative importance, the longest growth period (1 yr) has the strongest effect, then the "female" sex, then the "undifferentiated" sex, followed by the summer growth period and age class 2 (residual standard deviations from Table 5). If the best growth performance is wanted for eels in Les Garcines pond, 2-yr-old females should be grown for an entire annual cycle (or at least during the summer period).

Discussion

The high rate of recapture in this experiment enabled us to use marking with tetracycline to estimate the individual growth of eel otoliths. In a previous experiment, Dekker (1986) marked 3000 eels by tetracycline injection, but

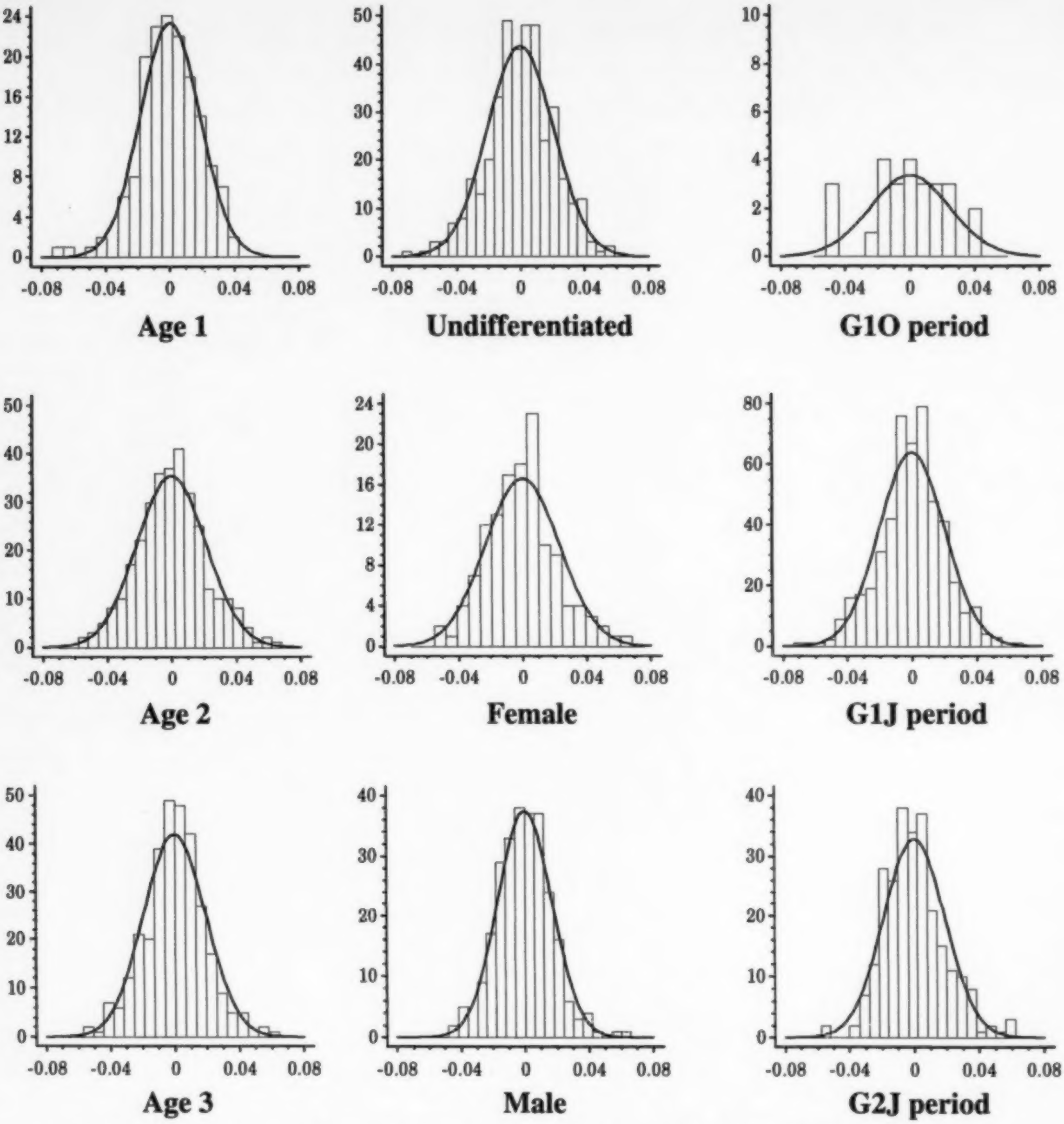

FIG. 5. Distributions (numbers of individuals) of centred residuals coming from the ANCOVA for each factor.

because of problems of recapture recovered too few individuals to be able to estimate growth. In marking experiments in which there is a high recapture rate, the main bias is that the marking itself may have an effect on subsequent growth of individuals. This bias is always difficult to detect because to do so requires an unmanipulated control group, subjected to the same conditions, but not having been manipulated beforehand. In addition, even if there is a real decrease in growth, the cause must still be determined – it could be due to the handling during marking or the inability of the fish to adapt to the new environment because of the density of fish, food availability, etc. For example, Peters (1982) showed that dominance relationships in eels lead to stress, and it is known that high densities in pisciculture affect growth (Degani and Levanon 1983; Degani et al. 1984). The initial population of eels in Les Garcines pond was, however, low and the quantity that was then released into the pond (50 kg·ha^{-1} in total) remained moderate compared with other Mediterranean lagoons (Tesch 1977; Rossi et al. 1988); the density recorded at the end of the experiment was 40.7 kg·ha^{-1}. Finally, a comparison of the values of the condition factors (Kc) of the natural population in the pond

TABLE 5. Statistics on centred residuals coming from the ANCOVA (Table 3) for the various factors (age, sex, and period) SD = standard deviation; CI (95%) = confidence interval for mean at 95%.

Factor	*n*	Mean	SD	CI (95%)
All residuals	788	0	0.01989	$-1.3909 \times 10^{-3} \ll 1.3909 \times 10^{-3}$
Age				
1	158	0	0.01843	$-2.8972 \times 10^{-3} \ll 2.8972 \times 10^{-3}$
2	316	0	0.02133	$-2.3615 \times 10^{-3} \ll 2.3615 \times 10^{-3}$
3	314	0	0.01913	$-2.1246 \times 10^{-3} \ll 2.1246 \times 10^{-3}$
Sex				
Undifferentiated	393	0	0.02070	$-2.0530 \times 10^{-3} \ll 2.0530 \times 10^{-3}$
Female	132	0	0.02301	$-3.9621 \times 10^{-3} \ll 3.9621 \times 10^{-3}$
Male	263	0	0.01680	$-2.0405 \times 10^{-3} \ll 2.0405 \times 10^{-3}$
Period				
G1O	26	0	0.02467	$-9.9669 \times 10^{-3} \ll 9.9669 \times 10^{-3}$
G1J	504	0	0.02021	$-1.7693 \times 10^{-3} \ll 1.7693 \times 10^{-3}$
G2J	258	0	0.01876	$-2.3011 \times 10^{-3} \ll 2.3011 \times 10^{-3}$

and of the marked fish showed no differences after 15 mo of growth (Panfili 1992). There appeared, therefore, to be little bias from the experimental manipulation in this study.

The overall back-calculated growth of the marked population over a cycle of slightly more than 1 yr (15 mo for G1J) was 6.6 cm, for all age classes and sizes combined. For these individuals having grown for an annual cycle, the mean growth of an age class *i* represents the growth between age *i*-1 and age *i*, and this can therefore be compared with data in the literature. The back-calculated growth in length was 6.7 cm for individuals in Les Garcines aged 2 yr (therefore, between 1 and 2 yr), 7.4 cm between 2 and 3 yr, and 5.1 cm between 3 and 4 yr. Published records of growth in length between 1 and 2 yr vary: 6.2 cm in a Spanish estuary (Arias and Drake 1985), 6.1 cm in a Portuguese lagoon (Gordo and Jorge 1991), between 4.5 and 8.4 cm in northern European rivers (Rasmussen and Therkildsen 1979; Moriarty 1983; Vøllestad and Jonsson 1988), and from 5.1 to 9.4 cm in lake environments (Berg 1985; Paulovits and Biró 1986; Nagiec and Bahnsawy 1990). The growth observed by marking in Les Garcines therefore falls within the range of growth values recorded across the whole of Europe. Our results are therefore within acceptable values and tend to show that growth was good even after marking.

There was great variability in individual otolith growth during the experimental periods, if all fish are taken into account. Age or size at marking had a pronounced influence on this growth. Although overall growth slowed with age, the differences became more pronounced after age 3 and increased in variability. A small proportion of large individuals showed no visible otolith growth even after spending 15 mo in the pond; this was not due to maturation of these individuals, since the percentage of silver eels captured remained very low. Growth was therefore rather fast in the first few years in Les Garcines. Elsewhere in Mediterranean habitats, particularly in lagoons and estuaries, and in contrast with more northerly freshwater habitats, younger fish also show rapid growth (Rossi and Villani 1980; Ardizzone and Corsi 1985; Arias and Drake 1985; Fernández-Delgado et al. 1989; Gordo and Jorge 1991).

In this experiment, only absolute otolith growth was measured and back-calculation was used to show the significant effect of size at marking on subsequent growth of the otolith. The use of back-calculation has, however, been the subject of controversy (Small and Taylor 1987; Campana 1990; Francis 1990). The bias produced by this method can be of three types: (1) a poor relation between fish length and otolith size, (2) variation in measurements recorded due to the preparation technique used on the calcified pieces (Panfili and Ximénès 1992), and (3) a poor calculation technique (Campana 1990; Francis 1990). Although some authors have shown uncoupling between otolith and somatic growth (Mosegaard et al. 1988; Reznick et al. 1989; Secor and Dean 1989, 1992; Secor et al. 1989; Wright et al. 1990), this has only been for very short growth periods (daily cycles). It is not certain that these differences occur at the seasonal scale. In addition, the decrease in growth of the otolith with fish size is very pronounced in Les Garcines and indirectly confirms the strong relation between fish length and that of the otolith. This relation is also confirmed by the correlation coefficient of the linear regression. Estimation of somatic growth by back-calculation from otolith growth is certainly sensitive to the method of calculation used. For this reason, our comparisons have concentrated on otolith growth.

Great variability in the growth of eels has been reported on several occasions in the literature (Vøllestad 1989, 1992; Fontenelle 1991). In our experiments over all growth periods, otolith growth was strongly influenced by age and sex class. It is remarkable that the variability within classes is great, in agreement with what has previously been reported in the literature. Growth was distinctly different between the various age and sex classes, with little overlap. In this experiment, variability in growth increased with age, but the effect of age was confounded by the passage from the undifferentiated stage to the male or female categories, which would have reduced the variance of individuals whose sexual identity became apparent but not for the others. In the latter, the variability was not the same in all age classes and could reflect the presence of successive cohorts within the same year. Differences in growth between sex categories of eels have been recorded in few cases in the natural environment (Vøllestad and Jonsson 1988; Tulonen 1989), but in pisciculture, these differences are very clear (Egusa 1979). In natural populations, a pronounced difference has often been recorded in the ages and mean lengths of males and females, the latter being larger and older (Lee 1979; Rossi 1979; Rossi and Villani 1980; Aprahamian 1986, 1988; Vøllestad and Jonsson 1988). Two hypotheses could explain why females are larger: either females reach larger sizes because they live longer or they have faster growth rates from the start and the difference in size is due both to longevity and to growth rate. This study supports the second hypothesis because the growth of females was notably greater than that of males over an annual cycle, even if age class, which would have accentuated the difference, is disregarded. In our closed population, a bias could be caused in the growth estimates of the various sex classes, since size could only increase among the undifferentiated class, as there was no recruitment of small fish in this population whereas such recruitment did occur among males and females as a result of undifferentiated fish becoming macroscopically sexually distinguishable. This maturation from a sexually undifferentiated stage to a differentiated stage can explain the inequalities in absolute growth between the periods for the undifferentiated fish.

In this Mediterranean pond, the most favorable period for growth is the spring, and especially the summer. Otolith growth in this study was slow at the start of spring, but did occur. In contrast, it is certain that winter growth was extremely slow or nonexistent. Over a long growth period of more than one annual cycle, growth variability was reduced, but was much more pronounced for periods of 7 or 8 mo. These results agree to some extent with those of Fernández-Delgado et al. (1989) on a population in a Spanish estuary, who noted that growth was fast in May, low from June to October, and zero from November to April. The most important difference between that study and ours is the fast growth in May, a phenomenon that was not recorded in Les Garcines pond, if a comparison is made of the growth in the first (G1J) and second groups (G2J). In this pond, growth is best between the end of spring (May–June) and the start of autumn (October), but smaller scale variations cannot be distinguished within this long period.

In pisciculture, the optimal temperatures for growth vary slightly from study to study but fall between 22 and 26.5°C (26.5°C, Kuhlmann 1979; 22–23°C, Sadler 1979; 26°C, Seymour 1989 and Holmgren et al. 1991). In Les Garcines pond, the temperature at the bottom exceeded 20°C from June 89 to September 89, but never exceeded 25°C except at the surface (Fig. 2). This is the period during which growth should be optimal, judging from the growth results obtained in pisciculture. This also corresponds exactly to the best period of growth recorded by marking otoliths with tetracycline. The period during the experiments when the temperature fell below 10°C was between November 89 and March 90 (Fig. 2): this corresponds closely to the very low otolith growth of marked individuals. The best period for growth in Mediterranean lagoons is therefore the summer period.

The three main factors having an effect on growth, age, sex, and season of growth, all have qualitatively similar effects. Growth is, however, always better in the summer period and/or for females and/or for young individuals. However, as sexual dimorphism does not occur in the eel, and the future sex of undifferentiated individuals cannot be determined, and is even difficult to determine macroscopically on mature individuals (Van de Wijdeven 1990), it is impossible to select females for rearing. In aquaculture, it is also known that males stop growing when they reach a length of about 30 cm (Van de Wijdeven 1990). The fish farmer who wants to obtain the best yield should therefore opt for the 2- to 3-yr-old age classes. But the selection of fish of this age based on their length will always pose problems because of the variability in length growth in eel.

Acknowledgements

We thank Madeleine Sagliocco (CEMAGREF, Montpellier) for her great help and her expertise, time, and effort in reading and measuring otoliths, Laurent Eon and Pascal Contournet (Station Biologique de la Tour du Valat) for their help in the field, and the Laboratoire de Biologie Marine et Continentale (Université de Montpellier II) and especially Patrice Got for loan of the fluorescent microscope.

References

APRAHAMIAN, M.W. 1986. Eel (*Anguilla anguilla* L.) production in the River Severn, England. Pol. Arch. Hydrobiol. 33: 373–389.

APRAHAMIAN, M.W. 1988. Age structure of eel, *Anguilla anguilla* (L.), population in the River Severn, England, and the River Dee, Wales. Aquacult. Fish. Manage. 19: 365–376.

ARDIZZONE, G.D., AND F. CORSI. 1985. Eel population structure, dynamics and fishing yield in a Mediterranean coastal lagoon. Oebalia 11: 547–560.

ARIAS, A.M., AND P. DRAKE. 1985. Estructura de la población y régimen alimentario de *Anguilla anguilla* L., 1758 (Osteichthyes, Anguillidae), en los esteros de San Fernando (Cádiz). Invest. Pesq. 49: 475–491.

BEAMISH, R.J., AND G.A. MCFARLANE. 1983. The forgotten requirement for age validation in fisheries biology. Trans. Am. Fish. Soc. 112: 735–743.

BEAMISH, R.J., AND G.A. MCFARLANE. 1987. Current trends in age determination methodology, p. 15-42. *In* R.C. Summerfelt and G.E. Hall [ed.] The age and growth of fish. The Iowa State University Press, Ames, Iowa. 544 p.

BERG, R. 1985. Age determination of eels, *Anguilla anguilla* (L.): comparison of field data with otolith ring patterns. J. Fish Biol. 26: 537–544.

BERG, R. 1986. Field studies on eel (*Anguilla anguilla*) in Lake Constance: tagging effects causing retardation of growth. Vie Milieu 36: 285–286.

CAMPANA, S.E. 1990. How reliable are growth back-calculations based on otoliths? Can. J. Fish. Aquat. Sci. 47: 2219–2227.

CHISNALL, B.L., AND J.W. HAYES. 1991. Age and growth of shortfinned eels (*Anguilla australis*) in the lower Waikato basin, North Island, New Zealand. N.Z. J. Mar. Freshwater Res. 25: 71–80.

DEGANI, G., AND D. LEVANON. 1983. The influence of low density on food adaptation, cannibalism and growth of eels (*Anguilla anguilla* (L.)). Bamidgeh 34: 53–60.

DEGANI, G., D. LEVANON, AND C. DOSORETZ. 1984. Growth of *Anguilla anguilla* in different densities in out door containers with *Tilapia aurea*. Prog. Fish-Cult. 47: 114–118.

DEKKER, W. 1986. Age reading of European eels using tetracycline labelled otoliths. ICES Anad. Catad. Fish Comm. C.M. 1986/M:16: 14 p.

EGUSA, S. 1979. Notes on the culture of the European eel (*Anguilla anguilla* L.) in Japanese farming ponds. Rapp. P.-v. Réun. Cons. int. Explor. Mer 174: 51–58.

FERNÁNDEZ-DELGADO, C., J.A. HERNANDO, M. HERRERA, AND M. BELLIDO. 1989. Age and growth of yellow eels, *Anguilla anguilla*, in the estuary of the Guadalquivir river (South-West Spain). J. Fish Biol. 34: 561–570.

FONTENELLE, G. 1991. Age et longueur moyenne des anguilles (*Anguilla anguilla*) en Europe: une revue critique. EIFAC Working Party on Eel, Dublin, Ireland. 16 p.

FRANCIS, R.I.C.C. 1990. Back-calculation of fish length: a critical review. J. Fish Biol. 36: 883–902.

GORDO, L.S., AND M.I. JORGE. 1991. Age and growth of the European eel, *Anguilla anguilla* (Linnaeus, 1758) in the Aveiro lagoon, Portugal. Sci. Mar. 55: 389–395.

HANSEN, R.A., AND A.G. EVERSOLE. 1984. Age, growth, and sex ratio of American eels in brackish-water portions of a South Carolina river. Trans. Am. Fish. Soc. 113: 744–749.

Holmgren, K., H. Wickstrom, and K. Fredga. 1991. Difficulties when estimating growth of eel in a meoscale experiment. EIFAC Working Party on Eel, Dublin, Ireland. 19 p.

Kuhlmann, H. 1979. The influence of temperature, food, initial size, and origin of elvers (*Anguilla anguilla* L.). Rapp. P.-v. Réun. Cons. int. Explor. Mer 174: 59–63.

Lee, T.-W. 1979. Dynamique des populations d'anguilles (*Anguilla anguilla* L.) des lagunes du Bassin d'Arcachon. Thèse 3ème cycle, Univ. Montpellier II, France. 218 p.

McEwan, A., and T. Hecht. 1984. Age and growth of the longfin eel, *Anguilla mossambica* Peters, 1852 (Pisces: Anguillidae) in Transkei rivers. S. Afr. J. Zool. 19: 280–285.

Meunier, F. 1974. La technique de marquage vital des tissus squelettiques des poissons. Bull. Fr. Piscic. 255: 51–57.

Meunier, F.J., and G. Boivin. 1974. Divers aspects de la fixation du chlorhydrate de tétracycline sur les tissus squelettiques de quelques Téléostéens. Bull. Soc. Zool. Fr. 99: 495–504.

Michaud, M., J.-D. Dutil, and J.J. Dodson. 1988. Determination of the age of young American eels, *Anguilla rostrata*, in fresh water, based on otolith surface area and microstructure. J. Fish Biol. 32: 179–189.

Moriarty, C. 1983. Age determination and growth rate of eels, *Anguilla anguilla* (L.). J. Fish Biol. 23: 257–264.

Mosegard, H., H. Svedang, and K. Taberman. 1988. Uncoupling of somatic and otolith growth rates in Arctic char (*Salvelinus alpinus*) as an effect of differences in temperature response. Can. J. Fish. Aquat. Sci. 45: 1514–1524.

Nagiec, M., and M.H. Bahnsawy. 1990. Age and growth of female eels, *Anguilla anguilla* L., in a Polish lake, Jeziorak lake, Mazurian lake district, Poland. Aquacult. Fish. Manage. 21: 459– 470.

Nielsen, J. 1988. A review on marking and tagging methods applied to eel (*Anguilla anguilla* (L.)). FAO EIFAC Occas. Pap. 21: 24 p.

Panfili, J. 1992. Estimation de l'âge individuel des poissons: méthodologies et applications à des populations naturelles tropicales et tempérées. Thèse doctorat, Univ. Montpellier II Sci. Tech. Languedoc, France. 456 p.

Panfili, J., and M.-C. Ximénès. 1992. Measurements on ground or sectioned otoliths: possibilities of bias. J. Fish Biol. 41: 201–207.

Panfili, J., M.-C. Ximénès, A.J. Crivelli, and T. Do Chi. 1992. Validation de l'âge de l'anguille européenne dans les lagunes méditerranéennes françaises (Camargue): résultats préliminaires, p. 119–127. *In* J.L. Baglinière, J. Castanet, F. Conand, and F.J. Meunier [ed.] Tissus durs et âge individuel des Vertébrés, Colloque National, Bondy, France, 4–6 mars 1991. Colloques et Séminaires ORSTOM-INRA, Paris. 459 p.

Paulovits, G., and P. Biró. 1986. Age determination and growth of eel, *Anguilla anguilla* (L.) in Lake Ferto, Hungary. Fish. Res. 4: 101–110.

Peters, G. 1982. The effect of stress on the stomach of the European eel, *Anguilla anguilla* L. J. Fish Biol. 21: 497–512.

Poole, R. 1991. The age and growth of eels (*Anguilla anguilla* L.) in two oligotrophic streams in the west of Ireland. EIFAC Working Party on Eel, Dublin, Ireland, 12 p.

Rasmussen, G., and B. Therkildsen. 1979. Food, growth, and production of *Anguilla anguilla* L. in a small Danish stream. Rapp. P.-v. Réun. Cons. int. Explor. Mer 174: 32–40.

Reznick, D., E. Lindbeck, and H. Bryga. 1989. Slower growth results in larger otoliths: an experimental test with guppies (*Poecilia reticulata*). Can. J. Fish. Aquat. Sci. 46: 108–112.

Ricker, W.E. 1992. Back-calculation of fish lengths based on proportionality between scale and length increments. Can. J. Fish. Aquat. Sci. 49: 1018–1026.

Rossi, R. 1979. An estimate of the production of the eel population in the Valli of Comacchio (Po Delta) during 1974–1976. Boll. Zool. 46: 217–223.

Rossi, R., A. Carrieri, M.G. Rizzo, and M. Lucchini. 1988. Use of intensive rearing systems as back-up for coastal lagoon aquaculture: an experience with eels, *Anguilla anguilla* L., in the Comacchio lagoons. Aquacult. Fish. Manage. 19: 355–361.

Rossi, R., and P. Villani. 1980. A biological analysis of eel catches, *Anguilla anguilla* L., from the lagoons of Lesina and Varano, Italy. J. Fish Biol. 16: 413–423.

Sadler, K. 1979. Effects of temperature on the growth and survival of the European eel, *Anguilla anguilla* L. J. Fish Biol. 15: 499–507.

Secor, D.H., and J.M. Dean. 1989. Somatic growth effects on the otolith – fish size relationship in young pond-reared striped bass, *Morone saxatilis*. Can. J. Fish. Aquat. Sci. 46: 113–121.

Secor, D.H., and J.M. Dean. 1992. Comparison of otolith-based back-calculation methods to determine individual growth histories of larval striped bass, *Morone saxatilis*. Can. J. Fish. Aquat. Sci. 49: 1439–1454.

Secor, D.H., J.M. Dean, and R.B. Baldevarona. 1989. Comparison of otolith growth and somatic growth in larval and juvenile fishes based on otolith length/fish length relationship. Rapp. P.-v. Réun. Cons. int. Explor. Mer 191: 431–438.

Seymour, E.A. 1989. Devising optimum feeding regimes and temperatures for warmwater culture of eel, *Anguilla anguilla* L. Aquacult. Fish. Manage. 20: 311–323.

Small, M.A., and W.W. Taylor. 1987. Sources of back-calculation error in estimating growth of lake whitefish, p. 189–202. *In* R.C. Summerfelt and G.E. Hall [ed.] The age and growth of fish. The Iowa State University Press, Ames, Iowa. 544 p.

Tesch, F.W. 1977. The eel. Biology and management of anguillid eels. Chapman and Hall, London. 435 p.

Tulonen, J. 1989. Growth and sex ratio of eels (*Anguilla anguilla*) of known age in four small lakes in southern Finland. EIFAC Working Party on Eel, Porto, Portugal. 15 p.

Van Coillie, R. 1967. Étude à l'aide de tétracyclines de la croissance périodique des écailles de Téléostéens. Naturaliste Can. 94: 29–58.

Van de Wijdeven, F. 1990. L'anguilliculture intensive en France: état et perspectives. Thèse doctorat Ingén, ENSAR, Rennes, France. 172 p.

Vøllestad, L.A. 1985. Age determination and growth of yellow eels, *Anguilla anguilla* (L.), from a brackish water, Norway. J. Fish Biol. 26: 521–525.

Vøllestad, L.A. 1989. Effect of growth rate on age at maturity of the European eel *Anguilla anguilla*. EIFAC Working Party on Eel, Porto, Portugal. 22 p.

Vøllestad, L.A. 1992. The geographic variation in age and length at metamorphosis of maturing European eel: environmental effects and phenotypic plasticity. J. Anim. Ecol. 61: 41–48.

Vøllestad, L.A., and B. Jonsson. 1988. A 13-year study of the population dynamics and growth of the European eel *Anguilla anguilla* in a Norwegian river: evidence for density-dependent mortality, and development of a model for predicting yield. J. Anim. Ecol. 57: 983–997.

Vøllestad, L.A., R. Lecomte-Finiger, and B. Steinmetz. 1988. Age determination of *Anguilla anguilla* and related species. EIFAC Occas. Pap. 21: 28 p.

Weber, D., and G.J. Rigway. 1967. Marking Pacific salmon with tetracycline antibiotics. J. Fish. Res. Board Can. 24: 849–865.

Wickins, J.F. 1985. Effects of size, culling and social history on growth of cultured elvers, *Anguilla anguilla* (L.). J. Fish Biol. 31: 71–82.

Wright, P.J., D. Rowe, and J.E. Thorpe. 1990. Otolith and somatic growth rates in Atlantic salmon parr, *Salmo salar* L.: evidence against coupling. J. Fish Biol. 36: 241–249.

Growth Rate of 0+ Fish in Relation to Temperature, Body Size, and Food in Shallow Eutrophic Lake Tjeukemeer

W.M. Mooij and E.H.R.R. Lammens[1]

Netherlands Institute of Ecology, Centre for Limnology, Rijksstraatweg 6, 3631 AC Nieuwersluis, The Netherlands

and W.L.T. Van Densen

Netherlands Institute of Ecology, Centre for Limnology, Rijksstraatweg 6, 3631 AC Nieuwersluis,. The Netherlands
and
Agricultural University Wageningen, Department of Fish Culture and Fisheries, P.O. Box 338, 6700 AH Wageningen, The Netherlands

Mooij, W.M., E.H.R.R. Lammens, and W.L.T. Van Densen. 1994. Growth rate of 0+ fish in relation to temperature, body size, and food in shallow eutrophic Lake Tjeukemeer. Can. J. Fish. Aquat. Sci. 51: 516–526.

The growth rate of young-of-the-year of the six most abundant fish species (smelt (*Osmerus eperlanus*), pikeperch (*Stizostedion lucioperca*), perch (*Perca fluviatilis*), ruffe (*Gymnocephalus cernua*), bream (*Abramis brama*), and roach (*Rutilus rutilus*)) in Lake Tjeukemeer was predicted from water temperature using the model $dW_t/dt = a \cdot W_t^b \cdot (T_t - c)$. For each species the model parameters were estimated using data from approximately 120 field observations of body size over a period of 13 yr; about 94% of the variance in body size could be explained by the model. The growth rate was correlated with temperature for all planktivorous species, except smelt. The relationship between growth rate and temperature was also significant for piscivorous pikeperch but not for benthivorous ruffe. These conclusions were corroborated by comparing the unexplained sum of squares of the temperature growth model with that of a temperature-neutral, logistic growth model. The abundance of food was not related to the temperature-corrected growth rate of planktivorous fishes, except in one year during which food conditions were extremely poor. We concluded that in most years the growth rate of 0+ planktivorous fish was not food limited. For piscivorous pikeperch, however, the variation in growth rate could be explained by the higher availability of smelt in warmer years.

Le modèle : $dW_t/dt = a \cdot W_t^b \cdot (T_t - c)$ a permis de prévoir le taux de croissance de jeunes de l'année appartenant aux six espèces de poisson les plus abondantes (éparlan (*Osmerus eperlanus*), sandre (*Stizostedion lucioperca*), perche (*Perca fluviatilis*), grémille (*Gymnocephalus cernua*), brème (*Abramis brama*) et gardon (*Rutilus rutilus*)) dans le lac Tjeukemeer à partir de la température de l'eau. Pour chaque espèce, les paramètres du modèle ont été évalués au moyen de données provenant d'environ 120 observations sur le terrain de la taille corporelle et portant sur une période de 13 ans; le modèle permettait d'expliquer environ 94 % de la variance de la taille corporelle. Le taux de croissance était corrélé à la température pour toutes les espèces planctonophages, à l'exception de l'éperlan. La relation entre le taux de croissance et la température était également importante dans le cas du sandre ichtyophage mais pas pour la grémille benthophage. Ces conclusions ont été corroborées en comparant la somme des carrés du modèle de croissance en fonction de la température, qui reste inexpliquée, à celle d'un modèle de croissance logistique, à température neutre. L'abondance de nourriture n'a pas été corrélée au taux de croissance corrigé en fonction de la température des poissons planctonophages, sauf pendant une année au cours de laquelle les conditions alimentaires étaient très mauvaises. Nous avons conclu que pendant la plupart des années, le taux de croissance des poissons planctonophages d'âge 0+ n'était pas limité par la nourriture. Dans le cas du sandre ichtyophage, cependant, la variation du taux de croissance pouvait être expliquée par la plus grande disponibilité d'éperlan les années plus chaudes.

Received November 27, 1992
Accepted October 25, 1993
(JB701)

Reçu le 27 novembre 1992
Accepté le 25 octobre 1993

The influence of prey availability on survival of 0+ fish is an important question in fish ecology (Cushing 1981; Henderson 1985; Cryer et al. 1986). Food limitation can affect survival in two ways: directly by starvation or indirectly by retarding growth rate and thus increasing vulnerability to predators (Backiel and Le Cren 1978). Food limitation can be tested by comparing growth rates in the field with rates reached at maximum rations in the laboratory (Elliott 1975; Wieser et al. 1988; Mooij and Van Tongeren 1990). However, such comparisons are complicated by the influence of other factors on growth rate, mainly body size and temperature (Brett 1979; Ricker 1979).

The relationship between growth rate (defined as individual length or weight increment per time unit) and the explanatory variables (food availability or abundance of competitors, water temperature, and body size) can be analysed by multiple regression (Henderson 1985; Henderson and Brown 1985; Mills et al. 1989b). This method has the advantage of straightforward testing of the significance of the explanatory variables. However, this approach is limited by the assumption that the effects of the causal factors are linear and additive. Interpretation of the parameters is also problematic. A special growth model, such as the Bertalanffy, Gompertz, or logistic curve (Guma'a 1978; Ricker 1979; Tong 1986; Weatherley 1987) can also be used. The advantage of using growth models is that the parameters are interpretable from the biological point of view. However, the lack of simple methods for significance testing is a disadvantage.

---

[1] Present address: Institute for Inland Water Management and Waste Water Treatment, P.O. Box 17, 8200 AA Lelystad, The Netherlands.

For this study the latter method was chosen. A three-parameter growth model was parameterized for the major 0+ species in shallow eutrophic Lake Tjeukemeer: cyprinids bream (*Abramis brama*) and roach (*Rutilus rutilus*), percids pikeperch (*Stizostedion lucioperca*), perch (*Perca fluviatilis*), and ruffe (*Gymnocephalus cernua*), and the smelt (*Osmerus eperlanus*). In this model (Elliott 1975, 1984, 1985), growth is viewed as the multiplicative effect of three functions, each with one parameter, describing the effect of temperature, body size, and food availability. Mooij and Van Tongeren (1990) have extended the model for use in natural situations with variable temperatures. The extended model has been used to compare the growth rate of roach in Tjeukemeer with the growth rate in the laboratory at maximum food rations. In the present study, the three parameters of the model were estimated from field data.

The significance of the relation between temperature and growth rate was analysed in two ways. First, a Monte Carlo permutation test (Sokal and Rohlf 1981) was performed on the results of the temperature growth model. Second, the fit of the temperature growth model was compared with that of a temperature-neutral logistic growth model. To determine the impact of food availability and 0+ food competition on growth rate, the deviations of the temperature model, which can be seen as temperature- and size-corrected growth rates, were compared with zooplankton biomass and 0+ fish abundance. Finally, the relationship between zooplankton abundance and temperature was analysed in a multiple regression analysis. Such a relationship might lead to an indirect effect of temperature on growth rate.

These tests have several possible conclusions: (1) if the only significant correlation is that between temperature and growth rate, the growth rate is limited by temperature and not by food conditions, (2) if the only significant correlation is that between food conditions and growth rate, the growth rate is limited by food conditions, and (3) if both temperature and food conditions are significantly correlated, the impact of temperature and food conditions on growth rate cannot be separated.

Material and Methods

Field Data from Tjeukemeer

From 1976 to 1988, 0+ fish were caught monthly from July to December at five sites in the open-water zone of Tjeukemeer (surface area 21.0 km^2, mean depth 1.5 m) using a 5-m beam trawl (cod end 5.5 mm knot-to-knot, Lammens et al. 1990). About 50–100 specimens of each species were measured to the nearest 0.5 cm forklength on each sampling day. A bimodality in the length frequency distribution of pikeperch was used to distinguish between planktivorous and piscivorous specimens (Van Densen 1985b).

During 1986–88, hoopnets (diameter 0.4 m and mesh size 0.5 mm) were used to determine the abundance and the growth rate of the younger stages. Weekly hauls were made until the middle of July in the open-water area (six sites) and close to the shoreline (nine sites). Fish were preserved in 4% formaldehyde, identified (cyprinids after Mooij 1989), and measured to the nearest millimetre forklength.

Zooplankton were collected with a 5-L Friedinger sampler at the five trawl sites. At each site, 5-L samples were taken from just below the surface and from 0.5 m above the bottom (average depth 1.5 m). The combined 50-L sample was concentrated using a 125-μm sieve. Densities and lengths of zooplankton in a representative subsample were determined (Van Densen and Vijverberg 1982). Zooplankton biomass was calculated on the basis of length – dry weight relationships (Bottrell et al. 1976; Vijverberg and Frank 1976).

Growth Model

The growth model used in this study (Mooij and Van Tongeren 1990) uses a differential equation to describe the absolute growth rate as a function of body size and temperature:

$$(1)\quad dW_t/dt = a \cdot W_t^b \cdot (T_t - c)$$

where W represents fresh weight (grams), T temperature (degrees Celsius), and t time (days) and a, b, and c are parameters. The "weight parameter" b describes the decrease in the relative growth rate with increase in weight. The "temperature parameter" c represents the lower temperature threshold for growth. At temperatures above c, a linear relationship between growth rate and temperature is assumed, limiting the use of the model to suboptimal temperatures. At water temperatures below the lower temperature threshold c, weight is assumed to remain constant. The parameter a represents the absolute growth rate of a fish of 1 g at a temperature of 1°C above the temperature threshold c. Parameter a should be considered as an index of all other factors influencing growth rate but mainly food, and is therefore referred to as the "food parameter".

Mean daily water temperatures were calculated from air temperatures using the model of Mooij and Van Tongeren (1990), calibrated using water temperature data from Tjeukemeer (De Boer et al. 1988). For each field observation, a separate predicted value was calculated using the first day of March of each year as a starting point.

The moment of onset of growth was predicted with a day-degree formula (Elliott et al. 1987):

$$(2)\quad \sum_{t=1}^{n} (T_t - c) = d$$

where T represents the environmental temperature (degrees Celsius) and n the number of days between 1 March and the onset of growth. For the temperature parameter c the value of the growth equation (1) was used. Parameter d represents the total heat sum necessary for the onset of growth, thus combining the temperature-induced timing of spawning and the duration of the egg and yolk-sac stage. The average initial length was set at 6 mm for all species on the basis of length measurements of hoopnet catches.

TABLE 1. Basic parameters for the six species studied: parameter f of the length–weight relationship $W = f \cdot L^{3.2}$, the total variance (Var) in the log-transformed mean fresh weights (g), and the number of observations n, each representing a sample of 50–100 measured fishes.

Species	$f(10^6)$	Var	n	Species	$f(10^6)$	Var	n
Smelt	3.24	2.536	156	Perch	5.75	4.133	133
Pikeperch total	3.47	5.912	148	Ruffe	5.62	0.899	107
Pikeperch plank.	3.47	4.712	138	Bream	5.62	4.449	157
Pikeperch pisci.	3.47	1.595	59	Roach	5.50	4.148	136

TABLE 2. Calibrated parameters and percentage of unexplained sum of squares (% Ssq) of the growth models for the six species studied: (A) parameters a, c, and d of the temperature growth model $dW_t/dt = a \cdot W_t^{0.6} \cdot (T_t - c)$ and (B) parameters $\ln(W_{incr})$, i, and j of the logistic model $\ln(W_t) = \ln(W_0 + \ln(W_{incr})/(1 + e^{-i(t-j)})$.

(A) Species	$a(10^3)$	c	d	% Ssq	Species	$a(10^3)$	c	d	% Ssq
Smelt	1.10	−3.60	552.0	4.5	Perch	4.40	9.8	46.1	2.6
Pikeperch total	5.26	10.0	69.8	5.9	Ruffe	3.26	7.6	48.9	10.9
Pikeperch plank.	4.07	9.8	59.9	4.0	Bream	5.62	12.8	16.9	3.0
Pikeperch pisci.	7.68	8.6	201.8	11.2	Roach	3.60	10.2	59.9	3.3
(B) Species	$\ln(W_{incr})$	$i(10^3)$	j	% Ssq	Species	$\ln(W_{incr})$	$i(10^3)$	j	% Ssq
Smelt	8.00	32.3	163	5.9	Perch	7.56	46.4	169	6.5
Pikeperch total	8.64	46.1	178	9.9	Ruffe	7.97	32.9	164	9.1
Pikeperch plank.	7.79	53.7	173	6.4	Bream	7.11	49.1	181	7.8
Pikeperch pisci.	10.28	30.0	173	11.5	Roach	6.95	52.8	176	5.8

The observed lengths were converted to fresh weight using the formula

$$(3) \quad W = f \cdot L^g$$

where W represents fresh weight (grams) and L forklength (millimetres) and f and g are parameters. For ease of interpretation the predicted weights were converted to lengths.

Parameter Estimation

Problems with interdependence between the parameters were minimized by holding the weight parameter b at a constant value of 0.6 (Brett and Shelbourn 1975; Jobling 1980, 1983). Values for the three parameters a, c, and d were optimized using an iterative fitting procedure. Optimum fit of the model was defined as that at which the sum of squared differences between the log-transformed observed and predicted weights – further called the unexplained sum of squares – was minimal (Mooij and Van Tongeren 1990). The parameter space around the values established thus was scanned for local minima.

The parameters of the length – fresh weight relationship were determined by nonlinear regression, using length and weight measurements of individual fish (range 40–80 mm, pikeperch 40–160 mm) caught in Tjeukemeer. To ensure the validity of this relationship when extrapolated to smaller stages, the parameter g was fixed at a value of 3.2 (Le Cren 1951; Biro 1972; Hellawell 1972; Rheinberger et al. 1986). Changes in the length–weight relationship of the youngest stages as observed in roach (Mooij and Van Tongeren 1990), with values of parameter g up to 3.9, were neglected. This simplified the approach. Comparable data for percids and smelt were not available. No correction was made for the underestimation of the arithmetic mean weight by applying an individual-based length–weight relationship to the arithmetic mean of normally distributed lengths.

Significance Testing

The relation between growth rate and temperature can be considered in two parts: (a) the relation between the general growth curve of a species in Tjeukemeer and the general course of temperature within years and (b) the relation between the differences in temperature and growth rate between years. The general courses of growth rate, temperature, and zooplankton abundance within years should all be correlated, as all these variables reach highest values in summer and lowest in winter. Thus, only the differences between years were tested. The relation of differences in zooplankton abundance and temperature between years was tested in a multiple regression analysis with the biomass of the four major zooplankton groups (*Daphnia*, *Bosmina*, *Chydorus*, and copepods) as dependent variables and the number of day-degrees above 12°C within a year as the independent variable. The relation of differences in temperature and growth rate between years was tested in a Monte Carlo permutation test (Sokal and Rohlf 1981). After parameterization and calculation of the unexplained sum of squares for the field data, this process was repeated 999 times with permutated data, that is, the growth data for one year were combined with the course of temperature in another year. Years were chosen randomly without replacement. Since 13! (approximately 6.23×10^9) different combinations are possible, the probability that two permutations were identical is very small. The significance of temperature as an explanatory variable was calculated from the rank of the unexplained sum of squares of the field data among the unexplained sum of squares of the 999 permutations.

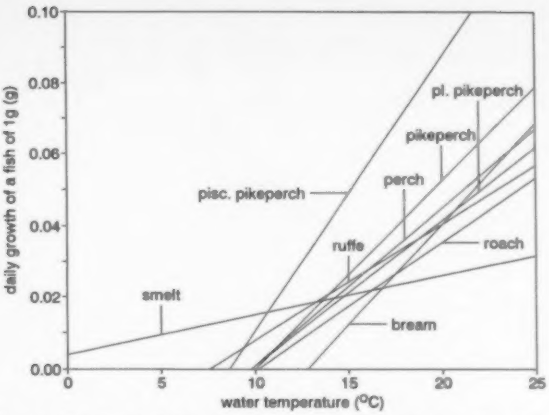

FIG. 1. Predicted daily growth rate of a fish of 1 g. The slope of each line represents food parameter *a* (equation (1)), while the intercept on the ordinate equals temperature parameter *c* (equation (1)).

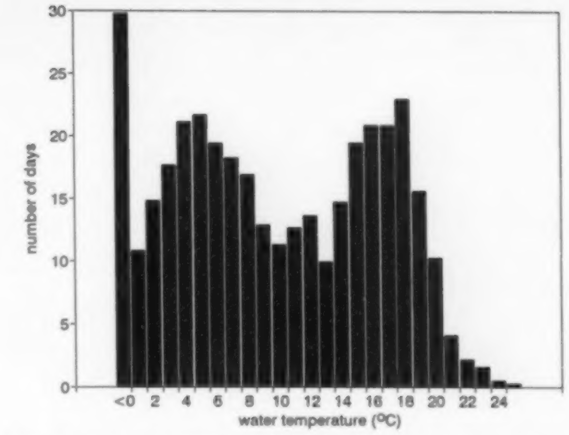

FIG. 2. Frequency distribution of days with a certain water temperature in Tjeukemeer. Values are means over the years 1971–88. Water temperatures were calculated from air temperatures.

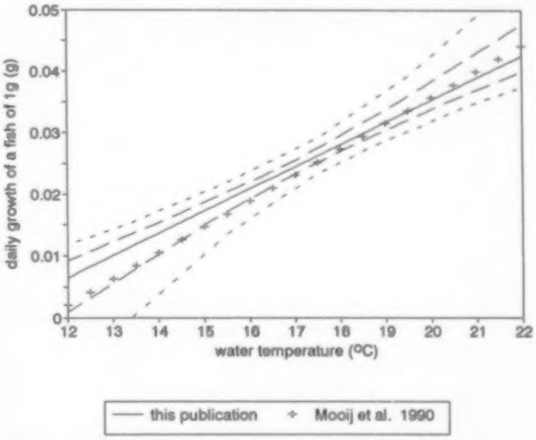

FIG. 3. Comparison of the relation between water temperature and growth rate derived from laboratory data (+) (Mooij and van Tongeren 1990) and from field data (this publication). The five lines represent the optimal value of the parameters (—) and the areas enclosing all lines with an unexplained variance that is at most 5% (– –) and 25% (----) higher than the minimal sum of squares.

Logistic Model

Another way to examine the validity of the model is to compare the results with a three-parameter model which does not account for yearly differences in temperature. A logistic growth curve was fitted to the natural logarithm of the observed weights as follows (Ricker 1979; Tong 1986):

$$(4)\quad \ln(W_t) = \ln(W_0) + \frac{\ln(W_{\text{incr}})}{(1+e^{-i\cdot(t-j)})}.$$

The parameters of the logistic model represent the average total increase in size during the season (W_{incr}), the slope at the point of inflection (i), and the corresponding day number (j). As with the temperature model, the parameters W_{incr}, i, and j were derived for each species from the field data in an iterative fitting procedure. This resulted in one curve for each species, describing the average growth in Tjeukemeer.

To describe the fit of the model, the unexplained sum of squares was calculated using the same approach adopted for the temperature model. The performances of the logistic model and the temperature model were compared by calculating the ratio of the unexplained sum of squares. There will, however, be autocorrelation between the deviations between the predicted and the observed body size within one year. Consequently, the number of degrees of freedom of both models was not clear and it was not possible to test the differences between the two models by standard procedures.

Food Parameters

To relate the deviations between the observed and predicted growth rates to food conditions, the food parameter *a* was calculated for each species for each year separately, keeping parameters *b*, *c*, and *d* constant. The deviations of these specific food parameters from the average value of the food parameter were expressed by their quotient, referred to as "relative food parameters".

Results

Parameters of the Temperature Model

The complete data set comprised 892 mean lengths (Table 1). Ruffe and piscivorous pikeperch were caught only in trawl nets. All the data for these species therefore refer to older stages and the variance in body size of these species is markedly lower (Table 1). In terms of the length–weight relationship (parameter *f*) the species can be divided into two groups: (1) slender species (smelt and pikeperch) and (2) species with a deeper body (perch, ruffe, bream and roach) (Table 1).

The range for the food parameter *a* was 1.10×10^{-3} to 7.68×10^{-3} $g^{0.4}\cdot{}^{\circ}C^{-1}\cdot d^{-1}$. The lowest value was for smelt and the highest for piscivorous pikeperch (Tabld 2A). For the other planktivorous fishes and ruffe, these values were in the range 3.26×10^{-3} to 5.62×10^{-3} $g^{0.4}\cdot{}^{\circ}C^{-1}\cdot d^{-1}$. The values of temperature parameter *c* ranged from −3.6 to 12.8°C (Table 2A). The lowest temperature parameter value found

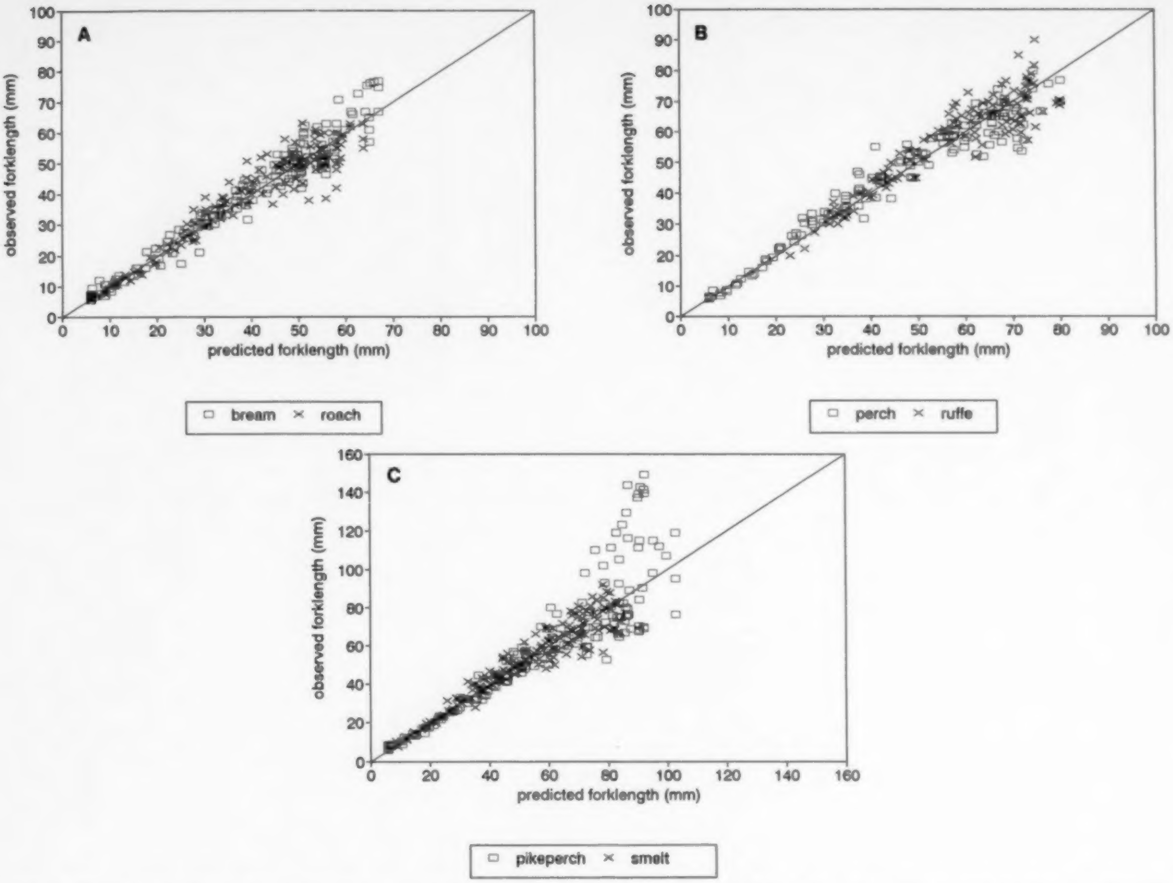

FIG. 4. Fit of the model to the observations on (A) bream and roach, (B) perch and ruffe, and (C) pikeperch and smelt in Tjeukemeer during 1976–88.

was for smelt, with higher values for the percids (7.6–10.0°C) and the highest values for the cyprinids (10.2–12.8°C).

Although smelt is the first species to spawn, it has the highest value for parameter *d* (Table 2A). This is due to its very low temperature threshold. The value of the heat sum parameter *d* for piscivorous pikeperch represents the number of day-degrees necessary for the onset of growth of pikeperch, this species being piscivorous from hatching. However, during its early development, pikeperch always has a planktivorous feeding mode. The range for parameter *d* for the other species was 16.9–71.1 day-degrees.

For a clear illustration of the combined effect of the food parameter and the temperature parameter, the absolute growth rate of a fish of 1 g (thus eliminating the effect of weight) was plotted against temperature over the entire range occurring in Tjeukemeer (Fig. 1). The intersects of the different lines with the *x*-axis represent the value of the temperature parameters.

As the parameters of the temperature model were estimated from field observations of growth rate in Tjeukemeer, their values will only be valid for the range of water temperatures that occur frequently in the lake. The frequency distribution of mean daily temperatures in Tjeukemeer is bimodal in shape with maxima at 5 and 18°C, representing the most frequent winter and summer water temperatures, respectively (Fig. 2). Temperatures between 10 and 13°C, which occur in spring and autumn, are relatively rare. Therefore, it can be concluded that most attention should be paid to the predicted growth rates (Fig. 1) in the range of 14–19°C.

Comparison with Laboratory Data

The parameters found for roach were compared with the experimental data for non-food-limited growth of this species (Mooij and Van Tongeren 1990). The temperature threshold of 11.5°C found in the laboratory is 1.3°C higher than that found in this study. Similarly, the laboratory-derived estimate of the food parameter by Mooij and Van Tongeren (1990) was $0.6 \times 10^{-3}\ g^{0.4} \cdot {}^{\circ}C^{-1} \cdot d^{-1}$ higher. As the data were analysed using a calibrated simulation model rather than by multiple regression, there was no simple way to test for the significance of these differences. However, the unexplained sum of squares of the model for a certain set of parameters can be compared with the minimal unexplained sum of squares found during calibration (Klepper and Rouse 1991). Application of this method provides the opportunity to quantify differences between sets of parameters in relative terms. However, the choice of criteria for acceptability of sets remains arbitrary.

TABLE 3. Statistical parameters describing the fit of the growth models for the six species studied. The table gives the rank of the unexplained sum of squares of the temperature model with the field data as input among the unexplained sum of squares of 999 runs of the model with permutated temperature data in a Monte Carlo test. Significance levels were calculated by dividing the rank of the run with the field data by the total number of runs (1000). Ranks and significance levels are given for the total data set and for the hoopnet (first part of the season, larvae) and trawl data sets (second part of the season, 0+) separately. The fit of the temperature and the logistic models was expressed as the ratio of the unexplained sum of squares (Ratio Ssq) of the logistic models and the unexplained sum of squares of the temperature model. ns, $P > 0.05$; $^{*}0.05 > P > 0.01$; $^{**}0.01 > P > 0.001$; $^{***}P < 0.001$.

Species	Rank			Ratio Ssq	Species	Rank			Ratio Ssq
	Hoop	Trawl	Total			Hoop	Trawl	Total	
Smelt	14^{*}	796 ns	63 ns	1.31	Ruffe	—	—	183 ns	0.83
Pikeperch	9^{**}	5^{**}	5^{**}	1.67	Bream	60 ns	1^{***}	1^{***}	2.60
Perch	1^{***}	15^{*}	1^{***}	2.52	Roach	30^{*}	6^{**}	1^{***}	1.71

TABLE 4. Mean zooplankton abundance (10^{-6} g dry weight/L) during July–September in Tjeukemeer of *Daphnia* sp. (Da), *Bosmina* sp. (Bo), *C. sphaericus* (Ch), and cyclopoid copepods (Co.) DD = day-degrees above 12°C.

Year	DD	Da	Bo	Ch	Co	Total	Year	DD	Da	Bo	Ch	Co	Total
1976	882	689	66	117	190[a]	1061	1984	602	1040	81	59	111[a]	1291
1977	639	1230	79	70	84[a]	1463	1985	714	1520	252	99	79[a]	1949
1978	643	239	161	207	106[a]	713	1986	647	78	107	88	58	331
1979	709	928	22	18	157[a]	1124	1987	618	649	223	82	137	1091
1980	730	102	45	39	85[a]	272	1988	715	4	27	15	31	76
1981	739	240	131	67	110[a]	549	Mean		834	134	82	117	1167
1982	842	1390	497	165	231[a]	2283	%		71	12	7	10	100
1983	815	2740	58	34	139[a]	2971							

[a] Calculated from the mean number in each year multiplied by the ratio of the mean biomass and the mean number during 1986–88.

TABLE 5. Mean length (L, mm forklength), number (n, 1000/haul) and biomass (B, kg/haul) of planktivorous fish (smelt, perch, bream, and roach) during July–October in Tjeukemeer (1976–88).

Month	L	n	B	Month	L	n	B
July	39.6	5.75	3.50	September	59.0	2.87	5.89
August	49.2	4.22	5.28	October	63.7	1.30	3.75

As part of the sensitivity analysis of the parameterization process, all combinations of a and c resulting in an unexplained sum of squares of <5% higher than the minimum unexplained sum of squares were calculated. This was also done for the 25% limits and the ranges were plotted (Fig. 3). Clearly, the prediction of the growth rate is most accurate at about 17.5°C, the mean summer temperature of Tjeukemeer. To compare the field and the laboratory-established parameters of roach, the temperature growth relationship of Mooij and Van Tongeren (1990) was plotted on the same graph. Although the temperature thresholds of both analyses differ markedly, the graph clearly shows that at a temperature of 17.5°C, both estimates of the growth rate are quite similar. The results of the sensitivity analysis can also explain the differences in temperature thresholds mentioned in literature: roach, 12°C (Mann 1973), 14°C (Broughton and Jones 1978), and 12–13°C (Muller and Meng 1986); perch, 14°C (Le Cren 1958).

Several authors have conducted laboratory experiments on cyprinid and percid egg and yolk-sac larvae development at different temperatures (Kokurewicz 1969; Herzig and Winkler 1986; Mooij and Van Tongeren 1990). However, the values of the heat sum parameter d derived from these studies cannot be compared with the value of d estimated from the field data because the latter value also accounts for the temperature-induced timing of spawning.

Fit of the Growth Models

The fit of the temperature model was expressed graphically by plotting the observed lengths against the predicted lengths (Fig. 4). For all species except pikeperch, the absolute deviation increases with body size, while the relative deviation between predicted and observed lengths remains fairly constant. Only for pikeperch does the model not account for the sharp increase in growth rate after the onset of piscivory (Fig. 4C).

The Monte Carlo permutation test showed that the yearly variation in body size of bream ($P < 0.001$), roach ($P < 0.001$), perch ($P < 0.001$), and finally pikeperch ($P < 0.01$) was significantly related to yearly variation in temperature (Table 3). For bream and roach, the correlation between temperature and growth rate was strongest for the larger fish. For perch and smelt, the correlation was strongest for the smaller fish. For pikeperch the correlation was similar for

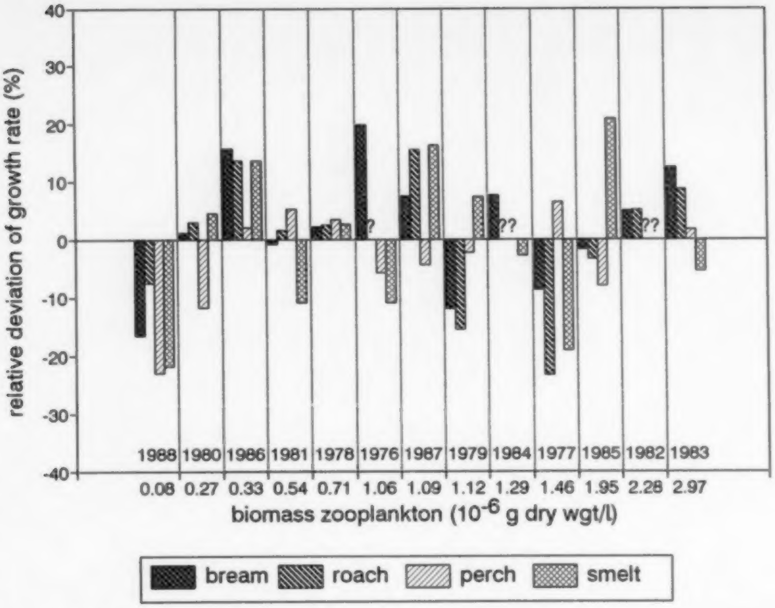

FIG. 5. Relative deviation of the optimal value of food parameter *a* for each year compared with its mean value during 1976–88. Only planktivorous fish are shown (bream, roach, perch, and smelt). Years were ordered according to the total biomass of zooplankton during July–September in Tjeukemeer.

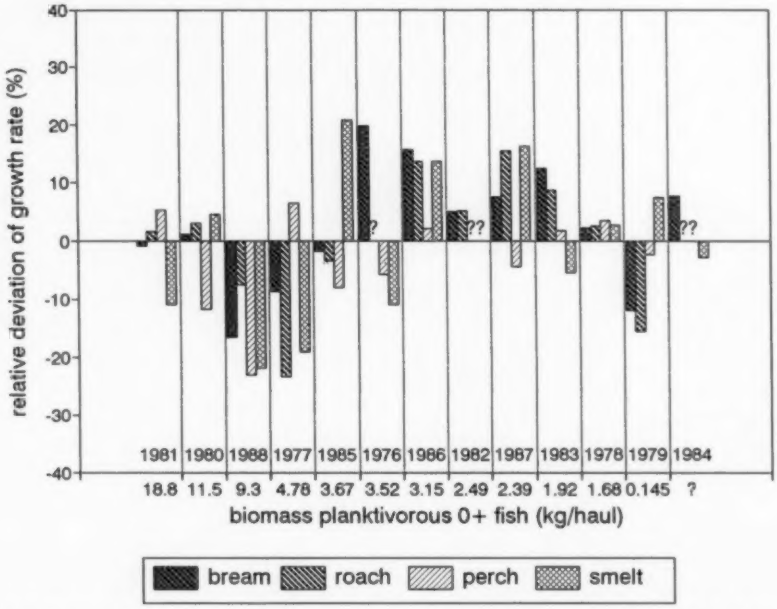

FIG. 6. Same as Fig. 5 except that years were ordered according to the abundance of planktivorous 0+ fish during July–September in Tjeukemeer.

all lengths, while no correlation between temperature and growth rate was found for ruffe.

Analysis of the ratio's between the unexplained sums of squares of the temperature model and the unexplained sum of squares of the logistic model leads to similar conclusions as the Monte Carlo analysis (Tables 2B and 3). The ratio was highest for bream, perch, roach, and pikeperch. Smelt has an intermediate value, while the ratio for ruffe is even less than 1, indicating a better fit of the logistic model compared with that of the temperature model.

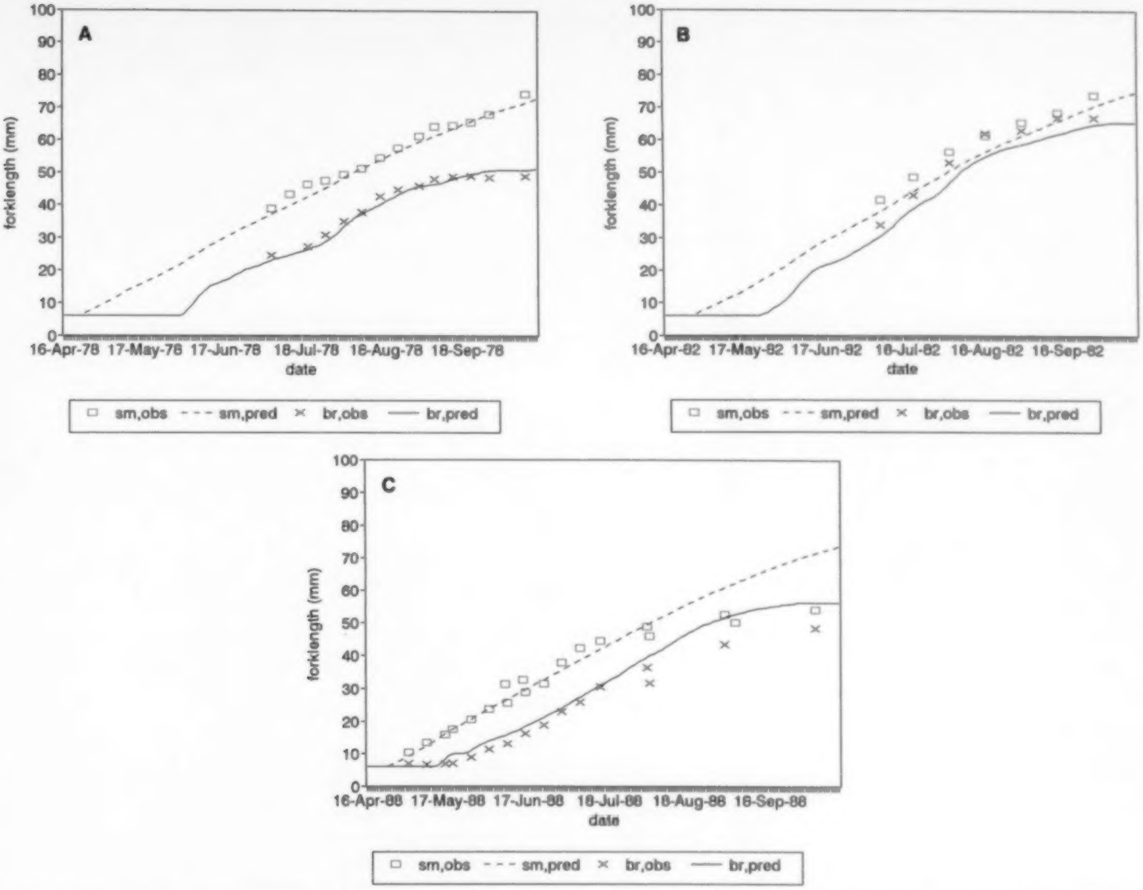

FIG. 7. Observed (obs) and predicted (pred) growth of smelt (sm) and bream (br) in Tjeukemeer in (A) 1978 (643 day-degrees above 12°C), 1982 (842 day-degrees above 12°C), and 1988 (715 day-degrees above 12°).

Food Parameters

To analyse the actual food conditions, the main zooplankton species were combined into four groups: (1) the large *Daphnia*, dominated by *Daphnia galeata*, (2) the middle-sized species, including *Bosmina coregoni* and *B. longirostris*, (3) the small-sized *Chydorus sphaericus*, and (4) the cyclopoid copepods (Table 4). The mean total biomass for each group was calculated for the months July, August, and September of each year. During this period, 0+ fish biomass reaches a maximum (Table 5). In most years, zooplankton biomass was dominated by *D. galeata* (70% mean relative abundance over the whole period), while the remaining biomass was evenly distributed among the other three groups. Highest zooplankton biomass was found in 1983 (2.9 mg dry weight/L) and the lowest in 1988 (0.08 mg dry weight/L).

Linear regression analyses relating zooplankton abundance to temperature were performed for all groups separately and for the total biomass. The number of day-degrees above 12°C was taken as a measure of temperature (Table 4). No significant relations were found ($P > 0.05$) except for the cyclopoid copepods ($r^2 = 0.59$, $P < 0.05$).

Relative food parameters were calculated only from the body size data for samples collected after 1 August, when food shortage is most likely to occur because of the high 0+ fish biomass. There was a highly significant correlation between the relative food parameters for bream and roach ($r = 0.85$, $P < 0.01$) but not for the other combinations of species. Multiple regression analysis did not yield a significant relationship between the relative food parameters of the fish species and either the biomass estimates of the four groups of zooplankton or the total zooplankton biomass (Table 4) for any of the food items for any fish species ($P > 0.05$).

Finally, as an indication of nonlinear relationships between growth rate and food conditions, the relative parameters for the different years and species were plotted after ranking on the basis of the total zooplankton biomass during July–September (Fig. 5). Only in 1988 did all planktivorous fishes show poor growth. In 1980, however, when zooplankton biomass was also low, only perch had poor growth, while the other four species did rather well. The relative parameters were also plotted after ranking on the basis of the total biomass of planktivorous 0+ fish during July–September in the lake (Fig. 6). In 1981, when 0+ fish were extremely abundant, temperature-corrected growth rates had average values and there were no indications of density-dependent growth.

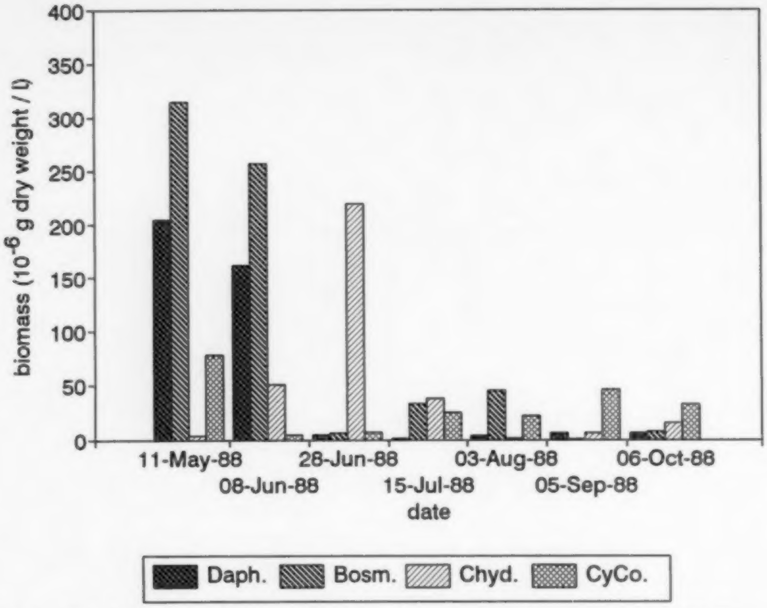

FIG. 8. Abundance of zooplankton (μg dry weight/L) in Tjeukemeer during 1988. Four groups are shown: *Daphnia* sp. (Daph.), *Bosmina* sp. (Bosm.), *C. sphaericus* (Chyd.), and cyclopoid copepods (CyCo.).

Discussion

A significant relation between temperature and the growth rate of bream, roach, perch, and small smelt – all planktivorous fishes – was found. The shape of the temperature – growth rate relationship for smelt shows a smaller increase in growth rate with rising temperatures than for the other species. This difference reflects the adaptation of the salmonid smelt to much lower temperatures (Belyanina 1969). This phenomenon might be the reason for the lack of a significant relationship between the yearly differences in growth rate and temperature for the larger smelt (trawl data). In a lake with lower summer temperatures than Tjeukemeer (10–15°C), growth of smelt is faster in a "warmer" year (Naesje et al. 1987). Apparently, smelt have a temperature optimum at about 15°C, which is normal for a salmonid (Elliott 1975). To describe the growth rate of this species more properly, a second temperature parameter should be included in the model (equation (1)). For the cyprinids and the percids, the optimum of the temperature–growth curve lies well above the temperature maxima occurring in Tjeukemeer (Hokanson 1977; Willemsen 1978; Elliott 1981; Jobling 1981; Hokanson and Koenst 1986).

The difference in growth rate between smelt and bream, showing the weakest and the strongest dependence of growth rate on temperature of the planktivorous species, respectively, is best illustrated by comparing observed and predicted growth rates in a cold year (1978, Fig. 7A) and a warm year (1982, Fig. 7B). Both the observed and the modelled growth curves for bream indicate that this species has an advantage over smelt during warm years.

Analysis of temperature-corrected growth rates and food conditions did not yield a significant correlation for any of the planktivorous fishes. Only in 1988, when the summer plankton biomass in Tjeukemeer was extremely low, were growth rates of all planktivorous species lower than would be expected based on the prevailing temperature. The observed growth rates for both bream and smelt after the middle of July are lower than the predicted rates (Fig. 7C). The most likely cause of this was the decline in zooplankton biomass after the end of June 1988 (Fig. 8).

The total biomass of zooplankton was not significantly correlated with temperature, although the abundance of copepods, which constitute only 10% of the total zooplankton biomass, shows a relation to temperature. Thus, there will probably be no indirect effect of temperature via food on the growth rate and, in most years, growth of planktivorous 0+ fish in Tjeukemeer is limited directly by temperature. This also holds for years with an extreme abundance of 0+ fish (Fig. 6), resulting in a change in the body size and species composition of the zooplankton community (Van Densen and Vijverberg 1982; Van Densen 1985a). This observation confirms the conclusion that the effect of food quality on 0+ fish growth rate, as observed by Mills et al. (1989a) for yellow perch (*Perca flavescens*), cannot be demonstrated in Tjeukemeer. Only if the total zooplankton biomass declines to values below 80 μg dry weight/L does food limitation occur (Fig. 7C and 8).

Ruffe and pikeperch, two of the major fish species of Tjeukemeer, were not included in the group of planktivores. Ruffe switches to a benthivorous feeding mode either during or after the larval phase (Van Densen 1985a). This behaviour explains the absence of this species in the hoopnet catches. For ruffe, growth rate and temperature were not correlated. Van Densen and Hadderingh (1982) also observed an increase in growth rate for bream, roach, and perch but not for ruffe in a Frisian lake, heated by waste water from a power station. Ruffe is probably food limited, but a complete analysis of the zoobenthos data from Tjeukemeer was beyond the scope of this study. The absence of a significant relation between growth and temperature for this species, however, might also be related to its intermittent spawning behaviour (Collette et al. 1977; Hokanson 1977), which can last for several weeks, and may obscure a relationship between growth and temperature. Moreover, ruffe is known to be a species that is not very sensitive to temperature (Bergman 1987).

Pikeperch, being the main predator on fish in Tjeukemeer, becomes piscivorous during the 0+ stage (Van Densen 1985a, 1985b). Probably as a result of the higher energy content of fish compared with zooplankton (Keast and Eadie 1985), the growth rate of this species increases sharply after it becomes piscivorous, resulting in a bimodal length frequency distribution of slow-growing planktivores and fast-growing piscivores (Van Densen 1985b). The Monte Carlo permutation test indicated a significant relation between growth rate and temperature for 0+ pikeperch. As the predominant effect of food on the growth rate is obvious, it should be concluded that the opportunity for developing a piscivorous feeding mode is better in warmer years. This phenomenon is well known (Biro 1972; Svardson and Molin 1973; Willemsen 1977; Van Densen 1985b). Within the scope of the present study, an analysis of the availability of prey from the field observations was not possible. From the results presented, however, a hypothesis can be formulated that explains the positive correlation between pikeperch recruitment and temperature. Pikeperch has a relatively higher growth rate than smelt in warmer years. Since small differences in body size between a 0+ predator and its 0+ prey are important, the availability of smelt for pikeperch may be higher in these years.

Acknowledgments

We thank all the people who participated over the years in the sampling programme, in particular Aafje Frank-Landman, Bertus Lemsma, Peter Mac Gillavry, Steven van Schendel, Koos Swart, Bauke Vlink, and Steven Visser. Moreover, we thank Maarten Boersma, Niels Daan, Ramesh Gulati, Onno van Tongeren, and Koos Vijverberg for commenting on the manuscript, Pete Shaw for correcting the English, and finally Anja van der Honig for typing the temperature data.

References

Backiel, T., and E.D. Le Cren. 1978. Some density relationships for fish population parameters, p. 279–302. *In* S.D. Gerking [ed.] Ecology of freshwater fish production. Blackwell Scientific Publications, Oxford.

Belyanina, T.N. 1969. Synopsis of biological data on smelt, Osmerus eperlanus (Linnaeus 1758). FAO Fish. Synop. 78.

Bergman, E. 1987. Temperature-dependent differences in foraging ability of two percids, *Perca fluviatilis* and *Gymnocephalus cernua*. Environ. Biol. Fishes 19: 45–53.

Biro, P. 1972. First summer growth of pikeperch (*Lucioperca lucioperca* L.) in Lake Balaton. Ann. Biol. Tihany 39: 101–113.

Bottrell, H.H., A. Duncan, Z.M. Gliwicz, E. Grygierek, A. Herzig, A. Hillbricht-Ilkowska, H. Kurasawa, P. Larsson, and T. Weglenska. 1976. A review of some problems in zooplankton production studies. Norw. J. Zool. 24: 419–456.

Brett, J.R. 1979. Environmental factors and growth, p. 599–675. *In* W.S. Hoar, D.J. Randall, and J.R. Brett [ed.] Fish physiology. Vol. VIII. Academic Press, New York, N.Y.

Brett, J.R., and J.E. Shelbourn. 1975. Growth rate of young sockeye salmon, *Oncorhynchus nerka*, in relation to fish size and ration level. J. Fish. Res. Board Can. 32: 2103–2110.

Broughton, N.M., and N.V. Jones. 1978. An investigation into the growth of 0-group roach (*Rutilus rutilus* L.) with special reference to temperature. J. Fish Biol. 12: 345–357.

Collette, B.B., M.A. Ali, K.E.F. Hokanson, M. Nagiec, S.A. Smirnov, J.E. Thorpe, A.H. Weatherley, and J. Willemsen. 1977. Biology of the percids. J. Fish. Res. Board Can. 34: 1890–1899.

Cryer, M., G. Peirson, and C.R. Townsend. 1986. Reciprocal interactions between roach, *Rutilus rutilus*, and zooplankton in a small lake: prey dynamics and fish growth and recruitment. Limnol. Oceanogr. 31: 1022–1038.

Cushing, D.H. 1981. Fisheries biology. A study in population dynamics. 2nd ed. University of Wisconsin Press, Madison, Wis.

De Boer, T., H.L. Hoogveld, H. Kramer, J. Schrotenboer, and J. Voerman. 1988. Hydrological, physical and chemical research in Tjeukemeer and surroundings; results over the period 1968–1987. Limnological Institute Oosterzee/Nieuwersluis Internal Rep. 81-4, 81-6/9, 81-13/14, 83-3/4, 84-2/3, 85-6, 86-3, 86-15, 87-5, 88-5.

Elliott, J.M. 1975. The growth rate of brown trout (*Salmo trutta* L.) fed on maximum rations. J. Anim. Ecol. 44: 805–821.

Elliott, J.M. 1981. Some aspects of thermal stress on freshwater teleosts, p. 209–245. *In* A.D. Pickering [ed.] Stress and fish. Academic Press, London.

Elliott, J.M. 1984. Growth, size, biomass and production of young migratory trout *Salmo trutta* in a Lake District stream, 1966–1983. J. Anim. Ecol. 53: 979–994.

Elliott, J.M. 1985. Growth, size, biomass and production for different life-stages of migratory trout *Salmo trutta* in a Lake District stream, 1966–83. J. Anim. Ecol. 54: 985–1001.

Elliott, J.M., U.H. Humpesch, and M.A. Hurley. 1987. A comparative study of eight mathematical models for the relationship between water temperature and hatching time of eggs of freshwater fish. Arch. Hydrobiol. 109: 257–277.

Guma'a, S.A. 1978. On the early growth of 0+ perch, *Perca fluviatilis*, in Windermere. Freshwater Biol. 8: 213–220.

Hellawell, J.M. 1972. The growth, reproduction and food of the roach (*Rutilus rutilus* L.) of the River Lugg, Herefordshire. J. Fish Biol. 4: 469–486.

Henderson, B.A. 1985. Factors affecting growth and recruitment of yellow perch, *Perca flavescens* Mitchill, in South Bay, Lake Huron. J. Fish Biol. 26: 449–458.

Henderson, B.A., and E.H. Brown Jr. 1985. Effects of abundance and water temperature on recruitment and growth of alewife (*Alosa pseudoharengus*) near South Bay, Lake Huron, 1954–82. Can. J. Fish. Aquat. Sci. 42: 1608–1613.

Herzig, A., and H. Winkler. 1986. The influence of temperature on the embryonic development of three cyprinid fishes, *Abramis brama*, *Chalcalburnus chalcoides mento* and *Vimba vimba*. J. Fish Biol. 28: 171–181.

Hokanson, K.E.F. 1977. Temperature requirements of some percids and adaptations to the seasonal temperature cycle. J. Fish. Res. Board Can. 34: 1524–1550.

Hokanson, K.E.F., and W.M. Koenst. 1986. Revised estimates of growth requirements and lethal temperatures limits of juvenile walleyes. Prog. Fish-Cult. 48: 90–95.

Jobling, M. 1980. Gastric evacuation in plaice, *Pleuronectes platessa* L.: effects of temperature and fish size. J. Fish Biol. 17: 547–551.

Jobling, M. 1981. Temperature tolerance and the final preferendum – rapid methods for the assessment of optimum growth temperatures. J. Fish Biol. 19: 439–455.

Jobling, M. 1983. Growth studies with fish – overcoming the problems of size variation. J. Fish Biol. 22: 153–157.

Keast, A., and J.M. Eadie. 1985. Growth depensation in year-0 largemouth bass: the influence of diet. Trans. Am. Fish. Soc. 114: 204–213.

Klepper, O., and D.I. Rouse. 1991. A procedure to reduce parameter uncertainty for complex models by comparison with real system output illustrated on a potato growth model. Agric. Syst. 36: 375–395.

Kokurewicz, B. 1969. The influence of temperature on the embryonic development of the perches: *Perca fluviatilis* L. and *Lucioperca lucioperca* L. Zool. Pol. 19: 47–67.

Lammens, E.H.R.R., W.L.T. van Densen, and R. Knijn. 1990. The fish community structure in Tjeukemeer in relation to fishery and habitat utilization. J. Fish Biol. 36: 933–945.

Le Cren, E.D. 1951. The length–weight relationship and seasonal cycle in gonad weight and condition in the perch (*Perca fluviatilis*). J. Anim. Ecol. 20: 201–219.

Le Cren, E.D. 1958. Observations on the growth of perch (*Perca fluviatilis*, L.) over twenty-two years with special reference to the effects of temperature and changes in population density. J. Anim. Ecol. 27: 287–334.

MANN, R.H.K. 1973. Observations on the age, growth, reproduction and food of the roach, *Rutilus rutilus* (L.) in two rivers in southern England. J. Fish Biol. 5: 707–736.

MILLS, E.L., M.V. POL, R.E. SHERMAN, AND T.B. CULVER. 1989a. Interrelationships between prey body size and growth of age-0 yellow perch. Trans. Am. Fish. Soc. 118: 1–10.

MILLS, E.L., R. SHERMAN, AND D.S. ROBSON. 1989b. Effect of zooplankton abundance and body size on growth of age-0 yellow perch (*Perca flavescens*) in Oneida Lake, New York, 1975–86. Can. J. Fish. Aquat. Sci. 46: 880–886.

MOOIJ, W.M. 1989. A key to the identification of larval bream, *Abramis brama*, white bream, *Blicca bjoerkna*, and roach, *Rutilus rutilus*. J. Fish Biol. 34: 111–118.

MOOIJ, W.M., AND O.F.R. VAN TONGEREN. 1990. Growth of 0+ roach (*Rutilus rutilus*) in relation to temperature and size in a shallow eutrophic lake: comparison of field and laboratory observations. Can. J. Fish. Aquat. Sci. 47: 960–967.

MULLER, R., AND H.J. MENG. 1986. Factors governing the growth rate of roach, *Rutilus rutilus* (L.) in prealpine Lake Sarner. Schweiz. Z. Hydrol. 48: 135–144.

NAESJE, T.F., B. JONSSON, L. KLYVE, AND O.T. SANDLUND. 1987. Food and growth of age-0 smelts, *Osmerus eperlanus*, in a Norwegian fjord lake. J. Fish Biol. 30: 119–126.

RHEINBERGER, V., R. HOFER, AND W. WIESER. 1986. Growth and habitat separation in eight cohorts of three species of cyprinids in a subalpine lake. Environ. Biol. Fishes 18: 209–217.

RICKER, W.E. 1979. Growth rates and models, p. 677–743. *In* W.S. Hoar, D.J. Randall, and J.R. Brett [ed.] Fish physiology. Vol. VIII. Academic Press, New York, N.Y.

SOKAL, R.R., AND F.J. ROHLF. 1981. Biometry. W.H. Freeman and Company, San Francisco, Calif. 859 p.

SVARDSON, G., AND G. MOLIN. 1973. The impact of climate on Scandinavian populations of the sander, *Stizostedion lucioperca* (L.). Inst. Freshwater Res. Drottningholm Rep. 53: 112– 139.

TONG, H.Y. 1986. A qualitative and quantitative description of the early growth of roach, *Rutilus, rutilus*, in the laboratory. Environ. Biol. Fishes 15: 293–300.

VAN DENSEN, W.L.T. 1985a. Feeding behaviour of major 0+ species in a shallow, eutrophic lake (Tjeukemeer, The Netherlands). Z. Angew. Ichthyol. 1: 49–70.

VAN DENSEN, W.L.T. 1985b. Piscivory and the development of bimodality in the size distribution of 0+ pikeperch (*Stizostedion lucioperca* L.). Z. Angew. Ichthyol. 1: 119–131.

VAN DENSEN, W.L.T., AND R.H. HADDERINGH. 1982. Effects of entrapment and cooling water discharge by the Bergum Power Station on 0+ fish in the Bergummermeer. Hydrobiologia 95: 351–368.

VAN DENSEN, W.L.T., AND J. VIJVERBERG. 1982. The relations between 0+ fish density, zooplankton size and the vulnerability of pikeperch, *Stizostedion lucioperca*, to angling in the Frisian lakes. Hydrobiologia 95: 321–336.

VIJVERBERG, J., AND TH.H. FRANK. 1976. The chemical composition and energy contents of copepods and cladocerans in relation to their size. Freshwater Biol. 6: 333–345.

WEATHERLEY, N.S. 1987. The diet and growth of 0-group dace, *Leuciscus leuciscus* (L.), and roach, *Rutilus rutilus* (L.), in a lowland river. J. Fish Biol. 30: 237–247.

WIESER, W., H. FORSTNER, F. SCHIEMER, AND W. MARK. 1988. Growth rates and growth efficiencies in larvae and juveniles of *Rutilus rutilus* and other cyprinid species: effects of temperature and food in the laboratory and in the field. Can. J. Fish. Aquat. Sci. 45: 943–950.

WILLEMSEN, J. 1977. Population dynamics of percids in Lake Ijssel and some smaller lakes in The Netherlands. J. Fish. Res. Board Can. 34: 1710–1719.

WILLEMSEN, J. 1978. Influence of temperature on feeding, growth and mortality of pikeperch and perch. Verh. Int. Ver. Limnol. 20: 2127–2133.

Metabolic Costs and Physiological Consequences of Acclimation to Aluminum in Juvenile Rainbow Trout (*Oncorhynchus mykiss*). 1: Acclimation Specificity, Resting Physiology, Feeding, and Growth

Rod W. Wilson[1]

Department of Biology, McMaster University, Hamilton, ON L8S 4K1, Canada

Harold L. Bergman

Fish Physiology and Toxicology Laboratory, University of Wyoming, Laramie, WY 82071-3166, USA

and Chris M. Wood

Department of Biology, McMaster University, Hamilton, ON L8S 4K1, Canada

Wilson, R.W., H.L. Bergman, and C.M. Wood. 1994. Metabolic costs and physiological consequences of acclimation to aluminum in juvenile rainbow trout (*Oncorhynchus mykiss*). 1: Acclimation specificity, resting physiology, feeding, and growth. Can. J. Fish. Aquat. Sci. 51: 527–535.

Juvenile rainbow trout (*Oncorhynchus mykiss*, 5–13 g) became acclimated (i.e., increased their resistance to lethal Al levels, 162 $\mu g \cdot L^{-1}$, pH 5.2) after only 5 d when exposed to sublethal Al (38 $\mu g \cdot L^{-1}$) in acidified soft water (Na^+ = 85, Ca^{2+} = 28 $\mu Eq \cdot L^{-1}$, pH 5.2). Acclimation was associated with reduced ionoregulatory and respiratory disturbances during lethal Al challenge and was maintained for at least 34 d. Acclimation was relatively specific to Al because no consistently improved resistance to lethal Cu (32 $\mu g \cdot L^{-1}$, pH 5.2) was observed. Exposure to sublethal acid alone (pH 5.2) did not result in acclimation to lethal $[H^+]$ (pH 4.0) and caused a pronounced reduction in whole-body Na^+ and Cl^-. Sublethal acid + Al resulted in a more rapid loss of ions than sublethal acid alone over the first 10 d, but both groups subsequently recovered ionoregulatory status after 34 d. Exposure to sublethal acid alone had a negligible effect on feeding or growth. However, growth was impaired by 29% in Al-exposed trout, primarily the result of reduced appetite during the first 10 d. Decreased growth must be considered one of the costs of acclimation during chronic sublethal exposure to Al.

Des truites arc-en-ciel (*Oncorhynchus mykiss*) juvéniles (5–13 g) se sont acclimatées (c.-à-d. ont accru leur résistance à des concentrations létales d'Al, 162 $\mu g \cdot L^{-1}$, pH 5,2) après 5 jours seulement lorsqu'elles ont été exposées à des doses sublétales d'Al (38 $\mu g \cdot L^{-1}$) dans de l'eau douce acidifiée (Na^+ = 85, Ca^{2+} = 28 $\mu Eq \cdot L^{-1}$, pH 5,2). L'acclimatement était associé à une réduction des troubles de l'ionorégulation et de la respiration pendant l'exposition à des concentrations létales d'Al, et s'est maintenu pendant au moins 34 jours. Cet acclimatement était relativement spécifique à l'Al, car on n'a observé aucune amélioration régulière de la résistance à des concentrations létales de Cu (32 $\mu g \cdot L^{-1}$, pH 5,2). L'exposition à une concentration sublétale d'acide uniquement (pH 5,2) n'a pas produit d'acclimatement à des concentrations létales de $[H^+]$ (pH 4,0) et a causé une réduction prononcée de Na^+ et Cl^- dans l'ensemble de la masse corporelle. L'exposition simultanée à des concentrations sublétales d'acide et d'Al a provoqué une perte plus rapide d'ions que la concentration sublétale d'acide seul pendant les 10 premiers jours, mais les deux groupes ont par la suite retrouvé une ionorégulation normale après 34 jours. L'exposition à une concentration sublétale d'acide seulement avait un effet négligeable sur l'alimentation ou la croissance. Toutefois, la croissance était réduite de 29 % chez les truites exposées à l'Al, ce qui est avant tout causé par une diminution de l'appétit pendant les 10 premiers jours. La réduction de la croissance doit être considérée comme l'un des coûts de l'acclimatement pendant l'exposition chronique à des concentrations sublétales d'Al.

Received February 8, 1993
Accepted October 6, 1993
(JB785)

Reçu le 8 février 1993
Accepté le 6 octobre 1993

Chronic exposure of freshwater fish to sublethal aluminum concentrations is frequently encountered in low-pH soft water due to the acid-induced leaching of Al from soils and sediments (Wright and Gjessing 1976; Cronan and Schofield 1979; Dickson 1980). It is now clear that at pH values between 4.7 and 5.5, fish kills may be primarily due to the presence of Al rather than the H^+ concentation, per se (Schofield and Trojnar 1980; Baker and Schofield 1982). Physiological studies have demonstrated that Al causes *acute* ionoregulatory and respiratory disturbances in this pH range (e.g., Neville 1985; Booth et al.

---

[1] Author to whom correspondence should be addressed. Present address: School of Biological Sciences, G.38 Stopford Building, University of Manchester, Oxford Road, Manchester M13 9PT, United Kingdom.

TABLE 1. Measured water chemistry variables (means ± SEM (*n*)) during the chronic exposure regimes.

Exposure group	$[Na^+]$ ($\mu Eq \cdot L^{-1}$)	$[Ca^{2+}]$ ($\mu Eq \cdot L^{-1}$)	pH	Total [Al] ($\mu g \cdot L^{-1}$)
6.5/0	85.4 ± 4.6 (32)	30.5 ± 1.5 (32)	6.45 ± 0.03 (36)	3.6 ± 0.6 (32)
5.2/0	85.3 ± 5.2 (32)	28.0 ± 1.0 (32)	5.37 ± 0.02 (36)	3.2 ± 0.7 (32)
5.2/Al	85.6 ± 5.3 (32)	26.5 ± 0.9 (32)	5.22 ± 0.01 (36)	38.1 ± 1.2 (35)

1988; Wood et al. 1988a) associated with surface binding and precipitation of Al on the gills (Playle and Wood 1989, 1991; Reid et al. 1991). However, laboratory studies on prolonged exposure to sublethal Al have shown that acclimation (i.e., increased resistance to lethal Al) occurs with time (Orr et al. 1986; Wood et al. 1988b, 1988c; McDonald et al. 1991) which may explain the continued presence of fish populations in acidified softwater lakes and rivers containing levels of Al in excess of 100 $\mu g \cdot L^{-1}$ (Wright and Snekvik 1978; Schofield and Trojnar 1980; Kelso et al. 1986).

The acclimation process results from a "damage/repair" phenomenon involving physiological, biochemical, and structural changes at the gills (McDonald et al. 1991; Mueller et al. 1991; McDonald and Wood 1992). In juvenile brook trout (*Salvelinus fontinalis*), the initial damage phase (lasting 4–5 d) was characterized by the accumulation of gill Al, reduction in whole-body electrolytes, severe gill histopathologies, and impaired oxygen delivery to tissues (whole-body lactate levels were elevated). Acclimation was observed from day 10 onwards and was accompanied by at least partial recovery of whole-body ion and lactate levels and a progressive reduction in total gill Al.

The specificity of acclimation to Al is unknown, i.e., whether it will simultaneously increase a fish's resistance to other metals. Because the mechanism of acclimation is probably designed to combat the mechanism of toxicity of a metal, it is possible that metals with similar modes of toxic action will elicit similar acclimatory responses and thus may exhibit crossover resistance (McDonald and Wood 1992). Cu has similar effects to Al in freshwater fish; both can impair respiratory gas exchange during acute exposure and both interfere with the active influx and passive efflux components of branchial ion transport (Laurén and McDonald 1985, 1986; Booth et al. 1988; Playle et al. 1989; Wilson and Taylor 1993). Therefore, Cu is a likely candidate for testing crossover resistance during acclimation to Al.

Estimates of metabolic rate in fish acclimated to Al showed increased energy requirements compared with control fish when swimming aerobically (Wilson et al. 1994). However, growth is a more sensitive indicator of subtle increases in energy demand, and impaired growth has indeed been documented for fish exposed to sublethal acid and Al (Sadler and Lynam 1987, 1988; Reader et al. 1988; Mount et al. 1988a, 1988b; Ingersoll et al. 1990a, 1990b; Wilson and Wood 1992). However, the relationship between energetic costs and growth cannot be defined without the quantification of energy input (feeding rate), in which appetite represents an equally important factor.

The present paper deals with three elements: (i) the specificity of acclimation to Al tested by challenge with lethal levels of Cu, (ii) the resting ionoregulatory, respiratory, and gill Al status during both chronic exposure to sublethal Al and acute challenge with lethal Al, and (iii) some of the potential costs of acclimation assessed by measuring growth and feeding rates and the relevance of appetite. The study was conducted in parallel with that described in our companion paper (Wilson et al. 1994), using juvenile rainbow trout (*Oncorhynchus mykiss*) exposed to pH 5.2 in the presence of 38 $\mu g \ Al \cdot L^{-1}$ for a period of 36 d. All measured variables were compared with two other groups exposed to either pH 5.2 or pH 6.5, both with no Al added. Exposures were carried out in a synthetic software medium relevant to the acid-threatened lakes and rivers of eastern North America and Europe.

Materials and Methods

Animal Holding

Juvenile rainbow trout (5–13 g) were obtained from the hatchery of the Wyoming Game and Fish Department, Wyoming, and transported to the Red Buttes Fish Physiology and Toxicology Laboratory, Laramie, Wyoming, where they were initially maintained in continuously flowing well water ($[Ca^{2+}] \approx 2.6$, ($[Na^+] \approx 0.3 \ mEq \cdot L^{-1}$) and fed ad libitum. During this holding period in hard water, fish were divided into three groups of approximately 400 individuals. At this stage, each individual was given a freeze-brand distinctive of its group (Mighell 1969) to allow identification during subsequent tests (see below).

Four weeks before starting the experimental regime the holding water was switched from hard well water to continuously flowing synthetic soft water (nominal $[Ca^{2+}] \approx 25$, ($[Na^+] \approx 80 \ \mu Eq \cdot L^{-1}$, pH 6.7–7.0, $P_{CO_2} < 0.13$ kPa) designed to be similar to the composition of acid-threatened lakes and streams in eastern North America and Europe. Soft water was generated by treating the hard well water with reverse osmosis followed by separate bed anion and cation deionization. The required amounts of reagent-grade $CaCl_2$ and NaCl were added via Mariotte bottles to the main head tank and pH adjusted to the appropriate level in secondary head tanks with either KOH or H_2SO_4 using Leeds and Northrup pH controllers. Fish were kept in circular 400-L tanks supplied with water at 3.5 $L \cdot min^{-1}$ (i.e., 12.6 volume addition per day). The study was conducted from January to March 1991 at 15°C (range ±0.5°C) under a photoperiod adjusted biweekly to follow the natural cycle for Laramie, Wyoming.

After softwater acclimation, rainbow trout were exposed to one of three conditions: (i) normal soft water at pH 6.5 (6.5/0 group), (ii) low-pH soft water (nominal pH 5.2)

(5.2/0 group), and (iii) low-pH soft water (nominal pH 5.2) with 38 μg Al·L^{-1} added (5.2/Al group). The elevated level of Al was achieved by adding an $AlCl_3 \cdot 6H_6O$ stock solution from Mariotte bottles into the appropriate softwater supply. Water variables (pH, [Ca^{2+}], [Na^+], and total Al) were measured on samples collected daily from each tank (Table 1).

Sampling Protocol

Thirty fish were sampled from each tank after 1, 5, 10, 17, 25, and 34 d of exposure to test for changes in tolerance to Al and Cu (by LT50 tests) and to determine whole-body ions and lactate and gill Al content. For Al LT50 tests, 10 fish from each group were transferred to a 400-L challenge tank receiving pH 5.2 soft water at 3.5 L·min^{-1} with 162 μg Al·L^{-1} added. For Cu LT50 tests, another 10 fish were transferred to an identical tank with 32 μg Cu·L^{-1} added (no added Al). Cumulative mortalities in each tank were recorded over the following 96 h or until all fish were dead. Fish were removed and weighed as soon as mortalities were observed. Using a single challenge tank for the Al LT50 tests and one tank for the Cu LT50 tests ensured identical "challenge" conditions for all three groups. Individual freeze-brand marks allowed identification of the origin of each fish. At the end of each test, LT50 values (time to 50% mortality) were estimated by log/probit analysis for each group. The background level of Cu in chronic exposure tanks was 1.45 ± 0.20 μg·L^{-1} (mean ± SEM of 34 water samples).

Ten of the 30 fish sampled from each tank were netted individually, killed by decapitation with a sharp knife, and the body portion immediately freeze-clamped between two aluminum plates in liquid nitrogen. The mass of the frozen body plus head was then measured to the nearest 0.01 g and the frozen body stored at −80°C until preparation for measurement of lactate and ion content. Gill baskets were dissected free from the unfrozen head portion, washed for 10 s in pH 5.2 Al-free soft water, and stored at −80°C for later analysis of Al content.

On day 36, two additional challenge tests were performed. First, 10 fish from each group were transferred to the Al challenge tank and then sampled after 10 h (i.e., before any mortality) for analysis of whole-body ions and lactate and gill Al content to assess their physiological status during Al challenge. A second group of 10 fish from each tank was transferred to a low-pH challenge tank (pH 3.99, no Al added) and LT50's determined as above in order to test for acclimation to acid alone. A further 10 fish from each exposure tank were sampled on day 36 to assess whole-body water content. These fish were individually killed, blotted dry in paper towels, weighed to the nearest 0.001 g, and dried at 85°C to a constant weight.

Feeding Regime and Growth

Fish were fed to satiation twice per day at approximately 8-h intervals using floating trout pellets (Purina Trout Chow ground and sieved manually to an average pellet size of 1.2 × 1.5 mm). For each exposure tank, a separate pre-weighed bag of pellets was used. At the start of each meal, food was offered in small aliquots (equivalent to less than 5% of the daily ration) once every minute. Feeding was stopped when uneaten pellets still remained after a period of 2 min, and the amount of food eaten per day was calculated from the difference in bag weight at the beginning and end of each day. Feeding rates (percent body weight per day) were calculated from the weight of food eaten and the biomass in each tank (equivalent to the product of average weight and total number of fish per tank). This feeding protocol was adopted during the last week of adjustment of softwater conditions and continued throughout the entire experimental exposure period. Exposure tanks were cleaned of organic debris daily by siphon. To assess growth rates, 50 fish from each tank were removed twice per week, weighed individually in a tared vessel containing the appropriate medium, and then returned to their original tank. Gross food conversion efficiencies were calculated as described by Brett and Groves (1979), using the weight of food eaten and the change in whole-body dry weight (assuming 73% water content) for the average fish in each group over the course of the study.

Analytical Techniques

For analysis of whole-body ions and lactate, frozen carcasses were ground to a fine powder under liquid nitrogen with a mortar and pestle. The frozen powder was weighed in 50-mL centrifuge tubes (once all residual liquid nitrogen had gassed off) and deproteinized by adding a precise volume (15–30 mL) of ice-cold 8% (w/v) perchloric acid. Homogenates were shaken thoroughly, allowed to stand for 2 h on ice, and centrifuged at 900*g* for 10 min. The concentration of lactate in the resultant supernatant was then measured on 67-μL aliquots using an enzymatic assay (L-lactate dehydrogenase/NADH method) and Sigma reagents. Supernatant Cl^- was measured directly on duplicate 200-μL aliquots by coulometric titration (Aminco-Cotlove). Supernatant Na was measured by atomic absorption spectophotometry (Perkin Elmer 2380) following 1:100 dilution with deionized water.

In preparation for the analysis of gill Al content, gill baskets were thawed, weighed, and digested with five times their weight of 1.0 N H_2SO_4 in 15-mL capped polypropylene centrifuge tubes at 80°C overnight. Gill digests were vortexed, centrifuged (900*g* for 5 min), and a sample of the supernatant diluted 1:10 in deionized water. Twenty-microlitre aliquots of the diluted supernatant were analyzed for Al content using an atomic absorption spectrophotometer (Perkin Elmer 2380) with graphite furnace attachment (Perkin Elmer HGA-400). Atomiser parameters were 2-s ramp to 120°C, 20 s at 120°C, 2-s ramp to 1700°C, 10 s at 1700°C, 0.1-s ramp to 2700°C, and 5.0 s at 2700°C. Argon was used as the carrier gas, and peak heights were read during the final 5.0 s at $\lambda = 309.3$ nm. Total [Cu] and [Al] in water samples from the LT50 tests were similarly analyzed by electrothermal atomic absorption spectrophotometry and water [Ca^{2+}]and [Na^+] by flame atomic absorption spectrophotometry.

Statistical Analysis

Mean values ± SEM (*n*) are generally reported throughout the text where *n* represents the number of fish or water samples. LT50 values were compared between groups using the nomographic methods of Litchfield (1949) and Litchfield and Wilcoxon (1949) at the 5% level of significance. Mean values of all other variables were compared between groups on each day using a Student's unpaired *t*-test at the 5% level of significance.

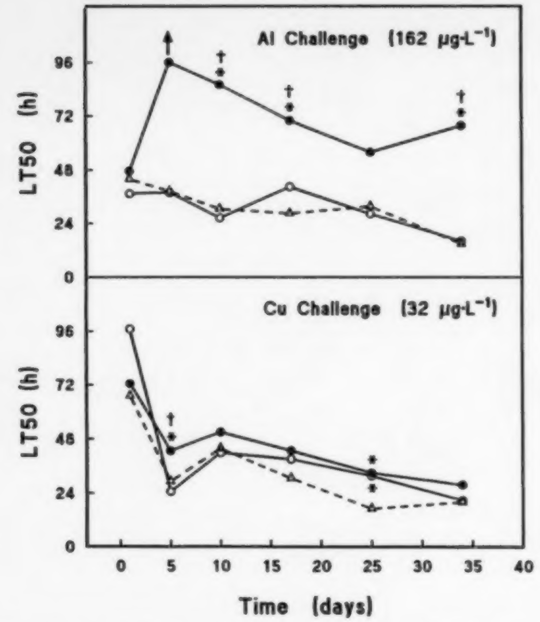

FIG. 1. Estimated times to 50% mortality (LT50's) during challenge with acutely lethal Al (162 µg·L^{-1}, pH 5.2) or Cu (32 µg·L^{-1}, at pH 5.2). The vertical arrow on day 5 indicates that less than 50% mortality occurred in the 5.2/Al group within the 96-h test. Asterisks indicate a significant difference from the 6.5/0 control group, and daggers indicate a significant difference from the 5.2/0 group.

Results

Mortality and Acclimation

Mortality was low in the chronic exposure groups (0.25, 0.5, and 5.5% in the control, 5.2/0, and 5.2/Al groups, respectively). Acclimation to lethal Al (161.7 ± 2.5 µg·L^{-1}, (n = 35); pH 5.25 ± 0.01, (n = 38)) was first observed in the 5.2/Al group on day 5 and persisted thereafter, with the 5.2/Al fish surviving at least 2.6 times longer than the other two groups (Fig. 1). Preexposure to acid alone did not result in acclimation to Al.

With the exception of day 1 (see Fig. 1), challenge with lethal Cu (32.2 ± 1.3 µg·L^{-1} (n = 33); pH ± 5.21 ± 0.01 (n = 37)) resulted in 50% mortality in all groups within about 48 h or less. On day 1 the Cu challenge LT50 values were substantially higher (67–96 h) but were associated with significantly lower measured ambient Cu levels during this particular toxicity test (20.8 ± 0.4 µg·L^{-1} (n = 4)). During all subsequent LT50 tests the average measured Cu levels in the Cu challenge tank ranged from 30.7 to 35.9 µg·L^{-1} and produced LT50 values comparable with those for unacclimated fish in the Al challenge tests. Thus, the levels of Cu and Al (32 and 162 µg·L^{-1}) were of approximately equivalent toxicity. On a molar basis ([Cu] = 0.52 and [Al] = 5.55 µmol·L^{-1}), Cu was therefore approximatly 10 times more toxic than Al at the ambient pH and Ca levels we used.

In Cu LT50 tests, significantly improved survival times were seen on days 5 and 25 for the 5.2/Al trout and on day 25 for the 5.2/0 trout when compared with the control group (Fig. 1). However, these differences were small (relative to the Al LT50 tests) and were inconsistent. On day 36, when challenged with lethal pH alone (pH 3.99 ± 0.04 (n = 4), no Cu or Al added), LT50's were similar in all three groups (14.8, 17.3, and 17.5 h for the control, 5.2/0, and 5.2/Al groups, respectively), indicating no acclimation to low pH itself in the absence of Al.

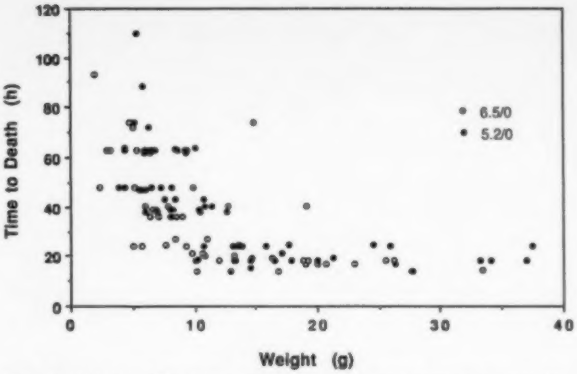

FIG. 2. Relationship between body mass and time to mortality in control (open circles) and 5.2/0 (solid circles) trout challenged with lethal Al (162 µg·L^{-1}, pH 5.25).

During the course of LT50 tests, it was noticed that larger fish tended to die earlier than smaller fish. Figure 2 shows this phenomenon using the data accumulated from Al toxicity tests during the 34-d experimental period for the two unacclimated groups (5.2/0 and 6.5/0). It is apparent that no fish larger than about 15 g survived for more than 40 h during the Al challenge. In contrast, 45% of fish smaller than 15 g survived for 40 h or longer, and some of these smaller fish were able to survive the full 96 h of the tests. Thus, size had a substantial effect on survival during lethal Al challenge.

Ionoregulatory and Respiratory Disturbances and Gill Al content

Both experimental groups suffered losses of whole-body Na$^+$ and Cl$^-$ over the first 5–17 d of exposure (Fig. 3). Initially, the losses were both more rapid and more severe in the 5.2/Al trout, being at least twofold greater on day 5. Whole-body ions subsequently stabilized in the 5.2/Al trout, but continued to fall in the 5.2/0 group until, by day 17, they had reached similar levels to those in the 5.2/Al trout, representing losses of about 24 and 32% of their whole-body Na$^+$ and Cl$^-$, respectively. Following day 17, ionic status gradually recovered, and by day 34, whole-body Na$^+$ and Cl$^-$ of both groups were not significantly different from the control group. In contrast with ionoregularoty status, the whole-body lactate contents of 5.2/0 and 5.2/Al trout were never significantly different from the control group (Fig. 3).

At the beginning of the sublethal exposures, total gill Al in the 5.2/Al trout increased almost linearly with time, reaching an initial peak on day 5 of around 29 µg·g^{-1} (Fig. 3). Gill Al burden subsequently declined between days 5 and 10, but thereafter increased again reaching a maximum of 37.9 ± 5.0 µg·g^{-1} on day 34. The peak gill Al levels on days 5

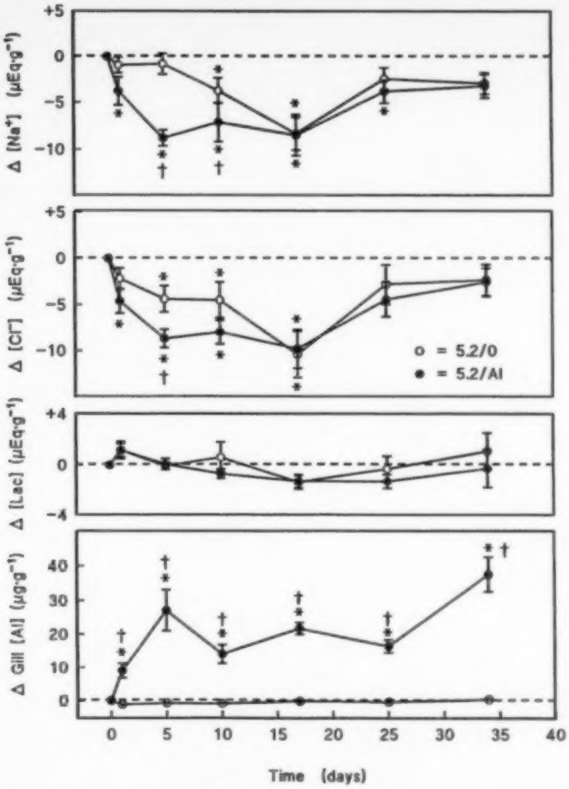

FIG. 3. Whole-body Na^+, Cl^-, and lactate and gill Al concentration (relative to the control group) during 34 d of exposure to pH 5.2 (open circles) or pH 5.2 with sublethal Al present (38 μg Al·L^{-1}) (solid circles). The broken line represents the combined mean values for control fish (maintained at pH 6.5, zero Al; $[Na^+] = 32.7 \pm 0.5$ ($n = 60$), $[Cl^-] = 29.0 \pm 0.6$ ($n = 60$), $[\text{lactate}] = 3.59 \pm 0.32$ ($n = 59$) μEq·g wet weight^{-1}, gill $[Al] = 1.09 \pm 0.27$ ($n = 60$) μg·g wet weight^{-1}). Asterisks indicate means significantly different ($P < 0.05$) from the 6.5/0 control group, and daggers indicate means significantly different from the 5.2/0 group. The two peaks of gill Al in the 5.2/Al group (days 5 and 34) were also significantly higher than the trough on day 5.

and 34 were both significantly higher ($P < 0.05$) than the trough on day 10 (Student's unpaired *t*-test). There was no accumulation of Al on the gills of the other two groups throughout the study.

Physiological Responses to Lethal Al Challenge

Figure 4 shows the changes in four variables (whole-body Na, Cl, and lactate and gill Al) in all three groups when subjected to 10 h of exposure to lethal Al at pH 5.2 on day 36. Whole-body losses of Na^+ and Cl^- and increases in lactate were significantly attenuated in the 5.2/Al group compared with the controls. In contrast, the accumulation of gill Al during lethal challenge was not different from that in the control group. In the 5.2/0 group, ion losses and lactate accumulation did not differ from those found in control fish (Fig. 4).

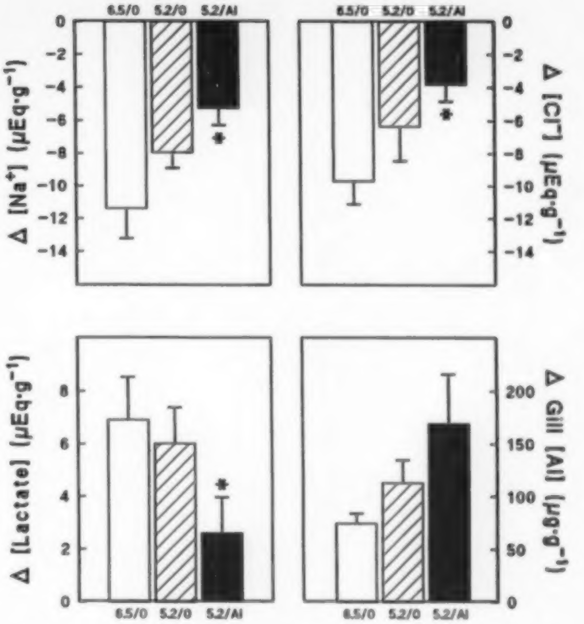

FIG. 4. Physiological changes (whole-body Na^+, Cl^-, and lactate and gill Al) following a 10-h challenge with lethal Al (162 μg·L^{-1}, pH 5.2) on day 36. Δ values ($n = 10$) were obtained by subtracting the mean value observed for each group on day 34 of the chronic sublethal exposure regimes. Open bars represent the control group (6.5/0), hatched bars the 5.2/0 group, and solid bars the 5.2/Al group.

Feeding and Growth

At the start of the exposure regimes, all three groups had feeding rates of around 1.4% body weight per day (Fig. 5). From day 0 onwards, feeding rates were similar in the 5.2/0 and 6.5/0 groups (although the 6.5/0 group was usually slightly higher), and both groups gradually increased their daily food intake over the course of the study, reaching 3.3% by day 36 (Fig. 5). Exposure to sublethal Al caused an immediate reduction in appetite and hence feeding rate, reaching a minimum of 0.4% on day 3. Food intake gradually recovered thereafter, but remained below 1.5% for the first 10 d. After day 10, daily food intake approached, but never really matched, the rates maintained by the 5.2/0 and 6.5/0 groups and was still approximately one full percentage point lower at day 34 (Fig. 5).

At the start of the study, average weights were very similar in the three groups at around 7.5–8.5 g. Growth occurred in all three exposure regimes and followed an exponential curve when plotted as wet weight versus time (Fig. 5). Overall, the control group had the largest increase in mass during the study, almost tripling their average to 21.1 ± 1.1 g on day 35. The 5.2/0 trout were slightly (but not significantly) smaller on day 35 (19.17 ± 1.07 g) whereas the 5.2/Al trout only managed to double their mass by this time (16.91 ± 1.01 g). However, this was the only occasion on which the weight of 5.2/Al trout was significantly lower than that of the control group. Interestingly, from day 21 to 28, the 5.2/0 trout actually appeared to be growing faster than the control trout and were significantly larger than the 5.2/Al trout on

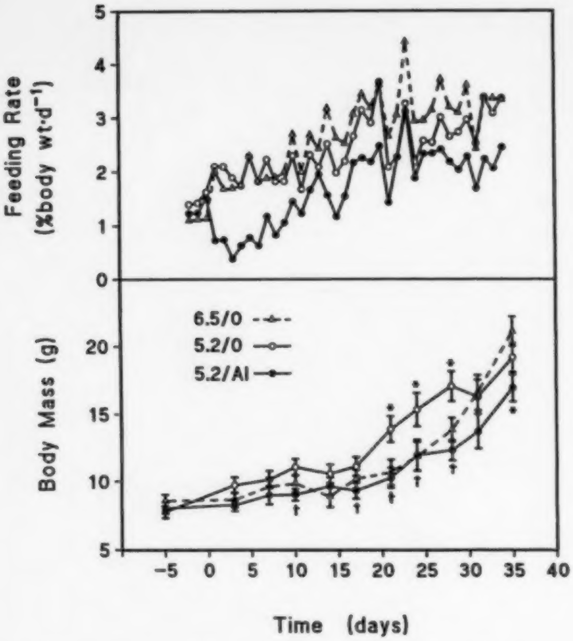

FIG. 5. Feeding rates and growth in the 6.5/0 group (broken line), 5.2/0 group (open symbols), and 5.2/Al group (solid symbols) during 34 d of the chronic sublethal exposyre regimes. The lower panel shows mean wet weight (± SEM, $n = 50–90$) with time during the chronic sublethal exposure regimes. Asterisks indicate significant difference from the 6.5/0 control group, and daggers indicate significant difference from the 5.2/0 group.

days 10, 17, 21, 24, and 28 (Fig. 5).To test whether these greater increases in wet mass in the 5.2/0 trout could be due to impaired water balance rather than growth, we measured the water contents of 10 fish from each group at the end of the study. On day 36, we found that whole-body water contents ranged from 72.4 ± 0.4% (5.2/0) to 74.6 ± 0.6% (controls), but no differences were found between any of the groups. The 5.2/Al group had the highest gross food conversion efficiency at 38.2% compared with 31.6% for the 6.5/0 control group and 28.3% for the 5.2/0 group.

Discussion

We have confirmed that acclimation is induced when trout are continuously exposed to sublethal Al and that this acclimation is a product of the ambient Al level rather than the simultaneous exposure to increased acidity (Orr et al. 1986; Wood et al. 1988b, 1988c; McDonald et al. 1991; Wilson and Wood 1992). The achievement of acclimation after just 5 d was slightly earlier than in most previous studies (see below).

Specificity of Acclimation

Cu and Al act primarily at the gills of fish and appear to have similar modes of toxic action; both disrupt Na^+ and Cl^- balance and cause respiratory disturbances during acutely lethal exposures (e.g., Playle et al. 1989; Wilson and Taylor 1993). The lack of cross-toxicant resistance between these two metals implies that acclimation to Al involves changes that are specific to Al rather than the toxic effects it produces. This is not the case for other toxic metals. For example, Zn and Cd both interfere with branchial control of Ca^{2+} balance, and acclimation to Cd has been shown to increase resistance to Zn and vice versa (Kito et al. 1982; Duncan and Klaverkamp 1983; Thomas et al. 1985; Klaverkamp and Duncan 1987). However, this may simply mean that Cd and Zn inhibit Ca^{2+} transport via very similar mechanisms. Cu and Al inhibit the Na^+ uptake mechanism in a similar if not identical manner, through the blockade of transport enzymes (reviewed by Wood 1992). However, they may disrupt tight junctions and stimulate passive Na^+ losses (J^{Na}_{out}), via subtly different mechanisms because J^{Na}_{out} is independent of the ambient [Ca^{2+}] during Cu exposure (Laurén and McDonald 1985, 1986) but is Ca^{2+} dependent during Al exposure (Booth et al. 1988; Wood et al. 1988a, 1988c; Playle et al. 1989). Perhaps this subtle difference between the mechanisms of Al and Cu toxicity is the basis for the lack of their crossover resistance. Whether this is true or not, it is apparent that the gross symptoms of toxicity are not sufficient in themselves to be able to predict mechanisms of toxicity and acclimation.

Size Effect

The observation that size has a critical effect on the acute toxicity of Al is not new (Baker and Schofield 1982; Brown 1983; Rosseland and Skogheim 1984; Cleveland et al. 1986; Hunn et al. 1987; Ingersoll et al. 1990b; Wood et al. 1990). However, these previous studies demonstrated this effect using different life stages or age groups of fish. All our fish were of the same age, and therefore, differential sensitivity to Al can *only* be attributed to size in this case. This age-independent size effect has not been previously reported and could obviously influence toxicity test results. However, there were no significant differences in the mean weight of fish used in LT50 tests between groups on any given day, so size cannot be considered a complicating factor in the acclimation observed in the 5.2/Al trout. Nevertheless, the general increase in weight in all three groups with time may explain why LT50 values all tended to decrease during the course of the study. One possible physiological explanation for the size effect during lethal Al challenge could be that cutaneous gas exchange is greater (proportionally) in smaller fish, making them less dependent on the gills (where most of the damage through Al precipitation is occurring) and therefore more tolerant to toxic Al concentrations. Some support for this may be the opposite size dependence found during exposure to ambient hypoxia (Shepard 1955) where gas transfer through the skin and gills would be affected equally.

Acclimation and Physiological Recovery

Peak respiratory and ionoregulatory disturbances consistently occur within the first 5 d of sublethal exposure to Al (Booth et al. 1988; Playle et al. 1989; McDonald et al. 1991; Wilson and Wood 1992; present study). In contrast, the time required for the development of acclimation varies considerably (5–17 d). This variability in the time to acclimation is not related to the concentration of Al used or, consequently, the severity of the initial damage caused. However, acclimation usually does precede the recovery of physiological status. The temporal seperation of these processes suggests that the underlying mechanisms behind acclimation and physiological recovery may be independent of each other. One observation previously linking acclimation to physiological recovery was that fish exposed to acid alone, which does not induce acclimation, did not recover ionoregulatory status but merely stabilized at a new reduced level (Audet et al. 1988; Audet and Wood 1988; Wood et al. 1988c; McDonald et al. 1991; Wilson and Wood 1992). We have now observed that trout exposed to acid alone or acid + Al can recover their ionic status to the same degree given time, even though fish exposed to acid alone still fail to acclimate to low pH itself. Clearly, increased resistance is not required for the recovery of ionoregulatory status, and vice versa. In terms of respiratory disturbances, we observed that resting whole-body [lactate] was unaffected, indicating negligible impairment of oxygen uptake under *routine* conditions. Although a prerequisite of acclimation may be some degree of disturbance to gill morphology and aerobic capacity (McDonald and Wood 1992; Wilson et al. 1994), the threshold for acclimation to Al obviously does not necessitate impaired gas transfer in the nonactive state.

Physiological Correlates of Acclimation

Fish chronically exposed to sublethal Al clearly showed reduced physiological disturbances, in terms of whole-body ion losses and lactate accumulation, when challenged with a potentially lethal Al concentration. This attenuation was similar to that described by McDonald et al. (1991) and Reid et al. (1991) in acclimated brook trout and is to be expected if acclimatory changes are directed at preventing the detrimental action of Al at the gills. Nevertheless, opposite to the expected trend, and in contrast with previous findings (McDonald et al. 1991; Reid et al. 1991), we observed that acclimated fish did not accumulate any less Al on their gills than nonacclimated fish during lethal Al challenge. This disagreement is difficult to explain, but may be a function of the different sampling protocols used; we measured gill Al on all fish after 10 h of exposure, prior to any mortality, whereas McDonald et al. (1991) and Reid et al. (1991) used only the surviving fish remaining after 24 or 40 h of lethal challenge.

A similar anomaly was observed during the sublethal Al exposure in our study, i.e., that acclimation was first observed on day 5 when gill Al content had reached an initial peak, and that acclimation remained despite a secondary, more gradual increase in the gill Al content with time. Earlier, we observed an almost identical, biphasic pattern of gill Al changes in the same species, under very similar conditions (Wilson and Wood 1992). We speculated at the time that this pattern represented two separate accumulations of Al in the gills: one that occurs rapidly and is externally located (on the gill surface and within the gill mucus) but that recovers with acclimation and the other internal (within the gill cells themselves) that is slower but eventually masks the decline of external [Al]. Both these studies with rainbow trout contrast with the findings of McDonald et al. (1991) who showed that brook trout only became acclimated as the gill Al burden was progressively reduced. This could reflect species differences in the mechanism of acclimation; however, the two studies are not directly comparable due to the higher level of Al (75–150 $\mu g \cdot L^{-1}$) used in the brook trout study (McDonald et al. 1991).

A change at the gill surface that prevents the deposition of Al is often cited as a key feature of acclimation to Al (McDonald et al. 1991; Reid et al. 1991; McDonald and Wood 1992). Several components of such acclimatory changes have been suggested. Respiratory problems probably result from precipitation of Al within the gill microenvironment (Playle and Wood 1991). The inflammatory response to this may be reduced when mucus turnover rates are increased such that clearance of insoluble Al is accelerated (McDonald et al. 1991). On the other hand, the disruption of ionoregulation is thought to result from the chemical binding of soluble, charged Al species to structural elements of the gill surface (Playle and Wood 1991). A second component of acclimation appears to be a change in ligand chemistry with a reduction in the affinity of the gill surface for Al, resulting in the restoration of normal ionoregulatory function (Reid et al. 1991).

In support of this "model" was the observation that a substantial hypertrophy of mucous cells coincided with the first apperance of increased resistance (Wilson et al. 1994). However, it is difficult to reconcile these ideas with our results concerning increases in gill Al content during both sublethal exposure and lethal challenge. Clearly, more work is required to provide a model of acclimation that satisfies all the existing observations.

Feeding and Growth

Previous investigations on brown trout (*Salmo trutta*) (Sadler and Lynam 1987, 1988; Reader et al. 1988), brook trout (Mount et al. 1988a, 1988b; Ingersoll et al. 1990a, 1990b), and rainbow trout (Wilson and Wood 1992) have documented reduced growth in Al-exposed fish. However, most studies have either used a fixed maintenance ration or given only anecdotal or semiquantitative reports of feeding behaviour. Here, we have clearly shown that when trout are fed to satiation, reduced growth after 34 d in Al-exposed fish can be at least partially accounted for by a reduction in appetite during the first 10 d. Increased energy expenditure seemed a likely additional factor involved in reduced growth based on our estimates of metabolic rate from forced swimming tests (Wilson et al. 1994). However, trout within the 5.2/Al exposure tanks were noticeably less active, even listless, compared with the other two groups. Indeed, reduced spontaneous activity has been quantitatively documented in cutthroat trout (*Oncorhynchus clarki*, previously *Salmo clarki*) (Woodward et al. 1989) and brook trout (Cleveland et al. 1986, 1989) exposed to sublethal Al. Ironically, this could be important in explaining the greater gross food conversion efficiency in 5.2/Al fish (38.2% compared with 31.6% in the control group). A lower overall *routine* metabolic rate could result in a greater percentage of the dietary protein being retained for growth. This will be true in the laboratory where food is supplied, but a decrease in routine activity in the wild would surely reduce an animal's overall fitness to feed and avoid predation. The apparent increase in food conversion efficiency should therefore be interpreted with caution, and appetite, rather than changes in metabolism, must be considered the principal cause of reduced growth in Al-exposed trout.

Feeding rates in trout exposed to acid alone were similar to those in control fish, indicating that the reduced appetite was solely due to the presence of Al. Acid pH levels lower than 5.2 have been found to impair growth in the absence of Al (Menendez 1976; Sadler and Lynam 1987; Ingersoll et al. 1990a). However, pH 5.2 had no significant impact on overall growth in the present study, similar to our findings in trout fed a constant maintenance ration of 1% body weight per day (Wilson and Wood 1992). Thus, regardless of the feeding regime adopted, it would appear that any increased energy expenditure associated with exposure to pH 5.2 has little impact on the total energy budget of the animal, and specifically the energy invested in growth. This is supported by the fact that the gross food conversion efficiencies of 5.2/0 and 6.5/0 trout were similar.

In summary, acclimation to Al clearly occurs when trout are chronically exposed to sublethal Al at low pH and is entirely due to the presence of Al because acidity alone does not result in increased resistance to either acid or Al. As one might expect, acclimation is associated with reduced physiological disturbances during lethal challenge with Al, but is relatively specific to the offending metal, rather than the symptoms it produces, because increased resistance to Cu was not consistently observed. Contrary to previous studies (Audet et al. 1988; Wood et al. 1988c; McDonald et al. 1991; Wilson and Wood 1992), we have found that trout exposed to acid alone (in addition to acid + Al) can recover their physiological status, given time, even though acclimation is not induced. Finally, while increased resistance to potentially lethal pulses of acid/Al is an obvious benefit of chronic sublethal exposure to acid + Al, there are some costs involved. Reduced feeding and growth rates (in addition to impaired aerobic scope and swimming performance; Wilson et al. 1994) have now been identified as major costs associated with chronic sublethal exposure and in the wild would limit the ability of fish to feed, avoid predation, and reproduce (Little and Finger 1990). These costs must be weighed against the benefits of increased resistance when considering the overall fitness of acclimated fish in real ecological situations.

Acknowledgements

This work was supported by a NSERC Strategic Grant in Environmental Quality to C.M.W. The authors wish to thank Joe Bobbit, Annie Narahara, Connie Boese, and Jose Fernandez for their invaluable help at the Red Buttes hostelry.

References

Audet, C., R.S. Munger, and C.M. Wood. 1988. Long-term sublethal acid exposure in rainbow trout (*Salmo gairdneri*) in soft water: effects on ion exchanges and blood chemistry. Can. J. Fish. Aquat. Sci. 45: 1387–1398.

Audet, C., and C.M. Wood. 1988. Do rainbow trout acclimate to low pH? Can. J. Fish. Aquat. Sci. 45: 1399–1405.

Baker, J.P., and C.L. Schofield. 1982. Aluminum toxicity to fish in acidic waters. Water Air Soil Pollut. 18: 289–309.

Booth, C.E., D.G. McDonald, B.P. Simons, and C.M. Wood. 1988. Effects of aluminum and low pH on net ion fluxes and ion balance in the brook trout (*Salvelinus fontinalis*). Can. J. Fish. Aquat. Sci. 45: 1563–1574.

Brett, J.R., and T.D.D. Groves. 1979. Physiological energetics, p. 279–352. *In* W.S. Hoar and D.J. Randall [ed.] Fish physiology. Vol. 8. Academic Press, Inc., New York, N.Y.

Brown, D.J.A. 1983. Effect of calcium and aluminum concentrations on the survival of brown trout (*Salmo Trutta*) at low pH. Bull. Environ. Contam. Toxicol. 30: 582–587.

Cleveland, L., E.E. Little, S.J. Hamilton, D.R. Buckler, and J.B. Hunn. 1986. Interactive toxicity of aluminum and acidity to early life stages of brook trout. Trans. Am. Fish. Soc. 115: 610–620.

Cleveland, L., E.E. Little, R.H. Wiedmeyer, and D.R. Buckler. 1989. Chronic no-observed effect concentrations of aluminum for brook trout exposed in low-calcium, dilute acidic water, p. 229–245. *In* T.E. Lewis [ed.] Environmental chemistry and toxicology of aluminum. Lewis Publishers, Inc., Chelsea, Mich.

Cronan, C.S., and C.L. Schofield. 1979. Aluminum leaching response to acid precipitation: effects of high elevation watersheds in the Northeast. Science (Wash., D.C.) 204: 304–306.

Dickson, W. 1980. Properties of acidified waters, p. 75–83. *In* D. Drablos and A. Tollan [ed.] Proc. Int. Conf. Ecol. Impact Acid Precip. SNCF Project, Norway.

Duncan, D.A., and J.F. Klaverkamp. 1983. Tolerance and resistance to cadmium in white suckers (*Catostomus commersoni*) previously exposed to cadmium, mercury, zinc, or selenium. Can. J. Fish. Aquat. Sci. 40: 128–138.

Hunn, J.B., L. Cleveland, and E.E. Little. 1987. Influence of pH and aluminum on developing brook trout in a low calcium water. Environ. Pollut. 43: 63–73.

Ingersoll, C.G., D.D. Gulley, D.R. Mount, M.E. Mueller, J.D. Fernandez, J.R. Hockett, and H.L. Bergman. 1990a. Aluminum and acid toxicity to two strains of brook trout (*Salvelinus fontinalis*). Can. J. Fish. Aquat. Sci. 47: 1641–1648.

Ingersoll, C.G., D.R. Mount, D.D. Gulley, J.D. Fernandez, T.W. LaPoint, and H.L. Bergman. 1990b. Effects of pH, aluminum, and calcium survival and growth of eggs and fry of brook trout (*Salvelinus fontinalis*). Can. J. Fish. Aquat. Sci. 47: 1580–1592.

Kelso, J.R.M., C.K. Minns, J.E. Gray, and M.L. Jones. 1986. Acidification of surface waters in eastern Canada and its relationship to aquatic biota. Can. Spec. Publ. Fish. Aquat. Sci. 87: 42 p.

Kito, H., T. Kazawa, Y. Ose, T. Sato, and T. Ishikawa. 1982. Protection by metallothionein against cadmium toxicity. Comp. Biochem. Physiol. 73: 135–139.

Klaverkamp, J.F., and D.A. Duncan. 1987. Acclimation to cadmium toxicity by white suckers: cadmium binding capacity and metal distribution in gill and liver cytosol. Environ. Toxicol. Chem. 6: 275–289.

Laurén, D.J., and D.G. McDonald. 1985. Effects of copper on branchial ionoregulation in the rainbow trout, *Salmo gairdneri* Richardson. Modulation by water hardness and pH. J. Comp. Physiol. 155B: 635–644.

Laurén, D.J., and D.G. McDonald. 1986. Influence of water hardness, pH, and alkalinity on the mechanisms of copper toxicity in juvenile rainbow trout, *Salmo gairdneri*. Can. J. Fish. Aquat. Sci. 43: 1488–1496.

Litchfield, J.T. 1949. A method for rapid graphic solution of time – percent effect curves. J. Pharmacol. Exp. Ther,. 97: 399–408.

Litchfield, J.T., and F. Wilcoxon. 1949. A simplified method of evaluating dose–effect experiments. J. Pharmacol. Exp. Ther,. 96: 99–113.

Little, E.E., and S.E. Finger. 1990. Swimming behaviour as an indicator of sublethal toxicity in fish. Environ. Toxicol. Chem. 9: 13–19.

McDonald, D.G., and C.M. Wood. 1992. Branchial mechanisms of acclimation to metals in freshwater fish, p. 295–319. *In* C. Rankin and F.B. Jensen [ed.] Fish ecophysiology. Chapman and Hall, London, England.

McDonald, D.G., C.M. Wood, R.G. Rhem, M.E. Meuller, D.R. Mount, and H.L. Bergman. 1991. Nature and time course of acclimation to aluminum in juvenile brook trout (*Salvelinus fontinalis*). 1. Physiology. Can. J. Fish. Aquat. Sci. 48: 2006–2015.

Menendez, R. 1976. Chronic effects of reduced pH on brook trout (*Salvelinus fontinalis*). J. Fish. Res. Board Can. 33: 118–123.

Mighell, J.L. 1969. Rapid cold-branding of salmon and trout with liquid nitrogen. J. Fish. Res. Board Can. 26: 2765–2769.

Mount, D.R., J.R. Hockett, and W.A. Gern. 1988a. Effect of long-term exposure to acid, aluminum, and low calcium on adult brook trout (*Salvelinus fontinalis*). 2. vitellogenesis and osmoregulation. Can. J. Fish. Aquat. Sci. 45: 1623–1632.

Mount, D.R., C.G. Ingersoll, D.D. Gulley, J.D. Fernandez, T.W. LaPoint, and H.L. Bergman. 1988b. Effect of long-term exposure to acid, aluminum, and low calcium on adult brook trout (*Salvelinus fontinalis*). 1. Survival, grwoth, fecundity, and progeny survival. Can. J. Fish. Aquat. Sci. 45: 1623–1632.

Mueller, M.E., D.A. Sanchez, H.L. Bergman, D.G. McDonald, R.G. Rhem, and C.M. Wood. 1991. Nature and time course of acclimation to aluminum in juvenile brook trout (*Salvelinus fontinalis*) 2. Histology. Can. J. Fish. Aquat. Sci. 48: 2016–2027.

Neville, C. 1985. Physiological response of juvenile rainbow trout, *Salmo gairdneri*, to acid and aluminum — prediction of field responses from laboratory data. Can.J. Fish. Aquat. Sci. 42: 2009–2019.

Orr, P.L. R.W. Bradley, J.B. Sprague, and N.J. Hutchinson. 1986. Acclimation-induced change in toxicity of aluminum to rainbow trout (*Salmo gairdneri*). Can. J. Fish. Aquat. Sci. 43: 243–246.

Playle, R.C., G.G.Goss, and C.M. Wood. 1989. Physiological disturbances in rainbow trout (*Salmo gairdneri*) during acid and aluminum exposures in soft water of two calcium concentrations. Can. J. Zool. 67: 314–324.

Playle, R.C., and C.M. Wood. 1989. Water pH and aluminum chemistry in the gill microenvironment of rainbow trout during acid and aluminum exposure. J. Comp. Physiol. 159B: 539–550.

Playle, R.C., and C.M. Wood. 1991. Mechanisms of aluminium extraction and accumulation at the gills of rainbow trout, *Oncorhynchus mykiss* (Walbaum), in acidic soft water. J. Fish. Biol. 38: 791–805.

Reader, J.P. T.R.K. Dalziel, and R. Morris. 1988. Growth, mineral uptake and skeletal calcium deposition in brown trout, *Salmo trutta* L., yolk-sac fry exposed to aluminium and manganese in soft acid water. J. Fish. Biol. 32: 607–624.

Reid, S.D., R.G. Rhem, and D.G. McDonald. 1991. Acclimation to sublethal aluminum: modifications of metal – gill surface interactions of juvenile rainbow trout (*Oncorhynchus mykiss*). Can. J. Fish. Aquat. Sci. 48: 1995–2004.

Rosseland, B.O., and O.K. Skogheim. 1984. A comparative study on salmonid fish species in acid aluminum-rich water. II. Physiological stress and mortality of one- and two-year-old fish. Inst. Freshwater Res. Natl. Swed. Board Fish. Rep. 61: 186–194.

Sadler, K., and S. Lynam. 1987. Some effects on the growth of brown trout from exposure to aluminium at different pH levels. J. Fish. Biol. 31: 209–219.

Sadler, K., and S. Lynam. 1988. The influence of calcium on aluminium-induced changes in the growth rate and mortality of brown trout, *Salmo trutta* L. J. Fish. Biol. 33: 171–179.

Schofield, C.L., and J.R. Trojnar. 1980. Aluminum toxicity to brook trout (*Salvelinus fontinalis*) in acidified waters, p. 341–363. *In* T.Y. Toribara, M.W. Miller, and P.E. Morrow [ed.] Polluted rain. Plenum Press, New York, N.Y.

Shepard, M.P. 1955. Resistance and tolerance of young speckled trout (*Salvelinus fontinalis*) to oxygen lack, with special reference to low oxygen acclimation. J. Fish. Res. Board Can. 12: 387–433.

Thomas, D.G., M.W. Brown, D. Shurben. J.F. del G. Solbe, A. Cryer, and J. Kay. 1985. A comparison of the sequestration of cadmium and zinc in the tissue of rainbow trout (*Salmo gairdneri*) following exposure to the metals singly or in combination. Comp. Biochem. Physiol. 82C: 55–62.

Wilson, R.W., H.L. Bergman, and C.M. Wood. 1994. Metabolic costs and physiological consequences of acclimation to aluminum in juvenile rainbow trout (*Oncorhynchus mykiss*). 2: gill morphology, swimming performance, and aerobic scope. Can. J. Fish. Aquat. Sci. 51: 536–544.

Wilson, R.W., and E.W. Taylor. 1993. The physiological responses of freshwater rainbow trout, *Oncorhynchus mykiss*, during acutely lethal copper exposure. J. Comp. Physiol. B 163: 38–47.

Wilson, R.W., and C.M. Wood. 1992. Swimming performance, whole body ions, and gill Al accumulation during acclimation to sublethal aluminium in juvenile rainbow trout (*Oncorhynchus mykiss*). Fish. Physiol. Biochem. 10: 149–159.

Wood, C.M. 1992. Flux measurements os indices of H^+ and metal effects on freshwater fish. Aquat. Toxicol. 22: 239–264.

Wood, C.M., D.G. McDonald, C.E. Booth, B.P. Simons, C.G. Ingersoll, and H.L. Bergman. 1988a. Physiological evidence of acclimation to acid/aluminum stress in adult brook trout (*Salvelinus fontinalis*). 1. Blood composition and net sodium fluxes. Can. J. Fish. Aquat. Sci. 45: 1587–1596.

Wood, C.M., D.G. McDonald, C.G. Ingersoll, C.R. Mount, O.E. Johannsson, S. Landsberger, and H.L. Bergman. 1990. Whole body ions of brook trout (Salvelinus fontinalis) alevins: responses of yold-sac and swim-up stages toowater acidity, calcium, and aluminum, and recovery effects. Can. J. Fish. Aquat. Sci. 47: 1604–1615.

Wood, C.M., R.C. Playle, B.P. Simons, G.G. Goss, and D.G. McDonald. 1988b. Blood gases, acid–base status, ions, and hematology in adult brook trout (*Salvelinus fontinalis*) under acid/aluminum exposure. Can. J. Fish. Aquat. Sci. 45: 1575–1586.

Wood, C.M., B.P. Simons, D.R. Mount, and H.L. Bergman. 1988c. Physiological evidence of acclimation to acid/aluminum stress in adult brook trout (*Salvelinus fontinalis*). 2. Blood parameters by cannulation. Can. J. Fish. Aquat. Sci. 45: 1597–1605.

Woodward, D.F., A.M. Farag, M.E. Mueller, E.E. Little, and F.A. Vertucci. 1989. Sensitivity of endemic snake river cutthroat trout to acidity and elevated aluminum. Trans. Am. Fish. Soc. 118: 630–643.

Wright, R.F., and E.T. Gjessing. 1976. Acid precipitation: changes in the chemical composition of lakes. Ambio 5: 219–223.

Wright, R.F., and E. Snekvik. 1978. Chemistry and fish populations in 700 lakes in southernmost Norway. Verh Int. Ver. Limnol. 20: 765–775.

Metabolic Costs and Physiological Consequences of Acclimation to Aluminum in Juvenile Rainbow Trout (*Oncorhynchus mykiss*). 2: Gill Morphology, Swimming Performance, and Aerobic Scope

Rod W. Wilson[1]

Department of Biology, McMaster University, Hamilton, ON L8S 4K1, Canada

Harold L. Bergman

Fish Physiology and Toxicology Laboratory, University of Wyoming, Laramie, WY 82071-3166, USA

and Chris M. Wood

Department of Biology, McMaster University, Hamilton, ON L8S 4K1, Canada

Wilson, R.W., H.L. Bergman, and C.M. Wood. 1994. Metabolic costs and physiological consequences of acclimation to aluminum in juvenile rainbow trout (*Oncorhynchus mykiss*). 2: Gill morphology, swimming performance, and aerobic scope. Can. J. Fish. Aquat. Sci. 51: 536–544.

Juvenile rainbow trout (*Oncorhynchus mykiss*, 5–13 g) were chronically exposed to sublethal Al (38 $\mu g \cdot L^{-1}$) in acidified soft water (Na^+ = 85, Ca^{2+} = 28 $\mu Eq \cdot L^{-1}$, pH 5.2–5.4) for 36 d. Acclimation (increased resistance to challenge with 162 μg $Al \cdot L^{-1}$ Al at pH 5.2) occurred after 5 d and was associated with a fourfold increase in gill mucous cell density and reduction in apparent lamellar surface area; initially elevated blood–water diffusion distances returned to normal after 34 d, but the reduction in apparent surface area persisted. Chronic exposure to acid alone (pH 5.2, same water chemistry) caused no morphometric changes but resulted in persistent impairment of U_{crit} (critical aerobic swimming speed) by about 10%. This was due to increased oxygen requirements at subcritical swimming speeds (loading stress) and was alleviated when trout were swum at pH 6.5 (zero Al) on day 36. In trout preexposed to sublethal Al, U_{crit} was chronically impaired by approximately 16% due to loading stresses and reduction in the maximum rate of oxygen uptake, $MO_{2\ max}$ (limiting stress); U_{crit} and $MO_{2\ max}$ remained depressed even when fish were swum at pH 6.5 (zero Al). Reduced gill area compromises the aerobic scope for activity but may be an unavoidable cost of acclimation to Al.

Des truites arc-en-ciel (*Oncorhynchus mykiss*) juvéniles (5–13 g) ont été exposées de façon chronique à une dose sublétale d'Al (38 $\mu g \cdot L^{-1}$) dans de l'eau douce acidifiée (Na^+ = 85, Ca^{2+} = 28 $\mu Eq \cdot L^{-1}$, pH 5,2–5,4) pendant 36 jours. L'acclimatement (résistance accrue à une concentration de 162 μg $Al \cdot L^{-1}$ à pH 5,2) s'est produire après 5 jours et elle était associée à une augmentation par un facteur de 4 de la densité des cellules muqueuses des branchies et à une réduction de la superficie apparente des lamelles branchiales; après 34 jours, les distances de diffusion sang–eau, élevées au départ, sont revenues à la normale, mais la réduction de la superficie apparente a persisté. Une exposition chronique à l'acide seulement (pH 5,2, mêmes propriétés chimiques de l'eau) n'a provoqué aucune modification morphométrique, mais une altération persistante de la valeur U_{crit} (vitesse de nage aérobique critique) d'environ 10 %. Cette modification est due à des besoins accrus en oxygène à des vitesses de nage sous-critiques (stress de charge) et a été atténuée lorsque les truites se trouvaient dans une eau à pH 6,5 (Al nul) le trente-sixième jour. Dans le cas de truites exposées au préalable à une dose sublétale d'Al, la valeur U_{crit} subissait une modification chronique d'environ 16 % en raison du stress de charge et une réduction du taux maximal de fixation de l'oxygène, $MO_{2\ max}$ (stress limitant); les paramètres U_{crit} et $MO_{2\ max}$ demeuraient réduits même lorsque les poissons étaient placés dans une eau à pH 6,5 (Al nul). Une surface branchiale réduite compromet la portée aérobique de l'activité, mais peut être un coût inévitable de l'acclimatement à l'Al.

Received February 8, 1993
Accepted October 6, 1993
(JB784)

Reçu le 8 février 1993
Accepté le 6 octobre 1993

Acclimation to aluminum (i.e., increased resistance to acutely toxic levels established through *continued* sublethal exposure) has been well documented (Orr et al. 1986; McDonald et al. 1991; Wilson et al. 1994). It has also been demonstrated that the acclimation process results from a "damage/repair" phenomenon involving physiological, biochemical, and structural changes at the gills (McDonald et al. 1991; Mueller et al. 1991; McDonald and Wood 1992). In juvenile brook trout (*Salvelinus fontinalis*) the inital damage phase (lasting 4–5 d) was accompanied by severe gill histopathologies and impared oxygen delivery to tissues (whole-body lactate levels were elevated (McDonald et al. 1991; Mueller et al. 1991)). Acclimation (increased tolerance to lethal Al) was observed from day 10 onwards and was accompanied by at least partial recovery of whole-body lactate levels. However, many gill histopathologies remained even after acclimation had been established. Indeed, they may well be an unavoidable component of acclimation. Although the resting aerobic metabolism was restored with time (Wood et al. 1988; Walker et al. 1991), the persistence of structural abnormalities at the gills suggests that the *capacity* of the respiratory gas exchange system may remain compromised during prolonged exposure to Al. This would only be apparent during increased aerobic activity such as sustained swimming.

---

[1] Author to whom correspondence should be addressed. Present address: School of Biological Sciences, G.38 Stopford Building, University of Manchester, Oxford Road, Manchester M13 9PT, United Kingdom.

Previous studies have shown that low environmental pH reduces swimming performance (Hargis 1976; Waiwood and Beamish 1978; Graham and Wood 1981; Ye and Randall 1991; Butler et al. 1992; Wilson and Wood 1992). However, only Wilson and Wood (1992) have addressed the problems of chronic acid exposure in combination with sublethal Al levels. From that study, it was apparent that one of the costs of acclimation to Al was a prolonged depression of swiming performance approximately twofold greater than that found in fish exposed to acid alone. The main objective of the present study was to assess whether the impairment of swimming performance is related to chronic changes in gill morphology and ultimately aerobic scope. To this end, aerobic swimming metabolism was assessed in juvenile rainbow trout (*Oncorhynchus mykiss*) at intervals during a 36-d exposure to either pH 6.5 (controls) or pH 5.2 in the presence and absence of sublethal Al (38 $\mu g \cdot L^{-1}$) in synthetic soft water. Morphometric analysis of the gills from these three groups was performed near the beginning ("damage phase") and at the end of the exposure regime. Water pH, Ca, and Na levels relevant to the acid-threatened watersheds in eastern North America and Europe were used. The present study was run in parallel with that of Wilson et al. (1994) using fish kept under identical exposure conditions.

Materials and Methods

Animal Holding

Juvenile rainbow trout (5–13 g) were obtained, held, and adapted to synthetic soft water ($[Ca^{2+}] = 28$, $[Na^+] = 85\ \mu Eq \cdot L^{-1}$, pH 6.5–7.0, 15°C) as described in Wilson et al. (1994). After 4 wk in circumneutral soft water, rainbow trout were exposed for 36 d to one of three conditions: (i) normal soft water at pH 6.5 (6.5/0 group), (ii) low-pH soft water at pH 5.2 (5.2/0 group), and (iii) low-pH soft water at pH 5.2 with 38 $\mu g\ Al \cdot L^{-1}$ added (5.2/Al group). Water variables (pH, $[Ca^{2+}]$, $[Na^+]$ and total Al) were measured daily on samples from each tank and are reported in Wilson et al. (1994).

Histological and Morphometric Techniques

On days 5 and 34 the second gill arch (left side only) was rapidly excised from four fish (stunned by a blow on the head) from each group and immediately placed in 10% neutral buffered formalin (NBF; pH 7.4) for 1 h. Each gill arch was then trimmed so as to include only the central portion containing approximately 10 paired filaments, and this was placed in fresh NBF for a further 24 h. Once fixed, gill tissues were washed overnight in tap water, dehydrated in graded ethanol solutions, and embedded in plastic (JB-4, Polysciences). Longitudinal 2-μm sections (parallel to the filaments and perpendicular to the lamellae) were cut using a Sorvall MT-2B microtome, mounted on glass slides, and stained with periodic acid-Schiff's reagent and then haematoxylin. Morphometric measurements were performed only on sections that had been cut along the portion of the filament lying between the efferent artery and the cartilaginous gill ray. This region has the most uniform filament thickness and cell composition and includes the central portion of respiratory lamellae (Leino and McCormick 1984). All gill measurements were made using an inverted miscroscope (Zeiss Axiovert 10) and video camera (Hamamatsu C2400) in conjunction with an image analysis system (Neotech, Image Grabber) on a MAC IIci computer. Calibrations were performed using a stage micrometer (Leitz).

The gill dimensions measured were total filament thickness, filament epithelium thickness, interlamellar distance, lamellar thickness, lamellar height, and water–blood diffusion distance. A transparency of a Mertz grid was fixed to the image analyzer screen in order to randomize the points from which all measurements were initiated (Hughes and Perry 1976). It has been shown that for morphometric measurements the within-individual variation is much greater than the between-individuals variation (Haines et al. 1986). Therefore, we used a relatively large number of measurements per individual from a relatively small number of individuals. For statistical purposes, each individual was assigned a single mean value for each of the above variables from the following number of measurements: (i) 10 measurements per tissue section, three sections per filament, from five different filaments per fish (for filament thickness, filament epithelium thickness, interlamellar distance, and lamellar height) and (ii) three measurements per lamella (basal, middle, and distal portions) on 10 lamellae per section, three sections per filament, from five different filaments (for lamellar thickness and water–blood diffusion distance). In addition the number of filamental and lamellar mucous cells per 200 μm of filament length was counted on five sections of five different filaments per fish.

The percentage differences in "apparent" lamellar surface area were approximated by comparing the average perimeters of lamellae, estimated from the mean values of lamellar height and thickness using

$$\text{Perimeter} = 2(\text{height} - [0.5 \times \text{thickness}] + (0.5 \times \pi \times \text{thickness}).$$

Comparing perimeters is only valid if it is assumed that lamellar length and density per filament remained constant in all groups. Although this is not an accurate evaluation of the actual respiratory surface area of the gills, it is a useful measure of percentage differences in "apparent" lamellar surface area between groups.

Swimming Performance and Metabolism Tests

On days 1, 5, 10, 17, 25, and 34, swimming performance and metabolism tests were carried out on eight fish from each group using small-volume (~3.2 L) Blazka-type respirometers similar to those described by Beamish et al. (1989). The soft water supplied to the respirometers was maintained at pH 5.2 when swimming the two acid-exposed groups (5.2/0 and 5.2/Al) with no Al added to the water. Respirometers were supplied with pH 6.5 soft water when swimming the control group (6.5/0). Water temperatures

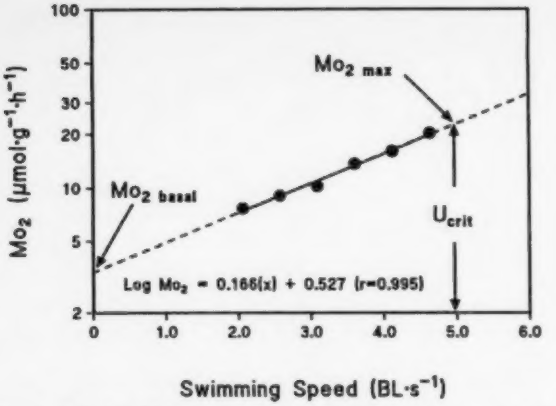

FIG. 1. Relationship between swimming speed and oxygen consumption for a single fish (No. 6, 6.5/0 group on day 5) plotted as a log function of Mo_2. The solid line represents the range over which measurements of Mo_2 were actually made, and the broken lines represents extrapolation to zero speed and U_{crit}, from which the $Mo_{2\,basal}$ and $Mo_{2\,max}$ are derived using the regression equation for log Mo_2 versus speed.

within the respirometers were maintained at 15°C (±0.5) by submerging them in a temperature-controlled water table. Fish were transferred to the swimming respirometers the evening before the swim test and maintained at a minimum water velocity (20 cm·s^{-1}) for 12–16 h. Water speed was then increased in 5 cm·s^{-1} stepwise increments every 60 min until fish became exhausted. Fish were considered exhausted once they became impinged on the rear screen, but only if they subsequently refused to swim again when the water velocity was temporarily lowered and then returned to the last speed reached. Critical swimming speed (U_{crit}) was then calculated for each fish according to Brett (1964):

$$U_{crit} = V_f + (T/t \cdot \delta V)$$

where U_{crit} is in centimetres per second, t is time increment (minutes), δV is velocity increment (centimetres per second), and T is the time elapsed at the final velocity (V_f) before exhaustion. Fish were quickly removed following exhaustion, killed with a blow to the head, measured to the nearest 0.1 cm fork length, freeze-clamped between aluminum plates in liquid nitrogen, weighed to the nearest 0.01 g, and stored at −80°C for later analysis for postexercise whole-body lactate content (see Wilson et al. 1994). Swimming velocities were not corrected for solid blocking effects because fish cross-sectional areas did not exceed 10% of the cross-sectional area of the swimming tube (Jones et al. 1974; Webb 1975). Individual U_{crit} values were then transformed to body lengths (BL) per second.

At each swimming speed, oxygen consumption was determined in a flow-through water system from measurements of water flow rate, respirometer volume, fish mass, and the oxygen partial pressure difference across the respirometers ($Po_{2\,in} - Po_{2\,out}$) at the beginning and end of each 1-h period at the new speed. Water Po_2 was measured using Radiometer oxygen electrodes (E5047) and a Cameron Instruments oxygen meter (OM-200) and coverted to oxygen content using tabulated values for the oxygen solubility coefficient in water of zero salinity (Boutilier et al. 1984). The equation given by Fry (1971) was used to account for the time lag between changing the water velocity and reaching a new steady-state outflow Po_2, and corrections were made for the oxygen consumption of individual respirometers in the absence of fish.

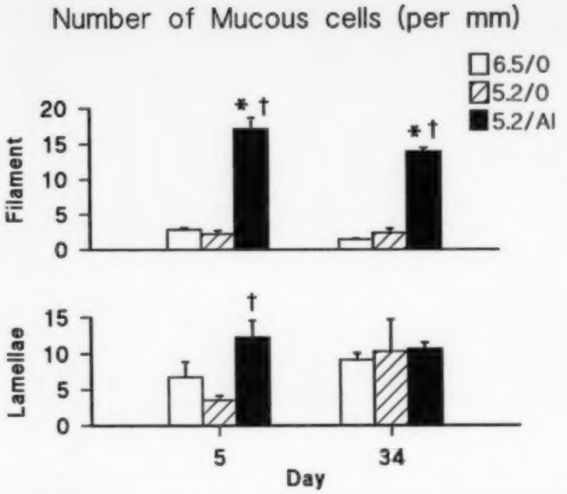

FIG. 2. Gill filamental and lamellar mucous cell densities expressed as number per millimetre along the filaments on days 5 and 34 in the three exposure groups (means ± SEM, n = 4). Asterisks indicate means significantly different ($P < 0.05$) from the 6.5/0 control group, and daggers indicate means significantly different from the 5.2/0 group.

For each fish, a regression equation was established for the logarithm of oxygen consumption versus swimming speed. Only data from fish that gave a significant regression correlation coefficient ($P < 0.05$) were used. Using these regression equations, predicted values for Mo_2 at 0 cm·$^{-1}$ (basal Mo_2) and U_{crit} (maximum Mo_2) were calculated for individual fish (Fig. 1). Aerobic scope was then calculated as the difference between basal and maximum Mo_2 for each fish.

On day 36, an additional test was performed in which U_{crit} and aerobic scope were again measured using fish from the two experimental groups (5.2/0 and 5.2/Al), but this time whilst swimming in soft water maintained at pH 6.5 instead of 5.2. The objective here was to differentiate between the effects caused by the acidity of the water during the swim test versus the exposure histories of fish prior to the test. The results from these tests were then compared with the control group (6.5/0) also swum at pH 6.5 on day 34. Throughout all the swimming tests, fish were exposed to continuous light in order to reduce diurnal fluctuations in metabolic rate (Chakraborty et al. 1992).

Statistical Analysis

Data are expressed as means ± SEM (n) where n refers to the number of fish. Regression analyses for individual swimming fish were performed by the method of least squares and the significance of the correlation coefficient assessed ($P < 0.05$). Multiple comparison and Tukey's statistic (Zar 1984) were used to test for differences between the group regression equations on day 34. For all other measured variables, one-way analysis of variance was used to assess significant differences between groups on each sam-

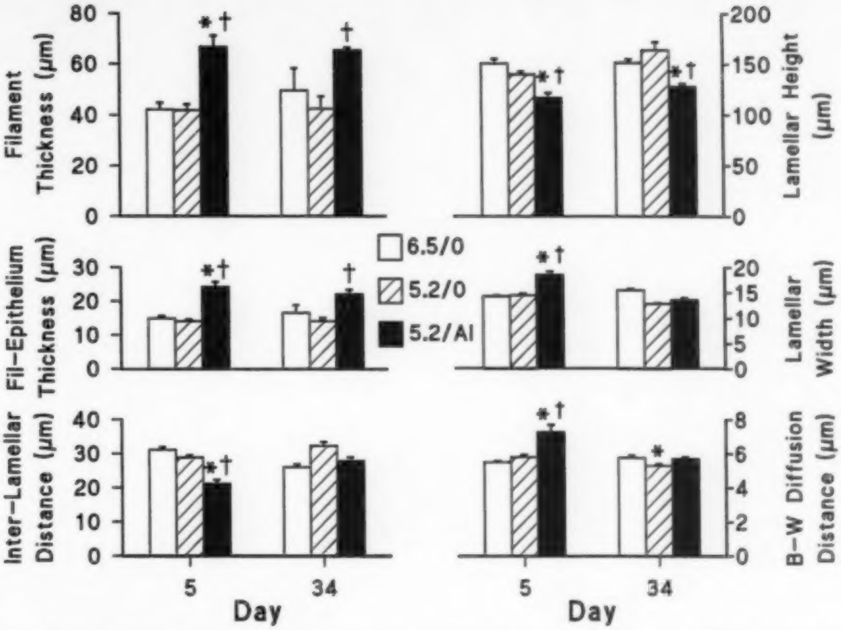

FIG. 3. Gill morphometric measurements of filament thickness, filamental epithelium thickness, interlamellar distance, lamellar height, lamellar thickness, and blood–water diffusion distance on days 5 and 34 in the three exposure groups (means ± SEM, $n = 4$). Asterisks indicate means significantly different ($P < 0.05$) from the 6.5/0 control group, and daggers indicate means significantly different from the 5.2/0 group.

pling day. Where appropriate, Fisher's protected least significant difference (PLSD) was then applied to establish specific differences (at the 5% level of significance).

Results

Gill Morphology

After 5 and 34 d of exposure to sublethal Al at pH 5.2 the number of mucous cells present in the filamental epithelium was five- and fourfold greater, respectively, than the corresponding mucous cell densities of the 5.2/0 and 6.5/0 trout (Fig. 2). The number of lamellar mucous cells in 5.2/Al trout on day 5 was twice the number found in the 5.2/0 trout, but not significantly different from the 6.5/0 trout. In fish exposed to Al the mucous cell densities remained at these elevated levels until day 34. However, on day 34 the density of mucous cells within the lamellar epithelium of both 5.2/0 and 6.5/0 trout was greater such that there were no longer significant differences among the three groups. However, the total number of mucous cells (lamellar plus filamental) in 5.2/Al trout was still at least twofold higher than in either the 5.2/0 or 6.5/0 controls, even after 34 d.

Morphometric differences between the gills of control (6.5/0) and 5.2/0 trout were limited to a small but significant reduction in the blood–water diffusion distance in the acid-exposed fish on day 34 (Fig. 3). In contrast, significant changes in the branchial morphology of Al-exposed fish were found in all variables measured on day 5 when compared with both the control and 5.2/0 groups (Fig. 3). These changes amounted to a 59% increase in filament thickness, a 71% increase in the filamental epithelium thickness, a 22% reduction in lamellar height, a 30% increase in lamellar thickness, a 32% decrease in the interlamellar space, and a 33% increase in the blood–water diffusion distance compared with the 6.5/0 control group on day 5 (Fig. 3). By day 34 the blood–water diffusion distance, lamellar thickness, and interlamellar space had returned to values similar to the control and 5.2/0 groups. Nevertheless, lamellae remained shorter and filaments thicker than those of the 5.2/0 fish (but not the 6.5/0 group) even after 34 d. Apparent lamellar surface area was approximately 22% lower than in the controls on both days 5 and 34 (Table 1).

TABLE 1. Calculated values (means ± SEM (n)) for mean lamellae perimeters (μm), used as an index of apparent lamellar surface area. Asterisks indicate means significantly different ($P < 0.05$) from the 6.5/0 control group, and daggers indicate means significantly different from the 5.2/0 group.

	6.5/0	5.2/0	5.2/Al
Day 5	323.1 ± 11.7 (4)	302.2 ± 8.7 (4)	253.1 ± 12.9*† (4)
Day 34	351.5 ± 10.2 (4)	347.1 ± 14.8 (4)	274.5 ± 15.2*† (4)

Swimming Performance

The U_{crit} of control fish swum in pH 6.5 soft water did not vary significantly over the time course of the study (U_{crit} ranged from 4.13 ± 0.21 $BL \cdot s^{-1}$ on day 0 to 4.48 ± 0.12 $BL \cdot s^{-1}$ on day 25; Fig. 4). There were no significant differences in body mass of swimming fish among the three

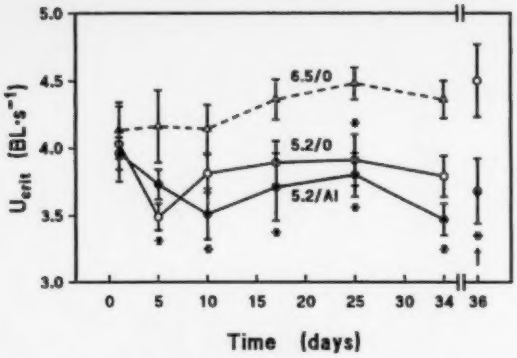

FIG. 4. Critical swimming velocities in juvenile rainbow trout at various intervals during the 36-d exposure regimes. All the control group (6.5/0) swim tests were performed at pH 6.5. From day 1 to 34 the two experimental groups (5.2/0 and 5.2/Al) were swum at pH 5.2 with *no* Al added. On day 36 the two experimental groups were swum at pH 6.5 (no Al added) and compared with the control group swum in the same medium on day 34. Means values ± SEM ($n = 8$) are shown. Asterisks indicate means significantly different ($P < 0.05$) from the 6.5/0 control group, and daggers indicate means significantly different from the 5.2/0 group.

groups on any particular day, but the averages did increase slightly in all groups with time (mean values increased from 5.85 ± 0.83 to 8.59 ± 1.23 g). In contrast, fork length was relatively constant in all groups throughout the study (mean values increased from 9.0 ± 0.3 to 9.7 ± 0.3 cm).

In general, there was a gradual reduction in U_{crit} from day 1 to 10 in the 5.2/Al group when swum at pH 5.2, following which U_{crit} stabilized (Fig. 4). The 5.2/0 group showed the greatest inhibition at day 5. With the exception of day 5, the 5.2/Al fish had the lowest U_{crit}. When swum in pH 5.2 soft water, neither group showed any sign of recovery of U_{crit} during the study.

When compared with that of the control group, the U_{crit} of 5.2/0 fish was reduced by 9–16% (significant on days 5, 25, and 34), except on day 1 when the reduction was only 3%. When fish from the 5.2/0 group were subsequently swum at circumneutral pH (6.5) on day 36, their U_{crit} was found to be almost identical to the U_{crit} found for control 6.5/0 fish on day 34 (Fig. 4).

Trout previously exposed to sublethal acid plus Al (5.2/Al) tended to have (not significant) greater reductions in U_{crit} than the 5.2/0 fish (Fig. 4). Compared with the control group, the inhibition increased progressively from day 1 (5%) to day 10 (17%), thereafter stabilizing at 15–21%. In contrast with the 5.2/0 group, U_{crit} did not recover when 5.2/Al fish were swum at pH 6.5 on day 36.

There was some variation in the mean whole-body [lactate] measured postexercise over the course of the study, but no differences were observed between groups at any time. The overall mean value for all groups, from all days, for postexercise [lactate] was 8.82 ± 0.51 $\mu mol \cdot g^{-1}$ ($n = 157$).

Oxygen Consumption

There was a trend for basal oxygen consumption to be highest in the 5.2/Al group and lowest in the control group (Fig. 5), but none of the differences between groups were statistically significant. $Mo_{2\ max}$ was always lowest in the 5.2/Al group, being significantly lower than in the control group on all days measured and lower than in the 5.2/0 group on days 34 and 36. Relative to the control group, the maximum reduction of $Mo_{2\ max}$ (35%) in the 5.2/Al trout was on day 5. $Mo_{2\ max}$ was also reduced in the 5.2/0 trout on days 5 and 25, but on day 34 the $Mo_{2\ max}$ of 5.2/0 trout (swum at pH 5.2) recovered to that of the control group (swum at pH 6.5), and on day 36 when the 5.2/0 group was also swum at pH 6.5, their $Mo_{2\ max}$ was similar to that of the control group swum on day 34. In contrast, $Mo_{2\ max}$ of 5.2/Al trout remained significantly depressed when swum at this circumneutral pH on day 36.

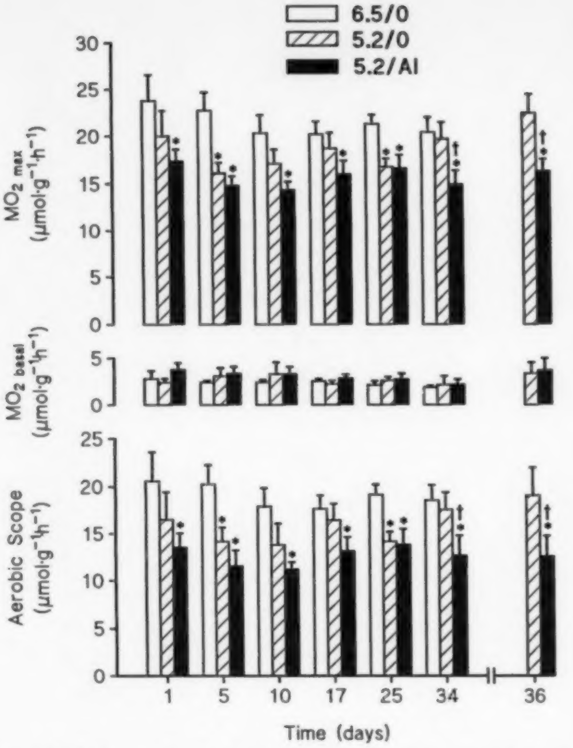

FIG. 5. Maximum and basal rates of oxygen consumption (means ± SEM, $n = 8$) and aerobic scope ($Mo_{2\ max} - Mo_{2\ basal}$) measured during swimming metabolism tests over the 36-d exposure regimes. See legend to Fig. 1 for further details. Asterisks indicate means significantly different ($P < 0.05$) from the 6.5/0 control group, and daggers indicate means significantly different from the 5.2/0 group.

Aerobic scope ($Mo_{2\ max} - Mo_{2\ basal}$) followed the same trend as found for the $Mo_{2\ max}$ values, but the differences between groups were more pronounced (Fig. 5). For example, when compared with the control group, the aerobic scope of the 5.2/Al trout was reduced by 43% on day 5, and even when swum in pH 6.5 soft water on day 36, it was still 36 and 34% lower than in either the control (on day 34) or the 5.2/0 group, respectively.

Discussion

Gill Morphology

The gill changes in response to pH 5.2 alone were consistent with the general trend found in rainbow trout (Youson and Neville 1987; Evans et al. 1988; Audet and Wood 1993), brook trout (Tietge et al. 1988; Mueller et al. 1991), brown trout (*Salmo trutta*) (Karlsson-Norrgren et al. 1986a, 1986b), minnow (*Phoxinus phoxinus*) (Norrgren et al. 1991), and fathead minnow (*Pimephales promelas*) (Leino et al. 1990) in which histopathologies due to sublethal acid were generally mild. However, in agreement with many of these same studies, sublethal Al combined with acid caused thickening of the respiratory epithelium, hyperplasia of the filamental epithelium, and a proliferation of mucous cells (Fig. 2 and 3). In the present study the changes caused by Al were not as severe or extensive as the damage observed in brook trout exposed to higher Al (75–150 $\mu g \cdot L^{-1}$) at pH 5.2 (Mueller et al. 1991). This was also consistent with the much lower mortality we observed. Although severe abnormalities such as lamellar fusion were not prevalent, we did find substantial changes in gill morphometrics that would be expected to have a significant impact on gas exchange capacity.

All the changes observed in the 5.2/Al trout after 5 d of exposure would increase the blood–water diffusion distance and/or reduce the total gill surface area available for gas exchange. Experimentally induced reductions in functional gill area are known to cause a proportional reduction in $Mo_{2\ max}$ (Duthie and Hughes 1987). We estimated a reduction in "apparent" lamellar surface area of approximately 22% on day 34. Accordingly, the corresponding reduction in $Mo_{2\ max}$ on day 34 was very similar (26%).

The hyperplasia of mucous cells seen by day 5 in 5.2/Al trout coincided with the first positive test for acclimation to Al (see Wilson et al. 1994) and persisted throughout the study. We consider this mucous cell response to be compensatory or protective rather than pathological and to be directly related to the acclimation to Al (McDonald et al. 1991; Mueller et al. 1991). The purpose of mucocyte hyperplasia is presumably to accelerate the secretion of mucus that preferentially bind and carries away Al from the sensitive gill surface (Playle and Wood 1989, 1991; McDonald et al. 1991; Mueller et al. 1991). Conversely, the increase in blood–water diffusion distance and the reduction in "apparent" gill area after 5 d of Al exposure are more likely to be the direct result of physical damage to epithelial cells typically encountered during the acute phase of sublethal metal exposures (Mallatt 1985; McDonald an Wood 1992). The subsequent recovery of diffusion distances we observed contrasts with previous morphological studies (e.g., Tietge et al. 1988; Mueller et al. 1991; Norrgren et al. 1991). This likely reflects the small amount of initial damage inflicted by the low level of Al we used and suggests that elevated diffusion distances may not be an obligatory part of the acclimation process for Al. However, apparent gill area did not return to normal, indicating that this may be an important part of acclimation to Al. Reduced gill area may offer some advantage by minimizing the amount of branchial epithelium susceptible to the surface binding of toxic metals (Mallatt 1985; McDonald and Wood 1992), but corresponding limitations to branchial gas exchange and ultimately aerobic scope are inevitable (see below).

Swimming Performance

With the exceptions of Cleveland et al. (1989), Butler et al. (1992), and Wilson and Wood (1992), studies on the effects of acidity on swimming performance in trout have not used water pH and Ca^{2+} levels relevant to the acid-threatened waters of eastern North America and Europe. Only Wilson and Wood (1992) and the present study have addressed the chronic effects of both low pH and Al on truly aerobic swimming performance. Both studies show that chronic exposure to sublethal low pH results in a sustained impairment of U_{crit}. This tends to be further exacerbated when trout are simultaneously exposed to sublethal Al, although the additional effect of Al was not statistically significant in the present study. As no differences in postexercise [lactate] were found, we have assumed that all groups reached their true aerobic maximum.

The same general pattern of impairment was observed whether the swimming tests were performed at pH 5.2 with 30 $\mu g\ Al \cdot L^{-1}$ either present (Wilson and Wood 1992) or absent (present study), and in both cases, no evidence of recovery was observed. However, the reductions in U_{crit} were smaller (by about one third) and took longer to occur (after 5 d instead of 1 d) in the present study where swimming tests were performed in the absence of Al. Clearly the choice of external medium used during swimming influences these tests. In the natural environment, fish will be swimming in the external milieu to which they have been previously exposed, suggesting that the differences between fish chronically exposed to acid alone and acid plus Al may be greater in the wild than in these laboratory studies.

Aerobic Scope in Relation to Swimming Performance

Aerobic swimming performance in fish can be affected by changes at any level of the oxygen transport system and/or muscle contraction process. Randall and Brauner (1991) demonstrated that disturbances in the ion and water balance in muscle of coho salmon (*Oncorhynchus kisutch*) reduced U_{crit} and suggested that this occurred via decreased muscle contractility. Similar changes could be involved during the initial stages of acid/Al exposure because both experimental groups experienced pronounced whole-body ion losses over the first 5–10 d (see Wilson et al. 1994). However, both groups recovered ionic balance, so it seems unlikely that alterations at the level of the muscle contraction were involved in the lower U_{crit} values after day 25.

In terms of oxygen transport and aerobic metabolism, Brett (1958) divided environmental stresses into two categories: "limiting" stresses that reduce the maximum aerobic capacity ($Mo_{2\ max}$) and "loading" stresses that increase the cost of routine maintenance ($Mo_{2\ basal}$). The reduction of U_{crit} in trout exposed to acid alone does not appear to be related to limitations in the branchial gas exchange capacity. For example, on day 34, $Mo_{2\ max}$ was almost identical to that of the control fish, and yet, U_{crit} was impaired (13%). Because we could detect no gill morphometric changes, this indicates that the reduced U_{crit} must be due to loading rather than limiting factors. The presence of loading factors is shown by the trend for $Mo_{2\ basal}$ in 5.2/0 trout to be higher than in the controls (although this was never statistically significant). However, this is shown more clearly by comparing the log Mo_2 versus swimming speed regression lines for the three groups on day 34 (Fig. 6). Equating swimming performance to aerobic scope alone on day 34 is most valid because reductions in U_{crit} due to muscle contratility changes would be minimal at this time (see above). For any given swimming speed, the 5.2/0 trout required more oxygen than the control trout (the regression line for 5.2/0 was signifi-

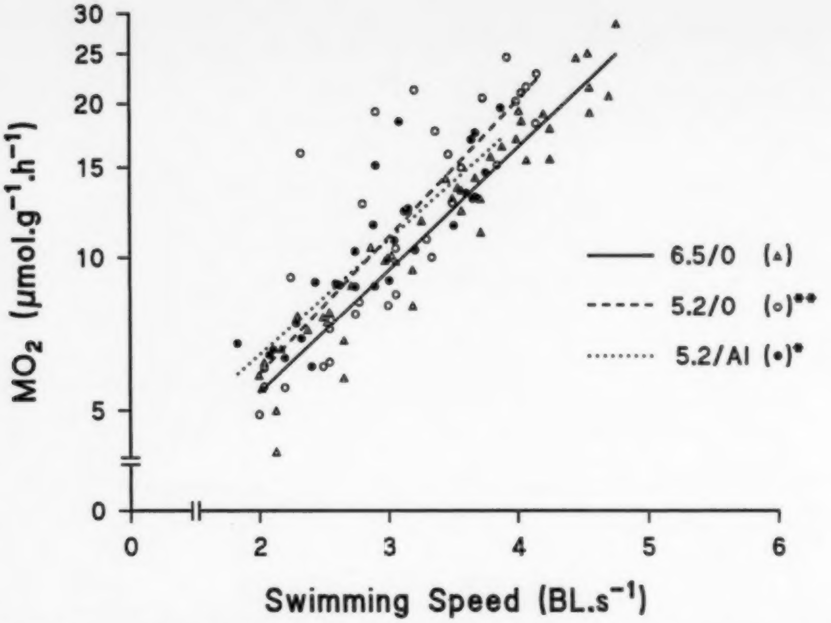

FIG. 6. Regression relationships between oxygen consumption (note log scale) and swimming speed for all three exposure groups on day 34. Group regression equations, where $y = \log \mathrm{Mo}_2$ and x = speed, were $y = 0.239x + 0.256$ ($r = 0.962$) in the 6.5/0 group, $y = 0.267x + 0.236$ ($r = 0.836$) in the 5.2/0 group, $y = 0.225x + 0.358$ ($r = 0.874$) in the 5.2/Al group. Multiple comparison revealed that the three slopes were not significantly different, having a common regression coefficient of 0.244. However, regression lines for both the 5.2/0 and 5.2/Al groups were significantly elevated above the control group ($P < 0.005$ and $P < 0.05$, respectively), indicating increased maintenance costs at all subcritical swimming speeds. Note also the additional depression of $\mathrm{Mo}_{2\,\max}$ in the 5.2/Al group.

cantly elevated ($P < 0.005$) relative to the control group; Fig. 6). We speculate that increased ionoregulatory costs associated with acid exposure act as a loading stress and lead to an increase in the metabolic rate needed for normal homeostatis. This loading stress thereby impairs U_{crit} by reducing the proportion of available oxygen that reaches the working aerobic muscle.

Perhaps the most interesting result with respect to loading stresses in acid-exposed trout was the complete recovery of U_{crit} when fish were swum at circumneutral pH on day 36. This suggests that their reduced swimming performance when swum at pH 5.2 was *entirely* due to the presence of increased [H^+] during the swim test itself rather than any accumulated physiological damage caused by the previous 36 d of exposure to low pH. The implication for fish in the wild is that even after prolonged exposure to acid water (uncontaminated with Al), a rapid restoration of more neutral pH (e.g., by liming) should result in an immediate recovery of aerobic swimming performance.

In contrast with acid alone, the reduction in swimming performance caused by preexposure to Al appears to be caused by a combination of both loading and limiting factors. Al-exposed trout had the highest basal metabolic rates and higher Mo_2 values at all subcritical speeds (Fig. 6), indicative of increased maintenance costs as in the 5.2/0 trout. However, limitations to the rate of oxygen uptake were also very apparent, as shown by the persistent depression of $\mathrm{Mo}_{2\,\max}$. The reduction in aerobic scope is not surprising considering the extent of the changes in gill morphology caused by preexposure to Al. Initially, limitations to oxygen uptake were probably the result of both reduced surface area and increased blood–water diffusion distances. However, by day 34 the reduced $\mathrm{Mo}_{2\,\max}$ was apparently the result solely of a smaller surface area for gas exchange, although increased mucus could additionally act as a diffusion barrier (e.g., see Ultsch and Gros 1979). Whatever the relative contributions of surface area and diffusion barrier alterations, the presence of limiting factors appears to be the major difference between 5.2/Al and 5.2/0 trout in terms of aerobic scope.

In addition to the elevated ionoregulatory costs due to acid alone, general gill repair, higher cell turnover, and mucus secretion rates are presumably other sources of loading stress faced by Al-exposed trout. The energetic cost of increased mucus defences may be considerable (Calow 1991), as is (presumably) the cost of gill repair. It is therefore somewhat surprising that their elevation of Mo_2 at subcritical swimming speeds was not substantially higher than for 5.2/0 trout. This observation implies that the increased metabolism associated with these acclimatory changes at the gills is small in comparison with that caused by the ionoregulatory stress induced by acid alone. This may be particularly relevant during swimming, as the cost of mucus secretion and gill repair is probably fixed, whereas Febry and Lutz (1987) have shown that the cost of osmoregulation in freshwater fish increases with swimming speed. Thus, at the swimming speeds used in our tests (20–50 $\mathrm{cm{\cdot}s^{-1}}$), elevated ionoregulatory costs may have masked any metabolic effects due to gill acclimatory processes.

We observed that the depression of both U_{crit} and $\mathrm{Mo}_{2\,\mathrm{max}}$ persisted even when the 5.2/Al trout were swum at pH 6.5 on day 36. This contrasts with the complete recovery of U_{crit} in 5.2/0 trout and suggests that the morphological limitations to branchial gas exchange capacity are only slowly reversed on return to neutral Al-free water. In support, Norrgren et al. (1991) demonstrated complete recovery of gill morphology only after 36 d in Al-free water at pH 7 following exposure of minnow to sublethal acid and Al for the previous 48 d.

The structural changes at the gill associated with long-term Al exposure, which appear to be an unavoidable consequence of the acclimatory process, probably account for the differences in swimming performance when compared with trout exposed to acid alone. While chronic sublethal background levels of Al may endow endogenous fish species with increased resistance to temporary pulses of potentially lethal Al, the mechanisms involved in acclimation carry a substantial cost in terms of scope for activity. In light of these costs, the overall benefits of acclimation may be slight in terms of the animal's fitness in the wild.

Acknowledgements

This work was supported by a NSERC Strategic Grant in Environmental Quality to C.M.W. The authors wish to thank Prof. F.W.H. Beamish for the respirometer design and R. Gilles for his help with their construction. Many thanks also to Dr. R. Jacobs and P. D'Amico for their assistance and use of the image analysis system and Joe Bobbit, Annie Narahara, Connie Boese, and Jose Fernandez for their invaluable help at the Red Buttes hostelry.

References

Audet, C., and C.M. Wood. 1993. Branchial morphological and endocrine responses of rainbow trout (*Oncorhynchus mykiss*) during a long sublethal acid exposure in which acclimation did not occur. Can. J. Fish. Aquat. Sci. 50: 198–209.

Beamish, F.W.H., J.C. Howlett, and T.E. Medland. 1989. Impact of diet on metabolism and swimming performance in juvenile lake trout, *Salvelinus namaycush*. Can. J. Fish. Aquat. Sci. 46: 384–388.

Boutilier, R.G., T.A. Heming, and G.K. Iwama. 1984. Physicochemical parameters for use in fish respiratory physiology. p. 403–430. *In* W.S. Hoar and D.J. Randall [ed.] Fish physiology. Vol. 10A. Academic Press, Inc., London.

Brett, J.R. 1958. Implications and assessments of environmental stress, p. 69–93. *In* P.A. Larkin [ed.] The investigation of fish-power problems. Institute of Fisheries, University of British Columbia, Vancouver, B.C.

Brett, J.R. 1964. The respiratory metabolism and swimming performance of young sockeye salmon. J. Fish. Res. Board Can. 21: 1183–1226.

Butler, P.J., N. Day, and K. Namba. 1992. Interaction of seasonal temperature and low pH on resting oxygen uptake and swimming performance of adult brown trout, *Salmo trutta*. J. Exp. Biol. 165: 195–212.

Calow. P. 1991. Physiological costs of combating chemical toxicants: ecological implications. Comp. Biochem. Physiol. 100C: 3–6.

Chakraborty, S.C., L.G. Ross, and B. Ross. 1992. The effect of photoperiod on the resting metabolism of carp (*Cyprinus carpio*). Comp. Biochem. Physiol. 101A: 77–82.

Cleveland, L., E.E. Little, R.H. Wiedmeyer, and D.R. Buckler. 1989. Chronic no-observed effect concentrations of aluminum for brook trout exposed in low-calcium, dilute acidic water, p. 229–245. *In* T.E. Lewis [ed.] Environmental chemistry and toxicology of aliminum. Lewis Publishers, Inc., Chelsea, Mich.

Duthie, G.G., and G.M. Hughes. 1987. The effects of reduced gill area and hyperoxia on the oxygen consumption and swimming speed of rainbow trout. J. Exp. Biol. 127: 349–354.

Evans, R.E., S.B. Brown, and T.J. Hara. 1988. The effects of aluminum and acid on the gill morphology in rainbow trout, *Salmo gairdneri*. Environ. Biol. Fishes 22: 299–311.

Febry, R., and P. Lutz. 1987. Energy partitioning in fish: the activity-related cost of osmoregulation in a euryhaline cichlid. J. Exp. Biol. 128: 63–85.

Fry, F.E.J. 1971. The effect of environmental factors on the physiology of fish, p. 1–98. *In* W.S. Hoar and D.J. Randall [ed.] Fish physiology. Vol. 7. Academic Press, New York, N.Y.

Graham, M.S., and C.M. Wood. 1981. Toxicity of environmental acid to the rainbow trout: interactions of water hardness, acid type, and exercise. Can. J. Zool. 59: 1518–1526.

Haines, T.A., S.J. Pauwels, and C.H. Jagoe. 1986. Predicting and evaluating the effects of acidic precipitation on water chemistry and endemic fish populations in the northeastern United States. U.S. Fish Wildl. Serv. Eastern Energy and Land Use Team, Biol. Rep. 80 (40.23): 139 p.

Hargis, J.R. 1976. Ventilation and metabolic rate of young rainbow trout (*Salmo gairdneri*) exposed to sublethal environmental pH. J. Exp. Zool. 196: 39–44.

Hughes, G.M., and S.F. Perry. 1976. Morphometric study of trout gills: a light-microscopic method suitable for the evaluation of pollutant action. J. Exp. Biol. 64: 447–460.

Jones, D.R., J.W. Kiceniuk, and O.S. Bamford. 1974. Evaluation of the swimming performance of several fish species from the Mackenzie river. J. Fish. Res. Board Can. 31: 1641–1647.

Karlsson-Norrgren, L., I. Bjorklund, O. Ljungberg, and P. Runn. 1986a. Acid water and aluminum exposure: experimentally induced gill lesions in brown trout, *Salmo trutta* L. J. Fish Dis. 9: 11–25.

Karlsson-Norrgren, L., W. Dickson, O. Ljungberg, and P. Runn. 1986b. Acid water and aluminum exposure: gill lesions and aluminum accumulation in farmed brown trout, *Salmo trutta* L. J. Fish Dis. 9: 1–18.

Leino, R.L., and J.H. McCormick. 1984. Morphological and morphometrical changes in chloride cells of the gills of *Pimephales promelas* after chronic exposure to acid water. Cell Tissue Res. 236: 121–128.

Leino, R.L., J.H. McCormick, and K.M. Jensen. 1990. Multiple effects of acid and aluminum on brood stock and progeny of fathead minnows, with emphasis on histopathology. Can. J. Zool. 68: 234–244.

Mallatt, J. 1985. Fish gill structural changes induced by toxicants and other irritants: a statistical review. Can. J. Fish. Aquat. Sci. 42: 630–648.

McDonald, D.G., and C.M. Wood. 1992. Branchial mechanisms of acclimation to metals in freshwater fish, p. 295–319. *In* C. Rankin and F.B. Jensen [ed.] Fish ecophysiology. Chapman and Hall, London, England.

McDonald, D.G., C.M. Wood, R.G. Rhem, M.E. Mueller, D.R. Mount, and H.L. Bergman. 1991. Nature and time course of acclimation to aluminum in juvenile brook trout (*Salvelinus fontinalis*). 1. Physiology. Can. J. Fish. Aquat. Sci. 48: 2006–2015.

Mueller, M.E., D.A. Sanchez, H.L. Bergman, D.G. McDonald, R.G. Rhem, and C.M. Wood. 1991. Nature and time course of acclimation to aluminum in juvenile brook trout (*Salvelinus fontinalis*) 2. Histology. Can. J. Fish. Aquat. Sci. 48: 2016–2027.

Norrgren, L., A. Wicklund Glynn, and O. Malmborg. 1991. Accumulation and effects of aluminium in the minnow (*Phoxinus phoxinus* L.) at different pH levels. J. Fish. Biol. 39: 833–847.

Orr, P.L. R.W. Bradley, J.B. Sprague, and N.J. Hutchinson. 1986. Acclimation-induced change in toxicity of aluminum to rainbow trout (*Salmo gairdneri*). Can. J. Fish. Aquat. Sci. 43: 243–246.

Playle, R.C., and C.M. Wood. 1989. Water pH and aluminum chemistry in the gill microenvironment of rainbow trout during acid and aluminum exposure. J. Comp. Physiol. 159B: 539–550.

Playle, R.C., and C.M. Wood. 1991. Mechanisms of aluminium extraction and accumulation at the gills of rainbow trout, *Oncorhynchus mykiss* (Walbaum), in acidic soft water. J. Fish. Biol. 38: 791–805.

Randall, D., and C. Brauner. 1991. Effect of environmental factors on exercise in fish. J. Exp. Biol. 160: 113–126.

Tietge, J., R. Johnson, and H.L. Bergman. 1988. Morphometric changes in gill secondary lamellae of brook trout (*Salvelinus fontinalis*) after long-term exposure to acid and aluminum. Can. J. Fish. Aquat. Sci. 45: 1643–1648.

Ultsch, G.R., and G. Gros. 1979. Mucus as a diffusion barrier to oxygen: possible role in O_2 uptake at low pH in carp (*Cyprinus carpio*) gills. Comp. Biochem. Physiol. 62A: 685–689.

Waiwood, K.G., and F.W.H. Beamish. 1978. Effects of copper, pH and hardness on the critical swimming performance of rainbow trout (*Salmo gairdneri* Richardson). Water Res. 12: 611–619.

WALKER, R.L., C.M. WOOD, AND J.L. BERGMAN. 1991. Effects of long-term preexposure to sublethal concentrations of acid and aluminum on the ventilatory response to aluminum challenge in brook trout (*Salvelinus fontinalis*). Can. J.Fish. Aquat. Sci. 48: 1989–1995.

WEBB, P.W. 1975. Hydrodynamics and energetics of fish propulsion. Bull. Fish. Res. Board Can. 190: 159.

WILSON, R.W., H.L. BERGMAN, AND C.M. WOOD. 1994. Metabolic costs and physiological consequences of acclimation to aluminum in juvenile rainbow trout (*Oncorhynchus mykiss*). 1: Acclimation specificity, resting physiology, feeding, and growth. Can. J. Fish. Aquat. Sci. 51: 527–535

WILSON, R.W., AND C.M. WOOD. 1992. Swimming performance, whole body ions, and gill Al accumulation during acclimation to sublethal aluminium in juvenile rainbow trout (*Oncorhynchus mykiss*). Fish. Physiol. Biochem. 10: 149–159.

WOOD, C.M., B.P. SIMONS, D.R. MOUNT, AND H.L. BERGMAN. 1988. Physiological evidence of acclimation to acid/aluminum stress in adult brook trout (*Salvelinus fontinalis*). 2. Blood parameters by cannulation. Can. J. Fish. Aquat. Sci. 45: 1597–1605.

YE, X., AND D.J. RANDALL. 1991. The effect of water pH on swimming performance in rainbow trout (*Salmo gairdneri*, Richardson). Fish Physiol. Biochem. 9: 15–21.

YOUSON, J., AND C. NEVILLE. 1987. Deposition of aluminum in the gill epithelium of rainbow trout (*Salmo gairdneri* Richardson) subjected to sublethal concentrations of the metal. Can. J. Zool. 65: 647–656.

ZAR, J.H. 1984. Comparing simple linear regression equations, p. 292–305. *In* H.J. Zar [ed.] Biostatistical analysis. Prentice-Hall Inc., Englewood Cliffs, N.J.

Developing a Raman Spectral Method for Measuring the Strontium and Calcium Concentrations of Fish Otoliths

R.W. Gauldie, K. Xi, and S.K. Sharma

Hawaii Institute of Geophysics, School of Ocean and Earth Science and Technology, University of Hawaii, 2525 Correa Road, Honolulu, HI 96822, USA

Gauldie, R.W., K. Xi, and S.K. Sharma. 1994. Developing a Raman spectral method for measuring the strontium and calcium concentrations of fish otoliths. Can. J. Fish. Aquat. Sci. 51: 545–551.

Surface-enhanced Raman scattering (SERS) spectra of Ca^{2+} and Sr^{2+} complexes of four dyes (*O*-cresolphthalein, PAN black, murexide, and eriochrome-black T(EBT) are reported. It has been demonstrated that SERS spectra of the murexide complex of Ca^{2+} can be used for the accurate determination of the cation in solutions at pH 12–8. Similarly, the SERS spectra of the EBT complex of Sr^{2+} can yield accurate determination of the cation concentration in solutions at pH 12–8. The SERS technique has linear resolutions of Sr^{2+} and Ca^{2+} concentrations down to 219 and 20 ppb, respectively. The chemistry of the otoliths of *Hyperoglyphe antarctica* (Centrolophidae: Teleostei) and *Beryx splendens* (Berycidae: Teleostei) proved to be similar. Using the SERS murexide complex technique for Ca and the SERS EBT complex for Sr, concentrations were 39.33% weight Ca and 272.7 ppm Sr for *H. antarctica* and 44.93% weight Ca and 273.133 ppm Sr for *B. splendens.*

Les spectres de l'effet Raman exalté de surface (SERS) de complexes entre les ions Ca^{2+} et Sr^{2+} et quatre colorants (*O*-crésolphtaléine, noir PAN, murexide et noir Erio au chrome T (EBT)) sont présentés. Il a été démontré que les spectres du complexe Ca^{2+}–murexide peuvent être utilisés pour mesurer avec précision la concentration de cations dans des solutions dont le pH est compris entre 12 et 8. De la même façon, les spectres SERS du complexe Sr^{2+}–EBT peuvent permettre une mesure exacte de la concentration de cations dans des solutions dont le pH varie de 12 à 8. La spectrométrie de l'effet Raman exalté de surface possède une résolution linéaire pour les concentrations de Sr^{2+} et de Ca^{2+} jusqu'à respectivement 219 et 20 $pp10^9$. Les propriétés chimiques des otolithes d'*Hyperoglyphe antarctica* (Centrolophidae: Teleostei) et de *Beryx splendens* (Berycidae: Teleostei) se sont révélées les mêmes. À l'aide de la technique SERS pour le complexe Ca–murexide et la technique SERS pour le complexe Sr–EBT, les concentrations étaient de 39,33 % de Ca en poids et 272,7 ppm de Sr pour *H. antarctica* et 44,93 % de Ca en poids et 273,133 ppm de Sr pour *B. splendens.*

Received November 25, 1992
Accepted October 6, 1993
(JB698)

Reçu le 25 novembre 1992
Accepté le 6 octobre 1993

The concentation of Sr in fish otoliths has been proposed as an indicator of the ambient temperature to which fish are exposed as well as other significant life-history characteristics of fishes (see reviews by Gauldie et al. 1992; Gunn et al. 1992). From a fisheries management perspective, the practical usefulness of the information coded in the Sr of the otolith depends almost entirely on having a sample that is statistically large enough to reveal any potential differences in life histories between not only different stocks, but also different cohorts within stocks. Because otoliths are often routinely collected for aging, they represent a source of information whose collection costs have already been met. The high costs of ship time and labor make otolith collections relatively expensive, further emphasizing the desirability of exhaustive sampling of all the information that otoliths might contain. However, the manager faces the problem of adding further analytical costs to programs by recovering life-history data to go with otolith age data. Cost must be added to the technical difficulties involved in determining low concentrations of Sr and Ca in large numbers of otoliths at sufficient precision to detect the small changes required to decode the life histories of fish. There is a need to develop a new method of analyzing otolith chemistry that is sufficiently sensitive and has a reasonable cost.

Otoliths are calcium carbonate concentrations of aragonite deposited on an organic matrix within the endolymphatic sac of the inner ear (Carlstrom 1963). Otolith deposition along the main growth axis of the fish otolith is in the form of microincremental layers laid down daily over most, if not all, of the life of the fish (Jones 1985; Ralston and Williams 1988). Microincrements vary in width, with those near the nucleus of the otolith being widest, and those deposited in the postjuvenile phase becoming progressively more narrow, decreasing in width over time (e.g., Smith and Kostlan 1992). Microincrement widths over most of the life of most fish species examined range from about 3 μm to less than 1 μm (Campana and Nielson 1985). The most powerful means of decoding life histories from otolith chemistry must therefore provide measurements of chemical concentration that can be made accurately at volumes that correspond to spatial resolution of the order of microincrements.

Techniques using charged particle beams have to draw many compromises between the accuracy of the chemical measurement and target area. For example, electron microprobe beams have potentially high physical resolution (subdaily microincrement width beam size) but relatively low chemical resolution. Various electron beam techniques have been reviewed by Gunn et al. (1992) and have chemical detection limits for Sr in the range of 500–1000 ppm. Although Sr levels in otoliths may be as high as 8000 ppm, the inherent sensitivity of the electron beam technique has proven to be too low to reliably track biologically significant changes in otolith Sr, e.g., those that are of the same order of magnitude as those expected to be induced by changes in temperature (Toole and Nielsen 1992).

Although the chemical sensitivity of the proton probe is much greater than that of the electron microprobe (Coote et al. 1982, 1991; Sie and Thresher 1992) the size of the target site is constrained by the width of the proton beam. Target sizes of the proton beam can be constrained to spots 10 × 10 μm (West et al. 1992). Targets of this size cannot reconstruct chemical life histories in the detail potentially provided by daily microincrements and, in the case of Sr, probably conceal significant amounts of variation (Gauldie et al. 1994).

In recent years, optical spectrophotometric techniques (e.g., Raman scattering fluorescence, fluorescent confocal microscopy) have become attractive as analytical tools for measuring the chemistries of small areas of material (see Bist et al. 1989 for a general review). Raman scattering arises from the molecular vibrations of various bonds induced by incident monochromatic (usually laser) light. The vibrational state of molecules provides a direct chemical way of analyzing the arrangement of atoms in the molecules in a sample irrespective of its state of aggregation (e.g., solid, liquid, or gas). The Raman scattering signal is limited by its low intensity, typically 10^{-6} of the intensity of the laser source. However, conjugation with certain metal surfaces (surface-enhanced Raman scattering, SERS) can increase signal strength by 10^7 times. SERS spectroscopy has both sensitivity and molecular specificity (Taylor et al. 1990; Xi et al. 1992). SERS techniques are used in general for detecting polyatomic anions and organic molecules; however, SERS techniques can be modified for analyzing cationic species by reacting the cations with suitable dyes (Pollard and Martin 1956; Carron et al. 1991). General reviews of the physics and applications of Raman spectroscopy are provided by Jawhari et al. (1990) and Hendra et al. (1991). Basic Raman spectroscopy and Fourier-transform (FT) Raman spectroscopy, as well as their variants such as SERS and resonance Raman scattering, have proved to be powerful analytical tools in mineralogy (Bischoff et al. 1985; Urmos et al. 1991), medicine, biology (Nie et al. 1991), and water chemistry (Xi et al. 1992).

In this study, we report the effectiveness of SERS techniques in detecting the Sr and Ca complexes with four different dyes and in providing quantitative measurements of Sr and Ca derived from, and at concentrations typical of, otoliths.

Materials and Methods

Sample Material

Otoliths of *Hyperoglyphe antarctica* (Centrolophide: Teleostei; common name bluenose) and *Beryx splendens* (Berycidae: Teleostei; common name alphonsino) were used to make two different species-specific test solutions. These two species were chosen because although they may be caught in the same water mass, *B. splendens* typically makes extensive vertical daily migrations in the upper 100–400 m (Galaktionov 1984), while *H. antarctica* is a demersal deep-water species found ranging from 200 to 800 m (Ayling and Cox 1982; Horn and Massey 1989). Species-specific test solutions were prepared using a pooled sample of 10 otoliths of each species dissolved in reagent-grade HCl in the ratio of 1 g of otolith in 20 mL of 1 M HCl solution. Large fragments of otolith organics were removed by centrifugation. This material would have been left in the test solutions to simulate otolith chemistry but tended to settle out of solution and was therefore removed. The otolith solutions were used as prepared for Sr determination (i.e., a 20× weight to weight dilution). Because of their very high Ca levels (50 000 ppm) the original solutions were diluted by 10^5 times to bring Ca sample solutions into the molar $\times 10^{-6}$ (micromolar) range reported for this technique by Carron et al. (1991).

Standard Solutions

Reagent-grade strontium carbonate and calcium carbonate solutions were prepared by dissolution in HCl to provide standard solutions for Sr^{2+} and Ca^{2+} in the molar $\times 10^{-6}$ (micromolar) range.

Dye Complex Preparation

Dyes were used as obtained from Aldrich Chemicals. All solutions were prepared with distilled and deionized water. The dye–metal complex was formed by the addition of dye solution to the metal ion (Sr^{2+} or Ca^{2+}) solutions. The dye concentrations were varied depending on the experiment.

Silver Colloid Preparation

We used silver colloids as a SERS-active substrate for the following reasons. First, they are easily and inexpensively prepared by standard chemical techniques. Second, colloidal silver hydrosols are easily characterized by their absorption spectra. Silver colloids were prepared according to a method modified by Taylor et al. (1990): 6 mL of 34 mM sodium citrate solution was added drop by drop over a 1-h period via buret to 1 L of rapidly boiling and stirred 0.3 mM silver nitrate. The solution was boiled for 1 h and the volume was adjusted to 1 L after cooling to room temperature. The sol formed by this process showed absorption maxima at approximately 410 nm. Prior to use, the sol was activated with 0.585 g of NaCl-filtered solution.

Instrumentation

Raman spectral were obtained on the stage of a Raman microscope that consisted of a modified Leitz Ortholux-I microscope optically coupled to a Spex Triplemate spectrograph (model 1877) with an optical multichannel detector (charge-coupled device) cooled to 153 K (Sharma et al. 1985; Sharma and Urmos 1987). Data storage and processing was handled with an IBM-XT computer with Spectra-Calc software (Galactic Industries). All measurements were made using a 180° scattering geometry whereby an incident laser beam was directed onto the sample via a beam splitter and an objective lens which also collects the scattered light. The 514.5-nm line of an Ar^+ ion laser (Spectra-Physics model 2020) was used for excitation. Laser power was set at 10–12 mW at the sample. Data were acquired with a 15-s integration time and accumulated for four scans by computer. This technique provided excellent signal-to-noise ratios without sample decomposition (e.g., Taylor et al. 1990). Spectra were recorded with 1–2 cm^{-1} (Raman shift) resolution. For SERS measurements, 2 mL of the sample solution

TABLE 1. Composition and intensities of SERS spectra, with metal complex intensities as ratios of dye intensities in parentheses.

Types of dye and Raman bands (cm^{-1})	Dye alone intensity × 10^3	Ca–dye intensity × 10^3	Sr–dye intensity × 10^3
O-Cresolphthalein (1294–1338)	69.1	23.1 (0.334)	64 (0.926)
PAN black (1340)	68.8	8.1 (0.118)	6.4 (0.093)
Murexide (725)	60	143.2 (2.38)	109.2 (1.827)
Eriochrome black T (1319)	34	56.3 (1.66)	103.6 (3.047)

was mixed with 2 mL of silver colloids. The mixture was then placed in a 1-cm disposable cuvette. The mixtures were allowed to equilibrate for about 1 min to achieve absorption equilibrium before Raman measurements were made.

Results

Resonance SERS spectral measurements were made on metal–dye complexes. The data are reported by dye species, and as various treatments to, and subsequent measurements of, the metal–dye complex.

O-Cresolphthalein

SERS spectra of *O*-cresolphthalein (*O*-CRES) and Sr– (Sr–CRES) and Ca–*O*-cresolphthalein (Ca–CRES) complex ions at pH 12 are shown in Fig. 1. The SERS spectrum of the *O*-CRES dye had spectral bands at 1627, 1294, and 1338 cm^{-1}. At pH 12 the effect of Ca binding was to reduce the intensity of the SERS spectrum of *O*-CRES, but with only small changes in spectral frequencies (Fig. 1). In contrast the effect of Sr binding to *O*-CRES was to produce changes in the intensity of the spectral bands at 1631, 1312, and 1334 cm^{-1}, respectively. The Sr–CRES complex gave rise to SERS spectra that were twice as intense as the spectrum of the Ca–CRES complex, so that the *O*-CRES reagent could be used for separate determinations of Ca^{2+} and Sr^{2+} concentrations (Table 1), but the SERS spectrum of the native *O*-CRES dye was more intense than both the Sr– and Ca–dye complexes.

PAN Black (PAN)

The SERS spectra of PAN and the Sr– and the Ca–PAN complex ions at pH 12 are shown in Fig. 2. The intensities of the spectra of the Sr– and Ca–PAN complexes were much weaker than the native dye. There were also additional bands in the spectrum of both the Ca– and Sr–PAN complexes. Because of the weak intensities of the Ca– and Sr–PAN complexes (Table 1), this dye was not considered suitable for determining low concentrations of Ca^{2+} and Sr^{2+} in aqueous solutions.

Murexide (Ammonium Purpurate)

The SERS spectra of murexide and the Sr– and Ca–murexide complexes are shown in Fig. 3. At pH 12, both the Ca– and the Sr–murexide complexes gave intense SERS spectra. The SERS spectra for Sr– and Ca–murexide complexes showed more or less parallel pH-dependent changes in the intensity of the spectral bands (Table 1). Murexide was considered suitable for separate determinations of low concentrations of Ca^{2+} and Sr^{2+}.

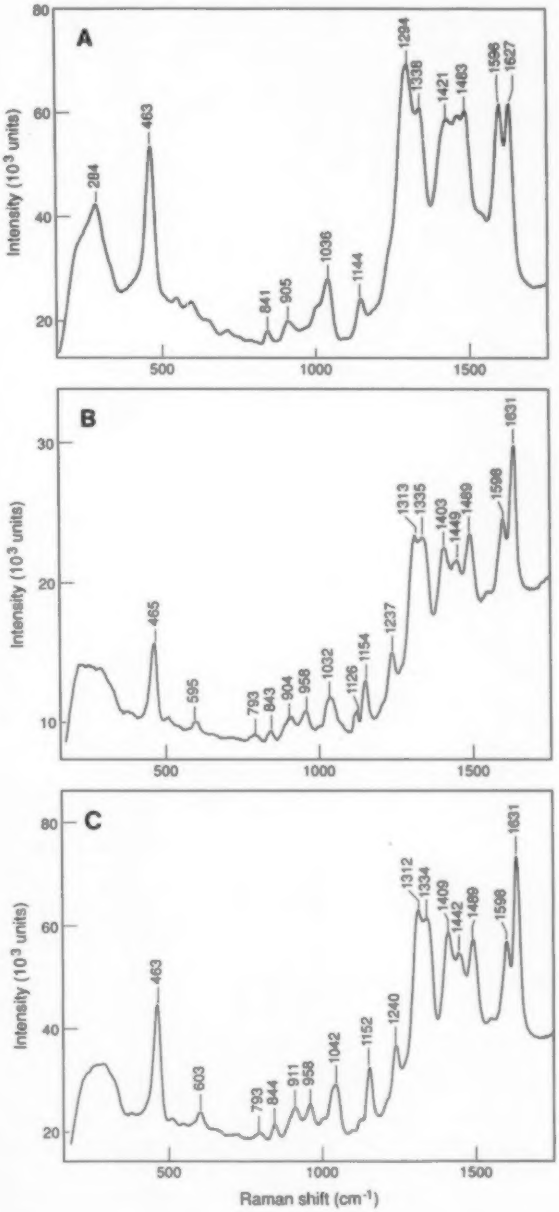

FIG. 1. SERS spectra of 1 μM solutions (pH 12) of (A) *O*-CRES, (B) Ca–CRES, and (C) Sr–CRES.

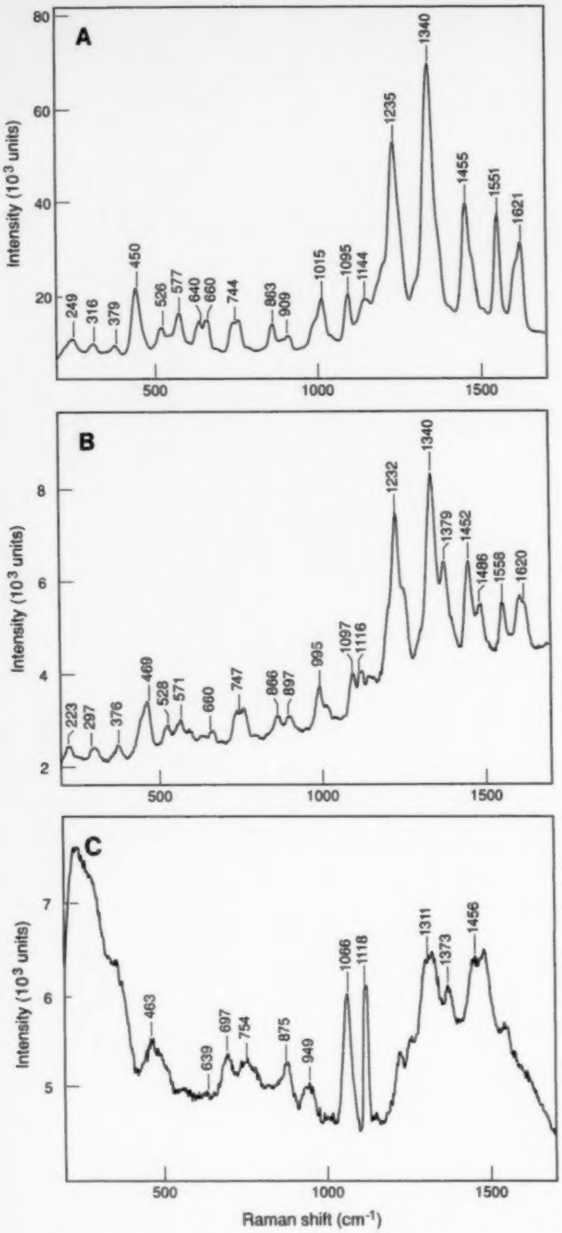

FIG. 2. SERS spectra of 1 μM solutions (pH 12) of (A) PAN, (B) Ca–PAN, and (C) Sr–PAN.

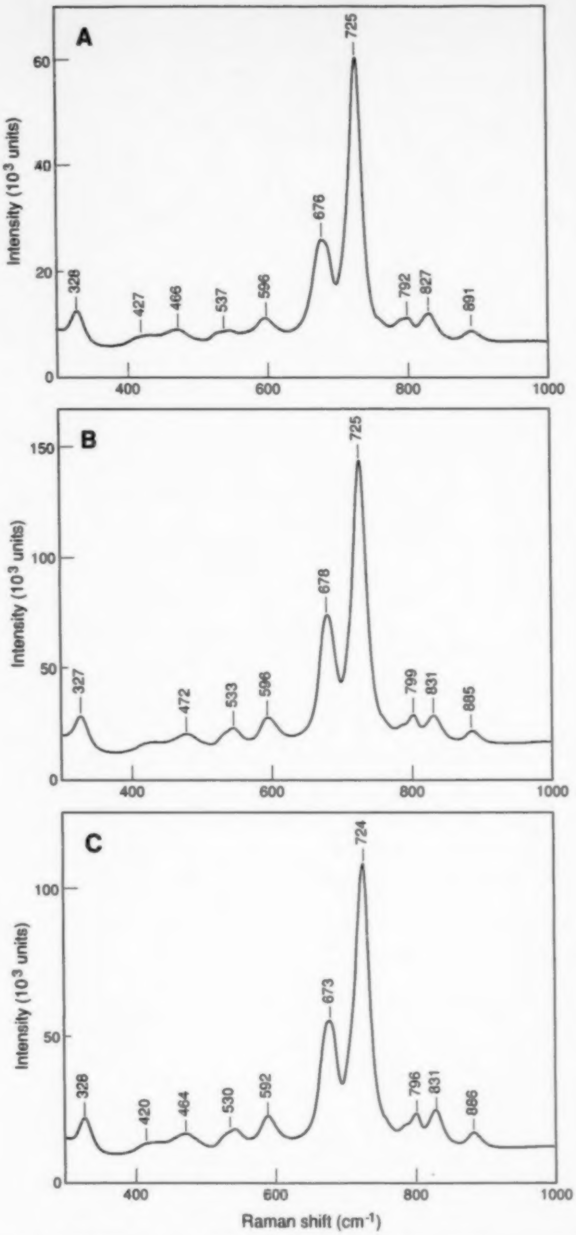

FIG. 3. SERS spectra of 1 μM solutions (pH 12) of (A) murexide, (B) Ca–murexide, and (C) Sr–murexide.

Eriochrome-black T (EBT)

The SERS spectra of EBT and Sr– and Ca–EBT complexes are shown in Fig. 4. The most significant change in Fig. 4 was loss of the shoulder of the 1274 cm^{-1} spectral peak of EBT and the change in the relative intensities of the 1319 and the 1355 cm^{-1} spectral peaks of the Ca– and the Sr–EBT complexes (Table 1). The changes were similar to those observed by Carron et al. (1991) in the SERS spectra of alkali-earth EBT complexes. EBT–metal complexes also showed inverse pH-dependent changes in the intensity of spectral peaks of the Sr– and Ca–EBT ion complexes (Fig. 5).

Standard Curves and Otolith Samples

Comparison of the relative intensities of dye complexes with dye alone (Table 1) shows that the Ca–murexide complex was the most sensitive for Ca and that the Sr–EBT complex was the most sensitive for Sr. Accordingly, standard solutions were used to develop concentration curves in the

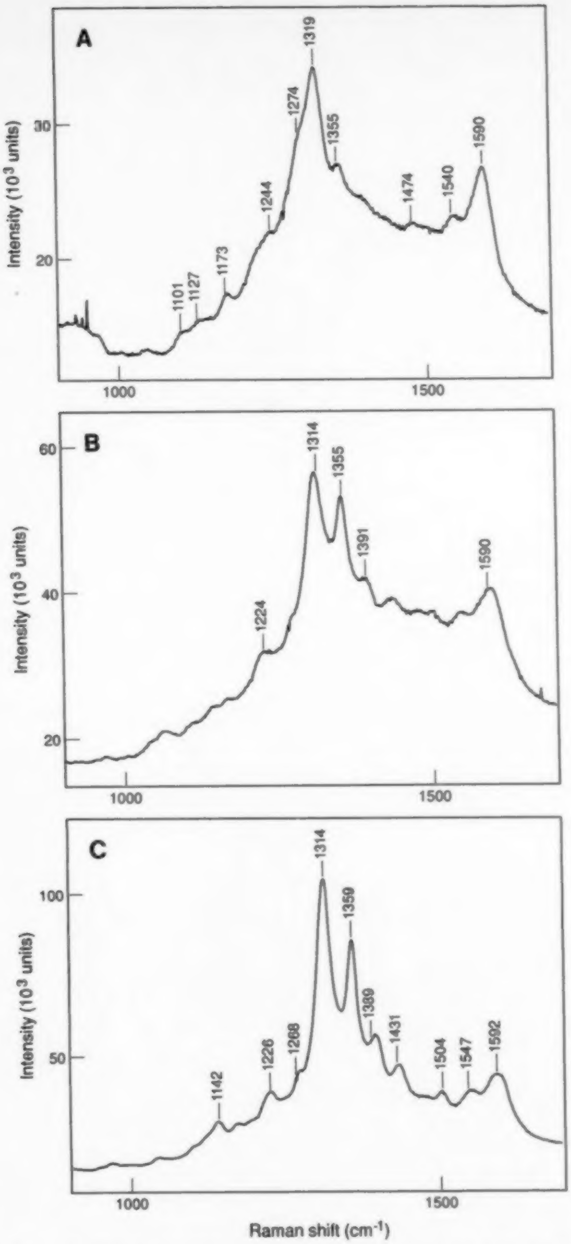

FIG. 4. SERS spectra of 10 μM solutions of (A) EBT, (B) Ca–EBT, and (C) Sr–EBT.

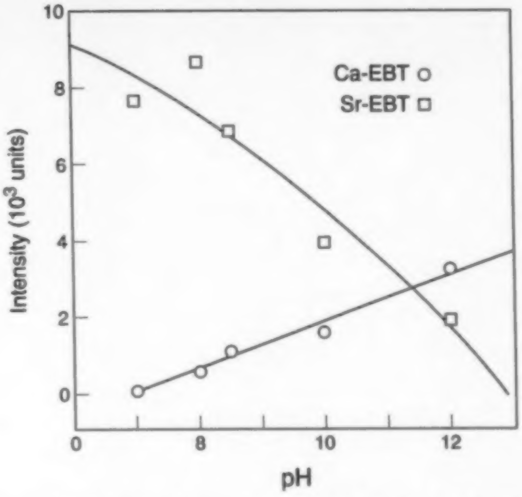

FIG. 5. pH-dependent changes in 10 μM solutions of Ca–EBT (circles) and Sr–EBT (squares).

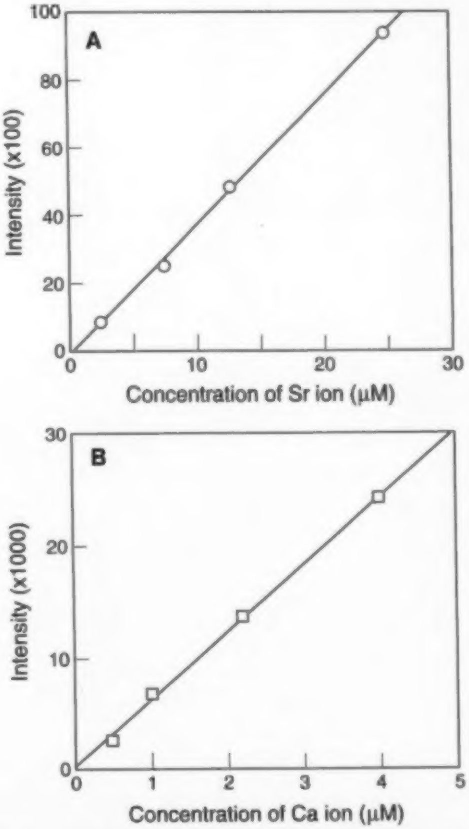

FIG. 6. Standard curves of intensity versus concentrations for (A) Sr–EBT and (B) Ca–murexide.

micromolar range using Ca–murexide and Sr–EBT. These curves are shown in Fig. 6 and are for all practical purposes straight lines passing through zero. The data points on the curve show measured detection limits of 0.5 μM (20 ppb) for Ca–murexide and 2.5 μM (219 ppb) for Sr–EBT.

Samples of the initial 20× dilution of otoliths for both *H. antarctica* and *B. splendens* were used to generate the Sr–EBT complex. The SERS spectra for the Sr–EBT complex for both species are shown in Fig. 7. The spectral peak for the Sr–EBT complex appears as an extension of the general fluorescent background requiring the baseline corrections indicated by the broken lines in Fig. 7. Similarly, sam-

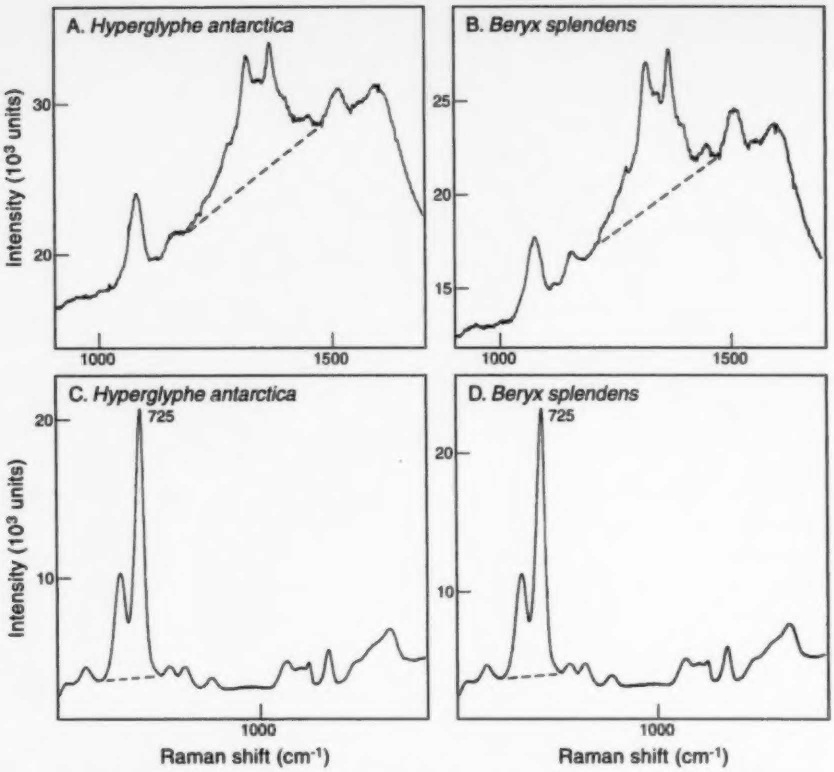

FIG. 7. SERS spectra of (A and B) Sr–EBT (pH 9) and (C and D) Ca–murexide (pH 12) in *H. antarctica* and *B. splendens*.

ples of the 20 × 10^{-5} dilution of otoliths were used to generate the Ca–murexide complex. The SERS spectra for the Ca–murexide complex for both species are shown in Fig. 7 with baseline corrections indicated by the broken lines. Both the Sr–EBT and the Ca–murexide SERS spectra generated by the otoliths of both species show peaks with high signal-to-noise ratios in the micromolar range of concentrations.

Measurements were made from the spectra in Fig. 7 to assess otolith composition for Ca and Sr. For *H. antarctica* the Ca^{2+} concentration was 19 664.54 ppm (39.33% of original weight of otolith) and the Sr^{2+} concentration was 272.7 ppm (0.545% of original otolith mass) giving a Sr^{2+}/Ca^{2+} ratio in the original otolith of 0.01386. For *B. splendens* the Ca^{2+} concentration was 22 462.53 ppm (44.93% of original weight of otolith) and the Sr^{2+} concentration was 273.133 ppm (0.546% of original otolith mass), giving a Sr^{2+}/Ca^{2+} ratio in the original otolith of 0.01215.

Discussion

The four dyes used in this study form complexes with Sr^{2+} and Ca^{2+} that have characteristic SERS spectra. For one of the dyes, EBT, the intensities associated with Sr– and Ca–EBT complexes were inversely related to pH. This inverse relationship has not been described previously and may under some circumstances allow measurements of both Sr^{2+} and Ca^{2+} concentrations to be made by changing the pH of the solution containing a mixture of Sr– and Ca–EBT complexes. However, it is evident from Table 1 that in dealing with otoliths, peak sensitivities for Sr^{2+} and Ca^{2+} were obtained by using the Ca–murexide and Sr–EBT complexes, respectively.

The calibration curves for the Sr–EBT and Ca–murexide complexes showed a linear relationship between SERS intensity and concentration down to about 0.5 μM (20 ppb) for Ca–murexide and about 2.5 μM (219 ppb) for Sr–EBT. These results are in the range of sensitivities described for ion–dye SERS spectra by Carron et al. (1991).

Pooled samples of 10 otoliths of *H. antarctica* and *B. splendens* were used to test the general applicability of the method to fish otoliths. Sr levels as a percentage of total otolith material were 0.55% for *H. antarctica* and 0.546% for *B. splendens*. These values are in the midrange of average weight % Sr reported for various marine aragonites (Morse and Mackenzie 1990, p. 213). Levels of otolith Sr reported in the literature as concentrations are lower in salmonids (0.014–0.3%) (Gauldie et al. 1980, 1986), *Chrysophrys auratus* (0.19–0.26%) (Edmonds et al. 1989), and *Gadus* sp, (0.3%) (Gauldie et al. 1986). The Ca level in *H. antarctica* was 39.33% of the original otolith weight, close to the 40% expected ratio of Ca in calcium carbonate. However, in *B. splendens* the Ca level is 44.93%, suggesting that in the otoliths of *B. splendens*, Ca is sequestered in some form other than the carbonate.

The difference between *H. antarctica* and *B. splendens* in Sr^{2+}/Ca^{2+} ratios of otoliths based on concentrations was about 14%. The Sr/Ca ratio in aragonitic corals decreases with temperature at a rate of about 1% per 1°C (Smith et al. 1979). If this observation could be transferred to the Sr/Ca ratios in otoliths, it would imply that the otoliths of *H. antarctica* were from colder water than the otoliths of *B. splendens* and that the average difference in ambient water temperature between the species was about 14°C. Generally, *H. antarctica* are taken in deeper and therefore colder water than *B. splendens*, but the maximum temperature difference implied by even the upper and lower limits of their respective ranges (200–800 m) is about 6°C (Heath 1976).

In this study, pooled whole otoliths were used. More detailed information about Sr distribution can be obtained by using the microdrilling technique developed for sampling material for isotope analysis by Prezbindowski (1984). The microdrilling method recovers volumes of material as small as 0.05 mm^3. Aragonite specific gravity is 2.5, so that 0.05 mm^3 yields 125 μg of otolith that contains 0.68 μg of Sr^{2+}. In a 4-mL cuvette, 0.68 μg of Sr^{2+} corresponds to 1.94 μmol of Sr^{2+} which is near the limit of detection using the Sr–EBT SERS method. Volumes of 0.05 mm^3 correspond to a cube of the dimensions of about 370 μm. A sample this size corresponds to time periods of the order of 6 mo in otoliths whose daily microincrements range in width from 1 to 3 μm. Samples of less than a year over the life of the fish would allow the Sr^{2+} components of the life history of fishes to be recovered in concentration units, thereby allowing the laws of physical chemistry to be applied directly to the analysis of Sr^{2+} variability in otoliths at relatively low cost.

Acknowledgements

The authors gratefully acknowledge NOAA Sea Grant (NA89AA-D-SG063) support for this study. The authors would also like to thank both the Office of Naval Research for providing support to develop SERS spectroscopic techniques at the University of Hawaii and the reviewers for their constructive comments. This is School of Ocean and Earth Science and Technology contribution No. 3520.

References

AYLING, T., AND G.J. COX. 1982. Sea fishes of New Zealand. Collins, Auckland and London. 343 p.

BISCHOFF, W.D., S.K. SHARMA, AND F.T. MACKENZIE. 1985. Carbonate ion disorder in synthetic and biogenic magnesian calcites: a Raman spectral study. Am. Mineral. 70: 581–589.

BIST, H.D., J.R. DURIG, AND D.J. SULLIVAN. 1989. Raman spectroscopy sixty years on. Vibrational spectra and structure. Vol. 17B. Elsevier, Amsterdam, The Netherlands. 645 p.

CAMPANA, S.E., AND J.D. NEILSON. 1985. Microstructure of fish otoliths. Can. J. Fish. Aquat. Sci. 42: 1014–1032.

CARLSTROM, D. 1963. A crystallographic study of vertebrate otoliths. Biol. Bull. 125: 441–463.

CARRON, K., K. MULLEN, M. LANOUTTE, AND H. ANGERSBACH. 1991. Selective-ultratrace detection of metal ions with SERS. Appl. Spectrosc. 45: 420–423.

COOTE, G.C., R.W. GAULDIE, AND I.F. WEST. 1991. Application of a nuclear microprobe to the study of fish otoliths and scales. Nucl. Instrum. Methods 54: 144–150.

COOTE, G.E., R.J. SPARKS, AND P. BLATTNER. 1982. Nuclear microprobe measurement of fluorine concentration profiles with applications in archeology and geology. Nucl. Instrum. Methods 197: 213–221.

EDMONDS, J.S., M.J. MORAN, N. CAPUTI, AND M. MORITA. 1989. Trace element analysis of fish sagittae as an aid to stock identification: pink snapper (*Chrysophrys auratus*) in Western Australian waters. Can. J. Fish Aquat. Sci. 46: 50–54.

GALAKTIONOV. G.V. 1984. Features of the schooling behaviour of the alfonsina *Beryx splendens* (Berycidae) in the thalassobathyal depths of the Atlantic Ocean. J. Ichthyol. 24: 148–151.

GAULDIE, R.W., G.C. COOTE, K.P. MULLIGAN, AND I.F. WEST. 1992. A chemical probe of the microstructural organization of fish otoliths. Comp. Physiol. Biochem. 102: 533–545.

GAULDIE, R.W., D.A. FOURNIER, D.E. DUNLOP, AND G. COOTE. 1986. Atomic emission and proton microprobe studies of the ion content of otoliths of chinook salmon aimed at recovering the temperature life history of individuals. Comp. Physiol. Biochem. 84: 607–615.

GAULDIE, R.W., E.J. GRAYNOTH, AND J. ILLINGWORTH. 1980. The relationship of the iron content of some fish otoliths to temperature. Comp. Physiol. Biochem. 66: 19–24.

GAULDIE, R.W., I.F. WEST, AND G.C. COOTE. 1994. Evaluating age estimates for *Hoplostethus atlanticus* by comparing patterns of checks, cycles in microincrement width and cycles in strontium and calcium composition. Bull. Mar. Sci. (In press)

GUNN, J.S., I.R. HARROWFIELD, C.H. PROCTOR, AND R.E. THRESHER. 1992. Electron probe microanalysis of fish otoliths — evaluation of techniques studying age and stock discrimination. J. Exp. Mar. Biol. Ecol. 158: 1–36.

HEATH, R.A. 1976. Estimates of the components of sea surface elevation contributing to the long-term variation of mean sea level around New Zealand. J. R. Soc. N.Z. 6: 95–105.

HENDRA, D., C. JONES, AND G. WARNER. 1991. Fourier-transform Raman spectroscopy: instrumentation and chemical applications. Ellis Wood, London.

HORN, P.L., AND B.R. MASSEY. 1989. Biology and abundance of alfonsino and bluenose off the lower east coast North Island, New Zealand. N.Z. Fish. Tech. Rep. 15: 32 p.

JAWHARI, T., P.J. HENDRA, H.A. WILLIS, AND M. JUDKINS. 1990. Quantitative analysis using Raman methods. Spectrochem. Acta 46: 161–170.

JONES, C. 1985. Determining age of larval fish with the otolith microincrement technique. Fish. Bull. U.S. 84: 91–103.

MORSE, J.W., AND F.T. MACKENZIE. 1990. Geochemistry of sedimentary carbonates. Elsevier, Amsterdam and New York. 707 p.

NIE, S., K.L. BERGBAUER, J.J. HO, J.F.R. KUCK, AND N.-T. YO. 1991. Applications of near-infrared Fourier transform Raman spectroscopy in biology and medicine. Spectroscopy 5: 24–32.

POLLARD, F.H., AND J.V. MARTIN. 1956. The spectrophotometric determination of the alkaline-earth metals with murexide, eriochrome black T and with *O*-cresolphthalein complexone. Analyst 81: 348–352.

PREZBINDOWSKI, D. 1984. Microsampling technique for stable isotopic analyses for carbonates. J. Sediment. Petrol. 50: 643–644.

RALSTON, S., AND H.A. WILLIAMS. 1988. Depth frequencies and growth characteristics of deep slope fishes of the Marianas Archipelago. NOAA Tech. Memo. NMFS-SWFC 113: 47 p.

SHARMA, S.K., H.K. MAO, P.M. BELL, AND J.A. XU. 1985. Measurement of stress in diamond anvil with micro-Raman spectroscopy. J. Raman Spectrosc. 16: 350–352.

SHARMA, S.K., AND J.P. URMOS. 1987. Micro-Raman spectroscopic study of materials at ambient and high pressures with CW and pulsed lasers, p. 133–136. *In* R.H. Geiss [ed.] Microbeam analysis 1987. San Francisco Press Inc., San Francisco, Calif.

SIE, S.H., AND R.E. THRESHER. 1992. Micro-PIXE analysis of fish otoliths: methodology and evaluation of first results for stock discrimination. Int. J. PIXE: 2: 357–359.

SMITH, M.K., AND E. KOSTLAN. 1992. Estimates of age and growth of Ehu (*Etelis carbunculus*) in four regions of the Pacific from the density of daily increments in otoliths. Fish. Bull. U.S. 89: 461–472.

SMITH, S.V., R.W. BUDDEMEIER, R.D. REDALJE, AND J.E. HOUCK. 1979. Strontium–calcium thermometry in coral skeletons. Science (Wash., D.C.) 204: 404–407.

TAYLOR, G.T., S.K. SHARMA, AND K. MOHANAN. 1990. Optimization of a flow injection sampling system for quantitative analysis of dilute aqueous solutions using resonance Raman and surface-enhanced Raman spectroscopy (SERRS). Appl. Spectrosc. 44: 635–840.

TOOLE, C.T., AND R.L. NIELSEN. 1992. Effects of microprobe precision on hypotheses related to otolith Sr:Ca ratios. Fish. Bull. 90: 421–427.

URMOS, J., S.K. SHARMA, AND F.T. MACKENZIE. 1991. Characterization of some biogenic carbonates with Raman spectroscopy. Am. Mineral. 76: 641–646.

WEST, I.F., G.E. COOTE, AND R.W. GAULDIE. 1992. Data smoothing techniques applied to proton microprobe scans of teleost hard parts. Int. J. PIXE 2: 313–323.

XI, K., S.K. SHARMA, G.T. TAYLOR, AND D.W. MUENOW. 1992. Determination of low concentrations of the azo-dye complex of nitrite in fresh water and seawater using surface-enhanced resonance Raman spectroscopy (SERRS). Appl. Spectrosc. 46: 819–826.

A Likelihood Method for Estimating Pacific Salmon Escapement based on Fence Counts and Mark–Recapture Data

M. Labelle[1]

Resource Ecology, University of British Columbia, Vancouver, BC V6T 1W5, Canada

Labelle, M. 1994. A likelihood method for estimating Pacific salmon escapement based on fence counts and mark–recapture data. Can. J. Fish. Aquat. Sci. 51: 552–566.

Pacific salmon escapements in natural streams are often determined by conducting fence counts in conjunction with mark–recapture operations. Typical field conditions are characterized by protracted floods, undetected immigration, variation in sampling rates, mortality during the census periods, small sample sizes, and few successive recaptures. Closed population models tend to overestimate escapement under such conditions, and traditional open population models cannot always be relied on due to the lack of sufficient data. A likelihood-based estimation method was specifically designed for such conditions. A distinguishing feature of this model is that individual recapture histories are not required for parameter estimation. The model is also structured to incorporate ancillary data in the estimation process to improve the precision and accuracy of the estimates. The model is described in detail, and suggestions are made to facilitate its application. Constructed data sets resembling those obtained under field conditions were used to evaluate the performance of the model. The estimates generated with simulated data and actual field data were compared with those based on visual foot surveys and other mark–recapture models.

Les échappées de saumon du Pacifique dans des cours d'eau naturels sont souvent établies par des dénombrements aux barrières et par des opérations de marquage–recapture. Les conditions pratiques typiques sont caractérisées par des crues prolongées, une immigration non déterminée, un taux d'échantillonnage variable, une mortalité pendant les périodes de dénombrement, des échantillons de petite taille et des recaptures successives peu nombreuses. Les modèles de population fermée tendent à surestimer l'échappée dans ces conditions, et on ne peut pas toujours se baser sur des modèles classiques de population ouverte en raison de l'insuffisance des données. Une méthode d'estimation fondée sur la vraisemblance a été conçue spécifiquement pour de telles conditions. Ce modèle se distingue par le fait que les antécédents de recapture individuelle pour l'estimation des paramètres ne sont pas nécessaires. Le modèle est également structuré de façon à incorporer des données auxiliaires dans le processus d'estimation afin d'augmenter la précision et la justesse des estimations. Le modèle est décrit en détail, et des propositions sont formulées pour en faciliter l'application. La performance du modèle a été évaluée par la construction d'ensembles de données ressemblant à ceux obtenus dans des conditions pratiques. Les estimations obtenues avec des données simulées et des données pratiques réelles ont été comparées à celles fondées sur des relevés visuels effectués à pied et d'autres modèles de marquage–recapture.

Received May 16, 1990
Accepted October 15, 1993
(JA577)

Reçu le 16 mai 1990
Accepté le 15 octobre 1993

Accurate escapement estimates are required to determine the exploitation rates, marine survival, and spawner–recruit relations of Pacific salmon stocks. The deficiencies of the current escapement enumeration system in British Columbia and their effects on various stock assessment estimates are well documented (Walters and Ludwig 1981; Cousens et al. 1982; Pearse 1982; Symons and Waldichuk 1984; Walters and Cahoon 1985). Escapement estimates of coho salmon (*Oncorhynchus kisutch*) have been described as "probably the most unreliable of all estimates for the five species of Pacific salmon" (Fraser et al. 1982). This situation can be attributed to several factors characterizing the ecology of this species. Adult coho usually return to their spawning grounds over a period of several weeks during autumn when floods are common. Once in the stream, they tend to remain sheltered under logjams, stream banks, and the bottom of deep pools and are difficult to see because of their cryptic coloration. Spawning takes place at various times and locations in the stream, so the entire population is rarely aggregated in one area. As a result, coho are particularly difficult to enumerate visually by fishery officers assessing escapement levels.

For small coastal streams without permanent counting facilities, the most reliable method for escapement estimation has traditionally been a two-stage process involving escapement enumeration and mark–recapture operations (Cousens et al. 1982). Typically, a small semipermanent fence is used to intercept, enumerate, and mark coho as they enter a stream. Seasonal fluctuations in water levels are pronounced in coastal streams, and because floods and fence damage are common, only a partial enumeration of the escapement is usually possible. Most of the coho intercepted at the fence are marked throughout the run, but since coho tend to enter streams during the first freshets, marks are often applied mainly during the early part of the run before floods occur.

---

[1] Present address: Fisheries Branch, B.C. Ministry of Environment, Lands and Parks, 780 Blanshard St., Victoria, BC V8V 1X4, Canada.

Censuses are conducted intermittently during the spawning period to determine the fraction of the population that is marked. Additional marking may take place during this period, but the fraction of the total population examined or marked at this stage is often much lower than at the fence. When conditions are not suitable for enumerating most of the escapement, mark–recapture estimates are relied upon heavily. This situation dictates that the mark–recapture model selected be suitable for the conditions encountered during the escapement period.

Methods for estimating population size by mark–recapture have developed considerably over the past 40 yrs (see reviews by Cormack 1968; Ricker 1975; Seber 1982). A few models have been used for estimating salmon escapements and abundance (Pritchard and Neave 1942; Chapman 1948; Howard 1948; Schaefer 1951; Salo and Noble 1953; Eames and Hino 1981; Eames et al. 1983). Simpson (1984) found that the Petersen model was the most commonly used model for escapement estimation based on mark–recapture data. Simpson (1984) noted that in most cases where Petersen estimates were evaluated against known counts, overestimation and large variation among replicates were observed. This is hardly surprizing, since Petersen-type estimators are not structured to account for the immigration, emigration, and death that can occur during extensive census periods.

Schaefer (1951) recognized the difficulties associated with obtaining reliable mark–recapture estimates of salmon escapement and devised a stratified mark–recapture model applicable to situations where salmon are marked and recovered along their migration route. This model is best designed for situations where the population size remains constant during the marking and census periods. Ricker (1975) noted that even under conditions where the Schaefer model is applicable, random marking or recovery would allow the simpler Petersen model to provide unbiased and consistent estimates of abundance. Accordingly, Eames et al. (1983) noted that in cases where the Schaefer method was applied, the escapement estimates obtained were not substantially different from those obtained with the simpler Petersen model.

Several other models could potentially serve as alternative estimators. DeLury (1951) proposed a modified Schnabel estimator to provide estimates of population size that are "undistorted" by the effect of natural mortality. This model is designed for situations where there is no immigration during the census period, mortality rates remain constant between censuses conducted at fixed time intervals, and no marked fish are added to the population except while conducting coho escapement enumeration. Unfortunately, such conditions are not commonly encountered when conducting coho escapement enumeration (Clark and Irvine 1989; Labelle 1990). Immigration can occur during the census period owing to floods or fence damage. Census periodicity and the number of coho examined for marks are often dictated by stream conditions and logistic constraints. Mortality rates can be constant within short time intervals, but may vary considerably during prolonged census periods.

DeLury (1958) proposed a modification of Shumacher and Eschemyer's (1943) model to account for mortality and recruitment, but failed to show that the model provided reliable estimates of abundance, recruitment, and mortality for a lake trout (*Salvelinus namaycush*) population. Ricker (1975) concluded from DeLury's bead-drawing trials that reliable estimates of mortality and recruitment would rarely be obtained by the proposed method. This model is also structured to use data as would be obtained if all coho examined during censuses were marked and released. The model is not tailored for situations such as described above where most of the marks are applied prior to the census period.

Gazey and Staley (1986) introduced a Bayesian algorithm that relies on sequential mark–recapture experiments to yield abundance estimates regardless of sample sizes or sampling procedure. According to these authors, the estimates are more reliable than those of the closed population models of Schnabel (1938) and Delury (1951) under conditions of small sample sizes and low recovery rates. However, the model is not structured to account for mortality during the census period, so in the context of escapement estimation, it is best applied when marked and unmarked coho have the same survival, fixed marking rates are used during the run, and all immigration occurs within a few days.

Several sophisticated stochastic models were developed specifically to estimate the abundance of populations subject to immigration and death. "Open" population models, derived from those of Jolly (1965) and Seber (1965), can potentially be used for escapement estimation. However, little use has been made of these models for such purposes, mainly because of the practical difficulties involved. To estimate migration and mortality rates, these models usually require information on successive recaptures obtained by means of serially numbered tags. Such tags may be unavailable for various reasons, or the number of recaptures may simply be insufficient for estimation purposes. For instance, Labelle (1990) reported cases where local residents objected to the application of external numbered tags, and only simple check marks on the operculum could be applied. Labelle also noted that in 12 mark–recapture operations, successive recaptures of marked coho were rarely obtained despite investing several hundred man-hours to mark 25–50% of the escapement at the fence and sample >10% of the escapement during censuses.

Lebreton et al. (1992) noted that the open population models available until recently were not sufficiently flexible and sometimes not robust to departures of the underlying assumptions. Minta and Mangel (1989) noted that the complex programs needed for parameter estimation and testing of the underlying assumptions of open population models often require large data sets to justify their use and are not generally suitable for the occasional user. Minta and Mangel concluded that there is a need for simple, inexpensive, alternative estimators to accommodate various experimental conditions. Minta and Mangel suggested that traditional probability models be incorporated into a simulation framework for estimating population sizes from mark–recapture data. When doing so, Hilborn (1990) noted that maximum likelihood estimates of the parameters can often be obtained with simple nonlinear search techniques that reduce the need for statistical derivations and tend to be more appealing to biologists with limited mathematical skills.

With this approach in mind, a simple likelihood method was developed for escapement estimation in situations where coho are marked at a fence as they enter the stream and are sampled subsequently throughout the period of stream residency. The underlying model is structured to account for

TABLE 1. Predicted coho escapement pattern, abundance levels, and marked proportions. Fence status is "out" when floods occur. Figures in columns 8–10 are the number of live coho available for sampling >24 h after passing the fence. All census counts rounded to the nearest integer.

1 Survey date	2 Day (d)	3 Fence status	4 Fence count (f_d)	5 Coho marked (m_d)	6 Coho missed $(\hat{e}_d)$	7 Escapement pattern $(\hat{f}_d)$	8 Total alive $(\hat{n}_d)$	9 Marked alive $(\hat{m}_d)$	10 Marked proportion $(\hat{m}_d/\hat{n}_d)$	11 Census time (t)	12 Sample size (c_t)	13 Marks recovered (r_t)	14 Marked proportion (r_t/c_t)
1 Oct.		Up	0	0									
2 Oct.		Up	0	0									
2 Oct.		Up	0	0									
2 Oct.		Up	0	0									
20 Oct.		Up	0	0									
21 Oct.	0	Up	100	80		100	0	0	0.00				
22 Oct.	1	Up	200	160		200	100	80	0.80				
23 Oct.	2	Up	400	320		400	299	240	0.80				
24 Oct.	3	Up	100	80		100	697	558	0.80				
25 Oct.	4	Up	50	40		50	790	632	0.80				
26 Oct.	5	Up	50	40		50	826	661	0.80				
27 Oct.	6	Up	50	40		50	854	683	0.80				
28 Oct.	7	Up	25	20		25	875	700	0.80				
29 Oct.	8	Up	25	20		25	865	692	0.80	1	43	35	0.81
30 Oct.	9	Up	0	0		0	850	680	0.80				
31 Oct.	10	Up	0	0		0	806	645	0.80				
1 Nov.	11	Up	0	0		0	761	609	0.80				
2 Nov.	12	Up	0	0		0	715	572	0.80				
3 Nov.	13	Out	0	0	300	300	669	535	0.80				
4 Nov.	14	Out	0	0	150	150	924	499	0.54				
5 Nov.	15	Out	0	0	50	50	1030	465	0.45	2	51	23	0.45
6 Nov.	16	Out	0	0	50	50	1034	432	0.42				
7 Nov.	17	Out	0	0	50	50	1036	401	0.39				
8 Nov.	18	Up	0	0		0	1035	372	0.36				
9 Nov.	19	Up	0	0		0	981	345	0.35				
10 Nov.	20	Up	0	0		0	927	319	0.34				
11 Nov.	21	Up	0	0		0	871	296	0.34				
12 Nov.	22	Up	0	0		0	816	274	0.34	3	41	14	0.34
13 Nov.	23	Up	0	0		0	763	254	0.33				
14 Nov.	24	Up	0	0		0	711	235	0.33				
15 Nov.	25	Up	0	0		0	662	218	0.33				
16 Nov.	26	Up	0	0		0	615	202	0.33				
17 Nov.	27	Up	0	0		0	571	187	0.33				
18 Nov.	28	Up	0	0		0	530	174	0.33				
19 Nov.	29	Up	0	0		0	492	161	0.33	4	25	8	0.32
20 Nov.	30	Up	0	0		0	456	150	0.33				
21 Nov.	31	Up	0	0		0	423	139	0.33				
22 Nov.	32	Up	0	0		0	392	130	0.33				
23 Nov.	33	Up	0	0		0	364	121	0.33				
24 Nov.	34	Up	0	0		0	338	112	0.33				
25 Nov.	35	Up	0	0		0	314	105	0.33				
26 Nov.	36	Up	0	0		0	291	97	0.33	5	15	5	0.33

TABLE 1. (*Concluded*)

1 Survey date	2 Day (d)	3 Fence status	4 Fence count (f_d)	5 Coho marked (m_d)	6 Coho missed ($\hat{e}_d$)	7 Escapement pattern ($\hat{f}_d$)	8 Total alive ($\hat{n}_d$)	9 Marked alive ($\hat{m}_d$)	10 Marked proportion ($\hat{m}_d/\hat{n}_d$)	11 Census time (t)	12 Sample size (c_t)	13 Marks recovered (r_t)	14 Marked proportion (r_t/c_t)
27 Nov.	37	Up	0	0		0	271	91	0.34				
28 Nov.	38	Up	0	0		0	252	85	0.34				
29 Nov.	39	Up	0	0		0	234	79	0.34				
30 Nov.	40	Up	0	0		0	218	74	0.34				
1 Dec.	41	Up	0	0		0	203	69	0.34				
2 Dec.	42	Up	0	0		0	189	65	0.34				
3 Dec.	43	Up	0	0		0	176	61	0.34	6	9	3	0.33
4 Dec.	44	Up	0	0		0	165	57	0.34				
5 Dec.	45	Up	0	0		0	154	53	0.35				
6 Dec.	46	Up	0	0		0	144	50	0.35				
7 Dec.	47	Up	0	0		0	134	47	0.35				
8 Dec.	48	Up	0	0		0	125	44	0.35				
9 Dec.	49	Up	0	0		0	117	41	0.35				
10 Dec.	50	Up	0	0		0	110	39	0.35	7	5	2	0.40
11 Dec.	51	Up	0	0		0	103	36	0.35				
12 Dec.	52	Up	0	0		0	97	34	0.36				
13 Dec.	53	Up	0	0		0	91	32	0.36				
14 Dec.	54	Up	0	0		0	85	30	0.36				
15 Dec.	55	Up	0	0		0	80	29	0.36				
16 Dec.	56	Up	0	0		0	75	27	0.36				
17 Dec.	57	Up	0	0		0	70	25	0.36	8	4	1	0.25
Sum			1000	800	600	1600					193	91	

the immigration of coho during floods, mortality during the sampling period, and variable sampling regimes. A distinguishing feature of this model (termed the ES model) is that knowledge of recapture histories is not essential for estimation purposes. Numbered tags should be used whenever possible to provide this information, quantify the population attributes, and assess departures from the assumptions. However, escapement estimates can be obtained with the ES model when such tags are not used, or when too few successive recaptures are obtained. The ES model can thus be used when traditional open population models cannot for lack of sufficient data and provides a superior alternative to closed population models which are not applicable.

The objectives of this paper are to describe the ES model, provide examples of its application, and assess its performance under various marking and sampling conditions, escapement patterns, mortality rates, and flood frequencies. Estimates generated with the ES model are compared with the actual parameter values used to construct the data sets and, in some cases, with those of closed population models to show the pitfalls of common practices. Examples are given to show how ancillary data from other sources can be used by the ES model to improve the reliability of the estimates.

Model Structure and Estimation Procedure

Symbols and Definitions

d = index used to distinguish each day in the escapement period ($d = 0, 1, \ldots, D$)
f_d = number of coho counted at the fence on day d ($F = \Sigma f_d$)
$\mathbf{f}$ = vector of f_d values (column 4, Table 1)
$\hat{f}_d$ = predicted number of coho passing by the fence on day d
m_d = number of coho counted and marked at the fence on day d ($M = \Sigma m_d$)
$\mathbf{m}$ = vector of m_d values (column 5, Table 1)
E = hypothesized number of undetected coho that entered during all floods
$\hat{e}_d$ = predicted number of undetected coho passing the fence on day d
p_d = hypothesized fraction of E that entered the stream during the flood on day d
$\mathbf{p}$ = vector of hypothesized p_d values. For days without floods, $p_d = 0$
N = hypothesized escapement ($=F + E$)
x = number of days elapsed since coho entered the stream
$Q(x)$ = probability of dying on the xth day after stream entry
$S(x)$ = probability of surviving after a stream residency period of x days
$\hat{n}_d$ = predicted number of live coho available for sampling on day d
$\hat{n}_t$ = predicted $\hat{n}_d$ at the corresponding time of census t
$\hat{m}_d$ = predicted number of marked live coho available for sampling on day d
$\hat{m}_t$ = predicted $\hat{m}_d$ at the corresponding time of census t
t = index used to distinguish each census ($t = 1, \ldots, T$)
c_t = number of live coho sampled during census t ($C = \Sigma c_t$)
$\mathbf{c}$ = vector of c_t values (column 12, Table 1)
r_t = number of live marked coho sampled during census t ($R = \Sigma c_t$)
$\mathbf{r}$ = vector of r_t values (column 13, Table 1)
ϕ = hypothesized median stream residency period
σ = hypothesized standard error of the $\log_e(x)$
Φ = full parameter vector (combination of E, $\mathbf{p}$, ϕ, and σ)

Background Information

A data set was constructed to illustrate what is "typically" obtained during a two-stage mark–recapture operation (Table 1). Coho were intercepted at the fence during 21–29 October, and 80% of those enumerated each day were marked prior to release. A flood occurred during 3–7 November, and a total of 600 coho entered the stream "undetected", i.e., without being enumerated. A total of 1600 coho escaped, and 50% of these were marked at the fence. For this example, it was assumed that coho required 24 h to distribute themselves throughout the stream after passing the fence, and all coho were subject to the same natural mortality rate irrespective of mark status. Figures in columns 8 and 9 of Table 1 thus represent the numbers of live coho and live marked coho *available* to surveyors at all locations, 1 d or more *after* passing the fence.

The proportion of the population bearing marks at any time is a function of marking rates used at the fence, natural mortality patterns, and the influx of coho during floods. In Table 1, a fixed fraction of the coho enumerated were marked each day, and marked and unmarked coho had identical survival patterns, so the predicted marked proportion (column 10) was 80%, until the influx of coho during the flood caused the proportion to decrease to ~34%. During each census, 5% of the live coho were examined, so 12.1% of the total escapement and 11.4% of all marked coho were sampled during the season. Note that surveyors do not sample 5.4 coho or find 3.7 marks, which is why census counts always end up being integers. As a result, the mark proportions based on census counts do not always match the predicted proportions because of the effects of rounding errors which tend to increase as sample sizes decrease.

The relation between the escapement pattern and the census data presented holds true when certain assumptions are met. The assumptions made when constructing this example must also hold for the ES model to perform optimally under similar conditions: (*i*) marking and sampling do not affect the catchability, behavior, and survival of coho, (*ii*) coho do not lose their marks prior to recovery, (*iii*) all marks observed in samples are reported, (*iv*) marked coho are sampled at random and have the same probability of recapture as unmarked coho after release, (*v*) groups of coho entering the stream on different days (*run segments*) are subject to the same survival pattern during the subsequent period of stream residency, and (*vi*) all coho entering the stream are intercepted and counted at the fence when it is operational. Under field conditions, some of these assumptions are inevitably violated to some extent, even when precautions are taken to minimize the violations. The robustness of the ES model to such deviations is therefore of interest and is assessed in the following sections.

Model Attributes

The ES model relies on a numerical simulation process to reconstruct the buildup of the population and its subsequent decline based on fence counts, the number of undetected coho, their immigration rate, and the survival patterns of marked and unmarked fish. For each set of parameter values (i.e., hypothesis), time series of total abundance and mark proportions are predicted. Discrepancies between the predicted proportions and those observed in all censuses are quantified by calculating the probability of the census data given the predicted and expected observations.

In the absence of empirical data on survival patterns from tagging operations, some survival pattern after stream entry must be hypothesized based on theoretical considerations. Field studies conducted on Vancouver Island during 1985–90 indicated that the mean stream residency period for coho ranged from 1 to 3 wk, with some coho surviving a few hours, and others as long as 6 wk (Labelle 1990; Irvine et al. 1992). Other investigators reported comparable figures and positively skewed distributions of survival periods (Willis 1954; Crone and Bond 1976; Johnston et al. 1986), but little is known on the shape of the distribution of stream residencies (Perrin and Irvine 1990). In the absence of an established standard, the ES model uses the log-normal to describe the probability of dying during the stream residency period. The log-normal has been used to model biological processes with skewed distributions and lower bounds ≥0, including the survival of salmonids over successive time periods (Hilborn and Walters 1992). The log-normal has two parameters (ϕ, σ), respectively set at 15 and 0.7 to construct the Table 1 example (Fig. 1). Unless the ES model user specifies otherwise, each run segment conforms to the same survival pattern irrespective of mark status. This assumption is not entirely unrealistic, particularly when most coho enter the stream within a few days, efforts are made to minimize marking stress, and there is no mark loss.

The total number of undetected immigrants (E) represents an ES model parameter that must be estimated. If two or more floods occur during the season, only a fraction of E may enter the stream during each day of flooding. Each corresponding fraction (p_d) is an ES model parameter that must be estimated if data from other sources (sonar data, fishway counts, snorkel counts, index counts, etc.) are not available to provide close approximations. In Table 1, there were 600 undetected immigrants, and the successive p_d were 0.5, 0.25, 0.083, 0.083, and 0.083.

Each hypothesis evaluated by the ES model thus consists of a prediction generated from several parameters to account for mortality rates (ϕ, σ), the number of undetected immigrants (E), and the immigration pattern of the undetected group (**p**). Based on the fence statistics and the hypothesized parameter values, the ES model "predicts" future trends in abundance and the corresponding mark proportions. As will be shown, the predicted trajectories provide the user with an important visual diagnostic tool, which can help assess the plausibility of each hypothesis. Ancillary data from field observations can also be used by ES model to further restrict the number of "unrealistic" hypotheses evaluated. The maximum likelihood hypothesis is found by searching over all hypotheses and provides the escapement estimate.

Mathematical Structure

Given the enumeration and marking statistics associated with the fence operations (vectors **f** and **m**), and the hypothesized set of parameter values (E, **p**, ϕ, σ), the number of coho entering the stream on each day d is predicted from

$$(1)\quad \hat{f}_d = f_d + (E \cdot p_d).$$

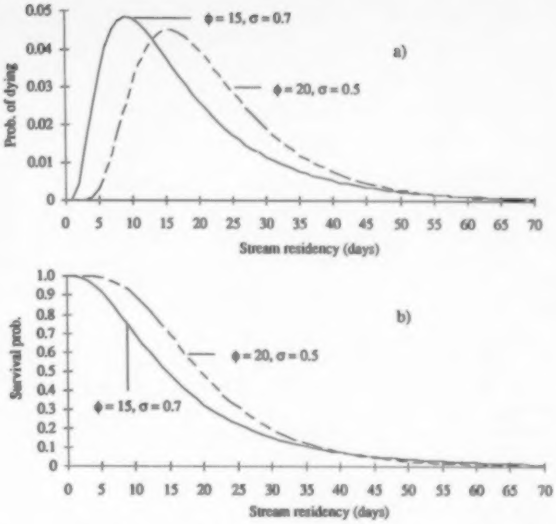

FIG. 1. (a) Probability of dying against time and (b) corresponding survival curves for two hypothetical populations with different stream residency parameters ϕ and σ.

If the probability of dying on the xth day after stream entry conforms to the log-normal, the numbers of live coho and marked coho available for sampling on day d are predicted from

$$(2)\quad Q(x) = \frac{1}{x\sigma\sqrt{2\pi}} \exp\left[\frac{-\{\log_e(x/\phi)\}^2}{2\sigma^2}\right]$$

$$(3)\quad S(x) = 1 - \int_0^x Q(x)\,dx$$

$$(4)\quad \hat{n}_d = \sum_{x=0}^{d-1} \hat{f}_x \cdot S(d-x)$$

$$(5)\quad \hat{m}_d = \sum_{x=0}^{d-1} m_x \cdot S(d-x).$$

When samples obtained during the subsequent censuses are independent of each other, and each fish has an independent and equal probability of capture during each census, the likelihood of the hypothesis data is given by

$$(6)\quad L(E, \mathbf{p}, \phi, \sigma, \mid \mathbf{f}, \mathbf{m}, \mathbf{c}, \mathbf{r}) = \prod_{t=1}^{T} \binom{c_t}{r_t} \left(\frac{\hat{m}_t}{\hat{n}_t}\right)^{r_t} \left(1 - \frac{\hat{m}_t}{\hat{n}_t}\right)^{c_t - r_t}$$

Ignoring terms that do not depend on the parameters, the log-likelihood function of the full parameter vector hypothesized reduces to

$$(7)\quad \ell(\Phi) \propto \sum_{t=1}^{T} \left\{ \log_e\left(\frac{\hat{m}_t}{\hat{n}_t}\right) + (c_t - r_t)\log_e\left(1 - \frac{\hat{m}_t}{\hat{n}_t}\right) \right\}.$$

Note here that the predictions $\hat{m}_t$ and $\hat{n}_t$ depend on the parameters through the accounting procedure illustrated in Table 1. The log-likelihood of various hypotheses can be obtained by evaluating Eq. 7 over a range of parameter values. This "grid search" method is sufficient when fitting simple models to data (Hilborn and Walters 1992, chap. 6). A simple search algorithm for escapement estimation is given in the appendix and works best when only E, ϕ, and σ must be estimated (one flood, so $p_d = 1.0$, or when every p_d is known a priori). When two or more floods occur during the season, $\mathbf{p}$ must be estimated if the number of undetected immigrants cannot be approximated from other sources. For such cases, nonlinear function minimization routines should be used to estimate all parameters more efficiently. The number of parameters estimated in such cases is equal to the number of floods plus 2 because for the last flood, the proportion is obtained indirectly (=1 minus the sum of p_d over all other flood days).

The parameter estimates are obtained by maximizing the log-likelihoods subject to the constraints $\phi > 0$, $\sigma > 0$, $\hat{n}_t \geq c_t$, and $\hat{m}_t \geq r_t$. The largest $\ell(\Phi)$ defines the maximum likelihood estimate ($\hat{\Phi} = \hat{E}, \hat{\mathbf{p}}, \hat{\phi}, \hat{\sigma}$) and the escapement estimate ($\hat{N} = F + \hat{E}$). Ancillary data can be used to impose further constraints and reduce the plausibility of "unrealistic" hypotheses. For instance, complementary field observations may indicate that on certain dates, the number of live coho in the stream is $\leq n_d^*$ or $\geq n_d^{**}$. A penalty function (Bard 1974) can be incorporated into the likelihood maximization procedure to make use of such observations. This will be illustrated in the next sections by penalizing the log-likelihoods of certain hypotheses as follows:

$$(8) \quad \ell'(\Phi) = \ell(\Phi) - \left\{ \begin{matrix} \sum e^{\hat{n}_d - n_d^*} & \text{if } \hat{n}_d > n_d^* \\ & + \\ \sum e^{n_d^{**} - \hat{n}_d} & \text{if } n_d^{**} > \hat{n}_d \end{matrix} \right\}.$$

Confidence intervals for the parameter estimate can be obtained from the variance–covariance matrix of Φ, but Lebreton et al. (1992) recommended that these be derived instead from the likelihood profile. Aitken et al. (1989) gave a general description of this procedure, which was also used by Garthwaite and Buckland (1990) to compute the bounds associated with the mark–recapture estimates of population sizes. The same procedure is used here, which involves sequentially computing $\ell(\Phi)$ for increasing values of E. This is done automatically when grid searches are conducted. When a function minimization routine is used, E must be held fixed during each minimization and is incremented prior to each successive one.

A critical contour of the log-likelihood function defines the likelihood-based confidence region. This contour is given by $\ell(\hat{\Phi}) - 0.5\chi^2_{1-\alpha,\mathrm{df}}$ for the critical chi-squares at probability $1 - \alpha$ and df degrees of freedom (i.e., the difference in the number of parameters between the models compared). Confidence intervals for all parameters are obtained from the minimum and maximum values of $\hat{\Phi}$ on the critical contour (Ross 1990). Considering $\mathbf{p}$, ϕ, and σ as nuisance parameters, the 95% confidence intervals for $\hat{N}$ are computed from the extreme values of $\hat{E}$ that satisfy the condition $\ell(\Phi) - \ell(\hat{\Phi}) \leq -1.92$. All hypotheses that satisfy this condition form the set of "plausible" hypotheses. The likelihood profile for N is obtained by plotting the range of escapement levels against their corresponding maximum log-likelihoods, or alternatively against $\ell(\Phi) - \ell(\hat{\Phi})$.

Model Testing Procedures

The performance of the ES model was assessed by means of numerical simulations using constructed data sets representing particular conditions of escapement patterns, marking, and sampling regimes. Each case describes a "true" population history from which samples are drawn and estimates are generated. Cases 1–4 are simple scenarios used to show the effects of single factors on the accuracy of the parameter estimates under fixed sampling rates. Cases 5–7 represent more complex conditions characterized by prolonged flood periods and stochastic variation in sampling and mortality rates. For cases 5–7, 1000 Monte Carlo data sets were drawn from the population history, and escapement estimates were generated each time. A frequency distribution of the estimates was then produced for each case separately to show the precision and accuracy of the estimator under specific conditions.

For each Monte Carlo experiment, binomial random deviates were generated with the rejection method described by Press et al. (1992). All parameter estimates were found with the Simplex algorithm described by Press et al. (1992), by including Eq. 1–5 and 7 into the function *funk* of the *amoeba* subroutine. The estimates were nearly identical to those found with the grid search algorithm if the grid search step size increment was relatively small, and at least three function minimizations were done with different starting values to reduce the possibility of converging on a false (i.e., local) minimum.

Case 1

Case 1 examines the effects of sampling rates on escapement estimates. Escapement pattern and census periods were as in Table 1, but only a single flood occurred on 3 November during which 300 coho entered undetected. The remaining 300 coho that entered during 4–7 November were considered as having been enumerated. As a result, 81.25% of the run was enumerated, and the actual trends in abundance were as in Table 1. Fixed daily sampling rates were used during all eight censuses. The rates were progressively increased from 1.5 to 22%. The actual values for N, ϕ, and σ are 1600, 15, and 0.7, respectively. For comparative purposes, a second set of estimates was generated with the model of Gazey and Staley (1986), using their recommended procedure. This sequential Bayesian algorithms is designed mainly for estimating the abundance of closed populations.

Case 2

Case 2 shows how ancillary data can be used to improve the reliability of the escapement estimates. Escapement pattern and census periods were as for case 1. A fixed daily sampling rate of 16% was used during all eight censuses. It was assumed that two snorkel surveys were conducted during the survey period. These indicated the presence of ≥500 live coho on 11 November and ≤50 live coho on 30 December. Escapement estimates were generated by incorporating the penalty function (Eq. 8) into the ES model after setting n_{21}^{**} to 500 and n_{70}^{*} to 50. The actual numbers of live coho on these two dates were 687 and 26, and the actual values for N, ϕ, and σ were still 1600, 15, and 0.7, respectively.

Case 3

Case 3 examines the effects of flood duration. Escapement pattern and census periods were as for case 1. The flood starts on 4 November, but its duration was progressively increased from 1 to 5 d. Coho entered during 4–7 November according to the pattern in Table 1, but each run segment was included in the undetected group if flooding occurred on the day of entry. Thus, the fraction of the escapement enumerated at the fence decreased from about 81 to 62% for the 1- to 5-d flood. The actual trends in abundance were as shown in Table 1. Eight censuses were conducted with fixed daily sampling rates set to 8, 12, and 16%. Escapement estimates were generated with and without the use of ancillary data as described for case 2.

Case 4

Case 4 examines the effects of flood periodicity. Conditions were as for case 2, with only one flood lasting 3 d. The first 2-d flood was on 4–5 November during which 450 coho entered (as in Table 1). Another 50 coho entered undetected on the third flood day that was on either 6, 7, or 8 November. The actual trends in abundance were as in Table 1. Eight censuses were conducted with fixed daily sampling rates set to 8, 12, and 16%. To show the merits of continued marking after floods, a second set of estimates was generated under the same conditions except that 20 coho were marked on each of the last 2 d of complete enumeration. The same overall marking effort was maintained by reducing the number of marks applied on 23 October to 280 instead of 320.

Case 5

Case 5 examines the combined effects of prolonged floods (5 d) and variation in daily sampling rates. Escapement pattern, census periods, and flood periods were as for Table 1. The three sampling conditions simulated were as follows:

(a) The fraction of the population sampled during each census was a binomially distributed random deviate centered around a mean sampling rate of 8%. The mark proportion in each sample was a binomially distributed random deviate centered on the actual mark proportion.

(b) The fraction of the population sampled during each census was a uniformly distributed random deviate within ±50% of a mean sampling rate of 8%. The mark proportion in each sample was a binomially distributed random deviate centered on the actual mark proportion.

(c) Inverse censuses (Ricker 1975, p. 76) are conducted, so sampling ends when a fixed number of marked coho are recovered. This number was set to 18, so that, on average, the total number of marked coho caught during all censuses was similar to that in a and b. The number of coho examined during each census was set to 18 times the reciprocal of the mark proportion, with the later being a binomially distributed random deviate centered on the actual mark proportion.

For a–c, escapement estimates were first generated without the use of ancillary data. A second set of estimates was then generated with the use of ancillary data as described under case 2.

Case 6

Case 6 examines the combined effects of prolonged floods (5 d) and variation in sampling rates and mortality rates. Conditions were as for case 5, except that stochastic variation in mortality rates was added. Each coho entering the stream was assigned a residency period of x days selected at random from the survival curve (Fig. 1b) with the transformation method described by Press et al. (1992). Monte Carlo trials were conducted as for case 5, for all three sampling conditions, with and then without the use of ancillary data.

Case 7

Case 7 examines the combined effects of prolonged floods (5 d), variation in sampling rates and mortality rates, and differential mortality of marked and unmarked coho. Conditions were as for case 6, except that the mortality parameters for the unmarked coho were set to $\phi = 15$ and $\sigma = 0.7$ and those of the marked coho were set to $\phi = 13$ and $\sigma = 0.7$. Thus the marked group had a lower mean stream residency as if the stress caused by marking had reduced the expected survival. Each coho entering the stream was assigned a residency period of x days selected at random from its respective survival curve. Monte Carlo trials were conducted for all three sampling conditions, with and then without the use of ancillary data.

Case 8

Case 8 examines the effects of prolonged floods (5 d), variation in sampling and mortality rates, and misrepresentation of the actual mortality patterns. Conditions were as for case 6, except that the actual residency period of each coho was a random deviate obtained from $N(16,0.5) \cdot e^{N(0,1)}$, which is a combination of a normal distribution ($\bar{x} = 16$ d, $s = 0.5$ d) and a normalized error. The error was added to ensure that the distribution of stream residencies for the population would be positively skewed as observed in various field studies. The mode, mean, and standard deviation of the resulting distribution were ~7, 20, and 17 d, respectively. Escapement estimates were generated with the ES model on the assumption that mortality rates conformed to the lognormal, so the investigator would be estimating escapement based on the "wrong" pattern. Monte Carlo trials were conducted for all three sampling conditions, with and then without the use of ancillary data. It was assumed that the two snorkel survey estimates indicated >600 and <200 live coho in the stream on 11 November and 30 December, respectively, with the actual numbers being 891 and 139.

When describing the simulation results, the discrepancy between the actual and estimated escapement will be termed relative error $\{= |(N - \hat{N}) \cdot N^{-1}|\}$. The discrepancy between the actual and the mean estimated escapement from the Monte Carlo trials will be termed relative bias $\{= |(N - \bar{\hat{N}}) \cdot N^{-1}|\}$. The 95% quantile range will refer to the 2.5 and 97.5% quantiles of the cumulative frequency distributions of the parameter estimates from the Monte Carlo trials.

Results

Case 1

Increasing sampling rates tended to reduce the relative error of the ES model escapement estimates (Fig. 2a). The relative error was within 13% at the lowest sampling rates, but decreased to 3% at the maximum sampling rates. Rounding errors that occur during the computations were largely responsible for the amount of relative error obtained. For sampling rates of 5%, the number of coho and marked coho examined should add up to 43.24 and 34.59 on 29 October, 51.48 and 23.25 on 5 November, and so on. When these figures were supplied to the ES model as sampling statistics, all parameter estimates matched the actual parameter values. However, since census data consist of integers, some rounding error is inevitable. The effects of rounding errors are minimized by increasing the sampling rates, but large errors are not always obtained with low sampling rates (see sampling rate = 1.5%).

The confidence intervals of the escapement estimates also decreased with increasing sampling rates. The lower bounds

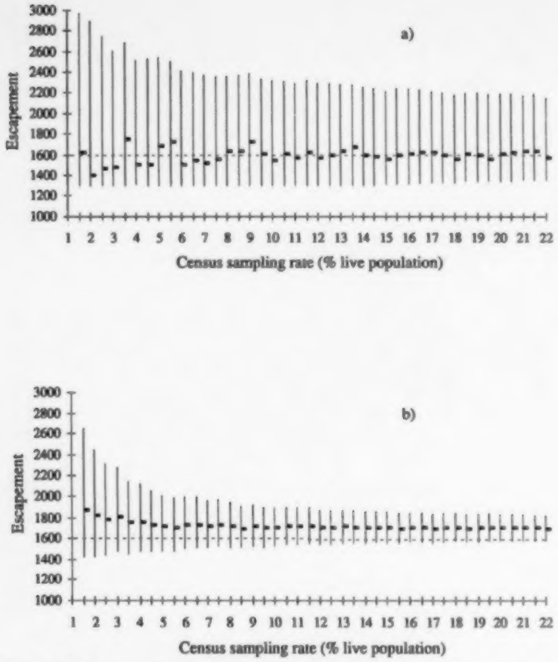

FIG. 2. Escapement estimates against census sampling rates for the (a) ES model and (b) Bayesian model. End points of the vertical bars indicate the upper and lower bounds of each escapement estimate (middle boxes). The horizontal broken line indicates the actual escapement.

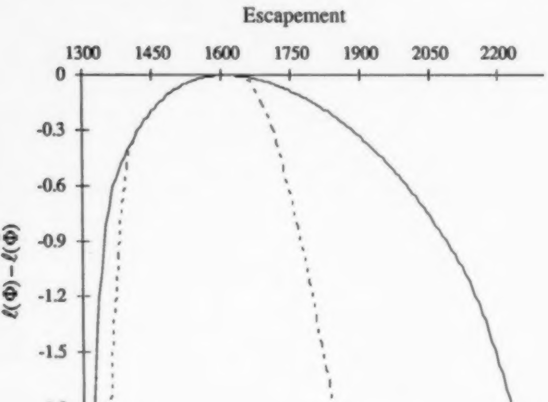

FIG. 3. Likelihood profiles obtained based on the conditions described in case 1 and a 16% daily sampling regime. The solid curve represents the profile obtained without any constraint. The broken line represents the profile obtained by implementing additional constraints based on ancillary data. The lower horizontal broken line marks the critical contour that crosses the upper and lower bounds of the escapement estimate.

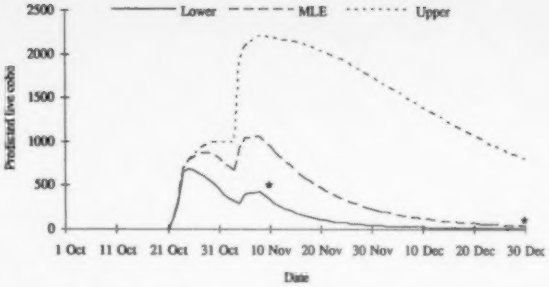

FIG. 4. Number of live coho in the stream during the census period as predicted by three hypotheses under conditions described in case 1, with a 16% daily sampling regime. The two stars represent the snorkel survey estimates of the numbers of live coho in the stream.

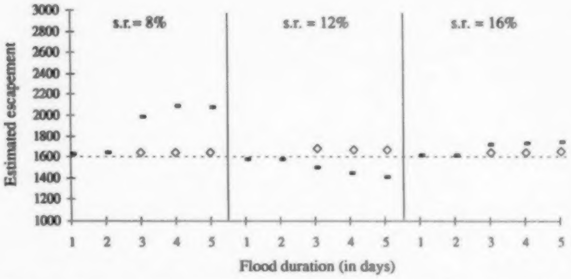

FIG. 5. Escapement estimates in relation to the flood duration and sampling rates (s.r.). The diamonds and boxes, respectively, correspond to the estimates obtained with and without the use of ancillary data. The horizontal broken line represents the actual escapement.

overlapped with the fence count until sampling rates reached ~15%, which often occurs when a large fraction of the escapement is enumerated and marked at the fence. In reality, when the number of unmarked coho examined during all censuses $(C - R)$ exceeds the number of unmarked coho enumerated at the fence $(F - M)$, the known minimum escapement is equal to $F + (F - M) + (C - R)$. For some sampling rates, the known minimum escapement was slightly larger than the lower bound computed solely from the likelihood function. The upper bounds decreased progressively with increasing sampling rates and were always wider than the lower bounds. Unsymmetrical bounds are a common feature of many traditional mark–recapture estimates of population sizes (see Ricker 1975, chap. 3).

Escapement estimates obtained with the closed population model always exceeded the actual escapement (relative error = 6–17%) and did not converge towards the actual escapement when daily sampling rates were >8.5% (Fig. 2b). The bounds decreased with increasing sampling rates and were narrower than those of the corresponding ES model estimates. The Bayesian model estimates and associated bounds were very similar to those obtained with Bailey's (1951) pooled Petersen-type estimator, with confidence intervals estimated by the method of Seber (1982, p. 63). Thus, even under fairly ideal conditions with a single flood, high mark proportions, no differential mortality, and large census sample sizes, closed population models can overestimate escapements. Additional simulations revealed that when a large portion of the run enters undetected several days after marking has ended, the relative error of the Bayesian estimates can be considerably larger, and the bounds may even fail to include the actual escapement.

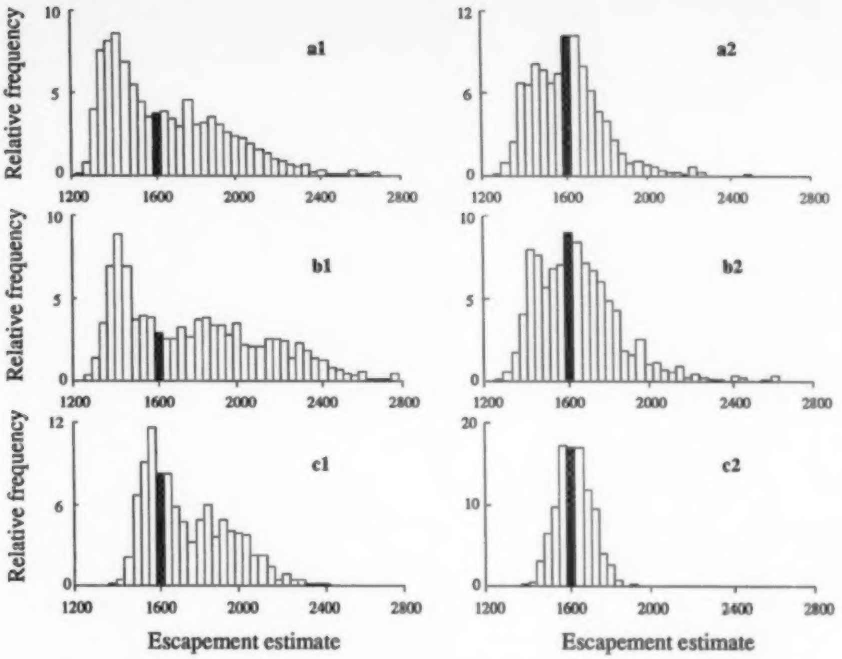

FIG. 6. Frequency distributions of escapement estimates from Monte Carlo trials based on (a) binomially distributed sampling rates, (b) uniformly distributed sampling rates, or (c) inverse censuses with binomially distributed sampling rates. Numeric suffixes indicate if ancillary data were used for estimation (1 = no, 2 = yes). The dark vertical bar represents the actual escapement.

Case 2

The likelihood profile generated by the ES model using no ancillary data and a fixed daily sampling rate of 16.0% is given in Fig. 3. An examination of the parameter values of "plausible" hypotheses within the bounds will often reveal some correlation between some parameters such that hypotheses with relatively low N have low ϕ and high σ values, while those with a relatively high N have higher ϕ and lower σ. Even in the absence of empirical data on survival patterns, the abundance patterns predicted by each hypothesis (column 8, Table 1) can help determine if the estimates of ϕ and σ are realistic. Figure 4 shows that the upper and lower bound hypotheses predicted radically different trajectories of abundance, which were considered plausible given the available census data. Note that the abundance predicted by the lower bound hypothesis on 10 November is lower than the snorkel survey estimate, while that of the upper bound hypothesis vastly exceeds the second snorkel survey estimate.

Incorporating the ancillary data into the estimation process lead to the elimination of hypotheses that predicted abundances lower than the first snorkel survey estimate and higher than the second survey estimate. This is reflected in the shape of the likelihood profile (Fig. 3), as the broken curve is considerably narrower than the solid curve. The range of parameter values associated with the set of "plausible" hypotheses was reduced from 7.3–23.7 and 0.57–0.82 to 9.62–22.4 and 0.51–0.72 for ϕ and σ, respectively. In this case, the estimated escapement did not change, but a considerable gain in precision was achieved.

Case 3

Only protracted floods (≥3 d) had substantial effects on the accuracy of escapement estimates, when coho entered the stream throughout the flood period (Fig. 5). The relative error was greatest at lower sampling rates for floods of comparable duration. The width of the associated bounds (not shown) increased with longer flood periods or lower sampling rates. Discrepancies between the actual and estimated escapements increased with longer flood periods. This results from there being less information on the overall immigration pattern. The function minimization converged towards an immigration pattern that provided the best fit to the mark proportions of the largest samples, since these have a greater effect on the overall likelihood. Under such conditions, it is not uncommon to have a best fitting hypothesis composed of parameter estimates with extreme values. The use of ancillary data can reduce the plausible parameter space, and in the process, prevent some local minima from blocking convergence towards the actual parameter values. Making use of the available ancillary data reduced the relative error of the escapement estimates for all three sampling rates under protracted flood conditions (Fig. 5). Using ancillary data can thus help increase both the precision and accuracy of escapement estimates generated by the ES model.

Case 4

The day on which the last group of undetected coho entered the stream had negligible effects on the relative error of the escapement estimates for sampling rates of 8, 12,

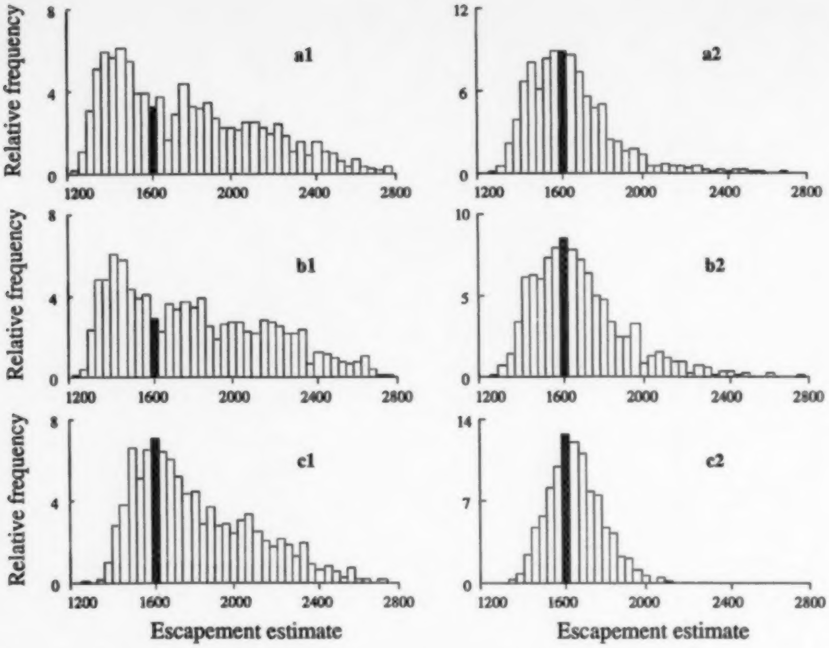

FIG. 7. Frequency distributions of escapement estimates from Monte Carlo trials involving variation in sampling and mortality rates (a–c as in Fig. 6). The dark vertical bar represents the actual escapement.

or 16%. Changes in relative error were not consistently larger or smaller. Applying 40 fewer marks on 23 October and marking instead 40 of the 100 coho that entered during 6–8 November generally improved in the accuracy of the escapement estimates. For instance, under fixed sampling rates of 8%, the relative error of the escapement estimate decreased from 21 to 9% when marks were applied. Additional simulations revealed that the influence of floods on the accuracy of escapement estimates is generally reduced if marking is continued after floods.

Case 5

When variation in sampling rates conformed to the binomial, the escapement estimates were biased by 3.3%, and the 95% quantile range was relatively wide (1240–2350, Fig. 6a1). When sampling rates varied uniformly about the mean rate, the escapement estimates were more biased (11.6%), and the 95% quantile range was wider (1310–2560, Fig. 6b1). With the inverse census regime, the bias was intermediate (8.7%), but the 95% quantile range was the narrowest (1440–2200, Fig. 6c1). The coefficients of variation (CV) for Fig. 6a1, 6b1, and 6c1 were 0.18, 0.21, and 0.12, respectively. The distributions associated with the three sampling conditions were positively skewed. Given the location of the modes, the investigator would have most likely underestimated the escapement, but less so if inverse censuses had been conducted. Incorporating ancillary data into the estimation process reduced the 95% quantile ranges by at least 300 coho for all three sampling conditions and reduced the relative biases to 6, 3, and 2% for Fig. 6a2, 6b2, and 6c2. The CVs were reduced to 0.11, 0.13, and 0.06, respectively, and all modes were well centered on the actual escapement.

Case 6

The frequency distributions of escapement estimates for specific conditions had similar shapes to their case 5 counterparts, but tended to have higher frequencies in the upper tails (Fig. 7). The 95% quantile ranges were larger, with CVs increasing to 0.22, 0.22, and 0.17 for Fig. 7a1, 7b1, and 7c1, respectively, and biases increasing to 11, 14, and 13%. Using ancillary data in the estimation process reduced the 95% quantile ranges, and CVs decreased to 0.13, 0.14, and 0.09 for Fig. 7a2, 7b2, and 7c2, respectively. The respective biases decreased to 9, 5, and 3%, and all three modes were well centered on the actual escapement. For the same overall sampling rates, more reliable estimates would have been obtained if inverse censuses had been conducted.

Case 7

Higher mortality rates on marked coho caused the ES model to substantially overestimate escapements under all conditions, with biases ranging from 24 to 50% (distributions not shown). The relative frequencies in the upper tails of each distribution increased even further to the right than shown in Fig. 7, and the upper limits of the 95% quantile ranges exceeded 3000 coho for all but the last condition (Fig. 7c2). The modes were generally located over the 1600–2000 range, indicating that the investigator would most likely have overestimated escapements. Using ancillary data to estimate escapements always reduced the quantile ranges, but did not always reduce the bias. The ES model is strongly affected by differential mortality under the conditions described.

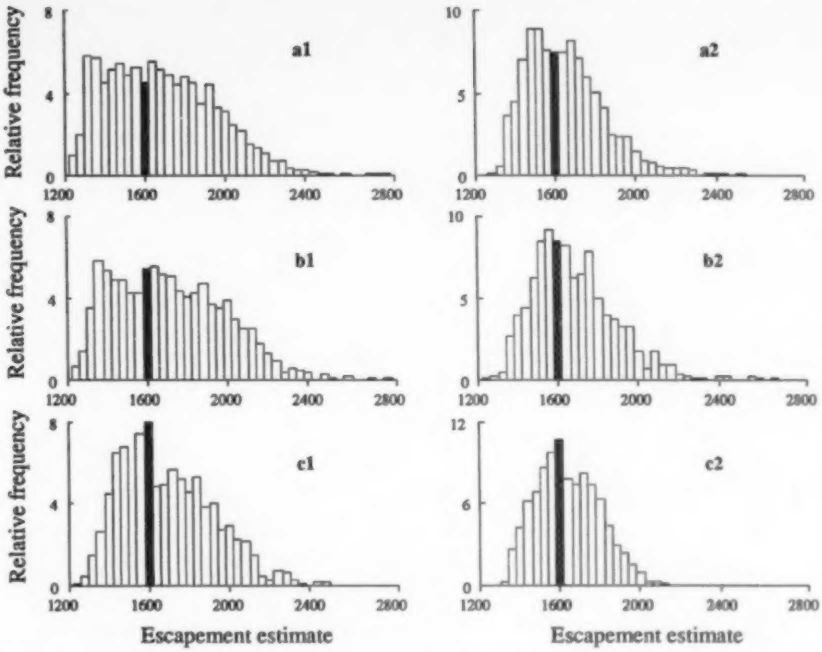

FIG. 8. Frequency distributions of escapement estimates from Monte Carlo trials involving variation in sampling and mortality rates, combined with misrepresentation of the actual survival pattern (a–c as in Fig. 6). The dark vertical bar represents the actual escapement.

Case 8

The frequency distributions of escapement estimates for specific conditions had similar shapes to their case 6 counterparts, but tended to be more platykurtic (Fig. 8). The 95% quantile ranges were slightly narrower, with CVs of 0.16, 0.16, and 0.13 for Fig. 8a1, 8b1, and 8c1, respectively, and biases of 4, 6, and 4%. Using ancillary data in the estimation process reduced the 95% quantile ranges, reduced the CVs to 0.12, 0.12, and 0.10 for Fig. 8a2, 8b2, and 8c2, respectively, and reduced the respective biases to 2, 4, and 1%. All three modes were well centered on the actual escapement. The locations of the modes indicate that when actual survival patterns are misrepresented, the actual escapement would most likely be underestimated under the conditions described, unless inverse sampling and ancillary data had been used jointly.

Discussion

The accuracy and precision of escapement estimates based on fence counts and mark–recapture surveys are a complex function of run sizes, immigration rates, flood patterns, marking and sampling regimes, census periodicity, and mortality rates. The mark–recapture model selected for estimation purposes should be structured to account for these processes. The ES model was designed to meet such criteria and to provide escapement estimates even when too few successive recaptures are obtained to use traditional open population models.

The simulation results confirm that accurate estimates of coho escapement can be obtained with the ES model under certain conditions despite protracted flood events and variation in daily sampling rates, mark proportions, and stream residencies. Incorporating ancillary data into the estimation process can substantially improve the accuracy and precision of the estimates. This should not be viewed as adding subjectivity into the estimation process, but rather as a way of capitalizing on external sources of data available to the investigator. The ES model provides a quantitative framework that uses these data to constrain the plausible parameter space. Bard (1974) recommended the generous imposition of such constraints, as it "exerts a beneficial influence on the convergence of an optimization algorithm" and "prevents it from bogging down in the irrelevant region of the parameter space."

Escapements were estimated here by making minimal use of the ancillary data. Under typical field conditions, there may be additional sources of ancillary data available. For instance, Labelle (1990) noted that in some Vancouver Island streams, >95% of the coho had died by January, irrespective of the season, run timing, or run size. Coho entering the stream often aggregated below the fence until freshets and floods and were counted visually while holding. Under such conditions, constraints could be incorporated into the ES model to reject hypotheses that predict excessive abundance levels after certain dates. The counts could also be considered sufficiently reliable to approximate **p**, or alternatively, set reasonable bounds on the permissible range for each p_d. The recovery of a few serially numbered tags could also provide sufficient data to set reasonable bounds on the permissible ranges for the two survival rate parameters. Other sources of ancillary data might include sonar indices, fishway counts, aerial survey indices, and even the number of carcasses.

The use of ancillary data combined with intensive marking and sampling is not always sufficient to obtain accurate escapement estimates. Differential mortality rates on marked and unmarked coho can affect of the performance of the ES model if not accounted for. This dictates that precautions be taken to minimize the possibility of differential mortality. Applying serially numbered tags (as opposed to opercular marks) can cause considerable stress on the marked group. Unless one expects to successfully quantify tagging effects, it might be advisable to minimize the number of serially numbered tags applied and rely on the ES model for estimation purposes.

Successive recaptures of tagged individuals are usually needed to determine the shape of the distribution of stream residencies and test for differences in mortality rates between marked and unmarked coho. In the absence of empirical data on the die-off patterns of various segments of the run, it is tempting to assume that survival patterns conform to those observed in neighboring streams or during past seasons. Unfortunately, several studies have indicated that the stream residency periods of coho may vary considerably among streams within a year and among years for a specific stream (Bocking et al. 1988; Perrin and Irvine 1990; Irvine et al. 1992).

In view of this situation, theoretical arguments were used to justify the use of the log-normal to represent the distribution of stream residencies in the ES model. Other skewed distributions (beta, Weibull, etc.) could be used instead, but it remains to be demonstrated that these are more suitable than the log-normal and that the distribution of stream residencies does not conform to the log-normal. The simulation results indicate that under certain conditions, the ES model can provide accurate estimates of escapement even when stream residencies are not log-normally distributed. If the shape of the distribution can be empirically determined, or if early and late run segments exhibit different stream residency periods (see Neilson and Geen 1981), investigators can simply substitute Eq. 2 accordingly. Certain run segments composed of marked or unmarked coho could also be assigned specific survival patterns if these are known to be subject to different mortality rates (see Hamilton 1978). The ES model can thus be adapted to a certain extent. However, this model is not tailored for situations where there is emigration of individuals during the census period (as noted by Labelle 1992) or for situations where distinct run segments congregate in different sections of the stream.

Because the ES model assumes that marked and unmarked coho are well mixed, efforts should be made to obtain representative samples of the population during each census. Howard (1948) suggested that sampling efforts be randomly distributed over time and areas to meet this objective, but doing so may be impractical due to the inaccessibility of certain areas and the difficulty of sampling under certain conditions. It is often more practical to intersperse sampling effort at least spatially, since this generally serves the same purpose as randomizing sampling efforts (Hurlbert 1984).

Ideally, censuses should be distributed throughout the stream residency period to keep track of the mark proportions. In practice, it is not always easy to allocate the limited sampling efforts early in the season. This process could be facilitated to a certain extent by generating predicted trajectories of abundances halfway through the season. Based on the shape of the trajectories, and a few numerical simulations, one could assess the value of focusing sampling efforts at specific times to help discriminate between alternative hypotheses.

Sample sizes should be as large as possible to increase the precision of the estimates, as this tends to minimize the effects of variation in sampling and mortality rates. Efforts should be made to minimize variation in sampling rates, presumably by controlling effort as much as possible. Under the conditions described, the ES model provided more reliable estimates when inverse censuses were conducted. The benefits of this approach have been shown for other mark–recapture models (Seber 1982, p. 118). This approach is easier to implement than one based on fixed sampling rates, but since the abundance levels decline as the season progresses, sampling rates must be increased accordingly. Coho often aggregate near the spawning grounds late in the season, so higher sampling rates might be achieved with the same level of effort by concentrating activities in such areas.

It was beyond the scope of this study to assess the performance of the ES model under the whole spectrum of scenarios that one can encounter in the field. However, insight into the performance of the ES model under actual field conditions was obtained through a comparative study of escapement estimation methods. In the study reported by Irvine et al. (1992), escapement enumeration was conducted concurrently in several streams and years, with the fence counts providing minimum escapement estimates. Coho were marked by means of simple opercular holes to minimize marking and handling stress. The visual foot survey data were used to provide escapement estimates by means of the area-under-the-curve method (English et al. 1992). Mark–recapture estimates of escapement were generated with the ES, Bayesian, and Petersen models.

The ES model estimates were always based on ancillary data (snorkel and visual survey counts) which were used to set constraints on the immigration rates and the maximum numbers of live coho at certain times. In 11 out of 12 comparisons, the escapement estimates of the closed population models exceeded those of the ES model. Because closed population models tend to overestimate escapements (Simpson 1984), one could surmise that the actual escapements were lower, and closer to the ES model estimates, in accordance with the results of the present study. Estimates based on visual surveys were considered less accurate than the ES model estimates because they were occasionally lower than the fence count, unlike those obtained with the ES model. Such results do not demonstrate that the ES model estimates were more accurate in all cases, but they suggest that the ES model estimates are at least as reliable as those obtained with the two other methods.

Selectivity during the marking stage is undoubtedly one of the most important factors affecting the performance of closed population models in the context of escapement estimation. In anticipation of floods, a large number of marks are often applied during the early part of the run when water levels are low and coho are easily caught at the fence. As a result, marked coho tend to die and be removed sooner than unmarked coho which can escape undetected during floods later in the season. This situation can translate into a substantial reduction in the relative availability of marked coho for sampling, which can lead to an overestimation of abundance. By contrast, the ES model is structured to account for the immigration, marking, and mortality processes that often operate concurrently during the survey period.

Unfortunately, adequate data sets have not yet been obtained to compare the performance of the ES model with that of other open population models such as the one recently proposed by Schwarz et al. (1993). Investigations currently being initiated should provide the necessary data to conduct such comparisons and provide more information on the distributions of stream residencies. In view of the simulation results presented, the ES model appears to have unique features which make it particularly useful under certain conditions. Despite its limitations, it still provides a valuable tool to those faced with the prospect of having to rely on a closed population model for lack of alternatives.

Acknowledgments

This study was partly funded by grants from the Natural Sciences and Engineering Research Council of Canada awarded to Dr. Carl Walters (strategic grant G1475 and operating grant A5869). Sincere thanks are owed to Drs. Carl Walters and Don Ludwig for their support, objective criticisms, and constructive comments.

References

Aitkin, M., D. Anderson, B. Francis, and J. Hinde. 1989. Statistical modelling in GLIM. Oxford Statistical Science Series 4. Clarendon Press, Oxford. 374 p.

Bailey, N.J.J. 1951. On estimating the size of mobile populations from recapture data. Biometrika 38: 293–306.

Bard, Y. 1974. Nonlinear parameter estimation. Academic Press, New York, N.Y. 341 p.

Bocking, R.C., J.R. Irvine, K.K. English, and M. Labelle. 1988. Evaluation of random and indexing sampling designs for estimating coho salmon (*Oncorhynchus kisutch*) escapement to three Vancouver Island streams. Can. Tech. Rep. Fish. Aquat. Sci. 1639: 95 p.

Chapman, D.G. 1948. A mathematical study of the confidence limits of salmon populations calculated by sample tag ratios. Int. Pac. Salmon Fish. Comm. Bull. 2: 67–85.

Clark, D.G., and J.R. Irvine. 1989. Enumeration and coded wire tagging of coho salmon (*Oncorhynchus kisutch*) smolts leaving Black Creek, Vancouver Island, during 1978 and 1979, their subsequent distribution in sport and commercial fisheries and escapement to the creek in 1978–1980. Can. MS. Rep. Fish. Aquat. Sci. 2017: 45 p.

Cormack, R.M. 1968. The statistics of capture–recapture methods. Oceanogr. Mar. Biol. Annu. Rev. 6: 455–506.

Cousens, N.B., G.A. Thomas, C.G. Swann, and M.C. Healey. 1982. A review of salmon escapement enumeration techniques. Can. Tech. Rep. Fish. Aquat. Sci. 1108: 122 p.

Crone, R.A., and C.E. Bond. 1976. Life history of coho salmon, *Oncorhynchus kisutch* in Sashin Creek, southeastern Alaska. Fish. Bull. 74: 897–923.

DeLury, D.B. 1951. On the planning of experiments for the estimation of fish populations. J. Fish. Res. Board. Can. 8: 281–307.

DeLury, D.B. 1958. The estimation of population size by marking and recapture procedure. J. Fish. Res. Board Can. 15: 19–25.

Eames, M., and M. Hino. 1981. A mark–recapture study of an enumerated coho spawning escapement. Wash. Dep. Fish. Prog. Rep. 148: 1–22.

Eames, M.J., T.J. Quinn, and M. Hino. 1983. 1977 Northern Puget Sound adult coho and chum tagging studies. Wash. Dep. Fish. Tech. Rep. 75: 1–239.

English, K.K., R.C. Bocking, and J.R. Irvine. 1992. A robust procedure for estimating salmon escapement based on the area-under-the-curve method. Can. J. Fish. Aquat. Sci. 49: 1982–1989.

Fraser, F.J., P.J. Star, and A.Y. Fedorenko. 1982. A review of the chinook and coho salmon of the Fraser River. Can. Tech. Rep. Fish. Aquat. Sci. 1126: 130 p.

Garthwaite, P., and S.T. Buckland. 1990. Analysis of a multiple-recapture census by computing conditional probabilities. Biometrics 46: 231–238.

Gazey, W.J., and M.J. Staley. 1986. Population estimation from mark–recapture experiments using a sequential Bayes algorithm. Ecology 67: 941–951.

Hamilton, R.E. 1978. Black Creek, Vancouver Island, B.C. Hydrology, fisheries resource and watershed development. Fish. Mar. Serv. MS. Rep. 1484: 42 p.

Hilborn, R. 1990. Determination of fish movement patterns from tag recoveries using maximum likelihood estimators. Can. J. Fish. Aquat. Sci. 47: 635–643.

Hilborn, R., and C.J. Walters. 1992. Quantitative fisheries stock assessment. Chapman and Hall, New York, N.Y. 570 p.

Howard, G.V. 1948. A study of the tagging method in the enumeration of sockeye salmon populations. Int. Pac. Salmon Fish. Comm. Bull. 2: 1–66.

Hurlbert, S.H. 1984. Pseudoreplication and the design of ecological field experiments. Ecol. Monogr. 54(2): 189–211.

Irvine, J.R., R.C. Bocking, K.K. English, and M. Labelle. 1992. Estimating coho salmon (*Oncorhynchus kisutch*) spawning escapements by conducting visual surveys in areas selected using stratified random and stratified index sampling designs. Can. J. Fish. Aquat. Sci. 49: 1972–1981.

Johnston, N.T., J.R. Irvine, and C.J. Perrin. 1986. A comparative evaluation of fence count, mark–recapture and Bendix sonar estimates of salmon escapements in the Keogh River, a variable-flow coastal B.C. stream. Can. Tech. Rep. Fish. Aquat. Sci. 1453: 44 p.

Jolly, G.M. 1965. Explicit estimates from capture–recapture data with both death and immigration — stochastic model. Biometrika 52: 225–247.

Labelle, M. 1990. A comparative study of coho salmon populations of S.E. Vancouver Island, British Columbia. Juvenile outmigration, coded wire tagging and recovery, escapement enumeration and stock composition at Black Creek, Trent River and French Creek, 1984–1988. Can. Tech. Rep. Fish. Aquat. Sci. 1722: 148 p.

Labelle, M. 1992. Straying patterns of coho salmon (*Oncorhynchus kisutch*) stocks from southeast Vancouver Island, British Columbia. Can. J. Fish. Aquat. Sci. 49: 1843–1855.

Lebreton, J-D., K.P. Burnham, J. Clobert, and D.R. Anderson. 1992. Modeling survival and testing biological hypotheses using marked animals: a unified approach with case studies. Ecol. Monogr. 62(1): 67–118.

Minta, S., and M. Mangel. 1989. A simple population estimate based on simulation for capture–recapture and capture–resight data. Ecology 70: 1738–1751.

Neilson, J.D., and G.H. Geen. 1981. Enumeration of spawning salmon from spawner residence time and aerial counts. Trans. Am. Fish. Soc. 110: 554–556.

Pearse, P.H. 1982. Turning the tide. A new policy for Canada's Pacific fisheries. The Commission on Pacific Fisheries Policy. Final Report. Department of Fisheries and Oceans, Ottawa, Ont. 292 p.

Perrin, C.J., and J.R. Irvine. 1990. A review of survey life estimates as they apply to the area-under-the-curve method for estimating the spawning escapement of Pacific salmon. Can. Tech. Rep. Fish. Aquat. Sci. 1733: 49 p.

Press, W.H., S.A. Teukolsky, W.T. Vetterling, and B.P. Flannery. 1992. Numerical recipes. The art of scientific computing. 2nd ed. Cambridge University Press, Cambridge, U.K. 963 p.

Pritchard, A.L., and F. Neave. 1942. What did the tagging of coho salmon at Skutz Falls, Cowichan River, reveal. Prog. Rep. Fish. Res. Board Can. 51: 8–11.

Ricker, W.E. 1975. Computation and interpretation of Biological statistics of fish populations. Bull. Fish. Res. Board Can. 191: 382 p.

Ross, G.J.S. 1990. Nonlinear estimation. Springer-Verlag, New York, N.Y. 189 p.

Salo, E.O., and R.E. Noble. 1953. Minter Creek Biological Station. Progress Report (September–December, 1952). State of Washington Department of Fisheries. 25 p.

Schaefer, M.B. 1951. Estimation of size of animal populations by marking experiments. U.S. Fish. Wildl. Serv. Fish. Bull. 69: 190–203.

Schnabel, Z.E. 1938. The estimation of the total fish population of a lake. Ann. Math. Mon. 45: 348–352.

Schumacher, F.X., and R.W. Eschmeyer. 1943. The estimation fish populations in lakes and ponds. J. Tenn. Acad. Sci. 18: 228–249.

Schwarz, C.J., R.E. Bailey, J.R. Irvine, and F.C. Dalziel. 1993. Estimating salmon spawning escapement using capture–recapture methods. Can. J. Fish. Aquat. Sci. 50: 1181–1197.

SEBER, G.A.F. 1965. A note on the multiple-recapture census. Biometrika 52: 249–259.

SEBER, G.A.F. 1982. The estimation of animal abundance and related parameters. 2nd ed. Oxford University Press, New York, N.Y. 654 p.

SIMPSON, K. 1984. The accuracy of mark–recapture estimates of escapement. Can. Tech. Rep. Fish. Aquat. Sci. 1326: 209–225.

SYMONS, P.E.K., AND M. WALDICHUK. 1984. Proceedings of the Workshop Stream Indexing for Salmon Escapement Estimation, West Vancouver, B.C., 2–3 February 1984. Can. Tech. Rep. Fish. Aquat. Sci. 1326: 258 p.

WALTERS, C.J., AND P. CAHOON. 1985. Evidence of decreasing spatial diversity in British Columbia salmon stocks. Can. J. Fish. Aquat. Sci. 42: 1033–1037.

WALTERS, C.J., AND D. LUDWIG. 1981. Effects of measurement errors on the assessment of stock–recruitment relations. Can. J. Fish. Aquat. Sci. 38: 704–710.

WILLIS, R.A. 1954. The length of time that silver salmon spent before death on the spawning grounds at Spring Creek, Wilson River in 1951–52. Oreg. Fish. Comm. Res. Briefing 5: 27–31.

Appendix: Simple Grid Search Algorithm for Escapement Estimation Using the ES Model

When a function minimization routine is not available for parameter estimation, the following stepwise procedure can be used to search for the best fitting combination of parameters. This simplified procedure is for cases where there was a single flood ($p_d = 1$) or when each proportion p_d is known a priori. This procedure can be easily implemented on a microcomputer.

(1) Set up the statistics as in Table 1. The dimensions of vectors **f**, **m**, **c**, and **r** should equal the maximum period of stream residency, which is given by the period (in days) between the dates when the first coho enters the stream and when the last coho dies.

(2) For days with complete enumeration, enter a 0.0 in the corresponding rows of vector **p**. Enter 1.0 in the row corresponding to the single flood day, or enter proportions for each p_d in the rows corresponding to the days of flooding or fence damage if these can be approximated from visual surveys or other sources.

(3) Supply *realistic* minimum and maximum values for the hypothesized E. This minimum can be $C - R - (F - M)$ if the expression is >0. Determine the increment size between the maximum and minimum values for E. Set E_i to the minimum.

(4) Supply *realistic* minimum and maximum values for the hypothesized survival rate parameters (ϕ, σ). For coho, realistic bounds are 3–50 d for ϕ and 0.1–1.2 for σ. Set the number of increments between the maximum and minimum values of each parameter. The range divided by the increments is the step size. For a start, try 1-d step sizes for ϕ and 0.025-d step sizes for σ, which translates into 37 increments for j and 44 for k. Set ϕ_j and σ_k to their minimum.

(5) Predict the $\hat{f}_d$ for each day from E_i and **p** (Eq. 1).

(6) Given ϕ_j and σ_k, calculate S_x for $x = 1, 2, \ldots, D$ days (Eq. 2 and 3).

(7) Predict $\hat{n}_d$ and $\hat{m}_d$ for each remaining day of the season (Eq. 4 and 5).

(8) If $c_t > \hat{n}_t$ or $r_t > \hat{m}_t$ (or other conditions not met), go to step 11.

(9) Calculate the log-likelihood of the full parameter vector (E, **p**, ϕ, σ) or hypothesis (Eq. 7).

(10) Store values to eventually determine the maximum log-likelihood and likelihood profiles.

(11) If $\sigma_k <$ maximum σ, add step size to σ, set $k = k + 1$, and go to 6.

(12) Set σ_k to minimum. If $\phi_j <$ maximum ϕ, add step size to ϕ, set $j = j + 1$, and go to 6.

(13) Set σ_k and ϕ_j to minimum. If $E_i <$ maximum E, add step size to E, set $i = i + 1$, and go to 5.

The above procedure yields an output matrix with records consisting of unique parameter combinations and the associated log-likelihood. Substitute the values under the parameter E column by $F + E$ to obtain escapement levels. Sort the matrix from the lowest to the highest escapement, and identify the greatest log-likelihood value associated with each escapement. Generate a plot of the greatest log-likelihoods against their corresponding escapement. This is the likelihood profile. The escapement with the maximum log-likelihood is the MLE of escapement. Determine the log-likelihood associated with the upper and lower bounds of the MLE by adding −1.92 to the log-likelihood of the MLE. Identify the escapement levels above and below the MLE which match the boundary value. These are the upper and lower bounds of the escapement estimate.

Inspect the parameter values and predicted trajectories of the MLE and its bounds. If anomalies are detected (extreme parameter values, unrealistic trends), impose further constraints (step 8) if possible to reduce the domain of the parameter space, and repeat the simulation process. If there is a discontinuity or sharp cutoff in the likelihood profile, respectively increase the level of resolution (more increments) and the parameter space, and repeat the simulation process.

If all p_d values for flood days cannot be approximated from other sources, modify the above routine as follows. Ignore step 2, and enter 0.0 in all rows of **p** except on the first flood day which gets 1.0. Go to step 3 and proceed onwards. After step 13 has been completed, enter a different combination of p_d values for the flood days in **p** using a maximum step size of 0.05 such that $\Sigma p_d = 1.0$. Go back to step 3 and proceed onwards. Repeat this loop until all possible combinations of p_d have been tested. It may be computationally more efficient to incorporate the ES model into a function minimizer to estimate all parameters. This procedure is too complex to describe here in detail, but a copy of the FORTRAN 77 computer code of the ES model with a built-in Simplex function minimization routine can be obtained from the author.

Liver Glycogen, Enzyme Activities, and Pancreatic Hormones in Juvenile Atlantic Salmon (*Salmo salar*) during Their First Summer in Seawater[1]

Erika M. Plisetskaya[2]

School of Fisheries HF-15, University of Washington, Seattle, WA 98195 USA

Thomas W. Moon

Department of Biology, University of Ottawa, Ottawa, ON K1N 6N5, Canada

Donald A. Larsen

Northwest Fisheries Science Center, 2725 Montlake Blvd. E., National Marine Fisheries Service, Seattle, WA 98112 USA

Glen D. Foster

Department of Biology, University of Ottawa, Ottawa, ON K1N 6N5, Canada

and Walton W. Dickhoff

School of Fisheries HF-15, University of Washington, Seattle, WA 98195 USA
and
Northwest Fisheries Science Center, 2725 Montlake Blvd. E., National Marine Fisheries Service, Seattle, WA 98112 USA

Plisetskaya, E.M., T.W. Moon, D.A. Larsen, G.D. Foster, and W.W. Dickhoff. 1994. Liver glycogen, enzyme activities, and pancreatic hormones in juvenile Atlantic salmon (*Salmo salar*) during their first summer in seawater. Can. J. Fish. Aquat. Sci. 51: 567–576.

Our observation of very low liver glycogen concentration in 1-yr-old feeding Atlantic salmon (*Salmo salar*) in seawater net-pens in Puget Sound, Washington, led to studies of their metabolic status. We assessed liver glycogen concentration, activities of some hepatic enzymes involved in glycogen synthesis, depletion, and gluconeogenesis, and plasma profiles of glucose and pancreatic hormones (insulin and glucagon) in yearling Atlantic salmon before and after seawater transfer. Liver glycogen concentration in Atlantic salmon during the several months after seawater entry was much lower than in coho salmon (*Oncorhynchus kisutch*) of the same age in seawater. Other metabolic and hormonal indices throughout the study did not differ substantially between the two species. During their first summer in seawater net-pens, seemingly healthy, feeding 1-yr-old Atlantic salmon smolts are prone to high mortality. We hypothesize that the virtual absence of glycogen reserves in the liver makes seawater-adapted 1-yr-old Atlantic salmon juveniles particularly susceptible to stress and may contribute to high summer mortality.

La présence d'une très faible concentration de glycogène dans le foie chez le saumon atlantique (*Salmo salar*) âgé de 1 an en phase d'alimentation et placé dans des parcs marins dans le Puget Sound (Washington) a permis la réalisation d'études sur leur état métabolique. Nous avons évalué la concentration de glycogène dans le foie, l'activité de certaines enzymes hépatiques participant à la synthèse du glycogène, à sa diminution et à la gluconéogenèse et les profils plasmatiques du glucose et des hormones pancréatiques (insuline et glucagon) chez les saumons atlantiques de l'année, avant et après leur transfert en milieu marin. La concentration de glycogène dans le foie chez le saumon atlantique pendant plusieurs mois après son entrée en mer était beaucoup plus faible que chez le saumon coho (*Oncorhynchus kisutch*) du même âge en milieu marin. D'autres indices métaboliques et hormonaux au long de l'étude différaient très peu entre les deux espèces. Pendant leur premier été dans des parcs en filet placés en milieu marin, des smolts de saumon atlantique en phase d'alimentation, âgés de 1 an et apparemment en santé son sujets à une mortalité élevée. Nous avons émis l'hypothèse selon laquelle l'absence virtuelle de réserves de glycogène dans le foie rend les juvéniles de saumon atlantique âgés de 1 an, adaptés à la mer particulièrement vulnérables au stress et peut être responsable d'une forte mortalité en été.

Received December 21, 1992
Accepted October 6, 1993
(JB734)

Reçu le 21 décembre 1992
Accepté le 6 octobre 1993

Atlantic salmon (*Salmo salar*) has become a highly desirable salmonid species for marine net-pen culture in the Pacific Northwest. However, frequent observation of high mortality of juveniles during their first summer in seawater remains a concern (Dickhoff et al. 1989). High losses among juvenile Atlantic salmon of 1 yr of age

---

[1] Reported in part at the Annual Meeting of American Society of Zoologists, Atlanta, GA, 1991

[2] Author to whom correspondence should be addressed.

TABLE 1. Groups of salmon used in the study

Group	Source (brood year)	Date of seawater entry (age)	Samples collected (age)	Tissue collected
1	Atlantic salmon, Fish Hatchery, Washington, Department of Fisheries (1989)	April 15, 1991 (1+)	July, August, September 1991 (1+)	Liver, blood
2	Atlantic salmon Sea Fresh Farm, reared through smoltification at the Northwest Fisheries Science Center (1989)	June 17, 1991 (1+)	February, March, April, May, June, July, August, September 1991 (1+)	Liver, blood
.	Atlantic salmon, Sea Farm, Washington (1989)	April 15, 1991 (1+)	July 1991 (1+)	Liver, blood
	Atlantic salmon, Sea Farm, Washington (1990)	April 15, 1992 (1+)	May 1992 (1+)	Liver, blood, skeletal muscle
4	Atlantic salmon, Sea Farm, Washington (1988)	April 1990 (1+)	July 1991 (2+)	Liver, blood
5	Atlantic salmon, Global Aquafarm (1990)	November 1991 (0+)	March, April, June 1992 (1+)	Liver, blood, skeletal muscle
6	Atlantic salmon, Global Aquafarm (1990)	February 1992 (1+)	March, April, June 1992 (1+)	Liver, blood, skeletal muscle
7	Atlantic salmon, Global Aquafarm (1989)	February 1991 (1+)	June 1992 (2+)	Skeletal muscle
8	Coho salmon, Issaqua hatchery, Washington, reared through smoltification at the Northwest Fisheries Science Center (1989)	June 17, 1991 (1+)	February, March, April, May, June, July, August, September 1991 (1+)	Liver, blood

in seawater net-pens have been reported elsewhere, for example, Norway and the United Kingdom (Bruno et al. 1989; Aldridge 1991, Stradmeyer 1991).

When it occurs, summer mortality plagues all groups of 1-yr-old Atlantic salmon regardless of the time of seawater transfer. Summer losses are not related to the initial mortality caused by incomplete smoltification and subsequent osmoregulatory incompetence (Dickhoff et al. 1989; Franklin et al. 1992). Although in some years, summer mortality could be associated with either disease (Stradmeyer 1991) or specific environmental events such as blooms of noxious phytoplankton (Bruno et al. 1989; Rensel 1991), no consistent abnormalities in examined tissues could be found and no pathogenic agents could be consistently isolated from dead or moribund fish (M. Kent, R. Ellston, Battelle Pacific Northwest, Sequim, Wash., personal communication; L.W. Harrel, Costal Zone and Estuarine Studies Division, National Marine Fisheries Service, personal communication). We have observed that neither Atlantic salmon smolts entering seawater at 2-yr of age, nor 1-yr-old Pacific salmon (*Oncorhynchus* sp.) smolts seem to suffer as marked summer mortality as do yearling Atlantic salmon.

There are many reports and reviews on various aspects of carbohydrate (Wendt and Saunders 1973), lipid (Rowe et al. 1991), and water (Usher et al. 1988) metabolism, osmoregulation (Langdon and Thorpe 1985), and feeding patterns and digestion (Usher et al. 1990, 1991) in Atlantic salmon during their first summer in seawater. Again, no specific disorder, other than the presence of "nonstarters" (i.e., fish that do not resume feeding after seawater entry), has been found that could be considered a cause of mortality, and the "nonstarter" population cannot account for 24–43% of summer losses that remain unspecified (Aldridge 1991).

During the summers of 1989 and 1990, we noted almost undetectable concentrations (from 0.01 to 0.3 g/100 g liver weight) of liver glycogen in various groups of Atlantic salmon smolts transferred to seawater. Virtual absence of glycogen was found not only in the nonfeeding or moribund fish, but also in feeding and growing fish that had already spent up to 3 mo in seawater net-pens (W.W. Dickhoff and E.M. Plisetskaya, unpublished data). Fish kept in fresh water during the summer months retained liver glycogen concentration in the range of 2–4 g/100 g liver weight.

Low glycogen concentration in the liver of seawater 1-yr-old Atlantic salmon might have various causes. Therefore, we decided to investigate in greater detail glycogen metabolism of 1-yr-old Atlantic salmon smolts. We measured liver glycogen content which represents energy store and the source of plasma glucose under acute stress conditions (Plisetskaya 1975), plasma glucose levels, and activities of several liver enzymes essential for glycogen synthesis, breakdown, and gluconeogenesis. We also assessed the profiles of two pancreatic hormones: insulin, which is known for its strong anabolic (glycogenic and lipogenic) action, and glucagon, which is mostly a catabolic (lipolytic, glycogenolytic, and gluconeogenic) hormone (Plisetskaya et al. 1988; Plisetskaya 1990). All these factors were examined before and after seawater transfer of Atlantic salmon. For comparison, we also examined a group of coho salmon (*Oncorhynchus kisutch*) which are not susceptible to summer mortality.

Materials and Methods

We studied seven groups of Atlantic salmon, mostly smolts, of ages 1+ and 2+ from four different hatcheries or fish farms. Information about each group of fish is pre-

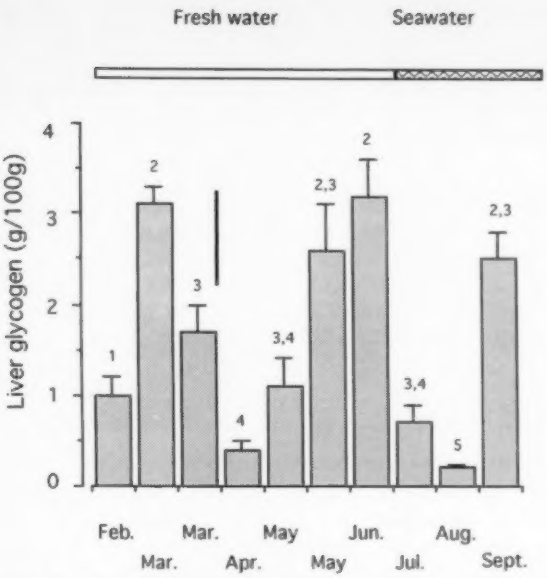

FIG. 1. Liver glycogen content in yearling Atlantic salmon (group 2, Table 1) during the parr-to-smolt transformation and subsequent transfer to seawater on June 17, 1991. Vertical bar: morphological smoltification. Here and in other figures, values are presented as mean ± SEM; values with a different superscript are significantly different from each other at $p < 0.05$.

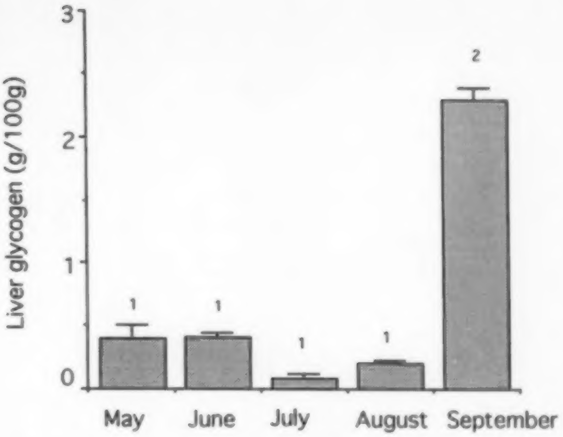

FIG. 2. Liver glycogen content in yearling Atlantic salmon (group 1, Table 1) in seawater (seawater transfer on April 15, 1991).

sented in Table 1. Most groups of Atlantic salmon were sampled one to three times between March and July. Group 5 consisted of fish transferred to seawater as underyearlings (see Saunders et al. 1990; Myrseth 1991) but sampled at age 1+. Group 7 was sampled only for glycogen in skeletal muscles. The samples were taken either 4–4.5 h (groups 3 and 4) or 12 h after last feeding. The surface water temperature in the net-pens ranged from 9.5°C in March to 11.0°C in July.

Two groups of fish, Atlantic salmon parr (group 2) and coho salmon parr (group 8), were reared through smoltification at the Northwest Fisheries Science Center, Seattle, under seasonally fluctuating water temperatures and natural photoperiod. Fish were fed standard rations of Oregon Moist Pellets (Moore Clarke Inc., La Conner, Wash.) at the rate of approximately 2% of body weight per day.

The developmental stages were determined according to Johnston and Saunders (1981) and Gorbman et al. (1982). Only fish with complete body silvering, darkened fin margins, and without parr marks were selected for the seawater transfer. Smolted coho and Atlantic salmon were transferred in aerated fresh water by tank truck (1-h travel time) to seawater (27–28‰) net-pens at Manchester. To minimize stress, fish were transferred directly to seawater in buckets (water-to-water transfer). The surface seawater temperature in the net-pens ranged from 9°C in April to 11.5°C in June and increased to the highest monthly average of 13°C during August–September. Atlantic and coho juveniles were sampled monthly from February to September 1991, except in March (before smoltification) and May (after smoltification), when they were sampled every 2 wk. The fish of both species were sampled simultaneously, approximately 12 h after last feeding.

All fish in groups 2 and 8 gained weight steadily except during the first month (July) in seawater when weights and lengths of Atlantic salmon increased by only 0.7 g and 3.7 cm, respectively. Coho salmon increased 0.6 g in weight and 0 cm in length. Although some individuals were observed to feed, many may have fasted for some time after seawater entrance (see Stradmeyer 1991). During the course of the experiment, group 2 Atlantic salmon increased from 78.4 ± 3.6 g in February to 227.4 ± 13.6 g in September; coho salmon weighed 13.2 ± 0.8 g in February and reached 93.9 ± 6.7 g in September.

The weights and lengths of group 1 Atlantic salmon were not measured during the first 2 mo in seawater, but the fish were observed to feed actively in seawater net-pens in May and throughout the rest of the experiment. During the course of the experiment, this group of fish grew from 89 g in April (average weight of 50 fish transferred to seawater by R. Hardy, Northwest Fisheries Science Center, Seattle, Wash., personal communication) to 348.2 ± 10.6 g (mean ± 1 SE; $n = 50$) in September.

Atlantic salmon in groups 3–7 were actively feeding in March–July when the samples were collected. The average weight of fish transferred to seawater in November at age 0 (group 5) in March was 341.0 ± 16.2 g and the final weight in June was 680 ± 72 g whereas fish that entered seawater as 1-yr-olds (group 6) had corresponding values of 123.8 ± 9.3 and 227.7 ± 22 g (10 fish for each sampling). Neither noxious phytoplankton blooms nor fish diseases were recorded during the summers of 1991 and 1992, and there was virtually no mortality of salmonids in seawater net-pens.

Tissue Samples

Twenty to 30 parr or 6–10 smolts were killed by a blow to the head. Fish weight and length were measured, and the presence of food in the stomach and intestine was noted.

In less than 2 min after removing fish from the water, the liver was excised and divided into two pieces with a cooled razor blade (for glycogen determination, we consistently used the section near the entrance of the hepatic portal vein). The liver samples were freeze-clamped on dry ice and transferred to a −60°C freezer for storage. Samples

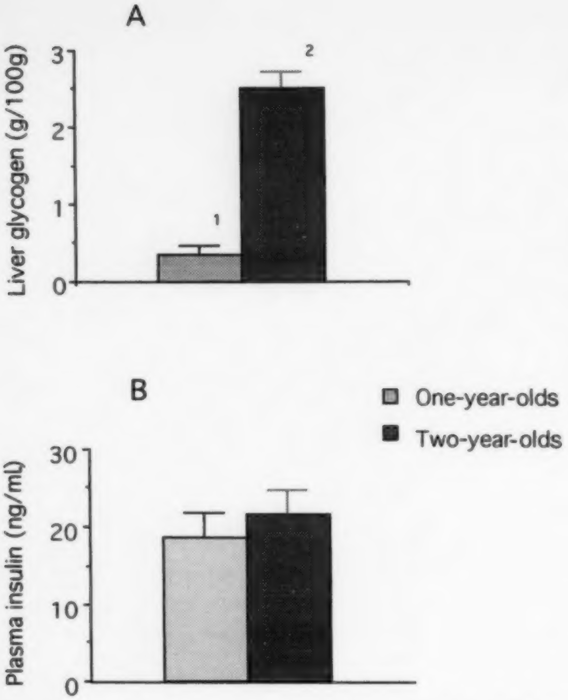

FIG. 3. (A) Liver glycogen content and (B) plasma insulin level 1- and 2-yr-old Atlantic salmon (groups 3 and 4, Table 1) after 3.5 mo in seawater (seawater transfer on April 15, 1991).

from the fish in fresh water were stored up to 3 mo, while samples from seawater fish were assayed within 1–5 d after collection. One half of each liver was used for glycogen assay in Seattle, while the other half was transported frozen to Ottawa, Ont., Canada, for enzyme assays. White skeletal muscles were collected for glycogen assay in a similar way.

Biochemical Assays

Frozen liver pieces were processed for glycogen content and enzyme activities. Glycogen was assayed according to Foster and Moon (1991). Frozen liver and muscles were sonicated for several seconds (Sonicator-Cell Disruptor, model W-225, Heat Systems-Ultrasonics, Inc. (mention of trade names does not imply endorsement by National Marine Fisheries Service)) in 6% perchloric acid and neutralized to pH 7.0 with K_2CO_3. Glycogen was hydrolyzed with amyloglucosidase and the resulting glucose assayed with a Trinder Kit (Sigma, St. Louis, Mo.). Glycogen values were corrected for preformed glucose in liver tissue.

To measure enzyme activities, frozen liver samples were homogenized for 5 s twice in a "stopping buffer" using a Polytron PCU-2 (Brinkmann Instruments Co.; setting 5). All activities were measured spectrophotometrically, unless noted, at 18°C under optimal assay conditions determined in preliminary experiments (Moon et al. 1989). Glycogen phosphorylase (GPase), pyruvate kinase (PK), glutamate-pyruvate transaminase (GPT), and lactate dehydrogenase (LDH) were estimated according to Moon et al. (1989). Glycogen synthase (GSase) was assayed according to Passonneau and Rottenberg (1973) using 20 mM uridine diphosphoglucose (UDPG) without added glucose 6-phosphate (G6P) for GSase "a" (active form) and 7 mM UDPG plus 5 mM G6P for total GSase activities. Neutral and acidic α-glucosidase (γ-amylase) activities were estimated using an umbelliferone and turanose fluorimetric assay according to Murat et al. (1978) at pH 7.0 (neutral) or 4.5 (acid).

Blood was collected from the caudal vessels into a heparinized syringe. A protease inhibitor, benzamidine-HCl (0.01 M, Sigma, St Louis, Mo.) was added to blood samples kept on ice. After centrifugation, plasma samples were pooled when necessary (three or four parrs) and aliquots for glucose, insulin, and glucagon assays were stored at −60 °C. Plasma glucose was assayed with a Trinder Kit (Sigma, St. Louis, Mo.). Plasma insulin and glucagon were measured by homologous radioimmunoassays (RIA) according to Plisetskaya et al. (1986; insulin) and Sundby et al. (1991b; glucagon).

Statistical Analysis

Data were evaluated by one-way analysis of variance (ANOVA) followed either by a Tukey (HSD) pairwise comparisons of means (Statistix 3.5 for PCs) for enzyme data or by Fisher protected least square differences test for the rest of the data. $P < 0.05$ was considered significant.

Results

Liver Glycogen

The parr-to-smolt transformation (late March to April) in group 2 Atlantic salmon was accompanied by a statistically significant depletion of liver glycogen (Fig. 1). Glycogen levels were restored in June, before seawater transfer, reaching 3.1 ± 0.4 g/100 g liver weight (Fig. 1). After these fish entered seawater in June, the liver glycogen concentration significantly diminished to less than 0.7 g/100 g liver weight and remained low until September (Fig. 1). In many individual Atlantic salmon, especially from group 1, liver glycogen content after 3–4 mo in seawater was found to be less than 0.1 g/100 g (Fig. 2). Low concentrations of liver glycogen, not exceeding 0.4 g/100 g, were found in yearling Atlantic salmon from groups 3 and 6 (Table 2). The most striking fact about fish from groups 3 (1 yr old) and 4 (2 yr old) was that all were sampled at 4–4.5 h after feeding and had very high systemic plasma insulin (18.6 ± 3.2 ng/mL; $n = 10$, in group 3 fish and 21.6 ± 3.1 ng/mL; $n = 6$, in group 4 fish), which should favor glycogen synthesis in both groups of fish. At the same time, 2-yr-old Atlantic salmon had up to fivefold higher glycogen concentration in liver than 1-yr-old fish (Fig. 3). Unlike liver glycogen, skeletal muscle glycogen concentration in 1-yr-old fish was in the normal range (Plisetskaya 1975) for salmonids and other teleost fish (Table 2).

In contrast with the significant glycogen depletion noted for seawater Atlantic salmon (groups 1 and 2), in coho salmon, comparatively low liver glycogen levels (1.0 ± 0.2 g/100 g) were observed only during the first month of seawater residence. Then glycogen content increased to 1.6 ± 0.3 and 3.0 ± 0.3 g/100 g during the second and third months, respectively. Similar trends in liver glycogen accumulation were observed in chinook salmon (*Oncorhynchus tshawytscha*) (A. Palmisano, Marrowstone Field Station, U.S. Fish and Wildlife Service, Norland, Wash., personal communication.)

TABLE 2. Glycogen, glucose and insulin concentrations (mean ± SEM) in farm-raised Atlantic salmon (10 fish in each group)

Group[a]	Date	Age	Liver glycogen (g/100 g)	Muscle glycogen (g/100 g)	Plasma glucose (mM)	Insulin (ng/mL)
3	July 31, 1991	1+	0.36 ± 0.11		4.1 ± 0.3	18.5 ± 3.2
4		2+[b]	2.50 ± 0.22		4.8 ± 0.2	21.6 ± 3.1
3	May 8, 1992	1+	0.38 ± 0.12	0.25 ± 0.23	4.0 ± 0.2.	13.8 ± 1.8
5	March 17, 1992	1+	0.79 ± 0.20	0.20 ± 0.32	5.0 ± 0.3	7.7 ± 1.2
6		1+	0.39 ± 0.12	0.13 ± 0.21	5.0 ± 0.4	13.5 ± 1.6
5	April 29, 1992	1+	0.37 ± 0.08		4.0 ± 0.3	10.0 ± 2.1
6		1+	0.34 ± 0.06		4.7 ± 0.4	10.1 ± 1.3
5	June 11, 1992	1+		0.14 ± 0.22		
6		1+		0.18 ± 0.27		
7		2+		0.30[c]		

[a] See Table 1 and Materials and Methods.

[b] Six fish sampled.

[c] Two fish sampled.

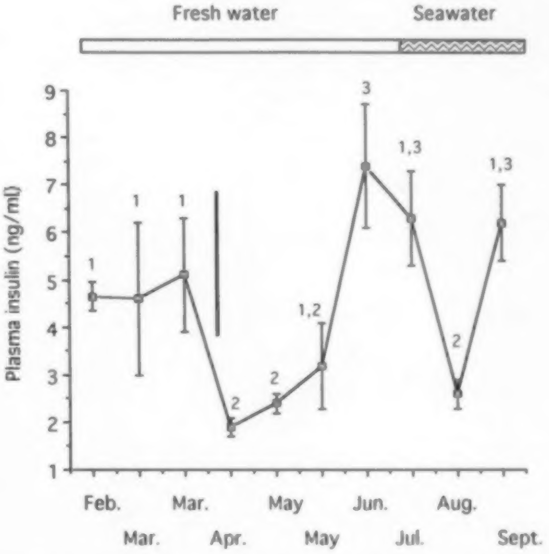

FIG. 4. Plasma insulin concentration in yearling Atlantic salmon (group 2, Table 1) during the parr-to-smolt transformation and subsequent transfer to seawater on June 17, 1991. Vertical bar: morphological smoltification.

Plasma Glucose

No substantial variations in plasma glucose levels were observed among groups 3–7 of Atlantic salmon in seawater (Table 2). Atlantic salmon of group 2 and coho salmon of group 8 had the highest plasma glucose concentrations (6.7 ± 0.4 mM, $n = 10$ and 5.4 ± 0.4 mM, $n = 8$, respectively) in July, soon after seawater transfer.

Pancreatic Hormones

Plasma insulin levels in group 2 Atlantic salmon significantly declined during smoltification period (late March–April) but were restored in June, before seawater transfer, reaching 7.3 ± 1.3 ng/mL. Afterwards, plasma insulin fluctuated, reaching the lowest point in August (Fig. 4). Plasma glucagon profiles in Atlantic salmon were similar to insulin profiles, although the concentration of glucagon remained less than 0.5 ng/mL. The highest glucagon concentrations (0.40 ± 0.13 and 0.39 ± 0.05 ng/mL) were observed before smoltification and before seawater entry, and the lowest values (0.14 ± 0.03 and 0.13 ± 0.02 ng/mL) were measured through the smoltification period and after entering seawater. Molar plasma ratios of insulin/glucagon (Fig. 5) suggest that during seawater residence, Atlantic salmon juveniles are primarily anabolic. However, no net liver glycogen accumulation has been observed in July–August.

Concentration of plasma pancreatic hormones in coho salmon was lower than in Atlantic salmon; insulin ranged from 1.0 to 3.5 ng/ml and glucagon from <0.1 to 0.2 ng/mL. There was only one sampling, on September 17, when systemic insulin and glucagon in coho salmon appeared to be higher than in Atlantic salmon, reaching 7.1 ± 0.9 ng/L for insulin and 0.3 ± 0.06 ng/L for glucagon. This may be because this was the only group of coho occasionally fed 2–3 h before sampling.

Hepatic Enzymes

Enzyme activities were estimated in Atlantic salmon (group 2) at five critical periods. Numerous significant changes were observed in the activities of the enzymes assayed (Table 3) but only some of them coincided with changes in either insulin or glycogen concentrations shown in Fig. 1 and 4. During smoltification (March and April), there were decreased total GSase activities, but these decreases were compensated for by changes in the percentage of the active ("a") form of the enzyme. Thus, throughout smoltification, activities of GSase changed very little. GPase activities remained unaffected by smoltification, but seawater transfer resulted in decreases in both total GPase and the percentage of GPase "a". Partial recovery of both total GPase and GPase "a" was achieved by September. Taken together, these results suggest that the potential for glycogen regulation is unaffected by smoltification, but seawater transfer leads to a predominance of glycogen synthesis over degradation. It is important to note, however, that glycogen breakdown should be generally favored, since the activity of GPase always exceeds that of GSase. Another enzyme of potential importance in glycogen breakdown is α-glucosidase (γ-amylase) (Murat et al. 1978). Activities of the neutral amylase showed no relation to either hormonal profiles, smoltification, or seawater transfer. These activities were 5–50 times below those of GPase "a"; activities of the acid or lysosomal amylase were at least 10 times lower than the neutral enzyme.

Activities of GPT and LDH generally fell at smoltification with some recovery noted by September. PK activities or activity ratios (activities at low compared with high phosphoenolpyruvate (PEP) concentrations) were again unrelated to developmental stage or hormonal profiles. These results suggest that gluconeogenic capacities may fall at smoltification, but the lack of correlation between changes in PK and GPT/LDH suggests that such changes are unlikely to affect gluconeogenic capacity in a significant manner.

The enzyme activities estimated in coho salmon livers were unrelated to either life stage, plasma insulin level, or liver glycogen content, but some changes related to seawater transfer could be seen (Table 4). Total activities of both GSase and GPase fell significantly with seawater transfer. This decline in GSase and GPase was compensated for by increases in the active form of GSase at least in July and September whereas changes in the GPase active form led to further decreases in the activity of GPase in fish in seawater. These results, as in the case of the Atlantic salmon, suggest that there is a relative increase in synthesis compared with breakdown of glycogen in July and September. Activities of γ-amylase were generally unaffected across the sampling period, but activities of the acid amylase were well above those found in the Atlantic salmon. There were no obvious trends in activities of PK, GPT, and LDH.

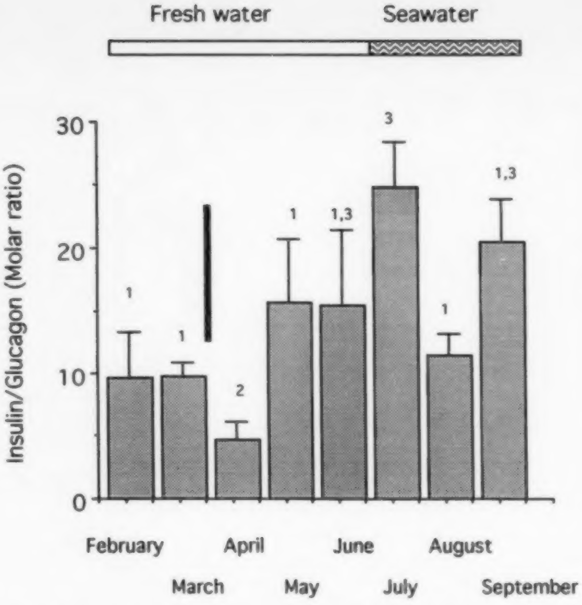

FIG. 5. Molar plasma ratios of insulin/glucagon in yearling Atlantic salmon (group 2, Table 1) during the parr-to-smolt transformation and subsequent transfer to seawater on June 17, 1991.

Discussion

While both juvenile Pacific and Atlantic salmon are catabolic during smoltification in fresh water (Fontaine and Hatey 1953; Sheridan et al. 1985; Plisetskaya et al. 1988; Gutiérrez and Plisetskaya 1991), the observation of extremely low concentration of liver glycogen in healthy, feeding Atlantic salmon several months after transfer to seawater was unexpected. We are not aware of any previous description of such a phenomenon. To the contrary, various fish fasting for several months through either winter periods or upstream spawning migrations usually do not deplete or do promptly replenish liver glycogen (reviewed by Plisetskaya 1975). Low liver glycogen concentrations observed by us could not be attributed to the prolonged storage of samples because, in contrast with Palace et al. (1990), we did not observe a decline in glycogen concentration depending on the duration of storage at −60°C. Moreover, samples from freshwater fish that had highest liver glycogen were stored for several months, while samples from seawater fish were often assayed the next day. The startling difference in glycogen concentration between 1- and 2-yr-old Atlantic salmon was observed in liver samples collected on the same day and measured in the same assay. There are numerous observations of sexual differences in liver glycogen concentration in teleost fishes, including salmonids, especially sexually maturing ones (reviewed by Plisetskaya 1975). Recently, Majewski et al. (1990) reported that liver glycogen concentration in 2-yr-old sexually maturing male Atlantic salmon is much higher than in females. This obviously does not relate to the immature 1-yr-old Atlantic salmon smolts in our study: no sexual difference in liver glycogen concentration was observed in these fish.

Thus, yearling Atlantic salmon seawater smolts appear to be a unique experimental model of a feeding animal that does not deposit much liver glycogen between food intakes. This pattern evidently does not represent a particular metabolic feature of Pacific Northwest Atlantic smolts because pilot measurement of liver glycogen in yearling Atlantic salmon in Rennes (France) during the summer of 1992 revealed a similar metabolic pattern (P. Prunet and E.M. Plisetskaya, unpublished data). Wendt and Saunders (1973), however, reported high liver glycogen content in 1-yr-old seawater Atlantic salmon smolts from New Brunswick, Canada. Interestingly, Atlantic salmon smolts in seawater near Halifax, N.S., Canada, have fourfold higher plasma insulin concentration than their counterparts from the Pacific Northwest (Lall et al. 1994).

Theoretically, low liver glycogen concentration might be a consequence of many different conditions but perhaps primarily of incomplete smoltification and poor ability to osmoregulate in seawater. In addition, changes in nutritional state, hormonal levels, enzyme activities, etc. (cf. Moon et al. 1989; Youn and Bergman 1990; Baanante et al. 1991; Foster and Moon 1991), may affect liver glycogen. According to morphological criteria (Johnston and Saunders 1981; Gorbman et al. 1982), salmon sampled by us during 1990–92 were transferred to seawater as smolts. Initial seawater mortality (usually caused by inadequate osmoregulation) was very low or absent. Nevertheless, it could be suggested that impaired feeding after seawater entry (Strademayer 1991; Usher et al. 1991) caused the drop in liver glycogen concentration. This too does not seem to be the case in our study, since fish kept in seawater for more than 1 mo fed actively, had food in their stomachs and guts, and steadily

TABLE 3. Activities of selected liver enzymes from yearling Atlantic salmon (group 2) during the parr-to-smolt transformation and subsequent transfer to seawater. Values (mean ± SEM (n)) are units per gram liver (except where noted). Activities are estimated under optimal conditions (V_{opt}), except where noted, and at 18°C. Superscript numbers that differ across rows are significantly different from each other at $p < 0.05$.

Enzyme	March 27	April 17	June 17	July 10	August 14	September 14
GSase (total)	0.49 ± 0.09 (4)^{1}	0.19 ± 0.05 (4)^{2,3}	0.19 ± 0.02 (6)^{2,3}	0.10 ± 0.04 (6)^{2,3}	0.09 ± 0.02 (7)^{3}	0.2 ± 0.03 (4)^{2,3}
% "a"	16.7^{1}	46.2^{1,2}	34.9^{1,2}	66.0^{2}	51.4^{1,2}	38.8^{1,2}
GPase (total)	1.80 ± 0.2 (4)^{1}	1.74 (2)^{1}	1.77 ± 0.2 (6)^{1}	0.44 ± 0.11 (6)^{2}	0.27 ± 0.07 (7)^{2}	0.64 ± 0.05 (4)^{2}
% "a"	81.3^{1,3}	60.2^{2,3,4}	82.4^{1,2}	54.8^{4}	64.9^{3,4}	98.1^{1}
γ-Amylase						
Neutral (milliunits)	18.9 ± 1.8 (4)^{1}	22.7 ± 1.0 (4)^{1,2}	ND^{a}	21.1 ± 1.3 (4)^{1,2}	27.3 ± 2.0 (6)^{2}	19.8 ± 1.5 (4)^{1}
Acid	1.1 ± 0.1 (4)^{1}	0.80 ± 0.3 (4)^{1}	1.6 ± 0.2 (4)^{1,2}	3.2 ± 0.5 (4)^{1,2}	1.3 ± 0.15(4)^{1}	1.1 ± 0.25 (4)^{1}
PK-V_{opt}	6.5 ± 0.5 (4)^{1,2}	4.1 ± 0.2 (4)^{2}	7.4 ± 0.5 (6)^{1}	6.0 ± 0.9 (6)^{1,2}	8.4 ± 0.4 (7)^{1}	6.7 ± 0.9 (4)^{1,2}
AR^{b}	0.16^{1,2}	0.07^{2,3}	0.13^{1,2,3}	0.17^{1}	0.08^{2,3}	0.18^{1}
GPT	63.5 ± 2.4 (4)^{1}	49.2 ± 5.7 (4)^{2}	28.4 ± 1.1 (6)^{3}	34.2 ± 2.6 (6)^{3}	34.7 ± 0.9 (7)^{3}	47.8 ± 2.2 (4)^{2}
LDH	232 ± 8.0 (4)^{1}	183 ± 24 (4)^{1,2,3}	122 ± 10 (6)^{3}	132 ± 23 (6)^{2,3}	141 ± 8 (7)^{1,2,3}	139 ± 14 (4)^{1,2,3}

[a] Not done.

[b] Activity ratio = activity at 0.2 mM compared with 5.0 mM PEP.

TABLE 4. Activities (mean ± SEM (n)) of selected liver enzymes from yearling coho salmon (group 2) during the parr-to-smolt transformation and subsequent transfer to seawater. Other designations as in Table 3.

Enzyme	March 27	April 17	June 17	July 10	August 14	September 14
GSase (total)	0.38 ± 0.05 (4)^{1,2}	0.46 ± 0.13 (4)^{1}	0.33 ± 0.03 (6)^{1,2,3}	0.09 ± 0.01 (6)^{3}	0.18 ± 0.01 (5)^{2,3}	0.2 ± 0.06 (4)^{1,2,3}
% "a"	14.4	11.2	12.1	43.0	8.5	24.4
GPase (total)	1.6 ± 0.4 (4)^{1}	1.6 ± 0.2 (4)^{1}	2.8 ± 0.2 (6)^{2}	0.5 ± 0.1 (6)^{3}	0.5 ± 0.03 (5)^{3}	0.5 ± 0.2 (4)^{3}
% "a"	71.3^{1,2}	66.9^{2}	90.4^{1}	61.9^{2}	80.1^{1,2}	66.4^{2}
γ-Amylase						
Neutral (milliunits)	18.3 ± 1.2 (4)	21.2 ± 1.2 (4)	ND	19.8 ± 1.0 (4)	23.0 ± 1.3 (4)	18.9 ± 2.0 (4)
Acid	16.6 ± 2.5 (4)^{1,2}	8.8 ± 1.0 (4)^{1}	16.0 ± 1.0 (4)^{1,2}	22.7 ± 2.9 (4)^{2,3}	ND	14.3 ± 1.4 (4)^{1,2}
PK-V_{opt}	13.0 ± 0.9 (4)^{1,2}	18.7 ± 1.4 (4)^{1,3}	15.7 ± 1.5 (6)^{1,2,3}	10.3 ± 0.3 (6)^{2}	18.1 ± 0.9 (5)^{1,3}	20.9 ± 2.5 (4)^{3}
AR	0.06^{1,2}	0.07^{1,2}	0.05^{2}	0.09^{1,3}	0.11^{1,3}	0.10^{1,3}
GPT	32.1 ± 2.1 (4)^{1,2}	35.8 ± 0.6 (4)^{1}	39.3 ± 1.0 (6)^{1}	35.5 ± 1.3 (6)^{1}	20.0 ± 3.0 (5)^{3}	24.9 ± 2.5 (4)^{2,3}
LDH	187 ± 7.0 (4)^{1,2}	196 ± 20.0 (4)^{1}	132 ± 13.0 (6)^{3}	124 ± 2.2 (6)^{3}	123 ± 2.2 (5)^{3}	148 ± 7.0 (4)^{1,2,3}

gained weight (in fish with the lowest glycogen concentration in the liver, the instantaneous growth rates were >1.0 and average feed conversion ratios around 0.6. (R. Hardy, Northwest Fisheries Science Center, National Marine Fisheries Service, personal communication)). Fish sampled at the fish farms (groups 3, 5, and 6) were in excellent physical condition, fed actively, and still had low liver glycogen concentration.

During the freshwater stage of development, plasma profiles of the major metabolic hormones insulin and glucagon were similar to those observed previously (Plisetskaya et al. 1988; Plisetskaya 1990). The only difference between Atlantic and coho salmon was the presence of an additional peak of insulin in Atlantic salmon after parr-to-smolt transformation was completed and fish were ready for seawater. The pattern of plasma glucagon during the freshwater stage was, in general, similar to that of insulin. Similar changes in hormones known for their opposite metabolic effects have been observed previously in Atlantic salmon (Sundby et al. 1991a, 1991c) and in starved rainbow trout (*Oncorhynchus mykiss*) (Moon et al. 1989). We have no explanation for the insulin and glucagon decline observed in August in both Atlantic and coho salmon juveniles.

To predict the metabolic state of fish, molecular ratios of major metabolic hormones are more valuable than their individual concentrations (Moon et al. 1989). The results shown in Fig. 5 suggest that although the plasma concentrations of both hormones diminish throughout smoltification of yearling Atlantic salmon, glucagon concentration diminishes relatively slowly, and consequently the ratio of insulin to glucagon declines. This suggests that the catabolic state of fish becomes enhanced.

Glycogen metabolism in the liver is known to be determined by the relative activities of GSase "a" (synthesis) and GPase "a" (breakdown) (Stalmans and van de Werve 1981). Smoltification in Atlantic salmon was accompanied by a decrease in total GSase activity, but this was compensated for by an increase in GSase "a " (Table 3). The mammalian data suggest that insulin activates the synthase only if the GPase "a" percentage falls below 10% of maximum (Stalmans and van de Werve 1981), a situation not observed in our study (Table 4). Seawater transfer did lead to a significant decrease in total GPase activities in both Atlantic and coho livers, and the latter were not compensated for by increases in the percentage of GPase "a". This could compromise glycogenolytic potential in the same manner as reported for fasting yelow perch (*Perca flavescens*) (Foster and Moon 1991). Relative to the fish during their freshwater period of life, the seawater Atlantic and coho salmon had a greater potential for glycogen synthesis which was realized to a much greater extent in coho than in Atlantic salmon. There is no indication that either form of γ-amylase plays a significant role in glycogen hydrolysis in salmon as suggested previously by Murat et al. (1978) and Castilla et al. (1980) for carp and trout.

If some Atlantic salmon smolts do not resume normal feeding for approximately 1 mo after seawater transfer (Stradmeyer 1991; Usher et al. 1991), glucose homeostasis should be supported by gluconeogenesis. According to studies by Rothman et al. (1991), if humans fast for up to 22 h, gluconeogenesis accounts for 64% and in the subsequent 18 h for 96% of total glucose production. Therefore, gluconeogenesis is considered to be a more important pathway for replenishing liver glycogen than glycogen synthesis from glucose. No similar studies comparing precursors for glycogen synthesis seem to have been conducted in fish.

Activities of enzymes that play a potential role in supplying substrates to the gluconeogenic pathway (GPT and LDH) and the gluconeogenic enzyme PK did not show consistent variation in this study. This is unlike the situation in fasting yellow perch (Foster and Moon 1991) and rainbow trout (Moon et al. 1989) where changes in these enzymes supported enhanced gluconeogenesis.

Since neither enzyme activities nor hormonal patterns seem to explain the "glycogen paradox" in Atlantic salmon, the continuation of this study should focus on measurement of key substrates of glycogen synthesis or gluconeogenesis, since it had been reported that such substrates can drastically influence liver glycogen content (Swallow and Fleming 1970; Mayer and Letsch 1989; Young and Bergman 1990; Baanante et al. 1991; López et al. 1991).

The novel peptide amylin, produced by the pancreatic B-cells and cosecreted with insulin, was reported to sharply diminish liver and especially muscle glycogen content in rats (Young et al. 1990). This effect is achieved by a countering of activation of GSase and of glucose incorporation into glycogen caused by insulin (Gómez-Foix et al. 1991). Furthermore, there are recent reports that amylin is more potent and more effective than glucagon in elevation of plasma glucose in fasted animals (Wang et al. 1991). Again, it seems not to be the case in our study, since in 1-yr-old seawater Atlantic salmon, muscle glycogen was not as drastically affected as liver glycogen.

The summer period when yearling Atlantic salmon have particularly low liver glycogen coincides with the high summer mortality of these fish in seawater. Such mortality was observed in some years but not in others. Liver glycogen stores are rebuilt in September when summer mortality usually subsides. Neither 2-yr-old Atlantic salmon nor yearling Pacific salmon display patterns of low liver glycogen and high summer mortality.

As a result of this study, we suggest a hypothesis to explain the summer mortality phenomenon. Yearling seawater Atlantic salmon smolts do not store liver glycogen during their first summer in seawater either as a result of some still unknown peculiarity of their metabolism or because of some metabolic disorder. Consequently, they are poorly adapted metabolically to potentially stressful environmental changes that may be encountered after entering seawater. Such stressors may be blooms of noxious phytoplankton, disease, abrupt changes in water temperature, and low dissolved oxygen, among other factors. In contrast, 2-yr-old Atlantic salmon smolts as well as yearling Pacific salmon smolts store liver glycogen between meals and maintain it at the level of 1–3% throughout the summer months. The stored energy can be promptly mobilized under stressful (especially anoxic) conditions to meet metabolic requirements for glucose including those of the brain. This hypothesis finds indirect support in the studies of Rensel (1991) who demonstrated that Atlantic salmon exposed to phytoplankton suffer significant reduction in blood oxygen. Thus, although *not causing* mortality, low energy stores in the liver of seawater Atlantic salmon smolts may enhance their susceptibility to any form of environmental stress. When the stressful conditions are absent, the fish remain alive and well as was observed by us in Puget Sound for the summers of 1991 and 1992.

One promising idea, proposed to increase Atlantic cod (*Gadus morhua*) survival during and after transportation stress, has been to modify the fish diet in order to build carbohydrate reserves (Hemre et al. 1991). Such reserves, in turn, may be expected to improve adaptation to a variety of stress factors (see Wendt and Saunders 1973) encountered by fish in seawater. Another approach already employed by some fish farms is to use underyearling smolts (Myrseth 1991) mentioned above. Although Atlantic salmon released at age 0 still have lower liver glycogen concentration than 2-yr-old fish (Table 2), they are much larger the following summer than fish of the same age but transferred to the seawater in spring.

In conclusion, we anticipate that further studies and a better understanding of the metabolic differences between 1- and 2-yr-old Atlantic smolts and between Atlantic and Pacific smolts will form the basis for the rational development of a method to improve the metabolic performance of farmed fish in the Pacific Northwest.

Acknowledgments

This study was supported by the National Marine Fisheries Service (NMFS), NSF grant DCB-8915935 to E.M.P., Washington Sea Grant R/A-63 to E.M.P. and W.W.D., and NSERC grant A-6944 to T.W.M. We thank Conrad V.W. Mahnken and Ron Sailor, NMFS, John Forster, Sea Farm Washington Inc., and Thor Erik, Global Aquafarm, for their helpful advice and permission to sample fish at their seawater facilities. We express special thanks to Dr. Ronald W. Hardy for his generous permission to use the control group of 1-yr-old Atlantic salmon smolts from his ongoing experiment.

References

ALDRIDGE, C. 1991. Smolt feature. Are we doing enough about early losses? Fish Farmer 14(No. 6): 11.

BAANANTE, I.V., P. GARCIA DE FRUTOS, L. BONAMUSA, AND F. FERNANDEZ. 1991. Regulation of fish glycolysis–gluconeogenesis: role of fructose 2,6P2 and PFK-2. Comp. Biochem. Physiol. 100B: 11–17.

BRUNO, D.W., G. DEAR, AND D.D. SEATON. 1989. Mortality associated with phytoplankton blooms among farmed Atlantic salmon, *Salmo salar* L., in Scotland. Aquaculture 78: 217–222.

CASTILLA, C., H. PARIS, A. CRESPO, AND J.C. MURAT. 1980. Comparative study of α-glucosidase activities in rat and trout tissues. Comp. Biochem. Physiol. 67B: 653–657.

DICKHOFF, W.W., C.V.W. MAHNKEN, W.S. ZAUGG, F.W. WAKNITZ, M.G. BERNARD, AND C.V. SULLIVAN. 1989. Effects of temperature and feeding on smolting and seawater survival of Atlantic salmon (*Salmo salar*). Aquaculture 82: 93–102.

FONTAINE, M., AND J. HATEY. 1953. Contribution a l'étude du metabolisme glucidique du salmon (*Salmo salar* L.) à diverses étapes de son developpement et de ses migrations. Physiol. Comp. Oecol. 3: 37–52.

FOSTER, G.D., AND T.W. MOON. 1991. Hypometabolism with fasting in the yellow perch (*Perca flavescens*): a study of enzymes, hepatocyte metabolism, and tissue size. Physiol. Zool. 64: 259–275.

FRANKLIN, C.E., M.E. FORSTER, AND W. DAVISON. 1992. Plasma cortisol and osmoregulatory changes in sockeye salmon transferred to seawater: comparison between successful and unsuccessful adaptation. Fish Biol. 41: 113–122.

GÓMEZ-FOIX, A.M., J.E. RODRIGUEZ-GIL, AND J.J. GUINOVART. 1991. Anti-insulin effects of amylin and calcitonin-gene-related peptide on hepatic glycogen metabolism. Biochem J. 276: 607–610.

GORBMAN, A., W.W. DICKHOFF, J.L. MIGHELL, E.F. PRENTICE, AND F.W.WAKNITZ. 1982. Morphological indices of developmental progress in the parr–smolt coho salmon, *Oncorhynchus kisutch*. Aquaculture 28: 1–19.

GUTIÉRREZ J., AND E.M. PLISETSKAYA. 1991. Insulin binding to liver plasma membranes of coho salmon during smoltification. Gen. Comp. Endocrinol. 82: 466–475.

HEMRE, G.-I., G. LAMBERSTEN, AND Ø. LIE. 1991. The effect of dietary carbohydrate on the stress response in cod (*Gadus morhua*). Aquaculture 95: 319–328.

JOHNSTON, C.E., AND L. SAUNDERS. 1981. Parr-smolt transformation of yearling Atlantic salmon (*Salmo salar*) at several rearing temperatures. Can. J. Fish. Aquat. Sci. 38: 1189–1198.

LALL, S.P., S.J. KAUSHIK, P.Y. LE BAIL, R. KEITH, J.S. ANDERSON, AND E. PLISETSKAYA. 1994. Quantitative arginine requirement of Atlantic salmon (*Salmo salar*) reared in sea water. Aquaculture. (In press)

LANGDON, J.S., AND J.E. THORPE. 1985. The ontogeny of smoltification: development patterns of gill Na +/K + -ATPase, SDH, and chloride cells in juvenile Atlantic salmon, *Salmo salar* L. Aquaculture 45: 83–95.

LÓPEZ, M. P., M.J. GÓMEZ-LECHÓN, AND J.V. CASTELL. 1991. Glucose: a more powerful modulator of fructose 2,6-bisphosphate level than insulin in human hepatocytes. Biochim. Biophys. Acta 1094: 200–206.

MAJEWSKI, H.S., S.B. BROWN, R.E. EWANS, H.C. FREEMAN, AND J.F. KLAVERKAMP. 1990. Responses of kidney, liver, muscle, and bone in Atlantic salmon (*Salmo salar*) to diet and liming in acidic Nova Scotia rivers. Can. J. Fish. Aquat. Sci. 47: 2441–2450.

MAYER, D., AND I. LETSCH. 1989. Glucose 6-phosphate plays a central role in regulation of glycogen synthesis in a glycogen-storing liver cell line. Cell Biochem. Funct. 7: 243–256.

MOON, T.W., G.D. FOSTER, AND E.M. PLISETSKAYA. 1989. Changes in peptide hormones and liver enzymes in the rainbow trout deprived of food for 6 weeks. Can. J. Zool. 67: 2189–2193.

MURAT, J.C., C. CASTILLA, AND H. PARIS. 1978. Comparative study of α-glucosidase activities in liver, plasma and urine of carp, rat and dog. Comp. Biochem. Physiol. 61B: 145–149.

MYRSETH, B. 1991. Smolts feature. The zero-year strategy. Fish Farmer 14(No. 6): 16–17.

PALACE, V.P., H.S. MAJEWSKI, AND J.F. KLAVERKAMP. 1990. Effect of sampling and storage conditions on the stability of biochemical parameters measured in rainbow trout (*Oncorhynchus mykiss*) liver. Comp. Biochem. Physiol. 95B: 51–55.

PASSONNEAU, J.V., AND D.A. ROTTENBERG. 1973. An assessment of methods for measurement of glycogen synthetic activity including a new direct one-step assay. Anal. Biochem. 51: 528–541.

PLISETSKAYA, E.M. 1975. Hormonal regulation of carbohydrate metabolism in lower vertebrates. Nauka, Leningrad, 215 p. (In Russian)

PLISETSKAYA, E.M. 1990. Recent studies of fish pancreatic hormones: selected topics. Zool. Sci. 7: 335–353.

PLISETSKAYA, E.M., W.W. DICKHOFF, T.L. PAQUETTE, AND A. GORBMAN. 1986. The assay of salmon insulin by homologous radioimmunoassay. Fish Physiol. Biochem. 1: 37–43.

PLISETSKAYA, E.M., P. SWANSON, M.G. BERNARD, AND W.W. DICKHOFF. 1988. Insulin in coho salmon (*Oncorhynchus kisutch*) during the parr to smolt transformation. Aquaculture 72: 151–164.

RENSEL J. E. 1991. Harmful effects of the diatom *Chaetoceros concavicornis* on Atlantic salmon. Can. Tech. Rep. Hydrogr. Ocean Sci. 135.

ROTHMAN, D.L., I. MAGNUSSON, L.D. KATZ, R.G. SHULMAN, AND G.L. SHULMAN. 1991. Quantitation of hepatic glucogenolysis and gluconeogenesis in fasting humans with ^{13}C NMR. Science (Wash., D.C.) 254: 573–576.

ROWE, D.K., J.E. THORPE, AND A.M. SHANKS. 1991. Role of fat stores in the maturation of male Atlantic salmon (*Salmo salar*) parr. Can. J. Fish. Aquat. Sci. 48: 405–413.

SAUNDERS, R.L., J. DUSTON; P.R. HARMON, D.E. KNOX, AND D.E. STEWART. 1990. Production of underyearling Atlantic salmon smolts. Bull. Aquacult. Assoc. Can. 90: 61–63.

SHERIDAN, M.A., N.Y.S. WOO, AND H.A. BERN. 1985. Changes in the rates of glycogenesis, glycogenolysis, lipogenesis, and lipolysis in selected tissues of coho salmon (*Oncorhynchus kisutch*) associated with parr–smolt transformation. J. Exp. Zool. 236: 35–44.

STALMANS, W. AND G. VAN DE WERVE. 1981. Regulation of glycogen metabolism by insulin, chap. 8, p. 119–138. *In* L. Hue and van de Werde [ed.] Short-term regulation of liver metabolism. Elsevier/North Holland Biomedical Press, New York, N.Y.

STRADMEYER, L. 1991. Smolts feature. Is feeding "non-starters" a waste of time? Fish Farmer 14(No. 6): 12–13.

SUNDBY, A., K. ELIASSEN, A.K. BLOOM, AND T. ÅSGÅRD. 1991a. Plasma insulin, glucagon, glucagon-like peptide and glucose levels in response to feeding, starvation and life long restricted feed ration in salmonids. Fish Physiol. Biochem. 9: 253–259.

SUNDBY, A., K. ELIASSEN, T. REFSTIE, AND E.M. PLISETSKAYA. 1991b. Plasma levels of insulin, glucagon and glucagon-like peptide in salmonids of different weights. Fish Physiol. Biochem. 9: 223–230.

SUNDBY, A., G-I. HEMRE, B. BORREBAEK, B. CHRISTOPHERSEN, AND A.K. BLOOM. 1991c. Insulin and glucagon family peptides in relation to activities of hepatic hexokinase and other enzymes in fed and starved Atlantic salmon (*Salmo salar*) and cod (*Gadus morhua*). Comp. Biochem. Physiol. 100B: 467–470.

SWALLOW, R.L., AND W.R. FLEMING. 1970. The effect of oxaloacetate, ACTH and cortisol on the liver glycogen levels of *Tilapia mossambica*. Comp. Biochem. Physiol. 36: 93–98.

USHER, M.L., C. TALBOT, AND F.B. EDDY. 1988. Drinking in Atlantic salmon smolts transferred to seawater and the relationship between drinking and feeding. Aquaculture 73: 237–246.

USHER, M.L., C. TALBOT, AND F.B. EDDY. 1990. Effects of transfer to seawater on digestion and gut function in Atlantic salmon smolts (*Salmo salar* L.). Aquaculture 90: 85–96.

USHER, M.L., C. TALBOT, AND F.B. EDDY. 1991. Effect of transfer to seawater on growth and feeding in Atlantic salmon smolts (*Salmo salar* L.). Aquaculture 94: 309–326.

WANG, M.W., P. CARLO, T.J. RINK, AND A.A. YOUNG. 1991. Amylin is more potent and more effective than glucagon in raising plasma glucose concentration in fasted, anesthetized rats. Biochem. Biophys. Res. Commun. 181: 1288–1293.

WENDT, C.A.G., AND R.L. SAUNDERS. 1973. Changes in carbohydrate metabolism in young Atlantic salmon in response to various forms of stress. Int. Atl. Salmon Symp. 1972 Spec. Publ. Ser. 4: 55–82.

YOUNG, J.H., AND R.N. BERGMAN. 1990. Enchancement of hepatic glycogen by gluconeogenic precursors: substrate flux or metabolic control? Am. J. Physiol. 258: E899–E906.

YOUNG, D.A., R.O. DEEMS, R.W. DEACON, R.H. MCINTOSH, AND J.E. FOLEY. 1990. Effects of amylin on glucose metabolism and glycogenolysis *in vivo* and *in vitro*. Am. J. Physiol. 259: E457–E461.

Homing, Straying, and Gene Flow among Seasonally Separated Populations of Chum Salmon (*Oncorhynchus keta*)

Ross F. Tallman[1]

Institute of Animal Resource Ecology, The University of British Columbia, 2075 Wesbrook Mall, Vancouver, BC V6T 1W5, Canada

and Michael C. Healey[2]

Department of Fisheries and Oceans, Pacific Biological Station, Nanaimo, BC V9R 5K6, Canada

Tallman, R.F., and M.C. Healey. 1994. Homing, straying, and gene flow among seasonally separated populations of chum salmon (*Oncorhynchus keta*). Can. J. Fish. Aquat. Sci. 51: 577–588.

To test the hypothesis that salmonids that stray into established populations can successfully reproduce, we compared the spatial and temporal pattern of return of marked individuals with the pattern of gene flow suggested by electrophoretic analysis in three populations of chum salmon (*Oncorhynchus keta*) on Vancouver Island. Substantial straying occurred between populations that spawned during the same season. Populations where there was both spatial and temporal isolation in spawning had little straying. Electrophoretic analysis suggested that gene flow was substantially lower than the rate of straying and that it was highest among populations in close geographic proximity. The results of analysis using a log-linear model showed that the probability of discovering an individual stray was dependent on the population sampled and whether one sampled by mark–recapture or using biochemical genetic analysis. We propose that the difference between the rate of straying as measured by mark–recapture and by the analysis of polymorphic enzymes could be accounted for if salmonids straying onto the spawning grounds of established populations of conspecifics had lower reproductive success than fish that return to their natal streams.

Dans le but de vérifier l'hypothèse selon laquelle des salmonidés qui errent dans des populations établies réussissent à se reproduire, nous avons comparé le profil spatio-temporel de retour d'individus marqués au profil du flux génique proposé par l'analyse électrophorétique de trois populations de saumon kéta (*Oncorhynchus keta*) de l'île de Vancouver. On relève un nombre important d'individus vagabonds dans les populations qui frayent pendant la même saison. Le phénomène de vagabondage est peu marqué dans les populations où il y avait un isolement spatio-temporel au moment de la fraye. D'après l'analyse électrophorétique, il semblait que le flux génique était beaucoup plus faible que le taux de vagabondage et qu'il était plus élevé dans les populations géographiquement très proches. Les résultats de l'analyse au moyen d'un modèle log-linéaire ont montré que la probabilité de trouver un vagabond dépendait de la population échantillonnée et si elle était échantillonnée par marquage–recapture ou par analyse génétique biochimique. Selon nous, la différence entre le taux de vagabondage mesuré par marquage–recapture et par l'analyse d'enzymes polymorphes pourrait être prise en compte si le succès de la reproduction des salmonidés qui vagabondent dans les frayères de populations établies de congénères était plus faible que celui des poissons qui retournent à leur cours d'eau d'origine.

Received February 8, 1991
Accepted October 15, 1993
(JA892)

Reçu le 8 février 1991
Accepté le 15 octobre 1993

In studies of genetic isolation, it is usually assumed that the movement of individuals between reproductive locations or seasons is an indication of gene flow between populations. Numerous studies have confirmed the tendency of salmonid fishes to home to their natal site to spawn (e.g., Foerster 1936; Lindsey et al. 1959; Hartman and Raleigh 1964). In recent years, researchers have also demonstrated that some salmonids stray from their natal streams and spawn elsewhere (Quinn 1984; Quinn and Fresh 1984; Klyashtorin 1989). Interpopulation and interspecific variation in straying levels ranges from 0.6 to 1.5% in sockeye salmon (*Oncorhynchus nerka*) (Foerster 1936, 1968), from 0.4 to 2.2% in pink salmon (*O. gorbuscha*) (Boyd 1964; Blair 1968), from 1.4 to 13% in chinook salmon (*O. tshawytscha*) (Snyder 1931; Sholes and Hallock 1979; Quinn and Fresh 1984), from 0.5 to 27% in coho salmon (*O. kisutch*) (Shapovalov and Taft 1954; Donaldson and Allen 1958), and from 2 to 46% in chum salmon (*O. keta*) (Sakano 1960, cited in Sano 1966; Harding 1981, cited in Lister et al. 1981). Straying has been described as an alternative survival tactic in dynamic equilibrium with homing (Quinn 1984). Selective breeding within hatcheries using gametes from returned migrants exclusively has been shown to result in an increase in percent return and a decrease in straying with time (Stabell 1984). The straying rate of Atlantic salmon (*Salmo salar*) at a hatchery in Iceland declined steadily from

---

[1] Present address: Department of Fisheries and Oceans, Freshwater Institute, 501 University Crescent, Winnipeg, MB R3T 2N6, Canada.

[2] Present address: Westwater Research Centre, University of British Columbia, Vancouver, BC V6T 1W5, Canada.

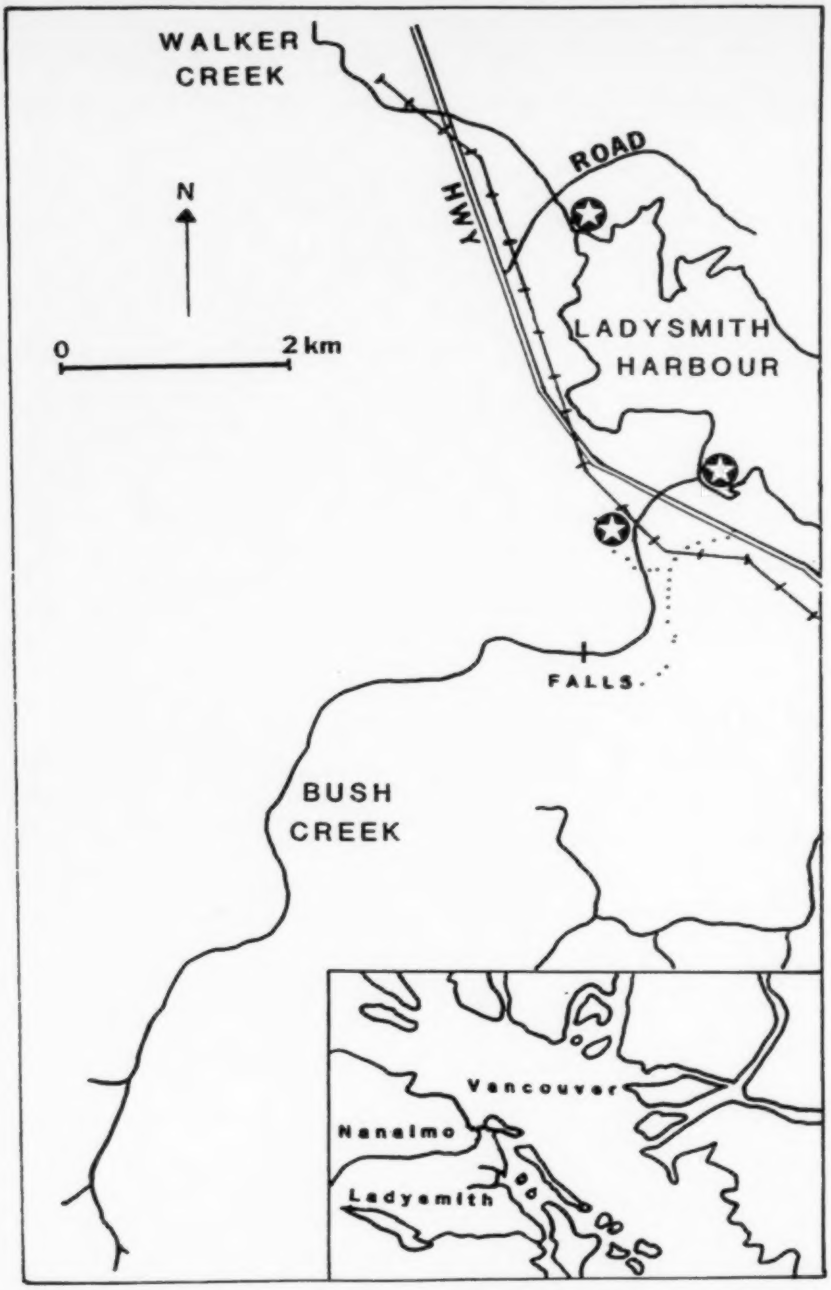
WALKER CREEK
ROAD
N
HWY
0
2 km
LADYSMITH HARBOUR
FALLS
BUSH CREEK
Vancouver
Nanaimo
Ladysmith

FIG. 1. Bush and Walker creeks of Vancouver Island showing the spawning areas and locations of traps for sampling of fry. Trap locations are marked by a star within a circle. The Autumn Bush stock spawning area lies between the two traps on Bush Creek, the Winter Bush spawning area lies between the upstream trap and the falls, and the Walker Creek stock spawning area is between the trap and the highway on Walker Creek.

20.8% in 1966 to 1.8% in 1973 (Guojonsson 1967 and Isaakson 1976, both cited in Stabell 1984). Thus, homing and, perhaps, straying appear to be under some degree of genetic control.

In most cases the basis for "homing" and "straying" was established by marking fish as they left their stream of origin. More recently, Heggberget et al. (1988) used ultrasonic tracking to examine homing in Atlantic salmon. Bartley and

Gall (1990) used electrophoretic analysis to estimate straying rate in chinook salmon. Quinn et al. (1987) also used electrophoretic analysis and "biological tags" (parasites) to infer the rate of homing and straying in sockeye salmon.

Straying has undoubtedly been of great importance in establishing the present distribution of salmonids. A classic example in which strays must have been important was the recolonization of the upper Fraser River by pink salmon following the Hell's Gate landslide of 1913 (Ricker 1987, 1989). Similarly, the colonization of watersheds around the Pacific rim following the retreat of the last ice age could only have been accomplished by strays spreading out from refugia (Neave 1958). Although outside the natural range of the species, the colonization of the North American Great Lakes by pink salmon serves as a modern example of the importance of straying (Kwain and Lawrie 1981). A single introduction of 21 000 fry resulted in the spread of this species throughout the Great Lakes (Kwain 1982; Withler and Kwain 1984). Furthermore, a breakdown in what had been thought to be a rigid 2-yr life cycle allowed pink salmon to develop even-year runs (Kwain and Chappel 1978; Kwain and Kerr 1984). The evolutionary payoff of straying as a mechanism of colonization must be great.

While it is certain that straying behaviour exists, it is not known if the strays are successful in transferring genetic material into an established population. Quinn et al. (1987) found the genetic transfer by strays to be less than 1% in two stock groups of sockeye salmon. This low percentage corresponds well with rates recorded by tagging studies. However, sockeye salmon are thought to have relatively precise homing compared with species such as chum salmon (Quinn 1984). In this paper, we test the hypothesis that salmonids, specifically chum salmon, that stray into established populations can successfully reproduce. To accomplish this, we compared the spatial and temporal pattern of return of marked individuals with the pattern of gene flow inferred from electrophoretic analysis in three populations of chum salmon on Vancouver Island, British Columbia.

Materials and Methods

The study populations spawned in Bush and Walker creeks near Ladysmith on Vancouver Island, British Columbia (Fig. 1). Walker Creek has a single population spawning between late November and early January; the majority of spawning occurs in December. Bush Creek has two temporarily and geographically separated spawning populations. The first population spawns in the lower reaches of Bush Creek between late September and early November with the maximum number of spawning fish appearing in the third week of October. The second spawns further upstream between late November and late December with most spawning occurring in the first and second weeks of December. The populations were designated Autumn Bush (AB), Winter Bush (WB), and Winter Walker (WW). See Tallman (1988) and Tallman and Healey (1991) for details regarding the study area and field sampling protocol to determine timing of reproduction. We employed two approaches to estimating straying rate among populations: an individual rate based on marked fish and a genetic rate based on analysis of protein polymorphisms.

To quantify individual straying among the populations, we marked fry migrating downstream during the spring of 1982 with fin clips. We clipped the right pelvic fin of 12 432 fry of the AB population, the left pelvic fin of 8053 fry of the WW population, and both pelvic fins of 2111 fry of the WB population. A portion of the fin-clipped fry was held in the laboratory for several weeks to establish that fry mortality was low (<2%) from the procedure.

Within Bush Creek there was the potential for mixing of fry, since fry migrations occur more or less synchronously between WB and AB offspring (Tallman and Healey 1991). Since the WB population spawned contiguously with but upstream from the AB population, the WB fry could be sampled without mixing from AB. The AB samples, however, could contain a small percentage of WB fry samples (<15%). This was reduced by marking downstream samples from nights when WB fry were not caught in large numbers in the upstream trap. See Tallman and Healey (1991) for further details on the capture of downstream migrants.

To determine the marking rate, we estimated the total number of fry migrating downstream for each population using the numbers caught in a trap each day (from an overnight sample) scaled by the estimate of trap efficiency. Trap efficiency was the ratio of the number of marked fry released upstream from the trap site that were recovered over the total marked. The total number of fry passing the trap was calculated as follows:

$$N = \frac{n \times M}{R}$$

where N = total number passing downstream, n = number of fry caught in the trap, M = total number of marked fry, and R = number of recaptured fry.

For nights that were not sampled, we estimated the number of fry expected to migrate by interpolation. The total number of fry from each population that migrated was calculated by summing up the nightly totals. Overnight samples were considered to be sufficient because virtually all fry migrated at night (Tallman 1988). The marking rate was the number of marked fry divided by the estimated total number of emigrants.

The carcasses of adults were examined for clipped or regenerated pelvic fins during the fall (September, October, and November) and winter (December and January) of 1984 and 1985, the first and second year of returning marks, respectively. The percentage of migrating fry marked was not equal among the populations. To adjust for the effect of unequal marking rates on the numbers of returning marks recovered in the field, we (1) calculated the combined marking rate for all populations, (2) divided the population specific marking rate by the combined marking rate to get an adjustment factor for each population, and (3) multiplied the recaptures from each population by the appropriate adjustment factor.

Even though Pacific salmon die after spawning, the number of carcasses examined fell well short of the total spawning population estimated by live counts. Carcasses may have fallen into deep pools, been removed from the stream by animals, or been swept downstream into Ladysmith Harbor. To account for the unobserved marks, we multiplied the number of marks of each population recovered at each location by the estimated spawning population size in the area divided by the number examined for marks. For example, the estimated number of marks moving into WB during 1984 that originated from AB was 9 × (1339/100) where

TABLE 1. Enzymes within tissues and buffer systems used in the electrophoretic analysis.

Tissue	Enzyme	Buffer[a]	Used in analysis
Muscle	*IDH-1,2*	AC	Yes
Muscle	*ME-1*	AC	Yes
Muscle	*LDH-1,2*	RW	Yes
Muscle	*LDH-3,4*	RW	Yes
Muscle	*LGG-1*	RW	Yes
Muscle	*AGP-1*	AC	No
Muscle	*MDH-3,4*	AC	No
Muscle	*6-PG*	AC	No
Muscle	*PGI-1*	RW	No
Muscle	*PGI-2*	RW	No
Muscle	*PGI-3*	RW	Yes
Muscle	*PGM-1*	RW	No
Muscle	*GL-1*	RW	No
Heart	*IDH-2*	AC	Yes
Heart	*AAT-1,2*	AC	Yes
Heart	*MDH-1,2*	AC	No
Heart	*MDH-3,4*	AC	Yes
Heart	*PMI*	AC	Yes
Heart	*AGP-1,2*	AC	Yes
Heart	*ACON-1,2*	AC	No
Heart	*ACON-3,4*	AC	No
Heart	*LDH-3*	MF	Yes
Heart	*PGM-1*	AC	No
Heart	*GL-1*	MF	Yes
Heart	*LGG-1*	MF	Yes
Liver	*IDH-3,4*	AC	Yes
Liver	*MDH-1,2*	AC	Yes
Liver	*PGM-1*	AC	Yes
Liver	*LDH-4*	RW	Yes
Liver	*PMI*	AC	No
Liver	*SDH*	RW	Yes
Eye	*IDH-3,4*	AC	Yes
Eye	*AAT-3*	AC	Yes
Eye	*MDH-1,2*	AC	No
Eye	*MDH-3,4*	AC	Yes
Eye	*GAP*	AC	No
Eye	*LDH-5*	MF	No
Eye	*GL-2*	MF	Yes
Eye	*LGG-1*	MF	Yes

[a] AC = amine–citrate buffer (Clayton and Tretiak 1972); MF = boric acid–Tris buffer (Markert and Faulhaber (1965); RW = discontinuous Tris buffer (Ridgeway et al. 1970).

9 is the number of AB fish recovered in the WB spawning time and location adjusted for differences in marking ratio, 1339 is the population size of spawning in WB, and 100 is the number examined for marks in WB. The answer rounds off to 121 marked fish.

To quantify genetic rates of straying based on protein polymorphism, we collected samples of hypaxial muscle, heart, liver, and eye tissue from spawning adults during 1981, 1982, and 1983. We transported tissues to the laboratory on ice and stored them at −20°C until the analysis was done in the winter of 1983–84. At the time of the analysis, tissue samples were ground and centrifuged. The supernatants were electrophoresed by the starch gel procedure of Allendorf and Utter (1979). A total of 39 loci were screened (Table 1). Fifteen of these were monomorphic or did not stain well. The results from the remaining 24 enzymes were used in the computations.

In scoring the electrophoresis results, we designated the most common allele as "100". Other alleles were scored according to the distance they travelled in the gel relative to the distance travelled by the most common allele. For example, if an allele travelled half the distance travelled by the most common allele, it was designated "50". If it travelled twice the distance travelled by the most common allele, it was designated "200".

We used Smith's (1970) H statistic to measure the divergence from Hardy–Castle–Weinberg (H-C-W) equilibrium and discriminate between an excess and a deficiency in the number of heterozygotes. For a two-allele system, Smith's (1970) statistic is defined as follows:

$$H = \frac{4n^2\hat{p}(1-\hat{p})-(2n-1)C}{4n(n-1)}$$

where n = number of individuals, $\hat{p}$ = estimated allele frequency, and C = number of heterozygotes. The H values can be summed without increasing the Wahlund effect using the formula

$$H = \frac{\Sigma(n_r - 1/2)H_r}{\Sigma(n_r - 1/2)}.$$

Tests were performed to compare the effect of years within populations. If no year effect was detected the data were pooled and the effect between populations tested.

Average heterozygosity was calculated using Nei's (1978) unbiased estimate based on conditional expectations.

To test the hypothesis that each population is in H-C-W equilibrium at each locus, a chi-square goodness of fit test was employed using the observed genotype frequencies and those expected under H-C-W equilibrium (Richardson et al. 1986). The chi-square test is suspect in cases where expected frequencies of some classes are low. Therefore, when more than two alleles were observed at a locus, the test was repeated using the genotypes pooled into three classes. Pooling was accomplished by considering all alleles except the common allele as a single allele. Three classes of genotype result: (1) homozygotes for the most common allele, (2) heterozygotes for the most common allele and one of the other alleles, and (3) all other genotypes. The resulting chi-square is used with 1 degree of freedom.

We used the fixation index (Wright 1969; Hartl 1981), F_{st}, to estimate the amount of gene flow among the populations:

$$F_{st} = \frac{H_T - H_S}{H_T}$$

where H_T = total heterozygosity and is the probability that two gametes chosen at random from the total population will carry different alleles and H_S = subpopulation heterozygosity, defined as the average heterozygosity among subpopulations.

Assuming that the populations are at equilibrium with respect to migration and that selection and mutation are negligible, the probability, m, that a randomly drawn allele is from a migrant depends on the degree of differentiation among the populations, F_{st}, and the effective population size, N_e. Thus, m can be estimated as

$$m = 1 - \left[\frac{F_{st}}{1/2N_e + (1 - 1/2N_e) \times F_{st}}\right]^{0.5} .$$

We used three different measures of effective population size. The first was simply the mean population size from the three years in which samples were collected (1981–83):

$$N_e = \frac{N_{81} + N_{82} + N_{83}}{3}.$$

As an alternative, we calculated the harmonic mean of the population sizes recorded from 1981 to 1985. Population sizes during 1981–83 were estimated from our field sampling whereas those of 1984 and 1985 were taken from Canadian Department of Fisheries and Oceans escapement records. We assumed that the fluctuation in the population size from year to year during this period would approximate the fluctuations from generation to generation:

$$\frac{1}{N_e} = \frac{1}{5}\left(\frac{1}{N_{81}} + \frac{1}{N_{82}} + \frac{1}{N_{83}} + \frac{1}{N_{84}} + \frac{1}{N_{85}}\right).$$

For the final estimate, we assumed that the average interval between generations was 3 yr and calculated the effective population size as the harmonic mean of the population sizes of 1981 and 1984:

$$\frac{1}{N_e} = \frac{1}{2}\left(\frac{1}{N_{81}} + \frac{1}{N_{84}}\right).$$

The sex ratio was near 1:1 in the populations (Tallman 1988).

The pattern among the populations of monomorphism and polymorphism at individual loci may be used to infer the most likely migration paths between the stocks. Six pathways exist: gene flow may be from AB to WB, WB to AB, AB to WW, WW to AB, WB to WW, and WW to WB. For the purpose of this analysis, we assume that these stocks are isolated from other stocks or that contributions from other stocks are negligible. There are 64 possible models of migratory exchange among these three populations ranging from complete exchange (that is, significant migration in all six directions) through various degrees of partial and complete isolation of the populations. If a locus is fixed in one population and polymorphic in another, then the only possible direction of genetic exchange is towards the polymorphic population.

We calculated 95% confidence limits on the percent probability of choosing a stray when sampling using the binomial distribution (Snedecor and Cochran 1967). The sample size used in calculations was the observed number of marks. A continuity correction term was applied to account for the small sample sizes.

We also used the binomial distribution to calculate the 95% confidence limits on *m*. The sample size was the number of fish scored for each population in the electrophoretic analysis.

We used a log-linear model (Sokal and Rohlf 1981) to analyse whether the rate of straying depended on the population and whether straying rate depended on the method of estimating possible genetic migration (by electrophoresis or by marking). The model was of the form

$$\ln Y_{ijk} = \mu + \alpha_i + \beta_j + \tau_k + \alpha\beta_{ij} + \alpha\tau_{ik} + \beta\tau_{jk} + a\beta\tau_{ijk} + \epsilon$$

where Y = predicted number of fish given the population i, the method of estimation j, and the fish type (stray or native), μ = overall parametric mean of the logarithms of expected frequencies, α_i, β_j, and τ_k = effects of population, method of estimation, and fish type, respectively, $\alpha\beta_{ij}$ = degree of dependence of method on population, $\beta\tau_{jk}$ = degree of dependence of fish type on method, $\alpha\tau_{ik}$ = degree of dependence of fish type on population, and $\alpha\beta\tau_{ijk}$ = three-way interdependence between effects α, β, and τ. For our interests the meaningful terms are the last three.

Results

The returns from marked fish indicated that straying among the three populations was substantial (Tables 2 and 3). The exchange was greatest between AB and WB with 15.3% of the returns spawned in AB returning to WB and 42.0% of the returns hatched in WB returning to AB. All strays from WW (54.0% of the returning marked fish) were found in the WB area. A small percentage (2.3%) of the returns from AB parents returned to WW.

The estimated return rates were 3.7, 2.8, and 1.4%, respectively, for AB, WB, and WW marked fish. Using the estimates of emigration and 3-yr-old population size the return rates were 3.5% for WB and 2.0% for WW fish. AB was composed of 3- and 4-yr-olds. We used the estimate of the percentage of age 4 fish, 42%, in the returning marks as an estimate of average percentage of age 4 fish in both years. Thus, 9161 × 0.58 = 5313 3-yr-olds returned in 1984 and 4843 × 0.42 = 2033 4-yr-old returned in 1985. The return rate for AB was 2.8%. From this information, there is no indication that fin-clipped fish had markedly poorer survival than the unmarked individuals.

Of those that returned in 1984, the composition of 3-yr-olds in the AB spawning population was 89.8% fish that originated from AB parents, 10.2% that originated from WB parents, and 0% that originated from WW parents (Table 3). In 1984, the composition of 3-yr-olds in the WB spawning population was 42.9% fish that originated from AB parents, 37.9% that originated from WB parents, and 19.1% fish that originated from WW parents. The composition of 3-yr-olds in the WW population was 29.9% from AB parents, 0% from WB parents, and 70.1% from WW parents. In 1985, only 4-yr-old fish marked as AB progeny were recovered. These were all observed to home to AB.

The 95% confidence limits of the probability of choosing a stray were very broad and included 0 in both AB and WW (Table 4). The probability of choosing a stray from WB remained well above 0. The 95% confidence interval for WW overlapped broadly with those of AB and WB. However, the intervals of AB and WB overlapped only slightly.

The percentage of polymorphic loci was similar among the populations. AB had the highest percentage of polymorphic loci (53.9%) compared with WB (43.6%) and WW (48.7%). The frequency of the most common allele was 0.95 or less at 38.5% of the loci of the WB samples compared with 35.9% of the loci of AB samples and 35.9% of the loci of WW samples.

Smith's (1970) *H* values were not significant between years with the confidence limits overlapping zero. Therefore, analyses were conducted on the pooled data between years for each stock. The allele frequencies of the polymorphic loci are shown in Table 5.

The average heterozygosity was less than 0.30. Mean heterozygosities were 0.208 (SE = 0.042), 0.218 (SE = 0.046),

TABLE 2. Marking rate of fry emigrating from Bush and Walker creeks in 1982. The marking ratio (WW) refers to the ratio of the marking rate for the WW population to the other populations. This value is used to adjust the numbers recovered to a common rate of marking.

Population	Total number of emigrants	Total marked	Marking rate (%)	Marking ratio (WW)	Marking ratio (AB)	Marking ratio (avg.[a])	Adjusted (WW) total marked	Adjusted (AB) total marked	Adjusted (avg.) total marked
AB	260 409	12 432	4.774	2.92	1.000	1.33	36 332	12 432	16 535
WB	38 342	2 111	5.506	2.53	0.867	1.15	5 439	1 830	2 428
WW	57 719	8 053	13.952	1.00	0.324	0.454	8 053	2 754	3 656

[a] Average marking ratio = 6.339%.

TABLE 3. Temporal and spatial pattern of return of marked fish to Bush and Walker creeks during 1984 and 1985.

Population of origin	Year	Recovery location			Adjustment by marking ratio			Number examined for marks	Adult population size	Recovery location			Return rate (%)	Straying rate (%)
		AB	WB	WW	AB	WB	WW			AB	WB	WW		
Using WW marking rate as the standard														
AB	1984	15	3	1	44	9	3	628	9161	642	121	23	3.76	18.3
	1985	3	0	0	9	0	0	75	4842	581	0	0		0.0
WB	1984	2	3	0	5	8	0	100	1339	73	107	0	3.199	38.5
	1985	0	0	0	0	0	0	20	708	0	0	0		—
WW	1984	0	4	7	0	4	7	150	1150	0	54	54	1.341	50.0
	1985	0	0	0	0	0	0	20	200	0	0	0		—
Using AB marking rate as the standard														
AB	1984	15	3	1	15	3	1	628	9161	219	40	8	3.781	18.0
	1985	3	0	0	3	0	0	75	4842	193	0	0		0.0
WB	1984	2	3	0	2	3	0	100	1339	29	40	0	3.253	42.0
	1985	0	0	0	0	0	0	20	708	0	0	0		—
WW	1984	0	4	7	0	1	2	150	1150	0	13	15	1.341	46.4
	1985	0	0	0	0	0	0	20	200	0	0	0		—
Using average marking rate as the standard														
AB	1984	15	3	1	20	4	1	628	9161	292	54	8	3.701	17.5
	1985	3	0	0	4	0	0	75	4842	258	0	0		0.0
WB	1984	2	3	0	2	3	0	100	1339	29	40	0	2.842	42.0
	1985	0	0	0	0	0	0	20	708	0	0	0		—
WW	1984	0	4	7	0	2	3	150	1150	0	27	23	1.368	54.0
	1985	0	0	0	0	0	0	20	200	0	0	0		—

TABLE 4. Probability that a spawner picked at random in 1984 will be a stray.

Population	Total estimated marks	Estimated strays	Probability of choosing a stray (%)	SD (%)	N	95%CI
AB	658	67	10.18	7.34	17	−7.15 to 27.51
WB	282	175	62.06	15.34	10	26.99 to 97.13
WW	77	23	29.87	16.19	8	−8.11 to 67.85

and 0.234 (SE = 0.044) for AB, WB, and WW, respectively. Heterozygosity varied greatly from locus to locus (Table 6). At some loci, H was very low or near fixation (e.g., *LGG-1* in eye).

Several loci were not in H-C-W equilibrium (Table 6). *ME-1*, *LDH-1,2*, and *LDH-3,4* in muscle tissue and *IDH-3,4* in eye tissue did not conform to H-C-W equilibrium in any of the populations. The AB population did not conform at the *MDH-3,4* and *GL-1* loci in heart tissue, *SDH* in liver tissue, and *GL-2* and *AAT-3* in eye tissue. The WW population did not conform at the *IDH-3,4*, *MDH-1,2*, *LDH-4*, and *SDH* loci in liver tissue and at the *AAT-3* locus in the eye.

Loci that were not in H-C-W equilibrium fell into three categories: those with a deficiency of heterozygotes relative to H-C-W expectations, those with an excess of heterozygotes, and those that were nearly monomorphic. In the latter case the chi-square was unusually high because the expected frequency of the less common homozygote was so low. *ME-1* in muscle had a deficiency of heterozygotes. In contrast, *LDH-1,2* and *LDH-3,4* from muscle, *IDH-3,4* from the eye in all populations and *SDH* from the liver, *AAT-3* from the eye in AB and WW, and *MDH-1,2* from liver tissue from WW samples all had an excess of heterozygotes. Loci close to fixation included *MDH-3,4* and *GL-1* from heart, *GL-2* from eye from AB, as well as *LDH-4* from liver tissue from WW.

Overall, the majority of loci in each population had more heterozygotes than predicted under H-C-W conditions. Twelve out of 21 loci in AB, 16 out of 17 in WB, and 15 out of 19 from WW showed an excess of heterozygotes.

The amount of genetic differentiation among the populations relative to a hypothetical group of subpopulations, each homozygous but having the same overall gene frequencies as the real populations, varied from locus to locus (Table 7). Three loci, heart *AGP-1,2*, liver *IDH-3,4*, and *PGM-1*, had F_{st} values in the range of 0.056–0.075, indicating moderate differentiation (Wright 1978; Hartl 1981). Other F_{st} values were less than 0.05. The overall mean F_{st} of 0.016 suggested that a limited amount of genetic differentiation had occurred among the populations.

Significant differences in allele frequency among the populations occurred at six loci: muscle *IDH-1,2*, heart *AGP-1,2*, liver *IDH-3,4*, *MDH-1,2*, and *LDH-4* and eye *AAT-3* (Table 8). The contingency chi-square indicated that at 16 of the 23 loci, genotype frequencies were out of H-C-W equilibrium. It is, therefore, unlikely that the samples were drawn from the same population. Subpopulation structuring appears to occur in this group of spawning populations.

There were seven loci that were polymorphic in one or two of the populations and not the remainder (Table 5). The *PGI-3* locus expressed in the muscle tissue and the *PGM-1* locus expressed in the liver were polymorphic in WW but not in WB or AB. Similarly, the *MDH-3,4* and *GL-1* loci expressed in heart tissue and the *GL-2* locus expressed in the eye were monomorphic in WB and WW but polymorphic in AB. The *AGP-1,2* locus expressed in heart tissue was polymorphic in AB and WW but fixed in WB. The *LDH-3* locus expressed in heart tissue was monomorphic in WW and polymorphic in the other two stocks. However, only five fish from WB were scored for this locus. Polymorphism might have been detected at this locus if more individuals had been sampled.

The mean probability, m, that an allele drawn at random will be from a stray was highest in the WB population (4.1–4.5%), next highest in the WW population (1.9–3.1%), and lowest in the AB population (0.38–0.45%) (Table 9). The 95% confidence limits for the m were above 0 for WB and WW (Table 10). All populations had overlapping intervals. The maximum probability of choosing an allele from a migrant ranged from 0.01 to 0.09.

The factors of population, the method of estimating exchange between the populations, and the frequencies of straying and homing fish were independent in terms of their three-way interaction ($p = 0.5281$). Thus, the interactions between straying and estimation method and between straying and the population could be considered independently of the three-way interaction in the ANOVA. The rates of straying were found to be dependent on the method of estimation ($p < 0.0001$) and the population ($p = 0.0016$). Dependence on the method of estimation means that mark–recapture showed greater rates of straying than electrophoresis. Also, regardless of method, straying rate depends on which population is observed, straying being greatest between WW and WB and least between AB and WW.

Discussion

In general the results may be summarized as follows:

(a) Marking suggested that straying rates were high (as much as 46% in the WB stock from other populations).

(b) Electrophoretic results suggested that the populations are genetically differentiated with low or moderate gene flow (under 5%) and that gene flow was greatest between populations in the same river system. The pattern of polymorphism and fixation observed among the populations could occur only if there was no interbreeding among the populations or if genetic migration occurred from the WB stock into the AB stock without migration in other possible directions.

(c) Both measures suggested that the intermediate population in time and space, WB, receives the greatest amount of genetic material from outside sources.

(d) Log-linear analysis indicates that the populations differ in their rates of straying and that the rate of straying

TABLE 5. Allele frequencies and sample sizes by population for loci used in the analysis.

			Stock							
			AB		WB		WW			
Tissue	Locus	Allele	*N*	Frequency	*N*	Frequency	*N*	Frequency	E.C. No.	Alternative name
Muscle	*IDH-1,2*	*100*	158	0.968	81	0.907	92	0.995	1.1.1.42	IDH
		64		0.032		0.093		0.005		
	ME-1	*100*	153	0.601	81	0.648	90	0.572	1.1.1.40	ME
		120		0.399		0.352		0.428		
	LDH-1,2	*100*	157	0.500	81	0.500	92	0.500	1.1.1.27	LDH
		136		0.500		0.500		0.500		
	LDH-3,4	*100*	158	0.513	81	0.500	92	0.500	1.1.1.27	LDH
		136		0.487		0.500		0.500		
	LGG-1(GAL)	*100*	153	0.889	81	0.821	85	0.847	3.2.1.23	GAL
		136		0.111		0.179		0.153		
	PGI-3	*100*	128	1.000	50	1.000	58	0.991	5.3.1.9	GPI
		80		0.000		0.000		0.009		
Heart	*IDH-1,2*	*100*	148	0.970	76	0.941	88	0.966	1.1.1.42	IDH
		110		0.030		0.059		0.034		
	AAT-1,2	*100*	138	0.819	76	0.757	79	0.823	2.6.1.1	AAT
		115		0.181		0.243		0.177		
	MDH-3,4	*100*	137	0.993	80	1.000	89	1.000	1.1.1.37	MDH
		120		0.007		0.000		0.000		
	PMI	*100*	127	0.807	72	0.840	72	0.889	5.3.1.8	MPI
		92		0.193		0.160		0.111		
	AGP-1,2	*100*	41	0.976	5	1.000	45	0.856	1.1.1.8	GPD
		93		0.024		0.000		0.144		
	LDH-3	*100*	156	0.997	81	0.994	90	1.000	1.1.1.27	LDH
		136		0.003		0.006		0.000		
	GL-1	*100*	120	0.983	73	1.000	87	1.000	4.4.1.5	GLO
		80		0.017		0.000		0.000		
	LGG-1	*100*	153	0.886	81	0.901	89	0.876	3.2.1.23	GAL
		75		0.114		0.099		0.124		
Liver	*IDH-3,4*	*100*	85	0.682	48	0.563	56	0.393	1.2.1.42	IDH
		27		0.035		0.063		0.036		
		40		0.176		0.135		0.429		
		83		0.106		0.240		0.143		
	MDH-1,2	*100*	153	0.931	80	0.881	91	0.775	1.1.1.37	MDH
		200		0.069		0.119		0.225		
	PGM-1	*100*	1	1.000	6	1.000	21	0.905	2.7.5.1	PGM
		110		0.000		0.000		0.095		
	LDH-4	*100*	103	0.927	80	0.994	91	0.956	1.1.1.27	LDH
		136		0.073		0.006		0.044		
	SDH	*100*	22	0.500	3	0.500	11	0.500	1.1.1.14	SDH
		90		0.500		0.500		0.455		
		80		0.000		0.000		0.045		

differs if one uses biochemical genetic or marking techniques to measure it.

Quinn (1984) hypothesized that straying is an evolutionary alternative to homing and that these two life-history strategies are in dynamic equilibrium with homing as the dominant strategy. However, to resolve our results, one must note that fish that stray (as inferred by recovered marks) do not necessarily successfully reproduce in the other population. They may face barriers in mate choice or their offspring may not survive. Possibly, they may mate only with other strays. Studies of sockeye salmon and its landlocked form, the kokanee, by Foote (1988, 1989) and Foote and Larkin (1988) demonstrated that male and female mate choice played an important role in maintaining the segregation between the forms of *O. nerka*. Foote et al. (1989) showed that kokanee were less adapted to marine conditions and suggested that this differentiation could adversely affect the survival of hybrids in the wild. Similarly, Taylor and Foote (1991) found that hybrids between sockeye and kokanee had lower swimming capabilities compared with

TABLE 5. (*Concluded*)

			Stock							
			AB		WB		WW			
Tissue	Locus	Allele	*N*	Frequency	*N*	Frequency	*N*	Frequency	E.C. No.	Alternative name
Eye	*IDH-3,4*	*100*	123	0.402	63	0.452	74	0.324	1.1.1.42	IDH
		27		0.020		0.032		0.014		
		40		0.492		0.397		0.595		
		83		0.085		0.119		0.068		
	AAT-3	*100*	120	0.837	74	0.932	80	0.781	2.6.1.1	AAT
		115		0.162		0.068		0.219		
	MDH-3,4	*100*	1	0.000	20	0.000	38	0.000	1.1.1.37	MDH
		120		1.000		1.000		1.000		
	GL-2	*100*	152	0.987	77	1.000	89	1.000	4.4.1.5	GLO
		80		0.013		0.000		0.000		
	LGG-1	*100*	120	0.946	62	0.903	69	0.957	3.2.1.23	GAL
		75		0.054		0.097		0.043		

TABLE 6. Heterozygosity and test of conformance to H-C-W equilibrium of polymorphic loci within each population (HUB = unbiased heterozygosity estimate (Nei 1978); p = p value for chi-square test).

		Population					
		AB		WB		WW	
Tissue	Locus	HUB	p	HUB	p	HUB	p
Muscle	*IDH-1,2*	0.061	0.681	0.169	0.358	0.011	0.958
	ME-1	0.481	0.001	0.459	0.001	0.492	0.001
	LDH-1,2	0.502	0.001	0.503	0.001	0.503	0.001
	LDH-3,4	0.501	0.001	0.503	0.001	0.503	0.001
	LGG-1	0.198	0.467	0.296	0.228	0.261	0.408
	PGI-3	0.000	1.000	0.000	1.000	0.017	0.947
Heart	*IDH-1,2*	0.059	0.703	0.112	0.583	0.066	0.741
	AAT-1,2	0.298	0.399	0.371	0.754	0.293	0.711
	MDH-3,4	0.015	0.001	0.000	1.000	0.000	1.000
	PMI	0.313	0.325	0.270	0.462	0.199	0.895
	AGP-1,2	0.048	0.873	0.000	1.000	0.250	0.257
	LDH-3	0.006	0.968	0.012	0.955	0.000	1.000
	GL-1	0.033	0.001	0.000	1.000	0.000	1.000
	LGG-1	0.203	0.110	0.179	0.324	0.218	0.183
Liver	*IDH-3,4*	0.494	0.102	0.610	0.720	0.646	0.018
	MDH-1,2	0.128	0.106	0.211	0.228	0.351	0.006
	PGM-1	0.000	1.000	0.000	1.000	0.177	0.630
	LDH-4	0.136	0.508	0.013	0.955	0.085	0.001
	SDH	0.512	0.001	0.600	0.083	0.567	0.012
Eye	*IDH-3,4*	0.591	0.001	0.628	0.001	0.540	0.030
	AAT-3	0.273	0.034	0.127	0.533	0.344	0.012
	MDH-3,4	0.000	1.000	0.000	1.000	0.000	1.000
	GL-2	0.026	0.001	0.000	1.000	0.000	1.000
	LGG-1	0.103	0.248	0.176	0.399	0.084	0.706

pure sockeye. They hypothesized that if variability in swimming performance is associated with differences in survival in nature, then such differences may promote divergence between sympatric sockeye and kokanee. The potential detrimental effects of interstock matings (such as mating with a stray from another stock) were also shown by Brannon (1967), who compared the reaction to current of three Fraser River sockeye salmon stocks: a lake-spawning stock (Cultus Lake), an outlet-spawning stock (Chilko River), and an inlet-spawning stock (Stellako River, tributary to Fraser Lake) and Chilko ♂ × Stellako ♀ hybrids. In Cultus Lake water, 86% of the Chilko fish moved upstream, 84% of the Stellako fish moved downstream, 62% of the Cultus fish moved upstream, and the hybrids went equally in either direction. For stocks such as Chilko or Stellako, hybridization would lead to fry failing to reach the appropriate rearing environ-

TABLE 7. Fixation index, F_{st} (Wright 1969), at all loci.

Tissue	Locus	F_{st}	Tissue	Locus	F_{st}
Heart	*IDH-1,2*	0.004	Muscle	*IDH-1,2*	0.032
	AAT-1,2	0.006		*ME-1*	0.004
	MDH-3,4	0.005		*LDH-1,2*	0.000
	PMI	0.009		*LDH-3,4*	0.000
	AGP-1,2	0.075		*LGG-1*	0.006
	LDH-3	0.002		*PGI-3*	0.006
	GL-1	0.011	Eye	*IDH-3,4*	0.017
	LGG-1	0.001		*AAT-3*	0.031
Liver	*IDH-3,4*	0.056		*MDH-3,4*	0.036
	MDH-1,2	0.036		*GL-2*	0.009
	PGM-1	0.066		*LGG-1*	0.009
	LDH-4	0.019		*SDH*	0.002

Overall mean = 0.016

TABLE 8. Contingency chi-square analysis at all loci. Chi-square and probability values are for the hypothesis that the samples were drawn from the same population.

Tissue	Locus	No. of alleles	Chi-square	df	*p*
Muscle	*IDH-1,2*	2	18.277	2	0.0001
	ME-1	2	2.089	2	0.3519
	LDH-1,2	2	0.000	2	1.0000
	LDH-3,4	2	0.106	2	0.9484
	LGG-1	2	4.417	2	0.1099
	PGI-3	2	3.076	2	0.2149
Heart	*IDH-1,2*	2	2.380	2	0.3043
	AAT-1,2	2	2.906	2	0.2339
	MDH-3,4	2	2.475	2	0.2901
	PMI	2	4.532	2	0.1037
	AGP-1,2	2	9.128	2	0.0104
	LDH-3	2	1.070	2	0.5857
	GL-1	2	5.372	2	0.0682
	LGG-1	2	0.533	2	0.7662
Liver	*IDH-3,4*	4	42.329	6	0.0000
	MDH-1,2	2	25.679	2	0.0000
	PGM-1	2	1.436	2	0.4878
	LDH-4	2	9.529	2	0.0085
	SDH	3	2.338	4	0.6739
Eye	*IDH-3,4*	4	11.522	6	0.0735
	AAT-3	2	13.819	2	0.0010
	GL-2	2	4.396	2	0.1110
	LGG-1	2	3.659	2	0.1605

ment. These studies all suggest that interstock matings should be less viable in nature. If the established population is able to suppress the introduction of allochthonous genetic material into its genome, this would be consistent with the observation that strays can colonize systems without conspecifics (e.g., the upper Fraser River by pinks after the Hell's Gate slide, the colonization through introduction of New Zealand, Chile, and the Great Lakes by chinook salmon, the Great Lakes by coho salmon, and especially the colonization of the Great Lakes by pink salmon) but that individual salmon populations in the natural home range of the species can maintain highly adapted and genetically unique populations. In the latter case, the success rate of strays is reduced. Our results suggest that such selection may be a powerful force in maintaining stock discreteness.

As in any study where fish are marked, we cannot completely discount the possibility that the marking procedure may have altered the subsequent behaviour of the fish. Fish could have strayed as a result of marking. However, salmon often experience wounds during the course of their feeding and spawning migrations. It is generally thought that the homing imperative is so great that the fish must be unable to function before it diverts from its course. It is also clear that the percent return of marked fish at age 3 (2.0–3.5%) is at least as high as the rate of return of unmarked animals. Thus, marked animals did not suffer substantial mortality or disorientation that prevented them from returning to the vicinity of their natal stream.

We have assumed that interannual variation in straying rates is not greater than the effects we measured. If this is not

TABLE 9. Estimated effective population size, N_e, and the mean probability, m, that a randomly chosen allele will be from a migrant individual assuming random mating no selection or mutation where population size is calculated by the algebraic mean, harmonic mean, and modified harmonic mean method.

	N_e			m		
Method	AB	WB	WW	AB	WB	WW
Algebraic	3800	318	775	0.00402	0.04506	0.01926
Harmonic	4078	325	478	0.00375	0.04416	0.03067
Modified harmonic	3417	356	594	0.00447	0.04062	0.02494

TABLE 10. The 95% confidence limits of m, the probability that an allele drawn at random from a population will be from a migrant.

Population	m	SD	N	CI
AB	0.00375	0.00318	369	−0.00384 to 0.01033
WB	0.04416	0.01755	137	0.00610 to 0.08771
WW	0.03067	0.01052	269	0.00878 to 0.05314

the case, then our interpretation is suspect because the estimates for gene flow and straying were done in separate years.

We have used the presence or absence of rare alleles to determine the direction of gene flow. Slatkin (1981, 1985) suggested that rare alleles could be useful in estimating gene flow. However, our conclusions are tempered with the knowledge that the frequencies of rare alleles can be affected by sampling error and genetic drift.

Although, the most parsimonius explanation is that strays do not reproduce, other possibilities exist. Chilcote et al. (1986) compared the reproductive success of naturally spawning summer run hatchery and wild steelhead trout (*Oncorynchus mykiss*) by electrophoretic examination of juveniles for a specific genetic marker. The hatchery strays had a lower success rate but they did produce significant numbers of smolts. One explanation for these results is that strays only mated with strays through some unknown mechanism of mate choice. If the offspring of these matings also stray, the genetic material represented by strays would not persist in the population. If this is the case the possibility raised by Chilcote et al. (1986) that naturally spawning hatchery fish would influence the genetic compositions of wild populations may need to be rescrutinized.

Kujima and Fujio (1982) concluded that the gene constitutions of two chum salmon populations separated by more than 600 km can be regarded as practically independent of each other. Beacham et al. (1985, 1987), in surveying British Columbia chum salmon stocks, found a range of interrelatedness between populations. Although a general pattern of increasing distinctness with increasing geographic separation is evident, some stocks located quite close together were very distinct whereas others that were geographically distant were apparently very similar in biochemical genetic composition. Our electrophorectic results suggest a very low exchange between the populations located within a few kilometres. These estimates are sensitive to the assumption that the operating sex ratio is one to one. This is probably not the case. Late-arriving males could not mate with females that have already spawned. An unbalanced sex ratio would lower the effective population size and increase m. We investigated the effects on m of lowering the effective population size and found that for AB, m changed from roughly 0.004 to 0.029 as N_e was lowered from 4000 to 500 whereas for WW and WB, m went from 0.035 to 0.12 as N_e went from 400 to 100. Thus, if N_e is substantially lower than observed in WW and AB, the real value of m could be close to the estimate from marking. For WB, N_e would have to be less than 5 to give a value for m close to that observed from tag returns. On the one hand, according to Spieth (1974) and Kujima and Fujio (1982), the rate of exchange recorded among the three populations, even assuming mixing, would still exceed the limit for differentiation. On the other hand, Tallman (1986) demonstrated substantial genetic differentiation between these populations in quantitative genetic traits. This result suggests the possibility that genetic differentiation does not require such stringent restrictions on the number of migrants.

In conclusion, it appears that the rate of straying as determined by marking does not reflect the true rate of genetic migration among these populations. Migration rates are much less than they appear. Therefore, studies that show high straying rates (i.e., Labelle 1990) should not be interpreted as demonstrating that the populations involved are panmictic.

Acknowledgements

We wish to thank R. Ball and F. Jordan who provided valuable technical assistance. T.A. Beacham and C.B. Murray, of the Department of Fisheries and Oceans in Nanaimo, B.C., provided helpful advice during the course of the study. D.P. Swain and S. Courtenay of the Department of Fisheries and Oceans, Moncton, N.B., and T. Quinn and C. Foote of the University of Washington, Seattle, Wash., provided helpful reviews of earlier versions of the manuscript.

References

ALLENDORF, K.W., AND F.M. UTTER. 1979. Population genetics, p. 407–454. *In* W.S. Hoar, D.J. Randall, and J.R. Brett [ed.] Fish physiology. Academic Press, New York, N.Y.

BARTLEY, D.M., AND G.A.E. GALL. 1990. Genetic structure and gene flow in chinook salmon populations in California. Trans. Am. Fish. Soc. 119: 55–71.

Beacham, T.D., A.P. Gould, R.E. Withler, C.B. Murray, and L.W. Barner. 1987. Biochemical genetic survey and stock identification of chum salmon (*Oncorhynchus keta*) in British Columbia. Can. J. Fish. Aquat. Sci. 44: 1702–1713.

Beacham, T.D., R.E. Withler, and A.P. Gould. 1985. Biochemical genetic stock identification of chum salmon (*Oncorhynchus keta*) in southern British Columbia. Can. J. Fish. Aquat. Sci. 42: 437–448.

Blair, A.A. 1968. Pink salmon find new home in Newfoundland. Fish. Can. 21(4): 9–12.

Boyd, F.C. 1964. Return of pink salmon to Robertson Creek shows promise of success. Can. Fish Cult. 32: 59–62.

Brannon, E.L. 1967. Genetic control of migrating behaviour of newly emerged sockeye salmon fry. Int. Pac. Salmon Fish. Comm. Prog. Rep. 16: 31 p.

Chilcote, M.W., S.A. Leider, and J.J. Loch. 1986. Differential reproductive success of hatchery and wild summer-run steelhead under natural conditions. Trans. Am. Fish. Soc. 115: 726–735.

Clayton, J.W., and D.N. Tretiak. 1972. Amino citrate buffer for pH control in starch gel electrophoresis. J. Fish. Res. Board Can. 29: 1169–1172.

Donaldson, L.R., and G.H. Allen. 1958. Return of the silver salmon, *Oncorhynchus kisutch* (Walbaum) to point of release. Trans. Am. Fish. Soc. 87: 13–22.

Foerster, R.E. 1936. The return from sea of sockeye salmon (*Oncorhynchus nerka*) with special reference to percentage survival, sex proportions and progress of migration. J. Biol. Board Can. 3: 26–42.

Foerster, R.E. 1968. The sockeye salmon. Bull. Fish. Res. Board Can. 162: 422 p.

Foote, C.J. 1988. Male mate choice dependent on male size in salmon. Behaviour 106: 63–80.

Foote, C.J. 1989. Female mate preference in Pacific salmon. Anim. Behav. 38: 721–723.

Foote, C.J., and P.A. Larkin. 1988. The role of mate choice in the assortative mating of anadromous and non-anadromous sockeye salmon (*Oncorhynchus nerka*). Behaviour 106: 43–61.

Foote, C.J., C.C. Wood, W.C. Clarke, and J. Blackburn. 1989. The saltwater adaptability of sympatric anadromous and non-anadromous sockeye salmon and their 'hybrids'. Aquaculture 82: 377.

Hartl, D. 1981. A primer of population genetics. Sinauer and Assoc. Inc., Sunderland, Mass. 191 p.

Hartman, W.L., and R.F. Raleigh. 1964. Tributary homing of sockeye salmon at Brooks and Karluk lakes, Alaska. J. Fish. Res. Board Can. 21: 485–504.

Heggberget, T.G., L.P. Hansen, and T.F. Naesje. 1988. Within river spawning migration of Atlantic Salmon (*Salmo salar*). Can. J. Fish. Aquat. Sci. 45: 1691–1698.

Kijima, A., and Y. Fujio. 1982. Correlation between geographic distance and genetic distance in populations of chum salmon, *Oncorhynchus keta*. Bull. Jpn. Soc. Sci. Fish. 48: 1703–1709.

Klyashtorin, L.B. 1989. Homing in pink salmon. Ryb. Khoz. 1: 56–58.

Kwain, W. 1982. Spawning behavior and early life history of pink salmon (*Oncorhynchus gorbuscha*) in the Great Lakes. Can. J. Fish. Aquat. Sci. 39: 1353–1360.

Kwain, W., and J.A. Chappel. 1978. First evidence for even-year spawning pink salmon, *Oncorhynchus gorbuscha*, in Lake Superior. J Fish. Res. Board Can. 35: 1373–1376.

Kwain, W., and S.J. Kerr. 1984. Return of 1-year-old pink salmon in Michipicoten River, eastern Lake Superior. N. Am. J. Fish. Manage. 4: 335–337.

Kwain, W., and A.H. Lawrie. 1981. Pink salmon in the Great Lakes. Fisheries 6: 2–6.

Labelle, M. 1990. A comparative study of coho salmon populations of S.E. Vancouver Island, British Columbia: juvenile outmigration, coded-wire tagging and recovery, escapement enumeration, and stock composition at Black Creek, Trent River and French Creek, 1984–1988. Can. Tech. Rep. Fish. Aquat. Sci. 1772: 148 p.

Lindsey, C.C., T.G. Northcote, and G.F. Hartman. 1959. Homing of rainbow trout to inlet and outlet spawning at Loon Lake, British Columbia. J. Fish. Res. Board Can. 16: 695–719.

Lister, D.B., D.G. Hickey, and I. Wallace. 1981. Review of the effects of enhancement strategies on the homing straying and survival of Pacific salmonids. Vol. 1. D.B. Lister and Associates Ltd., West Vancouver, B.C. 51 p.

Markert, C.L., and I. Faulhaber. 1965. Lactate dehydrogenase isozyme patterns of fish. J. Exp. Zool. 159: 319–332.

Neave, F. 1958. The origin and speciation of *Oncorhynchus*. Trans. R. Soc. Can. 52: 25–39.

Quinn, T.P. 1984. Homing and straying in Pacific salmon, p. 357–362. *In* J.D. McCleave, G.P. Arnold, J.J. Dodson, and W.H. Neill [ed.] Mechanisms of migration in fishes. Plenum Press, New York, N.Y.

Quinn, T.P., and K. Fresh. 1984. Homing and straying in chinook salmon (*Oncorhynchus tshawytscha*) from Cowlitz River Hatchery, Washington. Can. J. Fish. Aquat. Sci. 41: 1078–1082.

Quinn, T.P., C.C. Wood, L. Margolis, B.E. Riddell, and K.D. Hyatt. 1987. Homing in wild sockeye salmon (*Oncorhynchus nerka*) populations as inferred from differences in parasite prevalance and allozyme allele frequencies. Can. J. Fish. Aquat. Sci. 44: 1963–1971.

Richardson, B.J., P.R. Baverstock, and M. Adams. 1986. Allozyme electrophoresis. A handbook of animal systematics and population studies. Academic Press, Inc., San Diego, Calif.

Ricker, W.E. 1987. Effects of the fishery and of obstacles on the abundance of Fraser River sockeye salmon (*Oncorhynchus nerka*). Can. Tech. Rep. Fish. Aquat. Sci. 1522: 1–75.

Ricker, W.E. 1989. History and present state of the odd-year pink salmon runs of the Fraser River region. Can. Tech. Rep. Fish. Aquat. Sci. 1702: 1–37.

Ridgeway, G.J., S.W. Sherburne, and R.D. Lewis. 1970. Polymorphism in the esterases of Atlantic herring. Trans. Am. Fish. Soc. 99: 147–151.

Sano, S. 1966. Salmon of the north Pacific Ocean. Part III. A review of the life history of north Pacific salmon. 3. Chum salmon in the Far East. Int. North Pac. Fish. Comm. Bull. 18: 41–57.

Shapovalov, L., and A.C. Taft. 1954. The life histories of the steelhead rainbow trout (*Salmo gairdneri*) and silver salmon (*Oncorhynchus kisutch*). Calif. Dep. Fish Game Fish Bull. 98: 375 p.

Sholes, W.H., and R.J. Hallock. 1979. An evaluation of rearing fall-run chinook salmon (*Oncorhynchus tshawytscha*) to yearlings at Feather River Hatchery with a comparison of returns from hatchery and downstream releases. Calif. Fish Game 65: 239–255.

Slatkin, M. 1981. Estimating levels of gene flow in natural populations. Genetics 99: 323–335.

Slatkin, M. 1985. Rare alleles as indicators of gene flow. Evolution 39: 53–65.

Smith, C.A.B. 1970. A note on testing the Hardy–Weinberg law. Hum. Genet. 33: 377–383.

Snedecor, G.W., and W.G. Cochran. 1967. Statistical methods. 6th ed. Iowa State University Press, Ames, Iowa. 593 p.

Snyder, J.O. 1931. Salmon of the Klamath River, California. Calif. Dep. Fish Game Fish Bull. 34: 130 p.

Sokal, R.R., and F.J. Rohlf. 1981. Biometry. 2nd ed. Freeman and Co., New York, N.Y. 859 p.

Spieth, P.T. 1974. Gene flow and genetic differentiation. Genetics 78: 961–965.

Stabell, O.B. 1984. Homing of Atlantic salmon in relation to olfaction and genetics. Saumons 51: 21–25.

Tallman, R.F. 1986. Genetic differentiation among seasonally distinct spawning populations of chum salmon, *Oncorhynchus keta*. Aquaculture 57: 211–217.

Tallman, R.F. 1988. Seasonal isolation and adaptation among chum salmon, *Oncorhynchus keta* (Walbaum), populations. Ph.D. dissertation, University of British Columbia, Vancouver, B.C. 374 p.

Tallman, R.F., and M.C. Healey. 1991. Phenotypic differentiation in seasonal ecotypes of chum salmon, *Oncorhynchus keta*. Can. J. Fish. Aquat. Sci. 48: 661–671.

Taylor, E.B., and C.J. Foote. 1991. Critical swimming velocities of juvenile sockeye salmon and kokanee, the anadromous and non-anadromous forms of *Oncorhynchus nerka* (Walbaum). J. Fish Biol. 38: 407–419.

Withler, F.C., and W. Kwain. 1984. Survey of pink salmon in eastern Lake Superior, 1981. Can. Tech. Rep. Fish. Aquat. Sci. 1317: 1–39.

Wright, S. 1969. Evolution and the genetics of populations. Vol. 2: The theory of gene frequencies. University of Chicago Press, Chicago, Ill. 511 p.

Wright, S. 1978. Evolution and the genetics of populations. Vol. 4: Variability within and among natural populations. University of Chicago Press, Chicago, Ill. 580 p.

Identifying Habitat Associations of Marine Fishes Using Survey Data: An Application to the Northwest Atlantic

R. Ian Perry

Department of Fisheries and Oceans, Pacific Biological Station, Nanaimo, BC V9R 5K6, Canada

and Stephen J. Smith

Department of Fisheries and Oceans, Bedford Institute of Oceanography, Dartmouth, NS B2Y 4A2, Canada

Perry, R.I., and S.J. Smith. 1994. Identifying habitat associations of marine fishes using survey data: an application to the northwest Atlantic. Can. J. Fish. Aquat. Sci. 51: 589–602.

We present an objective method for identifying associations between environmental (habitat) conditions and the distributions of marine fishes using survey data. The method tests the null hypothesis of a random association between fish distribution and habitat conditions. We apply this method to bottom depth, temperature, and salinity data and to the distributions of four groundfish species (yellowtail flounder (*Pleuronectes ferruginens*, previously *Limanda ferruginea*), haddock (*Melanogrammus aeglefinus*), silver hake (*Merluccius bilinearis*), and Atlantic cod (*Gadus morhua*)) from trawl surveys of the eastern Scotian Shelf (northwest Atlantic) conducted in winter/spring (March) and summer (July) 1979–84. Haddock and silver hake maintained similar temperatures in winter and summer by changing their depth distributions (temperature-keepers), with haddock generally at cooler temperatures than silver hake. Yellowtail flounder (a depth-keeper) maintained similar depths between seasons while tolerating a wide range of temperatures and salinities. Atlantic cod were not consistently associated with particular depths in either spring or summer, and we were unable to distinguish between temperature or salinity as a single factor modifying their distributions, perhaps because of age-related effects. Identification of persistent habitat associations of marine fishes provides an opportunity to improve fisheries management procedures.

Nous présentons une méthode objective permettant d'identifier les associations entre les conditions environnementales (habitat) et les distributions des poissons marins en utilisant les données fournies par des relevés. La méthode teste l'hypothèse nulle d'une association aléatoire entre la distribution des poissons et des conditions de l'habitat. Nous appliquons cette méthode à des données sur la profondeur au fond, la température et la salinité et à la distribution de quatre espèces de poisson de fond (limande à queue jaune (*Pleuronectes ferruginens*, auparavant le *Limanda ferruginea*), aiglefin (*Melanogrammus aeglefinus*), merlu argenté (*Merluccius bilinearis*) et morue franche (*Gadus morhua*)) à partir de relevés effectués au chalut sur l'est de la plate-forme néo-écossaise (Atlantique nord-ouest) à deux périodes : hiver/printemps (mars) et été (juillet) de 1979 à 1984. L'aiglefin et le merlu argenté se maintenaient à des températures similaires en hiver et en été en changeant de profondeur (préférence pour la température), l'aiglefin se tenant généralement à des températures plus basses que le merlu argenté. La limande à queue jaune (préférence pour la profondeur) se maintenait à la même profondeur d'une saison à l'autre mais tolérait une fourchette large de températures et de salinité. La morue franche n'était pas associée de façon régulière à une température donnée ni au printemps ni en été, et nous n'avons pas pu faire la différence entre la température ou la salinité comme facteur modifiant leur répartition, ce qui est peut-être causé par des effets liés à l'âge. La connaissance des associations stables avec l'habitat chez les poissons marins donne l'occasion d'améliorer les méthodes de gestion des pêches.

Received March 8 1993
Accepted October 7, 1993
(JB837)

Reçu le 8 mars 1993
Accepté le 7 octobre 1993

Knowledge of the environmental conditions at which fish occur can lead to improved abundance estimates from trawl surveys (Smith 1990; Smith et al. 1991), identification of species assemblages (Mahon and Smith 1989), and understanding of environmental influences on fish distribution and migration patterns (e.g., Mysak 1986; Rose and Leggett 1988; Xie and Hsieh 1989). Reactions of freshwater fishes to temperature have received considerable attention, in particular regarding the impacts of thermal effluent (e.g., Coutant 1977; Richards et al. 1977). In the marine environment, the most common approach has been to determine environmental associations empirically using field studies and surveys. In the northwest (NW) Atlantic, Scott (1982a) examined depth, temperature, and salinity preferences of common groundfishes on the continental shelf off Nova Scotia from survey data collected during summer 1970–79. However, many fish species on the Scotian Shelf undertake seasonal migrations. Environmental conditions also change seasonally. It is unknown how fish in this area react to these changes, and whether associations with environmental conditions determined during summer can be applied to other seasons.

The objective of this paper is to identify significant associations between environmental (habitat) conditions and the

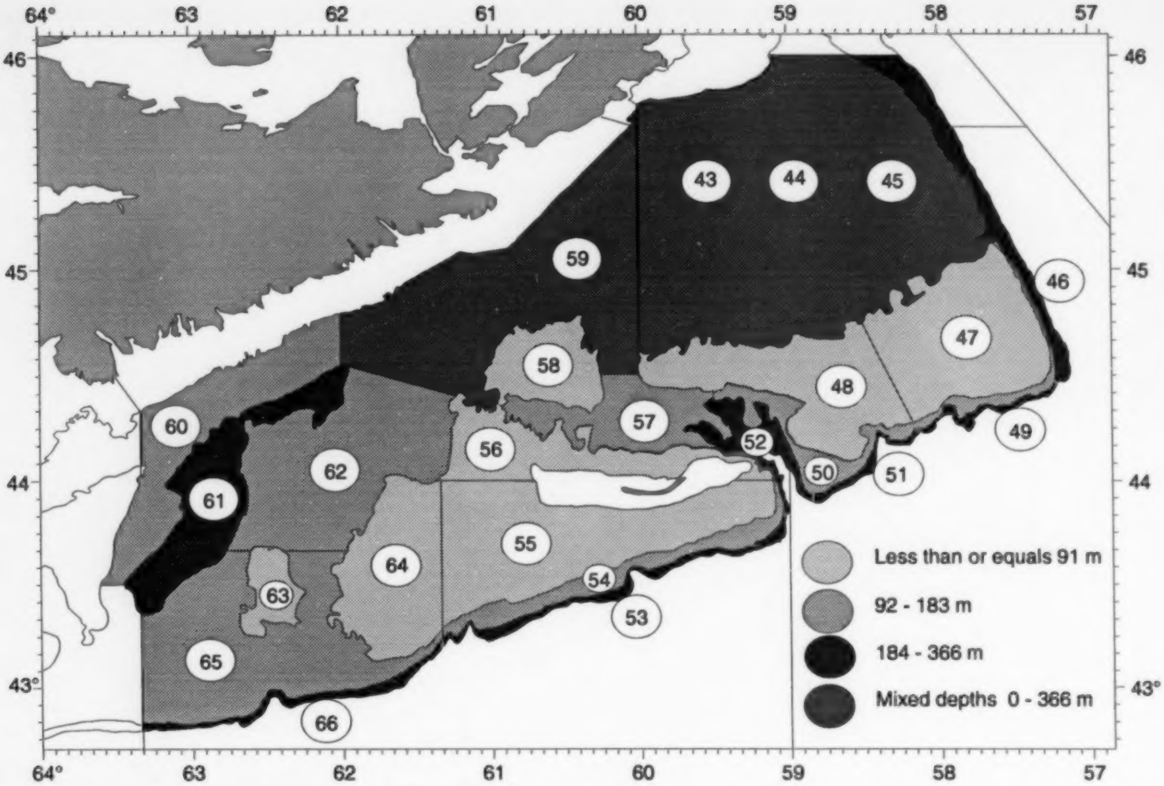

FIG. 1. Stratification scheme for spring and summer 1979–84 surveys of the eastern Scotian Shelf, NW Atlantic. Strata are identified by the numbers in circles and are based on the depth zones indicated.

distributions of four species of groundfish on the eastern Scotian Shelf in the NW Atlantic. To achieve this purpose, we develop an objective method to define fish–habitat associations which allows rigorous comparisons to be made with the ranges of environmental conditions available during the surveys. Strong associations with particular habitat conditions, especially those which may vary seasonally or interannually, will help predict changes in fish distributions as a response to changes in oceanographic conditions. For reasons of data availability, the habitat conditions we consider are temperature, salinity, and depth. The fish species we consider are yellowtail flounder (*Pleuronectes ferruginens*, previously *Limanda ferruginea*), haddock (*Melanogrammus aeglefinus*), silver hake (*Merluccius bilinearis*), and Atlantic cod (*Gadus morhua*). These are common groundfish species on the eastern Scotian Shelf and occur from shallow and intermediate depths with wide ranges of temperature and salinity (e.g., yellowtail flounder, Atlantic cod, haddock; mean conditions 60–90 m, 2–7°C, 31–34 psu) to deep depths and warm temperatures (e.g., silver hake; mean conditions 165 m and 7–10°C) (Scott 1982a; Smith et al. 1991).

Methods

Fish catch and hydrographic data were obtained from standard groundfish research trawl surveys of the eastern Scotian Shelf (NAFO Area 4VsW) conducted by the Marine Fish Division (Bedford Institute of Oceanography, Dartmouth, N.S., and Biological Station, St. Andrews, N.B.) of the Canadian Department of Fisheries and Oceans. The survey used a stratified random design, with strata based on depth boundaries of 91, 183, and 366 m (50, 100, and 200 fathoms) (Fig. 1). Inshore areas with bottom depths <28 m were not sampled. The survey sample unit was defined as the bottom area fished by a Western IIA trawl towed at a constant speed (3.5 kn) for a distance of 3.24 km (1.75 nautical miles). Locations of sample units (sets) were selected randomly within each stratum before each cruise. All species caught were identified, counted, and weighted to the nearest kilogram and expressed as catch per standard sample unit. Following each set, bottom-water samples were obtained with reversing bottles for measurements of temperature and salinity. Set depth was taken as the mean bottom depth during the tow determined from continuous echo sounder records. Further details of sample protocol are available in Halliday and Koeller (1981). Note that this protocol is unable to resolve variability and fish–environment associations at scales finer than the length of a tow, e.g., that might be caused by crossing frontal features. The summer survey has been conducted in July since 1970, while an additional survey was conducted in March (late winter/early spring) from 1979 to 1984. To compare seasons the analyses were restricted to the years 1979–84.

Our approach to identifying associations between catches of the four representative species and the environmental data from the surveys has three steps. First, we characterize

Table 1. Definitions of quantities associated with trawl survey calculations (Cochran 1977, p. 89–92; Smith 1988) and equations in the text.

n_h = number of hauls or sets in stratum h ($h = 1, \ldots, L$)

$n = \sum_{h=1}^{L} n_h$ (in the stratified case), total number of hauls

N_h = total number of possible sets in stratum h

$N = \sum_{h=1}^{L} N_h$, total number of possible sets overall

$W_h = N_h/N$, proportion of the survey area in stratum h

y_{hi} = number of fish of a particular species caught in set i ($i = 1, \ldots, n_h$) and stratum h; y_i is the same quantity but for the random (nonstratified) survey design

$\bar{y}_h$ = estimated mean abundance of a particular species of fish in stratum h; $\bar{y}$ is the same quantity but for the random (nonstratified) survey design

$\bar{y}_{st} = \sum_{h=1}^{L} W_h \bar{y}_h$, estimated stratified mean abundance for a particular species of fish

x_{hi} = measurement for a hydrographic variable in set i of stratum h; x_{hij} indexes the measurement for hydrographic variable j in set i of stratum h when more than one hydrographic variable is considered simultaneously

the general frequency distribution of the habitat variable (depth, temperature, or salinity) by constructing its empirical cumulative distribution function (cdf). Commonly, the probability associated with each observation in a cdf is $1/n$, but the stratified random survey design results in a probability of $1/n_h$ within each stratum (all symbols are defined in Table 1). Therefore the cdf for any habitat variable (x_{hi}) is constructed to incorporate the survey design as (Chambers and Dunstan 1986)

$$(1) \quad f(t) = \sum_h \sum_i \frac{W_h}{n_h} I(x_{hi})$$

with the indicator function

$$I(x_{hi}) = \begin{cases} 1, & \text{if } x_{hi} \leq t; \\ 0, & \text{otherwise.} \end{cases}$$

Here, t represents an index, ranging from the lowest to the highest value of the habitat variable at a step size appropriate for the desired resolution. Equation 1 is calculated over all values of t for each habitat measurement (x_{hi}) available. The cumulative distribution functions derived from equation 1 (e.g., depth; Fig. 2a) can be used to identify the proportion within any range of the habitat variable during the survey. For example, the range of depths that occurred within the central 50% (between the 25th and 75th percentiles) or the central 95% (between the 2.5th and 97.5th percentiles) of the area surveyed can be easily calculated from Fig. 2a.

Including the survey stratification scheme via the W_h/n_h terms ensures that we have an unbiased estimate of the frequency distribution for the habitat measurement. Ignoring the stratification by replacing W_h/n_h with $1/n$ would result in either under- or overestimating the area associated with any particular value of the habitat measurement. However, the term W_h/n_h does simplify to $1/n$ when the number of sets allocated to each stratum is proportional to the size of the stratum (i.e., $n_h = nW_h$). That is, stratification can be ignored when the allocation of sets is strictly proportional to stratum size.

Second, we associate the catch of fish (in numbers) of a particular species in each set with the habitat conditions at that set as a weight in the form

$$(2) \quad g(t) = \sum_h \sum_i \frac{W_h}{n_h} \frac{y_{hi}}{\bar{y}_{st}} I(x_{hi}).$$

Scaling the number of fish caught (Y_{hi}) by the stratified mean number of fish caught ($\bar{y}_{st}$) in equation 2 results in $g(t)$ summing to 1 over all values of t. If large values of $y_{hi}/\bar{y}_{st}$ are consistently associated with particular habitat conditions, then this suggests a strong association between the fish species and those habitat conditions. The cumulative distribution functions calculated from equation 2 illustrate the range of conditions at which the species occurred and can be compared with the habitat conditions available in the sampled area as calculated with equation 1. For example, 50% of the depths surveyed in March 1984 (curve $f(t)$, Fig. 2a) were less than 110 m, while 50% of the yellowtail flounder (curve $g(t)$, Fig. 2a) were caught at depths less than 60 m. The curve $g(t)$ can differ widely from the habitat curve $f(t)$ depending on the range of conditions occupied by the fish. At one extreme, if the fish were associated with one depth only (e.g., 100 m), $g(t)$ would be zero for $t < 100$ and equal to 1.0 for $t \geq 100$. If there was no particular association between fish distributions and the habitat variable within the area surveyed, for example if the fish were randomly distributed with respect to the habitat variable, then $g(t)$ and $f(t)$ would be almost identical.

The third step is to determine the strength of the association between catch and the habitat variable by assessing the degree of difference between the two curves, $g(t)$ and $f(t)$. Our test statistic is similar to that used for comparing empirical cdf's in Kolmogorov–Smirnov tests (see Conover 1980). We calculate the maximum absolute vertical distance between $g(t)$ and $f(t)$ as

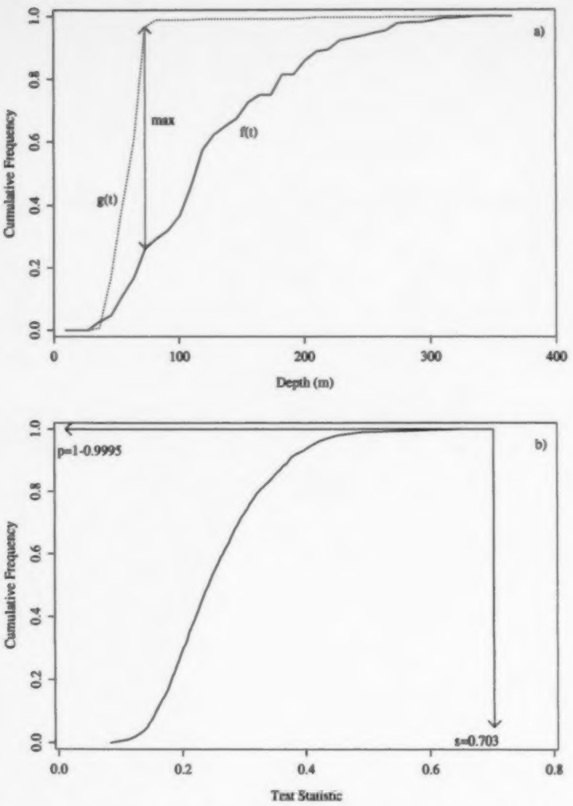

FIG. 2. (a) Cumulative distribution functions for observed depths ($f(t)$; equation 1) and depths as weighted by the number of yellowtail flounder caught ($g(t)$; equation 2) during the March 1984 bottom trawl survey on the eastern Scotian Shelf. The coordinate labelled "max" represents the depth at which the difference between the two curves ($|g(t) - f(t)|$) was maximum. (b) Cumulative distribution function for 2000 randomizations of the test statistic (equation 3) for yellowtail flounder depth distributions versus the observed depths from the March 1984 bottom trawl survey of the eastern Scotian Shelf. s represents the actual test statistic obtained from equation 3, while p represents its probability based on 2000 randomizations, i.e., a test statistic as large or larger than 0.703 was obtained in only 1 out of 2000 randomizations (see text for details).

$$(3)\quad \max_{\forall t}\left|g(t)-f(t)\right| = \max_{\forall t}\left|\sum_h\sum_i \frac{W_h}{n_h}\left(\frac{y_{hi}-\bar{y}_{\mathrm{st}}}{\bar{y}_{\mathrm{st}}}\right) I(x_{hi})\right|$$

where $|g(t) - f(t)|$ indicates the absolute value of the difference between $g(t)$ and $f(t)$ at any point t.

The stratified random survey design complicates distributional assumptions for the test statistic in equation 3, and therefore the standard tables for the Kolmogorov–Smirnov test, or indeed any goodness-of-fit test, cannot be used (see Rao and Thomas 1989). Instead, we developed a randomization procedure (Noreen 1989) to evaluate the significance of the test statistic. We modelled the distribution of the test statistic under the null hypothesis of random association between fish catch (numbers) and habitat variable through Monte-Carlo sampling. This was done by randomizing the pairings of $(W_h/n_h)[(y_{hi} - \bar{y}_{\mathrm{st}})/\bar{y}_{\mathrm{st}}]$ and x_{hi} over all h and i for the data within a survey and then calculating the test statistic in equation 3 for the new pairs. The x_{hi} for the pairings were obtained by sampling with replacement the observed x_{hi} with probability $W_h n_h$. This procedure was repeated a large number of times to give a pseudo-population of test statistics under the null hypothesis. The test statistic for yellowtail flounder and depth in March 1984 (Fig. 2b) was equal to 0.703 (also indicated as "max" in Fig. 2a) which was greater than or equal to 99.95% (2000 out of 2001) of the test statistics in the randomization distribution. There were 2001 test statistics when the original observed pairing of the data was included. Interpreting these results similar to a standard statistical hypothesis test, we note that the probability of obtaining a test statistic as large as 0.703 by chance is close to zero ($p = 0.0005$) and conclude that there was a very strong association by yellowtail flounder with a specific range of depths that was more restricted than the full range of depths available in the survey area during March 1984. This randomization test is a two-sided test, since it is the magnitudes of the absolute differences between $g(t)$ and $f(t)$ that are of interest.

However, environmental conditions are often correlated, for example where temperature decreases with increasing depth, which suggests that an association between a species and a particular depth range may also be confounded by an association with temperature. This problem can be explicitly considered by extending equations 2 and 3 to two (or more) habitat variables simultaneously. For k variables, equations 1 and 2 can be written as

$$(4)\quad \begin{aligned} f(\boldsymbol{t}) &= \sum_h\sum_i \frac{W_h}{n_h} I(\boldsymbol{x}_{hi}) \\ g(\boldsymbol{t}) &= \sum_h\sum_i \frac{W_h}{n_h}\frac{y_{hi}}{\bar{y}_{\mathrm{st}}} I(\boldsymbol{x}_{hi}) \end{aligned}$$

where

$$I(\boldsymbol{x}_{hi}) = \begin{cases} 1, & \text{if } (x_{hi1} \le t_1, x_{hi2} \le t_2, \ldots, x_{hik} \le t_k); \\ 0, & \text{otherwise.} \end{cases}$$

Boldface type for $\boldsymbol{t}$ and $\boldsymbol{x}$ indicates vectors of habitat variables. In the two-variable case, $g(\boldsymbol{t})$ can be represented as a three-dimensional surface in which the cumulative frequency forms the vertical axis. The test statistic (equation 3) is modified as

$$(5)\quad \max_{\forall t}\left|g(\boldsymbol{t})-f(\boldsymbol{t})\right| = \max_{\forall t}\left|\sum_h\sum_i \frac{W_h}{n_h}\left(\frac{y_{hi}-\bar{y}_{\mathrm{st}}}{\bar{y}_{\mathrm{st}}}\right) I(\boldsymbol{x}_{hi})\right|.$$

Results

Univariate cdf Results

Associations between the four groundfish species and bottom depth varied with species during the March 1984 survey. Atlantic cod were distributed in proportion to the available depths (Fig. 3a), and the test statistic derived from equation 3 indicated little difference between the two cdf's ($p = 0.98$). We conclude that Atlantic cod had no association with bottom depth within the sampled depth range (30–300 m) in March 1984. Haddock were distributed at shallower depths than the total range available (Fig. 3a), and the test statistic indicated a moderate association of haddock with these shallow depths ($p = 0.096$) during spring 1984. Both yellowtail flounder and silver hake had cumulative frequency distributions that reflected very strong associations with particular depths ($p < 0.01$ for both). Yellowtail flounder were associated with shallow depths; 97.5% of the population on the eastern Scotian Shelf occurred at bottom depths <74 m, which represented the shallowest 25% of the survey area. Silver hake were associated with deep depths; 97.5% occurred where bottom depths were deeper than 118 m, which represented the deepest 40% of the eastern shelf.

Three of the four groundfish species showed strong associations with temperature in March 1984 (Fig. 3b). Yellowtail flounder were associated with cooler temperatures ($p < 0.01$), as 97.5% of the population occurred at <4.9°C, at the lower 50% of available temperatures. Silver hake were associated with warmer temperatures ($p < 0.01$), as 75% of the population occurred above 7.5°C, the warmest 25% of observed temperatures. Haddock were associated ($p = 0.01$) with intermediate temperatures (4–6°C), but Atlantic cod had no association with temperature ($p = 0.34$) during the March 1984 survey.

The patterns of salinity associations in March 1984 were similar to those for depth (Fig. 3c). Yellowtail flounder were associated with lower salinities ($p < 0.01$) and silver hake with higher salinities ($p < 0.01$). Almost all yellowtail flounder (97.5%) occurred at salinities <32.9 (the lower 45% of observed salinities) whereas 75% of silver hake occurred at salinities >34.2 (the upper 25% of salinities observed on the eastern shelf). Haddock were weakly associated with salinity ($p = 0.13$), whereas Atlantic cod showed no association ($p = 0.70$).

These trends in March 1984 were consistent for March cruises from 1979 to 1984 (Table 2). Yellowtail flounder were always different from a random depth distribution, and generally different from temperature and salinity. Haddock were not strongly associated with depth, but were more strongly associated with temperature and salinity, and silver hake were generally different from a random association with all three habitat variables. Atlantic cod rarely showed strong associations with bottom depth, temperature, or salinity. Much of the variability in these test results can be attributed to interannual variability in bottom temperature, salinity, and depth (where variability in depth resulted from differences in set locations and missed sets due to sea ice). For example, yellowtail flounder were very weakly associated with temperature in March 1983 ($p = 0.27$), but strongly associated ($p < 0.01$) in March 1984 (Table 2). These differences were due to cooler conditions in 1983, when the median temperature for both habitat and yellowtail flounder distributions was 2.7°C, compared with 1984 when the median habitat temperature was 4.8°C whereas it was 1.9°C for yellowtail flounder (Fig. 4a). These temperature shifts occurred without any difference in depth distributions of yellowtail flounder between years (Fig. 4b).

Interannual variability of temperature and salinity presents the problem of distinguishing species with absolute or relative associations with particular conditions, e.g., species occur at relatively cooler or warmer temperatures rather than specific temperatures. Species having absolute associations should exhibit less variability among years compared with the variability of that habitat parameter itself. Three of the four species demonstrated such absolute associations with particular habitat conditions during the 1979–84 spring surveys. As shown by the relative error column of

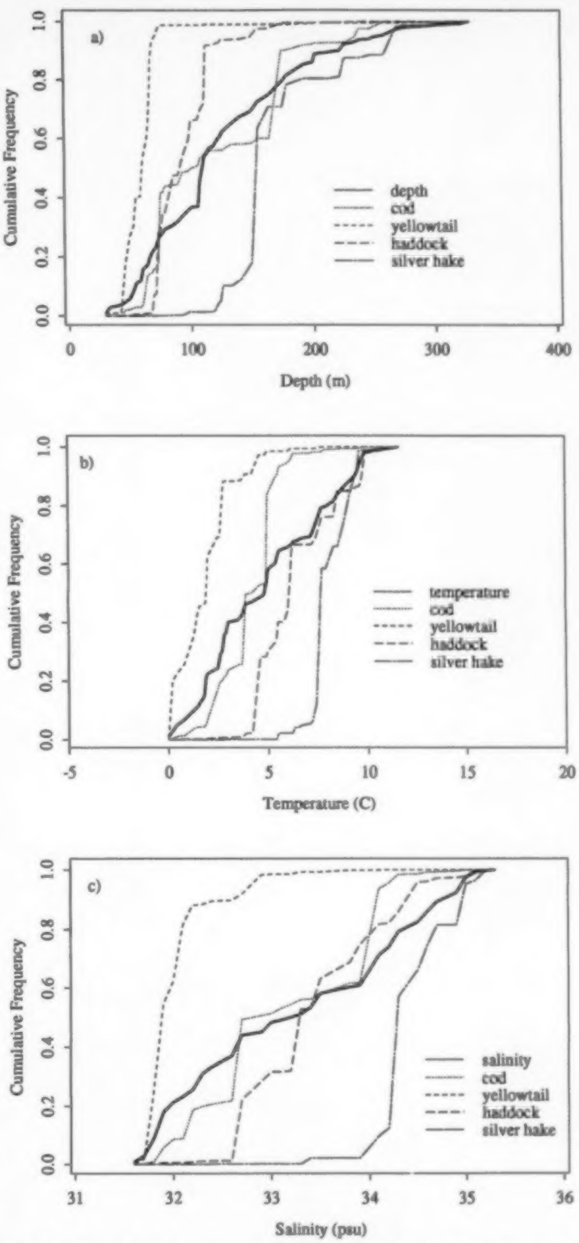

FIG. 3. Cumulative frequency distributions of habitat variables and catch-weighted data from the March 1984 trawl survey of the eastern Scotian Shelf for (a) bottom depth, (b) temperature, and (c) salinity. Test values for statistical significance are presented in Table 2.

TABLE 2. Test results for statistical differences in the catch-weighted cumulative frequency distributions compared with the unweighted cumulative frequency distributions of bottom depth, temperature, and salinity. Table entries are probability (p) values for having a test statistic (from the randomization procedure) as great or greater than that which was observed (equation 3).

Year	Habitat variable	Atlantic cod		Yellowtail flounder		Haddock		Silver Hake	
		March	July	March	July	March	July	March	July
1979	Depth	0.57	<0.01	<0.01	<0.01	0.97	0.01	0.02	0.02
1980		0.04	0.02	<0.01	<0.01	0.24	<0.01	<0.01	0.06
1981		0.53	0.13	<0.01	<0.01	0.22	0.16	0.54	0.20
1982		0.74	<0.01	<0.01	<0.01	0.33	0.02	0.20	0.01
1983		0.98	<0.01	<0.01	<0.01	0.10	<0.01	0.01	0.53
1984		0.98	0.52	<0.01	<0.01	0.10	<0.01	<0.01	0.40
1979	Temperature	0.24	0.25	<0.01	0.75	0.09	0.02	<0.01	<0.01
1980		0.32	0.02	<0.01	0.53	<0.01	0.08	<0.01	<0.01
1981		0.62	<0.01	0.02	0.46	0.25	<0.01	0.08	<0.01
1982		0.23	0.78	0.01	0.51	<0.01	0.02	0.02	<0.01
1983		0.66	0.47	0.27	0.17	0.02	0.09	<0.01	<0.01
1984		0.34	<0.01	<0.01	0.43	0.01	0.01	<0.01	<0.01
1979	Salinity	0.24	<0.01	<0.01	<0.01	0.08	0.02	<0.01	<0.01
1980		0.49	0.03	<0.01	<0.01	0.02	0.34	<0.01	<0.01
1981		0.11	<0.01	<0.01	<0.01	0.97	0.89	0.86	0.28
1982		0.33	0.42	0.21	<0.01	0.01	0.93	0.03	0.02
1983		0.67	<0.01	0.01	<0.01	<0.01	<0.01	<0.01	0.21
1984		0.70	0.15	<0.01	<0.01	0.13	0.60	<0.01	0.44

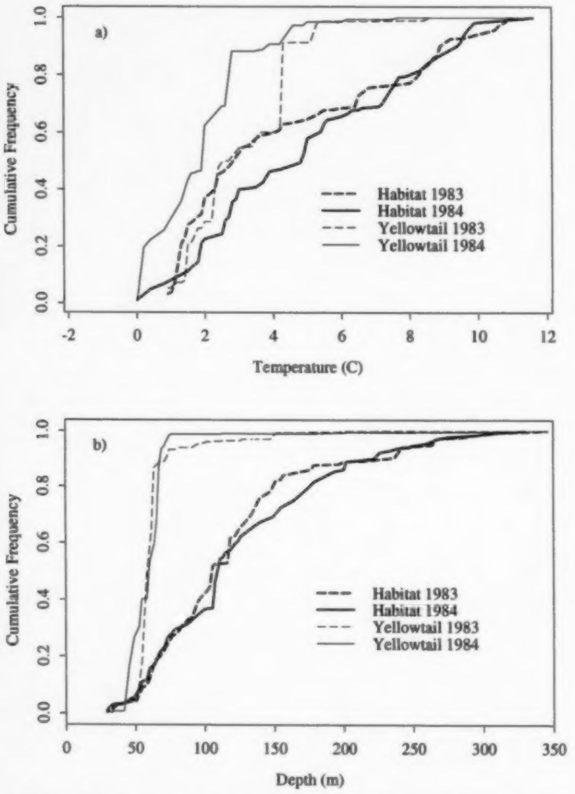

FIG. 4. Cumulative distribution functions for the observed (habitat) and yellowtail flounder (a) temperatures and (b) depths during surveys of the eastern Scotian Shelf in March 1983 and 1984.

Table 3, the median depth of yellowtail flounder was less variable than the median bottom depth, median temperatures for haddock and silver hake were less variable than the median available temperature, and the median salinity for yellowtail flounder was less variable than the median of the available salinities.

To investigate the effect of seasonal differences in fish behaviour (e.g., spring spawning versus summer feeding) on associations with water mass characteristics, the analysis was repeated using the summer (July) survey data for 1979–84. The cdf analysis clearly demonstrates the seasonal warming and freshening of bottom conditions during summer, the corresponding changes in temperature and salinity associations of yellowtail flounder despite little change of depth, and the movement of Atlantic cod to shallower depths in summer (Fig. 5). Yellowtail flounder showed strong associations with depth and salinity but not with temperature during summer, and haddock and silver hake were strongly associated with temperature (Table 2). However, Atlantic cod during the summer surveys were generally more associated with depth, temperature, and salinity than during the March surveys (Table 2). Variability and comparison of median conditions in summer (Table 4) were consistent with results from the spring surveys (Table 3). The median temperatures of haddock and silver hake varied less than the median of the available temperatures, and the median salinity of yellowtail flounder varied less than the median of the available salinities (Table 4). Although yellowtail flounder in summer were more variable with depth than the available habitat (larger relative error, Table 4), they were much less variable than the other three species, consistent with an absolute association with a particular depth range.

Bivariate cdf Results

The distributions of depth, temperature, and salinity on the eastern Scotian Shelf are not independent. The water mass

TABLE 3. Average value, standard deviation, and relative error (defined as the standard deviation/average value) of the median (50th percentile) of bottom depth, temperature, and salinity from the habitat and catch-weighted cumulative frequency curves calculated from March surveys over the period 1979–84. Asterisks indicate species–habitat associations for which the relative error was less than the habitat conditions.

Habitat variable	Habitat or species	Average value	Standard deviation	Relative error
Depth (m)	Habitat	116.2	8.8	0.0757
	Yellowtail flounder	61.1	2.9	0.0475*
	Atlantic cod	114.9	27.6	0.2402
	Haddock	92.4	10.6	0.1147
	Silver hake	147.5	15.2	0.1031
Temperature (°C)	Habitat	2.8	1.2	0.4286
	Yellowtail flounder	1.4	1.1	0.7957
	Atlantic cod	2.6	1.4	0.5385
	Haddock	5.0	1.4	0.2800*
	Silver hake	7.9	1.9	0.2405*
Salinity (psu)	Habitat	32.9	0.20	0.0061
	Yellowtail flounder	32.2	0.17	0.0053*
	Atlantic cod	32.8	0.42	0.0128
	Haddock	33.5	0.31	0.0093
	Silver hake	34.2	0.71	0.0208

TABLE 4. Average value, standard deviation, and relative error (defined as the standard deviation/average value) of the median (50th percentile) of bottom depth, temperature, and salinity from the habitat and catch-weighted cumulative frequency curves calculated from July surveys over the period 1979–84. Asterisks indicate species–habitat associations for which the relative error was less than the habitat conditions.

Habitat variable	Habitat or species	Average value	Standard deviation	Relative error
Depth (m)	Habitat	108.0	4.6	0.0426
	Yellowtail flounder	51.4	4.0	0.0778
	Atlantic cod	60.4	15.9	0.2632
	Haddock	63.3	19.0	0.3002
	Silver hake	142.2	38.6	0.2714
Temperature (°C)	Habitat	5.1	1.4	0.2745
	Yellowtail flounder	4.8	1.8	0.3750
	Atlantic cod	4.4	1.7	0.3864
	Haddock	6.7	1.1	0.1642*
	Silver hake	8.2	0.9	0.1098*
Salinity (psu)	Habitat	33.2	0.25	0.0075
	Yellowtail flounder	32.3	0.17	0.0056*
	Atlantic cod	32.5	0.25	0.0077*
	Haddock	32.8	0.68	0.0207
	Silver hake	34.0	0.84	0.0248

structure on the Scotian Shelf consists of an upper layer, a cold intermediate layer, and a warm deep layer (e.g., Hachey 1942), which leads to correlations among temperature, salinity, and depth. The effect of these correlated environmental variables on fish–habitat associations was examined using the bivariate form of the cdf analysis (equations 4 and 5).

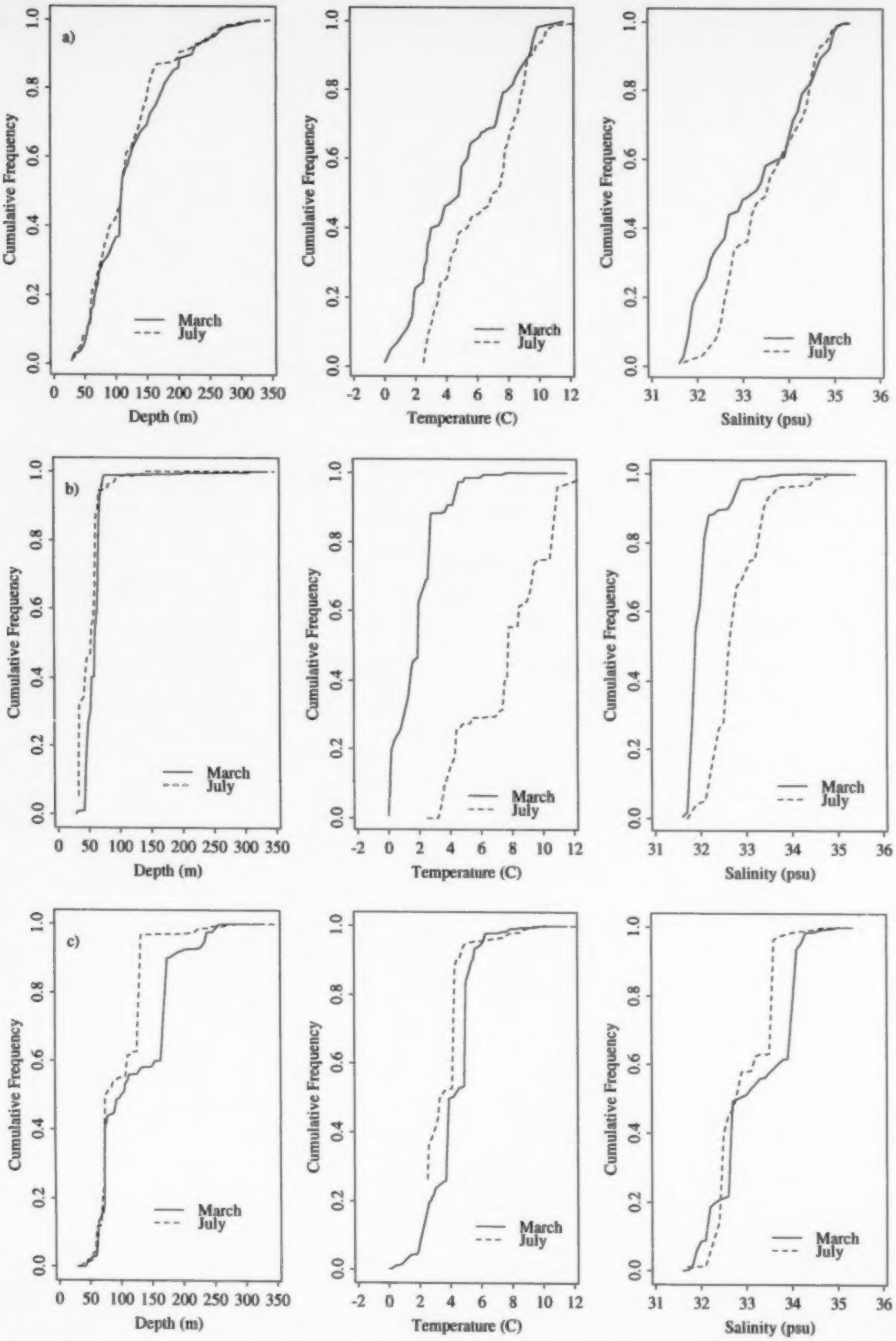

FIG. 5. Cumulative distribution functions for (a) observed (habitat) bottom depth, temperature, and salinity and as weighted by catches of (b) yellowtail flounder and (c) Atlantic cod from surveys of the eastern Scotian Shelf conducted in winter/spring (March) and summer (July) 1984.

The shapes and general locations of the bivariate cdf surfaces varied greatly among species within a season (Fig. 6). The available depths and temperatures were evenly distributed over the full range of conditions observed during March 1984, as indicated by the absence of large steps in the spring habitat panel of Fig. 6. In contrast, yellowtail flounder

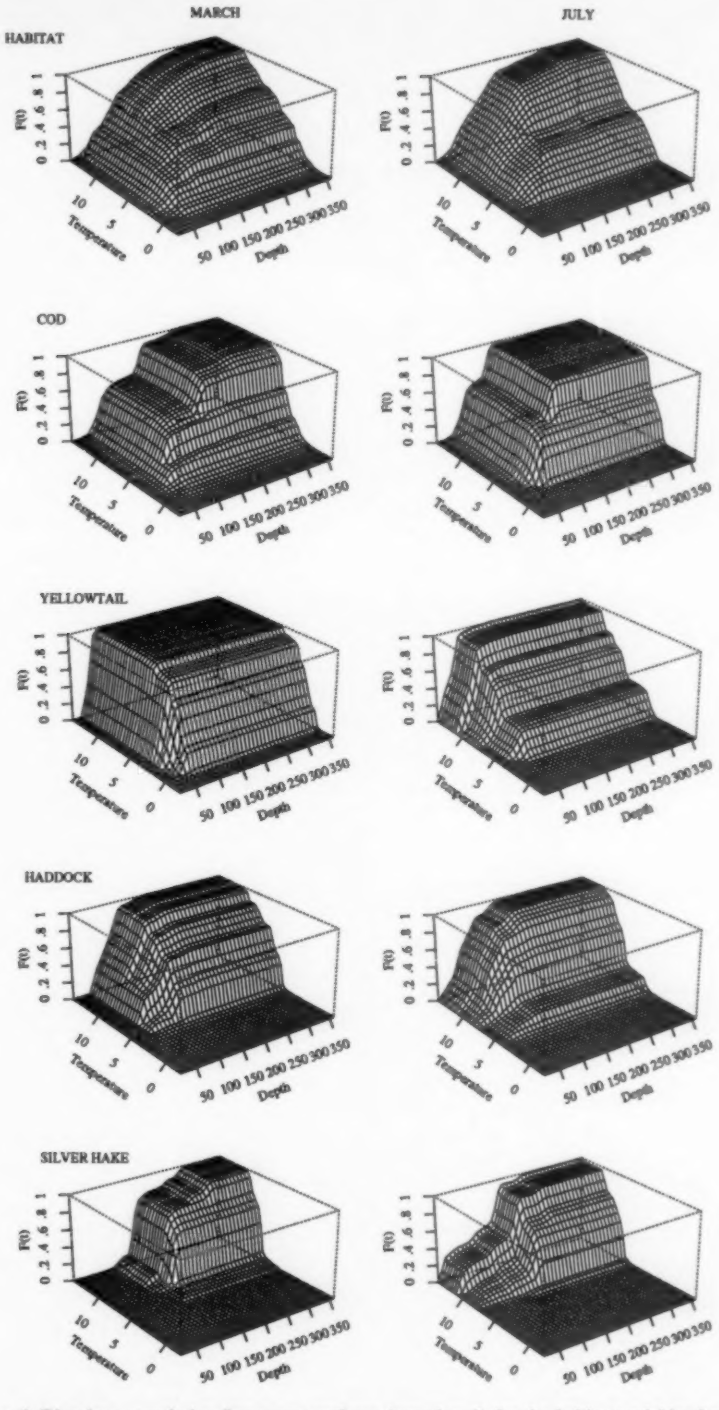

FIG. 6. Bivariate cumulative frequency surfaces (equation 4) for the habitat variables bottom depth and temperature and the four fish species from the March and July 1984 surveys of the eastern Scotian Shelf. Depths are in metres. "$F(t)$" refers to the bivariate cumulative frequency; $F(t) = 1$ represents the depth and temperature conditions up to which 100% of the fish populatin (or habitat) occurred as estimated by the survey. The back walls of the temperature or depth axes represent the same cumulative frequency distribution functions as calculated for the univariate cases (equations 1 and 2).

TABLE 5. Results from the randomization test (equations 4 and 5) for bivariate associations between catch and each of two hydrographic variables. Entries are p-values from tests which correspond to the probability of getting, by chance, a test statistic as large as was observed from the survey.

		Atlantic cod		Yellowtail flounder		Haddock		Silver Hake	
Year	Habitat variable	March	July	March	July	March	July	March	July
1979	Depth and temperature	0.92	<0.01	<0.01	<0.01	0.26	0.07	<0.01	0.01
1980		0.38	0.14	<0.01	<0.01	0.01	0.01	<0.01	0.04
1981		0.96	0.03	<0.01	<0.01	0.53	0.02	0.58	0.04
1982		0.58	<0.01	<0.01	<0.01	<0.01	0.12	0.18	0.01
1983		0.78	<0.01	<0.01	<0.01	0.10	<0.01	<0.01	0.06
1984		0.63	0.08	<0.01	<0.01	0.07	0.03	<0.01	0.04
1979	Depth and salinity	0.95	<0.01	<0.01	<0.01	0.28	0.06	<0.01	0.17
1980		0.38	0.15	<0.01	<0.01	0.24	0.03	<0.01	0.06
1981		0.96	<0.01	<0.01	<0.01	0.46	0.31	0.58	0.59
1982		0.58	0.02	<0.01	<0.01	0.14	0.32	0.19	0.12
1983		0.78	<0.01	<0.01	<0.01	0.02	<0.01	<0.01	0.46
1984		0.63	0.28	<0.01	<0.01	0.22	0.01	<0.01	0.29
1979	Temperature and salinity	0.63	0.01	<0.01	<0.01	0.18	0.03	<0.01	0.17
1980		0.71	0.12	<0.01	<0.01	<0.01	0.10	<0.01	0.02
1981		0.44	<0.01	<0.01	<0.01	0.40	<0.01	0.19	0.01
1982		0.42	0.55	<0.01	<0.01	<0.01	0.04	0.19	0.01
1983		0.60	<0.01	0.03	<0.01	<0.01	<0.01	<0.01	0.02
1984		0.41	0.05	<0.01	<0.01	0.02	0.02	<0.01	<0.01

occurred at low temperatures and shallow depths, silver hake occurred at high temperatures and deep depths, and haddock and Atlantic cod were intermediate (Fig. 6). For March 1984, these results indicate an association of yellowtail flounder with a narrow range of shallow depths (shown by the sharp increase without any "steps" in the shape of the cdf surface; Fig. 6) and an association with low temperatures although with a somewhat broader range than for depth. Silver hake in March 1984 were also associated with narrow ranges of temperature and depth, although the shape of the surface suggested that the association was stronger with temperature than with depth (i.e., the cdf surface was broader along the depth axis; Fig. 6). Haddock showed an association with depths between 50 and 100 m, but within this depth range there was also a relationship with temperature (the "step" shape of the surface along the temperature axis; Fig. 6). Atlantic cod was opposite to the results for haddock: most Atlantic cod were associated with a narrow (cool) temperature range, but there was also an effect of depth (Fig. 6). The strengths of these associations between fish catch and the joint distributions of depth and temperature were assessed by the bivariate randomization test (equation 5). Yellowtail flounder, silver hake, and haddock were all associated with particular ranges of depth and temperature ($p \leq 0.07$), but Atlantic cod appeared to be unrelated to the available combinations of the two variables ($p = 0.63$; Table 5).

The associations of these groundfish species with depth and temperature simultaneously during July 1984 are similar to those during March 1984. Yellowtail flounder were associated with shallow depths, but the association with temperature was weaker than in March 1984 (the more gradual slope along the temperature axis; Fig. 6). Silver hake were associated with temperature and depth, although more strongly with temperature; haddock were associated with ranges of depth and temperature similar to those during spring (Fig. 6). Atlantic cod were associated with shallower depths in summer than in spring (Fig. 6). The randomization test results for depth and temperature during July 1984 ($p \leq 0.04$; Table 5) were similar to those for March 1984 for yellowtail flounder, haddock, and silver hake but indicated that Atlantic cod were more strongly associated with particular ranges of temperature and depth during summer ($p = 0.08$; Table 5) than during spring.

The randomization test results for bivariate combinations of depth, temperature, and salinity from 1979 to 1984 (Table 5) refine the univariate habitat associations identified in Table 2. Yellowtail flounder were strongly associated ($p \leq 0.03$) with temperature and with salinity during spring and summer over all years when their joint distributions with depth were included (Table 5), in contrast with the univariate analysis (Table 2). Silver hake and haddock generally had stronger associations (smaller p-values; Table 5) with the joint distributions of temperature and depth, and with temperature and salinity, than with salinity and depth. However, the bivariate associations of Atlantic cod (Table 5) were similar to those from the univariate analysis (Table 2).

To identify which habitat variable was most influential in structuring the distributions of each of the four groundfish species in the presence of correlations among the habitat variables, we compared univariate and bivariate test results. The coordinates of the test statistic in equations 3 and 5 give the points of maximum difference between the catch-weighted cumulative curves and the cumulative curves for the habitat conditions (e.g., the point labelled "max" in Fig. 2a). In March 1984, the univariate cdf's for yellowtail flounder reached their maximum differences from the habitat cdf's at 75 m, 3.0°C, and 32.2 psu (Table 6a). However, when depth and temperature, and depth and salinity, were considered together in the bivariate analyses, the maximum differences increased for temperature and salinity but remained unchanged for depth (Table 6a). We assumed that the variable(s) with the strongest associations were those whose coordinates changed the least going from the univariate to the bivariate tests. Depth was the variable that changed the least for yellowtail flounder, followed by salinity (Table 6a). We conclude that depth was the most important variable because the salinities with which yellowtail flounder were associated were available at deeper depths, yet yellowtail flounder generally did not occur much deeper than 100 m. Haddock and silver hake were associated more with temperature than with salinity or depth (Tables 6b and 6c). In contrast, depth varied the most between univariate and bivariate analyses of Atlantic cod during March and July, but it is difficult to determine which of temperature or salinity was the least variable (Table 6d).

Discussion

Several methods have been used to identify habitat associations of marine fishes from survey data. Scott (1982a) defined habitat preferences of Atlantic groundfishes as those ranges of depth, temperature, and salinity with greater than 10% of the total species abundance. However, he took no account of the survey design (his data were derived from the same stratified-random design used in our study) or of the available habitat conditions. Murawski and Finn (1988) used data on fish catches, bottom depth, and temperature derived from a stratified-random survey to estimate habitat preferences of groundfishes on Georges Bank. Preferred conditions were defined as means and standard deviations of depth and temperature weighted by fish catch. Comparison of preferred conditions (i.e., weighted means) with available habitat conditions was done using scattergrams of the two habitat parameters (depth and temperature). Rose and Leggett (1988, 1989) compared the distributions of Atlantic cod and capelin (*Mallotus villosus*) (assessed acoustically) with temperature. They grouped data into 1°C categories and defined preference as those categories in which Atlantic cod occurrences were greater than expected based on the assumption of a random distribution with temperature. The observed distribution of Atlantic cod on temperature was compared with the expected (random) distribution using a χ^2-test. Rao and Thomas (1989) noted that in general, application of standard χ^2 tests to data from complex survey designs will result in the alternative hypothesis being rejected too often given the assumed type I error for the test.

The method we present has several advantages to estimating habitat associations of fish species. The use of cumulative distributions provides an objective method of estimating the proportion of a population that occurred within any range of habitat conditions, or conversely the conditions under which 50%, 95%, etc., of a population occurred. The method is nonparametric in the sense that no specific statistical distribution need be assumed for either the fish catch or habitat variables. It also allows quantitative comparisons with observed habitat conditions to identify species which are distributed randomly with respect to a particular habitat variable. The method takes explicit account of the survey design and can be applied to data collected with any sample-to-strata allocation scheme; it can therefore be used to estimate population-level responses. If the survey design is not stratified, using instead a simple random or regular scheme (or when a stratified design is used with proportional-to-area allocation), equations 1 and 2 for the calculation of the cumulative distribution functions reduce to

$$f(t) = \frac{1}{n}\sum_{i=1}^{n} I(x_i)$$

$$g(t) = \frac{1}{n}\sum_{i=1}^{n} \frac{y_i}{\bar{y}} I(x_i)$$

and

$$\max_{\forall t}\left|g(t) - f(t)\right| = \max_{\forall t}\left|\frac{1}{n}\sum_{i=1}^{n}\left(\frac{y_i - \bar{y}}{\bar{y}}\right) I(x_i)\right|$$

where $I(x_i)$ is the same as for equation 4 but without the stratification subscript h. This type of analysis could also easily be applied to fisheries data collected by other survey methods, for example acoustic surveys. Acoustic methods have the advantage of continuously monitoring fish biomass throughout the water column and, coupled with frequent water column measurements of hydrographic conditions, would be particularly important for assessing habitat associations of pelagic and semidemersal fish species.

One disadvantage of the method is that the randomization test (equations 3 and 5) is computationally more complex than applying any standard parametric or nonparametric test, but these can give erroneous results when applied to data from complex survey designs (Rao and Thomas 1989). In addition, Manly (1991) stated that randomization tests are often more powerful than their standard counterparts in nonstandard situations, such as the analyses we present here.

Several conclusions regarding winter/spring and summer habitat associations of the four eastern Scotian Shelf groundfish species examined in this study can be made based on the results of our analyses. Haddock and silver hake on the eastern Scotian Shelf can be considered as "temperature-keepers", in the sense that they maintained a similar temperature range between winter/spring and summer, but did this by changing their seasonal depth distributions. Yellowtail flounder, in contrast, can be considered as principally a "depth-keeper", implying that there was little alteration of their depth distribution between spring and summer and that they tolerated a wide range of temperature and salinity conditions. This relationship of yellowtail flounder with depth is consistent with the conclusions of Scott (1982a), who found that they tended to be located on the shallow banks on the eastern Scotian Shelf, and with the conclusions of Murawski and Finn (1988) for yellowtail flounder on Georges Bank. Murawski and Finn (1988) also concluded that silver hake on Georges Bank maintained a relatively narrow temperature range among seasons, but that haddock distributions on Georges Bank were more strongly related to depth than to temperature. The contrast with our results for haddock may be due to the reduced variation of depths sampled on Georges Bank (most full strata analysed by Murawski and Finn (1988) were <100 m) compared with the eastern Scotian Shelf.

In contrast, Atlantic cod were associated with particular ranges of depth, temperature, or salinity only during summer from 1979 to 1984, and we were generally unable to distinguish between temperature and salinity as the predominant single factor. The inability of the randomization test to detect consistent associations during March was likely due to the wider availability of the associated range of salinity during

TABLE 6. Coordinates of the test statistic for the univariate and bivariate randomization tests. The column labelled "Univ" under each habitat parameter represents the location of the maximum difference between the habitat and catch-weighted cumulative distribution functions in the univariate test (equation 3). The remaining two columns under each habitat parameter represent the locations of the maximum difference in the bivariate test (equation 5).

	Depth (m)			Temperature (°C)			Salinity (psu)		
Year	Univ	Temperature	Salinity	Univ	Depth	Salinity	Univ	Depth	Temperature
(a) Yellowtail flounder									
March									
1979	130	130	130	1.5	7.0	1.5	32.4	33.8	32.8
1980	90	90	90	1.5	2.5	1.5	32.2	32.4	32.4
1981	75	75	75	2.5	3.5	3.5	32.8	32.8	32.8
1982	90	90	75	0.0	0.0	0.0	32.4	32.6	32.8
1983	75	75	75	5.5	5.5	5.5	32.6	33.0	32.6
1984	75	75	75	3.0	5.0	3.0	32.2	33.0	32.2
July									
1979	75	90	90	2.5	9.5	9.5	32.8	33.4	32.8
1980	75	75	75	3.0	9.0	9.0	32.4	33.0	32.4
1981	90	90	90	8.0	12.0	12.5	32.8	33.6	32.8
1982	75	75	90	2.0	10.5	10.5	32.6	32.6	32.6
1983	75	75	75	2.5	8.5	8.5	32.8	33.2	32.8
1984	75	75	75	10.5	11.0	14.0	33.4	33.6	33.4
(b) Haddock									
March									
1979	90	300	240	2.5	2.5	2.5	33.2	33.2	35.0
1980	130	240	130	3.0	3.0	3.0	32.8	35.0	33.0
1981	110	110	110	3.0	7.5	3.0	33.8	34.2	33.8
1982	75	250	150	2.0	2.0	2.0	32.4	32.4	34.8
1983	110	275	250	3.0	3.0	3.0	32.8	32.8	32.8
1984	130	310	200	4.5	4.5	4.5	32.6	32.6	33.2
July									
1979	90	300	90	5.0	5.0	6.0	32.2	34.0	34.4
1980	75	75	75	4.5	8.0	4.5	32.6	34.0	34.0
1981	90	350	90	6.5	6.5	6.5	32.8	34.8	34.8
1982	130	240	130	2.0	2.0	2.0	32.6	34.4	33.2
1983	55	55	130	3.0	8.5	8.5	32.2	32.2	32.2
1984	110	110	110	7.0	11.0	7.0	34.2	34.4	35.0
(c) Silver hake									
March									
1979	150	350	275	8.0	8.0	8.0	34.4	34.4	35.0
1980	150	275	240	5.5	7.0	5.5	34.0	34.0	34.8
1981	130	310	130	3.5	3.5	3.5	32.6	33.4	33.8
1982	130	200	200	7.5	7.5	7.5	34.4	34.2	34.6
1983	110	250	310	6.0	6.0	6.0	33.6	33.6	34.6
1984	150	330	275	7.0	7.0	7.0	34.2	34.2	35.0
July									
1979	165	370	310	8.5	8.5	8.5	34.6	34.6	35.2
1980	90	310	240	6.5	6.5	6.5	33.6	33.6	34.8
1981	55	370	35	8.0	8.0	8.0	31.8	31.8	35.0
1982	130	250	290	5.5	6.0	5.5	34.0	34.0	34.8
1983	75	250	250	4.0	4.0	4.0	34.0	34.0	33.8
1984	35	310	35	7.5	7.5	7.5	33.2	32.4	35.0

March than during July. This is consistent with the widespread occurrence of Atlantic cod on the eastern Scotian Shelf (Scott 1988).

Age-specific differences and factors other than depth, temperature, or salinity can influence the distributions of marine fishes. These factors potentially include sediment type (e.g., Scott 1982b), oxygen (e.g., D'Amours 1993), and conceivably prey abundance and distribution. To some extent, depth may serve as a proxy for sediment type, while water mass (temperature and salinity) may act as a proxy for oxygen concentration and prey distributions. Therefore, while fish distributions may not be related to depth, tem-

TABLE 6. (*Concluded*)

Year	Depth (m)			Temperature (°C)			Salinity (psu)		
	Univ	Temperature	Salinity	Univ	Depth	Salinity	Univ	Depth	Temperature
				(d) Atlantic cod					
March									
1979	110	240	240	7.0	7.0	7.0	33.4	33.4	34.6
1980	150	150	150	2.5	10.5	2.5	33.0	35.0	32.8
1981	90	275	275	7.5	7.5	7.5	34.0	34.0	34.0
1982	55	160	160	1.5	1.0	1.5	33.2	33.2	33.2
1983	130	240	240	4.5	4.5	4.5	33.6	33.6	33.6
1984	160	180	180	6.5	6.5	6.5	34.2	34.2	34.2
July									
1979	75	75	75	7.5	9.5	14.0	33.4	33.4	33.4
1980	75	250	55	6.0	6.0	6.0	34.0	32.6	34.0
1981	150	150	150	5.0	4.5	12.5	33.4	33.6	33.4
1982	55	55	55	2.5	5.5	5.5	32.6	32.6	32.6
1983	90	55	90	7.5	8.5	8.5	32.6	32.6	32.2
1984	150	150	150	4.5	4.5	4.5	32.6	33.6	33.6

perature, or salinity alone, these may serve as reasonable first approximations. Fish distributions can also differ substantially among different age classes (e.g., Tremblay and Sinclair 1985; Sinclair 1992). Smith et al. (1991), using a slightly different approach, found a relationship between age-4 Atlantic cod distributions and the intermediate (cold) water mass (defined as water with salinities in the range 32–33.5 psu) within a specific depth range on the eastern Scotian Shelf during the March surveys, 1979–84. Stronger relationships between Atlantic cod and the salinities associated with the intermediate cold layer might have been obtained in our study had we analysed separate age classes using the present methods.

Identification of consistent habitat associations of marine fishes offers the opportunity to improve fisheries management and stock assessment methods in several ways. It can provide oceanographic bases for understanding changes in fish distributions, which ultimately may be predictable in advance or assessed by monitoring a few selected oceanographic or habitat parameters, provide corrections to the assumption of homogeneous conditions and distributions of fish within strata, leading to corrections to survey estimates of abundance (e.g., Smith et al. 1991), and provide a basis for understanding oceanographic effects on variations of catchability (e.g., Murawski and Finn 1988; Gordoa and Hightower 1991). Finally, the identification of strong associations with particular habitat conditions, i.e., an improved definition of habitat "space", is a prerequisite for expansion of spatially explicit models of fish distribution and growth (e.g., Brandt et al. 1992; Swartzman et al. 1992) to the marine environment.

Acknowledgments

We thank the vessel crews and scientific staff of the many cruises that were conducted for the groundfish survey program. Randy Losier performed much of the early data extractions and editing, and Scott Wilson constructed Fig. 1. We thank Drs. Jake Rice, Denis D'Amours, Fred Page, Peter Smith, George Rose, and Gordon Swartzman for suggestions during this study and comments on the manuscript. Much of the initial work was done while the first author was with the Marine Fish Division at the St. Andrews Biological Station, St. Andrews, N.B.

References

BRANDT, S.B., D.M. MASON, AND E.V. PATRICK. 1992. Spatially-explicit models of fish growth rate. Fisheries 17(2): 23–31.

CHAMBERS, R.L., AND R. DUNSTAN. 1986. Estimating distribution functions from survey data. Biometrika 73: 597–604.

COCHRAN, W.G. 1977. Sampling techniques. John Wiley & Sons, New York, N.Y. 428 p.

CONOVER, W.J. 1980. Practical nonparametric statistics. 2nd ed. John Wiley & Sons, New York, N.Y. 493 p.

COUTANT, C.C. 1977. Compilation of temperature preference data. J. Fish. Res. Board Can. 34: 739–745.

D'AMOURS, D. 1993. The distribution of cod (*Gadus morhua*) in relation to temperature and oxygen level in the Gulf of St. Lawrence. Fish. Oceanogr. 2: 24–29.

GORDOA, A., AND J.E. HIGHTOWER. 1991. Changes in catchability in a bottom-trawl fishery for Cape hake (*Merluccius capensis*). Can. J. Fish. Aquat. Sci. 48: 1887–1895.

HACHEY, H.B. 1942. The waters of the Scotian Shelf. J. Fish. Res. Board Can. 5: 377–397.

HALLIDAY, R.G., AND P.A. KOELLER. 1981. A history of Canadian groundfish trawling surveys and data usage in ICNAF Divisions 4TVWX, p. 27-43. *In* W.G. Doubleday and D. Rivard [ed.] Bottom trawl surveys. Can. Spec. Publ. Fish. Aquat. Sci. 58.

MAHON, R., AND R.W. SMITH. 1989. Demersal fish assemblages on the Scotian Shelf, Northwest Atlantic: spatial distribution and persistence. Can. J. Fish. Aquat. Sci. 46(Suppl. 1): 134–152.

MANLY, B.F.J. 1991. Randomization and Monte-Carlo methods in biology. Chapman and Hall, London. 281 p.

MURAWSKI, S.A., AND J.T. FINN. 1988. Biological bases for mixed-species fisheries: species co-distribution in relation to environmental and biotic variables. Can. J. Fish. Aquat. Sci. 45: 1720–1735.

MYSAK, L.A. 1986. El Niño, interannual variability and fisheries in the northeast Pacific Ocean. Can. J. Fish. Aquat. Sci. 43: 464–497.

NOREEN, E.W. 1989. Computer-intensive methods for testing hypotheses: an introduction. John Wiley & Sons. New York, N.Y.

RAO, J.N.K., AND D.R. THOMAS. 1989. Chi-squared test for contingency tables, p. 89–114. *In* C.J. Skinner, D. Holt, and T.M.F. Smith [ed.] Analysis of complex surveys. John Wiley & Sons. New York, N.Y.

RICHARDS, F.P., W.W. REYNOLDS, AND R.W. MCCAULEY [ED.] 1977. Temperature preference studies in environmental impact assessments: an overview with procedural recommendations. J. Fish. Res. Board Can. 34: 728–761.

ROSE, G.A., AND W.C. LEGGETT. 1988. Atmosphere–ocean coupling and Atlantic cod migrations: effects of wind-forced variations in sea temperatures and currents on nearshore distributions and catch rates of *Gadus morhua*. Can. J. Fish. Aquat. Sci. 45: 1234–1243.

ROSE, G.A., AND W.C. LEGGETT. 1989. Interactive effects of geophysically-forced sea temperatures and prey abundance on mesoscale coastal distributions of a marine predator, Atlantic cod (*Gadus morhua*). Can. J. Fish. Aquat. Sci. 46: 1904–1913.

SCOTT, J.S. 1982a. Depth, temperature and salinity preferences of common fishes of the Scotian Shelf. J. Northwest Atl. Fish. Sci. 3: 29–40.

SCOTT, J.S. 1982b. Selection of bottom type by groundfishes of the Scotian Shelf. Can. J. Fish. Aquat. Sci. 39: 943–947.

SCOTT, J.S. 1988. Seasonal spatial distributions of groundfishes of the Scotian Shelf and Bay of Fundy, 1974–79 and 1980–84. Can. Tech. Rep. Fish. Aquat. Sci. 1653.

SINCLAIR, A. 1992. Fish distribution and partial recruitment: the case of eastern Scotian Shelf cod. J. Northwest Atl. Fish. Sci. 13: 15–24.

SMITH, S.J. 1988. Abundance indices from research survey data. *In* D. Rivard [ed.] Collected papers on stock assessment methods. CAFSAC Res. Doc. 88/61: 16–43.

SMITH, S.J. 1990. Use of statistical models for the estimation of abundance from groundfish trawl surveys. Can. J. Fish. Aquat. Sci. 47: 894–903.

SMITH, S.J., R.I. PERRY, AND L.P. FANNING. 1991. Relationships between water mass characteristics and estimates of fish population abundance from trawl surveys. Environ. Monit. Assess. 17: 227–245.

SWARTZMAN, G., C. HUANG, AND S. KALUZNY. 1992. Spatial analysis of Bering Sea groundfish survey data using generalized additive models. Can. J. Fish. Aquat. Sci. 49: 1366–1378.

TREMBLAY, M.J., AND M.M. SINCLAIR. 1985. Gulf of St. Lawrence cod: age-specific geographic distributions and environmental occurrences from 1971 to 1981. Can. Tech. Rep. Fish. Aquat. Sci. 1387: 43 p.

XIE, L., AND W.W. HSIEH. 1989. Predicting the return migration routes of the Fraser River sockeye salmon (*Oncorhynchus nerka*). Can. J. Fish. Aquat. Sci. 46: 1287–1292

Simple Size-Structured Models of Recruitment and Harvest in Pacific Salmon (*Oncorhynchus* spp.)

L. Scott Forbes[1] and Randall M. Peterman

School of Resource and Environmental Management, Simon Fraser University, Burnaby, BC V5A 1S6, Canada

Forbes, L.S., and R.M. Peterman. 1994. Simple size-structured models of recruitment and harvest in Pacific salmon (*Oncorhynchus* spp.). Can. J. Fish. Aquat. Sci. 51: 603–616.

Growing evidence suggests that in Pacific salmon (*Oncorhynchus* spp.), components of reproductive success besides fecundity are size dependent. However, managers setting escapement goals usually estimate reproductive potential of a stock in terms of total number of spawners, number of female spawners, or potential egg deposition given a mean size of spawners. Interannual variation in size composition of spawners may thus result in errors in assessing reproductive potential. Here, we develop models of recruitment and harvest and determine optimal size-selective harvesting strategies. These optimal strategies range from the current large-fish harvests (larger-than-average fish are caught, leaving smaller fish to spawn) to small-fish harvests, where the reverse is true. If the body mass (M) of individual spawners increases more rapidly than reproductive success (RS) with respect to increasing length of adult females (e.g., if number of eggs alone best measures RS), then sustainable biomass yield is maximized by the current large-fish harvest. However, if RS/M increases with increasing length of females (e.g., if total biomass of eggs best measures RS), then small-fish harvest maximizes sustainable yield. Evidence suggests that some salmon populations show this latter pattern; thus, large-fish harvests may generate suboptimal yields.

Il semble de plus en plus évident que chez le saumon du Pacifique (*Oncorhynchus* spp.), les éléments du succès de la reproduction, en plus de la fécondité, dépendent de la taille. Toutefois, les gestionnaires qui établissent les objectifs de l'échappée estiment en général le potentiel reproductif d'un stock en fonction du nombre total de géniteurs, du nombre de génitrices ou du potentiel de ponte étant donné une taille moyenne des géniteurs. La variation interannuelle de la composition selon la taille des géniteurs peut donc entraîner des erreurs d'évaluation du potentiel reproductif. Nous avons élaboré des modèles de recrutement et de captures, et déterminé des stratégies optimales de pêche sélective selon la taille. L'éventail de ces stratégies optimales va du mode actuel des captures visant les poissons de grande taille (on capture des poissons plus grands que la moyenne, en laissant les petits poissons pour la fraye) aux captures des poissons de petite taille, auquel cas le contraire est vrai. Si la masse corporelle (M) de chaque géniteur augmente plus rapidement que le succès de la reproduction (SR) par rapport à l'augmentation de la longueur des femelles adultes (p. ex., si le nombre d'oeufs seul mesure mieux le SR), alors le rendement durable de la biomasse est maximisé par les captures actuelles de poissons de grande taille. Toutefois, si SR/M augmente avec l'augmentation de la longueur des femelles (p. ex., si la biomasse totale des oeufs mesure mieux le SR), la capture des poissons de petite taille maximise le rendement durable. Il semble que certaines populations de saumon présentent ce dernier profil; donc, les captures de poisson de grande taille peuvent entraîner des rendements sous-optimaux.

Received June 21, 1991
Accepted October 6, 1993
(JB097)

Reçu le 21 juin 1991
Accepté le 6 octobre 1993

The use of stock–recruitment theory to estimate optimal escapement rests upon the assumption that the parent stock and resulting recruitment are well measured. Errors in measuring the parent stock will inevitably result in errors in identifying the underlying relationship between these two variables. For example, in many marine fish populations, spawning stock biomass is used as a proxy for the abundance of eggs, but Rothschild and Fogarty (1989) showed that by doing so, a true underlying relationship between stock and recruitment can be obscured by density-dependent production of eggs per unit of female biomass.

Management of Pacific salmon (*Oncorhynchus* spp.) is usually based upon a policy of constant escapement of some abundance of spawners, which is expected to generate the maximum sustainable yield (MSY) (Ricker 1975). This optimal escapement is usually defined in units of either (1) total number of spawners, (2) number of female spawners, or (3) potential egg deposition. These ways of expressing optimal escapement represent a hierarchy of increasing refinement of the definition of reproductive potential. The second definition is a refinement of the first, in that it implicitly recognizes that the sex ratio of spawners is not always 1:1 and that females are more important to overall spawning success than males (e.g., Mathisen 1962 has shown that there are usually enough male salmon to fertilize all eggs). The third definition of escapement represents a further refinement; it accounts for variation in fecundity among females within a spawning population, which fisheries biologists have long recognized as potentially important (Foerster and Pritchard 1941; Rounsefell 1957).

---

[1] Present address: Department of Biology, University of Winnipeg, 515 Portage Avenue, Winnipeg, MB R3B 2E9, Canada.

However, even the third and most refined definition of escapement, potential egg deposition, may be an inadequate measure of reproductive potential (Hankin and McKelvey 1985). Growing evidence suggests strongly that the effects of body size go beyond the simple effect on fecundity (number of eggs). Egg size increases with female body size, resulting in larger, faster growing alevins and fry (e.g., Brown 1946; Bagenal 1969; Bilton 1970a, 1971; Bilton and Smith 1973; Beacham and Murray 1985; West and Larkin 1987; Fleming and Gross 1990). Moreover, larger females are more successful in intraspecific competition for nest sites, and they dig deeper redds less vulnerable to scouring and/or dig-up by other females and defend nests longer (van den Berghe and Gross 1984, 1986, 1989; Lewis 1987; Fleming and Gross 1989). Helle (1989) showed for chum salmon (*Oncorhynchus keta*) in Olsen Creek, Prince William Sound, Alaska, that the brood-class survival rate of progeny to adulthood was significantly positively correlated ($P < 0.01$) with the mean body size of their parent population. This was due to more than the simple effect of parental size on fecundity. Helle (1989) compared the largest and smallest size-classes of parents in the 13-yr data set and found only a 1.2-fold difference in fecundity per parent but a fourfold difference in surviving offspring per parent. Similarly, van den Berghe and Gross (1989) estimated that the largest females within a spawning population of coho salmon (*Oncorhynchus kisutch*) had a 23-fold fitness advantage (measured to the time of fry emergence) as the smallest females. About one third of this reproductive differential was attributable to differences in fecundity (70-cm females carried seven times as many eggs as 40-cm females) and the remainder was due to the competitive advantages of large body size such as acquiring better nest sites and defending nests against dig-up.

Thus, we can ask, "For Pacific salmon, what is the best measure of reproductive potential?" The answer is important for at least three reasons. First, determining the best measure of reproductive potential is likely to permit better estimates of optimal escapement through improved estimates of the parameters of stock–recruitment relationships. Typically, stock–recruitment relationships use annual abundance of individual spawners or females as the units of measurement. Doing so ignores potential variation in reproductive capabilities among individual spawners and the resulting total reproductive potential of the spawning population caused by year-to-year changes in age and size composition of spawners. Ignoring this component of the variance of reproductive potential contributes (some unknown amount) to the variance in observed stock–recruitment relationships. This is one example of the measurement error or errors-in-variables problem outlined by Walters and Ludwig (1981).

Second, with better measures of reproductive potential, we will be better able to evaluate the effects of traditional and experimental harvest strategies that affect the size distribution of spawners. If all individuals are not equally valuable in terms of reproductive potential, and if reproductive potential varies with size, then we may be able to meet the management objective of ensuring a target reproductive potential and at the same time increase biomass yields from the fishery through certain size-selective harvests that leave the most productive individuals to spawn. One example of this type of approach is Reed (1982), who expanded upon Mathisen's (1962) earlier work with sockeye salmon (*Oncorhynchus nerka*) and suggested that considerable potential exists for increasing the biomass yield from stocks of Pacific salmon through the preferential harvest of males.

Third, proper definition of reproductive potential is essential to the development of life-history models of age and size at maturity (e.g., Healey and Heard 1984; Hankin and McKelvey 1985; Healey 1986, 1987). Such models may provide managers with a better understanding of causes of interannual variability in abundance and age structure of returns of Pacific salmon.

In this paper, we explore alternative measures of reproductive potential and examine their implications for optimal harvest strategies. In particular, we show that if certain measures of reproductive potential are valid, then the current widely used troll gear and gill nets, which tend to remove the largest individuals in the population (Ricker 1981), are optimal. However, if other measures of reproductive potential are more valid, then the best approach would be to use a size-selective fishery that leaves the largest (and apparently most productive) individuals to spawn while harvesting smaller fish. We begin by reviewing available information on the relationship between body size and reproductive success in Pacific salmon. We then develop a series of simple models of recruitment (and the complementary models of optimal harvest) based upon four different measures of reproductive potential.

Body Size and Reproductive Success

A schematic summary of the effects of body size on growth and survival of the different life-history stages of Pacific salmon is presented in Fig. 1. These size-dependent effects are discussed below implicitly in the context of given fixed abundances to isolate these effects from the density-dependent growth and survival processes that are well documented for Pacific salmon (see Peterman 1987 for a review). These density-dependent relationships often have large variances around them, and the growing literature on size-dependent processes suggests that some of that variance may be explainable by sizes of spawning females and eggs.

Egg and Female Size: Maternal Effects

In Pacific salmon, larger females produce more and larger eggs on average than small females (e.g., Foerster and Pritchard 1941; Rounsefell 1957; Galbreath and Ridenhour 1964; Bilton and Jenkinson 1966; Beacham 1982; Hankin and McKelvey 1985; Healey and Heard 1985; Manzer and Miki 1986), a phenomenon studied most closely in coho salmon (Holtby and Healey 1986; Fleming and Gross 1989, 1990; van den Berghe and Gross 1989). In female coho, fecundity increases more slowly than female mass with increasing length (larger females produce fewer eggs/unit body mass than small females), but total egg mass (egg number × biomass/egg) increases faster than female mass (Fleming and Gross 1990). The same pattern holds for other Pacific salmon (Bilton 1970b; Bilton and Smith 1973; Hankin and McKelvey 1985; Lewis 1987). Thus, larger female salmon, with fewer eggs per unit biomass, apparently sacrifice fecundity for increased egg size compared with small salmon, for reasons discussed below.

Effects of Egg Size on Juvenile Growth and Survival

Small eggs have lower metabolic requirements and are more likely to survive incubation in low-quality gravel than

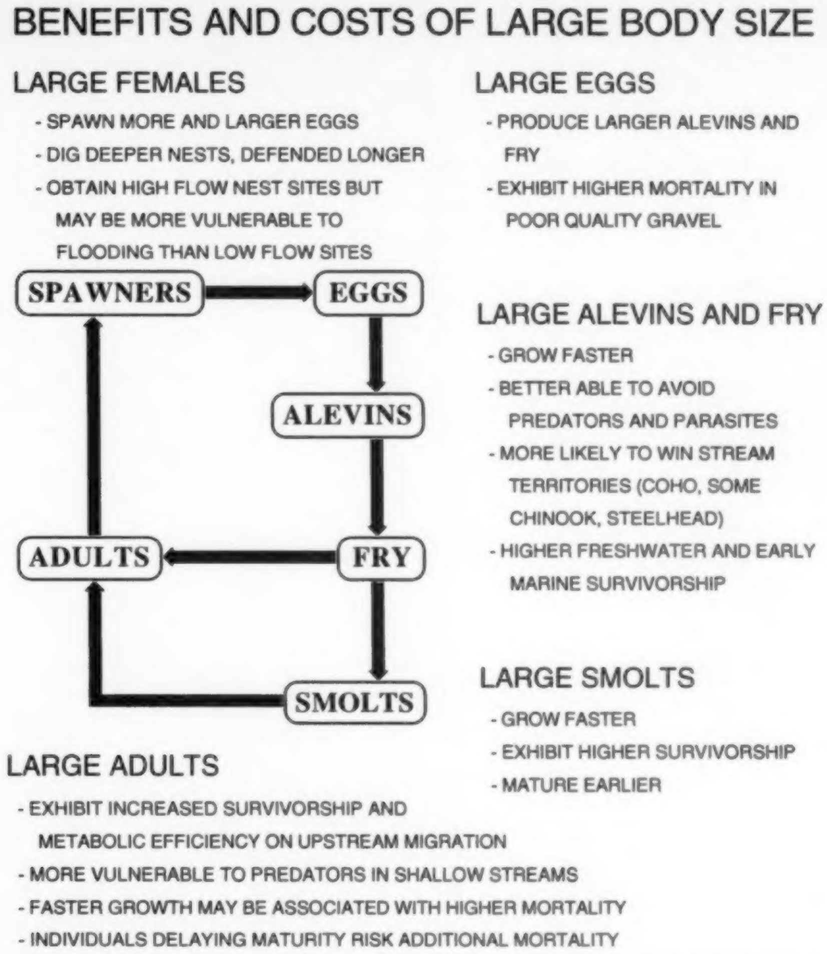
BENEFITS AND COSTS OF LARGE BODY SIZE
LARGE FEMALES
- SPAWN MORE AND LARGER EGGS
- DIG DEEPER NESTS, DEFENDED LONGER
- OBTAIN HIGH FLOW NEST SITES BUT MAY BE MORE VULNERABLE TO FLOODING THAN LOW FLOW SITES
LARGE EGGS
- PRODUCE LARGER ALEVINS AND FRY
- EXHIBIT HIGHER MORTALITY IN POOR QUALITY GRAVEL
SPAWNERS
EGGS
ALEVINS
ADULTS
FRY
SMOLTS
LARGE ALEVINS AND FRY
- GROW FASTER
- BETTER ABLE TO AVOID PREDATORS AND PARASITES
- MORE LIKELY TO WIN STREAM TERRITORIES (COHO, SOME CHINOOK, STEELHEAD)
- HIGHER FRESHWATER AND EARLY MARINE SURVIVORSHIP
LARGE SMOLTS
- GROW FASTER
- EXHIBIT HIGHER SURVIVORSHIP
- MATURE EARLIER
LARGE ADULTS
- EXHIBIT INCREASED SURVIVORSHIP AND METABOLIC EFFICIENCY ON UPSTREAM MIGRATION
- MORE VULNERABLE TO PREDATORS IN SHALLOW STREAMS
- FASTER GROWTH MAY BE ASSOCIATED WITH HIGHER MORTALITY
- INDIVIDUALS DELAYING MATURITY RISK ADDITIONAL MORTALITY

FIG. 1. Schematic outline of the effects of body size on growth and survival during different life-history stages of Pacific salmon. References are given in the text.

large eggs (van den Berghe and Gross 1989). Large egg size therefore bears an evolutionary cost in environments with low-quality gravel. Holtby and Healey (1986) indeed found that in years of low stream flow, smaller adult females, which are better able to exploit "marginal" spawning sites, enjoyed a reproductive advantage.

The potential disadvantage of large egg size, however, may be counterbalanced by the frequency with which large eggs are deposited in high-quality gravel and by other life-history stages because large eggs give rise to larger alevins and fry than small eggs (Brown 1946; Bagenal 1969; Bams 1969; Bilton 1970a; Fowler 1972; Kazakov 1981; Iwamoto et al. 1984; Wallace and Aasjord 1984; Beacham and Murray 1985; Beacham et al. 1985). Larger fry grow faster (Brown 1946; Bagenal 1969) and are better able to withstand food deprivation (Bagenal 1969) and avoid predators and parasites than small fry (Mead and Woodall 1968; Boyce 1974; Taylor and McPhail 1985; West and Larkin 1987).

One exception to this literature is the work of Holtby and Healey (1986) who studied coho salmon in Carnation Creek on Vancouver Island and failed to detect any statistically significant advantage for the progeny of large females. They did find a negative, but nonsignificant, correlation between the mean size of spawning females and subsequent egg mortality rate ($r = -0.41$, $n = 12$). In this case, a real effect may be present but simply not detected because of low statistical power due to small sample size and/or large variability (see Peterman 1990). In fact, we calculated (Cohen 1988) that the power of this test was only 0.26 with their sample size even if the true correlation were -0.41. For their small-sample test to have been high power (≥ 0.8), the true correlation would have to have been ≤ -0.73. We note parenthetically that Holtby and Healey's (1986) claim that there were *no* reproductive advantages of large body size for female coho in Carnation Creek overlooked the obvious differences in fecundity between small and large females (M.C. Healey, personal communication).

West and Larkin (1987) examined growth and survivorship of juvenile sockeye in relation to size of fry at emergence from the gravel. Larger fry grew faster and left the lake as larger smolts, and this growth advantage over small fry increased during freshwater life. Fry that emerged relatively small tended to stay in the lower end of the size distribution of their cohort and became progressively smaller relative to individuals at the large end of the size distribution. Moreover, smaller fry had a lower survival rate (fry-to-smolt survivals of fry above and below the mean size at emergence were 63.6 and 8.9%, respectively (West and Larkin 1987)).

Considerable variation in egg size occurs within populations of Pacific salmon. For example, spawning populations of chinook salmon (*Oncorhynchus tshawytscha*) frequently have threefold variation in egg size, attributable in part to differences in female size (Rombough 1985). There are three possible reasons why egg size increases with female body size. First, large egg size is simply an evolutionary constraint (i.e., not an adaptive trait) for large salmon; body size and egg size are simply correlated traits.

Second, large salmon derive a reproductive benefit from large eggs, i.e., the fitness returns (e.g., number of surviving offspring) per unit egg biomass for large eggs are at least equivalent to the fitness returns per unit egg biomass for small eggs. Larger eggs give rise to larger juveniles, which may exhibit higher survivorship (see above). But why then is egg size correlated with female body size? Fleming and Gross (1990) suggested that variation in success in female competition for breeding sites may explain differences in egg size. Large eggs survive less well than small eggs in nests of poor gravel quality, but large females tend to acquire better quality nest sites than small females through competitive interactions.

Third, egg size may reflect density-dependent competition as above but may currently be maladaptive. That is, females with large eggs and offspring derive fitness benefits from large body size and eggs when significant intraspecific competition exists (large females tend to acquire better nest territories, and large juveniles fare better in acquiring food and avoiding parasites or predators), as one would expect in high-abundance, unharvested populations. However, large salmon may pay a penalty for large egg size when intraspecific competition is relaxed, as in harvested populations where escapements tend to generally be at an abundance well below the unfished equilibrium. Because most Pacific salmon populations are currently harvested, levels of intraspecific competition are likely relaxed relative to that during most of their evolutionary history.

The validity of these three alternative explanations of increased egg size with body size has important implications for fishery managers. If the first is true, fecundity per se is the best measure of reproductive potential because there is no selective advantage to large egg size. If the second is true, egg biomass will represent a better measure of reproductive potential because it will reflect, at least in part, the reproductive advantages of large egg size. If the third explanation is true, the best measure of reproductive potential will likely lie somewhere between the first (small eggs favoured) and second (large eggs favoured). Note that if larger females derive greater fitness benefits per unit egg biomass than small females, then egg biomass per se will underestimate the reproductive potential of large females. As yet, there is no adequate measure of survivorship of offspring from females of different size.

Juvenile Size and Marine Survival

Several studies show that larger juvenile salmon tend to survive in the ocean better than smaller ones. Predation on juveniles entering salt water tends to be biased toward removing smaller individuals (Parker 1971; Healey 1982; Hargreaves and LeBrasseur 1986). Experiments in which hatchery chum and pink salmon (*Oncorhynchus gorbuscha*) fry were fed for 30–90 d before release have resulted in up to twofold increases in adult returns (Kobayashi 1980). In chinook, sockeye, and coho salmon, larger smolts are more likely to return as adults due to increased survivorship and/or earlier age at maturity (Foerster 1954; Clutter and Whitesel 1956; Ricker 1962; Garrison 1971; Hager and Noble 1976; Mathews and Buckley 1976; Bilton 1978, 1984; Bilton et al. 1982; Macdonald et al. 1987; Martin and Wertheimer 1989).

Holtby et al. (1991), in a detailed study of smolt size and early ocean survival in coho salmon, found that large smolt size conferred an advantage in years when marine survival was poor, but the large size was not a consistent advantage across all years. They suggested that ocean conditions affect rates of smolt growth, which in turn affect susceptibility to size-selective predators.

Adult Size and Survival on Upstream Migration

Long upstream migrations in rivers may favour large body size in salmonids because of the large energetic requirement for overcoming currents, turbulence, and obstacles (Schaffer and Elson 1975 (but see Myers and Hutchings 1987); Beamish 1978; Bernatchez and Dodson 1987). For example, female sockeye salmon, which were on average smaller than males, were much less successful than males in negotiating obstacles on their upstream migration in the Fraser and Babine rivers (Ricker 1987). Similarly, pink salmon, which are on average smaller than sockeye, are less able to cope with the same obstacles on the Fraser and Babine rivers than sockeye salmon (Ricker et al. 1978; Ricker 1989). However, larger body size may make individuals more vulnerable to predators such as bears and gulls, particularly in small, shallow streams (Konovalov and Shevlyakov 1978; Beacham and Murray 1987; Rogers 1987).

Adult Size and Spawning Behaviour

Large body size confers several advantages to spawning females. First, large females dig deeper nests than small females and those nests are less vulnerable to scouring by flood waters and redd superimposition (dig-up) by subsequently spawning small females (van den Berghe and Gross (1984, 1989). Second, large females may defend nests longer (van den Berghe and Gross 1986), although Schroder (1973) and Lewis (1987) did not observe this behaviour in chum salmon. Third, large females are more likely to obtain and defend nest territories in high-flow sites (Holtby and Healey 1986; van den Berghe and Gross 1986, 1989; Lewis 1987). Conversely, small eggs deposited by small females in gravel with lower flow may be less susceptible to scouring during years with heavy flooding than eggs deposited by large females (Holtby and Healey 1986).

Evolutionary Fitness versus Reproductive Success

Although considerable evidence suggests that larger spawners, particularly females, have higher reproductive success, we do not necessarily suggest that larger females always have higher evolutionary fitness. Indeed, if such were the case, we might expect populations composed entirely of large females. Undoubtedly, some size variation within populations is a result of environmental variability (i.e., not heritable) and thus has no selective consequences: some individuals grow faster because they are lucky in finding food.

Even if variation in body size is heritable, large females may still *not* enjoy higher evolutionary fitness if greater initial reproductive success is counterbalanced at other life-history stages. Reproductive success is only one component of fitness; survival to reproduction is another. Where large body size is achieved by delayed maturity (e.g., feeding in the ocean for an additional year), individuals risk additional mortality by remaining in the ocean longer (see Healey 1986, 1987 for comprehensive discussions of growth–mortality trade-offs in Pacific salmon). Similar arguments may hold when females of the same age mature at different sizes, if individuals growing faster and larger take more risks to seek food (see Holtby and Healey 1990; Holtby et al. 1991).

Frequency-dependent selection may also underlie variation in body size among spawning populations. Such variation may be maintained as mixed evolutionarily stable strategies (sensu Maynard Smith 1982) if life-history trade-offs are frequency dependent. Gross (1985), for example, suggested that coho jacks (males maturing after one winter at sea) and hooknoses (males maturing after two winters at sea) exhibit equal fitness, but hooknoses still enjoy higher spawning success than jacks (subject to frequency-dependent competition). This spawning advantage, however, is counterbalanced by a lower probability of survival of offspring to spawning age. Holtby and Healey (1986) have similarly suggested that alternative female phenotypes in coho salmon may be maintained by frequency-dependent selection.

Phenotypic variation may also arise from selection for bet-hedging strategies (sensu Seger and Brockmann 1987), where phenotypic diversification may allow for temporal or spatial escape from locally unfavourable conditions, reducing the probability of extinction for a given genotype, e.g., variation in age at maturity in Pacific salmon might serve as a hedge against occasional recruitment failure, due to drought or flooding (Murphy 1968; Healey 1982; Quinn 1982).

Absolute versus Density- and Frequency-Dependent Effects of Body Size

While some evidence thus exists that reproductive potential may increase with body size in Pacific salmon, increasing the productivity of Pacific salmon stocks is not necessarily a simple matter of pursuing harvest strategies that result in an increase in the mean body size of spawners. This is because some of the benefits of large body size are "relative" benefits and others are "absolute" benefits. That is, some benefits of large body size are density or frequency dependent; others are independent of those factors. Frequency-dependent benefits of large body size are at least partly dependent upon the relative frequency of sizes of individuals in the population (see Gross 1985). An example occurs in brown trout (*Salmo trutta*) fry, where larger individuals grow faster due to social dominance. However, where the large individuals were removed from the population, the smaller individuals showed increased growth rates (Brown 1946). Similarly, larger coho salmon fry are more likely to win stream territories, but when owners of territories are removed, smaller nomadic individuals take their place (Chapman 1962; Mason and Chapman 1965). Here, large body size per se appears less important than large body size *relative* to the size of other members of the population. In addition, Healey and Heard (1985) suggested that the reproductive potential of smaller, younger age-classes of chinook salmon may increase in the absence of competition from older, larger spawners, as now occurs in heavily exploited populations.

The importance of relative size effects may also be mediated by population density. van den Berghe and Gross (1989) found that reproductive success in a dense spawning population of coho salmon depended strongly upon success in female–female competition, which depended strongly upon female size. However, we expect the effects of female–female competition to be diminished at lower spawner densities. Indeed, Fleming and Gross (1989) suggested that relaxed competition due to lowered abundance of spawners caused by exploitation might explain the apparent lack of a relationship between female size and reproductive success in Carnation Creek coho found by Holtby and Healey (1986).

However, regardless of the presence or absence of these "relative" benefits of large body size, some benefits reviewed in previous sections seem likely to be independent of success in intraspecific competition. There are at least six "absolute" advantages of large body size: larger fry are (i) more resistant to starvation, (ii) better at avoiding predators, and (iii) reach threshold sizes where they are not vulnerable to certain gape-limited predators more quickly than smaller fry, resulting in lower juvenile mortality, and larger adult females (iv) carry more energy stores to succeed at upstream migration (as do larger adult males), (v) carry more and larger eggs, and (vi) dig their eggs deeper into gravels, thereby reducing mortality from stream scouring and dig-up by other spawners.

Managers of Pacific salmon fisheries have traditionally not incorporated either such frequency-dependent or absolute size-dependent processes into analyses of optimal harvesting strategies. Instead, they have usually only included effects of population density through stock–recruitment analyses. While we might expect diminished importance of the frequency- or density-dependent benefits of large body size because of reduced spawning densities due to harvested compared with unharvested conditions, the weight of evidence on the absolute effects of body size on reproductive success is now sufficient to warrant an examination of how such effects might influence our choice of harvesting strategies.

Alternative Models of Recruitment and Harvest

In this section, we first examine in greater detail the relationship among female body mass, fecundity, and egg size. These relationships lead to the development of four measures of reproductive potential and their associated models of recruitment, as well as distinct optimal harvest strategies. Here, we make no assumptions about the source of variation in size and age at maturity in Pacific salmon populations; we simply assume that such variation exists and ask the question "Can we increase biomass yield from the fishery while maintaining optimal spawning populations via size-selective fishing?" The source of variation in size and age at maturity, be it environmental or genotypic (heritable) in origin, *does* become important in assessing whether increased yields from the fishery are sustainable over the long run. We address this question later.

Size and Number of Eggs versus Female Size

The fecundity of a female of a given size and the biomass of eggs carried by a given female are two easily quantified measures of reproductive success that might be used to estimate the value of the exponent C in the relationship

$$(1) \quad \mathrm{RS} = kL^{C}$$

where RS is a measure of reproductive success, L is the length of adults, and k and C are positive constants. Relationships between egg biomass and female length and between fecundity and female length have been examined in detail in coho salmon by Fleming and Gross (1990). In 21 coho populations, the exponent C for the length–fecundity relationship ranged between 0.99 and 2.91 (mean = 2.27) and C was greater than 2.0 in 17 of the 21 populations. For those same 21 populations, the value of C for the length – egg biomass relationship ranged between 2.68 and 4.29 (mean=3.35); C ranged between 3.0 and 4.0 in 16 of 21 cases (the more extreme values tended to be associated with very small sample sizes). Thus, fecundity generally increased more slowly with respect to female length than female mass (assuming that female mass increases approximately as the cube of length, i.e., isometric growth), and egg biomass rose more rapidly than female mass. We note that the exponent in the length–mass relationship in Pacific salmon may be greater than 3.0 (e.g., Bilton 1985 reported mean values of 3.30, 3.35, and 3.46 for sockeye, pink, and chum salmon, respectively). We therefore suggest that when comparing the rates of increase of reproductive potential and individual biomass with female length, the exponent for the length–mass relationship for the particular stock in question should be used.

Unfortunately, detailed information such as Fleming and Gross' (1990) on relationships among egg biomass, fecundity, and female length is not available for other species of Pacific salmon, but the limited information available agrees qualitatively with their results for coho (summarized in Table 1). In 21 of 23 cases in Table 1, fecundity increased more slowly with changes in female length than female mass (i.e., C for the length–fecundity relationship is less than C for the female biomass relationship). Data on egg biomass, however, are scarce. In Klamath River chinook salmon, fecundity increased more slowly than female mass ($C = 1.166$), but ovary biomass increased more rapidly than female mass ($C = 4.083$) (Hankin and McKelvey 1985). In Walker Creek chum salmon, the body mass of age 4 females was 30.7% greater than that of age 3 females, but the egg biomass of age 4 females was 60.8% greater than that of age 3 females (Lewis 1987) (i.e., $C > 3.0$), once again indicating that egg biomass increases more rapidly with respect to female length than female mass.

Measures of Reproductive Potential

From this review, four categories of measures of reproductive potential in Pacific salmon were apparent.

(1) Spawner index: reproductive potential is measured as the number of female spawners.

(2) Fecundity index: reproductive potential is measured as the potential number of eggs deposited by spawning adults [(fecundity/female adult) × number of female adults].

(3) Egg biomass index: reproductive potential is measured as the potential biomass of eggs deposited by spawning adults [(egg biomass/female adult) × number of female adults]. The egg biomass index accounts for variation in egg size not included in the fecundity index.

(4) Progeny index: reproductive potential is measured as the potential number of progeny produced to some specified life stage by spawning adults [(potential progeny/adult female) × number of adult females]. The progeny index accounts for potential variation in offspring survival rate attributable to differences in size of eggs or female spawners, among other factors.

Relationships among Measures of Reproductive Potential

Clearly, these four measures of reproductive potential are examples of a larger set. However, they provide a range of alternative measures, two of which include the effects suggested in the literature of female body size on reproductive potential that go beyond the simple effect on fecundity. The four indices differ in the extent to which they account for differential reproductive success among individuals in a spawning population. If all individuals within a spawning population are reproductively equivalent (e.g., a single age-class of adults with very little size variation among them, as might occur in some pink salmon stocks), then all four model indices converge, and the spawner index is the most parsimonious measure of reproductive potential.

The fecundity index is an obvious improvement over the spawner model because it accounts for potential variation in the number of eggs carried by individual spawners. Variation in fecundity will clearly be more important where year-to-year variation in the size of spawners is large, as can occur in stocks where adults mature at different ages, or where the intensity of size-selective fishing varies. In Pacific salmon, considerable variation in fecundity does occur across age-classes (Table 1). As well, fecundity in Atlantic salmon (*Salmo salar*) is highly correlated ($r \geq 0.78$) with the sea age (number of winters in the ocean) of spawners, and using data from 10 populations in eastern Canada, Randall (1989) found a threefold range in the number of spawners (5–16 spawners/ha) required to meet egg deposition requirements (2.4×10^{4} eggs/ha) for different age structures of spawning populations.

The fecundity index, however, does not account for variation in egg size among spawners of different size. As noted above, such variation in egg size may be considerable. However, no one has estimated from field data the influence of female size or total biomass of eggs on recruitment of adults to the next generation due to logistical constraints (although Holtby and Healey (1986) and van den Berghe and Gross (1989) examined female size in relation to the number of surviving fry). Therefore, for the purpose of our analysis of the egg biomass model, we made the simplest assumption that the number of surviving offspring is directly related to the biomass of eggs deposited on the spawning grounds because that biomass reflects the combination of both number and size of eggs. If this is true in nature, then the egg biomass index will provide a better measure of reproductive potential than either the spawner or fecundity index.

If, however, the survival rate of offspring rises more rapidly than egg biomass with increasing length of adult females for a given abundance of spawners, then the prog-

TABLE 1. Comparison of fecundity and female biomass in different age-classes of Pacific salmon within the same stock. Percent increase in fecundity or female biomass is shown for the older age-class compared with the younger one. In most cases (those indicated by an asterisk), mean female mass was not reported but mean female length was. In these cases the percent increase in female biomass was calculated as $\{[(L_{i+1})^3 - (L_i)^3]/(L_i)^3\} \times 100$ where L_i is the mean length of the younger age-class and L_{i+1} is the mean length of the older age-class. We assumed isometric growth (i.e., mass increases as the cube of length). In fact, the exponent in the length–mass relationship may be greater than 3.0, making the values under "female biomass" too low. Literature sources: 1, Elson et al. (1986); 2, Rosberg et al. (1986); 3, Manzer and Miki (1986); 4, Bilton (1970b); 5, Hanamura (1966); 6, Helle (1979); 7, Lewis (1987); 8, Beacham (1982); 9, Snyder (1921); 10, Galbreath and Ridenhour (1964); 11, Yancey and Thorsteinson (1963).

		Percent increase in:		
Stock	Age-classes compared	fecundity	female biomass	Literature source
Sockeye				
British Columbia				
Chilko River	4_2–5_2	15.0	37.1*	1
Nadina River	4_2–5_2	33.3	42.7*	1
Upper Pitt River	4_2–5_2	22.3	38.9*	1
Weaver Creek	4_2–5_2	17.7	34.0*	2
Gates Creek	4_2–5_2	20.3	24.5*	2
Great Central Lake	4_2–5_2	32.0	58.4*	3
Sproat Lake	4_2–5_2	31.0	54.3*	3
Henderson Lake	4_2–5_2	34.0	43.4*	3
Ian Lake	4_2–5_2	8.1	12.4*	3
Awun Lake	4_2–5_2	16.4	40.0*	3
Babine Lake	4_2–5_2	20.9	44.4*	4
Russia				
Ozernaia River	5_3–6_3	13.6	30.9	5
	6_3–7_3	19.0	16.4	5
	6_4–7_4	12.7	30.3	5
Chum				
Alaska				
Olsen Creek	3_1–4_1	5.1	13.3*	6
	4_1–5_1	0.9	2.2*	6
British Columbia				
Walker Creek	3_1–4_1	39.9	30.7	7
Big Qualicum	3_1–4_1	11.6	16.8*	8
	4_1–5_1	1.1	8.3*	8
Pallant Creek	3_1–4_1	21.1	23.6*	8
Chinook				
California				
Klamath River	4_1–5_1	25.6	40.3	9
Washington				
Columbia River	4_2–5_2	34.1	73.4*	10
Alaska				
Cook Inlet	5–6	17.1	25.3	11

eny index will provide an even better measure of reproductive potential, all else being equal.

Of course, if fishing is not size selective, and if there is little variation in the size distribution of eggs across years or stocks, then it will not matter which measure of reproductive potential is used in determining optimal harvest or escapement policies. However, if managers impose size-selective fisheries, then a biased size distribution of the recruiting population will be allowed to spawn, and the different indices of reproductive potential will therefore lead to different decisions about how many fish should be allowed to spawn, even if sizes of fish prior to fishing are relatively constant each year.

To explore this topic further, we develop size-structured models of recruitment and optimal harvest in the following section, using the four measures of reproductive potential described above. We define the optimal harvest as that maximizing the sustainable biomass yield (MSY) to the fishery.

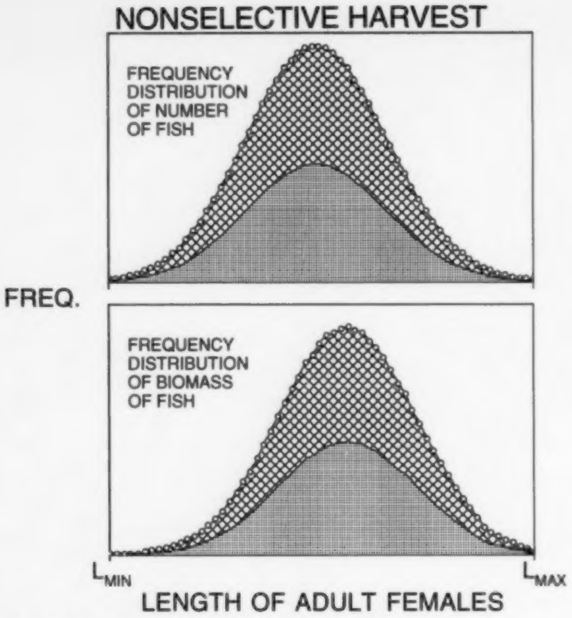

FIG. 2. Distributions for the case of nonselective harvest of a Pacific salmon stock with a unimodal length–frequency distribution of adult females in the returning population prior to fishing (recruits) (top panel). L_{MIN} and L_{MAX} are the minimum and maximum lengths of adult females in the population, respectively. The bottom panel represents the distribution of biomass of adult females in the recruits with respect to adult female length. Because longer adults are heavier, the mode of the adult biomass–frequency distribution lies to the right of the adult length–frequency distribution. In this example, one half of the returning adult females are harvested (cross-hatched area) and the remaining half are allowed to escape to spawn (shaded area). Because the harvest is nonselective for size, the proportional frequency distributions of sizes of adults in the catch and escapement are identical.

Models of Recruitment

Imagine a stock in which the population dynamics are described by a standard Ricker (1975) stock–recruitment relationship:

$$(2)\quad R = S\exp\{\alpha(1 - S/\beta)\}$$

where R is the number of recruits, S is the number of spawners, and α and β are model parameters. Assume that eq. 2 is stationary (i.e., the α and β parameters are unchanging across time). Now also imagine that we have a very long time series of stock (spawners) and recruitment (adult returns) data from which the α and β parameters of eq. 2 are well estimated. The optimal number of spawners, S^*, for that stock–recruitment relationship is then found iteratively by searching for the escapement that generates the MSY harvest.

This optimum escapement S^* will be composed of some average size distribution of spawners:

$$(3)\quad S^* = \Sigma_i\, S_i$$

where S_i is the abundance of spawners of size-class i and Σ_i is the sum across all size-classes, i. This S^* is valid if the total number of spawners is the best measure of reproductive potential. However, if it is not, we can also easily calculate the optimal value of the other measures of reproductive potential because they are simple linear transformations of S^* (the authors may be contacted for a proof). The optimum escapement in terms of the number of female spawners, S_f^*, is simply

$$(4)\quad S_f^* = S^*\,\overline{P} = \Sigma_i\, S_i\, P_i$$

where P_i is the proportion of females in a size-class i and $\overline{P}$ is the weighted average proportion of females across all size classes. Similarly, for the fecundity index, the optimum egg deposition, E^*, is

$$(5)\quad E^* = \Sigma_i\, S_i\, P_i\, F_i$$

where F_i is the fecundity of a female in size-class i. The optimum biomass of eggs, B^*, for the egg biomass index is found by substituting B_i, the biomass of eggs of females of size i, for F_i in the previous equation:

$$(6)\quad B^* = \Sigma_i\, S_i\, P_i\, B_i.$$

The optimum progeny strategy, O^*, in the progeny index of reproductive success is simply eq. 5 multiplied by a term accounting for differential survivorship among progeny from different size-classes of females:

$$(7)\quad O^* = \Sigma_i\, S_i\, P_i\, F_i\, O_i$$

where O_i is the survivorship of offspring from females of size-class i. Depending on the life stage at which offspring are measured, O_i can reflect many sources of mortality.

Note that where detailed information on the size structure of the population is not known, but where data on age structure are available, one might substitute age-classes for size-classes.

Models of Optimal Harvest

To estimate optimal harvests for each of these four measures of reproductive potential, we begin by specifying functional relationships between female length, L, and (i) female biomass, M, (ii) fecundity, F, and (iii) egg biomass, B. We expect female biomass, M, to increase approximately as the cube of female length, L:

$$(8)\quad M = k_1\, L^{q1}$$

where k_1 is some constant and $q1$ is a number close to 3. We expect fecundity, F, to increase with female length, but at a rate slower than female biomass, as noted above:

$$(9)\quad F = k_2\, L^{q2}$$

where k_2 is a constant and $q2$ is less than 3. We expect egg biomass, B, to increase more rapidly than female biomass:

$$(10)\quad B = k_3\, L^{q3}$$

where k_3 is a constant and $q3$ is greater than 3. Current data are too limited to specify a function relating length of females to abundance of early-life-stage progeny, O, for a given abundance of females. Therefore, the progeny model developed here is more speculative than the others. But the literature review above suggests that effects of body size of female spawners may affect production of offspring more than reflected by total egg biomass, so the progeny model is worth considering for future research. Finally, we specify a continuous probability density function, $f(L)$, which describes the length–frequency distribution of females in the recruits prior to fishing in greater detail than the discrete size classes, i, discussed above. For simplicity, we

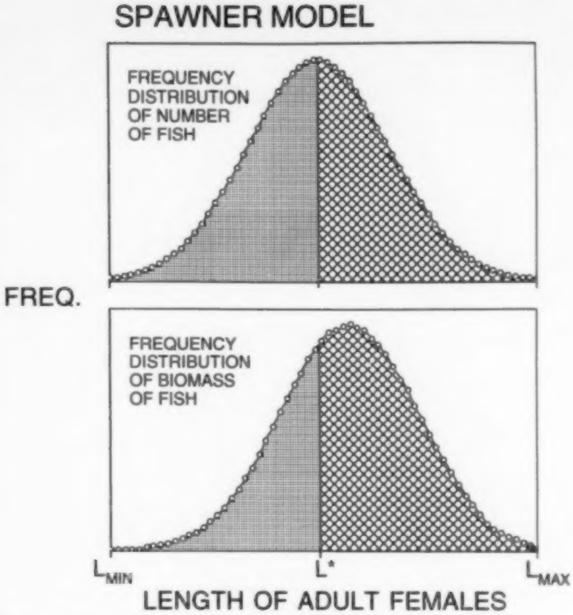

FIG. 3. Distributions for a size-selective harvest for the spawner model in which the number of female spawners is used as the measure of reproductive potential. The top panel represents the length–frequency distribution of the number of adult females in the recruits (i.e., prior to fishing). The bottom panel represents the distribution of biomass of adult females in the recruits. L_{MIN} and L_{MAX} are the minimum and maximum lengths of adult females in the population, respectively. L^* represents an example threshold size of harvested adult females that might maximize sustainable biomass yield to the fishery for a stock with particular α and β values (eq. 2). All females smaller than L^* are allowed to spawn (shaded area) and all females larger than L^* are harvested (cross-hatched area).

illustrate $f(L)$ as a normal distribution in Fig. 2–5, although we recognize that nonnormal distributions will often be the case in nature, e.g., multimodal distributions are likely when returning populations are composed of more than one age-class. Nevertheless, our qualitative results are not dependent upon the exact form of the length–frequency distribution, as long as the sex ratio is similar along the distribution. However, where sex ratio varies among age/size-classes, the optimal harvest strategy is likely to be affected. For example, a higher proportion of males is found among the younger age-classes of spawning Atlantic salmon, which favours the harvest of small fish (Randall 1989; see also Reed 1982).

For each of the alternative reproductive potential models, the goal of the harvest strategy is to maximize the sustainable biomass of harvestable adults while minimizing the biomass of spawners necessary to meet the optimum escapement requirements. As demonstrated below, some measures of reproductive potential imply different optimal harvest strategies than other measures. A nonselective harvest, illustrated in Fig. 2, is presented for comparison with the size-selective harvest strategies. In the nonselective harvest, the relative frequency distributions of the fish in the catch and escapement are identical.

Spawner model

For any given stock, some fixed number of spawners, S_f^*, will represent the optimum escapement, maximizing harvestable biomass. The distribution of female biomass as a function of female length in the returns (recruits) is presented in Fig. 3. Because of the exponential relationship between length and mass, the distribution of female biomass in the returning population is shifted to the right. In the case of the spawner model, in which all females are assumed to be equally productive, the optimal harvest strategy is obvious: we should selectively harvest the largest individuals and allow the smallest individuals to spawn. This is current practice in most salmon gillnet fisheries. That is, individuals between length L_{MIN} and L^* are allowed to spawn (Fig. 3), where

$$(11)\quad S_f^* = \int_{L_{\text{MIN}}}^{L^*} f(L)\,dL,$$

leaving the remainder to be harvested by the fishery. L^* that gives the maximum sustainable biomass harvest is found iteratively by trial for a particular stock–recruitment relationship (eq. 2), $f(L)$, and form of eq. 8. While we assume that a "knife-edge" size-specific harvest threshold of L^* is attainable for the sake of derivation of our models, in practice this will not be the case (i.e., some fish smaller than L^* will be caught, and some fish larger than L^* will escape to spawn). The theoretical maximum harvest that occurs in the "knife-edge" case will therefore be greater than that achievable in practice. Nevertheless, the relative comparisons of different models remain valid. The sustainable biomass of females harvested for this spawner model, H_s^*, (Fig. 3) is

$$(12)\quad H_s^* = \int_{L^*}^{L_{\text{MAX}}} M(L)\,f(L)\,dL.$$

Fecundity model

Recall that for the fecundity index of reproductive potential, E^* represents the optimum number of eggs deposited. The optimal harvest strategy derived below allows an escapement of females such that E^* eggs are deposited on the spawning grounds, which will maximize harvest biomass. The literature review above showed that fecundity increases more slowly than female mass with respect to female length, i.e., $q2 < q1$ in eq. 8 and 9. Thus, the frequency distribution of eggs in the returning population lies intermediate between the distributions of biomass and number of fish (Fig. 4). Those relationships between fecundity and length and between female mass and length further imply that smaller females carry more eggs per unit female mass than larger females. Thus, the optimal harvest strategy once again involves selective harvesting of the largest individuals, allowing the smallest, most "efficient" producers to spawn. In other words, if the number of eggs is the best measure of reproductive potential, smaller individuals contribute a disproportionately larger share of the reproductive potential of the spawning population than large fish. Thus, individuals between length L_{MIN} and L^* (Fig. 4) should be allowed to spawn:

$$(13)\quad S_E^* = \int_{L_{\text{MIN}}}^{L^*} f(L)\,dL,$$

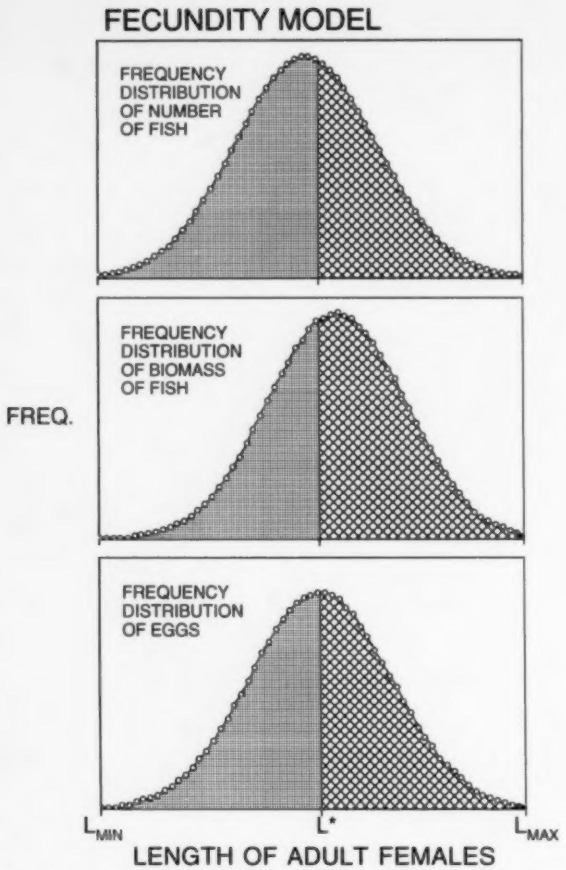

FIG. 4. Distributions for a size-selective harvest for the fecundity model in which the number of eggs deposited on the spawning grounds is used as the measure of reproductive potential. The top panel represents the length–frequency distribution of the number of adult females in the recruits. The middle panel represents the distribution of biomass of adult females in the recruits. The bottom panel represents the distribution of reproductive potential in the recruits, in this figure measured by the abundance of eggs. Because fecundity rises more slowly with increasing female length than individual mass, the mode of the egg–frequency distribution lies to the left of the mode of the adult biomass–frequency distribution. L^* represents an example threshold size of harvested adult females that might maximize sustainable biomass yield to the fishery; the L^* shown is merely an example reference point for comparing the three distributions. All females smaller than L^* are allowed to spawn (shaded area) and all females larger than L^* are harvested (cross-hatched area). The shaded area in the bottom panel represents the fraction of total reproductive potential that will result from that L^*. That "escapement" of eggs will generate the maximum sustainable yield.

leaving the remainder to be harvested by the fishery. Once again, L^* is found numerically. The biomass of females available for harvest in this fecundity model, H_E^* (Fig. 4) is thus

$$(14)\quad H_E^* = \int_{L^*}^{L_{\mathrm{MAX}}} M(L)\, f(L)\, dL.$$

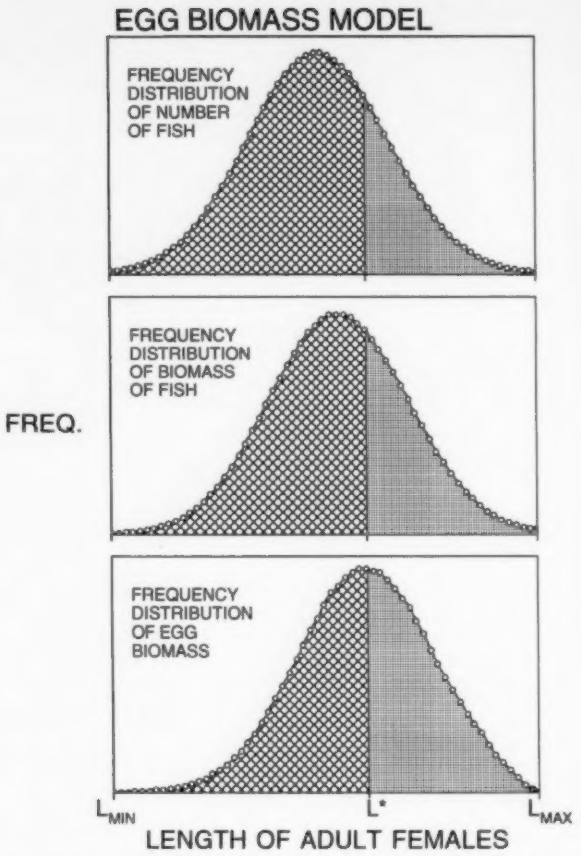

FIG. 5. Distributions for a size-selective harvest for the egg biomass model in which the total biomass of eggs deposited on the spawning grounds is used as the measure of reproductive potential. Because egg biomass increases with increasing female length more rapidly than female biomass, the mode of the egg biomass–frequency distribution (bottom panel) lies to the right of the adult biomass–frequency distribution (middle panel). The format is the same as in Fig. 3 and 4 except that here the smallest females are harvested (all fish smaller than L^*) and the largest females are allowed to spawn (all fish larger than L^*). The shaded area in the bottom panel represents the fraction of total reproductive potential that will result from the L^*. That "escapement" of egg biomass will generate the maximum sustainable yield for a particular situation. The progeny model (not shown) is qualitatively similar to the egg biomass model (i.e., the largest fish are allowed to spawn), although the exact value of L^* is likely to differ.

Egg biomass model

Recall that for the egg biomass index of reproductive potential, B^* is the optimum "escapement" of egg biomass. The optimal harvest strategy derived below will be the one that allows B^* egg biomass on the spawning grounds while maximizing harvestable fish biomass. If larger females carry more egg biomass per unit female mass as noted above, i.e., $q3 > q1$ in eq. 8 and 10, then egg biomass will be a better measure of reproductive success than egg abundance. In this case, the optimal harvest strategy will be exactly opposite to that under the spawner and fecundity models:

the smallest individuals should be harvested and the largest individuals should be allowed to spawn. This is because the largest individuals contribute the greatest reproductive success per unit mass of adult females when reproductive success is best reflected by total egg biomass. Thus, unlike the previous two situations, the largest fish should be allowed to spawn and the smallest ones harvested. Specifically, individuals between length L^* and L_{MAX} (Fig. 5) should be allowed to spawn:

$$(15) \quad S_B^* = \int_{L^*}^{L_{MAX}} f(L)\,dL.$$

Again, L^* is found numerically for the specific situation. The biomass of females available for harvest in this egg biomass model, H_B^* (Fig. 5), is thus

$$(16) \quad H_B^* = \int_{L_{MIN}}^{L^*} M(L)\,f(L)\,dL.$$

Progeny model

For the progeny index of reproductive potential, O^* represents the optimum "escapement" of potential progeny as measured at some life stage. Once again, the optimal harvest strategy derived below will be the one that allows only enough spawners to escape to produce O^* potential progeny while maximizing harvestable biomass. As with the egg biomass index of reproductive potential, for a given density, survivorship of progeny should increase with increasing female length more rapidly than female mass because of the size-dependent processes reviewed above. That is, larger females carry more potential progeny per unit female biomass than smaller females. As in the egg biomass model, the optimal harvest strategy will involve allowing the largest individuals to spawn (see Fig. 5) and harvesting the smallest individuals, i.e., individuals between length L^* and L_{MAX} are allowed to spawn:

$$(17) \quad S_O^* = \int_{L^*}^{L_{MAX}} f(L)\,dL,$$

leaving the remainder to be harvested by the fishery. The biomass of females available for harvest in this progeny model, H_O^*, is thus

$$(18) \quad H_O^* = \int_{L_{MIN}}^{L^*} M(L)\,f(L)\,dL.$$

Discussion

Risks and Rewards of Size-Selective Harvests

Our analysis has focussed on differing measures of reproductive potential in stocks of Pacific salmon. Strong evidence of size-dependent reproductive success in Pacific salmon suggests that the number of spawners per se may not be the most appropriate measure. Thus, gathering further data on the relationship between the size and reproductive success of individuals is key to determining the best measure of reproductive potential and the resulting optimal harvest strategy. If reproductive success increases more slowly than individual mass as the length of adult females increases (e.g., as does fecundity; $q2 < q1$), then the selective harvest of the largest individuals in a stock will, in the absence of an evolutionary response, maximize the sustainable harvest biomass. Conversely, if reproductive success increases more rapidly than individual mass with increasing female length (e.g., as does egg biomass; $q3 > q1$), then the selective harvest of the *smallest* individuals will maximize harvest biomass.

The choice of an incorrect measure of reproductive potential may lead to reduced yields because the MSY harvest biomass differs for those various measures under size-selective harvests that are common in Pacific salmon fisheries (Ricker 1981). These differences in MSY's occur because for a given abundance of spawners, the reproductive success of individuals is not directly proportional to their mass. Note, however, that under a nonselective harvest regime, the MSY biomass is the same for different measures of reproductive success. Clearly, if fishery managers use an inappropriate measure of reproductive potential, then a suboptimal management strategy will be chosen, given that size-selective fisheries are common.

Consequences of the Current Harvest Policy

Some authors suggest that the dramatic decrease in mean size of many salmon stocks observed over the past several decades may be at least partly attributable to fishing (e.g., Ricker 1981; Hankin and Healey 1986). If so, there are potentially important effects of the reproductive potential of such stocks. Younger, smaller spawners carry many fewer and smaller eggs, which led Hankin and McKelvey (1985) to suggest that stocks composed of smaller fish are likely to exhibit considerably diminished reproductive potential. In contrast, Healey and Heard (1985) speculated that smaller spawners would exhibit increased reproductive success in the absence of competition from larger individuals. The key to resolving this difference in predictions lies in distinguishing between the components of reproductive potential that are density or frequency dependent and those that are density or frequency independent (see Questions for Future Research below). The latter (-independent processes) will likely significantly influence the reproductive potential of most of the major wild salmon stocks in British Columbia because they generally tend to be heavily harvested (harvest rates = 50–80%/yr, e.g. Starr and Hilborn 1988; Collie et al. 1990; Farlinger et al. 1990). In those cases, abundance of spawners is reduced considerably below the unfished equilibrium values, and density- and frequency-dependent processes thus likely play a diminished role under relaxed intraspecific competition. Although smaller spawners will indeed exhibit increased reproductive success when released from competition with larger spawners (i.e., due to density/frequency-dependent effects), there will still remain a substantial reproductive differential between small and large spawners due to density- and frequency-independent effects such as differences in egg size and number.

Potential Risks of Size-Selective Harvests

As shown above, size-selective harvests offer the potential for increased harvest biomass, depending upon the relationship between individual size and reproductive success. One possible cost of a size-selective harvest is an alteration of the maturity schedule of the stock through maternal effects. The principal risk is that larger offspring (progeny produced from large eggs) may mature earlier and hence at a smaller size, potentially reducing the biomass harvest to the fishery. The latter effect might be expected because instantaneous growth rates generally exceed instantaneous mortality rates, and earlier age at maturity would result in a loss in the potential biomass harvest from a brood-class (Ricker 1976). Experimental releases of different sizes of smolts from hatcheries generally result in an inverse relationship between size at release and age at maturity (Bilton 1978, 1984) and wild populations also show this relationship (e.g., Peterman 1982).

The relative extent to which size variation among adults is maintained by genotypic or environmental influences will be an important determinant of the evolutionary effects of size-selective harvests. Unfortunately, current information is unclear about the relative importance of these two sources of variation. Evidence is accumulating that growth rate is heritable (Gall 1975; Beacham and Murray 1988). Thus, we can expect an evolutionary response to size-selective fishing. For instance, size-selective harvests of pink salmon have been implicated as the cause of a long-term decline in mean body size (Ricker et al. 1978), although Healey (1986) noted that other explanations for the decline are also plausible (e.g., changing oceanographic conditions). In contrast, there is evidence of a strong influence of the marine environment on interannual variability in mean age (and hence mean size) at maturity of sockeye salmon stocks (Peterman 1985). Where size variation is largely environmentally driven, size-selective fishing will result in little evolutionary response. Further information on the heritable and nonheritable components of growth variation in Pacific salmon is needed to assess responses to size-selective fishing.

A second possible cost of a size-selective harvest strategy is a reduction in the *diversity* of reproductive potential. A reduced range of body sizes within a spawning population due to size-selective fishing may diminish stock productivity. For instance, if relatively few large fish remain in a population after fishing, and if occasional high water flow conditions require large fish to successfully negotiate certain portions of a river during upstream migration, then few spawners will reach the spawning grounds in those years. Conversely, if a spawning population is mainly composed of large fish, relatively low reproductive success may occur in years of drought as a result of low water flow through spawning beds. This low success would occur because smaller individuals have higher reproductive success in "marginal" spawning habitat than either medium- or large-sized fish (large eggs survive less well in low flow sites; van den Berghe and Gross 1989; see also Holtby and Healey 1986).

Questions for Future Research

The central question for fishery managers arising from our work concerns the definition of the relationship between reproductive potential and body size in salmon in a manner relevant to the fishery: large spawners may produce more surviving offspring than small spawners. However, due to the interaction of several density- and frequency-dependent and -independent processes, this may or may not translate into an increase in harvestable biomass. An important question involves quantifying the relationship between female size and subsequent survival of offspring for a given density of spawners. Our four measures of reproductive potential (number of female spawners, number of eggs, biomass of eggs, and potential progeny) are all indirect measures of reproductive success. It is not clear which is best, although it seems unlikely that the simple number of female spawners or number of eggs is adequate.

What are the absolute effects of large egg size on subsequent juvenile survival? Larger juveniles do better within groups, but do groups that are on average larger in size exhibit higher mean survivorship than groups composed of small-sized fish? The effects of juvenile size at release on survival have been investigated in hatcheries (e.g., Hager and Noble 1976; Mathews and Buckley 1976; Bilton 1978, 1984; Martin and Wertheimer 1989), but the results of such studies are often confounded by variation in age at maturity and time of release. Moreover, the size of juveniles released from hatcheries often exceeds that normally observed in the wild and thus may not be representative of wild stocks. Detailed studies of the relationship between adult size and juvenile size and between juvenile size and survival to maturity in wild stocks are badly needed. Such studies should be facilitated by new techniques such as DNA fingerprinting which will allow researchers to measure the reproductive success of individuals more easily. For example, while there may be other variables in Helle's (1989) work causing both parental size and survival rate of their offspring to covary, his results strongly suggest that researchers should take a closer look at techniques that might be able to identify offspring from particular parents. Those methods will be a more powerful test than simply dealing with population means.

Optimal escapements are usually determined for Pacific salmon stocks by estimating parameters of the stock–recruitment relationship using a univariate measure of reproductive potential for stock abundance (Ricker 1975). However, it seems likely that more than one factor determines the reproductive potential of such stocks and a multivariate approach may therefore be more appropriate. For instance, current evidence suggests that size-dependent effects exist. In that case, the size as well as abundance of individual spawners and/or eggs likely interact and also make independent contributions to the reproductive potential of a particular stock. This set of variables should therefore be taken into account when estimating optimal escapements. Further research using this multivariate approach is needed to give a better understanding of the population dynamics of Pacific salmon and ultimately improve management performance.

Acknowledgments

Many thanks are due to C.C. Graham and F.E.A. Wood of the Department of Fisheries and Oceans, Vancouver, B.C., whose funding through a research contract helped to start this project with a review of the literature on effects of body size. Subsequent funding to support this project was provided by an NSERC operating grant to R.M.P. and by a Canadian Networks of Centres of Excellence grant to R.M.P. through OPEN, the Ocean Production Enhancement Network. We thank J.L. Anderson for an early review and Mart Gross, Eric van den Berghe, Ian Fleming, and Darren Gillis for early discussions of effects of body size. R.G. Randall, Mike Lapointe, Murdoch McAllister, Darren Gillis, Robert Crittenden, and an anonymous reviewer made many helpful comments on the manuscript.

References

Bagenal, T.B. 1969. Relationship between egg size and fry survival in brown trout *Salmo trutta* L. J. Fish Biol. 1: 349–353.

Bams, R.A. 1969. Adaptations in sockeye salmon associated with incubation in stream gravels, p. 71–87. *In* T.G. Northcote [ed.] Symposium on salmon and trout in streams. H.R. MacMillan Lectures in Fisheries, University of British Columbia, Vancouver, B.C.

Beacham, T.D. 1982. Fecundity of coho salmon (*Oncorhynchus kisutch*) and chum salmon (*Oncorhynchus keta*) in the northeast Pacific Ocean. Can. J. Zool. 60: 1463–1469.

Beacham, T.D., and C.B. Murray. 1985. Effect of female size, egg size, and water temperature on developmental biology of chum salmon (*Oncorhynchus keta*) from the Nitinat River, British Columbia. Can. J. Fish. Aquat. Sci. 42: 1755–1765.

Beacham, T.D., and C.B. Murray. 1987. Adaptive variation in body size, age, morphology, egg size, and developmental biology of chum salmon (*Oncorhynchus keta*) in British Columbia. Can. J. Fish. Aquat. Sci. 44: 244–261.

Beacham, T.D., and C.B. Murray. 1988. A genetic analysis of body size in pink salmon (*Oncorhynchus gorbuscha*). Genome 30: 31–35.

Beacham, T.D., R.E. Withler, and R.B. Morley. 1985. Effect of egg size on incubation time and alevin and fry size in chum salmon (*Oncorhynchus keta*) and coho salmon (*Oncorhynchus kisutch*). Can. J. Zool. 63: 847–850.

Beamish, F.W.H. 1978. Swimming capacity, p. 101–187. *In* W.S. Hoar and D.J. Randall [ed.] Fish physiology. Vol. 7. Academic Press, New York, N.Y.

Bernatchez, L., and J.J. Dodson. 1987. Relationship between bioenergetics and behavior in anadromous fish migrations. Can. J. Fish. Aquat. Sci. 44: 399–407.

Bilton, H.T. 1970a. Maternal influences on the age of maturity of Skeena River sockeye salmon (*Oncorhynchus nerka*). Fish. Res. Board Can. Tech. Rep. 167.

Bilton, H.T. 1970b. Comparison of the fecundity of sockeye salmon (*Oncorhynchus nerka*) in the Skeena River catch with the fecundity of those in the escapement. Fish. Res. Board Can. MS Rep. Ser. 1096: 8 p.

Bilton, H.T. 1971. A hypothesis of alternation of age of return in successive generations of Skeena River sockeye salmon (*Oncorhynchus nerka*). J. Fish. Res. Board Can. 28: 513–516.

Bilton, H.T. 1978. Returns of adult coho salmon in relation to mean size and time at release of juveniles. Can. Fish. Mar. Serv. Tech. Rep. 832.

Bilton, H.T. 1984. Returns of chinook salmon in relation to juvenile size at release. Can. Tech. Rep. Fish. Aquat. Sci. 1245.

Bilton, H.T. 1985. Length–weight relations for adult sockeye, chum, and pink salmon. Can. MS Rep. Fish. Aquat. Sci. 1846.

Bilton, H.T., D.F. Alderdice, and J.T. Schnute. 1982. Influence of time and size at release in juvenile coho salmon (*Oncorhynchus kisutch*) on returns at maturity. Can. J. Fish. Aquat. Sci. 39: 426–447.

Bilton, H.T., and D.W. Jenkinson. 1966. Relationship between egg size and fish size in sockeye salmon (*Oncorhynchus nerka*). Fish. Res. Board Can. MS Rep. Ser. 848: 3 p.

Bilton, H.T., and H.D. Smith. 1973. Relationship between egg size and fish size in pink salmon (*Oncorhynchus gorbuscha*) from the lower Babine River in 1966 and 1967. Fish. Res. Board Can. MS Rep. Ser. 1235.

Boyce, N.P.J. 1974. Biology of *Eubothrium salvelini* (Cestoda: Pseudophyllidea), a parasite of juvenile sockeye salmon (*Oncorhynchus nerka*) of Babine Lake, British Columbia. J. Fish. Res. Board Can. 31: 1735–1742.

Brown, M.E. 1946. The growth of brown trout (*Salmo trutta* Linn.). I. Factors influencing the growth of trout fry. J. Exp. Biol. 22: 118–129.

Chapman, D.W. 1962. Aggressive behavior in juvenile coho salmon as a cause of emigration. J. Fish. Res. Board Can. 19: 1047–1080.

Clutter, R.I., and L.E. Whitesel. 1956. Collection and interpretation of sockeye salmon scales. Int. Pac. Salmon Fish. Comm. Bull. 9.

Cohen, J. 1988. Statistical power analysis for the behavioral sciences. 2nd ed. Lawrence Erlbaum Associates, Inc., Hillsdale, N.J.

Collie, J.S., R.M. Peterman, and C.J. Walters. 1990. Experimental harvest policies for a mixed-stock fishery: Fraser River sockeye salmon, *Oncorhynchus nerka*. Can. J. Fish. Aquat. Sci. 47: 145–155.

Elson, M.S., J.D. Pugh, and M. Graves. 1986. A review of International Pacific Salmon Fisheries Commission bioreconnaissance data, with reference to proposed Fraser River system sockeye and pink salmon enhancement projects. Report prepared for New Projects Unit, Salmonid Enhancement Program, Department of Fisheries and Oceans, Vancouver, B.C. 200 p.

Farlinger, S., N. Bourne, B. Riddell, D. Chalmers, and A. Tyler [ed.] 1990. Pacific Stock Assessment Review Committee (PSARC) Annual Report for 1989. Can. MS Rep. Fish. Aquat. Sci. 2064: 236 p.

Fleming, I.A., and M.R. Gross. 1989. Evolution of adult female life history and morphology in a Pacific salmon (coho: *Oncorhynchus kisutch*). Evolution 43: 141–157.

Fleming, I.A., and M.R. Gross. 1990. Latitudinal clines: a trade-off between egg number and size in Pacific salmon. Ecology 71: 1–11.

Foerster, R.E. 1954. On the relation of adult sockeye salmon (*Oncorhynchus nerka*) returns to known smolt seaward migrations. J. Fish. Res. Board Can. 11: 339–350.

Foerster, R.E., and A.L. Pritchard. 1941. Observations on the relation of egg content to total length and weight in the sockeye salmon (*Oncorhynchus nerka*) and the pink salmon (*O. gorbuscha*). Trans. R. Soc. Can. Sect. V 35: 51–60.

Fowler, L.G. 1972. Growth and mortality of fingerling chinook salmon as affected by egg size. Prog. Fish-Cult 34: 66–69.

Gall, G.A.E. 1975. Genetics of reproduction in domesticated rainbow trout. J. Anim. Sci. 40: 19–28.

Galbreath, J.L., and R.L. Ridenhour. 1964. Fecundity of Columbia River chinook salmon. Oreg. Fish Comm. Res. Brief 10: 16–27.

Garrison, R.L. 1971. Effect of rapid smolt growth on coho maturation. J. Wildl. Manage. 35: 762–766.

Gross, M.R. 1985. Disruptive selection for alternative life histories in salmon. Nature (Lond.) 313: 47–48.

Hager, R.C., and R.E. Noble. 1976. Relation of size at release of hatchery-reared coho salmon to age, size, and sex composition of returning adults. Prog. Fish-Cult. 38: 144–147.

Hanamura, N. 1966. Sockeye salmon in the far east, p. 1–28. *In* Salmon of the North Pacific Ocean. Part II. A review of the life history of North Pacific salmon. Int. North Pac. Fish. Comm. Bull. 18.

Hankin, D.G., and M.C. Healey. 1986. Dependence of exploitation rates for maximum yield and stock collapse on age and sex structure of chinook salmon (*Oncorhynchus tshawytscha*) stocks. Can. J. Fish. Aquat. Sci. 43: 1746–1759.

Hankin, D.G., and R. McKelvey. 1985. Comment on fecundity of chinook salmon and its relevance to life history theory. Can. J. Fish. Aquat. Sci. 42: 393–394.

Hargreaves, N.B., and R.J. LeBrasseur. 1986. Size selectivity of coho (*Oncorhynchus kisutch*) preying on juvenile chum salmon (*O. keta*). Can. J. Fish. Aquat. Sci. 43: 581–586.

Healey, M.C. 1982. Timing and relative intensity of size-selective mortality of juvenile chum salmon (*Oncorhynchus keta*) during early sea life. Can. J. Fish. Aquat. Sci. 39: 952–957.

Healey, M.C. 1986. Optimum size and age at maturity in Pacific salmon and effects of size selective fisheries, p. 39–52. *In* D.J. Meerburg [ed.] Salmonid age at maturity. Can. Spec. Publ. Fish. Aquat. Sci. 89.

Healey, M.C. 1987. The adaptive significance of age and size at maturity in female sockeye salmon (*Oncorhynchus nerka*), p. 110–117. *In* H.D. Smith, L. Margolis, and C.C. Wood [ed.] Sockeye salmon (*Oncorhynchus nerka*) population biology and future management. Can. Spec. Publ. Fish. Aquat. Sci. 96.

Healey, M.C., and W.R. Heard. 1984. Inter- and intra-population variation in fecundity of chinook salmon (*Oncorhynchus tshawytscha*) and its relevance to life history theory. Can. J. Fish. Aquat. Sci. 41: 476–483.

Healey, M.C., and W.R. Heard. 1985. Reply to comment on fecundity of chinook salmon and its relevance to life history theory. Can. J. Fish. Aquat. Sci. 42: 394–395.

Helle, J.H. 1979. Influence of marine environment on age and size at maturity, growth, and abundance of chum salmon, *Oncorhynchus keta* (Walbaum), from Olsen Creek, Prince William Sound, Alaska. Ph.D. thesis, Oregon State University, Corvallis, Oreg. 118 p.

Helle, J.H. 1989. Relation between size-at-maturity and survival of progeny in chum salmon, *Oncorhynchus keta* (Walbaum). J. Fish Biol. 35(Suppl. A): 99–107.

Holtby, L.B., B.C. Anderson, and R.K. Kadowaki. 1991. Importance of smolt size and early ocean growth to interannual variability in marine survival of coho salmon (*Oncorhynchus kisutch*). Can. J. Fish. Aquat. Sci. 47: 2181–2194.

Holtby, L.B., and M.C. Healey. 1986. Selection for adult size in female coho salmon (*Oncorhynchus kisutch*). Can. J. Fish. Aquat. Sci. 43: 1946–1959.

Holtby, L.B., and M.C. Healey. 1990. Sex-specific life history tactics and risk-taking in coho salmon. Ecology 71: 678–690.

Iwamoto, R.N., B.A. Alexander, and W.K. Hershberger. 1984. Genotypic and environmental effects on the incidence of sexual precocity in coho salmon (*Oncorhynchus kisutch*). Aquaculture 43: 105–121.

Kazakov, R.V. 1981. The effect of the size of Atlantic salmon, *Salmo salar* L., eggs on embryos and alevins. J. Fish Biol. 19: 353–360.

Kobayashi, T. 1980. Salmon propagation in Japan, p. 91–109. *In* J.E. Thorpe [ed.] Salmon ranching. Academic Press, London. 441 p.

Konovalov, S.M., and A.G. Shevlyakov. 1978. Natural selection in Pacific salmon (*Oncorhynchus nerka*) (Walb.)) by body size. Zh. Obshch. Biol. 39: 194–206.

Lewis, A.F.J. 1987. The effects of breeding competition and abiotic factors on the behavior and reproductive success of female chum salmon (*Oncorhynchus keta*). M.Sc. thesis, Simon Fraser University, Burnaby, B.C. 186 p.

Macdonald, P.D.M., H.D. Smith, and L. Jantz. 1987. The utility of Babine smolt enumerations in management of Babine and Skeena River sockeye salmon (*Oncorhynchus nerka*) stocks, p. 280–295. *In* H.D. Smith, L. Margolis, and C.C. Wood [ed.] Sockeye salmon (*Oncorhynchus nerka*) population biology and future management. Can. Spec. Publ. Fish. Aquat. Sci. 96.

Manzer, J.I., and I. Miki. 1986. Fecundity and egg retention of some sockeye salmon (*Oncorhynchus nerka*) stocks in British Columbia. Can. J. Fish. Aquat. Sci. 43: 1643–1655.

Martin, R.M., and A. Wertheimer. 1989. Adult production of chinook salmon reared at different densities and released as two smolt sizes. Prog. Fish-Cult. 51: 194–200.

Mason, J.C., and D.W. Chapman. 1965. Significance of early emergence, environmental rearing capacity, and behavioral ecology of juvenile coho salmon in stream channels. J. Fish. Res. Board Can. 22: 173–190.

Mathews, S.B., and R. Buckley. 1976. Marine mortality of Puget Sound coho salmon (*Oncorhynchus kisutch*). J. Fish. Res. Board Can. 33: 1677–1684.

Mathisen, O.A. 1962. The effect of altered sex ratios on the spawning of red salmon, p. 137–246. *In* T.S. Koo [ed.] Studies of Alaska red salmon. University of Washington Press, Seattle, Wash.

Maynard Smith, J. 1982. Evolution and the theory of games. Cambridge University Press, Cambridge.

Mead, R.W., and W.L. Woodall. 1968. Comparison of sockeye salmon fry produced by hatcheries, artificial channels and natural spawning areas. Int. Pac. Salmon Fish. Comm. Prog. Rep. 20.

Murphy, G.I. 1968. Pattern in life history and the environment. Am. Nat. 102: 391–403.

Myers, R.A., and J.A. Hutchings. 1987. A spurious correlation in an interpopulation comparison of Atlantic salmon life histories. Ecology 68: 1839–1843.

Parker, R.R. 1971. Size selective predation among juvenile salmonid fishes in a British Columbia inlet. J. Fish. Res. Board Can. 28: 1503–1510.

Peterman, R.M. 1982. Model of salmon age structure and its use in preseason forecasting and studies of marine survival. Can. J. Fish. Aquat. Sci. 39: 1444–1452.

Peterman, R.M. 1985. Patterns of interannual variation in age at maturity of sockeye salmon (*Oncorhynchus nerka*) in Alaska and British Columbia. Can. J. Fish. Aquat. Sci. 42: 1595–1607.

Peterman, R.M. 1987. Review of the components of recruitment of Pacific salmon, p. 417–429. *In* M. Dadswell, R. Klauda, C. Moffitt, R. Saunders, R. Rulifson, and J.E. Cooper [ed.] Common strategies of anadromous and catadromous fishes. Am. Fish. Soc. Symp. 1.

Peterman, R.M. 1990. Statistical power analysis can improve fisheries research and management. Can. J. Fish. Aquat. Sci. 47: 2–15.

Quinn, T.P. 1982. Homing and straying in Pacific salmon, p. 357–362. *In* E.L. Brannon, and E.O. Salo [ed.] Proceedings of the Salmon and Trout Migratory Behavior Symposium. School of Fisheries, University of Washington, Seattle, Wash.

Randall, R.G. 1989. Effect of sea-age on the reproductive potential of Atlantic salmon (*Salmo salar*) in eastern Canada. Can. J. Fish. Aquat. Sci. 46: 2210–2218.

Reed, W.J. 1982. Sex-selective harvesting of Pacific salmon: a theoretically optimal solution. Ecol. Model. 14: 261–271.

Ricker, W.E. 1962. Comparison of ocean growth and mortality of sockeye salmon during their last two years. J. Fish. Res. Board Can. 19: 531–560.

Ricker, W.E. 1975. Computation and interpretation of biological statistics of fish populations. Bull. Fish. Res. Board Can. 191.

Ricker, W.E. 1976. Review of the rate of growth and mortality of fishing. J. Fish. Res. Board Can. 33: 1483–1524.

Ricker, W.E. 1981. Changes in the average size and average age of Pacific salmon. Can. J. Fish. Aquat. Sci. 38: 1636–1656.

Ricker, W.E. 1987. Effects of the fishery and of obstacles to migration on the abundance of Fraser River sockeye salmon (*Oncorhynchus nerka*). Can. Tech. Rep. Fish. Aquat. Sci. 1522: 75 p.

Ricker, W.E. 1989. History and present state of the odd-year pink salmon runs of the Fraser River region. Can. Tech. Rep. Fish. Aquat. Sci. 1702: 37 p.

Ricker, W.E., H.T. Bilton, and K.V. Aro. 1978. Causes of the decline in size of pink salmon (*Oncorhynchus gorbuscha*). Can. Dep. Environ. Fish. Mar. Serv. Tech. Rep. 820: 93 p.

Rogers, D.E. 1987. The regulation of age at maturity in Wood River sockeye salmon (*Oncorhynchus nerka*), p. 78–89. *In* H.D. Smith, L. Margolis, and C.C. Wood [ed.] Sockeye salmon (*Oncorhynchus nerka*) population biology and future management. Can. Spec. Publ. Fish. Aquat. Sci. 96.

Rombough, P.J. 1985. Initial egg weight, time to maximum alevin wet weight, and optimal ponding times for chinook salmon (*Oncorhynchus tshawytscha*). Can. J. Fish. Aquat. Sci. 42: 287–291.

Rosberg, G.E., K.J. Scott, and R. Rithaler. 1986. Review of the International Pacific Salmon Fisheries Commission's sockeye and pink salmon enhancement facilities on the Fraser River. Report prepared for Bio Program Unit, Enhancement Operations Division, Salmonid Enhancement Program, Department of Fisheries and Oceans, Vancouver, B.C. 184 p. + 3 appendices.

Rothschild, B.J., and M.J. Fogarty. 1989. Spawning-stock biomass: a source of error in recruitment/stock relationships and management advice. J. Cons. int. Explor. Mer 45: 131–135.

Rounsefell, G.A. 1957. Fecundity of North American salmonidae. U.S. Fish Wildl. Serv. Fish. Bull 122: 451–468.

Schaffer, W.M., and P.E. Elson. 1975. The adaptive significance of variations in life history among local populations of Atlantic salmon in North America. Ecology 56: 577–590.

Schroder, S.L. 1973. Effects of density on the spawning success of chum salmon (*Oncorhynchus keta*) in an artificial spawning channel. M.S. thesis, University of Washington, Seattle, Wash. 78 p.

Seger, J., and H.J. Brockmann. 1987. What is bet-hedging? Oxf. Surv. Evol. Biol. 4: 182–211.

Snyder, J.O. 1921. How many eggs does a salmon lay? Calif. Fish. Game 7: 63–64.

Starr, P., and R. Hilborn. 1988. Reconstruction of harvest rates and stock contribution in gauntlet salmon fisheries: application to British Columbia and Washington sockeye. Can. J. Fish. Aquat. Sci. 45: 2216–2229.

Taylor, E.B., and J.D. McPhail. 1985. Burst swimming and size-related predation of newly emerged coho salmon *Oncorhynchus kisutch*. Trans. Am. Fish. Soc. 114: 546–551.

van den Berghe, E.P., and M.R. Gross. 1984. Female size and nest depth in coho salmon (*Oncorhynchus kisutch*). Can. J. Fish. Aquat. Sci. 41: 204–206.

van den Berghe, E.P., and M.R. Gross. 1986. Length of breeding life of coho salmon (*Oncorhynchus kisutch*). Can. J. Zool. 64: 1482–1486.

van den Berghe, E.P., and M.R. Gross. 1989. Natural selection resulting from female breeding competition in a Pacific salmon (coho: *Oncorhynchus kisutch*). Evolution 43: 125–140.

Wallace, J.C., and D. Aasjord. 1984. An investigation of the consequences of egg size for the culture of Arctic charr, *Salvelinus alpinus* (L.). J. Fish Biol. 24: 427–435.

Walters, C.J., and D. Ludwig. 1981. Effects of measurement errors on the assessment of stock–recruitment relationships. Can. J. Fish. Aquat. Sci. 38: 704–710.

West, C.J., and P.A. Larkin. 1987. Evidence for size-selective mortality of juvenile sockeye salmon (*Oncorhynchus nerka*) in Babine Lake, British Columbia. Can. J. Fish. Aquat. Sci. 44: 712–721.

Yancey, R.M., and F.V. Thorsteinson. 1963. The king salmon of Cook Inlet, Alaska. U.S. Fish Wildl. Serv. Spec. Sci. Rep. Fish. 440: 18 p.

Zooplankton Biomass in the Southern Gulf of St. Lawrence: Spatial Patterns and the Influence of Freshwater Runoff

Yves de Lafontaine

Centre Saint-Laurent, Environment Canada, 105 McGill, Montréal, QC H2Y 2E7, Canada

de Lafontaine, Y. 1994. Zooplankton biomass in the southern Gulf of St. Lawrence: spatial patterns and the influence of freshwater runoff. Can. J. Fish. Aquat. Sci. 51: 617–635.

The role of advection of freshwater input in zooplankton distribution was evaluated from 16 surveys carried out in the southern Gulf of St. Lawrence during 1967–71. Biomass was structured according to two main patterns: large-scale gradients (>150 km) over the entire area and mesoscale (≈25km) patches. Patterns exhibited seasonal and interannual variability without any sign of recurrence through time, unlike the spatial structure of surface water temperature and salinity which was typical of large-scale dispersion gradients resulting from the seasonal input of freshwater into the area. In most cases, overall distribution patterns of biomass and hydrographic variables were not significantly correlated, indicating that biomass patterns in the southern Gulf were not related to water mass characteristics and advection of freshwater runoff over the entire area. Although mesoscale patchiness was unrelated to hydrographic processes, patch size (≈25km) was similar to estimates obtained for the northern Gulf and for other coastal shelf areas. Large-scale gradients in biomass may correspond to species changes in relation to the salinity gradient and/or topography and bathymetric features. I conclude that biomass alone is not an adequate predictor for monitoring changes and variability of zooplankton in response to runoff variability.

Le rôle de l'apport d'eau douce par advection sur la répartition du zooplancton a été évalué à partir de 16 relevés effectués dans le sud du golfe du Saint-Laurent entre 1967 et 1971. La biomasse était structurée selon deux patrons principaux : des gradients à grande échelle (>150 km) couvrant toute la région et une répartition en nuages à moyenne échelle (≈25 km). Les patrons présentaient une variabilité saisonnière et interannuelle sans aucun signe de récurrence dans le temps, contrairement à la structure spatiale de la température et de la salinité de l'eau de surface qui était caractéristique des gradients de dispersion à grande échelle découlant de l'apport saisonnier d'eau douce dans la région. Dans la plupart des cas, il n'existait pas de corrélation significative au niveau des patrons de répartition généraux de la biomasse et des variables hydrographiques, ce qui montre que les patrons de la biomasse dans le sud du Golfe n'étaient pas reliés à des caractéristiques de la masse d'eau et à l'apport d'eau douce par advection dans toute la région. Les répartitions à moyenne échelle n'étaient pas reliées à des processus hydrographiques, pourtant la taille des nuages (≈25 km) était similaire aux estimations obtenues dans le nord du Golfe et pour d'autres régions côtières de la plate-forme. Les gradients à grande échelle dans la biomasse peuvent correspondre à des modifications des espèces par rapport aux gradients de salinité ou à des éléments topographiques et bathymétriques. On conclut que la biomasse seule n'est pas une variable prédictive appropriée pour surveiller les modifications et la variabilité du zooplancton en réponse à la variabilité de l'apport d'eau douce.

Received January 28, 1993
Accepted October 6, 1993
(JB770)

Reçu le 28 janvier 1993
Accepté le 6 octobre 1993

Since Cassie's (1963) work on sampling variability, studies of plankton distribution have led to a consensus that plankton patchiness is primarily related to numerous physical and biological processes which interact with different relative influences at variable scales (Fager and McGowan 1963; Steele 1976; Harris 1980; Omori and Hamner 1982; Legendre and Demers 1984; Mackas 1984; Mackas et al. 1985; Wiens 1989; Taggart and Frank 1990). One prevailing concept asserts that mesoscale (1–100 km) and large-scale (>100 km) distribution patterns in zooplankton composition and biomass are primarily related to water mass structure resulting from advective forces (Mackas et al. 1985). In physically dynamic coastal regions, the distribution and abundance of plankton in a given area are often influenced by the variable advection of organisms from adjacent areas caused by variable circulation patterns (Cox and Wiebe 1979; Peterson et al. 1979; Chelton et al. 1982; Smith and Vidal 1984; Weikert 1984; Lindahl and Perissinotto 1987; Schneider 1987; Taggart and Frank 1987; Lindahl and Hernroth 1988; Springer et al. 1989; Coyle et al. 1990). Similarly, variable freshwater runoff may greatly influence zooplankton distribution and dynamics in coastal waters (Skreslet and Red 1986; Govoni et al. 1989). For example, it has been recently shown that part of the supply of zooplankton on the Scotian Shelf in eastern Canada originates from Gulf of St. Lawrence populations which drift out of the Gulf and become entrained within the Nova Scotia coastal current (Herman et al. 1991; Sameoto and Herman 1992).

Alternatively, variations in the community structure and biomass of zooplankton at various scales have often been ascribed to biological interactions, including selective predation (Kimmerer and McKinnon 1987, 1989; Frost 1988; Miller and Daan 1989; Suthers and Frank 1990), food-

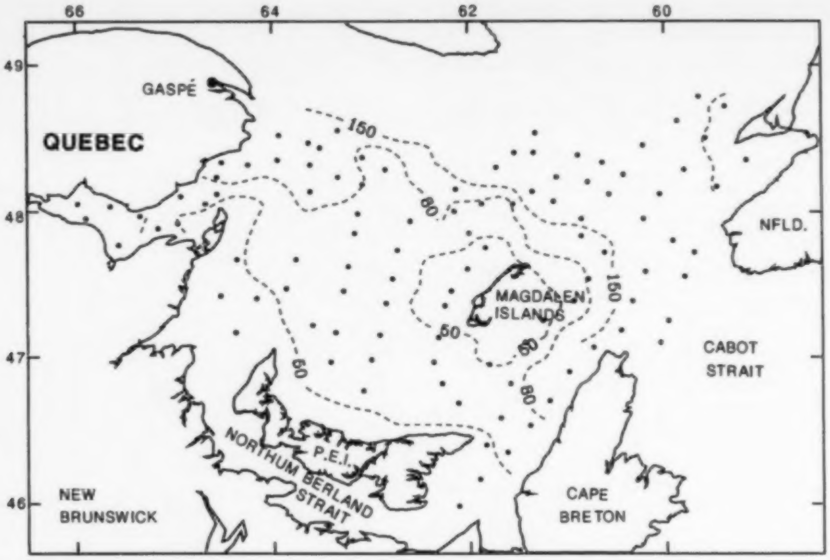

FIG. 1. Sampling area and station location for the various plankton surveys between 1967 and 1971. Bathymetric contours are in metres.

limiting growth (Paffenhoffer and Stearns 1988), and reproduction and life-cycle characteristics (Paffenhoffer and Stearns 1988; Runge and Simard 1990). The significant differences between the mesoscale (1–100 km) spatial patterns of phytoplankton and zooplankton during the same survey within a given area have been attributed to differences in the type and the effectiveness of patch-generating biological processes such as population dynamics, specific behaviour, and species interactions (Mackas 1984). Based on correlation analyses, Suthers and Frank (1990) argued that the persistent inshore–offshore gradient in zooplankton size composition and biomass off southwest Nova Scotia was determined by predation pressure rather than by water mass characteristics. In a series of experiments to assess the role of physical and biological processes on zooplankton dynamics, Kimmerer and McKinnon (1987, 1989) concluded that predation, as opposed to advective forces or water mass structure, was the main factor controlling the observed difference in the species composition of copepods inside and outside a marine embayment. These examples point out, as previously argued by Legendre and Demers (1984), that most studies of zooplankton distribution have not permitted unambiguous identification of the physical and biological factors generating and controlling patchiness. The controversy may indeed reflect the relative importance of both classes of processes according to the variable sampling scales used in relation to local hydrodynamics.

Spatial variability in the species composition and abundance of zooplankton may translate into spatial differences in secondary production (Omori and Hamner 1982; Frank 1988; Lobel and Robinson 1988; Miller and Daan 1989). Given the predominant role of zooplankton in the transfer of energy to higher trophic levels, as well as the close association between biomass and production of zooplankton (Davis 1987), it is important to clearly understand the factors determining the distribution and biomass of zooplankton in specific areas.

In the present study, I investigated the influence of physical dispersion forces, specifically freshwater input, on zooplankton biomass in the southern Gulf of St. Lawrence. To assess if biomass distribution is primarily controlled by advection of specific water masses, I tested the null hypothesis that spatial patterns of zooplankton biomass are not related to water mass characteristics over the study area.

Gulf of St. Lawrence

The Gulf of St. Lawrence is a highly stratified, semi-enclosed sea subjected to large freshwater runoff which drives the general circulation of surface water (Koutitonsky and Bugden 1991). The Gulf has been divided into four "biological zones" which take into account the large-scale spatial variability observed in community structure and size composition of the plankton (de Lafontaine et al. 1991). The reasons for this variability as well as the processes maintaining these spatial patterns, however, remain poorly understood. The highest zooplankton biomass in the area has been measured over the Magdalen Shallows in the southern Gulf, which was identified as the zone of maximum secondary production in the Gulf of St. Lawrence (Steven 1974). It has been hypothesized that this high biomass is produced locally by growing zooplankton populations which depend on the transport of materials issued from primary production occurring upstream (Steven 1974). The influence of freshwater runoff and advective processes on the spatial distribution of plankton remains unresolved and may depend on the type of relationship between runoff and entrainment of nutrients for primary producers (Bugden et al. 1982). Interannual fluctuations in the summer abundance of copepods in the southern Gulf have been shown to be positively related to sea surface temperature during springtime (de Lafontaine et al. 1991). Two sources of variability have been postulated to explain these fluctuations: recruitment variability from the spring generation (local enhancement) and interannual variability in advective processes at the sampling sites.

Despite the large number of plankton samples collected to date (review by de Lafontaine et al. 1991), spatial patterns and variability of zooplankton distribution within the southern Gulf have been only crudely described. The influence of advective processes and water mass movements on zooplankton dynamics remains speculative. This lack of adequate, detailed information has hindered any conclusive evaluation of the above hypothesized explanations for plankton distribution and dynamics in the area.

Materials and Methods

Zooplankton biomass data were obtained from plankton collections as part of the egg and larval survey program conducted in the Gulf of St. Lawrence by the Department of Fisheries and Oceans between 1965 and 1975 (Kohler et al. 1974a, 1974b, 1975, 1976). From this extensive data set, I have limited the present analysis to cruises conducted during five consecutive years (1967–71) for which seasonal coverage was sufficient to allow both intra- and interannual comparison. The sampling area included most of the Magdalen Shallows (<150 m depth) except for Northumberland Strait (Fig. 1). In some cruises, sampling extended over the deep waters of the Laurentian Channel (>150 m depth) and the coastal region of western Newfoundland. Therefore, the number of sampling stations and the cruise track differed between cruises (Table 1).

Zooplankton samples were collected using two standard 1-m-diameter ring nets, a 6-ft Isaacs-Kidd midwater trawl (IKMT) equipped with a 1-m-diameter cod end net (Aron 1959; Friedl 1971), and Miller high-speed samplers (Miller 1961). The two 1-m ring nets were towed simultaneously at surface and 15-m depths at a ship speed of 2.5 kn to sample plankton from the surface layer. The 6-ft IKMT was hauled at 5 kn in a stepped-oblique tow from near bottom (maximum sampling depth = 225 m) to the surface yielding water column averaged samples. High-speed Miller nets were stacked on the towing wire at predetermined depths (usually 9-m intervals) and towed at 2.5 kn to sample the vertical distribution of plankton. All nets were 471-μm-mesh Nitex and the tow duration was 30 min for all sampling. During some cruises, but not all, a TSK flowmeter provided estimates of the volume of water strained by the 1-m ring nets. No flowmeter was mounted on the IKMT or on the Miller samplers. Surface temperature and salinity were measured at every station. Zooplankton samples were preserved in 5–10% formalin solution after removing large gelatinous plankton. Settled volume (expressed in cubic centimetres) of the whole sample was measured to estimate the total biomass of zooplankton. Complete details of sampling protocols, gear deployment, cruise tracks, and station locations for particular cruises are contained in reports by Kohler et al. (1974a, 1974b, 1975, 1976). The number of stations, types of gear used, and general information on specific cruises are summarized in Table 1.

In order to standardize the information for statistical comparisons among cruises, all zooplankton biomass estimates were expressed in plankton volumes (cubic centimetres) per 30-min tow for each gear type. As these estimates were not corrected for gear differences in tow speed and mouth area, between-gear comparison for biomass (in absolute terms)

TABLE 1. Zooplankton sampling during plankton surveys conducted between 1967 and 1971. Time indicates daytime sampling only (D) or day and night sampling (D/N). Number of sampling stations (*n*), mean biomass (*X*) of zooplankton ($cm^3 \cdot 30\text{-min tow}^{-1}$), and CV (CV = 100·SD/mean) are listed for each sampling gear. Mean and standard error (SE) of surface temperature and salinity during each survey are also provided.

			Zooplankton samples											
			1-m net (0 m)			1-m net (15 m)			Isaacs–Kidd			Temperature	Salinity	
Cruise	Date	Time	*n*	*X*	CV	*n*	*X*	CV	*n*	*X*	CV	Mean SE	Mean SE	CV
P006	May 25 – June 7, 1967	D/N	83	292	172	82	632	158	65	208	126	4.14 (0.32)	29.90 (0.13)	4.01
H089	July 20–28, 1967	D	43	302	135	41	961	90	40	980	56	19.10 (0.22)	28.42 (0.12)	2.77
H091	Aug. 22–31, 1967	D							46	661	84	18.00 (0.20)	28.57 (0.05)	1.19
P014	Oct. 2–8, 1967	D/N	32	461	81	31	348	141				12.00 (0.19)		
P027	May 23 – June 04, 1968	D/N	90	180	116	83	212	138	25	271	171	6.45 (0.17)	30.47 (0.12)	3.74
P029	June 18–25, 1968	D/N	60	604	88	62	438	85	58	411	76	10.04 (0.20)	30.19 (0.14)	3.65
H094	July 27 – Aug. 5, 1968	D	51	352	192	46	1708	65	44	607	97	15.54 (0.19)	29.79 (0.16)	3.84
P033	Aug. 17–31, 1968	D/N							56	671	62	14.30 (0.25)	29.86 (0.11)	2.76
P045	May 12–25, 1969	D/N	86	215	150							3.90 (0.14)	30.64 (0.12)	3.63
P047	June 11–20, 1969	D/N	97	394	93				88	360	152	9.76 (0.21)	29.33 (0.18)	6.04
H097	July 17–29, 1969	D/N				86	976	92	91	324	105	14.85 (0.15)	28.95 (0.15)	4.94
P052	Aug. 19–30, 1969	D/N	27	443	120	25	1256	120	100	431	72	16.10 (0.13)	29.06 (0.11)	3.79
P071	May 20–30, 1970	D/N	98	308	106				61	274	135	6.18 (0.13)	30.11 (0.12)	3.95
P078	Aug. 19–29, 1970	D/N				71	1103	135	84	928	87	17.43 (0.08)	28.64 (0.11)	3.52
P085	May 10–20, 1971	D/N	92	227	105				90	783	90	4.56 (0.13)	29.66 (0.14)	4.53
P090	Aug. 24 – Sept. 3, 1971	D/N				55	1062	127	89	602	87	14.65 (0.19)	29.04 (0.09)	2.92

TABLE 2. Comparison between zooplankton biomass indices ($cm^3 \cdot 30$-min tow^{-1} and $cm^3 \cdot 1000\ m^{-3}$) using a conical 1-m ring net. Values in parentheses are CV's (CV = 100·SD/mean). All coefficients of correlation (*r* and tau) are significant at $P < 0.001$.

Cruise	Sampler depth (m)	Filtered volumes (m^3)	Biomass ($cm^3 \cdot 30$-min tow^{-1})	Biomass ($cm^3 \cdot 1000\ m^{-3}$)	Pearson *r*	Kendall tau
P006	15	1204.7 (44.5)	632 (158)	581.0 (142)	0.953	0.760
P006	0	1743.0 (24.1)	292 (172)	191.2 (184)	0.943	0.921
P027	15	1521.4 (29.2)	212 (138)	154.8 (116)	0.903	0.806
P027	0	1556.5 (25.3)	180 (116)	148.2 (208)	0.602	0.865
P029	15	1880.5 (16.1)	438 (85)	232.9 (82)	0.975	0.889
P029	0	1820.4 (13.3)	604 (88)	344.9 (96)	0.969	0.949
P045	0	1670.8 (32.6)	215 (150)	135.3 (157)	0.941	0.833
P047	0	1857.1 (27.1)	394 (93)	225.5 (94)	0.933	0.885
P071	0	1180.4 (34.4)	308 (106)	317.2 (106)	0.885	0.818
P085	0	968.0 (45.0)	227 (105)	276.2 (119)	0.769	0.652

is not recommended. This arbitrary index of biomass was chosen because flowmeter readings were available only for a small number of samples. This biomass index is strongly positively correlated with a biomass estimate expressed in cubic centimetres per 1000 m^3 in 12 cases (gears and cruises) for which estimates of filtered volumes were available (Table 2). The strong correlations were primarily due to the fact that among-station variability in filtered volumes (coefficient of variation (CV) = 13.3–45.0%) was much lower than volumetric biomass variability (CV = 77–172%) during any particular cruise (Table 2). Biomass estimates expressed in cubic centimetres per 30-min tow were therefore considered to be a valid representation of the spatial variability in zooplankton.

Spatial Analysis

Contour maps of temperature, salinity, and zooplankton biomass were produced by kriging (SURFER version 4, Golden Software Inc.). Analysis of spatial distribution patterns, hydrographic variables, and zooplankton data from the 1-m ring nets to detect spatial structures and correlations was performed using procedures recommended by Legendre and Troussellier (1988) and Legendre and Fortin (1989) and recently applied to other macrozooplankton (i.e., shrimp) (Ouellet et al. 1990; Simard and Savard 1990).

As a first step of the analysis, the normality of data was evaluated with a Kolmogorov–Smirnov test (Lilliefors 1967). Logarithmic ($\ln X + 1$) transformation was applied to normalize the zooplankton biomass data, while the Box–Cox method (Sokal and Rohlf 1981) was preferably used for temperature and salinity data. A spatial matrix of the geographic distances (kilometres) among the various stations was then computed from the coordinates of the sampling stations for each cruise. Geographic distances between pairs of stations were grouped in 25-km distance classes. The first distance class (25 km) includes distances between 0 and 25 km. The minimum spatial scale that the sampling grid can resolve is about 20 km. Spatial autocorrelation of univariate data (temperature, salinity, and biomass) was measured by calculating Moran's *I* coefficients for each variable at different distance classes. Moran's *I* values usually vary between 1 and −1, but larger values have also been reported (Legendre and Fortin 1989). The null hypothesis of Moran's *I* test is that there is no significant spatial autocorrelation at a given distance class. Spatial autocorrelograms were constructed by plotting Moran's *I* values as a function of distance class to detect significant spatial structures which allowed rejection of the null hypothesis that variables were randomly distributed in space (Legendre and Troussellier 1988; Legendre and Fortin 1989). The significance of each spatial correlogram was evaluated by the Bonferroni method (Legendre and Fortin 1989). The correlograms are all-directional because they were computed over all directions of the study area. This assumes that the phenomenon is isotropic, which means that the autocorrelation function is similar for each direction considered. The analysis of anisotropic cases requiring two-directional correlograms and variograms was beyond the scope of this paper.

Distance matrices of hydrographic and biological data were created by calculating the euclidian distance among observations of a variable for all possible pairs of stations (Legendre and Legendre 1983). The Mantel test was applied to data matrices to evaluate the null hypothesis that distances among data of a matrix **X** are not linearly correlated with distances among data of a matrix **Y**. In cases where matrix **Y** contains only geographic distances among pairs of stations, the Mantel test is equivalent to an autocorrelation test for a spatial gradient of the matrix **X** variable. Partial correlations (partial Mantel test, see Legendre and Troussellier 1988) were also calculated to control for spatial effects and to assess the probability of spurious correlation between zooplankton biomass and hydrographic variables resulting from common spatial position. As in a simple Mantel test, the null hypothesis of a partial Mantel test is that distances in a matrix **X** are not linearly correlated with distances in a matrix **Y**, after filtering the effect of the geographic distance matrix **W**.

More details of statistical computations and interpretation of Moran's *I* autocorrelation and Mantel tests are given in Legendre and Fortin (1989). All calculations were made using the R statistical package (Legendre and Vaudor 1991).

Results

Hydrographic Conditions

The distribution of sea surface temperature and salinity in the southern Gulf throughout the spring and summer months (Fig. 2–5) indicated a general freshening and a grad-

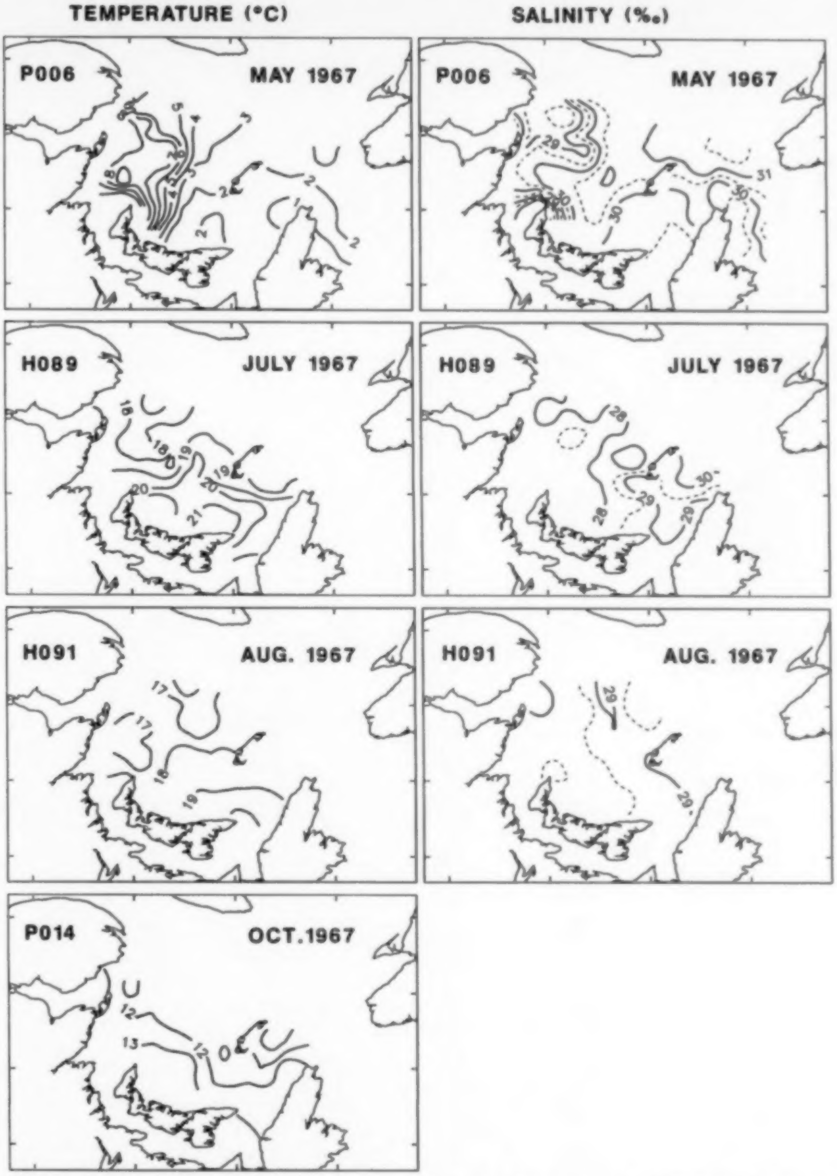

FIG. 2. Isopleths of surface temperature and salinity during four cruises in 1967. No salinity measurements were taken during cruise P014 in October 1967.

ual warming of the surface water as a result of the seasonal freshwater input and solar heating. The intrusion of low-salinity water near the Gaspé Peninsula was already evident in late May and early June due to the spring runoff dominated by the St. Lawrence River discharge (Petrie 1990; Koutitonsky and Bugden 1991). As the summer progressed, the low-salinity water, as indicated by the extension and the displacement of the 29-ppt isohaline, moved from the western end to the eastern side of the Magdalen Shallows (Fig. 2–5). This gradual dispersion induced a wide and relatively strong gradient in surface salinity over the entire area. The orientation of this gradient, as depicted by the salinity and temperature isolines, shifted from a west–east gradient in the spring to a north–south gradient (parallel to the Laurentian Channel) during the summer. The orientation of these gradients would remain the same down to a depth of 30 m (Petrie 1990).

Surface water over the deep offshore Laurentian Channel (>150 m) was significantly (ANOVA with *G*-test of independence) colder and more saline than that over the Magdalen Shallows (Table 3). When restricting the analysis to shallow (<150 m) stations only, surface salinity at stations west of the Magdalen Islands (west of 62° longitude and north of 47° latitude) was significantly lower than at eastern sta-

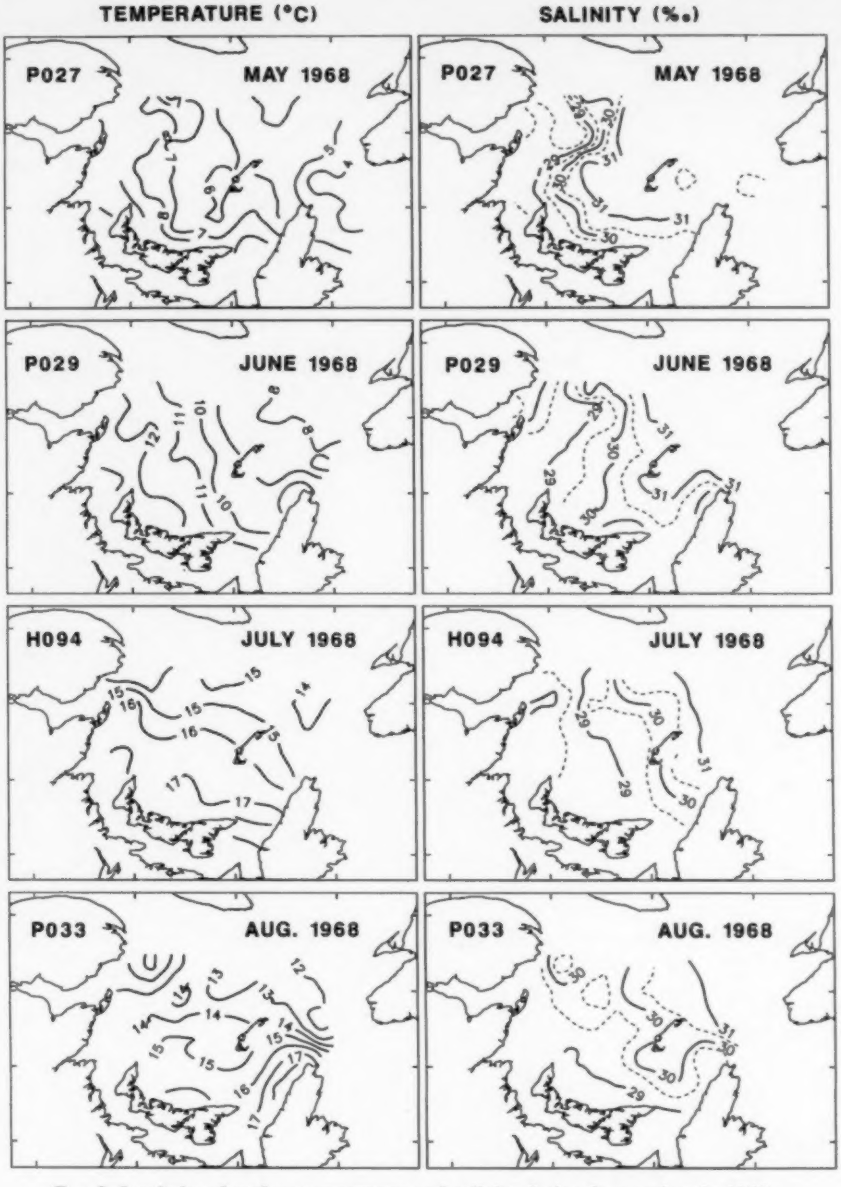

FIG. 3. Isopleths of surface temperature and salinity during four cruises in 1968.

tions. Surface temperature was significantly warmer in the western sector during the spring, but the gradient was reversed (warmer on the eastern side) in late summer and early fall (Table 3). An analysis of the correlation coefficients between hydrographic variables and the distance from Cabot Strait clearly indicated a seasonal shift in the relationships for temperature but not for salinity (Fig. 6). The reversal in the sign of coefficients for temperature was associated with the seasonal reversal of the surface gradient over the Magdalen Shallows. The lack of seasonal variation in the negative relationship between surface salinity and distance from Cabot Strait suggests that the salinity gradient resulting from the freshwater input on the western side of the southern Gulf was maintained throughout the summer.

Mean temperature and salinity also varied among years (Table 3). As pointed out by Bugden et al. (1982), the position and the offshore extension of the 29-ppt isohaline reveal year-to-year variability in the freshwater intrusion over the Magdalen Shallows. In 1968 (Fig. 3), the 29-ppt isohaline remained relatively inshore throughout the summer and did not reach the Magdalen Islands area, while in August 1971 the isohaline extended beyond the northern tip of the Magdalen Islands (Fig. 5). Although only five different years were considered here, the ranking of mean salinity recorded in May and August followed closely that of runoff

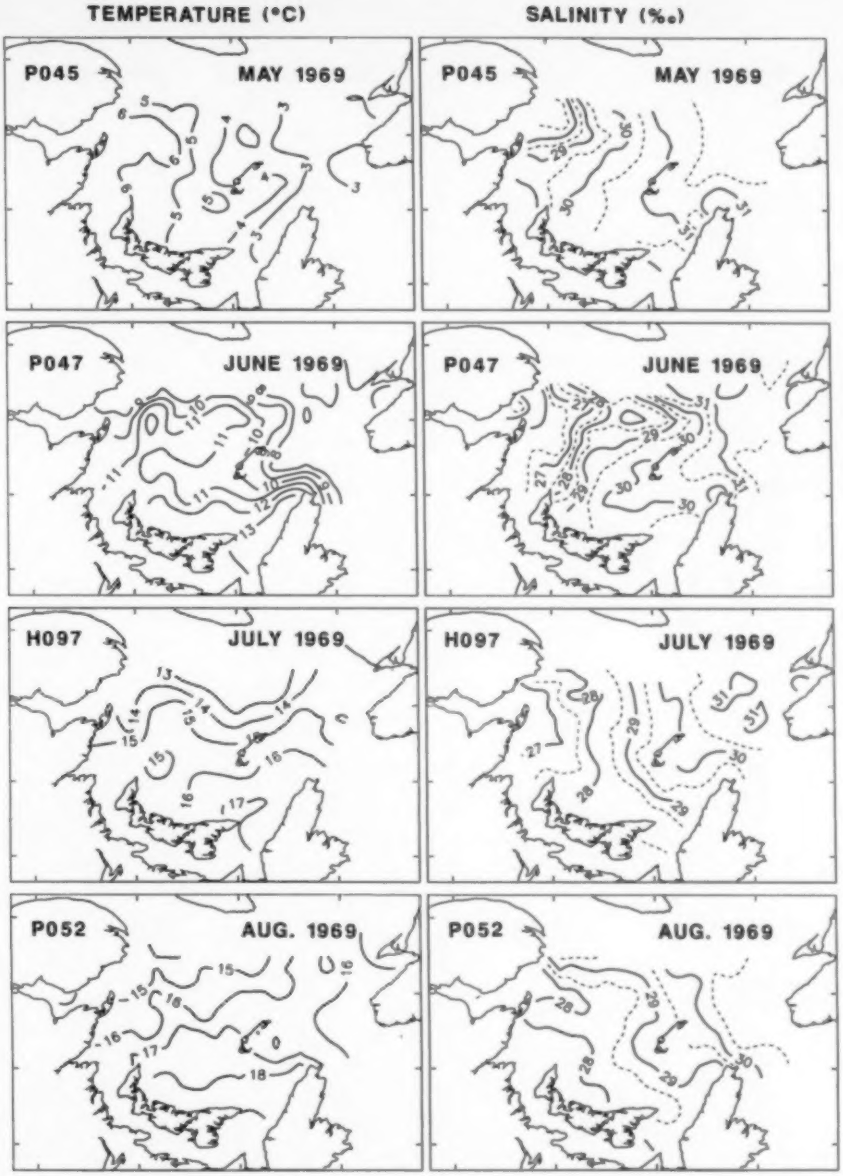

FIG. 4. Isopleths of surface temperature and salinity during four cruises in 1969.

values (Table 3) indicating that the interannual variability in mean salinity of surface water is related to the annual discharge from the St. Lawrence River and that spring runoff is largely responsible for the movement and the spatial extension of the low-salinity water over the Magdalen Shallows. Although sea surface temperature and salinity were significantly and negatively correlated within any particular cruise (Spearman r_s, $P < 0.001$ for each cruise), no definite relationship was found between mean temperature and mean salinity among years. Years with high salinity (i.e., low runoff, 1968) did not necessarily have colder waters and vice versa (Table 3). This suggests that the mean temperature in the southern Gulf during the summer is not directly or solely controlled by the freshwater runoff.

Zooplankton

Vertical distribution

Zooplankton biomass from the 1-m net collections was generally higher at 15 m than at the surface (Table 4). This difference was more pronounced during the summer (July–August) than at other times of the year. Plankton biomass at the two sampling depths, however, were significantly and positively correlated in all but one cruise (Table 4, H094), where biomass at 15 m greatly exceeded that at sur-

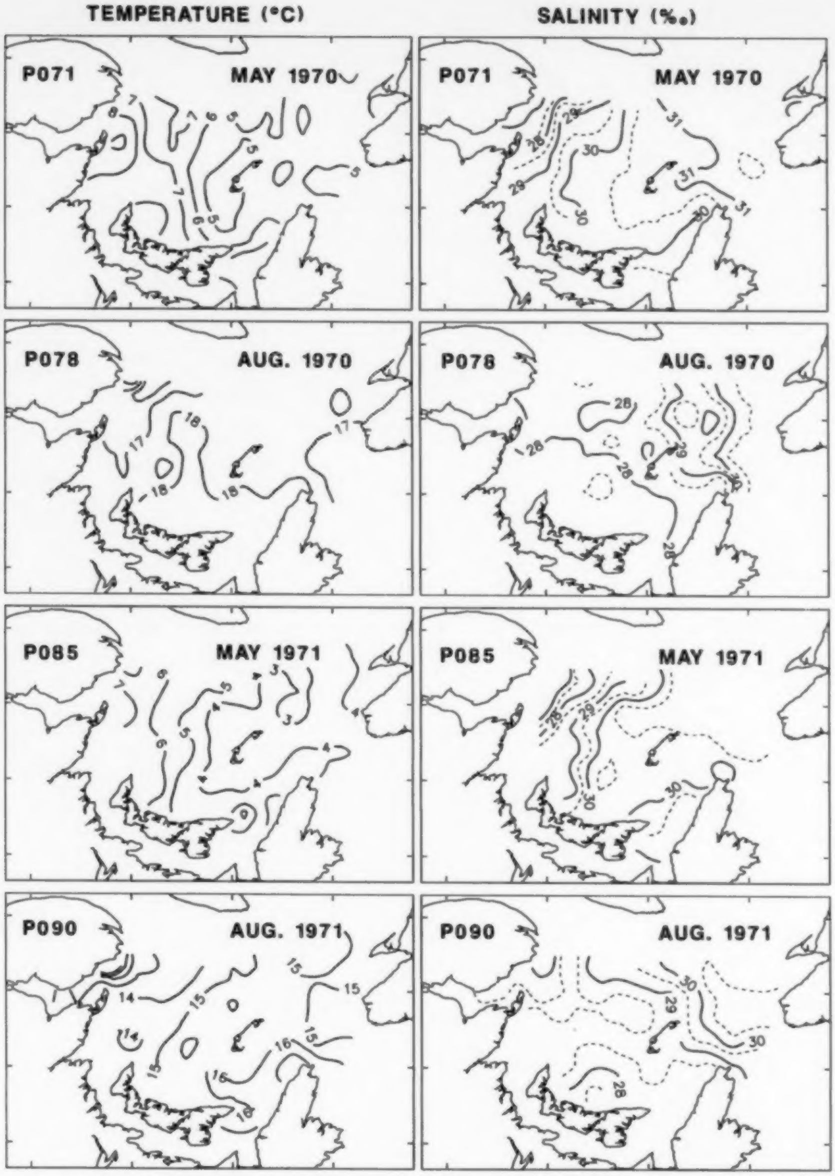

FIG. 5. Isopleths of surface temperature and salinity during the May and August cruises in 1970 and 1971.

face. The vertical distribution patterns derived from the Miller net samples also indicated a slightly larger biomass of zooplankton at depth than at the surface (Fig. 7). Ratios of middepth (9 and 18 m) to surface (0 m) biomass varied between 0.9 and 1.5 and were close to those calculated for the two sampling depths by the 1-m net at similar time periods (Table 4). Seasonal variation was evident both in the depth of the centre of mass of the vertical distribution (Z_{cm}, calculated as in de Lafontaine and Gascon 1990) and in the proportion of biomass at the surface relative to other depths (Fig. 7). The magnitude of these variations was, however, considered small and the vertical distribution was, on average, relatively homogeneous during the various cruises. Biomasses measured at 0 and 15 m are therefore representative of the zooplankton biomass of the well-mixed surface layer (above the pycnocline, 0–20 m) in the southern Gulf of St. Lawrence. For the horizontal distribution analyses (see below), zooplankton biomass for 1-m nets samples at the two sampling depths was therefore averaged, except for cruise H094, when samples from 15 m were judged to be more representative and were used without 0-m samples.

Horizontal distribution

Isopleths of biomass did not reveal a temporally persistent pattern in the spatial distribution of zooplankton in the southern Gulf of St. Lawrence (Fig. 8 and 9). Several cen-

TABLE 3. Mean surface temperature and salinity for three zones in the southern Gulf: (1) west: the shallow western zone (stations <150 m and west of 62°W and north of 47°N), (2) east: the shallow eastern zone (stations <150 m and east of 62°W and south of 47°N), and (3) offshore: the deep offshore zone (>150 m). Underlined values are significantly different from the other zones during a given cruise (ANOVA and multiple comparison test, $P < 0.05$). St. Lawrence River discharge (RIVSUM) data are from Budgen et al. (1982).

		Temperature			Salinity		
Cruise	Date	West	East	Offshore	West	East	Offshore
P006	May 1967	6.21	2.05	2.78	29.49	30.31	30.21
P027	May 1968	7.55	6.47	4.90	29.62	30.73	31.28
P045	May 1969	5.44	3.46	2.77	29.50	30.90	31.55
P071	May 1970	7.02	5.87	5.25	29.10	30.52	31.17
P085	May 1971	5.70	4.13	3.60	28.50	30.11	30.64
P029	June 1968	11.22	9.76	8.36	29.20	30.63	31.24
P047	June 1969	10.24	10.53	8.11	27.63	29.97	31.02
H089	July 1967	18.70	19.57		28.06	28.80	
H094	July 1968	15.52	16.06	14.49	28.85	30.11	31.27
H097	July 1969	14.55	15.66	14.07	27.74	29.48	30.58
H091	Aug. 1967	17.22	18.93		28.44	28.72	
P033	Aug. 1968	13.70	15.60	13.10	29.62	29.59	30.93
P052	Aug. 1969	15.48	17.30	15.90	28.22	29.21	30.50
P078	Aug. 1970	17.15	17.95	17.24	28.03	28.51	29.71
P090	Aug. 1971	13.56	15.85	15.13	28.58	28.89	30.11
P014	Oct. 1967	11.99	12.03	12.00			

RIVSUM (10^3 $ft^3 \cdot s^{-1}$)

Year	May	June	July	Aug.	Total Apr.–Aug.
1967	422	389	343	323	1477
1968	370	339	348	350	1407
1969	467	456	404	396	1723
1970	459	430	416	388	1693
1971	485	379	338	331	1533

tres of abundance were often clearly evident, and patches of high biomass were at times contiguous with areas of low biomass. In 8 out of 11 surveys, the spatial distributions of biomass in the surface layer (1-m net) were positively and significantly correlated (Spearman r_s, $P < 0.05$) with those derived from the IKMT samples which integrated plankton from bottom to surface.

In May, biomass was relatively low over the entire area. Concentrations were slightly (but not significantly) higher over the Laurentian Channel (Table 5, cruises P045, P071, and P085) and at a few central locations over the Magdalen Shallows. Except for cruise P045 where the orientation of biomass isolines ran parallel to the Laurentian Channel (Fig. 9), there was generally no clear delineation or transition in biomass between the Magdalen Shallows and the Laurentian Channel during the spring. Low biomass was often encountered in the coastal region (Fig. 8 and 9), especially near the Gaspé Peninsula and Miscou Island, both under the influence of the freshwater input (Fig. 2–5). However, a different pattern characterized by high biomass within the low-salinity plume near Gaspé was observed during cruise P006 (Fig. 8), which was conducted slightly later (late May and early June 1967) than spring cruises in subsequent years. The overall pattern of zooplankton distribution in the spring therefore appeared to be highly variable between years and was generally associated with a high degree of spatial heterogeneity.

With the advent of the summer, biomass increased rapidly and peaked in late July and August. Higher biomass occurred consistently in the western sector of the Magdalen Shallows (Table 5) where the main centres of abundance were located. Minimum biomass was commonly observed at deep stations offshore (Table 5), and sharp gradients in biomass were noticed along the margin between the Magdalen Shallows and the Laurentian Channel. By midautumn (cruise P014, October 1967), biomass had declined to spring levels and maximum concentrations still occurred on the western part of the Magdalen Shallows (Fig. 8). Consequently, the increase in zooplankton biomass from mid-May until the end of August was more prominent over the Magdalen Shallows than over the deep (>150 m) offshore area. A patchiness index ($1 + ((\sigma^2 - m)/m)$, where m and σ are, respectively, the mean and variance of biomass for each cruise; Pielou 1974; Hewitt 1981) indicated that spatial heterogeneity within the surface layer was relatively high in the spring, reached a minimum in midsummer, and increased again in August (Table 5). Patchiness of zooplankton integrated over the water column (IKMT samples) was also higher in the spring than in the summer. Due to the lack of measurements or to the interannual variability in the filtered volumes

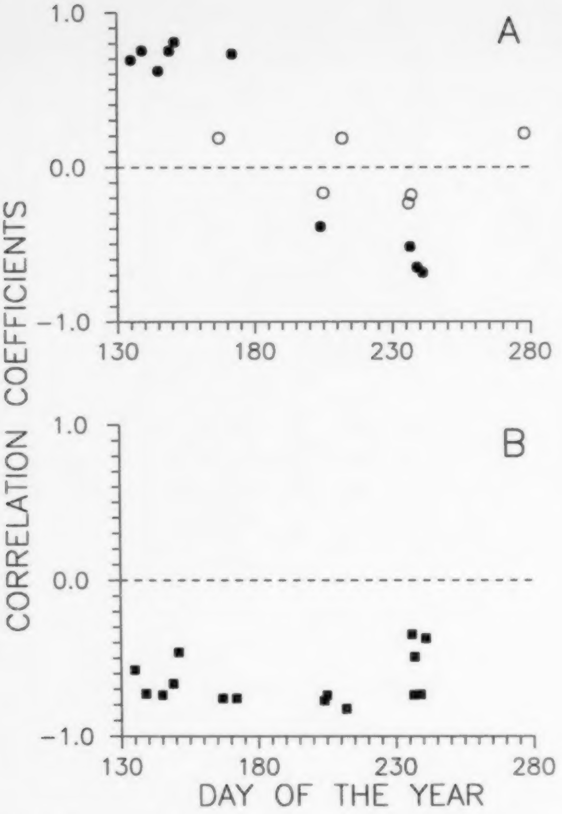

FIG. 6. Seasonal variation in correlation coefficients between the geographic distance from Cabot Strait and (A) surface water temperature and (B) salinity. Solid symbols indicate significant correlations at $P < 0.05$.

(Table 2), comparison of zooplankton biomass between years should be treated with caution. On the other hand, because filtered volumes varied much less than zooplankton biomass, and because it has no dimension, the patchiness index provides a reliable index of the inter- and intraannual variation in spatial heterogeneity of zooplankton in the southern Gulf of St. Lawrence.

Spatial Correlations

Spatial correlograms for zooplankton biomass over the Magdalen Shallows clearly show that zooplankton distribution patterns varied between surveys (Fig. 10 and 11). The correlograms were significant in all but four surveys (P033, August 1968; P045, May 1969; H097, July 1969; P085, May 1970). Significant correlograms are interpreted as evidence for nonrandom spatial patterns in zooplankton biomass during those surveys. The spatial structure of zooplankton biomass in the southern Gulf was typical either of a large-scale gradient (indicated by the significant positive correlations at small distance classes and negative correlations at large distance) or of small patches (significant positive correlations at small distances and nonsignificant correlations at larger distances). In most correlograms, the most positive and significant coefficient is at the first distance class (=25 km) which means that neighbouring stations (within a distance of 25 km) had the most similar zooplankton biomass. Dispersion gradients were more commonly observed and were evident during 1967 (P006, H089, and P014) and 1970 (P071 and P078) surveys and in July 1968 (H094) and August 1969 (P052). The transition between positive and negative coefficients is usually between 100 and 150 km, indicating a relatively large-scale dispersion gradient. For surveys characterized by small patches (P027, May 1968; P047, June 1969; H091 and P090, August 1967 and 1971), the first zero crossing of the autocorrelation is between 25 and 50 km and corresponds to the radius of

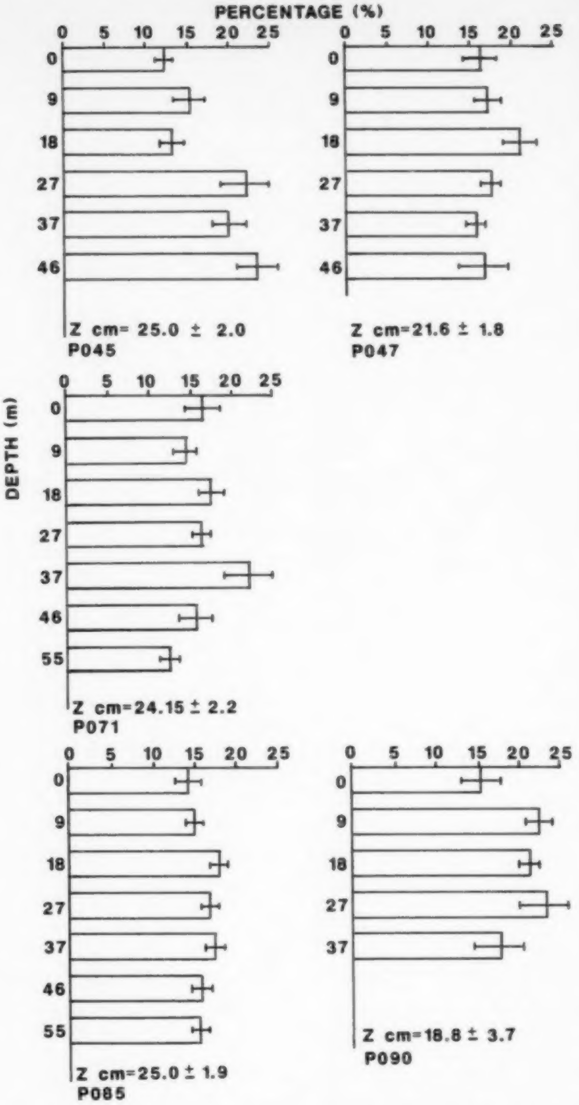

FIG. 7. Vertical distribution of zooplankton biomass during the various cruises in the southern Gulf of St. Lawrence. Mean and standard errors of proportion at depth were calculated from all stations sampled. Average depths of centre of mass (Z_{cm}) are also indicated.

TABLE 4. Correlation between zooplankton biomass (CV = 100·SD/mean, in parentheses) from 0 and 15 m sampling depths for different cruises ($*P < 0.05$; $**0.05 < P < 0.01$; $***0.01 < P < 0.001$). Mean ratios of biomass measured at 15 m relative to surface (0 m) with percentage of ratios exceeding 1.0 and percentage of ratios between 0.5 and 2.0.

			Biomass (CV%)			Ratios (15 m/0 m)		
Cruise	Date	n	0 m	15 m	Pearson r	Mean	Values >1	Values 0.5–2
P006	May 1967	82	295 (171)	632 (159)	0.580***	2.14	40.7	72.0
P027	May 1968	82	156 (101)	211 (139)	0.396***	1.35	64.6	58.5
P029	June 1968	58	624 (85)	440 (85)	0.308*	0.70	39.6	50.0
H089	July 1967	41	297 (137)	961 (90)	0.853***	3.23	97.5	12.2
H094	July 1968	44	348 (207)	1718 (66)	0.137 ns	4.93	85.7	12.8
P052	Aug. 1969	24	482 (114)	1296 (118)	0.605*	2.69	87.5	33.3
P014	Oct. 1967	31	474 (78)	348 (141)	0.812***	0.73	22.5	51.6

these biomass patches (Legendre and Fortin 1989). Secondary positive bumps in the correlograms are present, although not always significant, at a distance between 100 and 175 km or over 250 km. The tendency for positive autocorrelations at a very large distance (>250 km) is common for data from August surveys (Fig. 10 and 11). These secondary peaks in the correlograms correspond to the distances between the centres of patches in the distribution of zooplankton biomass (Legendre and Fortin 1989).

The slope and shape of the correlograms for hydrographic properties (temperature and salinity) are indicative of large-scale spatial gradients during most cruises (Fig. 10 and 11). Nonsignificant correlograms occur in only 2 out of 31 cases (temperature in H089 and P014). As expected for purely dispersive processes, maximum positive and significant coefficients are always observed at the smallest distance class (25 km) confirming that neighbouring stations have the highest degree of similitude in water properties. The transition between positive and negative coefficients is consistently between 100 and 175 km with a slight decline from May (150–175 km) to August (100–125 km). Large-scale spatial heterogeneity in water properties in the southern Gulf is therefore primarily associated with gradients probably induced by the freshwater input.

The similarity in correlograms of zooplankton and hydrographic variables as observed in some cases cannot be interpreted as evidence for a direct relationship or causal link. In theory, two variables characterized by independent patchy distribution could plausibly produce similar correlograms, but two variables with very different distribution patterns have very little probability of being associated. The Mantel test reveals significant correlation between zooplankton biomass and geographic location (variable SPACE) in 7 out of 16 surveys (Table 6). These significant relationships correspond to significant Moran's correlograms typifying large-scale gradients and confirm that zooplankton distribution was spatially structured during those cruises. Significant correlations between zooplankton and hydrographic variables (either salinity or temperature) are rare (Table 6). Moreover, because hydrographic variables are strongly correlated with geographic distance (Table 6), the partial correlations (partial Mantel test) between hydrographic variables and zooplankton diminish and become nonsignificant in some cases. Globally, significant relationships between zooplankton and salinity were observed in only two surveys, both in the spring (P027, May 1968; P071, May 1970). During two summer cruises (H089, July 1967; P047, June 1969), the distribution of zooplankton biomass was significantly related to temperature. In all other cases, results suggest that the distribution of zooplankton biomass over the entire southern Gulf was independent of the distribution of surface temperature and salinity.

Discussion

Omori and Hamner (1982) stated that animal aggregations are rarely accidental and exhibit a general series of temporal and spatial attributes. According to this premise, and given the extensive literature on marine plankton heterogeneity (see the introduction), the result that zooplankton biomass within the surface layer (0–15 m) of the southern Gulf of St. Lawrence was highly aggregated and characterized by nonrandom spatial structures should be regarded as typical. Zooplankton biomass was structured according to two main spatial patterns: (1) large-scale (≈150 km) gradients and (2) mesoscale (≤25 km) patches. A second, and probably more important, finding is that these patterns, as defined by spatial autocorrellograms (Fig. 10 and 11), were apparently not persistent or recurrent over time, but seemed to vary unpredictably both seasonally and between years.

In contrast, spatial patterns in hydrographic properties were smoother and more recurrent than patterns of zooplankton biomass and may be more predictable, via spatial modelling (e.g., Johnson 1989). The recurrence and stability in patterns characterized by a large-scale gradient are attributed to the influence of the freshwater input contributing to most of the kinetic energy of the system (Koutitonsky and Bugden 1991). Hydrographic results presented here are consistent with the proposed general circulation pattern of the Gulf where the intrusion of low-salinity water from the Gaspé current is primarily restricted to the Magdalen Shallows and is slowly advected eastward by the residual southeasterly flow during the summer months (El-Sabh 1976; Petrie 1990; Koutitonsky and Bugden 1991). The occurrence of lower salinity over the Shallows resulting from the Coriolis effect and geostrophic forces (Koutitonsky and Bugden 1991) contributes to maintain inshore–offshore or depth-related differences in hydrographic properties (Table 3). Advection of offshore surface waters onto the shallow area is not evident in the present analysis and is presumably minimal during the summer months. By the end of the summer and in early fall, the low-salinity surface

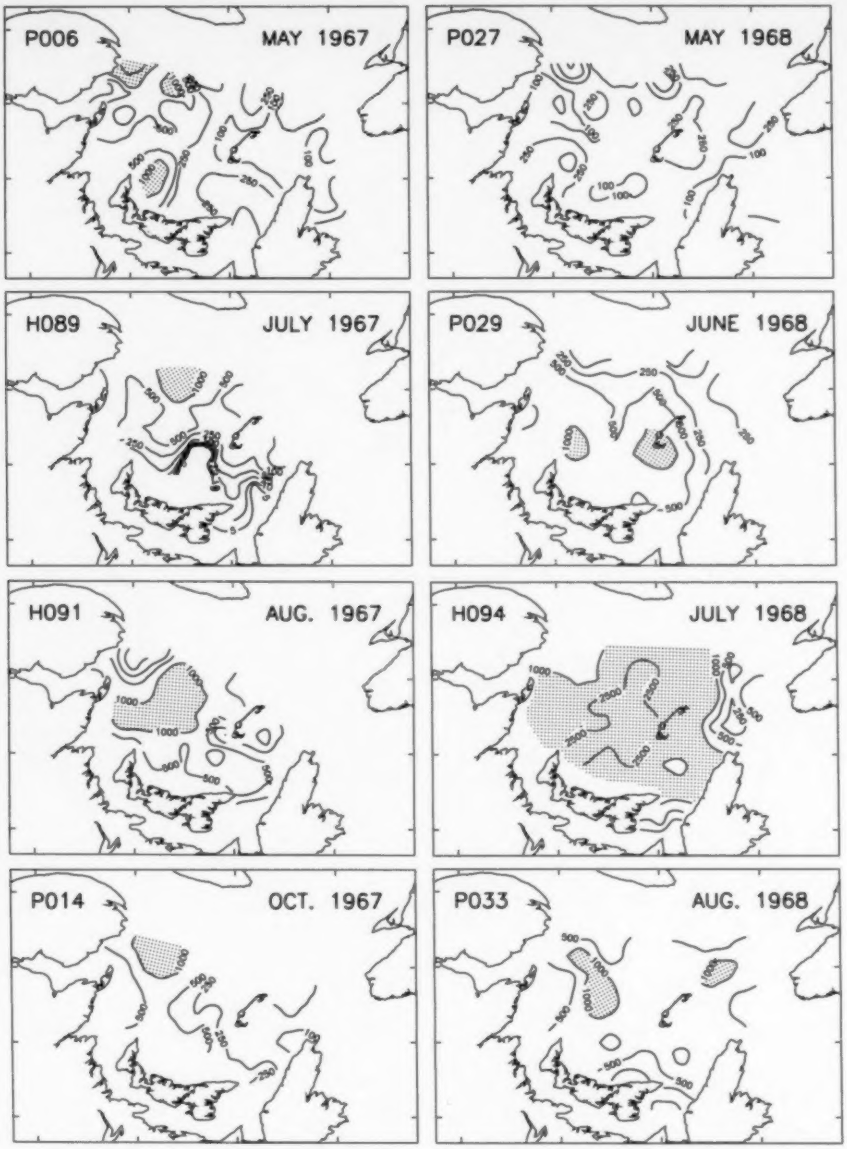

FIG. 8. Isopleths of zooplankton biomass ($cm^3 \cdot 30\text{-min tow}^{-1}$) during the 1967 and 1968 surveys. Isopleths are from 1-m net samples except for cruises H091 and P033 which are based on IKMT samples.

water has reached the Cape Breton coast and will eventually be advected outside the Gulf through Cabot Strait. El-Sabh (1977) showed that the outflow of Gulf surface waters through Cabot Strait is primarily concentrated on the south side and is maximal in late summer (August–September) at the time of lowest salinity, as supported by the above results.

By definition, plankton horizontal transport is generally considered to be mostly passive, and the meso- and large-scale (10–1000 km) distribution patterns are expected to follow patterns of some conservative physical property of water. The null hypothesis that zooplankton biomass within the surface layer (0–15 m) was not related to water mass characteristics could not be rejected in a majority of cases (Table 6). This indicates that, over the entire area and at the sampling scale used here, the spatial structures of zooplankton biomass are not directly linked or controlled by the spatial hydrographic structures in the southern Gulf. Similar results showing no significant relationship between spatial patterns of larval shrimp and hydrographic variables in the northern Gulf of St. Lawrence have also been reported by Ouellet et al. (1990).

In 15 surveys analyzed, significant relationships between salinity and plankton biomass were noted for the two mid-spring (end of May) cruises (Table 6) when freshwater intru-

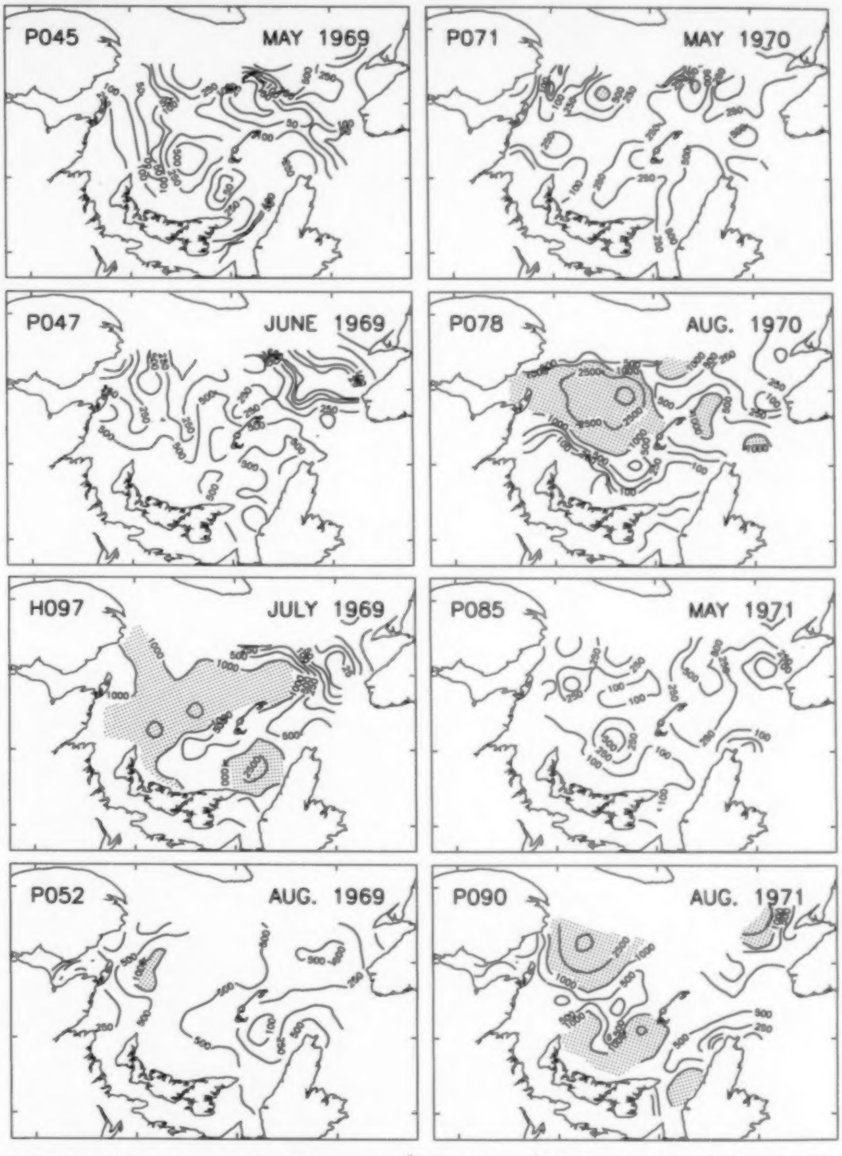

FIG. 9. Isopleths of zooplankton biomass (cm^3·30-min tow^{-1}) during the 1969, 1970, and 1971 surveys. Isopleths are from 1-m net samples except for cruise P052 which is based on IKMT samples.

sion was still spatially restricted (Fig. 2–5) and when zooplankton biomass was low, but relatively patchy (Fig. 8 and 9). The positive relationship would suggest that low zooplankton biomass was associated with low-salinity surface water; the freshwater plume does not support higher zooplankton biomass to be advected over the Magdalen Shallows at the end of May. The lack of strong relationships between plankton patterns and salinity during the summer months indicates that the distribution of zooplankton biomass was not related to advective processes induced by freshwater runoff and responsible for the salinity and water mass distribution in the area.

Biomass was significantly correlated with surface temperature in the three surveys conducted at the end of June and in July (Table 6; H089, H094, and P047). The exact nature of this relationship is difficult to explain, but could be associated with the inshore–offshore gradients of temperature and biomass during the summer months. Although warmer temperatures may enhance production and biomass locally (McLaren 1978; McLaren and Corkett 1981; Vidal and Whitledge 1982; Davis 1987), the fact that temperature isolines are oriented with the general topography of the Magdalean Shallows makes it difficult to separate the effect of temperature and topography on the biomass distribution.

TABLE 5. Mean zooplankton biomass for stations grouped into three zones within the southern Gulf (see Table 3). Underlined values are significantly different (ANOVA and multiple comparison test, $P < 0.05$) from mean values of other zones during a given cruise. Spatial patterns for each cruise as interpreted from statistical analysis are either large-scale gradients (G) or small-scale patches (P). Calculated patchiness index is given for each gear.

		1-m net samples				Isaacs–Kidd samples			
Cruise	Pattern	West	East	Offhore	Patchiness	West	East	Offhore	Patchiness
P006	G	$\underline{696.5}$	261.6	155.7	3.24	$\underline{299.2}$	151.0	116.1	2.64
P027	P	238.1	179.1	194.7	2.26				
P045	n.s.	226.9	136.7	302.3	3.32				
P071	G	259.2	324.6	$\underline{366.8}$	2.13	163.9	206.9	$\underline{466.6}$	2.87
P085	n.s.	214.6	197.2	277.6	2.10	891.1	$\underline{502.6}$	948.1	1.82
P029	G	587.5	599.5	$\underline{176.1}$	1.54	353.5	416.3	512.9	1.59
P047	P	380.8	522.4	$\underline{257.3}$	1.86	448.4	303.0	317.4	3.32
H089	G	871.3	$\underline{377.4}$		1.99	1023.0	937.8		1.32
H094	G	$\underline{1206.8}$	$\underline{908.3}$	$\underline{546.2}$	1.54	618.9	721.3	328.6	1.96
H097	n.s.	1322.1	957.0	$\underline{372.4}$	1.86	264.7	300.5	$\underline{460.2}$	2.11
H091	P					$\underline{798.0}$	498.3		1.71
P033	n.s.					734.7	589.5	690.9	1.38
P052	G					475.0	378.1	401.2	1.52
P078	G	$\underline{1882.7}$	485.9	647.5	2.87	$\underline{1083.7}$	739.4	740.0	1.76
P090	P	1409.1	658.3	1039.1	2.65	634.4	604.2	491.6	1.76
P014	G	$\underline{576.9}$	236.0						

Off southwestern Nova Scotia, inshore–offshore gradients in zooplankton biomass were noted in the absence of any cross-shore gradient in temperature and appeared to be primarily related to depth variability in predation pressure (Suthers and Frank 1990). The strong correlation between zooplankton biomass and geographic distances (variable SPACE in Table 6) and the lower coefficients in partial Mantel correlations between temperature and biomass suggest that the relationship between temperature and zooplankton biomass is not causal. My results are supported by additional correlation analysis between temperature and total zooplankton biomass showing no significant correlation in 16 out of 18 midsummer cruises in the southern Gulf between 1982 and 1991 (M. Castonguay, Y. de Lafontaine, and J. Runge, unpublished data). Therefore, the horizontal structure of zooplankton biomass in the southern Gulf may be independent of the hydrodynamic processes responsible for the water mass distribution in the area, and other factors may be responsible for the existence of the observed spatial patterns. This conclusion implies that the distribution of zooplankton biomass cannot be inferred from the analysis of surface hydrographic variables in the Gulf.

The weak association between hydrography and zooplankton spatial patterns may seem contradictory to the current paradigm linking the meso- and large-scale distribution of plankton to hydrographic regime and water mass movements. Evidence in support of this paradigm comes, to a large extent, from studies of short-term temporal variation or time-series analysis at a few locations (e.g., Cox and Wiebe 1979; Peterson et al. 1979; Chelton et al. 1982; Rothlisberg and Jackson 1982; Smith and Vidal 1984; Weikert 1984; Lindahl and Perissinotto 1987; Schneider 1987; Taggart and Frank 1987; Lindahl and Hernroth 1988; Krause and Kattner 1989; Springer et al. 1989; Coyle et al. 1990). Although it cannot be dismissed that the temporal variability observed in those studies was related to water movements and advection of different water masses, results of the present analysis are based on spatial sampling and are therefore not directly comparable. With the exception of the study by Ouellet et al. (1990) who also found no relationship between hydrography and spatial patterns for larval shrimp, the statistical analysis adopted here has still not been widely used in other studies for testing similar relationships.

The grouping of stations into three sectors (Tables 3 and 5) reveals significant differences in biomass which parallel the observed differences in mean salinity, but not in mean temperature. The occurrence of highest biomass in the western sector (Table 5) and the measurement of higher biomass over the Magdalen Shallows relative to the Laurentian Channel area (except for during the spring period) are both consistent with the existence of large-scale gradients in zooplankton abundance within the southern Gulf as suggested by Steven (1974). These differences between sectors are interpreted as evidence for relatively large-scale (>100 km) spatial structures which may be determined directly or indirectly by the salinity gradient.

Despite the fact that the slope and shape of correlograms differ, at times greatly, between hydrographic variables and zooplankton, it is noteworthy that, in most cases, the transition between positive and negative coefficients (Fig. 10 and 11) is between 100 and 150 km for both variables. On the other hand, autocorrelation analyses (Fig. 10 and 11) show maximum correlations in biomass at the smallest distance class (25 km) followed by rapid decline and nonsignificant correlations at larger distances, which indicate that small patches with length scales of 25–50 km are the dominant feature of the spatial distribution of zooplankton biomass in the southern Gulf. Mesoscale patches of 25–50 km radius have also been observed for both pelagic adult and larval shrimp in the northern Gulf (Ouellet et al. 1990; Simard and Savard 1990). Moreover, values for the Gulf are close to

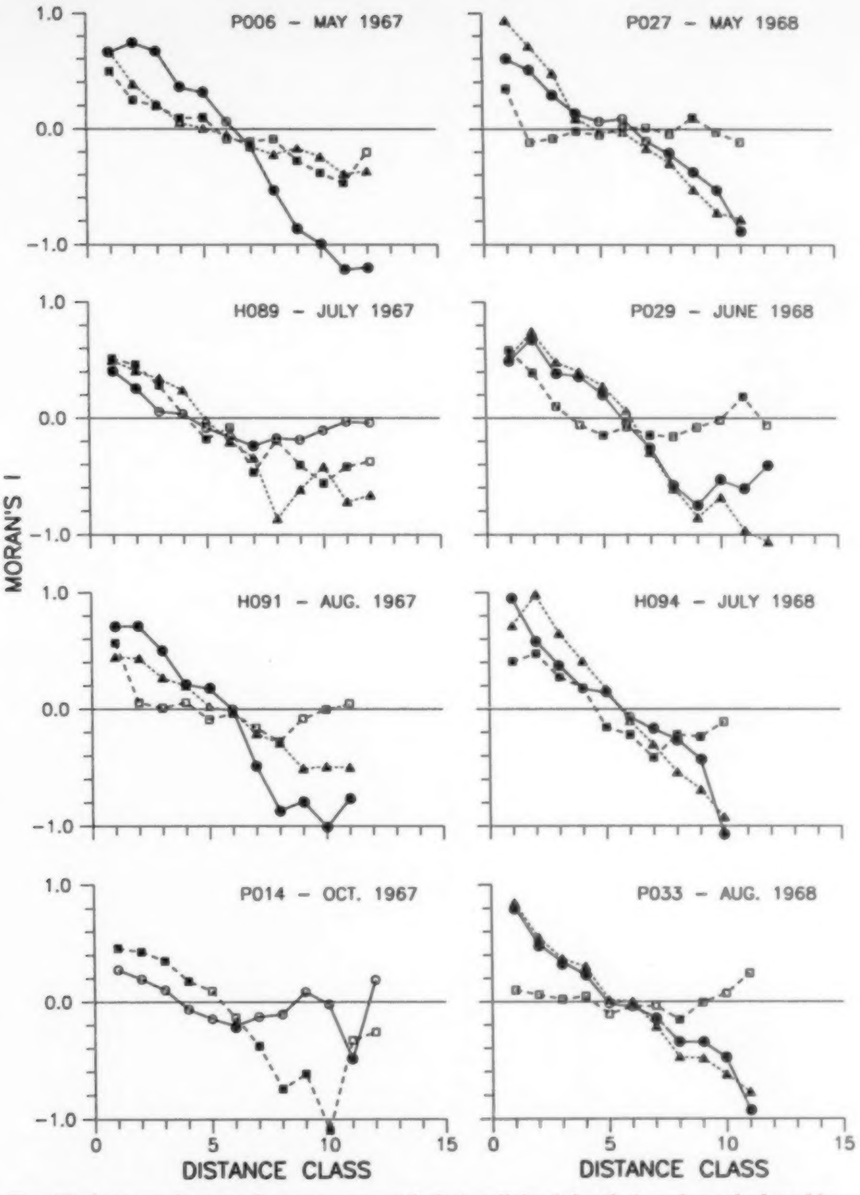

FIG. 10. Autocorrelograms for temperature (circles), salinity (triangles), and zooplankton biomass (squares) during the 1967–68 surveys. Each distance class is equivalent to 25 km spatial distance. Significant coefficients are indicated by solid symbols.

the 25-km scale estimated by Mackas (1984) for zooplankton biomass patches on the Pacific coastal shelf. The similarity of these estimates suggests that biomass patches of 25–50 km may be typical of coastal regions as opposed to smaller patch sizes (1–10 km) in stable oceanic regions (Star and Mullin 1981). The lack of direct or significant association between hydrographic variables and plankton distribution over the entire southern Gulf would therefore be due to the strong component of mesoscale patchiness (≈25km) in zooplankton which overwhelms the relationships at a large scale (Mackas et al. 1985). Verification of this hypothesis requires computation and analysis of Mantel correlograms obtained by calculating biomass-hydrography Mantel tests for each distance class (Legendre and Fortin 1989). Such analysis is beyond the scope of this paper.

The present study was based solely on biomass estimates without reference to size or species composition of zooplankton. Zooplankton biomass is generally characterized by more abrupt variation over space (greater patchiness) and by a shorter length scale (≈25 km) than zooplankton community assemblages (length scale ≈ 100–175 km) (Mackas 1984). The copepod community in the southeastern

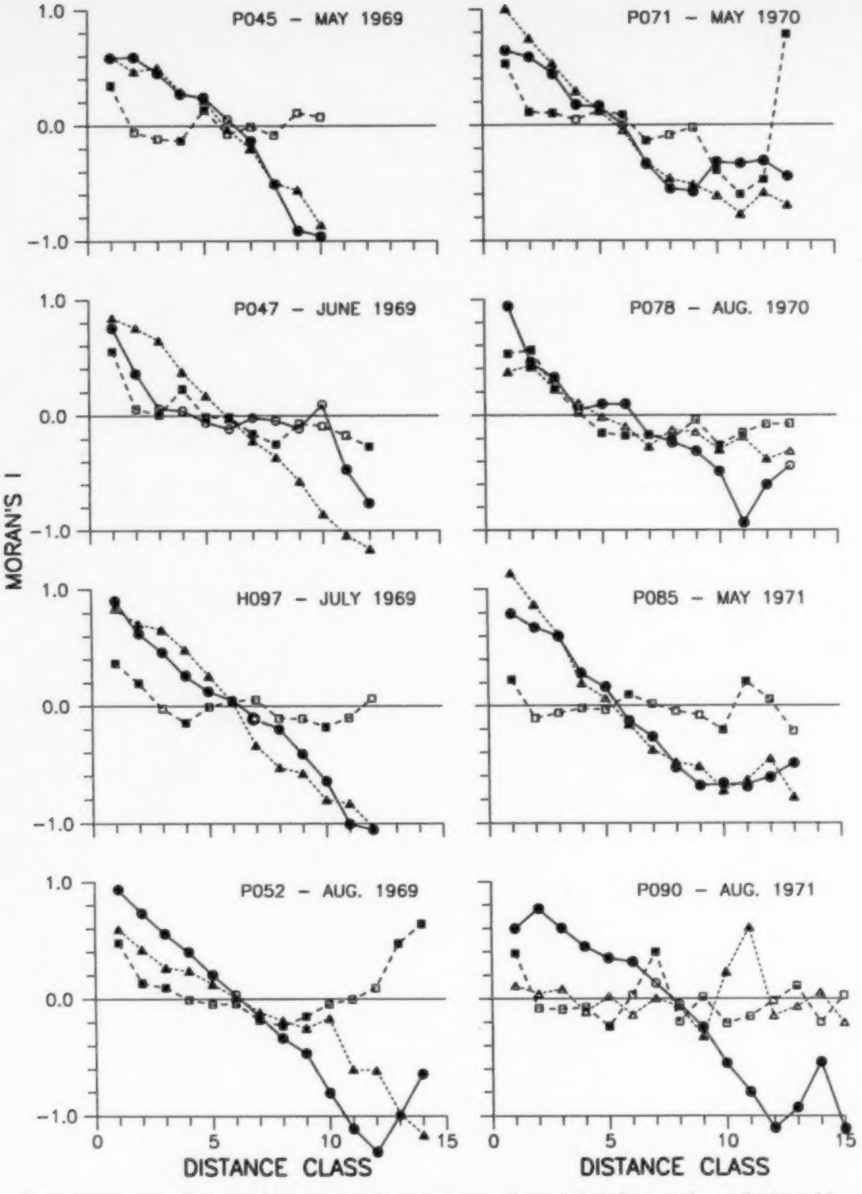

FIG. 11. Autocorrelograms for temperature (circles), salinity (triangles), and zooplankton biomass (squares) during the 1969–71 surveys. Each distance class is equivalent to 25 km spatial distance. Significant coefficients are indicated by solid symbols.

part of the Magdalen Shallows is composed by *Temora*, *Tortanus*, and the small *Centropages*, while large *Calanus* and small *Oithona* dominate in the western part and in the offshore waters over the Laurentian Channel (de Lafontaine et al. 1991). The relatively large mesh size (471 μm) used here has probably restricted the species composition and diversity to larger copepod species such as *Calanus*, *Temora*, and possibly *Tortanus*. In midsummer, zooplankton >1000 μm (sieve size) represent 65–80% of the overall biomass collected in 333-μm-mesh nets (M. Castonguay, Y. de Lafontaine, and J. Runge, unpublished data). The spatial variation in species composition over the entire area could, therefore, correspond to the regional, large-scale (>100 km) differences observed in biomass (Table 5). Spatial patterns of zooplankton communities and size classes in the southern Gulf remain to be described and compared with biomass patterns.

The observation of higher biomass over the Magdalen Shallows relative to the offshore deeper waters of the Laurentian Channel contrasts with the situation prevailing in southwestern Nova Scotia where the biomass of large zooplankton increases with distance from shore (Suthers and

TABLE 6. Mantel test correlation coefficients between zooplankton (Zoop) and geographic (SPACE) or hydrographic (Sal, Temp) distance matrices and between salinity and geographic distance matrices for each cruise. Asterisks denote probability levels (*$P < 0.05$; **$P < 0.01$; ***$P < 0.001$). Values in parentheses are partial Mantel tests between zooplankton and hydrographic variables controlling for the effect of geographic location (SPACE).

Cruise	Zoop-SPACE	Zoop-Sal	Zoop-Temp	SPACE-Sal
P006	0.189***	0.075	0.072	0.203***
H089	0.194***	−0.044	0.402*** (0.40***)	0.307***
H091	0.033	0.133*	−0.040	0.393***
P014	0.343*		−0.038	
P027	0.005	0.112** (0.123**)	−0.047	0.423***
P029	0.023	0.001	−0.008	0.593***
H094	0.160*	0.069	0.218* (0.190)	0.583***
P033	0.072	0.012	0.039	0.432***
P045	−0.029	−0.034	−0.028	0.533***
P047	0.119*	0.065	0.209*** (0.18***)	0.555***
H097	0.040	0.053	0.008	0.551***
P052	−0.008	−0.045	−0.066	0.566***
P071	0.206***	0.334*** (0.276***)	0.096* (0.033)	0.446***
P078	0.098*	−0.043	0.065	0.242***
P085	0.046	0.048	0.024	0.475***
P090	−0.007	−0.120	0.133	0.100

Frank 1990). These authors concluded that the lower biomass in shallow waters was due to higher predation pressure by gelatinous organisms. The inshore–offshore gradient off southwestern Nova Scotia, however, was associated with significant changes in water column stratification, where higher biomass was encountered in more stratified waters (Suthers and Frank 1990). Water properties at depths below the pycnocline (>20 m) are less spatially variable than at the surface in the Gulf (El-Sabh 1976; Petrie 1990). Under these conditions, spatial variations in surface temperature and salinity correspond to spatial variability in stratification. Consequently, the distribution of zooplankton biomass would correspond to the level of stratification over the entire area. In this view, results from the present study can be reconciled with those of Kiorboe and Johansen (1986) and Suthers and Frank (1990) showing an increase in zooplankton biomass in more stratified waters.

Seasonal Change in Abundance and Patchiness

The fivefold increase in biomass throughout the summer months and the higher increase in biomass over the Magdalen Shallows relative to the offshore waters of the Laurentian Channel are consistent with Steven's (1974) results. Interannual differences in summer biomass were relatively large and were not linked to spring biomass, which suggests that zooplankton population growth was probably determined during the spring-summer transition period. The lack of significant *positive* correlation between salinity and biomass during midspring and early summer (Table 6) does not support the suggestion that interannual variability in advective processes under the control of freshwater runoff contributes to the transport (or seeding) of significant quantities of large zooplankton over the Magdalen Shallows (de Lafontaine et al. 1991). Interannual (and seasonal) variability in spatial structures and in patchiness of zooplankton appeared unrelated to interannual variability in hydrographic properties and freshwater runoff. The influence of water mass movements on interannual biomass variations has been documented in other areas (Chelton et al. 1982; Smith and Vidal 1984, 1986; Lindahl and Hernroth 1988; Coyle et al. 1990). Although a longer time-series of data at a fixed time of year would be desirable to fully evaluate the influence of freshwater runoff on zooplankton dynamics in the southern Gulf, results presented here indicate that the summer increase of zooplankton biomass in the Magdalen Shallows is independent of hydrographic conditions. The absence of strong, recurrent spatial biomass patterns in the southern Gulf over 5 consecutive yr cannot be explained on the basis of available hydrographic information.

During the summer, the Magdalen Shallows is a favourite feeding area for numerous fish species, notably Atlantic herring (*Clupea harengus*) and Atlantic mackerel (*Scomber scombrus*) (MacKay 1967; Winters 1976; Winters and Beckett 1978; Grégoire and Castonguay 1989). Spawning grounds and preferred summer feeding zones for these two pelagic species are concentrated primarily in the western sector of the Magdalen Shallows which sustains the highest zooplankton biomass. In this context, it is interesting to note that Steven (1974) was not able to model the seasonal development of rich zooplankton populations in the Magdalen Shallows accurately without the incorporation of a predation parameter increasing mortality. Bioenergetic models predict that optimal swimming speed for foraging fish is 1–2 body lengths$\cdot s^{-1}$ (Ware 1978). In the case of Atlantic herring and Atlantic mackerel, this corresponds to 15–40 km$\cdot d^{-1}$. Therefore, pelagic fish whose food selection is primarily determined by the prey size (Koslow 1981) can quickly detect and remain in zooplankton prey concentrations. Zooplankton patchiness can be altered rapidly by fish foraging and then become unrelated to the hydrographic regime. While the selection for spawning and feeding grounds may be partly related to large-scale distribution in zooplankton biomass and possibly species or size composition, smaller scale fish movement would be linked to patch distribution (Mackas 1984). Unfortunately, fish movements and aggregations at the scales necessary to demonstrate their effects on zooplankton patchiness are poorly described for the Gulf, and until such information becomes available, the effects of fish predation will remain untested.

In conclusion, results of the present study show that spatial structures of zooplankton biomass in the southern Gulf of St. Lawrence are temporally variable, both at the seasonal and interannual level, and appear to be unpredictable from surface water characteristics. The lack of a strong and positive relationship between biomass and salinity *over the entire area* implies that freshwater runoff has no direct effect on biomass distribution at the sampling scale used in the present study. Zooplankton species or size composition may be a better predictor than biomass alone for monitoring changes and variability of zooplankton in response to runoff variability.

Acknowledgements

The author wishes to thank M. Castonguay, M. Levasseur, D. Mackas, I.A. McQuinn, and an anonymous referee for comments on and criticism of an earlier version of the manuscript. I am also grateful to P. Jalbert for providing the digitized map of the Gulf of St. Lawrence used in the figures. This study was financially supported by the Department of Fisheries and Oceans, Institut Maurice-Lamontagne, Mont-Joli, Qué., and by Environment Canada, Centre Saint-Laurent, Montréal, Qué.

References

Aron, W. 1959. Midwater trawling studies in the North Pacific. Limnol. Oceanogr. 4: 409–418.

Bugden, G.L., B.T. Hargrave, M.M. Sinclair, C.L. Tang, J-C. Therriault, and P.A. Yeats. 1982. Freshwater runoff effects in the marine environment: the Gulf of St. Lawrence example. Can. Tech. Rep. Fish. Aquat. Sci. 1078: 89 p.

Cassie, R.M. 1963. Microdistribution of plankton. Oceanogr. Mar. Biol. Annu. Rev. 1: 223–252.

Chelton, D.B., P.A. Bernal, and J.A. McGowan. 1982. Large-scale interannual physical and biological interaction in the California Current. J. Mar. Res. 40: 1095–1125.

Cox, J., and P.H. Wiebe. 1979. Origins of oceanic plankton in the Middle Atlantic Bight. Estuarine Coastal Mar. Sci. 9: 509–527.

Coyle, K.O., A.J. Paul, and D.A. Ziemann. 1990. Copepod populations during the spring bloom in an Alaskan subarctic embayment. J. Plankton Res. 12: 759–797.

Davis, C.S. 1987. Components of the zooplankton production cycle in the temperate ocean. J. Mar. Res. 45: 947–983.

de Lafontaine, Y., S. Demers, and J. Runge. 1991. Pelagic food web interactions and productivity in the Gulf of St. Lawrence: a perspective. *In* J-C. Therriault [ed.] The Gulf of St. Lawrence: small ocean or big estuary? Can. Spec. Publ. Fish. Aquat. Sci. 113: 99–123.

de Lafontaine, Y., and D. Gascon. 1990. Ontogenetic variation in the vertical distribution of eggs and larvae of Atlantic mackerel (*Scomber scombrus*). Rapp. P.-v. Réun. Cons. int. Explor. Mer 191: 137–145.

El-Sabh, M.I. 1976. Surface circulation pattern in the Gulf of St. Lawrence. J. Fish. Res. Board Can. 33: 124–138.

El-Sabh, M.I. 1977. Oceanographic features, currents, and transport in Cabot strait. J. Fish. Res. Board Can. 34: 516–528.

Fager, E.W., and J.A. McGowan. 1963. Zooplankton species groups in the North Pacific. Science (Wash., D.C.) 140: 144–151.

Frank, K.T. 1988. Independent distributions of fish larvae and their prey: natural paradox or sampling artifact? Can. J. Fish. Aquat. Sci. 45: 48–59.

Friedl, W.A. 1971. The relative sampling performance of 6- and 10-foot Isaacs-Kidd midwater trawl. Fish. Bull. U.S. 69: 427–432.

Frost, B.W. 1988. Variability and possible adaptative significance of diel vertical migration in *Calanus pacificus*, a planktonic marine copepod. Bull. Mar. Sci. 43: 675–694.

Govoni, J.J., D.E. Hoss, and D.R. Colby. 1989. The spatial distribution of larval fishes about the Mississippi River plume. Limnol. Oceanogr. 34: 178–187.

Grégoire, F., and M. Castonguay. 1989. L'alimentation du maquereau bleu (*Scomber scombrus*) dans le golfe du St-Laurent et sur le plateau néo-écossais, avec une application du test de Mantel. Rapp. tech. can. sci. halieut. aquat. 1673: 23 p.

Harris, G.P. 1980. Temporal and spatial scales in phytoplankton ecology. Mechanisms, methods, models, and management. Can. J. Fish. Aquat. Sci. 37: 877–900.

Herman, A.W., D.D. Sameoto, C. Shunnian, M.R. Mitchell, B. Petrie, and N. Cochrane. 1991. Sources of zooplankton on the Nova Scotia Shelf and their aggregations within deep-shelf basins. Continental Shelf Res. 11: 211–238.

Hewitt, R. 1981. The value of pattern in the distribution of young fish. Rapp. P.-v. Réun. Cons. int. Explor. Mer 178: 229–236.

Johnson, D.L. 1989. Spatial autocorrelation, spatial modelling, and improvements in grasshopper survey methodology. Can. Entomol. 121: 579–588.

Kimmerer, W.J., and A.D. McKinnon. 1987. Zooplankton in a marine bay. II. Vertical migration to maintain horizontal distributions. Mar. Ecol. Prog. Ser. 41: 53–60.

Kimmerer, W.J., and A.D. McKinnon. 1989. Zooplankton in a marine bay. III. Evidence for influence of vertebrate predation on distributions of two common copepods. Mar. Ecol. Prog. Ser. 53: 21-35.

Kiorboe, T., and K. Johansen. 1986. Studies of a larval herring (*Clupea harengus* L.) patch in the Buchan area. IV. Zooplankton distribution and productivity in relation to hydrographic features. Dana 6: 37–51.

Kohler, A.C., D.J. Faber, and N.J. McFarlane. 1974a. Eggs, larvae and juveniles of fishes from plankton collections in the Gulf of St. Lawrence during 1965, 1966 and 1967. Fish. Res. Board Can. Tech. Rep. 285: 164 p.

Kohler, A.C., D.J. Faber, and N.J. McFarlane. 1974b. Eggs, larvae and juveniles of fishes from plankton collections in the Gulf of St. Lawrence during 1968. Fish. Mar. Serv. Res. Dev. Tech. Rep. 490: 105 p.

Kohler, A.C., D.J. Faber, and N.J. McFarlane. 1975. Eggs, larvae and juveniles of fishes from plankton collections in the Gulf of St. Lawrence during 1969. Fish. Mar. Serv. Res. Dev. Tech. Rep. 521: 154 p.

Kohler, A.C., D.J. Faber, and N.J. McFarlane. 1976. Eggs, larvae and juveniles of fishes from plankton collections in the Gulf of St. Lawrence during 1970–1971. Fish. Mar. Serv. Res. Dev. Tech. Rep. 645: 139 p.

Koslow, J.A. 1981. Feeding selectivity of northern anchovy, *Engraulis mordax*, in the Southern California Bight. Fish. Bull. U.S. 79: 131–142.

Koutitonsky V.G., and G.L. Budgen. 1991. The physical oceanography of the Gulf of St. Lawrence: a review with emphasis on the synoptic variability of the motion. *In* J-C. Therriault [ed.] The Gulf of St. Lawrence: small ocean or big estuary? Can. Spec. Publ. Fish. Aquat. Sci. 113: 57–90.

Krause, M., and G. Kattner. 1989. The influence of water exchange on zooplankton dynamics and species development in a south Norwegian fjord. J. Plankton Res. 11: 85-103.

Legendre, L., and S. Demers. 1984. Towards dynamic biological oceanography and limnology. Can. J. Fish. Aquat. Sci. 41: 2–19.

Legendre, P., and M-J. Fortin. 1989. Spatial pattern and ecological analysis. Vegetatio 80: 107–138.

Legendre, L., and P. Legendre. 1983. Numerical ecology. Elsevier, Amsterdam, The Netherlands. 419 p.

Legendre, P., and M. Troussellier. 1988. Aquatic heterotrophic bacteria: modelling in the presence of spatial autocorrelation. Limnol. Oceanogr. 33: 1055–1067.

Legendre, P., and A. Vaudor. 1991. Le logiciel R, analyse multidimensionnelle, analyse spatiale. Département de sciences biologiques, Université de Montréal, Montréal, Qué. 145 p.

Lilliefors, H.W. 1967. The Kolmogorov–Smirnov test for normality with mean and variance unknown. J. Am. Stat. Assoc. 62: 399–402.

Lindahl, O., and L. Hernroth. 1988. Large-scale and long-term variations in the zooplankton community of the Gullmar Fjord, Sweden, in relation to advective processes. Mar. Ecol. Prog. Ser. 43: 161–171.

Lindahl, O., and R. Perissinotto. 1987. Short-term variations in the zooplankton community related to water exchange processes in the Gullmar Fjord, Sweden. J. Plankton Res. 9: 1113–1132.

Lobel, P.S., and A.R. Robinson. 1988. Larval fishes and zooplankton in a cyclonic eddy in Hawaiian waters. J. Plankton Res. 10: 1209–1223.

Mackas, D.L. 1984. Spatial autocorrelation of plankton community composition in a continental shelf ecosystem. Limnol. Oceanogr. 29: 451–471.

Mackas, D.L., K.L. Denman, and M.R. Abbott. 1985. Plankton patchiness: biology in the physical vernacular. Bull. Mar. Sci. 37: 652–674.

MacKay, K.T. 1967. An ecological study of mackerel, *Scomber scombrus* in coastal waters of Canada. Fish. Res. Board Can. Tech. Rep. 31: 127 p.

McLaren, I.A. 1978. Generation lengths of some temperate marine copepods: estimation, predation, and implication. J. Fish. Res. Board Can. 35: 1330–1342.

McLaren, I.A., and C.J. Corkett. 1981. Temperature-dependent growth and production of a marine copepod. Can. J. Fish. Aquat. Sci. 38: 77–83.

Miller, D. 1961. A modification of the small Hardy plankton sampler for simultaneous high-speed plankton hauls. Bull. Mar. Ecol. 45: 165–172.

Miller, R.J., and R. Daan. 1989. Planktonic predators and copepod abundance near the Dutch coast. J. Plankton Res. 11: 263–282.

Omori, M., and W.M. Hamner. 1982. Patchy distribution of zooplankton: behaviour, population assessment and sampling problems. Mar. Biol. 72: 193–200.

Ouellet, P., D. Lefaivre, and V. Koutitonsky. 1990. Distribution of shrimp (*Pandalus borealis*) larvae and hydrographic pattern in the northern Gulf of St. Lawrence. Can. J. Fish. Aquat. Sci. 47: 2068–2078.

Paffenhoffer, G-A., and D.E. Stearns. 1988. Why is *Acartia tonsa* (Copepoda: Calanoida) restricted to nearshore environments? Mar. Ecol. Prog. Ser. 42: 33–38.

Peterson, W.T., C.B. Miller, and A. Hutchinson. 1979. Zonation and maintenance of copepod populations in the Oregon upwelling zone. Deep-Sea Res. 26: 467–494.

Petrie, B. 1990. Monthly means of temperature, salinity and sigma-t for the Gulf of St. Lawrence. Can. Tech. Rep. Hydrogr. Ocean Sci. 126: 137 p.

Pielou, E.C. 1974. Population and community ecology. Principles and methods. Gordon & Breach Sci. Publ., New York, N.Y. 424 p.

Rothlisberg, P.C., and C.J. Jackson. 1982. Temporal and spatial variation of plankton abundance in the Gulf of Carpentia, Australia 1975–1977. J. Plankton Res. 4: 19-40.

Runge, J.A., and Y. Simard. 1990. Zooplankton of the St. Lawrence estuary: the imprint of physical processes on its composition and distribution, p. 296–320. *In* M.I. El-Sabh and N. Silverberg [ed.] Oceanography of a large-scale estuarine system, the St. Lawrence. Coastal and Estuarine Studies. Vol. 39. Springer-Verlag, New York, N.Y.

Sameoto, D.D., and A.W. Herman. 1992. Effect of outflow from the Gulf of St. Lawrence on Nova Scotia shelf zooplankton. Can. J. Fish. Aquat. Sci. 49: 857–869.

Schneider, G. 1987. Role of advection in the distribution and abundance of *Pleurobrachia pileus* in Kiel Bight. Mar. Ecol. Prog. Ser. 41: 99–102.

Simard, Y., and L. Savard. 1990. Variability, spatial patterns, and scales of similarity distributions of the northern shrimp (*Pandalus borealis*) and its migrations in the Gulf of St. Lawrence. Can. J. Fish. Aquat. Sci. 47: 794–804.

Skreslet, S., and N.A. Red. 1986. Advection of *Calanus finmarchicus* between habitats in Norwegian coastal waters, p. 375–388. *In* S. Skreslet [ed.] The role of freshwater outflow in coastal marine environments. NATO ASI Ser. G: Vol 7. Springer-Verlag, Berlin, Germany.

Smith, S.L., and J. Vidal. 1984. Spatial and temporal effects of salinity, temperature and chlorophyll on the communities of zooplankton in the southeastern Bering Sea. J. Mar. Res. 42: 221–257.

Sokal, R.R., and F.J. Rohlf. 1981. Biometry. 2nd ed. W.H. Freeman Co., San Francisco, Calif. 859 p.

Springer, A.M., C.P. McRoy, and K.R. Turco. 1989. The paradox of pelagic food webs in the northern Bering Sea — II. Zooplankton communities. Continental Shelf Res. 9: 359–386.

Star, J.L., and M.M. Mullin. 1981. Zooplankton assemblages in the areas of the North Pacific as revealed by continuous horizontal transects. Deep-Sea Res. 28: 1303–1322.

Steele, J.H. 1976. Patchiness, p. 98–115. *In* D.H. Cushing and J.J. Walsh [ed.] The ecology of the seas. Saunders, Philadelphia, Penn.

Steven, D.M. 1974. Primary and secondary production in the Gulf of St. Lawrence. Mar. Sci. Centre Manuscr. Rep. No. 26, McGill University, Montreal, Que. 116 p.

Suthers, I.M., and K.T. Frank. 1990. Zooplankton biomass gradient off south-western Nova Scotia: nearshore ctenophore predation or hydrographic separation? J. Plankton Res. 12: 831–850.

Taggart, C.T., and K.T. Frank. 1987. Coastal upwelling and *Oikopleura* occurrence ("slub"): a model and potential application to inshore fisheries. Can. J. Fish. Aquat. Sci. 44: 1729–1736.

Taggart, C.T., and K.T. Frank. 1990. Perspectives on larval fish ecology and recruitment processes. Probing the scales of relationships, p. 151–164. *In* K. Sherman and L.M. Alexander [ed.] Patterns, process, and yields of large marine ecosystems. AAAS Selected Symposium Series, Washington, D.C.

Vidal, J., and T.E. Whitledge. 1982. Rates of metabolism of planktonic crustaceans as related to body weight and temperature of habitat. J. Plankton Res. 4: 77–84.

Ware, D.M. 1978. Bioenergetics of pelagic fish: theoretical change in swimming speed and ration with body size. J. Fish. Res. Board Can. 35: 220–228.

Weikert, H. 1984. Zooplankton distribution and hydrography in the Mauritanian upwelling region off northwestern Africa, with special reference to the calanoid copepods. Meeresforschung 30: 155–171.

Wiens, J.A. 1989. Spatial scaling in ecology. Funct. Ecol. 3: 385–397.

Winters, G.H. 1976. Recruitment mechanisms of the southern Gulf of St. Lawrence Atlantic herring (*Clupea harengus*). J. Fish. Res. Board Can. 33: 1751–1763.

Winters, G.H., and J.S. Beckett. 1978. Migrations, biomass and stock interrelationships of southwest Newfoundland – southern Gulf herring from mark-recapture experiments. Int. Comm. Northwest. Atl. Fish. Res. Bull. 13: 67–79.

Assessment of Fin Erosion by Comparison of Relative Fin Length in Hatchery and Wild Trout in Utah

Thomas Bosakowski and Eric J. Wagner

Utah Division of Wildlife Resources, Fisheries Experiment Station, 1465 West 200 North, Logan, UT 84321, USA

Bosakowski, T., and E.J. Wagner. 1994. Assessment of fin erosion by comparison of relative fin length in hatchery and wild trout in Utah. Can. J. Fish. Aquat. Sci. 51: 636–641.

We measured all fins of 600 hatchery trout sampled from all 10 state fish hatcheries in Utah, and of wild fish sampled as controls comprising 58 rainbow trout (*Oncorhynchus mykiss*), 33 cutthroat trout (*O. clarki*), and 54 brown trout (*Salmo trutta*). A strong linear correlation was found between fin length and total body length (100–300 mm) for all fins of wild rainbow trout. "Relative fin length" (fin length/total body length × 100) proved to be a useful comparative measure, as this statistic was not biased by fish length in the wild fish sampled (all slopes <0.01%). Interspecific comparison of wild rainbow, cutthroat, and brown trout showed slight but statistically significant differences in some fin lengths. In intraspecific comparisons, hatchery fish had significantly shorter (10–50%) rayed fins than wild fish. The dorsal fin was most severely eroded in rainbow and brown trout, followed by the pectoral, anal, ventral, and caudal fins. In cutthroat trout the pattern was the same except that pectoral fins had more extensive erosion than dorsal fins. No species was clearly more susceptible to fin erosion in hatcheries, but the Fish Lake – DeSmet strain of rainbow trout had significantly shorter fins than other rainbow trout strains.

Nous avons mesuré toutes les nageoires de 600 truites d'élevage prélevées dans les 10 écloseries d'État de l'Utah, et de poissons sauvages prélevés comme témoins : 58 truites arc-en-ciel (*Oncorhynchus mykiss*), 33 truites fardées (*O. clarki*) et 54 truites brunes (*Salmo trutta*). Nous avons trouvé une forte corrélation linéaire entre la longueur des nageoires et la longueur totale du corps (100–300 mm) pour toutes les nageoires des truites arc-en-ciel sauvages. La «longueur relative des nageoires» (longueur de la nageoire/longueur totale du corps × 100) s'est révélée une mesure comparative utile, car cette donnée n'est pas biaisée par la longueur des poissons chez les spécimens sauvages échantillonnés (toutes les pentes <0,01 %). La comparaison interspécifique des spécimens sauvages de truite arc-en-ciel, de truite fardée et de truite brune a révélé des différences légères mais statistiquement significatives dans la longueur de certaines nageoires. Dans les comparaisons intraspécifiques, les poissons d'élevage présentaient des nageoires rayonnées nettement plus courtes (10–50 %) que les poissons sauvages. C'est la nageoire dorsale qui était la plus érodée chez la truite arc-en-ciel et la truite brune, suivie par les nageoires pectorales, anales, ventrales et caudales. Chez la truite fardée, le schéma était le même, mais les nageoires pectorales étaient plus érodées que les nageoires dorsales. Aucune espèce ne semblait nettement plus vulnérable que les autres à l'érosion des nageoires dans les écloseries, mais la souche Fish Lake – DeSmet de truite arc-en-ciel présentait des nageoires nettement plus courtes que les autres souches de la même espèce.

Received March 19, 1993
Accepted October 7, 1993
(JB850)

Reçu le 19 mars 1993
Accepté le 7 octobre 1993

Fin erosion is a common problem in hatchery-raised salmonids both in Utah and worldwide. This condition is so pervasive that it is often used as an indicator in the field to identify recently stocked fish. Studies have shown that fins clipped from one half of two thirds their length will regenerate in approximately 6 mo with only minor deformities (Eipper and Forney 1965), but fins reduced to the point of attachment with the bone will usually not regenerate (Stuart 1958; Eipper and Forney 1965; Jones 1979). Heimer et al. (1985) found no difference in survival of rainbow trout (*Oncorhynchus mykiss*) missing pectoral fins due to erosion when compared with control fish with intact pectoral fins. Gjerde and Refstie (1988) have also reported no significant differences in survival between fin-clipped and unclipped fish.

However, other studies have described detrimental effects on survival (Saunders and Allen 1967; Weber and Wahle 1969; Nicola and Cordone 1973; Mears and Hatch 1976). Because active fin erosion in hatchery fish is often accompanied by microbial infection and hemorrhage (Schneider and Nicholson 1980; Goede and Barton 1990), the ability to survive in the wild could be compromised, even if the effects of partial fin loss on swimming ability may be marginal. The lack of aesthetic appeal of fish with fin erosion is also a management and marketing problem with regard to satisfaction levels of discriminating anglers and consumers.

The purpose of this investigation was to (1) quantify the extent of fin erosion in the Utah State hatchery system, (2) compare the degree of erosion in hatchery-reared fish with that in wild populations, (3) determine the extent of affliction for individual fins, (4) evaluate the relationship between fin length and body length, and (5) compare fin erosion among hatcheries, strains, and species.

Materials and Methods

At total of 600 hatchery trout were sampled from 17 March 1992 to 1 May 1992 at all 10 state hatcheries in Utah. During this period, fish loads were near their maximum just prior to spring stocking. At each of the 10 hatcheries, two to four samples of 20 fish were taken from raceways or ponds. This sampling included 22 groups of rainbow trout, two groups of albino rainbow trout, four groups of cutthroat trout (*O. clarki*), and one group each of brown trout (*Salmo trutta*) and brook trout (*Salvelinus fontinalis*). Overall, the survey included a mixture of fish 200–300 mm long (catchables) and 100–200 mm long (subcatchables), all fish being no older than 22 mo. All fish were fed the same brand of food, but there may have been subtle differences in food storage conditions, feeding methods, and ration levels that could not be accounted for.

Fish were temporarily immobilized with tricaine methanesulfonate (MS-222), weighed to the nearest 0.1 g, and measured for total length to the nearest millimetre. All rayed fins were subsequently measured to the nearest millimetre by taking the maximum length reading, parallel to the fin rays (Fig. 1). Adipose fins were measured for maximum length from the anterior point of attachment to end of the posterior lobe. One of the authors (T.B.) made all of the fin measurements to avoid any possible observer bias. To determine the pattern and extent of fin wear, fin length measurements of hatchery trout were divided by total body length × 100 (Kindschi 1987) to obtain relative fin lengths for comparison with wild populations.

Using electrofishing equipment, 58 wild rainbow trout (113–285 mm) were sampled in August 1992 from Summit Creek, Cache County, Utah. A total of 33 wild cutthroat trout (139–297 mm) and 54 wild brown trout (116–297 mm) were sampled in January 1993 from the East Fork of the Little Bear River, Cache County, Utah. Identical procedures were used to measure these fish.

Ordinary least-squares linear regression of fin length or relative fin length against total length was performed with the SAS statistical software program (SAS Institute, Inc. 1988). For comparison of fin erosion between hatchery and wild fish, all hatchery rainbow trout ($N = 440$) data were pooled. Comparisons of relative fin length among the hatchery and the wild populations were made for each fin with the SAS procedure "NPAR1WAY WILCOXON", a nonparametric rank test (SAS Institute, Inc. 1988). This test was also used to evaluate differences among strains of rainbow trout, controlling for hatchery. The GLM procedure (general linear models; SAS Institute, Inc. 1988) was used in a two-way analysis to analyze rank transformed data for differences among hatcheries, species, and their interaction. For comparison of fin erosion among species within a hatchery, one-way analysis of variance (ANOVA) of rank transformed data was used. A significance level of $p < 0.05$ was used for each comparison.

Results

Linear regression plots were constructed by comparing fin lengths with total body length of wild rainbow trout (Fig. 2). Results showed a clear linear relationship for all fins within the size range of fish sampled (100–300 mm). High correlation coefficients ($r > 0.88$) indicated a strong correlation for all fins. All slopes were significantly greater than zero ($p < 0.0001$).

Relative fin lengths were generated and regressed against total body length (Table 1). These relationships were generally stable as fish length increased for wild rainbow trout, with the exception of the slightly negative slope (0.006%) for caudal fin values. Results for wild brown and cutthroat trout revealed slightly less stable relationships for relative fin length as body length increased, but slopes were minimal (all slopes < 0.01%).

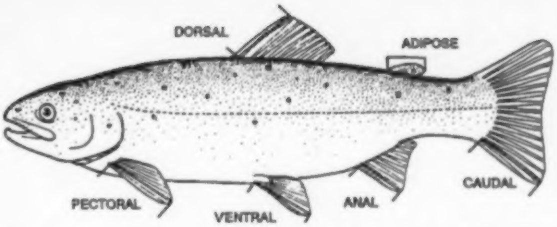

FIG. 1. Location of measurements taken for maximum fin length.

Intraspecific comparison of relative fin length for hatchery and wild fish showed that all rayed fins were significantly shorter in the hatchery rainbow, cutthroat, and brown trout (Fig. 3). In contrast with rayed fins, relative fin length for adipose fins was either the same (brown and cutthroat) or longer (rainbow) for hatchery fish. For rainbow and brown trout, fin erosion was most severe for dorsal fins, followed by the pectoral, anal, caudal, and ventral fins. The pattern for cutthroat trout was similar except that pectoral fins had greater erosion than dorsal fins.

Interspecific comparison of the wild populations (Fig. 4) showed that relative fin lengths for rainbow and brown trout tended to be the same for all rayed fins whereas for cutthroat, relative fin lengths were typically shorter for all rayed fins, except the caudal fin. The adipose relative fin length was unique for each species.

Among hatchery fish, species differences in relative fin length were examined within hatcheries to eliminate the effect of hatchery differences (Table 2). At the Egan Hatchery, there was an overall difference among the four trout species for each of the fins (ANOVA, $p < 0.0001$). Similarly, at the Kamas Hatchery, there was an overall difference for each of the fins of rainbow, albino rainbow, and cutthroat trout (ANOVA, $p < 0.0001$). At the Midway and Kamas hatcheries, relative dorsal and anal fin lengths of albino rainbow trout were significantly longer than the corresponding fins of pigmented rainbow trout, but the other fins were variable, with no consistent differences across both hatcheries.

In three of four hatcheries, relative dorsal fin lengths of rainbow trout were significantly shorter than those of cutthroat trout. On the other hand, cutthroat trout had greater erosion of the pectoral fins than rainbow trout at three of four hatcheries. In the Egan Hatchery, there was no significant difference in pectoral fin erosion as a result of the poorer condition of the rainbow trout fins, as opposed to the better condition of fins of the cutthroat trout. Differences in erosion of the ventral fins of cutthroat and rainbow trout were variable, with neither species clearly better or worse than the other.

Individual fin lengths were also compared by strain, but the number of statistically valid comparisons was limited to only four comparisons (Table 3). Rainbow trout of the Fish Lake – DeSmet (FD) strain generally had significantly shorter rayed fins than the albino (AB), Sand Creek (SC), and Shepherd of the Hills (SH) strains. Exceptions were the rel-

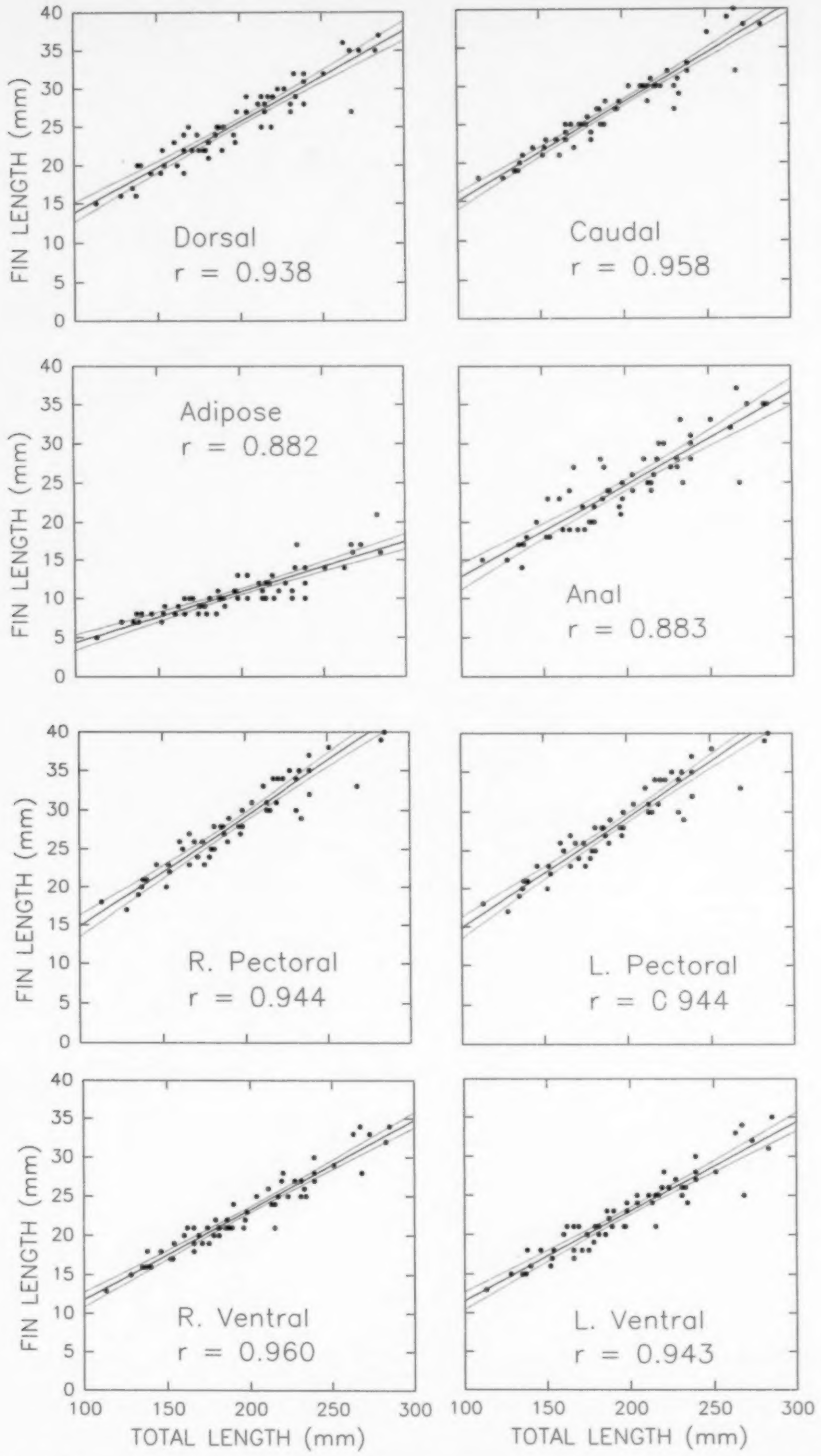

FIG. 2. Linear regression plots of fin length against total body length for wild rainbow trout ($N = 58$) from Summit Creek, Utah. Solid line = regression line; dotted lines = 95% confidence interval of the mean.

TABLE 1. Results of regression of relative fin length (%) with total body length for rainbow, cutthroat, and brown trout from wild populations. r = correlation coefficient, p = ANOVA probability that slope equals zero, m = slope (percent change per millimetre), b = y-intercept (relative fin length), DR = dorsal, CD = caudal, AD = adipose, AN = anal, RP = right pectoral, LP = left pectoral, RV = right ventral, LV = left ventral.

Species	DR	CD	AD	AN	RP	LP	RV	LV
Rainbow	r = 0.216	0.336	0.287	0.082	0.062	0.010	0.082	0.028
(N = 58)	p = 0.1027	0.0099	0.0287	0.5412	0.6457	0.9353	0.5378	0.8291
	m = −0.0048	−0.0065	0.0047	−0.0025	−0.0015	−0.0003	−0.0014	−0.0006
	b = 13.86	15.27	4.46	12.87	14.90	14.59	11.93	11.61
Cutthroat	r = 0.449	0.586	0.455	0.114	0.049	0.026	0.462	0.222
(N = 33)	p = 0.0088	0.0003	0.0001	0.5284	0.7887	0.8870	0.0068	0.2148
	m = −0.010	−0.0086	0.0058	0.0018	−0.0007	−0.0003	−0.0041	−0.0020
	b = 14.10	16.19	4.97	11.66	13.82	13.69	12.12	11.45
Brown	r = 0.380	0.491	0.432	0.347	0.491	0.523	0.190	0.070
(N = 54)	p = 0.0046	0.0002	0.0010	0.0102	0.0002	0.0001	0.1900	0.6142
	m = −0.0042	−0.0055	−0.0063	0.0050	−0.0092	−0.0094	−0.0018	−0.0006
	b = 14.25	15.39	8.35	11.26	17.21	17.27	12.13	11.84

TABLE 2. Species differences in relative fin lengths (%) of trout from five Utah hatcheries. CT = cutthroat trout, RT = rainbow trout, BK = brook trout, BN = brown trout, AB = albino rainbow trout, TL = total body length (mm); other abbreviations listed in Table 1. A common superscript letter among species within a hatchery indicates no significant difference ($p > 0.050$). ***No comparison because these cutthroat trout were adipose fin clipped.

Hatchery	Species	N	TL	DR	CD	AD	AN	RP	LP	RV	LV
Egan	CT	20	172.2^{a}	8.3^{a}	10.9^{a}	6.3^{a}	9.8^{a}	6.9^{a}	7.2^{a}	8.6^{a}	8.6^{a}
	RT	20	190.9^{b}	6.3^{b}	9.0^{b}	6.5^{a}	7.1^{b}	6.8^{a}	6.9^{a}	7.7^{b}	7.6^{b}
	BK	20	207.1^{c}	8.0^{abc}	11.2^{a}	6.2^{a}	9.8^{a}	11.3^{b}	10.5^{b}	7.3^{b}	6.8^{b}
	BN	20	186.5^{b}	7.0^{c}	11.1^{a}	7.1^{b}	9.9^{a}	9.9^{b}	9.8^{b}	9.9^{c}	9.5^{c}
Kamas	CT	20	143.4^{a}	7.3^{a}	11.2^{a}	6.2^{a}	9.6^{a}	6.8^{a}	6.5^{a}	7.2^{a}	6.9^{a}
	RT	40	157.2^{a}	8.6^{b}	12.4^{b}	6.8^{b}	10.2^{a}	11.3^{b}	11.5^{b}	9.9^{b}	9.9^{b}
	AB	20	217.2^{b}	9.7^{c}	12.5^{b}	6.2^{a}	10.8^{b}	9.4^{c}	9.5^{c}	9.3^{c}	9.1^{c}
Ft. Green	CT	20	177.3^{a}	8.1^{a}	12.1^{a}	***	10.3^{a}	10.5^{a}	10.5^{a}	8.2^{a}	8.6^{a}
	RT	40	243.0^{b}	6.2^{b}	11.5^{b}	***	9.7^{b}	11.2^{a}	11.3^{b}	9.9^{b}	9.9^{b}
Mantua	CT	20	308.9^{a}	8.4^{a}	10.1^{a}	***	9.3^{a}	6.2^{a}	6.4^{a}	8.4^{a}	8.3^{a}
	RT	20	203.6^{b}	6.5^{b}	10.3^{a}	***	7.8^{b}	8.4^{b}	8.4^{b}	8.6^{a}	8.2^{a}
Midway	AB	20	227.0^{a}	10.5^{a}	12.9^{a}	6.6^{a}	11.1^{a}	11.0^{a}	10.9^{a}	10.4^{a}	10.4^{a}
	RT	60	209.0^{b}	7.9^{b}	12.8^{a}	5.9^{b}	10.4^{b}	11.8^{a}	11.9^{a}	10.2^{a}	10.1^{a}

TABLE 3. Comparison of relative fin length (%) between different strains of rainbow trout within hatcheries. AB = albino, FD = Fish Lake – DeSmet, SH = Shepherd of the Hills, SC = Sand Creek; other abbreviations listed in Table 1. *Significant difference between strains within the hatchery ($p < 0.050$).

Hatchery	Strain	N	TL	DR	CD	AD	AN	RP	LP	RV	LV
Midway	AB	20	227.0	10.4	12.9	6.6	11.0	11.0	10.9	10.4	10.4
	FD	20	209.0*	7.9*	12.7	5.9	10.4*	11.7	11.9*	10.1*	10.1*
White Rocks	SH	20	232.6	8.2	12.0	6.5	10.3	11.2	11.4	10.5	10.5
	FD	20	182.3*	5.9*	11.2*	6.1	9.2*	9.9*	10.0*	9.2*	9.0*
Mammoth Creek	FD	20	228.8	5.0	10.6	6.3	8.6	3.9	4.1	9.4	9.3
	SC	20	121.9*	3.5*	11.7*	7.7*	9.6*	10.4*	10.6*	9.5	9.4
Loa	FD	20	227.2	2.6	9.4	6.9	5.7	4.7	4.6	9.3	9.2
	SC	40	146.8*	3.8*	11.3*	7.8*	8.4*	11.6*	11.2*	9.5	9.7*

ative dorsal fin and left pectoral fin lengths of the SC and AB trout strains, respectively, which were significantly greater in the FD strain.

Discussion

The proportion of fin length over total body length, termed "relative fin length" in this paper, was proposed by Kindschi (1987) as a method for quantifying fin erosion. However, questions arose concerning the stability of this ratio over a range of fish sizes. A comparison of relative fin length among fish of different sizes would be biased if the relationship was not linear. In this study, we determined that there was a clear linear relationship between fin length and total body length in wild rainbow, brown, and cutthroat trout ranging from 100 to 300 mm in length. The stability of rel-

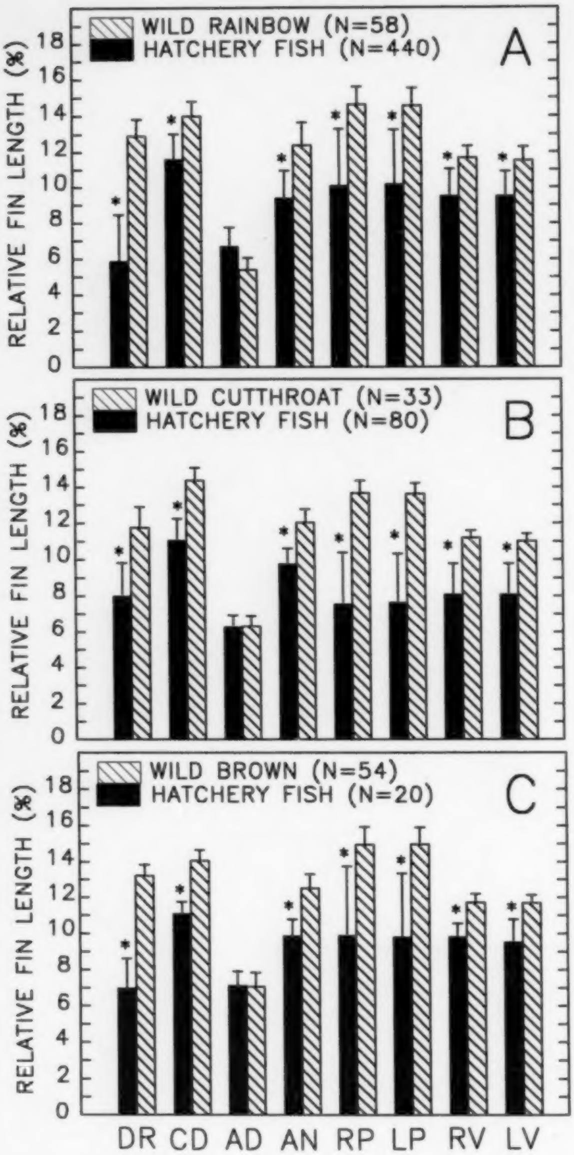

FIG. 3. Comparison of relative fin length between wild and hatchery (A) rainbow, (B) cutthroat, and (C) brown trout. Bar heights represent the mean, with error bars indicating the standard deviation. An asterisk indicates significant difference ($p > 0.05$) between hatchery and wild trout. Fin abbreviations are given in Table 1.

ative fin length, as size increases, was demonstrated for nearly all fins of the wild rainbow trout examined. Exceptions for cutthroat and brown trout fins were minor; all slopes were <0.01%. At least within the typical size range of hatchery trout (100–300 mm), this level of accuracy should be sufficient for quantifying fin erosion. In this investigation, average erosion was 10–50% for rayed fins.

Relative fin length for adipose fins was either the same (brown and cutthroat) or longer (rainbow) for hatchery fish.

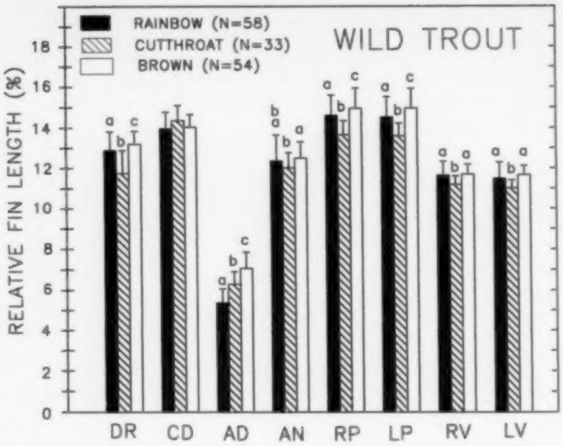

FIG. 4. Comparison of relative fin length among wild populations of rainbow, cutthroat, and brown trout. Bar heights represent the mean, with error bars indicating the standard deviation. A different letter indicates significant difference ($p > 0.05$). Fin abbreviations are given in Table 1.

This result demonstrates that the adipose fin is not subject to erosion and may even increase in size in hatchery fish. Simpson et al. (1992) found that adipose fin length and five body morphometrics could be used in a multiple regression model to successfully predict fat levels of hatchery Atlantic salmon (*Salmo salar*).

In using relative fin length, we document for the first time that all rayed fins of hatchery trout were significantly shortened by the fin erosion process. Intraspecific comparison between wild and hatchery fish showed that the dorsal fin of rainbow and brown trout was the most severely eroded, followed by the pectoral, anal, ventral, and caudal fins. Kindschi et al. (1991a) examined only the dorsal fins of wild and hatchery juvenile steelhead trout and found significant erosion in hatchery fish between 28 and 200 mm in length. Abbott and Dill (1985) observed that fin nipping in juvenile steelhead trout was primarily directed at the dorsal fin. Kindschi et al. (1991a) noted that steelhead trout held in isolation had excellent fins, indicating that fin erosion was a result of aggressive interaction, stress, or some water quality factor correlated with low density. Nutrition was clearly not involved in this particular case although it can influence fin erosion (Halver 1954; Ketola 1983; Lemm et al. 1988; Kindschi et al. 1991b).

In the wild populations, species differences in relative fin length were slight, but statistically significant in most cases. Fins of rainbow and brown trout were most similar, but most fins of cutthroat were usually slightly shorter. Our results for hatchery fish showed that all trout species (including brook trout) were susceptible to fin erosion, although no species showed greater susceptibility. Fin erosion has not been previously quantified in either brook, brown, or cutthroat trout. However, there were significant interspecific differences for fin susceptibility to erosion. For example, rainbow trout generally had greater erosion of the dorsal fin than cutthroat trout, but the reverse was true for pectoral fins. This result may be related to differences in aggressive behavior that have been noted for these two species (Nilsson and Northcote 1981).

There were significant differences in fin erosion among different strains of rainbow trout. The FD strain generally had the most severe fin erosion. Statements regarding strain differences are tempered by the possibility that there are genetically based differences in fin lengths that could affect the interpretation of strain comparisons. For example, research on intraspecific morphological variation has documented local adaptation in fin size for both chum (*O. keta*) and pink salmon (*O. gorbuscha*) (see review by Taylor 1991). Whether significant intraspecific variation occurs in the fin size of trout has not yet been established.

Under current hatchery practices (generally following those outlined in Piper et al. 1989 and Brannon 1991), the problem of fin erosion in trout from Utah hatcheries still appears to be widespread. Furthermore, the problem is not confined to dorsal fins, but significantly affects all rayed fins. Such findings demonstrate the need for continued research into reducing hatchery-induced fin erosion. The present study demonstrates that relative fin length can be used to accurately quantify the degree of fin erosion in hatchery and wild trout. This method represents a viable parametric alternative to the use of subjective categorical "fin scores, fin grades, or fin index" (Soderberg and Meade 1987; Lemm et al. 1988; Mork et al. 1989; Goede and Barton 1990). Statistical "power" is always decreased with categorical statistical tests (Zar 1974), so relative fin length may represent a more powerful tool for assessing fin erosion damage in hatchery trout.

Acknowledgments

We thank John Wullschleger for leading the electrofishing crews and all of the Utah fish hatchery staff for their assistance. We also thank Bruce Schmidt, Joe Valentine, Russ Lee, Christopher Wilson, and Ron Goede for their review of the manuscript. Research was supported by the Federal Aid in Sport Fish Restoration Program, project No. F-35-R, and the Utah Division of Wildlife Resources.

References

Abbott, J.C., and L.M. Dill. 1985. Patterns of aggressive attack in juvenile steelhead trout (*Salmo gairdneri*). Can. J. Fish. Aquat. Sci. 42: 1702–1706.

Brannon, E.L. 1991. Rainbow trout culture, p. 21–55. *In* R.R. Stickney [ed.] Culture of salmonid fishes. CRC Press, Boca Raton, Fla.

Eipper, A.W., and J.L. Forney. 1965. Evaluation of partial fin clips for marking largemouth bass, walleyes and rainbow trout. N.Y. Fish Game J. 12: 233–240.

Gjerde, B., and T. Refstie. 1988. The effect of fin-clipping on growth rate, survival and sexual maturity of rainbow trout. Aquaculture 73: 383–389.

Goede, R.W., and B.A. Barton. 1990. Organismic indices and an autopsy-based assessment as indicators of health and condition of fish, p. 93–108. *In* S.M. Adams [ed.] Biological indicators of stress in fish. Symp. 8. American Fisheries Society, Bethesda, Md.

Halver, E. 1954. Fish diseases and nutrition. Trans. Am. Fish. Soc. 98: 762–771.

Heimer, J.T., W.M. Frazier, and J.S. Griffith. 1985. Poststocking performance of catchable-size hatchery rainbow trout with and without pectoral fins. N. Am. J. Fish. Manage. 5: 21–25.

Jones, R. 1979. Materials and methods used in marking experiments in fishery research. Fish. Tech. Pap. No. 190 (FIRM/T190). Food and Agriculture Organization of the United Nations, Rome, Italy.

Ketola, H.G. 1983. Requirement for dietary lysine and arginine by fry of rainbow trout. J. Anim. Sci. 56: 101–107.

Kindschi, G.A. 1987. Method for quantifying degree of fin erosion. Prog. Fish-Cult. 49: 314–315.

Kindschi, G.A., H.T. Shaw, and D.S. Bruhn. 1991a. Effects of baffles and isolation on dorsal fin erosion in steelhead trout (*Oncorhynchus mykiss*). Aquacult. Fish. Manage. 22: 343–350.

Kindschi, G.A., H.T. Shaw, and D.S. Bruhn. 1991b. Effect of diet on the performance, fin quality, and dorsal skin lesions in steelhead. J. Appl. Aquacult. 1: 113–120.

Lemm, C.A., D.V. Rottiers, D.S. Dropkin, and B.A. Dennison. 1988. Growth, composition, and fin quality of Atlantic Salmon fed different diets at seasonal temperatures in a laboratory and hatchery. U.S. Fish Wildl. Serv. Biol. Rep. 88: 1–12.

Mears, H.C., and R.W. Hatch. 1976. Overwinter survival of fingerling brook trout with single and multiple fin clips. Trans. Am. Fish Soc. 6: 669–674.

Mork, J., T. Jarvi, and L.P. Hansen. 1989. Lower prevalence of fin erosion in mature than in immature Atlantic salmon (*Salmo salar*) parr. Aquaculture 80: 223–229.

Nicola, S.J., and A.J. Cordone. 1973. Effects of fin removal on survival and growth of rainbow trout (*Salmo gairdneri*) in a natural environment. Trans. Am. Fish. Soc. 102: 753–758.

Nilsson, N.A., and T.G. Northcote. 1981. Rainbow trout (*Salmo gairdneri*) and cutthroat trout (*S. clarki*) interactions in coastal British Columbia lakes. Can. J. Fish. Aquat. Sci. 38: 1228–1246.

Piper, R.G., I.B. McElwain, L.E. Orme, J.P. McCraren, L.J. Fowler, and J.R. Leonard. 1989. Fish hatchery management. 4th ed. U.S. Fish and Wildlife Service, Washington, D.C.

SAS Institute, Inc. 1988. SAS/STAT user's guide, 6.03 edition. SAS Institute, Inc., Cary, N.C.

Saunders, R.L., and K.R. Allen. 1967. Effects of tagging and fin-clipping on the survival and growth of Atlantic salmon between smolt and adult stages. J. Fish. Res. Board Can. 24: 2595–2611.

Schneider, R., and B.L. Nicholson. 1980. Bacteria associated with fin rot disease in hatchery-reared Atlantic salmon (*Salmo salar*). Can. J. Fish. Aquat. Sci. 37: 1505–1513.

Simpson, A.L., N.B. Metcalfe, and J.E. Thorpe. 1992. A simple nondestructive biometric method for estimating fat levels in Atlantic salmon, *Salmo salar* L., parr. Aquacult. Fish. Manage. 23: 23–29.

Soderberg, R.W., and J.W. Meade. 1987. Effects of rearing density on growth, survival, and fin condition of Atlantic salmon. Prog. Fish-Cult. 49: 280–283.

Stuart, T.A. 1958. Marking and regeneration of fins. Freshwater and Salmon Fisheries Research Publication 22, Scottish Home Department, Edinburgh, Scotland.

Taylor, E.B. 1991. A review of local adaptation in Salmonidae, with particular reference to Pacific and Atlantic salmon. Aquaculture 98: 185–207.

Weber, D., and R.J. Wahle. 1969. Effect of fin clipping on survival of sockeye salmon (*Oncorhynchus nerka*). J. Fish. Res. Board Can. 26: 1263–1271.

Zar, J.H. 1974. Biostatistical analysis. Prentice-Hall, Inc., Englewood Cliffs, N.J.

Age- and Sex-Specific Survival of Northern Grand Bank Capelin (*Mallotus villosus*)

Nancy L. Shackell, Peter A. Shelton, John M. Hoenig, and James E. Carscadden

Department of Fisheries and Oceans, P.O. Box 5667, St. John's, NF A1C 5X1, Canada

Shackell, N.L., P.A. Shelton, J.M. Hoenig, and J.E. Carscadden. 1994. Age- and sex-specific survival of northern Grand Bank capelin (*Mallotus villosus*). Can. J. Fish. Aquat. Sci. 51: 642–649.

Age-specific, sex-specific survival rates for immature and mature capelin (*Mallotus villosus*) were estimated by linear least-squares models, using abundance data derived from annual acoustic/trawl research surveys conducted from 1982 to 1990 on the northern Grand Bank. Survival estimates for age 2 immature fish were comparable between sexes (annual survival equals approximately 40%). Survival estimates for age 4 mature fish differed between sexes, with females having a higher (25–51%) average survival estimate than males (6%). Survival estimates for immature and mature age 3 fish were equivocal; immature males and females had comparable rates (30.3–32.3 and 15.2–26.6%, respectively) whereas a greater proportion of mature females (25–50%) survived than of mature males (2.5–13%). The stated ranges denote survival estimates including and excluding an influential data point, respectively. Higher average survival of mature females than of mature males may be a result of sex-specific behavior during beach spawning. The average annual contribution of surviving mature females to the total number of female spawners was estimated as 24–47%.

Nous avons calculé les taux de survie spécifiques à l'âge et au sexe pour les capelans (*Mallotus villosus*) immatures et matures par des modèles linéaires des moindres carrés, en nous servant des données sur l'abondance tirées de relevés annuels de recherche menés par des méthodes acoustiques et au chalut, de 1982 à 1990, sur le nord du Grand Banc. Les taux de survie estimés pour les poissons immatures d'âge 2 étaient comparables d'un sexe à l'autre (le taux annuel de survie est égal à environ 40 %). Les taux de survie estimés pour les poissons matures d'âge 4 différaient entre les sexes, celui des femelles étant supérieur en moyenne (25–51 %) à celui des mâles (6 %). Les taux de survie estimés pour les poissons immatures et matures d'âge 3 étaient équivoques; les mâles immatures et matures avaient des taux comparables (30,3–32,3 et 15,2–26,6 % respectivement), tandis qu'une proportion plus forte de femelles matures (25–50 %) survivaient par rapport aux mâles matures (2,5–13 %). Les fourchettes ainsi établies indiquent que les estimations du taux de survie incluent ou excluent un point de données d'importance. Le fait que le taux moyen de survie des femelles matures soit plus élevé que celui des mâles matures peut être lié à un comportement spécifique au sexe pendant la ponte sur les grèves. On estime à 24–47 % la proportion annuelle moyenne des femelles matures survivantes par rapport au nombre total de génitrices.

Received March 25, 1993
Accepted October 7, 1993
(JB859)

Reçu le 25 mars 1993
Accepté le 7 octobre 1993

Capelin (*Mallotus villosus*) is an abundant cold-water fish inhabiting northern oceans around the globe. It is generally characterized by small body size, short generation time, high variability in population size, and semelparity. On the basis that capelin is a principal forage species in northern ecosystems, it is possible that semelparity evolved in response to a high adult mortality rate. However, postspawning survival may occur in the Northwest Atlantic Ocean. Females have been observed with residual eggs 4–5 mo after the spawning period (Templeman 1948; Winters 1971), and the inshore fishery data consistently show higher proportions of females than males at the oldest ages (Nakashima and Harnum 1992). The possibility of iteroparous female capelin is intriguing from both a life history perspective, in that a sex-specific life history strategy may have evolved, and a fishery perspective, in that iteroparous individuals contribute to the spawning stock and fishery. We adopt a fishery perspective in this paper.

It has been difficult to estimate the degree of iteroparity in Northwest Atlantic populations of capelin in the absence of separate survival estimates of immature and mature fish. Carscadden et al. (1985) indirectly estimated spawning mortality by using the average total mortality rate estimated from Canadian and Russian catch data, the proportions mature estimated in Winters and Campbell (1974), and assuming a natural mortality of 0.3 for all age groups. However, the authors emphasized that the spawning mortality estimates may be imprecise and were derived to demonstrate the primary topic of the paper, which was an indirect method of estimating capelin maturation rates.

Recently, Shelton et al. (1993) used the acoustic/trawl research survey data of Miller and Carscadden (1991), in which the proportions of mature fish were estimated directly, to estimate average annual survival rates separately for immature and mature capelin from the northern Grand Bank. In this paper, we show that much of the residual variability from the fit of the model in Shelton et al. (1993) is accounted for by age and sex, and we use those results to estimate the contribution of iteroparous individuals to the total spawning stock.

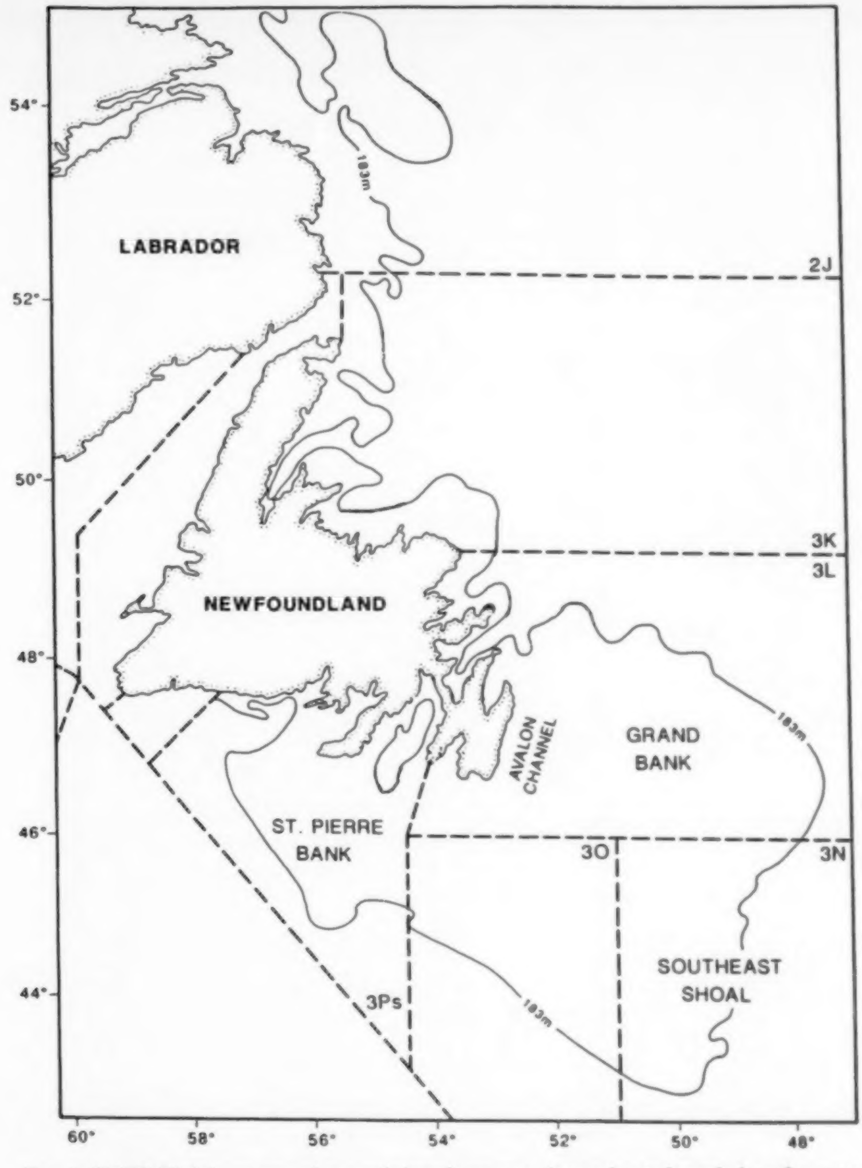

FIG. 1. NAFO Divisions: annual acoustic/trawl surveys. Approximate boundaries of survey area: 46°N to 49°N, 49°30′W to 52°45′W.

Material and Methods

Acoustic/Trawl Research Survey Database

Annual acoustic surveys of capelin are conducted for the purpose of recommending total allowable catches based on a projection of the numbers of mature capelin expected inshore in the following year (see Miller and Carscadden 1991). The survey area was located on the northern Grand Bank, roughly bounded by 46°N to 49°N and 49°30′W to 52°45′W, within Northwest Atlantic Fisheries Organization Division 3L (NAFO Div. 3L) (Fig. 1). Acoustic survey methods (data acquisition/echo integration systems, calibration parameters, etc.) and survey design are described in Miller (1985) and Miller and Carscadden (1989, 1991).

Midwater trawls were used to verify species identity and sample capelin length, age, and maturity throughout the survey area each year. Two hundred fish per trawl were randomly sampled and their lengths measured. From this random sample, stratified samples of two fish per half-centimetre group for each sex were used to construct age–length relationships. Length composition and the age–length key were used to determine the age composition in subdivided areas (strata) within the larger survey area. Total survey age composition and proportion of mature fish for each year were calculated by weighting each stratum by its estimated biomass.

TABLE 1. Numbers-at-age (millions) (N) and percent mature (P) of males and females for 1982–90 at ages 2–6 as estimated from the acoustic/trawl surveys. The total of each N column denotes the sum over all years; the total of each P column denotes % (total number of mature animals/total N). The average is the sum of P/total number of years.

	Age (yr)									
	2		3		4		5		6	
Year	*N*	*P*	*N*	*P*	*N*	*P*	*N*	*P*	*N*	*P*
					Males					
1982	4.13	4.82	7.83	74.51	0.63	95.95	0.19	97.98	0.00	0.00
1983	1.68	1.15	0.81	30.14	0.25	94.61	0.00	—	0.00	0.00
1984	9.31	2.38	2.32	68.86	0.98	98.06	0.07	98.30	0.00	0.00
1985	168.37	0.48	35.63	27.63	0.91	82.54	0.15	100.00	0.00	0.00
1986	32.68	0.17	73.01	20.52	7.12	90.67	0.00	—	0.00	0.00
1987	40.75	0.29	6.89	40.96	18.09	99.06	0.48	99.41	0.00	0.00
1988	176.58	0.67	34.01	65.53	5.98	100.00	1.13	100.00	0.00	0.00
1989	138.89	0.17	39.73	34.12	3.92	97.63	0.00	—	0.00	0.00
1990	161.21	0.26	62.24	21.84	18.76	94.25	0.11	100.00	0.00	0.00
Total	733.59	0.44	262.47	32.29	56.64	96.08	2.14	99.63	0.00	0.00
Average *P*		1.15		42.68		94.75		99.28		0.00
					Females					
1982	5.42	9.06	8.28	87.69	1.74	97.66	0.58	99.26	0.18	99.55
1983	1.74	23.43	1.12	73.38	0.52	90.29	0.06	86.62	0.00	—
1984	11.73	13.43	3.90	93.94	2.16	99.23	0.39	99.66	0.02	98.12
1985	201.15	4.84	44.84	56.04	2.89	92.33	2.14	100.00	0.03	100.00
1986	26.69	1.35	85.05	50.18	14.17	94.82	0.71	100.00	0.31	100.00
1987	47.32	2.71	11.41	96.82	20.83	99.75	3.43	99.76	0.08	100.00
1988	203.86	3.08	31.64	87.83	3.69	97.97	14.17	99.21	1.53	100.00
1989	175.83	2.45	56.43	62.01	7.13	97.79	0.43	97.25	0.96	100.00
1990	191.96	6.88	106.72	68.93	36.84	97.17	1.85	65.31	0.00	—
Total	865.71	4.35	349.39	64.95	89.95	97.34	23.76	96.69	3.10	100.00
Average *P*		7.16		74.18		96.44		94.38		99.96

We used information from surveys conducted in April–May, just prior to the inshore spawning migration, from 1982 to 1990. In April and May, the gonads of mature and immature capelin are visually distinguishable. Estimates of proportions of mature fish and numbers-at-age (Table 1) were used to calculate age-specific, sex-specific survival rates.

The population structure of capelin off the Newfoundland and Labrador coasts is unresolved. The regulatory agencies use the current designation of two to three separate spawning populations along a north–south gradient, but that designation is based largely on circumstantial evidence (summarized in Nakashima 1992). A recent study of capelin migration patterns indicated that mature capelin from northern (NAFO Div. 3K) and southern (NAFO Div. 3L) areas may be mixing during their spawning migration (Nakashima 1992). Nonetheless, capelin in NAFO Div. 3L are still treated as a separate unit stock for management purposes.

Gulland (1983) stated that "a group of fish can be treated as a unit stock if possible differences within the group and interchanges with other groups can be ignored without making the conclusions reached [from the model] depart from reality to an unacceptable extent." For the purpose of estimating survival rates, we could assume that capelin in the 3L survey area behaved as a unit stock for the following reasons. The average annual age structure estimated from the research trawls consists of few 1-yr-olds, abundant 2-yr-olds, followed by decreasing abundances of ages 3, 4, 5, and 6. Thus, the offshore samples are not representative of the abundance of fish less than 2 yr old (Nakashima 1990). In contrast, abundance estimates of males and females of ages 2–6 were judged consistent over time on the basis that strong (relatively abundant) year classes in year t corresponded to strong year classes in year $t + 1$. Further, acoustic abundance estimates of mature capelin are correlated with inshore fishery catch rate data a few months later (Carscadden 1992).

We could assume the survey data were representative of a single stock until 1991, in which year the capelin biomass detected in the acoustic survey was exceedingly low and the estimated age distribution changed dramatically relative to former years (Miller and Carscadden 1991). Capelin in 1991 were suspected to have been missed by the acoustic survey perhaps because of a change in capelin distribution. Thus, we assume that the annual acoustic surveys were representative of the stock of ages 2–6 in the northern Grand Bank stock for the years 1982–90 only.

Survival Estimation

Shelton et al. (1993) proposed a simple model for the survival of capelin cohorts on the basis that the fishery captures mature fish only:

TABLE 2. Age-specific, sex-specific survival rates of the northern Grand Bank capelin stock as estimated by linear regression. R^2 is the amount of variability explained by model (2) for ages 2, 4, and 5 and Model (1) for age 3. S is the regression coefficient (estimate of survival rate). SE is the standard error of the regression coefficient. $n = 8$ for each analysis except $n = 7$ in analyses excluding an influential datum.

	R^2	S	SE
Age 2			
Male	0.826	0.366	0.064
Female	0.853	0.428	0.067
Age 3			
Male	0.854		
Immature		0.322	0.100
Mature		0.130	0.216
Female	0.816		
Immature		0.152	0.360
Mature		0.497	0.273
Age 3, excluding influential datum			
Male	0.944		
Immature		0.303	0.050
Mature		0.025	0.111
Female	0.973		
Immature		0.266	0.089
Mature		0.250	0.072
Age 4			
Male	0.896	0.057	0.007
Female	0.843	0.511	0.083
Age 4, excluding influential datum			
Female	0.853	0.250	0.042
Age 5			
Male		0	
Female	0.519	0.089	0.033

$$(1)\quad N_{a+1,t+1} = N_{a,t}(1 - p_{a,t})S_i + (N_{a,t}p_{a,t} - C_{a,t})S_m + \epsilon_{a+1,t+1}$$

where N is the number of fish estimated from the acoustic survey, C is the commercial catch by number (taken during a fishery lasting about 4 wk), p is the proportion mature by number, S_i is the average annual (finite) survival rate of immature fish, S_m is the average annual (finite) survival rate of mature fish, and ϵ is randomly distributed error. The subscripts a and t denote age and year, respectively. Shelton et al. (1993) estimated S_i as 0.35 (SE = 0.043) and S_m as 0.227 (SE = 0.239). These results were considered practical for potential use in assessment models (Shelton et al. 1993).

It subsequently became apparent that the proportion of females increases with age. Below are the total numbers-at-age (millions) estimated from the acoustic/trawl surveys and summed over the years 1982–90 and percent female at each age from 2 to 6:

	2	3	4	5	6
Total abundance	1599.3	611.9	146.6	25.9	3.1
% female	54.1	57.1	61.4	91.7	100.0

Since the older age classes are largely mature and the sex ratio becomes progressively more skewed with age, it appears that mature females have a higher survival than mature males. Model (1) can be fitted separately to each sex or to each sex–age combination. Based on the predominance of females in older age classes, we (i) analyzed ages and sexes separately and (ii) examined age–sex–year-specific survival rates.

Regression estimates

We first fitted equation (1) separately for each sex with all age groups combined. We then analyzed each sex–age combination. Since landings averaged only 4% of the predicted biomass from 1982 to 1990 (Shelton et al. 1993), we eliminated the catch term for simplicity. Most (>94%) 2-yr-old capelin are immature, so all fish were assumed immature in the analysis of survival of age 2 fish. Most (>96%) 4 and most (>97%) 5-yr-old capelin are mature; so all fish were assumed mature in the analysis of survival of 4- and 5-yr-olds. Survival rates of 2-, 4-, and 5-yr-olds were estimated separately for each age by sex from the simple regression model

$$(2)\quad N_{a+1,t+1} = N_{a,t}\,S_i + \epsilon_{a+1,t+1}$$

where the symbols are as described previously.

Estimating survival of 3-yr-olds involved accounting for the varying proportion mature among years. Separate estimates for immature and mature 3-yr-olds for each sex were obtained from model (1) excluding commercial landings.

Survival ratios

Age-specific, sex-specific survival rates were estimated for each pair of adjacent years by computing the ratio of female, or male, capelin at a given age in a given year to the number of capelin at the previous age in the previous year ($N_{a+1,t+1}/N_{a,t}$).

Contribution of surviving mature females to the spawning stock

The relative contribution (RC) of surviving mature females to the total spawning stock from 1982 to 1990 was estimated from

$$(3)\quad \mathrm{RC} = \frac{\sum_{t=82}^{90}\sum_{a=3}^{6} N_{a,t}^{M}\,S_{m,a}}{\sum_{t=82}^{90}\sum_{a=3}^{6} N_{a,t}^{M}}$$

where $N^{M}_{a,t}$ is the number of mature females at age a in year t and $S_{m,a}$ is the survival estimate of mature females at age a. This is simply an estimate of the proportion of spawing females that will survive to the next spawning season averaged over the 9-yr period.

Results

When ages are combined, the sex-specific survival estimates ($n = 24$) are 0.427 (SE = 0.043) and 0.358 (SE = 0.194) for immature and mature females, respectively, and 0.365 (SE = 0.037) and 0.073 (SE = 0.280) for immature and mature males, respectively.

When ages are analyzed separately, survival of immature 2-yr-old male capelin does not appear to differ from that of immature 2-yr-old females (Table 2; Fig. 2–4). In the mature age classes, survival of age 4 females is higher than that of age 4 males. Annual estimates of survival (ratio of $N_{a+1,t+1}/N_{a,t}$) of age 4 females are consistently higher than those of males (Fig. 4, $p = 0.008$ for a two-sided sign test with $n = 8$ comparisons). The pattern for 3-yr-olds is less clear but consistent with the above. Overall, survival of

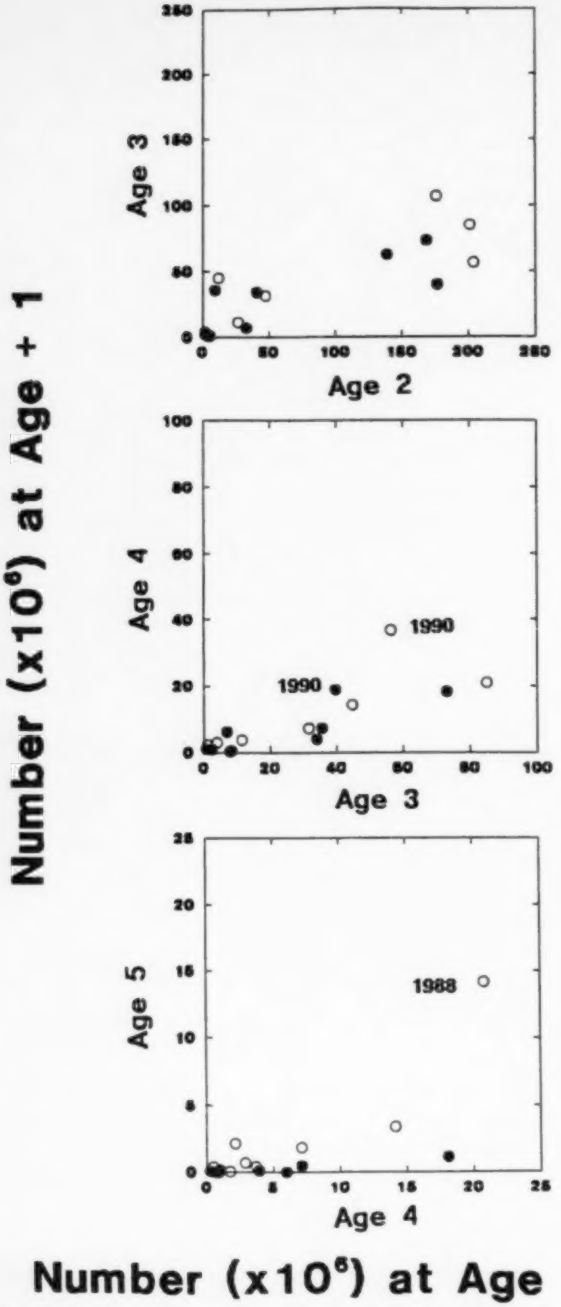

FIG. 2. Number-at-age + 1 as a function of number-at-age for ages 2–5 for each sex. The 1988 and 1990 survey points are denoted as influential data points assuming a linear function between the dependent and independent variables (see text). Solid circles refer to males and open circles to females.

mature age 3 and 4 females appears to be higher than that of mature age 3 and 4 males. Further, there are virtually no males that survive from age 5 to 6 whereas a small fraction of females do (Table 1; Fig. 3).

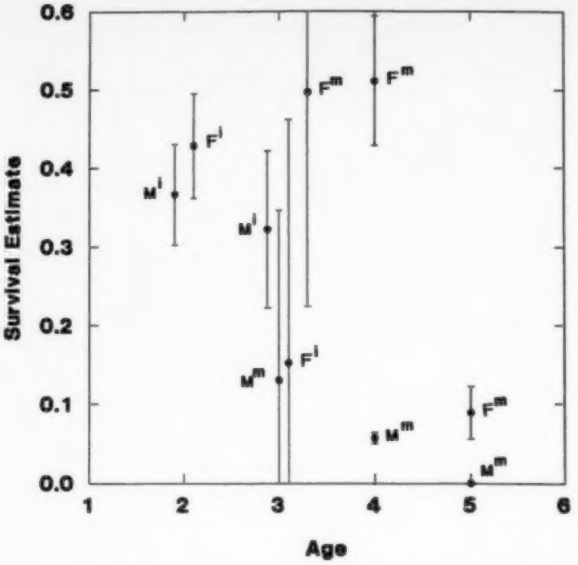

FIG. 3. Survival from age a to age $a + 1$, as estimated from models (1) and (2) described in the text. M^i refers to immature males, M^m to mature males, F^i to immature females, and F^m to mature females. Vertical bars are ±1 SE.

Examination of the residual variation and original plots of dependent and independent variables made it apparent that one datum in each analysis of age 3 male and females and one datum in analysis of age 4 females were influencing survival estimates more than other data. Subsequent analyses excluding those data confirmed their influence. Given that the stability of our results is low partially due to the low number of data points, and that one datum can substantially change the results, we present survival estimates with and without the most influential datum. When age 3 females and males are analyzed without the most influential datum (labelled in Fig. 2), survival estimates change notably, standard errors become smaller, and the amount of variance explained increases (Table 2). The survival estimate for age 4 females drops from 0.511 (SE = 0.083; $n = 8$) to 0.250 (SE = 0.042; $n = 7$) when an influential datum (labelled in Fig. 2) is excluded from the analysis. Nonetheless, age 4 females still have a higher survival rate than males.

The relative contribution of surviving mature females to the total female spawning stock, as estimated from equation (3), is 47% when survival rates estimated from all the data were used and 24% when survival rates were estimated from data excluding the influential data points.

Discussion

Sex-Specific Survival

Survival of mature age 4 and 5 female capelin is clearly higher than that of mature males; whether differential survival between sexes occurs at age 3 is equivocal. Mature female capelin may survive longer than mature males as a result of differential spawning behavior. Male capelin typically rest close inshore waiting for females, who stay farther offshore until ready to spawn. Waiting males meet successive

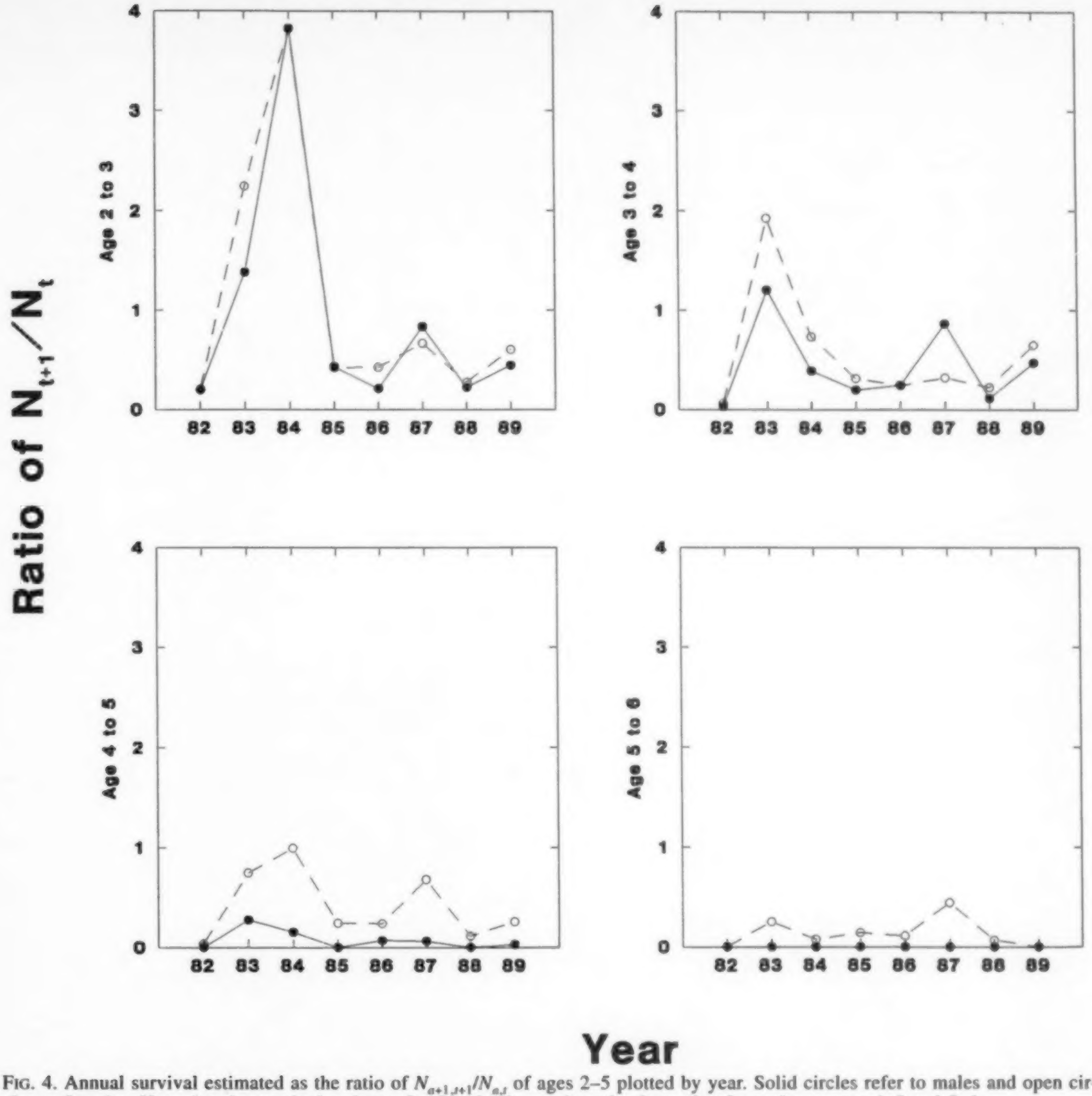

FIG. 4. Annual survival estimated as the ratio of $N_{a+1,t+1}/N_{a,t}$ of ages 2–5 plotted by year. Solid circles refer to males and open circles to females. Note that the survival estimate for females is consistently above that for males at ages 4–5 and 5–6.

waves of incoming females and most of the males die close to, or on, the beach whereas females return back offshore (Templeman 1948). We interpret this behavior to indicate that males spawn more than females within a season and, consequently, are at greater risk to mortality due to greater physiological stress from multiple spawnings and/or greater physical trauma sustained in the surf zone.

Skewed sex ratios observed in fish populations have been attributed to sampling bias due to physical segregation of the sexes, to size-selective sampling, or to differential exploitation of the sexes (Hoenig and Lawing 1983; Mason and Phillips 1985; Botha 1986; Young et al. 1987). We have no evidence that sampling factors account for our results. Skewed sex ratios have also been attributed to differences in level of predation (e.g., Clarke 1983) which is one of the factors that can lead to sex-specific life history strategies (Brown et al. 1987; Holtby and Healey 1990; Bowen et al. 1991; Mullan et al. 1992). We believe that differences in spawning behavior, moreso than predation, account for the skewed sex ratio in the NAFO Div. 3L capelin stock. Whether spawning behavior has caused a sex-specific life history strategy to evolve cannot be addressed by our analyses.

Contribution of Surviving Mature Females to the Total Female Spawning Stock and Fishery

The contribution of surviving mature females to the total spawning stock could be considerable: 24–47% (excluding and including influential data points, respectively) of the mature spawning stock over the years 1982–90 were estimated to be mature females that had survived at least one spawning season. The contribution of older age classes may also be an important factor in regulation of capelin populations. If we assume that larval/juvenile survival is largely due to unpredictable environmental variability (Leggett et al. 1984; Frank and Leggett 1981a, 1991b), then a greater diversity of life history traits (e.g., egg size and quality, timing and/or choice of spawning location, etc.) may lead to a decreased variance in year class strength. Older females differ from younger females in various ways, such as having a greater fecundity (Nakashima 1987). Winters (1971) proposed that repeat spawners, as distinguished by otolith characteristics, had a greater fecundity than did first-time spawners of equal age and size. In essence, simply considering the number of fish may underestimate the contribution of older females to the spawning potential.

Model Adequacy

Models (1) and (2) assume interannual variability in the survival rates because the independent variables are assumed known without error in a linear regression model. Furthermore, abundance estimates act as both independent and dependent variables and are assumed known. Thus, the random error term has to refer to the variability in survival rates. In reality, considerable measurement error probably exists in the estimates of numbers and of the proportions of mature fish. To study interannual variability in survival and survival estimates, we would need to estimate the variability in each input variable (acoustic estimates, age composition, proportion of mature fish). This has yet to be undertaken. Therefore, the estimated standard errors of our estimates of survival rates are only indicative of relative precision.

The survival estimates from the regression models are survival rates averaged over time, and these estimated averages will become more precise as more years of data are obtained. In the interim, we have developed a model for future data analyses. The present analyses with and without influential survey data points illustrate the degree of stability of the results. Certain aspects of survival are clear regardless of whether or not influential points are considered in the analysis. Thus, survival rates of immature fish appear to be comparable among the sexes, survival of mature females at ages 4 and 5 appears to be higher than that of mature males of the same age, and 4-yr-old fish appear to have higher survival than 5-yr-olds of the same sex. The greatest uncertainty concerns the survival rates of 3-yr-olds. When the influential data point is excluded, immature 3-yr-old fish have survival rates not significantly different from those of immature 2-yr-olds whereas mature fish have survival rates similar to that of mature 4-yr-olds of the corresponding sex.

We also examined interannual variability in survival rates by computing survival ratios. The observed variability in the estimates reflects both measurement error and actual interannual variability in survival. The observed variability is therefore overestimated, which is conservative. If information becomes available on the measurement errors, then we could determine if survival rates can be estimated with a given level of precision. The annual estimates of survival are imprecise as evidenced by the large fraction of estimates greater than 100%. Although we cannot obtain precise estimates, we can still test hypotheses about the effects of age and sex. The estimate of survival for females was higher than the corresponding estimate for males at both age 4 and 5 in every year; therefore, older females have a higher survival rate than older males.

This paper provides estimates of capelin survival rates that differ from those currently being used for stock assessment in the Northwest Atlantic (see Carscadden et al. 1985) and, in the case of mature survival, those used for assessment in the Barents Sea (Tjelmeland 1985). The current NAFO Div. 3L stock assessment model, combined with the existing 10% harvest rate, has been shown to be reasonably risk averse (Shelton et al. 1993). Nevertheless, we advocate the use of the recently estimated survival rates in the future development of assessment models. The higher survival rates of mature females, and therefore the greater degree of iteroparity than previously assumed, should not be taken to imply that higher exploitation rates are acceptable. The estimates of survival rate are associated with considerable uncertainty, and this should be taken into account in an assessment procedure that quantifies the risk associated with management decisions.

Acknowledgements

We thank Dan Miller who coordinated the acoustic/trawl surveys and the many individuals of the Department of Fisheries and Oceans and of the crew the *Gadus Atlantica* who have participated in the offshore capelin surveys. The research and computer facilities were funded by the Northern Cod Science Program of the Department of Fisheries and Oceans. The constructive comments of G.H. Winters and two anonymous reviewers were used to revise an earlier version of the manuscript.

References

BOTHA, L. 1986. Reproduction, sex ratio and rate of natural mortality of cape hakes *Merluccius capensis* Cast. and *M. paradoxus* Franca in the Cape of Good Hope area. S. Afr. J. Mar. Sci. 4: 23–35.

BOWEN, S.H., D.J. D'ANGELO, S.H. ARNOLD, M.J. KENIRY, AND R.J. ALBRECHT. 1991. Density-dependent maturation, growth, and female dominance in Lake Superior lake herring (*Coregonus artedii*). Can. J. Fish. Aquat. Sci. 48: 569–576.

BROWN, E.J., JR., R.L. ARGLE, N.R. PAYNE, AND M.E. HOLEY. 1987. Yield and dynamics of destabilized chub (*Coregonus* spp.) populations in Lakes Michigan and Huron, 1950–84. Can. J. Fish. Aquat. Sci. 44 (Suppl. 2): 371–383.

CARSCADDEN, J. 1992. Capelin in NAFO Division 2JK3L. CAFSAC Res. Doc. 92/18: 14 p.

CARSCADDEN, J.E., G.H. WINTERS, AND D.S. MILLER. 1985. An indirect method of estimating maturation rates of cohorts of capelin (*Mallotus villosus*). J. Northwest Atl. Fish. Sci. 6: 135–140.

CLARKE, T.A. 1983. Sex ratios and sexual differences in sizes among mesopelagic fishes from the Central Pacific Ocean. Mar. Biol. 73: 201–209.

FRANK, K.T., AND W.C. LEGGETT. 1981a. Wind regulation of emergence times and early larval survival in capelin (*Mallotus villosus*). Can. J. Fish. Aquat. Sci. 38: 215–223.

FRANK, K.T., AND W.C. LEGGETT. 1981b. Prediction of egg development and mortality rates in capelin (*Mallotus villosus*) from meteorological, hydrographic, and biological factors. Can. J. Fish. Aquat. Sci. 38: 1327-1338.

GULLAND, J.A. 1983. Fish stock assessment: a manual of basic methods. FAO/Wiley series on food and agriculture, Vol. 1. John Wiley & Sons, New York, N.Y. 223 p.

HOENIG, J.M., AND W.D. LAWING. 1983. Using incomplete tagging data to estimate the total mortality rate when the sex ratio is skewed. ICES C.M. 1983/D:24: 18 p.

HOLTBY, L.B., AND M.C. HEALEY. 1990. Sex-specific life history tactics and risk-taking in coho salmon. Ecology 71: 678–690.

Leggett, W.C., K.T. Frank, and J.E. Carscadden. 1984. Meteorological and hydrographic regulation of year-class strength in capelin (*Mallotus villosus*). Can. J. Fish. Aquat. Sci. 41: 1193–1201.

Mason, J.C., and A.C. Phillips. 1985. Biology of the bathylagid fish, *Leuroglossus schmidti*, in the Strait of Georgia, British Columbia, Canada. Can. J. Fish. Aquat. Sci. 42: 1144–1153.

Miller, D.S. 1985. The use of hydroacoustic surveys to estimate capelin biomass in NAFO divisions 2J + 3KLNO. NAFO SCR Doc. 85/105 Ser. No. N1081: 18 p.

Miller, D.S., and J.E. Carscadden. 1989. Biomass estimates from two hydroacoustic surveys for capelin (*Mallotus villosus*) in NAFO Divisions 3L and 3N and observation of the Soviet fishery for capelin in Division 3NO. NAFO SCR Doc. 89/52 Ser. No. N1631: 15 p.

Miller, D.S., and J.E. Carscadden. 1991. Results of two acoustic surveys for capelin (*Mallotus villosus*) in NAFO Divisions 3L in 1991. NAFO SCR Doc. 91/123 Ser. No. N2016: 6 p.

Mullan, J.W., A. Rockhold, and C.R. Chrisman. 1992. Life histories and precocity of chinook salmon in the mid-Columbia River. Prog. Fish-Cult. 54: 25–28.

Nakashima, B.S. 1987. Regional and temporal variations in fecundity of capelin in Newfoundland waters. Trans. Am. Fish. Soc. 116: 864–873.

Nakashima, B.S. 1990. Escapement from a Diamond IX midwater trawl during acoustic surveys for capelin (*Mallotus villosus*) in the Northwest Atlantic. J. Cons. Int. Explor. Mer 47: 76–82.

Nakashima, B.S. 1992. Patterns in coastal migration and stock structure of capelin (*Mallotus villosus*). Can. J. Fish. Aquat. Sci. 49: 2423–2429.

Nakashima, B.S., and R.W. Harnum. 1992. The inshore capelin fishery in NAFO Division 3L in 1991. NAFO SCR Doc. 92/3 Ser. No. N2036: 16 p.

Shelton, P.A., J.E. Carscadden, and J.M. Hoenig. 1993. Risk evaluation of the 10% harvest rate procedure for capelin in NAFO Division 3L, p. 193–201. *In* S.J. Smith, J.J. Hunt, and D. Rivard [ed.] Risk evaluation and biological reference points for fisheries management. Can. Spec. Publ. Fish. Aquat. Sci. 120: 442 p.

Templeman, W. 1948. The life history of the caplin (*Mallotus villosus* O.F. Muller) in Newfoundland waters. Bull. Nfld. Gov. Lab. No. 17: 1–151.

Tjelmeland, S. 1985. The capelin assessment model – a documentation, p. 31–43. *In* H. Gjosœter [ed.] The Proceedings from the Soviet–Norwegian Symposium on Barents Sea Capelin, Bergen, August 1984. Institute of Marine Research, Bergen, Norway. 236 p.

Winters, G.H. 1971. Fecundity of the left and right ovaries of Grand Bank capelin (*Mallotus villosus*). J. Fish. Res. Board Can. 28: 1029–1033.

Winters, G.H., and J.S. Campbell. 1974. Some biological aspects and population parameters of Grand Bank capelin. ICNAF Res. Doc. 74/76: 23 p.

Young, J.W., S.J.M. Blaber, and R. Rose. 1987. Reproductive biology of three species of midwater fishes associated with the continental slope of Eastern Tasmania, Australia. Mar. Biol. 95: 323–332.

Impacts of Flounder Trawls on the Intertidal Habitat and Community of the Minas Basin, Bay of Fundy

Michael Brylinsky and Jamie Gibson

Acadia Centre for Estuarine Research, Acadia University, Wolfville, NS B0P 1X0, Canada

and Donald C. Gordon Jr.

Department of Fisheries and Oceans, Habitat Ecology Division, Bedford Institute of Oceanography, Dartmouth, NS B2Y 4A2, Canada

Brylinsky, M., J. Gibson, and D.C. Gordon Jr. 1994. Impacts of flounder trawls on the intertidal habitat and community of the Minas Basin, Bay of Fundy. Can. J. Fish. Aquat. Sci. 51: 650–661.

Four experimental trawls were made at highwater over the intertidal zone of the Minas Basin and the effects assessed when the tide was out to determine the physical and biological impacts of groundfish trawling on the benthos. The trawl doors made furrows 30–85 cm wide and up to 5 cm deep. The rollers compressed surficial sediments but did not scour a depression. The bridle caused no obvious disturbance. Door furrows and roller marks remained visible for 2–7 mo. No significant impacts were observed on either benthic diatoms or macrobenthos. The macrobenthos was dominated by polychaetes, some of which may have the ability to take evasive action as a trawl approaches. There were few molluscs, crustaceans, or echinoderms present; these taxa have been shown to be more susceptible to trawling damage in studies done elsewhere. Nematode numbers were initially depressed in the door furrows but did recover with time. It is not known whether nematodes were killed or displaced but the latter is thought more likely. Overall, the impacts in this particular environment are judged to be minor, especially since the intertidal sediments of the Minas Basin are already exposed to similar natural stresses imposed by storms and winter ice.

Nous avons effectué quatre traits de chalut expérimentaux à marée haute au-dessus de la zone intertidale du bassin des Mines, et nous en avons évalué les effets à marée basse pour déterminer les impacts physiques et biologiques sur le benthos du chalutage du poisson de fond. Les panneaux du chalut ont creusé des sillons de 30–85 cm de largeur et d'une profondeur allant jusqu'à 5 cm. Les rouleaux comprimaient les sédiments superficiels mais n'ont pas creusé de dépression. Les bras ne semblent pas avoir causé de perturbation. Les sillons creusés par les panneaux et les marques des rouleaux sont restés visibles pendant 2 à 7 mo. Nous n'avons observé aucun impact notable sur les diatomées benthiques ni sur le macrobenthos. Ce dernier était dominé par les polychètes, dont certains peuvent avoir la possibilité de s'éloigner quand le chalut approche. Il y avait peu de mollusques, de crustacés ou d'échinodermes sur place; on a montré dans des études réalisées ailleurs que ces taxons sont plus vulnérables aux dommages causés par le chalutage. L'effectif des nématodes a été réduit au départ dans les sillons des panneaux, mais s'est rétabli avec le temps. On ne sait pas si les nématodes ont été tués ou déplacés, mais il est plus vraisemblable qu'ils ont été déplacés. En gros, les impacts sur ce milieu particulier sont jugés peu importants, d'autant plus que les sédiments intertidaux du bassin des Mines sont déjà exposés à des stress naturels similaires imposés par les tempêtes et par les glaces d'hiver.

Received April 1, 1993
Accepted October 6, 1993
(JB865)

Reçu le 1 avril 1993
Accepté le 6 octobre 1993

For centuries, fishermen have used various kind of trawls, rakes, and dredges to capture bottom-dwelling finfish and shellfish. It has long been recognized that such mobile fishing gear may affect benthic habitat and communities, but few quantitative studies have been done to determine the kind and scale of potential impacts. This issue has been of concern in Canada since at least the mid-1940s (Ketchen 1947). It has been suggested that the species composition and production rate of benthic communities may be altered in heavily trawled areas. Recently, investigations with different types of mobile gear have been conducted in both European (e.g., de Groot 1984; Krost et al. 1990; Rumohr and Krost 1991; Bergman and Hup 1992) and North American (e.g., Caddy 1973; Peterson et al. 1987; Langton and Robinson 1990) waters. Reviews of the issue have recently been prepared by Messieh et al. (1991) and Jones (1992). It is clear from the limited amount of research conducted so far that mobile gear can change the physical properties of surficial sediments, influence chemical exchanges between sediments and water, and alter the composition of benthic communities. These impacts must be understood and addressed by both habitat and fisheries managers to ensure the long-term sustainability of commercial fisheries and the habitats supporting them.

In 1990, the Department of Fisheries and Oceans began a new research program to investigate the potential environmental impacts of mobile fishing gear in marine benthic habitats in eastern Canada. An initial field project was conducted in the Minas Basin of the Bay of Fundy, in collaboration with the Acadia Centre for Estuarine Research at

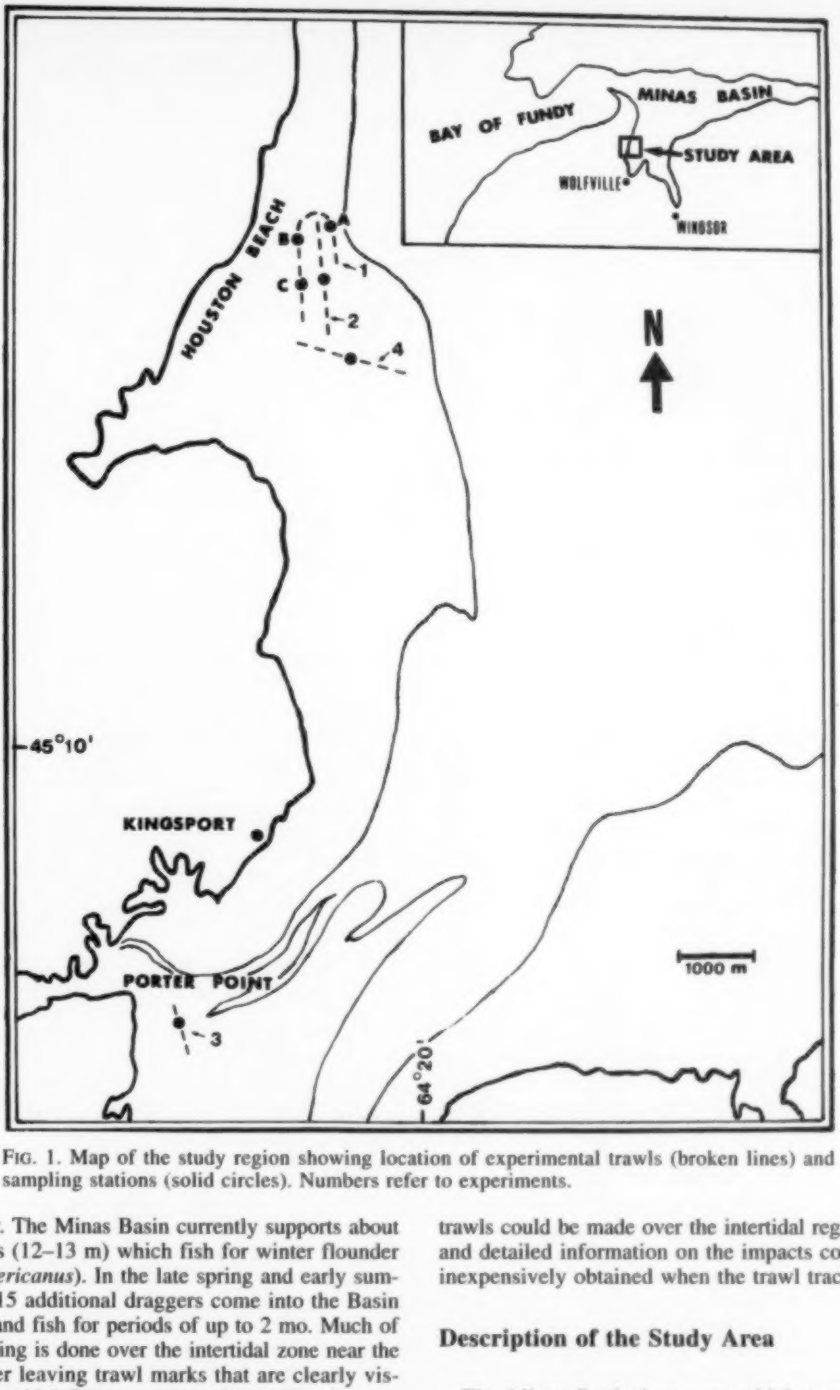

FIG. 1. Map of the study region showing location of experimental trawls (broken lines) and sampling stations (solid circles). Numbers refer to experiments.

Acadia University. The Minas Basin currently supports about six small draggers (12–13 m) which fish for winter flounder (*Pleuronectes americanus*). In the late spring and early summer, as many as 15 additional draggers come into the Basin from other areas and fish for periods of up to 2 mo. Much of the flounder trawling is done over the intertidal zone near the time of high water leaving trawl marks that are clearly visible when the intertidal flats are exposed (see Fig. 2).

The objectives of the project were to evaluate the initial extent of physical and biological disturbance caused by flounder dragging activities in the intertidal and to document the recovery processes over time. The Minas Basin was selected for this study because its macrotidal character affords a unique sampling opportunity; experimental trawls could be made over the intertidal region at high water, and detailed information on the impacts could be easily and inexpensively obtained when the trawl tracks were exposed.

Description of the Study Area

The Minas Basin is a macrotidal estuary in the upper reaches of the Bay of Fundy, Nova Scotia, Canada (Fig. 1). Tidal range averages about 11 m but can reach 16 cm on exceptional spring tides. Tidal current velocities frequently exceed 1 m/s. The extensive intertidal zone, often several kilometres wide, is characterized by saltmarshes and mudflats in protected areas and by sandflats and sandbars in the more

TABLE 1. Details of trawling impact experiments. Initial date indicates the day that experimental trawling was conducted. Gear was towed at approximately 1 m/s following usual fishing procedures.

Experiment	Gear	Duration
1 (Houston Beach)	18-m trawl and 180-kg Westpick wooden doors	22 Oct. – 18 Dec. 1990
2 (Houston Beach)	18-m trawl and 180-kg Westpick wooden doors	28 May – 15 July 1991
3 (Porter Point)	18-m trawl and No. 2½ (200-kg) metal Bison doors	29 May – 2 Oct. 1991
4 (Houston Beach)	24-m trawl and No. 6 (270-kg) metal Bison doors	16 June – 3 Oct. 1991

exposed locations. The general environmental setting is described in more detail in Bleakney (1972).

Experimental studies were conducted at two areas within the midintertidal zone along the western shoreline of the Basin: off Houston Beach and Porter Point (Fig. 1). The site off Houston Beach was characterized by relatively coarse sand overlain by a silty layer which varied in thickness from one to several centimetres. The site off Porter Point had siltier sediment which was relatively uniform to a depth of at least 10 cm. At both sites the intertidal area is about 1.5 km wide and the midintertidal zone is exposed for 2–4 h each low tide (every 12.5 h).

Methods

Trawling

Four separate trawling experiments were conducted at high water. Trawls were made roughly parallel to the shoreline (Fig. 1) at water depths of 6–8 m using procedures normally employed during fishing operations (speed about 1 m/s). Two types of flounder trawls and three types of doors were used (Table 1). The footline of all trawls was equipped with spherical, 29-cm-diameter, 4-6-kg rubber rollers (12 on the 18-m trawl and 16 on the 24-m trawl). None of the trawls was equipped with tickler chains. As soon as the tide receded, the fresh trawl tracks were examined and sampling stations established at representative locations.

Physical Disturbance

Qualitative assessments of the initial physical disturbance to surficial sediments as well as the rate of recovery over time were made by eye. Numerous photographs were also taken during all experiments, both from the ground and from a helicopter at an altitude of about 150 m. Quantitative information was obtained using a 150-cm-long aluminum metering bar which was set horizontally on two reference stakes across the door track. The distance from the bar to the sediment surface was measured at 5-cm intervals across the track on each sampling date. During Experiment 1, the metering bar was left in position between sampling dates and this resulted in considerable erosion within the area immediately under the bar. Hence, it was not possible to quantitatively document the physical recovery of the door furrow. During later experiments, the bar was placed in position only when measurements were being made. Measurements of the distance between doors and the area impacted by the net and footline rollers were also made.

Biological Effects

Samples for chlorophyll *a* analysis, an estimate of benthic diatom abundance, were collected with a 1.2-cm-diameter syringe which was modified to sample the upper 5 mm of sediment. Samples were stored frozen in scintillation vials until analysis. Chlorophyll was extracted by adding 5 mL of 90% acetone to the vial, shaking vigorously by hand, and allowing extraction to proceed for 24 h in the dark under refrigeration. The supernatant was then transferred to a 1-cm-pathlength cuvette and measurements of absorbance made at wavelengths of 664 mm for chlorophyll and 750 nm for turbidity before and after acidification with 0.1 mL of 10% Hcl. Chlorophyll *a* concentration was calculated according to Lorenzen (1967). The sediment weight of each sample was determined after oven drying at 70°C for 24 h.

Meiofaunal samples, which consisted almost exclusively of nematodes (>99%), were collected using a 2.6-cm-diameter syringe modified to sample the top 2 cm of sediment. Samples were transferred to vials and preserved in 10% formalin. Prior to enumeration, samples were diluted, stained and homogenized by transferring each sample to a beaker containing 75 mL of filtered seawater containing rose bengal. Numbers were determined by subsampling the mixture while it was slowly stirred, transferring the subsample (0.5–2.0 mL depending on turbidity) to a petri dish, and counting under a binocular microscope. Subsampling continued until further analysis produced little change in the mean number of nematodes per sample. In most cases, five subsamples proved adequate.

Samples for benthic macrofauna were collected with a 10-cm-diameter metal core that was inserted into the sediment to a depth of 10 cm. Samples were gently sieved in the field through a 850-μm-mesh screen, preserved in 70% alcohol, and later sorted and enumerated by species.

The number, kind, and frequency of samples collected varied with the experiment. During Experiment 1 (Houston Beach), sampling was conducted at three stations along the trawl track (Fig. 1). At each station, three locations were sampled in triplicate: within the furrow created by the door, within the area compacted by the rollers, and within an undisturbed area immediately outside the track (i.e., control). Sampling interval ranged between 2 and 9 d. Meiofaunal samples were not collected. During Experiments 2–4 (Houston Beach and Porter Point), one sampling station was established along each trawl track (Fig. 1). Replicate samples (three for macrofauna, three for meiofauna, six for chlorophyll) were collected from within the door furrow and from an adjacent control area on each sampling date. The area compacted by the rollers was not sampled. The sampling interval varied according to the rate of physical recovery and differences in biological variables between door furrow and control samples. It averaged about 1 wk during the first few months and declined to about 3 wk thereafter.

All samples at a given location were taken in close proximity to minimize large-scale differences in sediment characteristics and biology. Areas disturbed by previous sampling were avoided.

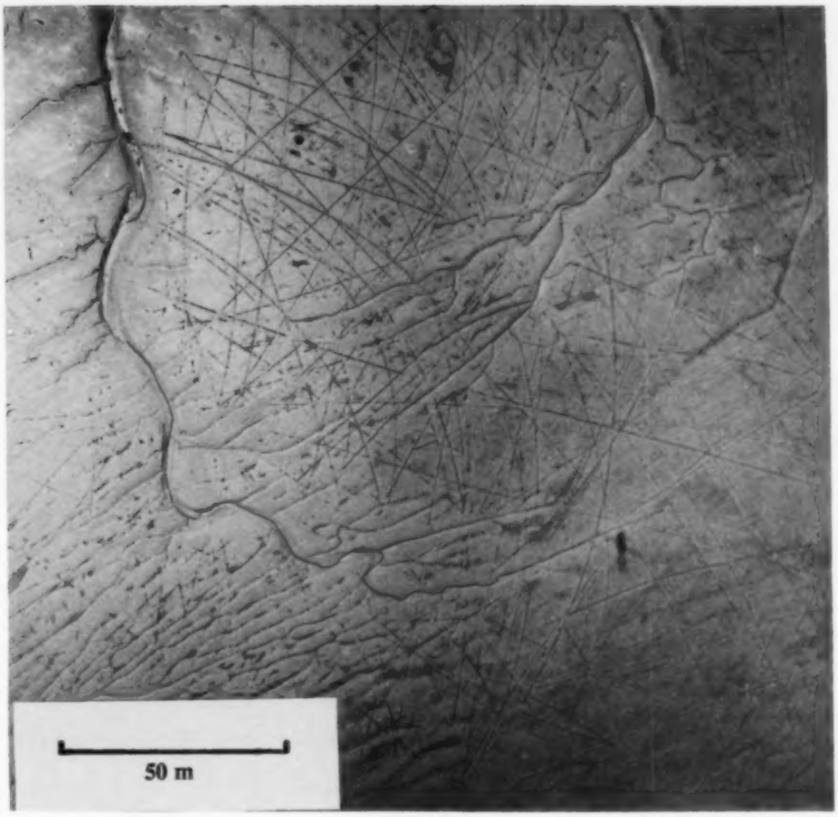

FIG. 2. Aerial photograph of trawl marks resulting from normal fishing activity off Porter Point taken in June 1991 from an altitude of approximately 150 m. (Courtesy of BIO Photo Laboratory).

Statistical Analysis

For each parameter, differences between treatments (control, roller, and door for Experiment 1 and control and door for Experiments 2–4) were investigated using analysis of variance (ANOVA). Bonferroni-adjusted probabilities (Neter and Wasseman 1974) were used in multiple comparisons of treatment effects. All data were log $(x + 1)$ transformed before analysis. Bartlett's test (Winer 1971) was used to test for homogeneity of variances of the transformed data.

Results

Physical Disturbance

Initial

The flounder trawls produced two kinds of physical disturbance. Most visible were the two parallel furrows made by the doors which keep the net spread open during towing. The door passes over the bottom at an angle, the front of the door being outward of the tail end, and tends to move sediments toward the inside of the trawl track. The furrows were about 23 m apart with the 18-m trawl used in Experiments 1–3. Less pronounced marks, about 10 cm wide, were made by each of the rollers on the trawl's footline. The bridle left no visible mark. About 12% of the total seafloor area between the outer edges of the doors was visibly disturbed.

Aerial photographs taken during June 1991 indicate that considerable commercial trawling activity took place off Porter Point in the spring of 1991 (Fig. 2). A 100 × 100 m area in the most heavily disturbed area was crossed by approximately 12 trawls. Since each trawl disturbs an area approximately 3 m wide (two doors plus the rollers), 12 trawls would disturb on the order of one third the sediment surface. The amount of disturbance could be expected to be greater by the end of the summer, since commercial trawling often continues until early August. Examination of aerial photographs also indicated that in some instances, door furrows never filled in and became incorporated into the natural drainage system.

The extent of the initial physical disturbance varied widely (Fig. 3 and 4). In Experiment 1 (Houston Beach), both the door furrow and roller marks were clearly visible immediately after the trawl was conducted. The door scoured a furrow about 85 cm wide and 2–4 cm deep (Fig. 3), while the roller marks appeared to be caused more by compression than scouring. The initial physical disturbance in Experiment 2 (Houston Beach) was much less, even though the same gear was used. Sediment appeared to have been compressed to a depth of 1–2 cm over a width of 50–80 cm by the doors

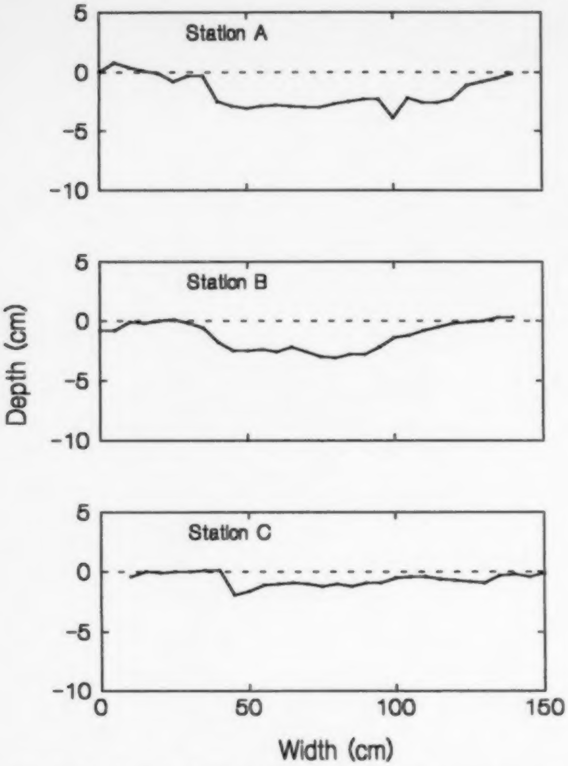

FIG. 3. Profiles of door furrows on day 1 in Experiment 1 (Houston Beach) (outside of trawl track on right).

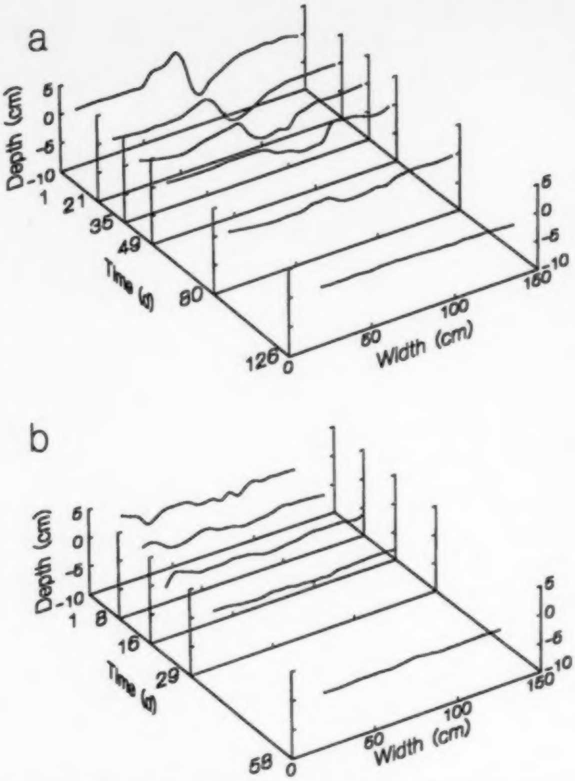

FIG. 4. Changes in the profiles of door furrows with time (outside of trawl track on right) in (a) Experiment 3 (Porter Point) and (b) Experiment 4 (Houston Beach).

but there was little evidence of actual scouring, and the roller marks were not discernible. The third experiment at Houston Beach (Experiment 4), using larger and heavier gear, created an intermediate level of initial disturbance. The doors left a furrow about 80 cm wide which varied in depth to a maximum of about 2 cm (Fig. 4a). At Porter Point (Experiment 3) the doors created a furrow about 30 cm wide and 5 cm deep and deposited the displaced sediment as a mound about 5 cm high and 30 cm wide along the inside edge of the furrow (Fig. 4a). Although the total width of sediment surface disturbed was less than at the Houston Beach experiments, the amount of disturbance appeared greater as a result of deeper penetration by the doors over a wider portion of the door furrow. Roller marks were clearly visible and, as at Houston Beach, seemed to be the result of sediment compression rather than scouring.

Recovery

Physical recovery during Experiment 1 (Houston Beach) was slow despite numerous periods of strong wind and wave activity. For example, a week after the experiment started, a storm removed the upper 1–2 cm layer of silty sediment and created bedforms in the exposed sandy sediments. While some degradation had taken place, both the furrows made by the doors and the roller marks were clearly visible from the air after 47 d and from the ground after 57 d (the last day of sampling). In June 1991, 7 mo later, portions of the door furrows could still be observed from the air. Despite minimal initial disturbance, the trawl tracks in Experiment 2 (Houston Beach) remained clearly visible for about 40 d. They began to degrade thereafter and could no longer be seen from the ground after 130 d.

The rate of recovery in Experiments 3 and 4 was determined quantitatively using the metering bar. Recovery in Experiment 3 (Porter Point) took over 80 d (Fig. 4a). After 49 d, the furrow created by the door was half filled in and the mound beside the furrow had disappeared. After 126 d, the furrow was completely filled in, but was still visible from the ground. The most rapid recovery occurred during Experiment 4 (Houston Beach) (Fig. 4b). After just 16 d, the door track was less than 1 cm deep and it was no longer visible after 58 d.

Collectively, these data clearly indicate that the physical disturbance caused by flounder trawls in the Minas Basin intertidal sediments can persist for at least 2–7 mo.

Biological Effects

Nature of the biological community

The dominant groups of marine organisms present at both study sites are benthic diatoms, nematodes, and polychaete worms. With the exception of low densities ($<2\ m^2$) of the mud snail (*Ilyanassa obsoleta*), epibenthic macrofauna were absent. No large invertebrates were collected in the experimental trawls. Benthic diatom abundance, as estimated by chlorophyll *a*, and nematode abundance were about twice as great at Porter Point compared with Houston Beach which

TABLE 2. Macrofauna present at study sites (in order of decreasing abundance).

Houston Beach (1991), Experiment 1	Houston Beach (1992), Experiment 2	Porter Point (1992), Experiment 3	Houston Beach (1992), Experiment 4
Clymenella torquata	*Clymenella torquata*	*Heteromastus filiformis*	*Clymenella torquata*
Glycera dibranchiata	*Spiophanes bombyx*	*Corophium volutator*	*Spiophanes bombyx*
Phyllodoce mucosa	*Nephytys caeca*	*Streblosoma benedicti*	*Nephytys caeca*
Crangon septemspinosa	*Phyllodoce mucosa*	*Spiophanes bombyx*	*Phyllodoce mucosa*
Nereis diversicolor	*Pygospio elegans*	*Cerebratulus lacteus*	*Heteromastus filiformis*
Odostomia bisuturalis	*Nereis diversicolor*	*Tharyx acutus*	*Crangon septemspinosa*
Chiridotea ceoca	*Heteromastus filiformis*	*Eteone heteropoda*	*Eteone trilineata*
Idotea phosphorea	*Streblosoma benedicti*	*Glycera dibranchiata*	*Spiophanes benedicti*
Crenella glandula	*Nassarius trivittatus*	*Eteone lactea*	*Nassarius trivittatus*
Glycera robusta	*Eteone trilineata*	*Eteone trilineata*	*Oxyurostylis smithi*
Ophioglycera gigantia	*Glycera dibranchiata*	*Phyllodoce mucosa*	*Buccinium totteni*
Cancer borealis	*Mercenaria mercenaria*	*Gemma gemma*	*Gammarus duebeni*
Corophium volutator	*Ilyanassa obsoleta*	*Crangon septemspinosa*	*Turbonilla interrupta*
Nassarius trivittatus		*Mya arenaria*	*Euclymena zonalis*
Cancer irroratus		*Scoloplos armiger*	*Corophium volutator*
Cerebratulus lacteus		*Ilyanassa obsoleta*	*Nereis diversicolor*
Ilyanassa obsoleta			*Ilyanassa obsoleta*

TABLE 3. Summary of *F* values for time, treatment (control, door, and roller), and interaction effects on sediment chlorophyll *a* concentration, total number of polychaetes, and number of dominant polychaetes for Experiment 1. Levels of significance: ns, $P > 0.05$; *$0.01 < P \leq 0.05$; **$P \leq 0.01$.

	df	Sediment chlorophyll *a*	Total no. of polycheates	No. of *C. torquata*	No. of *G. dibranchiata*
Station A					
Time	10	10.25**	2.84**	2.58*	1.52 ns
Treatment	2	13.12**	1.41 ns	0.77 ns	2.09 ns
Interaction	20	1.71 ns	1.00 ns	0.71 ns	3.05*
Bartlett's (χ^2)	32	37.03**	29.18**	50.24**	49.86*
Station B					
Time	11	5.95**	2.16**	0.67 ns	1.51 ns
Treatment	2	3.84*	1.90 ns	0.16 ns	3.95*
Interaction	22	1.90*	1.42 ns	0.90 ns	0.69 ns
Bartlett's (χ^2)	35	39.42**	36.09**	22.73**	43.47*
Station C					
Time	11	16.09*	1.57 ns	2.03*	4.04*
Treatment	2	1.54 ns	0.77 ns	0.56 ns	1.66 ns
Interaction	22	12.31 ns	1.43 ns	1.62 ns	1.63 ns
Bartlett's (χ^2)	35	58.09*	43.17**	34.45**	61.57 ns

is in keeping with the finer nature of the sediment. At all sites the dominant macrofauna were polychaetes (Table 2). At Houston Beach, the dominant polychaete was *Clymenella torquata*, a nonselective deposit feeder which forms long vertical tubes of sand and mucus and occurs mainly subtidally. During Experiment 1, *Glycera dibranchiata*, a deep burrowing carnivorous polychaete, was also abundant. Although *G. dibranchiata* occurs mainly intertidally, it can be found to depths of 400 m. During Experiments 2 and 4, *C. torquata*, *Spiophanes bombyx*, a selective surface deposit feeder, and *Nephytys caeca*, a highly mobile predacious burrowing polychaete, were the dominant species. Both *S. bombyx* and *N. caeca* occur subtidally to depths of 100 m. These polychaete species constituted about 90% of the total number of macrofauna at all Houston Beach sampling locations. Macrofauna at Porter Point was dominated by a single polychaete species, *Heteromastus filiformis*, a tube-building, nonselective deposit feeder commonly found in fine sediments around the Bay of Fundy both intertidally and to depths of 60 m.

Impact on benthic diatoms and recovery

Trawling does appear to have some minor impacts on benthic diatoms (Fig. 5 and 6). In Experiment 1 (Houston Beach), an initial ANOVA indicated significant differences in sediment chlorophyll *a* concentration between stations; therefore, the data for each station were subjected to a separate ANOVA (Table 3). Significant treatment effects were observed for Stations A and B, but not for Station C. An analysis of Bonferroni-adjusted pairwise comparisons indicated that at Station A, chlorophyll *a* concentrations were significantly lower in both the door furrow and roller marks, and at Station B, chlorophyll *a* concentrations were significantly less in only the door furrow. All three stations showed

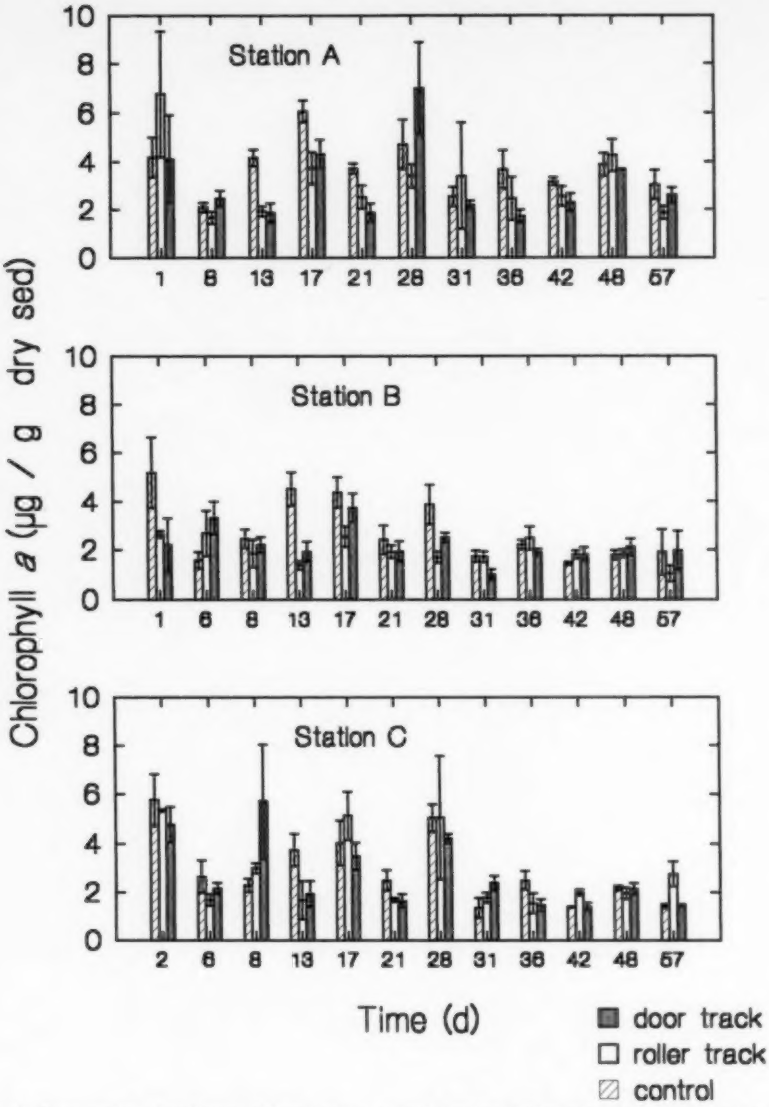

FIG. 5. Time series of sediment chlorophyll *a* at each station in Experiment 1 (Houston Beach). Error bars are 1 SE of the mean.

decreasing chlorophyll *a* concentrations with time which was presumably due to the decreasing levels of solar radiation at this time of year (October–December).

In contrast, chlorophyll *a* was lower in the door furrows than in control samples (Table 4) at the beginning of Experiments 2–4 (which were conducted during the late spring and summer) and remained so for approximately 1 mo (Fig. 6). However, after 80 d, a reverse trend occurred in Experiment 3 (Porter Point) where chlorophyll *a* in the door furrow was about twice that in control samples. On the final sampling day (day 126) the difference was fourfold, and this apparent bloom of algae in the furrow was clearly visible to the naked eye.

Impact of nematodes and recovery

Experiments 2–4 indicate that trawling can have impacts on nematodes (Fig. 7; Table 4). In all cases, nematode numbers were markedly lower in the door furrows than in control samples at the beginning of the experiments. However, after 4–6 wk, numbers returned to levels similar to controls. The impacts appeared to be greater at Porter Point which had higher initial concentrations of nematodes.

Impact on polychaetes and recovery

There was little evidence that trawling had any impact on either the species composition or number of polychaetes that dominated the benthic macrofauna community at the Houston Beach sites. In Experiment 1, there were very few differences in polychaete numbers which could be attributed to trawling (Fig. 8). An initial ANOVA showed significant differences among stations in the total number of polychaetes, so the data for each station were analyzed sep-

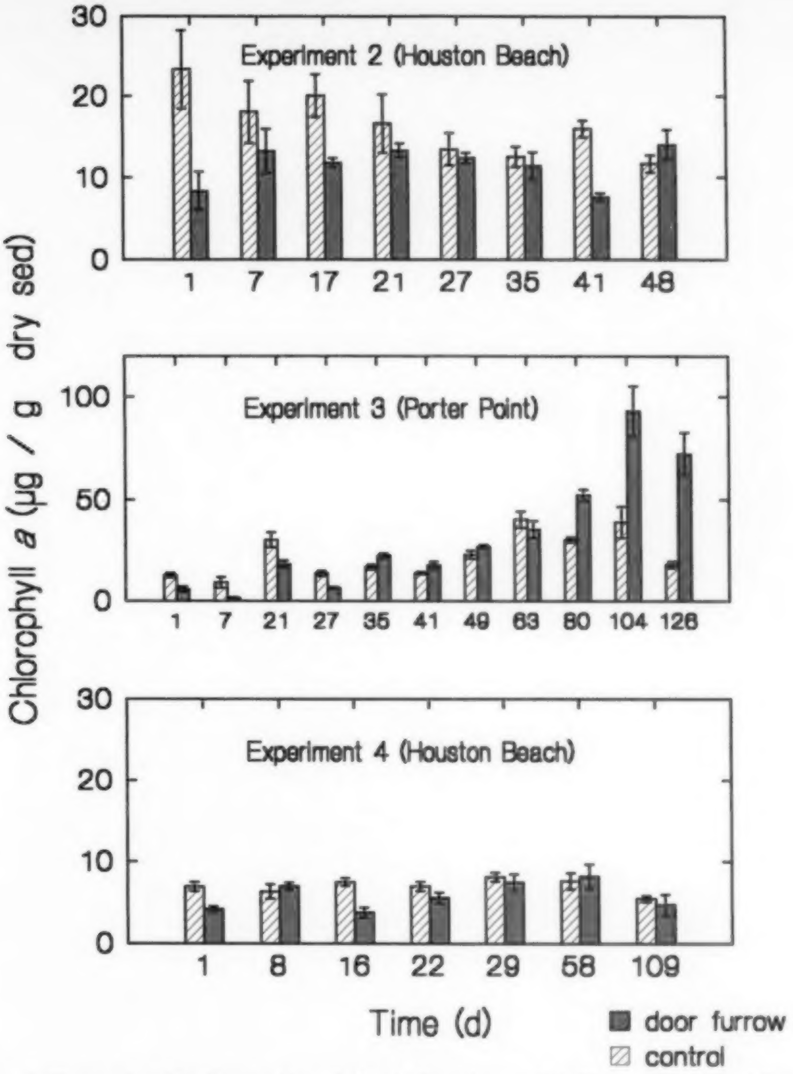

FIG. 6. Time series of sediment chlorophyll *a* in Experiments 2–4 (Houston Beach and Porter Point). Error bars are 1 SE or the mean.

arately. An ANOVA for each station (Table 3) revealed no significant treatment effect on the total number of polychaetes, and in only one instance (*G. dibranchiata* at Station B) was there a significant treatment effect (greater number in the control) on one of the dominant polychaetes. In Experiments 2 and 4, polychaete numbers were slightly lower in the door furrows on day 1 (Fig. 9), but these differences were not statistically significant. There were no consistent differences between the door furrows and controls for the rest of the experiments.

Polychaete numbers were very low at the beginning of Experiment 3 (Porter Point) and there was no sign of any initial impact (Fig. 9). After about 1 mo, polychaetes began to increase in both door furrow and control samples. At first, the rate of increase was greater in control samples, but after about 7 wk, there was little difference between control and door furrow samples.

Discussion

The amount of initial physical disturbance caused by trawling varied markedly and seemed to be influenced primarily by the kind of sediment and the type of doors used. Disturbance was greater in the finer sediments off Porter Point and with the heavier doors used in Experiments 3 and 4. Even though the maximum depth of scour recorded was only 5 cm, the disturbance left by the doors and the rollers was easily visible from both the ground and the air when the intertidal area was exposed. The data collected during these experiments indicate that trawl tracks on the intertidal flats of the Minas Basin can persist for 2–7 mo. This persistence of trawl tracks in the intertidal zone is somewhat surprising considering that the tracks are exposed to wave activity twice within a 12.5-h period, tidal currents inundation, and the erosive effects of precipitation during

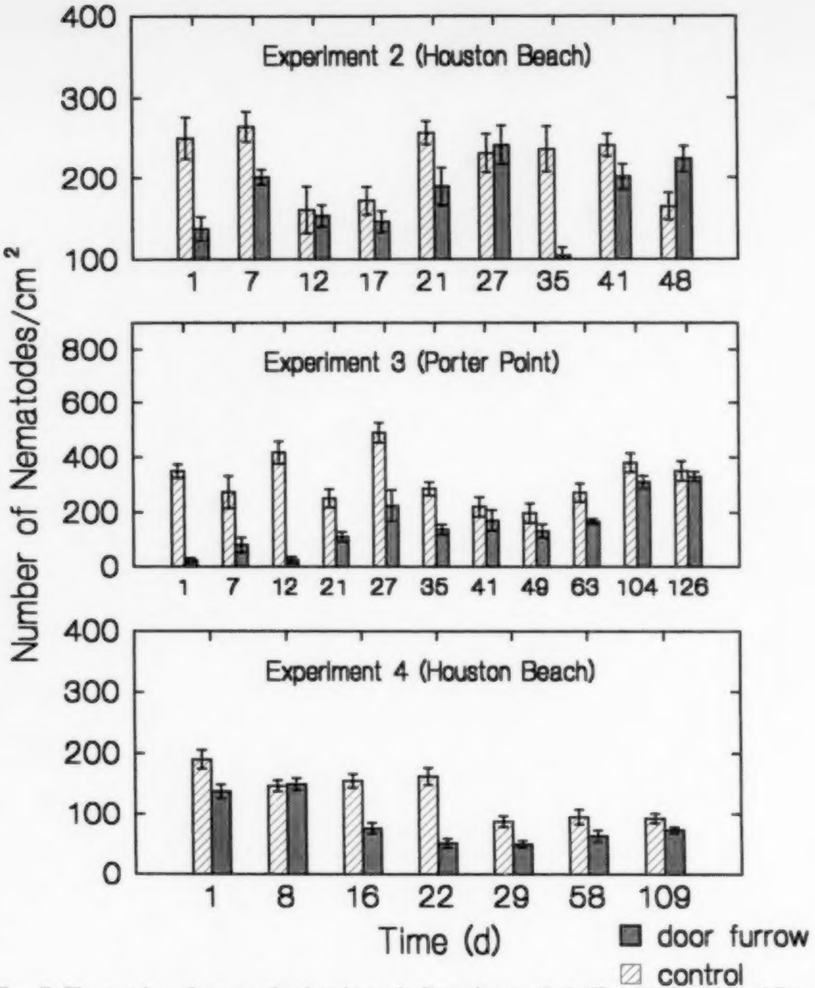

FIG. 7. Time series of nematode abundance in Experiments 2–4 (Houston Beach and Porter Point). Error bars are 1 SE of the mean.

TABLE 4. Summary of *F* values for time, treatment (control and door), and interaction effects on sediment chlorophyll *a* concentration, total number of nematodes, total number of polychaetes, and number of dominant polychaetes for Experiments 2, 3, and 4. Levels of significance: ns, $P > 0.05$; *$0.01 < P \leq 0.05$; **$P \leq 0.01$.

	df	Sediment chlorophyll *a*	Total no. of nematodes	Total no. of polychaetes	No. of *C. torquata*	No. of *S. bombyx*	No. of *N. caeca*
Experiment 2							
Time	7	17.25**	2.46*	0.70 ns	0.92 ns	7.84**	1.75 ns
Treatment	1	15.56**	9.14**	1.20 ns	2.18 ns	0.83 ns	0.09 ns
Interaction	7	2.21 ns	2.36*	2.84*	2.58*	1.20 ns	0.87 ns
Bartlett's (χ^2)	15	27.47*	29.13*	29.29*	24.73**	27.46*	38.13 ns
Experiment 3							
Time	10	77.34**	3.08**	25.37**			
Treatment	1	33.71**	42.02**	23.46**			
Interaction	10	14.73**	3.91*	4.35**			
Bartlett's (χ^2)	21	29.09*	38.08*	38.90*			
Experiment 4							
Time	6	8.71**	10.92**	2.14 ns	1.54 ns	7.19**	1.32 ns
Treatment	1	4.21**	37.19**	3.15 ns	0.89 ns	1.35 ns	0.49 ns
Interaction	6	5.03**	3.30**	1.50 ns	0.96 ns	1.63 ns	1.47 ns
Bartlett's (χ^2)	13	25.75*	12.48**	27.59*	43.41 ns	15.58**	26.02*

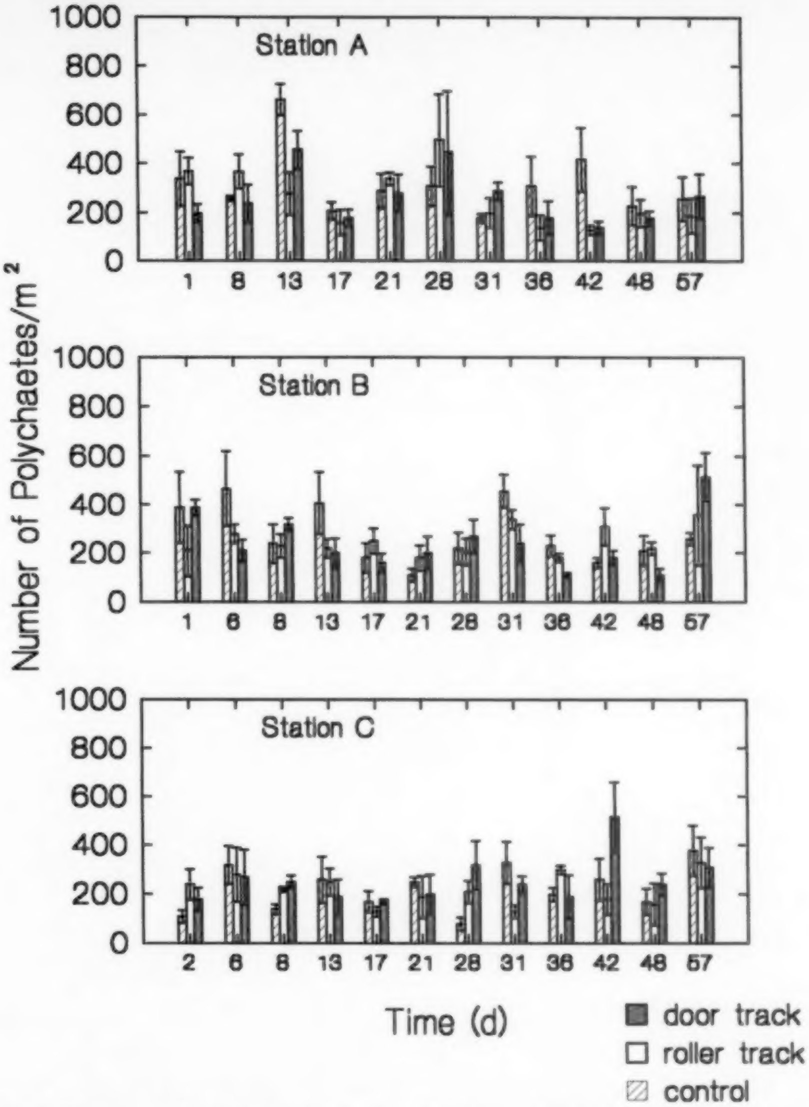

FIG. 8. Time series of polychaete abundance in Experiment 1 (Houston Beach). Error bars are 1 SE of the mean.

inundation, and the erosive effects of precipitation during exposure.

Although there was some evidence of depression of sediment chlorophyll *a* levels at Station A in Experiment 1, there was little indication that the rollers had any biological impact. The only biological impacts observed, which were quite minor, were caused by the doors. In the three Houston Beach experiments, there was generally little difference between control samples and door furrows in chlorophyll *a* levels or macrofauna abundance, either immediately after the trawl was made or as long as the disturbance was visible. There were also no obvious differences, other than the amount of physical disturbance created, that could be related to the time the trawls were made or the type of trawl used. In the Porter Point experiment, the initial impact was more obvious, probably because of the finer sediment and greater initial physical disturbance. Chlorophyll *a* levels in the door furrow were initially depressed relative to the control and this persisted for about 1 mo. After that time, however, chlorophyll *a* levels increased at a much faster rate within the door furrow and eventually became 2–4 times as great as the control, perhaps as a result of increased nutrient availability resulting from disturbance of the sediments. Polychaetes, however, differed little between the door furrow and control samples in either abundance or rate of increase in abundance. The greatest biological impact of the flounder trawls was the depression in the number of nematodes within the door furrow relative to the control samples. This was obvious in Experiments 2–4 but was most pronounced in Experiment 3 (Porter Point) where it persisted for almost 2 mo.

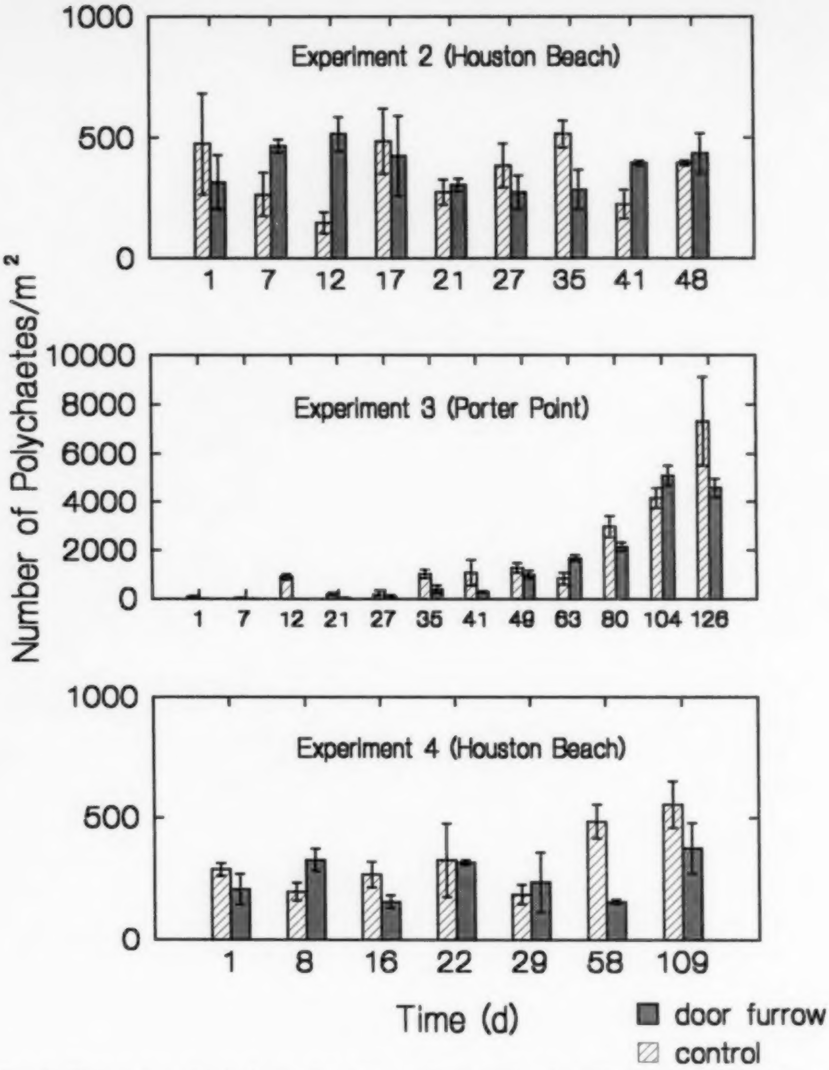

FIG. 9. Time series of polychaete abundance in Experiments 2–4 (Houston Beach and Porter Point). Error bars are 1 SE of the mean.

The general lack of a significant impact on benthic diatoms is not surprising, since they have a very rapid division rate (on the order of once a day) and are subject to suspension and redistribution during periods of strong winds (de Jonge and van den Bergs 1987). The fate of the nematodes lost from the door furrows is unknown. While some may have been killed by the doors, it is more likely that most of them were resuspended or displaced with the sediment. If this is true, the nematodes may have continued to live and thus the overall impact may be less than the data suggest.

At first, the lack of impact on the macrofauna may seem surprising, since other studies have demonstrated that at least some species of polychaetes can be affected by trawling, for example, *Lanice conchilega*, *Magelona papillicornis*, and *S. bombyx* in the North Sea (Bergman and Hup 1992). However, the polychaetes dominant at the Minas Basin study sites (Table 2) were predominantly tube-dwelling, upside-down-feeding, nonselective deposit feeders or burrowing carnivores. These species may be able to better sense the approach of the trawl doors and take evasive action by either moving down their tubes (which generally extend deeper than 5 cm) or burrowing deeper. Selective surface deposit feeding species, such as *S. bombyx*, may be more susceptible to damage. The fact that *S. bombyx* was not noticeably impacted in this study, but was in the North Sea (Bergman and Hup 1992), could be explained by the type of gear used. The latter study employed a beam trawl equipped with tickler chains which affects an area 12 m wide and at least 6 cm deep. In general, polychaetes are well known for their ability to withstand stress and there is evidence that their relative abundance in the Wadden Sea is increasing due to habitat disturbance (Reise 1982). Impacts on the macrofauna would probably have occurred if other classes of infaunal organisms or epibenthic organisms had been present at the study sites. For example, crustaceans, molluscs, and echinoderms appear to be much more susceptible to trawl damage (e.g., de Groot 1984; Langton and Robinson 1990; Rumohr and Krost 1991; Bergman and Hup 1992).

The results of this study indicate that the impact of flounder draggers on the intertidal benthic community of the Minas Basin is minor and not cause for serious concern at the present time. This conclusion, however, should not be applied to other benthic habitats which have quite different sedimentological conditions and biological communities and which can be disturbed by other kinds of fishing gear (scallop rakes, clam dredges, etc.). Further investigations in subtidal areas are necessary. If trawl marks can last for 2–7 mo in intertidal sediments, which are subjected to the various physical stresses discussed above, they could last longer in subtidal sediments, except perhaps in areas of strong tidal currents. However, some of the results of this intertidal study may be applicable to subtidal habitats. For example, the dominant polychaete species in this study also occur subtidally to depths of at least 60 m, so it is unlikely that they would be affected by trawling in deeper water.

While trawling does appear to cause a substantial amount of physical disturbance, it must be appreciated that this activity is superimposed upon a variety of natural processes that make the intertidal zone of the Minas Basin a heavily stressed environment due to wave action and storms. Storms can cause very high levels of mortality in benthic organisms (Yeo and Risk 1979). During the winter, the intertidal zone is subjected to the erosive effects of moving ice (Knight and Dalrymple 1976) which create abundant furrows on the order of several centimetres deep (Gordon and Desplanque 1983). Therefore, it is not surprising that the intertidal benthic community in the Minas Basin is little affected by the additional stress of trawling. Another anthropogenic disturbance which has taken place in recent years in the Minas Basin is bait digging for blood worms (*G. dibranchiata*) but this has not been quantified. Visual impressions suggest that this activity is likely to have far more impact on the sediments, bottom morphology, and the benthos in areas where it takes place.

Acknowledgements

We thank L. Dickie for first bringing the presence of trawl marks in the intertidal zone of the Minas Basin to our attention. His perceptive observations while digging clams one weekend led to the initiation of this project. Numerous colleagues assisted in the initial field work and design of this project, especially P. Vass and T. Rowell. We thank R. Belanger and K. Bentham for their assistance with the aerial photography. K. Mahwinney and P. Burke assisted in field work and identification and enumeration of macrobenthos. B. Millet carried out the experimental trawls. T. Rowell and J. Prena critically reviewed an early version of the manuscript. Funding was provided by the Department of Fisheries and Oceans (DFO) Atlantic Fisheries Adjustment Program (AFAP) and DFO/NSERC Subvention Grant CRD 115371. Publication No. 27 of the Acadia Centre for Estuarine Research, Acadia University, Wolfville, Nova Scotia, Canada.

References

Bergman, M.J.N., and M. Hup. 1992. Direct effects of beamtrawling on macrofauna in a sandy sediment in the southern North Sea. ICES J. Mar. Sci. 49: 5–11.

Bleakney, J.S. 1972. Ecological implications of annual variation in tidal extremes. Ecology 53: 933–938.

Caddy, J.F. 1973. Underwater observations of tracks of dredges and trawls and some effects of dredging on a scallop ground. J. Fish. Res. Board Can. 30: 173–180.

de Groot, S.J. 1984. The impact of bottom trawling on benthic fauna of the North Sea. Ocean Manage. 9: 177–190.

de Jonge, V.N., and J. van den Bergs. 1987. Experiments on the resuspension of estuarine sediments containing benthic diatoms. Estuarine Coastal Shelf Sci. 24: 725–740.

Gordon, D.C. Jr., and C. Desplanque. 1983. Dynamics and environmental effects of ice in the Cumberland Basin of the Bay of Fundy. Can. J. Fish. Aquat. Sci. 40: 1331–1342.

Jones, J.B. 1992. Environmental impact of trawling on the seabed: a review. N.Z. J. Mar. Freshwater Res. 26: 59–67.

Ketchen, K.S. 1947. An investigation into the destruction of grounds by otter trawling gear. Fish. Res. Board Can. Prog. Rep. 73: 55–56.

Knight, R.J., and R.W. Dalrymple. 1976. Winter conditions in a macrotidal environment, Cobequid Bay, Nova Scotia. Rev. Geogr. (Montreal) 30: 65–85.

Krost, P., M. Bernhard, F. Werner, and W. Hukriede. 1990. Otter trawl tracks in Kiel Bay (Western Baltic) mapped by side-scan sonar. Meeresforschung 32: 344–353.

Langton, R.W., and W.E. Robinson. 1990. Faunal associations on scallop grounds in the western Gulf of Maine. J. Exp. Mar. Biol. Ecol. 144: 157–171.

Lorenzen, C.J. 1967. Determination of chlorophyll and phaeo-pigments: spectrophotometric equations. Limnol. Oceanogr. 12: 343–346.

Messieh, S.N., T.W. Rowell, D.L. Peer, and P.J. Cranford. 1991. The effects of trawling, dredging and ocean dumping on the eastern Canadian continental shelf seabed. Continental Shelf Res. 11: 1237–1263.

Neter, J., and W. Wasserman. 1974. Applied linear statistical models: regression, analysis of variance and experimental design. Richard D. Irwin, Inc., Homewood, Ill. 842 p.

Peterson, C.H., H.C. Summerson, and S.R. Fegley. 1987. Ecological consequences of mechanical harvesting of clams. Fish. Bull. 85: 281–298.

Reise, K. 1982. Long-term changes in the macrobenthic invertebrate fauna of the Wadden Sea: are polychaetes about to take over? Neth. J. Sea Res. 16: 29–36.

Rumohr, H., and P. Krost. 1991. Experimental evidence of damage to benthos by bottom trawling with special reference to *Arctica islandica*. Meeresforschung 33: 340–345.

Winer, B.J. 1971. Statistical principles in experimental design. McGraw-Hill Book Co., New York, N.Y. 907 p.

Yeo, R.K., and M.J. Risk. 1979. Intertidal catastrophes: effect of storms and hurricanes on intertidal benthos of the Minas Basin, Bay of Fundy. J. Fish. Res. Board Can. 36: 667-669.

Development and Evaluation of a Biological Model to Assess Regional-Scale Effects of Acidification on Atlantic Salmon (*Salmo salar*)

Josh Korman[1] and David R. Marmorek

ESSA Environmental and Social Systems Analysts Ltd., 3rd Floor, 1765 W. 8th Avenue, Vancouver, BC V6J 5C6, Canada

Gilles L. Lacroix

Department of Fisheries and Oceans, Biological Station, St. Andrews, NB E0G 2X0, Canada

Peter G. Amiro, John A. Ritter, Walton D. Watt, and Richard E. Cutting

Department of Fisheries and Oceans, Biological Sciences Branch, Halifax, NS B3J 2S7, Canada

and Donald C.E. Robinson

ESSA Environmental and Social Systems Analysts Ltd., 3rd Floor, 1765 W. 8th Avenue, Vancouver, BC V6J 5C6, Canada

Korman, J., D.R. Marmorek, G.L. Lacroix, P.G. Amiro, J.A. Ritter, W.D. Watt, R.E. Cutting, and D.C.E. Robinson. 1994. Development and evaluation of a biological model to assess regional-scale effects of acidification on Atlantic salmon (*Salmo salar*). Can. J. Fish. Aquat. Sci. 51: 662–680.

We developed an age-structured simulation model incorporating pH-dependent mortality to assess impacts of acidification on Atlantic salmon (*Salmo salar*) populations at the reach and river system level. Applied to the LaHave River, Nova Scotia, acidic reaches (mean annual pH 4.6–5.1) were predicted to have 0–15% of the annual smolt production and 0–31% of the maiden spawner production compared with circumneutral reaches (pH ≥ 5.6) and increased juvenile growth due to lower parr densities. The benefit of increased growth (earlier age of smoltification and increased early marine survival) was not sufficient to outweigh impacts of higher freshwater juvenile mortality. Simulated removal of acidic conditions resulted in a 41% increase in recruits, but only after several decades following complete chemical recovery. Circumneutral reaches were predicted to be 4–12 times more efficient at producing smolts and 3–7 times more efficient at producing adults from hatchery fingerlings compared with acidic reaches. To maintain current target egg deposition rates of 240 eggs/100 m^2, circumneutral reaches could withstand grilse exploitation rates of up to 65%, while acidic reaches, even without harvesting mortality, could not maintain this level. Fisheries management strategies need to account for variability in freshwater production both within and between river systems.

Nous avons élaboré un modèle de simulation à structure par âge intégrant la mortalité dépendante du pH pour évaluer les impacts de l'acidification sur les populations de saumon atlantique (*Salmo salar*) au niveau d'un tronçon de cours d'eau et au niveau du réseau, modèle que nous avons appliqué à la rivière LaHave (Nouvelle-Écosse). Nous avons prédit que les tronçons acidifiés (pH annuel moyen 4,6–5,1) représenteraient 0–15 % de la production annuelle de smolts et 0–31 % de la production de géniteurs vierges par rapport aux tronçons presque neutres (pH ≥ 5,6) et connaîtraient une croissance plus forte des juvéniles à cause des densités plus faibles de tacons. Le gain représenté par la croissance supérieure (smoltification précoce et accroissement de la survie au début de la phase marine) ne suffisait pas à contrebalancer les impacts de la mortalité plus forte des juvéniles en eau douce. La simulation de la disparition des conditions acides a donné une hausse de 41 % du recrutement, mais seulement après plusieurs décennies faisant suite à un rétablissement complet sur le plan chimique. Nous avons prédit que les tronçons presque neutres seraient 4–12 fois plus efficaces pour la production de smolts et 3–7 fois plus efficaces pour la production d'adultes à partir d'alevins provenant de piscicultures par rapport aux tronçons acidifiés. Si l'on veut maintenir les taux cibles actuels de ponte de 240 oeufs/100 m^2, les tronçons presque neutres pourraient soutenir des taux d'exploitation des madeleineaux pouvant aller jusqu'à 65 %, tandis que les tronçons acidifiés, même exempts de mortalité par pêche, ne pourraient maintenir ce niveau. Les stratégies de gestion des pêches doivent tenir compte de la variabilité dans la production des eaux douces, tant au sein d'un même réseau que d'un réseau à l'autre.

Received March 2, 1993
Accepted October 7, 1993
(JB828)

Reçu le 2 mars 1993
Accepté le 7 octobre 1993

---

[1] Author to whom correspondence should be addressed. Current address: School of Resource and Environmental Management, Simon Fraser University, Burnaby, BC V5A 1S6, Canada.

Acidification of rivers in southwestern Nova Scotia has been associated with significant losses of Atlantic salmon (*Salmo salar*) (Farmer et al. 1980; Watt et al. 1983; Lacroix 1987, 1989a). This acidification is due to the combined effects of acid deposition and natural organic acids from peatland and bogs (Gorham et al. 1986; Kerekes et al. 1986). Preliminary estimates suggest that acidification may be responsible for a 50% decrease in salmon production in southwestern Nova Scotia (Watt 1986), with over 30 rivers affected. Since 1980, several ecological and toxicological studies have documented the life stages of salmon affected, the physiological mechanisms of effect, the responses to acidic episodes, and the chemical factors responsible (reviewed by Lacroix 1989a). Concerns remain about the long-term prognosis for salmon production, the loss of biological diversity, and the potential for recovery of damaged salmon runs. These concerns raise many questions including (1) How much salmon production has been lost due to acidic deposition, and what changes in salmon production can be anticipated from future acidic deposition?, (2) Do compensatory, density-dependent effects mitigate the impact of acidification on salmon populations?, (3) How does the effectiveness of alternative stocking and harvesting levels vary in systems of different acidity?, and (4) How does habitat preference of juvenile salmon affect our ability to "scale-up" site-specific investigations or predictions to an entire river? The Atlantic Salmon Regional Acidification Model (ASRAM) was designed to help address these questions. ASRAM is a dynamic fisheries model whose juvenile mortality rates are modified by measurements of stream acidity. ASRAM differs from other Atlantic salmon models (e.g., Elson 1975; Symons 1979; Evans et al. 1984) in that it explicitly simulates a density-independent factor (i.e., pH) which is recognized as being an important determinant of production in acidified rivers (Watt 1986; Lacroix 1989b).

In this paper, we describe the structure of ASRAM to highlight the key assumptions and functional relationships used in the model. We apply ASRAM to the LaHave River, Nova Scotia, at site and watershed levels and illustrate how the dynamics of the model vary in systems of different acidity. A validation exercise is presented to assess how well the model fits observed stock–recruitment relationships for the LaHave River. A sensitivity analysis is used to determine the influence of different density-dependent and -independent parameters on model projections. Finally, we evaluate the potential for biological recovery from acidification impacts in the LaHave River and the effectiveness of different stocking and harvesting levels in reaches of different acidity.

The LaHave River location was chosen primarily because of the availability of both fisheries and hydrochemical data. The river contains habitat with a wide range of acidity and also represented a situation where the behaviour of the model could be fully assessed. The model results are applicable to other acidified rivers in Nova Scotia for which physical, chemical, and biological data are available, and are relevant to understanding the impacts of other stresses affecting the early life history of salmonids.

Model Description

ASRAM is a habitat- and pH-sensitive age-structured salmonid life history model designed to examine alternative management scenarios in Atlantic salmon rivers of the Maritimes. The model combines pH-dependent toxicity relationships, habitat-preference models, density-dependent processes, and natural and fishing mortality estimates to predict annual smolt production and adult returns at site and river system levels.

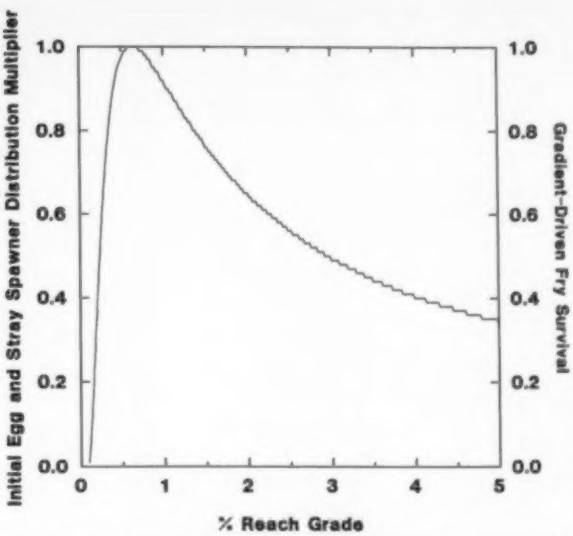

FIG. 1. Relationship used to distribute initial egg numbers and stray spawners to other than home reaches for the LaHave River simulation based on percent reach grade (from Amiro 1993). The same relationship is used to calculate gradient-driven fry mortality rates for each reach.

The spatial structure of the model is consistent with the Department of Fisheries and Oceans (Scotia–Fundy Region) Atlantic salmon stream habitat database (P.G. Amiro, Department of Fisheries and Oceans, Scotia–Fundy Region, Halifax, N.S., unpublished data) and uses river systems divided into tributaries consisting of multiple reaches separated at 5-m contour intervals. The area and water surface grade of each reach (percent reach grade), used as input data for the model, are based on information obtained from aerial photographs and orthophotographic maps (Amiro 1993). Annual pH time series collected from monitoring stations distributed throughout a river system are assigned to a set of spatially linked reaches to predict tributary-specific pH-driven mortality rates.

Juvenile Model

The spatial distribution of juvenile Atlantic salmon has been shown to be strongly related to stream surface grade in the Stewiacke, Musquodolboit, and St. Mary's rivers, with high densities of parr occurring in moderate to higher gradient sections of streams and very low densities or absence of parr in lower gradient sections (Amiro 1993). To reproduce this habitat distribution in simulated river systems, the total initial input egg deposition is distributed among reaches at the beginning of a model run according to the following weighting factor:

$$\text{(1)}\quad \text{Weight} = 9.67 \times \text{AwSg}^{0.97} \times e^{-\text{AwSg}}$$

where AwSg, the area-weighted stream surface grade (percent), is calculated from

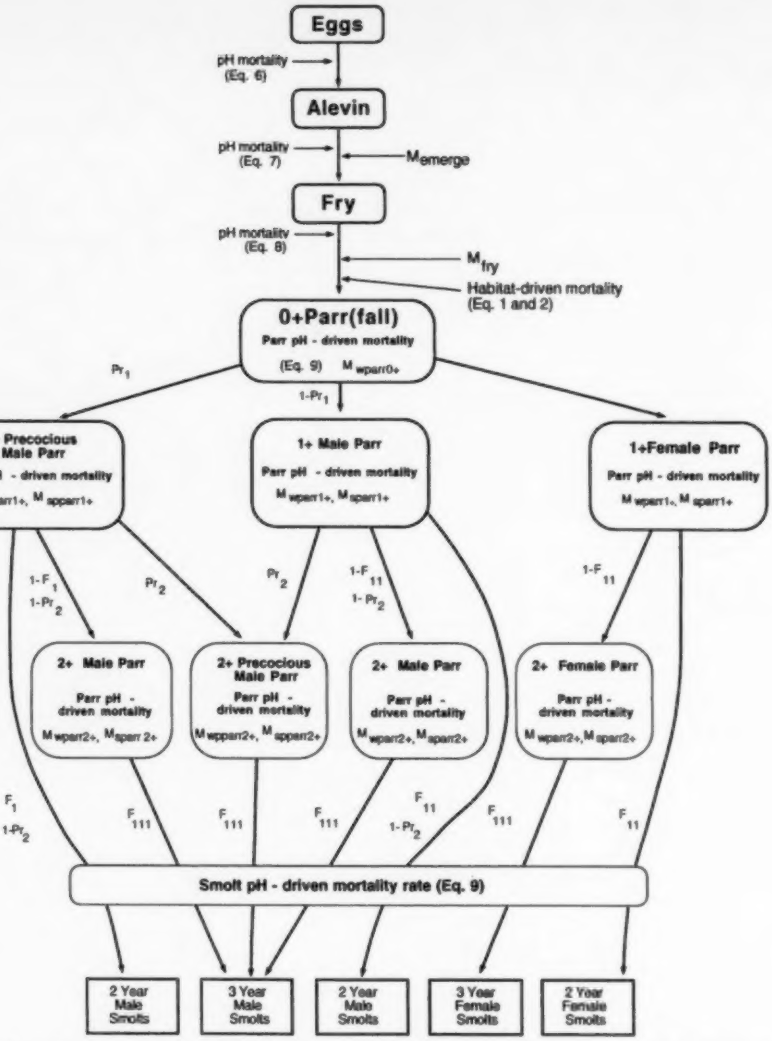
Eggs
pH mortality (Eq. 6)
Alevin
pH mortality (Eq. 7)
M emerge
Fry
pH mortality (Eq. 8)
M fry
Habitat-driven mortality (Eq. 1 and 2)
0+Parr(fall)
Parr pH - driven mortality
(Eq. 9) M wparr0+
Pr 1
1-Pr 1
1+ Precocious Male Parr
Parr pH - driven mortality
M wpparr1+, M spparr1+
1+ Male Parr
Parr pH - driven mortality
M wparr1+, M sparr1+
1+Female Parr
Parr pH - driven mortality
M wparr1+, M sparr1+
1-F 1
1-Pr 2
Pr 2
Pr 2
1-F 11
1- Pr 2
1-F 11
2+ Male Parr
Parr pH - driven mortality
M wparr2+, M sparr 2+
2+ Precocious Male Parr
Parr pH - driven mortality
M wpparr2+, M spparr2+
2+ Male Parr
Parr pH - driven mortality
M wparr2+, M sparr2+
2+ Female Parr
Parr pH - driven mortality
M wparr2+, M sparr2+
F 1
1-Pr 2
F 111
F 111
F 111
F 11
1- Pr 2
F 111
F 11
Smolt pH - driven mortality rate (Eq. 9)
2 Year Male Smolts
3 Year Male Smolts
2 Year Male Smolts
3 Year Female Smolts
2 Year Female Smolts

FIG. 2. Conceptual representation of the egg-to-smolt component of ASRAM. Refer to Table 2 for a description of the symbols.

$$\text{(2)} \qquad \text{AwSg} = 1.201 + 0.505 \times (\%\ \text{reach grade})$$

which is an empirically derived transformation to correct for bias in gradient estimates based on remote survey data (Amiro 1993). Combining Eq. 1 and 2 produces a gradient – habitat preference function (Fig. 1). This relationship explained 17–27% of the variability in parr density in the Stewiacke, Musquodolboit, and St. Mary's rivers between 1984 and 1990 (n = 236, 59, 64, $p \leq 0.01$) without accounting for year or tributary effects.

A juvenile age-structured model (Fig. 2) incorporating natural mortality, pH-driven mortality functions, and simulated density-dependent processes is used to determine the number of 2- and 3-yr smolts produced from every reach within a modelled river system. Following the application of egg and alevin toxicity functions (Table 1, Eq. 6 and 7) to determine pH-driven mortality, surviving alevins are subject to a natural emergence mortality rate, M_{emerge} (Table 2). The surviving emerging individuals, termed fry, are subject to another pH-dependent mortality rate (Table 1, Eq. 8) and a natural mortality rate, M_{fry} (Table 2).

We use a gradient-driven mortality function to reduce fry production in circumneutral reaches with nonoptimal grade. This habitat-dependent rate is calculated for every reach by combining Eq. 1 and 2 and standardizing the output so that fry in reaches with gradients at the peak of the preference curve experience no gradient-dependent mortality (Fig. 1).

Two sets of factors control the developmental fate of parr (Fig. 2): (1) "destiny parameters" which are globally defined for all reaches (Table 2) and (2) the density of total parr (1^+ and 2^+ parr) within each reach. The proportion of male fall parr potentially developing into 1^+ or 2^+ precocious parr is controlled by Pr_x, the 0^+ or 1^+ parr precocity rates. The remaining males (the $1-Pr_x$ fraction) can potentially develop into nonprecocious male parr or smolts. Because the egg sex ratio is assumed to be 50/50, half of the 0^+ fall

TABLE 1. Toxicity functions used in the model to estimate egg-to-smolt pH-driven mortality rates over the specified application periods. TD denotes toxic debt accumulation per week which is equivalent to the proportion dying per week.

Life stage	Function	Eq.	Application period	Source
Interstitial pH	Avg. interstitital pH = 0.515 + 0.908 × (avg. surface pH)	5	November–April	Lacroix 1985
Egg	% Egg mortality = 456.849 − 86.893 × (avg. interstital pH)	6	November–April	Lacroix 1985
Alevin	% Alevin mortality = $4.545 \times 10^7 \times e^{(-3.12 \times \text{avg. pH})}$	7	May	R.H. Peterson, unpublished data; Lacroix et al. 1985
Fry	% Fry mortality = $6.50 \times 10^6 \times e^{(-2.33 \times \text{avg. pH})}$	8	June	Lacroix et al. 1985; Farmer et al. 1980
Parr	TD accumulation = $7 \times (4.7 \times 10^{17} \times e^{(-9.5 \times \text{avg. weekly pH})})$	9	All year	Lacroix and Townsend 1987; G.L. Lacroix, unpublished data
Wild smolt	TD accumulation = $7 \times (4.7 \times 10^{17} \times e^{(-9.5 \times \text{avg. weekly pH})})$		May	Lacroix and Townsend 1987; G.L. Lacroix, unpublished data
Hatchery smolt	TD accumulation = $7 \times (4.7 \times 10^{17} \times e^{(-9.5 \times \text{avg. weekly pH})})$		May 15–25	Lacroix and Townsend 1987; G.L. Lacroix, unpublished data

TABLE 2. Summary of juvenile natural mortality rates and destiny parameters used in ASRAM. Unless otherwise specified, summer and winter mortality rates denote proportion lost between May–October and November–April, respectively. The symbols used in this table correspond to those in Fig. 2. *Dynamic parameters calculated as a function of total parr density.

Parameter	Symbol	Value	Source
Gravel emergence mortality rate (Nov.–May)	M_{emerge}	0.85	Meister 1962; Symons 1979; Lacroix 1985
Natural summer fry mortality rate (June–Nov.)	M_{fry}	0.40	Elson 1962
Natural winter 0^+ parr mortality rate	M_{wparr0^+}	0.40	Elson 1962
Natural summer 1^+ parr mortality rate	M_{sparr1^+}	0.40	Elson 1962
Natural winter 1^+ parr mortality rate	M_{wparr1^+}	0.40	Elson 1962
Natural summer 2^+ parr mortality rate	M_{sparr2^+}	0.40	Elson 1962
Natural winter 2^+ parr mortality rate	M_{wparr2^+}	0.40	Elson 1962
Natural summer 1^+ precocious parr mortality rate	M_{spparr1^+}	0.50	Elson 1962; Power 1969
Natural winter 1^+ precocious parr mortality rate	M_{wpparr1^+}	0.50	Elson 1962
Natural summer 2^+ precocious parr mortality rate	M_{spparr2^+}	0.50	Elson 1962
Natural winter 2^+ precocious parr mortality rate	M_{wpparr2^+}	0.50	Elson 1962
Proportion 1^+ precocious male parr potentially developing into 2-yr smolts	F_1	0.33	P.G. Amino, unpublished data
Proportion 1^+ parr potentially developing into 2-yr smolts	F_{11}	*	
Proportion 2^+ parr potentially developing into 3-yr smolts	F_{111}	*	
Proportion 0^+ parr potentially developing into 1^+ precocious male parr	Pr_1	0.10	Assumed value
Proportion 1^+ parr potentially developing into 1^+ precocious male parr	Pr_2	0.25	Assumed value

parr are destined to develop into 1^+ female parr. F_1 controls the proportion of 1^+ precocious males destined to become 2-yr smolts. F_{11} and F_{111} are density-dependent parameters which control the proportion of 1^+ and 2^+ parr (male and female) destined to become 2- and 3-yr smolts, respectively. With this approach the sex ratio and age structure of smolts produced from every reach are controlled by the "destiny parameters" as well as the pH-driven and natural mortality rates (Table 2) which influence parr density.

The proportions of 1^+ and 2^+ parr destined to become

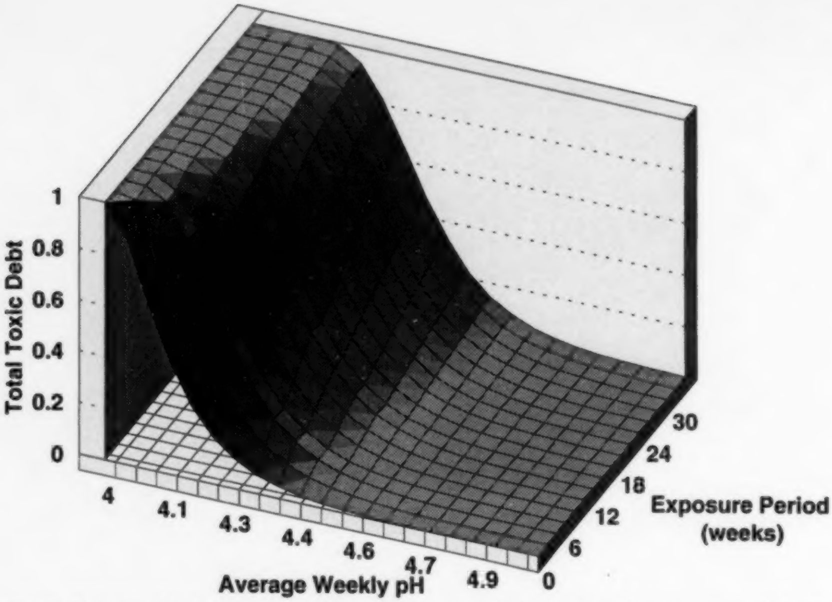

FIG. 3. Relationship between toxic debt (TD) accumulation, pH, and exposure period. The total exposure periods allowed in the model for parr and wild and hatchery smolts are 26, 4, and 1.5 wk, respectively. The pH axis denotes the effective range for the TD function using an average weekly pH.

2- (F_{II}) and 3-yr smolts (F_{III}) act as a density-dependent control affecting smolt age structure. Total parr density (1^+ and 2^+ parr/100 m^2) in each reach is used to predict the average fall fork lengths of 1^+ and 2^+ parr using the following relationships developed for the Stewiacke River (P.G. Amiro, unpublished data):

(3) Average 1^+ parr length = 11.26 − 0.75 × log (total parr density)

(4) Average 2^+ parr length = 13.468 − 0.585 × log (total parr density).

The 1^+ and 2^+ length–density functions weighted by total age 1^+ and 2^+ parr densities explained 46% ($n = 232$, $p \leq 0.001$) and 20% ($n = 195$, $p \leq 0.001$) of the variability in parr fork length measured between 1984 and 1991 at 29 sampling sites in the Stewiacke River. We use predicted average sizes in each reach to generate separate normal distributions of 1^+ and 2^+ parr lengths with a standard deviation of 0.78 cm. Criterion fall fork lengths of 9.7 cm for 1^+ parr and 10.7 cm for 2^+ parr (P.G. Amiro, unpublished data) are overlaid on the predicted length distributions to determine the proportion of each age-class large enough to smolt (as in Evans et al. 1984) at 2 and 3-yr, respectively. Increases in total parr densities within a reach, therefore, increase the proportion of individuals subject to an additional year of natural and pH-driven mortality and lead to a reduction in total smolt production. The cost of remaining in the freshwater environment an additional year depends partially on the pH-driven mortality rates in each reach.

Because early marine survival rates have been shown to be influenced by smolt size (Isaksson 1976; Chadwick 1987; Eriksson et al. 1987; Ritter 1989), we predict 2- and 3-yr smolt size by multiplying the predicted 1^+ and 2^+ fall parr fork lengths by 1.5 and 1.26, factors developed from Little River, a tributary of the Stewiacke River (P.G. Amiro, unpublished data). The fate of smolts from each reach is tracked separately in the adult component of the model to determine the number of returning adults.

Toxicity Relationships

The pH-driven mortality functions derived for egg, alevin, fry, and parr (Table 1) were developed using *in situ* bioassays and population density estimates from acidic rivers in Nova Scotia (Farmer et al. 1980, 1989; Lacroix 1985, 1989b; Lacroix et al. 1985; Lacroix and Townsend 1987; G.L. Lacroix and R.H. Peterson, Department of Fisheries and Oceans, St. Andrews, N.B., unpublished data). We use weekly average pH values for the fixed development schedule specified in Table 1 as input to estimate egg, alevin, and fry pH-driven mortality rates. We convert surface water pH to interstitial pH (Table 1, Eq. 5) to estimate egg mortality (Eq. 6), but use surface water pH for all other freshwater-stage toxicity functions.

We calculate annual pH-driven parr mortality rates (0^+, 1^+, and 2^+) based on weekly toxic debt accumulation (Table 1, Eq. 9). The annual mortality rate is calculated by multiplying the weekly survival values from the toxic debt function and then subtracting the total survival from 1. The rate of toxic debt accumulation (TD) for 0^+, 1^+ and 2^+ parr (precocious and nonprecocious) is assumed to be equivalent. A TD of 1 is equivalent to a 100% mortality rate. Parr mortality is a function of both pH and the length of exposure to each episode (Fig. 3). The function does not directly account for short episodes of extremely low pH (e.g., pH < 4 for several hours), but the use of an average weekly pH does incorporate some of the daily and hourly variability that

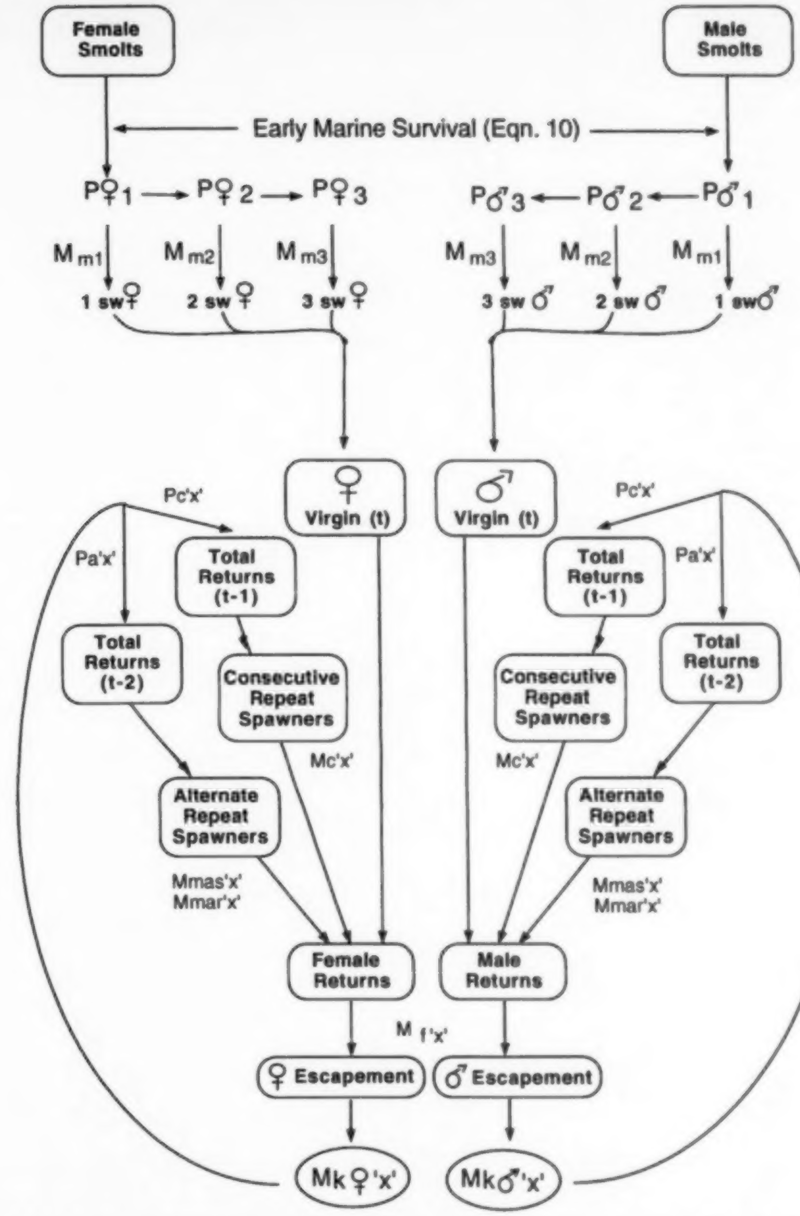
Female Smolts
Male Smolts
Early Marine Survival (Eqn. 10)
P♀1
P♀2
P♀3
P♂3
P♂2
P♂1
M m1
M m2
M m3
1 sw♀
2 sw♀
3 sw♀
3 sw♂
2 sw♂
1 sw♂
♀ Virgin (t)
♂ Virgin (t)
Pc'x'
Pa'x'
Total Returns (t-1)
Total Returns (t-2)
Consecutive Repeat Spawners
Alternate Repeat Spawners
Mc'x'
Mmas'x'
Mmar'x'
Female Returns
Male Returns
M f'x'
♀ Escapement
♂ Escapement
Mk♀'x'
Mk♂'x'

FIG. 4. Conceptual representation of the smolt-to-adult component of ASRAM. Refer to Table 3 for a description of the symbols. *t* denotes the maiden spawning year.

occurred during the bioassays done under natural and fluctuating pH regimes. The TD rate for smolts is assumed to be equivalent to that for parr (Farmer et al. 1989), but the relationship is applied for a shorter duration (Table 1, Eq. 9).

Adult Model

The adult component of ASRAM tracks the fate of fish on a reach-by-reach basis between emigration and adult return and spawning. The conceptual representation of the model (Fig. 4) summarizes how mortality rates and "destiny parameters" are used to predict the numbers, sex ratio, and age structure of returning adults. The structure of the adult model allows it to be applied to any river system. Mortality rates, destiny parameter values, fecundity, and adult sizes used here are specific to the LaHave River (Table 3).

Early marine survival of smolts is calculated as a sigmoidal function of predicted smolt fork lengths (Eq. 3 or 4 combined with smolt growth multipliers) and the following function:

TABLE 3. Summary of adult destiny parameters and annual freshwater and marine mortality rates. The symbols used in this table correspond to those in Fig. 4. Parameter values are based on life history characteristics for salmon of the LaHave River. SW = sea winter.

Parameter	SW age	Symbol	Value	Source
Proportion of smolts potentially developing into "*x*" SW ♂/♀ virgin spawners	1	$P_{♂1}/P_{♀1}$	0.96/0.64	J.A. Ritter, unpublished data
	2	$P_{♂2}/P_{♀2}$	1/1	
	3	$P_{♂3}/P_{♀3}$	1/1	
Proportion of surviving "*x*" SW spawners potentially developing into consecutive-year repeat spawners	1	P_{c1}	0.1	J.A. Ritter, unpublished data
	2	P_{c2}	0.1	
	3	P_{c3}	0.1	
	4	P_{c4}	0.1	
Proportion of surviving "*x*" SW spawners potentially developing into alternate-year repeat spawners	1	P_{a1}	0.9	J.A. Ritter, unpublished data
	2	P_{a1}	0.9	
	3	P_{a1}	0.9	
Fork length (cm)				
				R.E. Cutting,
Maiden spawners	1		50	unpublished data
	2		68	
	3		75	
Consecutive-repeat spawners	2		60	R.E. Cutting, unpublished data
	3		71	
	4		80	
	5		85	
Alternate-repeat spawners	3		72	R.E. Cutting,
	4		92	unpublished data
	5		95	unpublished data
Annual virgin "*x*" SW marine mortality rate	1	M_{m1}	0.1	J.A. Ritter, unpublished data
	2	M_{m2}	0.7	
	3	M_{m3}	0.9	
Annual "*x*" SW consecutive-year repeat spawner marine mortality rate	1	M_{mc1}	0.1	J.A. Ritter, unpublished data
	2	M_{mc2}	0.1	
	3	M_{mc3}	0.1	
	4	M_{mc4}	0.1	
Annual "*x*" SW alternate-year repeat spawner marine mortality rates (at-sea-year and return-year)	1	M_{mas1}/M_{mar1}	0.55/0.1	J.A. Ritter, unpublished data
	2	M_{mas2}/M_{mar2}	0.7/0.1	
	3	M_{mas3}/M_{mar3}	0.7/0.1	
Annual "*x*" SW freshwater mortality rate (excluding kelt mortality following spawning	1	M_{f1}	0.3	J.A. Ritter, unpublished data
	2	M_{f2}	0.15	
	3	M_{f3}	0.15	
	4	M_{f4}	0.15	
	5	M_{f5}	0.15	
Annual ♂/♀ "*x*" SW kelt mortality	1	$M_{k♂1}/M_{k♀1}$	0.90/0.80	J.A. Ritter, 1989;
	2	$M_{k♂2}/M_{k♀2}$	0.90/0.80	J.A. Ritter, unpublished data
	3	$M_{k♂3}/M_{k♀3}$	0.90/0.80	
	4	$M_{k♂4}/M_{k♀4}$	0.90/0.80	

$$(10)\qquad \text{Survival} = \frac{\text{SurvMax} \times \text{fork length}^{\beta}}{\text{HalfSize}^{\beta} + \text{fork length}^{\beta}}$$

where SurvMax is the maximum possible survival rate, HalfSize is the smolt fork length at which survival is 50% of SurvMax, and β is the coefficient controlling the sigmoidal character of the curve. To calculate the coefficients for this relationship for the LaHave River, we assumed that the estimated mean smolt-to-prerecruit survival of 22% represented the average smolt size determined for the sample captured in 1992 (R.E. Cutting, Department of Fisheries and Oceans, Halifax, N.S., unpublished data). Using these data in conjunction with the assumption that smolts averaging 12 cm survived at a 0.5% rate, we defined the parameters for Eq. 10 (HalfSize = 15.5 cm, SurvMax = 0.44, β = 15) using a Simplex nonlinear estimation procedure (Wilkinson 1990). We assume a maximum smolt size of 20 cm (G.L. Lacroix, unpublished data) to limit the predicted size of smolts and prerecruit marine survival produced from very low parr densities. There is considerable evidence that survival as a function of size reaches a plateau at 20 cm for both wild (Ward et al. 1989) and hatchery smolts (Carlin 1968; Isaksson 1976; Ritter 1977). The slope of Eq. 10 is consistent with changes in marine survival in the midsize smolt ranges observed in many other investigations (Carlin 1968; Murray 1968; Isaksson 1976; Ritter 1977; Chadwick 1987; Eriksson et al. 1987; Ward and Slaney 1988; Ward et al. 1989).

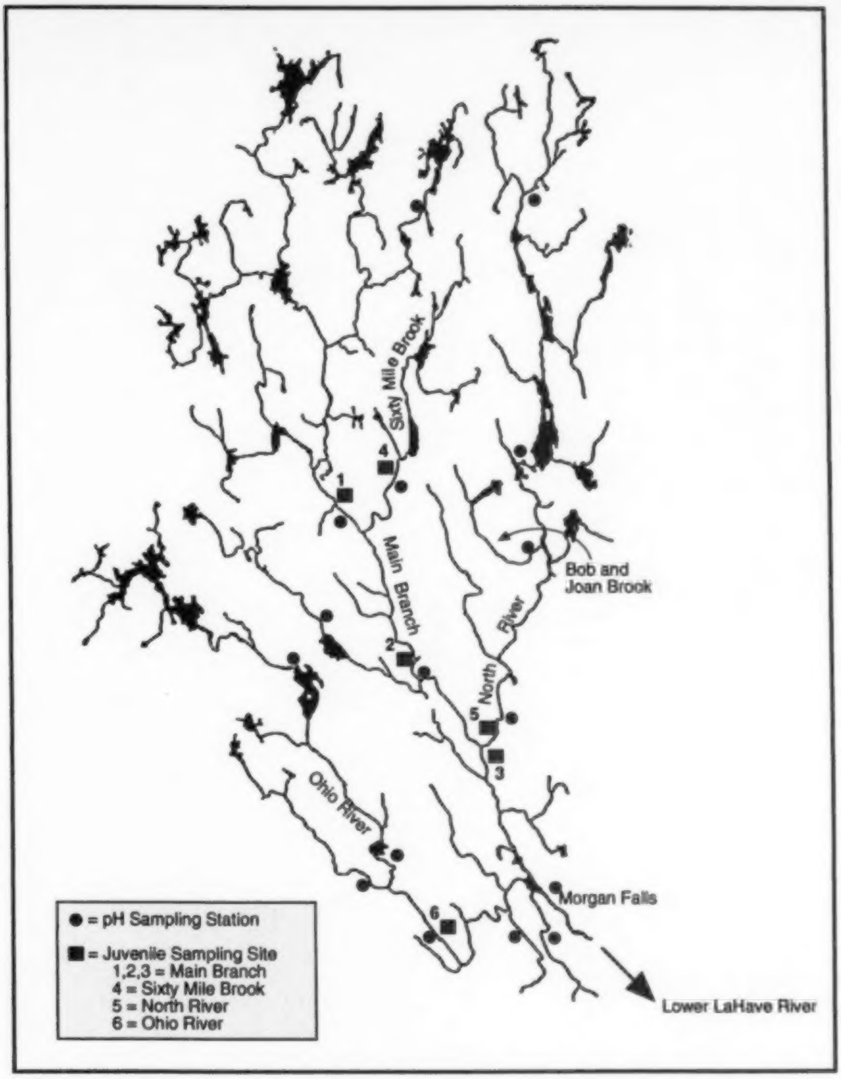

FIG. 5. Map of the LaHave River draining over Morgan Falls. Locations of pH and juvenile salmon sampling stations and the Morgan Falls fish ladder are shown.

To simplify the adult model, age-at-maturity is assumed to be independent of growth or smolt age and is determined by sex-specific destiny parameters (Fig. 4; Table 3). Age-specific marine and freshwater mortality rates (Table 3) include both natural and exploitation mortalities. Mortality rates following spawning (kelt mortality rates, Table 3) are applied to all spawners to estimate the number of individuals surviving until the end of the reacclimatization period in the marine environment.

Consecutive-year repeat spawners return every year and alternate-year repeat spawners return every second year following first sea age-at-maturity (Fig. 4). Sex-specific repeat spawner destiny parameters and marine mortality rates (Table 3) control the proportion of repeat spawners in the escapement. The differences in marine mortality rates between maiden, consecutive-, and alternate-year repeat spawners reflect different rates of exploitation associated with alternative marine migration patterns.

Fecundity is determined as a function of female fork length (centimetres) using the power relationship

$$\text{(11)}\quad \text{Eggs/female} = 446.54 \times e^{(0.0362\times \text{fork length})}$$

developed for the LaHave River stock (Cutting et al. 1987). Female fork lengths for maiden and repeat spawners for all age-classes (one to five sea-winters) are based on sizes measured at the Morgan Falls fish ladder on the LaHave River (Cutting et al. 1987). We calculate egg deposition in each reach from the number of eggs supplied by spawners returning to their home reach as well as egg contributions from stray spawners originating from other reaches in the system (20%). Stray spawners are distributed throughout the reaches in the river system according to the habitat prefer-

TABLE 4. Equilibrium (i.e., replacement) juvenile and spawner projections and pH-driven mortality rates at circumneutral (LaHave River mainstem) and acidic (Ohio River) sites and for the entire LaHave River system above Morgan Falls. The LaHave River system indicators % female spawners and smolts/spawner are an adult number-weighted average, and the pH-driven mortality rates are a reach area-weighted average.

Indicator	LaHave River mainstream (circumneutral)	Ohio River (acidic)	LaHave River system
Eggs	$411/100\ m^2$	$139/100\ m^2$	6 601 200
Total parr	$11.6/100\ m^2$	$1.3/100\ m^2$	136 550
Total smolts	$2.3/100\ m^2$	$0.3/100\ m^2$	31 000
% 2-yr smolts	36	96	50
% female smolts	54	57	54
2-yr smolt fork length (cm)	14.1	16.6	15.0
Total spawners	$21.9/\ 10\ 000\ m^2$	$6.8/10\ 000\ m^2$	3 450
Maiden spawners	$19.2/10\ 000\ m^2$	$6.0/10\ 000\ m^2$	3 040
% female spawners	49	54	51
Smolt/spawner ratio	10.6	5.0	9.0
Egg–fry pH-driven mortality	0.03	0.44	0.16
Parr pH-driven mortality	0	0.44	0.17
Smolt pH-driven mortality	0	0.06	0.02

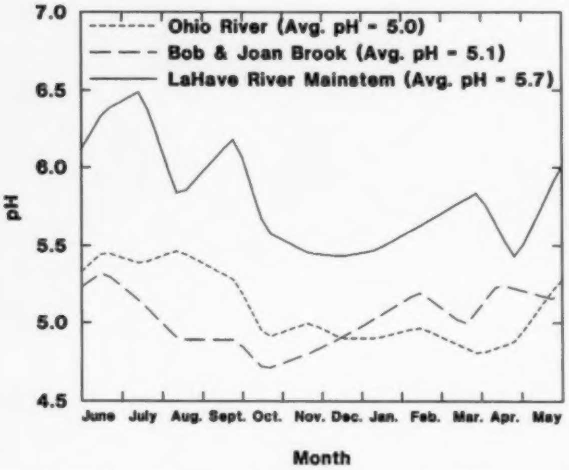

FIG. 6. Weekly pH interpolated from monthly measurements for three sites on the LaHave River above Morgan Falls (W.D. Watt, unpublished data). The annual pH averages are shown in parentheses.

ence function (Fig. 1, Eq. 1 and 2). The juvenile model uses predicted egg deposition as input to calculate the number of parr and smolts in the following 3 yr.

Application of ASRAM to the LaHave River

ASRAM was applied to the LaHave River above Morgan Falls because of the availability of physical, chemical, and biological information (Cutting et al. 1987; Gray et al. 1989; P.G. Amiro, unpublished data; R.E. Cutting, unpublished data; W.D. Watt, Department of Fisheries and Oceans, Halifax, N.S., unpublished data). The upper LaHave basin, with an estimated drainage area of 1668 km^2, consists of monzo-granite and granodiorite, hard rocks which yield water of low alkalinity (Gray et al. 1989). The total river system is made up of five major tributaries: Main Branch, West Branch, North Branch, Ohio River, and North River, and more than 100 lakes (Fig. 5) with a total surface area of 7516 ha (Gray et al. 1989). The West and North branches enter the LaHave mainstem below Morgan Falls and were not included in this study or in Fig. 5. The escapement and adult age structure for the upper river population are monitored by a fishway at Morgan Falls. Instream pH was monitored at monthly intervals at 17 locations above Morgan Falls (W.D. Watt, unpublished data).

To apply ASRAM to the LaHave River above Morgan Falls, we divided the river system into 55 tributaries consisting of multiple reaches as defined by 5-m contour intervals. Based on this method, the LaHave River upstream of Morgan Falls was dissected into 534 reaches, of which 362 were classified as suitable for Atlantic salmon production. This represents a potential production area of 28 395 × 100 m^2. Since our rule for dividing reaches is based on elevation gain, reach lengths in the LaHave are variable and range from 21 m (percent surface grade = 9.3) to 5.6 km (percent surface grade = 0.07) with an average length of 731 m. We assembled monthly pH data for the 17 monitoring stations from March 1988 to February 1989. If a month's data were not available, we substituted the next year's data for that month and station. Weekly pH values for each station were linearly interpolated from the monthly measurements. We assigned all of the reaches within each of the 55 tributaries above Morgan Falls to one of the 17 monitoring sites, choosing the nearest monitoring station downstream of each reach. Figure 6 shows the weekly interpolated pH for three stations which span the range of chemistry regimes observed above Morgan Falls.

The model was calibrated to the LaHave River data set as follows: (1) 1^+ and 2^+ parr criterion fork lengths were adjusted (9.7 and 10.7 cm, respectively) to reproduce observed average parr densities for circumneutral sampling sites during 1985–87, and (2) marine mortality rates and adult destiny parameters were "tuned" so that the predicted smolt output for the LaHave River above Morgan Falls (based on 1984–86 egg depositions) reproduced maiden and repeat spawner numbers and sex ratios observed during 1987–90.

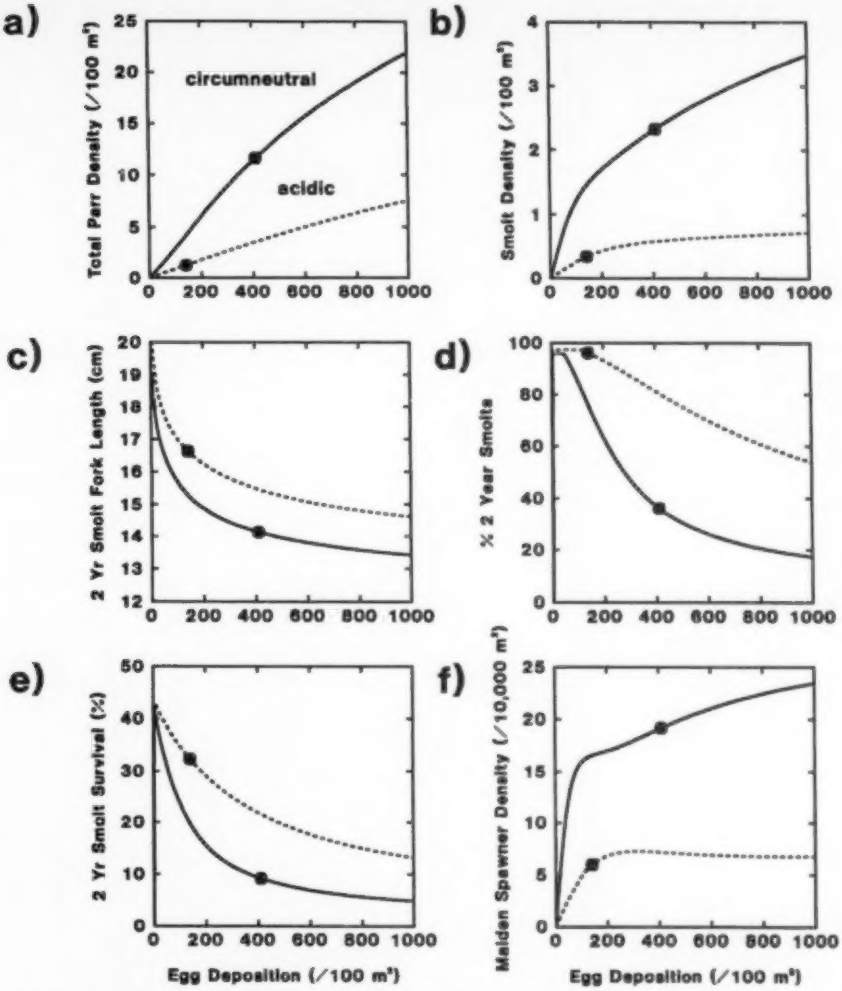

FIG. 7. Juvenile and maiden spawner return projections across a range of input egg deposition rates at circumneutral (LaHave River mainstem) and acidic (Ohio River) sites. Circles on the lines represent equilibrium (i.e., replacement) projections (values summarized in Table 4).

Model Behaviour

The behaviour of ASRAM was summarized under different density conditions and in systems of different acidity to convey important aspects of the dynamics of the model. The responses of predicted total parr and smolt density, mean smolt fork length, smolt age composition, early marine survival, and maiden spawner density (recruits) to a range of theoretical egg densities were compared in reaches in the LaHave River mainstem (circumneutral, mean annual pH = 5.7) and in the Ohio River (acidic, mean annual pH = 5.0) (Fig. 7). The dynamic behaviour of the model as egg deposition increases is shown, and the equilibrium values (i.e., replacement level for egg deposition) are highlighted. Only one equilibrium condition can exist for each site. A summary of equilibrium values is given in Table 4. We assumed that a simulation had reached equilibrium when total parr density in 5 consecutive yr was within 10% of the preceding 5-yr moving average.

In the model, circumneutral reaches have higher densities than acidic reaches, but show much greater evidence of density-dependent effects. Total parr (Fig. 7a) and smolt density (Fig. 7b) increase with egg deposition, although densities are considerably lower at the acidic site. At an egg deposition rate of 240 eggs/100 m^2, smolt and recruit densities in the acidic site are 26 and 41% of the densities in the circumneutral site, respectively. As total parr densities increase, growth is reduced (Fig. 7c) and the proportion of 2-yr smolts (Fig. 7d) and early marine survival (Fig. 7e) decline. Recruit density (Fig. 7f) is influenced by changes in both smolt age structure and early marine survival; however, smolt density (Fig. 7b) is only influenced by changes in smolt age. At the acidic site, the effects of density-dependent processes on model behaviour are seen at higher egg densities compared with the circumneutral site because of elevated pH-driven mortality rates.

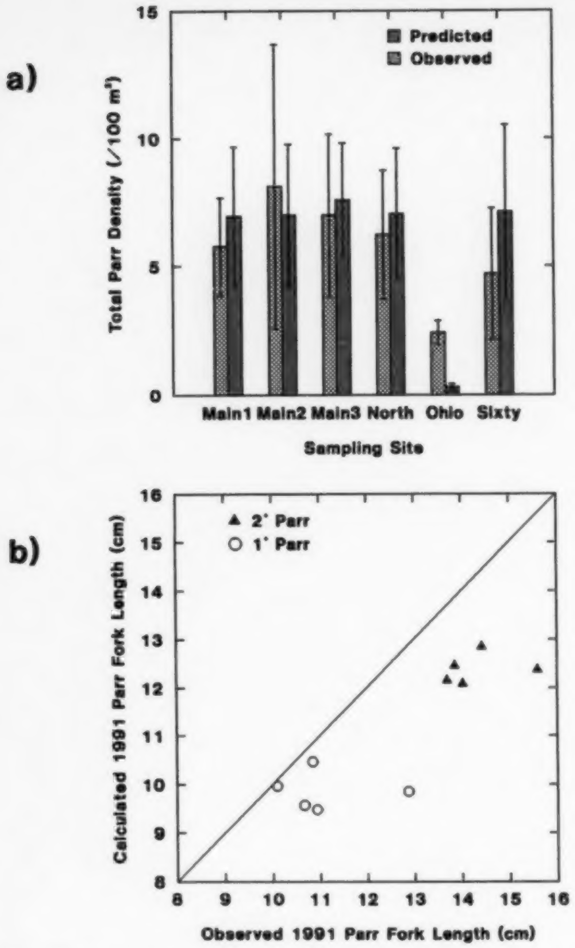

FIG. 8. (a) Comparison of predicted and average observed (1978–91) total parr densities for six juvenile sampling sites in the LaHave River system. The error bars denote one standard deviation. (b) The 1991 average observed 1^+ and 2^+ fall parr fork lengths for five of these sites are compared with calculated values using the observed total parr densities for 1991 as input to Eq. 3 and 4.

Validation

Model validation is essential to test hypothesized representations of physical and biological processes represented in the model and to improve the confidence of decision makers in model projections. In this analysis, we compared model projections at site and river system levels. As some of the LaHave River data were used to calibrate the model, the following validation is, for the most part, a confirmation that our tuning procedure provides a reasonable fit to the observed patterns between egg deposition and the resulting production of parr and adults in the LaHave.

A comparison of predicted total parr and smolt densities in circumneutral sites with values reported in the literature can be used to determine how well ASRAM operates in tributaries with no pH impacts. Lacroix (1987, 1989b) reported 6.6 1^+ presmolts/100 m^2 in the North River mainstem (1982–83) produced from an estimated egg deposition of 190 eggs/100 m^2 (see Fig. 5 for site location). Using the 1988–89 pH regime for the North River and the same egg deposition, the predicted 1^+ and 2^+ parr density is 5.8 fish/100 m^2, 0.8 presmolt/100 m^2 lower (−12%) than that reported by Lacroix. The predicted smolt density from this egg deposition rate is 1.7 smolts/100 m^2, an underestimate (−37%) compared with the 2.7 smolts/100 m^2 calculated by Lacroix. At low egg deposition rates (45 eggs/100 m^2) observed in the Pollet River, New Brunswick (Elson 1975), ASRAM underpredicts the observed smolt density (1.7 smolts/100 m^2) by 1 smolt/100 m^2 (−59%). This river produces predominantly 2-yr smolts, but at higher egg deposition rates (725 eggs/100 m^2), our model predicts a considerable increase in the proportion of 3-yr smolts (up to 78% 3-yr smolts). At these higher egg deposition rates, ASRAM underestimates the observed smolt density in the Pollet River (5.8 smolts/100 m^2) by as much as 2.8 smolts/100 m^2 (−48%). For a given egg deposition, the model predicts considerably lower smolt density (Fig. 7b) compared with the relationship presented by Symons (1979) for 2^+ smolts, but most of this discrepancy is related to the shift in smolt age structure predicted by ASRAM. Such changes in smolt age have been observed in the Matamek River, Quebec, where reduced numbers of spawners resulted in lower parr densities, increased growth rates, and a reduction in mean smolt age (Gibson 1978, 1983).

To test the model's predictions in an acidic system, we compared predicted juvenile densities with 1983 observed values in the Westfield River, Nova Scotia (1982–83 average pH = 5.0). The pH measurements from 1982 and 1983 (Lacroix 1989b) were used to calculate pH-driven mortality rates for egg-to-fry and 0^+ parr life stages, respectively, and 1982 measured egg densities of 690 eggs/100 m^2 were used as starting values for the model runs (Lacroix 1987, 1989a). Based on these input data, the model predicts a fall 1^+ presmolt density of 1.7 fish/100 m^2, a value 70% higher than the observed density of 1.0 fish/100 m^2.

The average fall parr fork length – total parr density functions (Eq. 3 and 4) used to determine smolt age structure and size determine the magnitude of the density-dependent responses in the model. Since predicted total parr density is used as input for these functions, we compared predicted densities at juvenile sampling sites in the LaHave River (Fig. 5) system (LaHave River Mainstem (three sites), Ohio River (one), Sixty Mile Brook (one), and North River (one)) based on 1975–88 egg depositions for the area upstream of Morgan Falls with the observed parr densities (R.E. Cutting, unpublished data) resulting from this egg deposition (Fig. 8a). On average (all sites combined), the model overpredicts total parr densities by 0.44 parr/100 m^2; however, the mean differences for each site were not significant (paired *t*-test, $p = 0.05$). Our predictions are within one standard deviation of the observed means for all sites except the Ohio River (annual average pH 5.0). It is difficult to make inferences regarding model biases from this comparison because (1) the number of sampling sites was very limited and (2) there is some question as to the representativeness of the samples within these reaches (R.E. Cutting and P.G. Amiro, personal observation). Nevertheless, based on these limited data, total parr density projections of the model agree reasonably well with observations in the LaHave River.

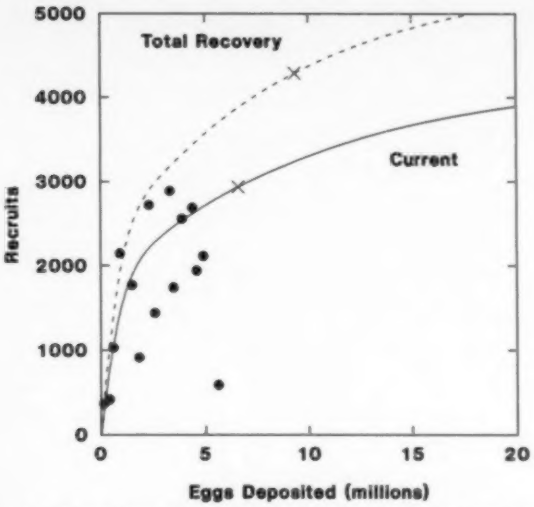

FIG. 9. Comparison of predicted and observed (circles) recruits above Morgan Falls as a function of egg deposition. The solid line represents the current predicted relationship. The broken line represents the relationship if all pH-driven mortality in the river system were eliminated. The lines were generated by determining the predicted recruits across a range of egg depositions. The crosses on the lines represent the equilibrium (i.e., replacement) levels.

To determine how well the parr length – total parr density relationships developed for the Stewiacke River (Eq. 3 and 4) predict fall parr fork lengths in the LaHave River, we compared 1991 observed fall fork lengths of 1^+ and 2^+ parr (R.E. Cutting, unpublished data) from five of the six sampling sites used in the previous analysis (fork lengths were not available for one mainstem site) with fork lengths calculated from Eq. 3 and 4 using the observed 1991 densities (Fig. 8b). The parr size–density relationships tended to underpredict mean 1^+ and 2^+ parr fork lengths by 1.2 and 1.4 cm, respectively, for the five sampling sites.

As a final test of overall model performance in the LaHave River, we compared observed egg depositions (1973–86) and resulting recruits to Morgan Falls with predicted recruits across the same range of deposition rates (Fig. 9, solid line). The model did well in predicting returns based on observed egg deposition; the mean paired difference between predicted and observed maiden returning spawners, 328 recruits, was not significantly different from zero (paired t-test, $p = 0.11$, $n = 15$). Observed and predicted recruit numbers were significantly correlated ($r^2 = 0.35$, $p = 0.02$, $n = 15$).

In summary, our validation of model projections at the site and river system level in the LaHave demonstrates that (1) the combined assumptions of the model reproduce the observed stock (egg deposition) and recruitment (smolt and adult) patterns in the LaHave quite well and (2) the values of criterion lengths (9.7 and 10.7 cm for 1^+ and 2^+ parr, respectively) and adult mortality rates and destiny parameters (Table 2) used to calibrate the model are well within observed ranges.

Sensitivity Analysis

Monte Carlo methods (O'Neil et al. 1980) were used for examining the sensitivity of the model because they allow

TABLE 5. Summary of model sensitivity to biological parameters controlling natural mortality rates, growth, and density dependence. The ranges presented in the table represent parameter values which resulted in equilibrium (i.e., replacement) projections of total smolts and recruits (maiden spawners) within ±20% of the value calculated from the base parameter values. The smolt density and ±20% ranges for the LaHave River mainstem and the Ohio River are 2.3 (1.8–2.8) and 0.34 (0.27–0.41) smolts/100 m^2, respectively. The recruit densities and ±20% ranges for the LaHave River mainstem and the Ohio River are 19.2 (15.4–23.0) and 6.0 (4.8–7.2) fish/10 000m^2, respectively. The parameter ranges for the Ohio River shown in the right two columns are calculated using ±20% ranges for smolt density (±0.5 smolt/100 m^2) and recruit density (±3.8 fish/10 000 m^2) of the circumneutral system.

		LaHave River mainstem (circumneutral)		Ohio River (acidic)			
		Relative change		Relative change		Absolute change	
Parameter	Default (range for analysis)	Smolts	Recruits	Smolts	Recruits	Smolts	Recruits
Emergence mortality rate	0.85 (0.5–1)	0.79–0.90	0.76–0.96	0.83–0.87	0.5–0.87	0.5–0.92	0.5–0.89
Natural summer fry mortality rate	0.40 (0–1)	0.28–0.59	0.14–0.82	0.31–0.49	0.03–0.51	0.01–0.61	0.01–0.58
Natural 1^+ parr winter mortality rate	0.40 (0–1)	0.33–0.50	0.29–0.53	0.35–0.46	0.34–0.48	0.01–0.61	0.14–0.56
1^+ parr criterion fork length (cm)	9.7 (7–13)	9.5–10.2	9.1–13	9.5–10	9.2–10	7–13	7–10.8
1^+ parr fork length (cm at 10 fish/100 m^2)	9.5 (7.3–11.8)	9.3–9.7	7.3–9.7	9.4–9.6	9.4–9.6	7.3–10.5	8.8–9.9
1^+ parr–2-yr smolt growth multiplier	1.5 (1–2)	1.3–1.7	1.4–1.6	1.4–1.6	1.5–1.6	1–2	1.4–1.7
Early marine survival rate (std. to 14 cm)	0.08 (0–1)	0.05–0.11	0.07–0.09	0.05–0.12	0.06–0.11	0.03–0.44	0.03–0.22

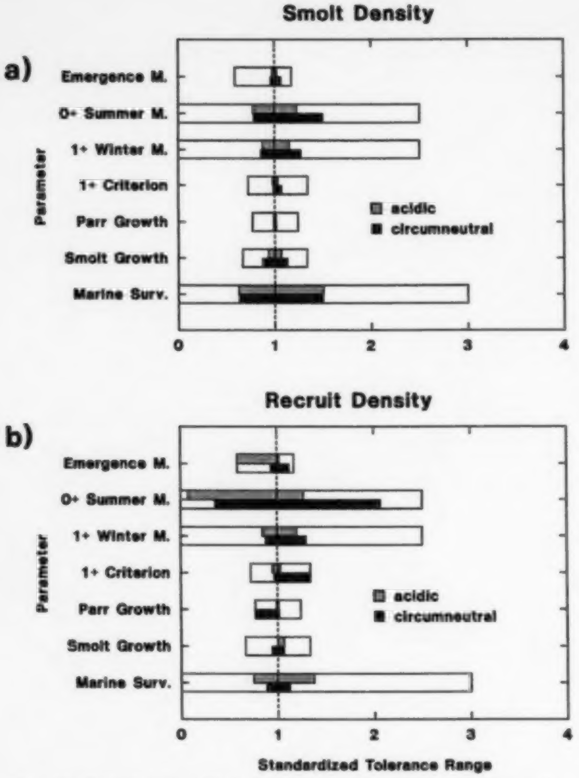

FIG. 10. Relative sensitivity of (a) smolt and (b) recruit predictions to parameters controlling mortality, growth, and density dependence in circumneutral (LaHave River mainstem) and acidic (Ohio River) reaches. The open bars show the relative range of parameter values used in the analysis; the solid and hatched boxes represent the range of standardized variation which produces smolt and recruit density estimates within ±20% of the baseline predictions.

explicit evaluation of the relative influence of model parameters. The approach involves running a large number of simulations of the same model to equilibrium while varying a single parameter from one simulation to the next within a prespecified uniform distribution; all other parameters are held at their default values. The range of parameter values which generate predictions within an acceptable range of the baseline value provides an indication of the sensitivity of the model to that parameter.

The equilibrium criterion used in this analysis is based on year-to-year variation in total parr density and is identical to that used to calculate the default equilibrium projections summarized in Table 4. In the following analysis, we consider a parameter value to have no significant effect on model predictions if the projected equilibrium smolt and recruit densities or smolt/spawner ratios are within ±20% of the baseline values summarized in Table 4.

Model Sensitivity to Natural Mortality Rates and Parameters Controlling Density Dependence

Uncertainties in parameters affecting natural mortality, growth, and density-dependent processes can affect absolute production estimates as well as the projected magnitude of responses to fisheries management actions and changes in water chemistry. We chose parameters for this analysis based on their position within the sequence of life history stages and compensatory mechanisms (Fig. 2 and 4) because the position of a parameter within the age structure of the model affects its level of influence on projections.

We carried out a Monte Carlo analysis by running the model 500 times for each of the selected parameters using both circumneutral and acidic sites. The acceptable parameter ranges (e.g., emergence mortality rate) which generated equilibrium smolt and recruit densities within ±20% of the baseline projection for reaches of identical gradient in the LaHave River mainstem and the Ohio River (Fig. 5 and 6) were summarized (Table 5). To compare the relative sensitivity of the model to different parameters, we standardized acceptable parameter ranges by dividing these ranges by the appropriate default parameter value (Fig. 10). In addition, because of differences in production between the acidic and circumneutral sites, we also described the sensitivity of the acidic site in terms of the acceptable absolute change in smolt and recruit densities of the circumneutral site (Table 5).

The upper range of values for most of the parameters in Table 5 within acceptable bounds for recruit density is more often larger than for smolts because of the additional compensatory mechanism between smolts and adults (better early marine survival resulting from lower density rearing conditions). As expected, smolt density is more sensitive to parameters influencing juvenile age structure and mortality, while recruit density is more sensitive to parameters affecting smolt growth and survival (Fig. 10). The model is most sensitive to variation in emergence mortality, 1^+ parr criterion fork length, and parr and smolt growth (Fig. 10).

The extent of model sensitivity to parameter variation is greatly influenced by pH. The acidic site is extremely sensitive to variation in parr growth and the 1^+ parr criterion length, presumably because the impacts of smolt age structure changes are magnified in a system with higher pH-driven mortality (Fig. 10; Table 5). In the circumneutral site, where total parr densities are higher, the model is very sensitive to changes in parr and smolt growth and is more resilient to overestimates of freshwater natural mortality, since the carrying capacity for simulated circumneutral systems is limited more by density-dependent growth processes than by in-stream mortality (Fig. 10; Table 5).

In absolute terms, model runs under acidic conditions have a much lower sensitivity to parameter variation relative to simulations under circumneutral ones. While the acidic site seems much more sensitive to parameters influencing density-dependent responses (parr and smolt growth and 1^+ parr criterion length) compared with the circumneutral site (Fig. 10), it is important to realize that this analysis measures relative and not absolute changes in density to facilitate between-site comparisons. Our significance levels (±20%) for smolt and recruit densities at the acidic site in absolute terms (±0.07 smolt/100 m^2, ±1.2 recruits/10 000 m^2) are 7.1 and 3.2 times smaller than those of the circumneutral system (±0.5 smolt/100 m^2, ±3.8 recruits/10 000 m^2), respectively. If we apply the absolute circumneutral significance level to the acidic site (Table 5, last two columns), the range of acceptable parameter values for the acidic site is much larger compared with the circumneutral range for all para-

TABLE 6. Summary of model sensitivity to pH-driven mortality projections for Bob and Joan Brook (very acidic) and the Ohio River (acidic). The ranges (expressed as mortality rates and relative change from baseline mortality projections) presented in the table represent predicted mortality rates which resulted in equilibrium projections (i.e., replacement) of smolts/spawner within ±20% of the baseline projections. The smolts/spawner ratios and ±20% ranges for Bob and Joan Brook and the Ohio River are 2.9 (2.3–3.5) and 5.0 (4.0–6.0), respectively.

	Bob and Joan Brook (very acidic)			Ohio River (acidic)		
Life stage	Baseline Mortality	Mortality Range	Relative Range	Baseline Mortality	Mortality Range	Relative Range
Egg	0.15	0–0.30	−100–100	0.25	0–0.49	−100–100
Alevin	0.04	0–0.09	−100–100	0.05	0–0.09	−100–100
Fry	0.30	0.1–0.48	−65–60	0.22	0–0.43	−100–95
Parr	0.62	0.59–0.65	−5–5	0.44	0.33–0.51	−25–15
Smolt	0.06	0–0.01	−100–100	0.01	0–0.02	−100–100

meters except the early marine survival rate. This overall behaviour highlights that parameter uncertainty at acidic sites will have little effect on total density estimates.

Sensitivity to pH-Driven Mortality Projections

We examined the overall effect of uncertainty in pH-driven mortality by varying the rates for each freshwater life stage through a range of ±100% of the projected values using a 1% increment. Reaches of identical gradient in Bob and Joan Brook and the Ohio River (Fig. 5 and 6) were used to compare the sensitivity in a very acidic system, which is predicted to be unable to support any production, with that in an acidic system with predicted depressed production. We considered pH-driven mortality rates to have no significant effect on model projections when the equilibrium smolt/spawner ratio was within ±20% of the baseline condition. The smolt/spawner return ratio is inherently less sensitive to changes in equilibrium projections compared with smolt or recruit density indicators used in the previous analysis, but this indicator highlights how errors in pH-driven mortality estimates influence the productive efficiency of a system.

The effects of errors in pH-mortality estimates are highly variable among life stages (Table 6). Variability in egg, alevin, and smolt mortalities has no effect on model projections in either site within a ±100% range because the pH-driven mortalities for these life stages are relatively low even in the very acidic system. Small errors in parr mortality rates caused significant departures from baseline smolt production/spawner ratios at both sites. This result is not surprising because pH-driven parr mortality rates are applied 2–3 times to a cohort within the model (see Fig. 2), while egg, alevin, and fry mortalities are applied only once. In addition, application of egg, alevin, and fry pH-driven mortality rates occurs prior to density-dependent functions so the population has more "slack" that can be taken up by compensatory mechanisms.

Bob and Joan Brook shows a higher sensitivity to errors in parr pH-driven mortality rates compared with the Ohio River (Table 6). The greater sensitivity of more acidic sites to errors in pH-driven mortality rates results from two site-specific differences: (1) pH-driven mortality rates are higher in the acidic site; thus, a relative increase from the baseline pH-driven mortality rate will generate a larger absolute change in the rate applied to the population; and (2) the projected total parr densities in very acidics sites are much lower than projections for less acidic ones. Sensitivity to underestimates of pH-driven mortality rates in the former system will not be buffered by compensatory effects as much as underestimates in less acidic systems.

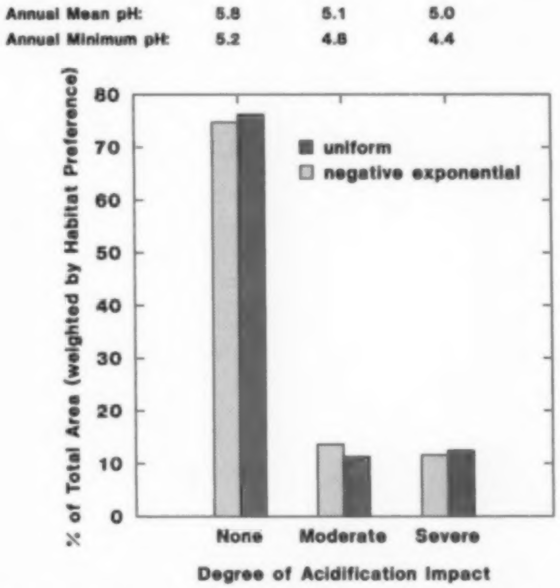

FIG. 11. Distribution of habitat-preference-weighted area for 362 producing reaches in the LaHave River (above Morgan Falls) as a function of the extent of acidification impacts on smolt density (none = 2.3 smolts/100 m^2, moderate = 0.5–1 smolts/100 m^2, severe = <0.5 smolts/100 m^2. The annual average and minimum weekly pH (interpolated from monthly measurements) for each impact category are shown for reference.

Sensitivity to River System Parameters

A key structural assumption of ASRAM is that individual fish remain in their home reach for the entire duration of their juvenile life cycle. This assumption is based on the increasing residency of parr as a function of time after June 1 and during the period of growth (Gibson 1973; Randall and Paim 1982; Lacroix 1989b). However, in streams where

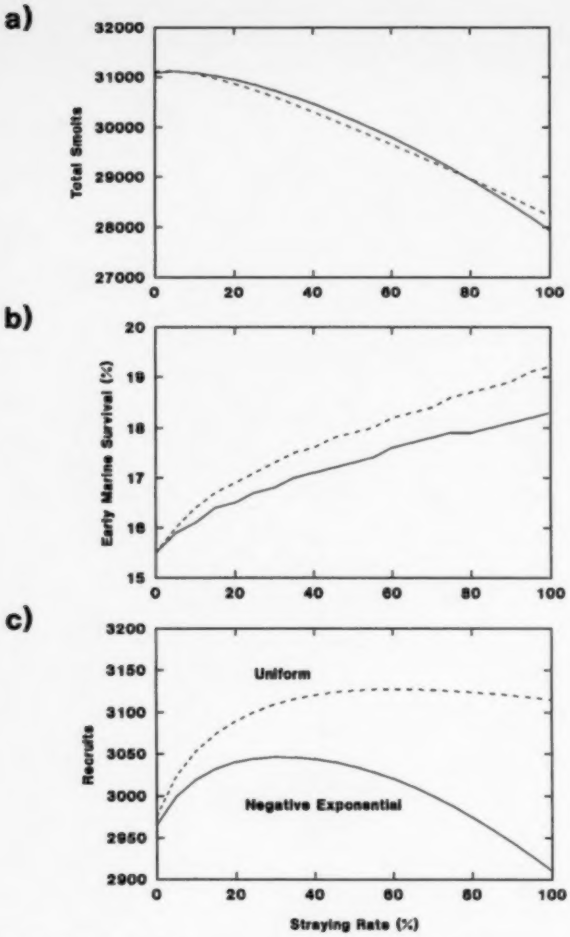

FIG. 12. Predicted (a) total smolt numbers, (b) early marine survival, and (c) recruit numbers above Morgan Falls as a function of straying rate of returning spawners to other than home reaches assuming negative exponential (solid line) or uniform-gradient (broken line) preference models.

acute acidic episodes occur, parr may emigrate in response to the episodes (G.L. Lacroix, personal observation).

The initial egg deposition pattern and stray spawner distribution over a river system are driven by an empirically derived gradient function (Fig. 1, Eq. 1 and 2) to reproduce an observed pattern of parr habitat preference (Amiro 1993) in the model. Errors in the assumed gradient preference pattern or the straying rate (affecting the distribution of adults to other than home reaches) could potentially influence projected smolt and adult production estimates for an entire river. Straying of spawners to chronically acidic headwater streams, which often contain the best spawning habitat, can reach significant proportions (>60%, Lacroix 1987) and could also be a source of error in model simulations, especially in the most acidic areas. To examine the potential effects of these errors, we ran the model for all reaches within the LaHave River cycling through the entire range of possible straying rates (0–100%) using a 5% increment. We compared the equilibrium results under both uniform (equal preference for all gradients within 0.12–5% reach grades) and negative exponential gradient-preference (Fig. 1, Eq. 1 and 2) assumptions affecting initial egg and stray spawner spatial distribution.

Differences in the proportion of low-pH-preferred habitat between the two gradient-preference models were expected to significantly influence the sensitivity of model projections to variation in the straying rate parameter. The relative distribution of rearing area (weighted by gradient preference for both patterns) as a function of the degree of acidification impacts on smolt densities for all modelled tributaries in the LaHave River above Morgan Falls indicated that (Fig. 11) (1) three quarters of the river's total production area has no acidity problems and (2) this conclusion holds for either preference model.

The rate of spawner redistribution (straying rate) and gradient preference model had only minor effects on the LaHave River simulation. Under either distribution pattern, increasing the straying rate resulted in a decline in total smolt numbers (Fig. 12a) and in increased early marine survival as a result of better growth (Fig. 12b). Under the uniform distribution pattern, recruit numbers remained relatively constant with straying rates higher than the 20% default value, while under the negative exponential pattern, recruit numbers declined (Fig. 12c). As straying rate increased, the fraction of spawners from circumneutral reaches that strayed to acidic ones increased. While the fraction of spawners from acidic reaches that strayed to circumneutral ones also increased, circumneutral-to-acidic straying dominated the observed patterns because circumneutral reaches had much higher annual adult production (see Table 4). Thus, as straying rates increased, smolt densities declined as more adults originating from healthy reaches deposited their eggs in acidic ones. While the decrease in spawner numbers to circumneutral reaches lowered total smolt densities, the average early marine survival of these smolts increased due to lower total parr densities. The benefit of increased growth equalled the impact of decreased annual smolt production on recruits under the uniform distribution, and accordingly, recruit numbers remained constant at straying rates beyond 20%. Under the negative exponential pattern, the decreased annual smolt production was not adequately compensated by increased early marine survival; thus, recruit numbers declined with increases in straying rate above 20%. The decrease in total parr densities was more dramatic under the uniform stray distribution pattern, since there was no spawner preference for reaches with gradients between 0.12 and 5%. Consequently, the average smolt-weighted early marine survival rates increased more quickly under the uniform-gradient preference model and resulted in a larger increase in recruit numbers per unit increase in straying rate.

While it is clear that assumptions about straying rate and habitat preference can have an effect on model projections, the impact is very small. Using the worst case scenario of a 100% straying rate with a uniform distribution pattern, the differences between predicted smolt and recruit numbers and predicted baseline values (negative exponential distribution, 20% straying rate) were only −9 and +3%, respectively. In modelled systems with proportionately more acidic area, the effects would be more significant.

In summary, our sensitivity analysis highlights three significant aspects of the behaviour of the model: (1) sensitivity to biological parameters is influenced by acidity and, in terms of absolute levels of production, acidic sites are less sensitive to parameter errors than circumneutral ones, (2) model projections are most sensitive to density-dependent parameters and pH-driven mortality estimates for parr, and (3) model projections for the upper LaHave River are relatively insensitive to errors in the assumed straying rate or the preference model used to distribute stray spawners. However, sensitivity would increase in relation to the proportion of acidic habitat in a system.

Analysis of Management Actions

The key purpose for developing ASRAM is to provide a tool which can be used to assess management actions in systems of different acidity and to estimate the recovery potential of acidified rivers. Fisheries managers need information on the most effective spawning targets in order to adjust harvest rates for removing only fish that are surplus to growing or maintaining salmon production, depending on the particular river management status. To assess the effectiveness of alternative stocking policies, replacement (i.e., equilibrium) smolt and recruit densities were plotted as a function of stocking rates of fall fingerlings (0^+ parr) in the LaHave River mainstem (circumneutral), the Ohio River (acidic), and Bob and Joan Brook (very acidic) (Fig. 5 and 6). The stocking was assumed to have been made in barren reaches with no natural production and that all returning adults were removed before spawning. Smolt and recruit densities are therefore solely driven by acidity and stocking rate (Fig. 13).

Smolt densities increased with stocking rate at all three sites, although it was clear that acid-stressed systems are much less efficient at producing smolts compared with circumneutral ones (Fig. 13a). At a stocking rate of 100 fingerlings/100 m^2, the circumneutral site (5.9 smolts/100 m^2) was 4.5 and 11.8 times more efficient at producing smolts compared with the acidic (1.3 smolts/100 m^2) and very acidic sites (0.5 smolt/100 m^2), respectively. In terms of recruits, the circumneutral site (28 fish/10 000 m^2) was 3.2 and 7.2 times more efficient compared with the acidic (8.7 fish/10 000 m^2) and very acidic sites (3.9 fish/10 000 m^2), respectively. Optimal stocking rates to produce the maximum number of recruits at the circumneutral (28 fish/10 000 m^2), acidic (10 fish/10 000 m^2), and very acidic sites (5 fish/10 000 m^2) occurred at densities of 116 fingerlings/100 m^2, 232 fish/100 m^2, and 366 fish/100 m^2, respectively (Fig. 13b).

The effects of freshwater exploitation rates on the viability of reaches of different acidity were examined by varying the grilse freshwater mortality rate across a range of 0–100% (default value 30%) for sites in the LaHave River mainstem, Bob and Joan Brook, and the Ohio River (Fig. 5 and 6) and then computing the equilibrium egg deposition which evolved under these conditions (Fig. 14). The 30% freshwater mortality rate is predominantly based on angling exploitation, but also includes a correction for poaching and nonreporting as well as within-stream natural adult mortality (J.A. Ritter, unpublished data). Thus, a given change from the default value is closely equivalent, but not identical, to changes in the grilse exploitation rate.

Acid-stressed systems were much less resilient to exploitation compared with circumneutral ones. To maintain a "target" egg deposition of 240 eggs/100 m^2 (Elson 1975), the circumneutral site could support a 65% freshwater grilse exploitation rate and yield 5.1 fish/10 000 m^2. In comparison, the acidic site, even in the absence of any harvesting, could only maintain an egg deposition rate of 210 eggs/100 m^2, while the very acidic site could not support a viable population (Fig. 14a). An examination of the equilibrium annual number of grilse taken as a function of the exploitation rate highlights the difficulty of setting harvesting regulations in a river system with tributaries of different acidity (Fig. 14b). At the circumneutral site, the grilse exploitation rate which maximized yield (46%) provided 6 fish/10 000 m^2 and maintained deposition rates at 330 eggs/100 m^2. At the acidic site, the optimal exploitation rate was lower (36%), yielded one third the number of fish (1.7 fish/10 000 m^2), and only provided a deposition rate of 127 eggs/100 m^2.

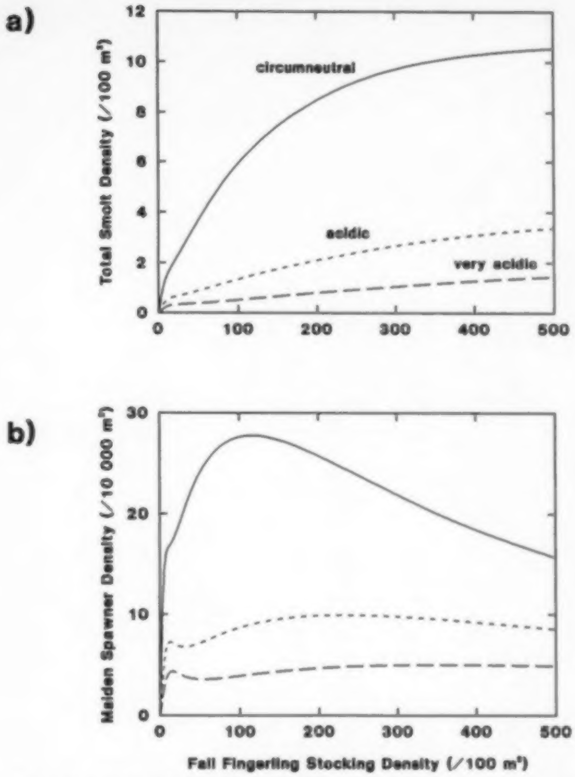

FIG. 13. Predicted equilibrium (i.e., replacement) (a) smolt and (b) maiden spawner density as a function of fall fingerling stocking density at sites representing pH conditions in the LaHave River mainstem (circumneutral), Ohio River (acidic), and Bob and Joan Brook (very acidic).

A simple assessment of the magnitude of acidification impacts on the LaHave River stock was made by comparing projections for the entire river system above Morgan Falls based on observed current pH with projections generated in the absence of any pH-driven mortality for all tributaries. In this analysis, we compared the predicted recruits with those of Morgan Falls generated from a range of egg depositions under both scenarios (Fig. 9). The predicted equilibrium values (i.e., replacement) for the "best case" recovery scenario (9.35 million eggs producing 4296 recruits) represented a 41% increase in maiden spawner returns

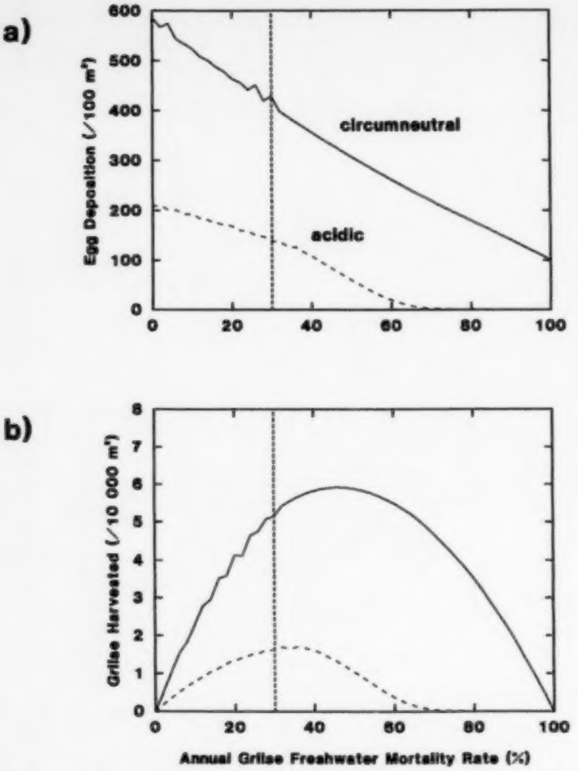

FIG. 14. Predicted equilibrium (i.e., replacement) (a) egg deposition and (b) grilse harvest for circumneutral (LaHave River mainstem), acidic (Ohio River), and very acidic (Bob and Joan Brook) reaches across a range of grilse freshwater mortality rates. The baseline mortality rate (30%) is represented by the broken vertical line.

(1256 recruits) and egg deposition (2.7 million eggs) compared with current (6.6 million eggs, producing 3040 recruits) predictions (values denoted by the crosses on the lines in Fig. 9). Assuming an instantaneous recovery in chemical conditions, the model predicts that it would take 36 yr to reach this new equilibrium with 80% of the increased production occurring in 14 yr. Under current observed healthy egg deposition rates of 5 million eggs above Morgan Falls (R.E. Cutting, unpublished data), our recovery scenario predicted an increase of 837 recruits (31%) above current predicted recruitment levels. We stress that our recovery estimate is very optimistic. In eliminating all pH-driven mortality across the entire river system, we have assumed that (1) there is total replenishment of base cations in the watershed to completely neutralize future reduced levels of acidic deposition and (2) base cation supply is large enough to eliminate any pH-driven mortality caused by natural inputs of dissolved organic carbon from wetlands within the LaHave watershed (Lacroix 1989b; W.D. Watt, unpublished data).

Discussion

We initially posed four questions regarding the effects of acidification on Atlantic salmon. The experience of building and testing ASRAM has given preliminary answers to these questions and insights on what is required to produce better answers.

How much salmon production has actually been lost to acidic deposition, and what changes can be anticipated from future acidic deposition? In the LaHave River simulation, removal of all pH-driven mortality resulted in a 41% increase in recruitment, slightly higher than the increase one would expect based strictly on the proportion of habitat with current mean pH ≤ 5.1 (34%, see Fig. 11). Our results for the LaHave River are therefore consistent with the area-proportional approach taken by Watt (1986) to estimate total production losses over all Atlantic salmon rivers in Nova Scotia. Simulated LaHave reaches in the 4.6–5.1 pH range comprised 0–15% of the annual recruit production of reaches with mean annual pH ≥ 5.6. Watt (1986) asumed that rivers with mainstem mean annual pH 4.7–5.0 had 10% of the production of rivers with pH > 5.0. Other rivers in southwestern Nova Scotia (e.g., Tusket, Clyde, Medway, Jordan, and East rivers) have a greater proportion of low-pH reaches and have greater potential for recovery compared with the LaHave River.

The simulations suggest that without additional management actions (e.g., stocking), biological recovery of Atlantic salmon populations may require several decades beyond the time required to restore natural chemical conditions. Even assuming instantaneous removal of all pH effects (i.e., ignoring the time lags associated with implementation of emission controls, desorption of sulphur stored in soils and wetlands, and replenishment of cation exchange capacity by weathering), it took 14 yr for the populations of previously acidified reaches to reach 80% of the level of production of circumneutral reaches. The intrinsic rate of population growth is slow for the LaHave stock; however, populations with a higher proportion of surviving repeat spawners, higher within-river straying rates, lower angling exploitation rates, or higher fecundities would be expected to recover faster.

At this point, we have only addressed the question of biological recovery for hypothetical past or future pH levels in the LaHave River. Our estimates for the LaHave provide an upper limit for potential recovery, since we have not considered production limitations arising from natural organic acidity and have assumed that there is total replenishment of base cations in the watershed to completely neutralize future reduced levels of acid deposition. We are currently developing a steady-state hydrochemical model which accounts for these processes in order to provide more realistic recovery scenarios.

Do compensatory, density-dependent effects mitigate the impact of acidification on salmon populations? Parr densities at acidic sites were shown to be controlled by elevated pH-driven mortality rates, and the predicted increase in growth reduced density-dependent mortality. Our comparison of circumneutral and acidic sites indicated that the reduced density-dependent mortality at the acidic site resulted in higher smolt-to-recruit survival (18% = 6 recruits/10 000 m^2 from 34 smolts) than at the circumneutral site (8.3% = 19.2 recruits/10 000 m^2 from 230 smolts). In addition, the acidic site produced a much higher proportion of 2-yr smolts (96%) compared with the circumneutral system (36%). The decrease in density-dependent early marine mortality at the acidic site resulted in smolt-to-recruit production which was 2.2-fold higher compared with the circumneutral site. However, these differences were insufficient to compensate for a

6.8-fold reduction in smolt production relative to the circumneutral site (0.34 versus 2.3 smolts/100 m^2). The net result is that the acidic site had only 31% of the annual recruit production compared with the circumneutral site.

How does the effectiveness of alternative stocking and harvesting levels vary in systems of different acidity? ASRAM simulations showed that acidic tributaries had higher optimal stocking densities because of elevated pH-driven mortality and, at realistic stocking densities, hatchery fingerlings did not show significant growth reduction. Acidic tributaries (e.g., Ohio River) were only about one half as efficient as circumneutral tributaries in producing recruits from parr, and more acidic streams (e.g., Bob and Joan Brook) were only one third as efficient. There are obviously "diminishing returns" from stocking the most acidic streams. Acidic tributaries were much more vulnerable to overharvesting and could not maintain current target egg deposition rates (240 eggs/100 m^2), even if grilse exploitation was completely eliminated. Regulating harvest control in systems with multiple tributaries of different pH is similar to managing mixed-stock fisheries. As harvest rates in the mainstem of the LaHave River increase, stocks from acidic tributaries become increasingly vulnerable.

How does habitat preference of juvenile salmon affect our ability to "scale-up" site-specific investigations or predictions to an entire river? Quantifying the extent of acidification impacts on Atlantic salmon production over an entire river was one of the key reasons for developing ASRAM. Straying of spawners to other than home reaches and selection of habitat by juvenile salmon (i.e., gradient preference) limit our ability to scale-up the results of site-specific investigations to entire rivers. These two processes, as represented in ASRAM, had negligible effects on the model's predictions for the LaHave River (Fig. 12), but could be important in other systems with a greater proportion of acidic habitat.

Projections of ASRAM for parr and smolt production are generally consistent with data from circumneutral sites in the LaHave River. This should come as no surprise, since juvenile density measurements were used to calibrate freshwater density-dependent parameters (criterion fork lengths), and maximum recruitment observations at Morgan Falls were used to adjust marine mortality rates and adult destiny parameters. The comparison of model projections with stock and recruitment data confirmed that our combined assumptions about density dependence provided a realistic estimate of the productive capacity for the LaHave River within the observed data range. However, higher egg depositions together with monitoring of smolt and adult production are required to determine the true potential capacity of this river.

The validation presented in this paper was only intended to confirm that we had adequately tuned the model to the LaHave River. In order to apply ASRAM to other rivers where calibration data are not available, further work on the parr length–density and early marine survival – length functions is necessary. Our sensitivity analysis highlighted the importance of parameters controlling density dependence on model projections. Although negative relationships between parr density and growth have been observed in other systems (Gibson and Dickson 1984; Gibson et al. 1987), there is considerable uncertainty in the shapes of these functional relationships (Eq. 3 and 4) and a recognized need to include important covariates such as stream temperature, productivity, or habitat quality. It is likely that the relationship between early marine survival and size as well as the criterion fall fork length for smoltification and parr–smolt growth multipliers will vary between river systems. Analyses of existing data from other river systems and long-term monitoring of adult, smolt, and parr populations will be required to regionalize these key parameters and functions if the model is to be applied at a broader geographic scale.

The requirement of ASRAM for weekly pH readings for all tributaries in a river system also creates difficulties with respect to regional application. Collecting such data is certainly not feasible for each of the 60 river systems flowing through the southwestern portion of Nova Scotia and is probably unnecessary because only the "transition reaches" at pH 4.7–5.1 require such accurate chemical data. Use of monthly data for the LaHave River, interpolated to weekly values and extrapolated to upstream reaches without measurements, potentially adds considerable error to production estimates for these transition reaches. Provided there is no systematic bias in sampling over the course of a year, errors in assigning pH to individual reaches may offset one another over the whole river. The sensitivity of the model to the spatial/temporal resolution of pH data will be examined to provide guidance for future chemical monitoring of other rivers and to assess its influence on our productivity estimates for acidic reaches.

ASRAM fills a unique niche in the set of quantitative tools developed to assess acidification impacts on fisheries at a regional scale. Most previous regional-scale models have focussed on lakes rather than streams (e.g., Baker et al. 1990; Minns et al. 1990). These other approaches have also relied on average water chemistry rather than the time series of pH changes throughout the year. Dose–response relationships have been largely empirical regressions developed from regional surveys of average lake chemistry and physical characteristics, designed to predict the probability of fish species presence or fish species richness. The work of Christensen et al. (1988) and Baker et al. (1990) has some parallels with our approach, in that they combined the results of laboratory experiments, age-structured population models, and field survey data to guide both the structure and calibration of their models. Representation of toxicity processes in ASRAM is based on both field acidification experiments and broad-scale surveys and explicitly recognizes the importance of seasonal variation in chemical conditions. The finer time scale of the model increases its biological realism, but comes at a cost of greater input data requirements.

ASRAM provides a scientific basis for estimating the shift in the stock–recruitment curve as habitat is improved; this is an important tool for fisheries management (Hilborn and Walters 1992). It is a step forward in the development of management strategies which account for tributary- and river-specific variability in production capacity. As chemistry data from other rivers become available through continued monitoring, and our knowledge of density dependence in early life stages improves, it should be possible to apply ASRAM on a wide geographic scale. This application would provide a regional assessment of the recovery potential for Atlantic salmon populations in acidified Maritime rivers.

Acknowledgements

The mechanism for dynamic stability of the juvenile component of ASRAM was adapted from a model proposed by

P.G. Amiro in 1988 (unpublished data). We thank S. Barbour, P. Boudreau, M. Chadwick, K. Eshelman, G. Farmer, G. Howell, P. Keiter, L. Marshall, D. Meerburg, R. Peterson, W. Silvert, and W. White for their contributions during the initial design of ASRAM. C.K. Minns and an anonymous reviewer provided helpful suggestions to improve the manuscript. Copies of the software and user's guide to run ASRAM on MS-DOS IBM-PC compatible computers are available from the Department of Fisheries and Oceans (Dr. J.A. Ritter, Halifax, N.S.). The work was funded by the Department of Fisheries and Oceans under contract to ESSA Ltd.

References

AMIRO, P.G. 1993. Habitat measurement and population estimation of juvenile Atlantic salmon (*Salmo salar*). *In* R.J. Gibson and R.E. Cutting [ed.] Production of juvenile Atlantic salmon, *Salmo salar*, in natural waters. Can. Spec. Publ. Fish. Aquat. Sci. 118: 81–97.

BAKER, J.P., D.P. BERNARD, S.W. CHRISTENSEN, M.J. SALE, J. FREDA, K. HELTCHER, D. MARMOREK, L. ROWE, P. SCANLON, G. SUTER, W. WARREN-HICKS, AND P. WELBOURN. 1990. Biological effects of changes in surface water acid–base chemistry. NAPAP Report 13. *In* National Acid Precipitation Assessment Program, Acidic Deposition: State of Science and Technology. Vol. II. 1990.

CARLIN, B. 1968. Tagging experiments in Sweden. Atlantic Salmon Association Centennial Award Fund, University of New Brunswick, Fredericton, N.B.

CHADWICK, E.M.P. 1987. Causes of variable recruitment in a small Atlantic salmon stock. Am. Fish. Soc. Symp. 1: 390–401.

CHRISTENSEN, S.W., J.E. BRECK, AND W. VAN WINKLE. 1988. Predicting acidification effects on fish populations, using laboratory data and field information. Environ. Toxicol. Chem. 7: 735–747.

CUTTING, R.E., E.M. JEFFERSON, AND S.F. O'NEIL. 1987. Status of the Atlantic salmon of the LaHave River, Nova Scotia, in 1986 and forecast of returns in 1987. Can. Atl. Sci. Advisory Comm. Res. Doc. 87/106: 18 p.

ELSON, P.F. 1962. Predator–prey relationships between fish-eating birds and Atlantic salmon. Bull. Fish. Res. Board Can. 133: 87 p.

ELSON, P.F. 1975. Atlantic salmon rivers, smolt production and optimal spawning: an overview of natural production. Int. Atl. Salmon Found. Spec. Publ. Ser. 6: 96–119.

ERIKSSON, T., L.-O. ERIKSSON, AND J. LUNDQVIST. 1987. Adaptive flexibility in life history tactics of mature male Baltic salmon parr in relation to body size and environment. Am. Fish. Soc. Symp. 1: 236–243.

EVANS, G.T., J.C. RICE, AND E.M.P. CHADWICK. 1984. Patterns in growth and smolting of Atlantic salmon (*Salmo salar*) parr. Can. J. Fish. Aquat. Sci. 41: 783–797.

FARMER, G.J., T.R. GOFF, D. ASHFIELD, AND H.S. SAMANT. 1980. Some effects of the acidification of Atlantic salmon rivers in Nova Scotia. Can. Tech. Rep. Fish. Aquat. Sci. 972: 13 p.

FARMER, G.J., R.L. SAUNDERS, T.R. GOFF, C.E. JOHNSTON, AND E.B. HENDERSON. 1989. Some physiological responses of Atlantic salmon (*Salmo salar*) exposed to soft, acidic water during smolting. Aquaculture 82: 229–244.

GIBSON, R.J. 1973. Interactions of juvenile Atlantic salmon (*Salmo salar* L.) and brook trout (*Salvelinus fontinalis* Mitchill). Int. Atl. Salmon Found. Spec. Publ. Ser. 4: 181–202.

GIBSON, R.J. 1978. Recent changes in the population of juvenile Atlantic salmon in the Matamek River, Quebec, Canada. J. Cons. int. Explor. Mer 38: 201–207.

GIBSON, R.J. 1983. Large Atlantic salmon parr (*Salmo salar*) of a boreal river in Quebec. Naturaliste can. 110: 135–141.

GIBSON, R.J., AND T.A. DICKSON. 1984. The effects of competition on the growth of juvenile Atlantic salmon. Naturaliste can. 111: 175–191.

GIBSON, R.J., T.R. PORTER, AND K.G. HILLIER. 1987. Juvenile salmonid production in the Highlands River, St. George's Bay, Newfoundland. Can. Tech. Rep. Fish. Aquat. Sci. 1538: v + 109 p.

GORHAM, E., J.K. UNDERWOOD, F.B. MARTIN, AND J.G. OGDEN III. 1986. Natural and anthropogenic causes of lake acidification in Nova Scotia. Nature (Lond.) 324(6096): 451–453.

GRAY, R.W., J.D. CAMERON, AND E.M.J. JEFFERSON. 1989. The LaHave River: physiography and potential for Atlantic salmon production. Can. Tech. Rep. Fish. Aquat. Sci. 1710: 58 p.

HILBORN, R., AND C.J. WALTERS. 1992. Quantitative fisheries stock assessment: choice, dynamics and uncertainty. Chapman and Hall, London, U.K. 570 p.

KEREKES, J.H.S. BEAUCHAMP, R. TORDON, AND T. POLLOCK. 1986. Sources of sulphate and acidity in wetlands and lakes in Nova Scotia. Water Air Soil Pollut. 31: 207–214.

ISAKSSON, A. 1976. The results of tagging experiments at the Kollafjorour experimental fish farm from 1970 through 1972. J. Agric. Res. Icel. 1976 (8, 1–2): 3–13.

LACROIX, G.L. 1985. Survival of eggs and alevins of Atlantic salmon (*Salmo salar*) in relation to the chemistry of interstitial water in redds in some acidic streams of Atlantic Canada. Can. J. Fish. Aquat. Sci. 42: 292–299.

LACROIX, G.L. 1987. Model for loss of Atlantic salmon stocks from acidic brown waters of Canada, p. 516–521. *In* R. Perry, R.M. Harrison, J.N.B. Bell, and J.N. Lester [ed.] Acid rain: scientific and technical advances. Selper Ltd., London.

LACROIX, G.L. 1989a. Ecological and physiological responses of Atlantic salmon in acidic organic rivers of Nova Scotia, Canada. Water Air Soil Pollut. 46: 375–386.

LACROIX, G.L. 1989b. Production of juvenile Atlantic salmon (*Salmo salar*) in two acidic rivers of Nova Scotia. Can. J. Fish. Aquat. Sci. 46: 2003–2018.

LACROIX, G.L., D.J. GORDON, AND D.J. JOHNSTON. 1985. Effects of low environmental pH on the survival, growth, and ionic composition of postemergent Atlantic salmon (*Salmo salar*). Can. J. Fish. Aquat. Sci. 42: 768–775.

LACROIX, G.L., AND D.R. TOWNSEND. 1987. Responses of juvenile Atlantic salmon (*Salmo salar*) to episodic increases in acidity of Nova Scotia rivers. Can. J. Fish. Aquat. Sci. 45: 1475–1484.

MEISTER, A.L. 1962. Atlantic salmon production in Cove Brook, Maine. Trans. Am. Fish. Soc. 91: 208–212.

MINNS, C.K., J.E. MOORE, D.W. SCHINDLER, AND M.L. JONES. 1990. Assessing the potential extent of damage to inland lakes in eastern Canada due to acidic deposition. III. Predicted impacts on species richness in seven groups of aquatic biota. Can. J. Fish. Aquat. Sci. 47: 821–830.

MURRAY, A.R. 1968. Smolt survival and adult utilization of Little Codroy River, Newfoundland, Atlantic salmon. J. Fish. Res. Board Can. 25: 2165–2218.

O'NEIL, R.V., R.H. GARDNER, AND J.B. MANKIN. 1980. Analysis of parameter error in a nonlinear model. Ecol. Model. 8: 297–311.

POWER, G. 1969. The salmon of Ungava Bay. Arct. Inst. N. Am. Tech. Pap. No. 22: 72 p.

RANDALL, R.G., AND U. PAIM. 1982. Growth, biomass, and production of juvenile Atlantic salmon (*Salmo salar* L.) in two Miramichi River, New Brunswick, tributary streams. Can. J. Zool. 60: 1647–1659.

RITTER, J.A. 1977. Relationship between smolt size and tag return rate for hatchery-reared Atlantic salmon (*Salmo salar*). ICES Res. Doc. C.M. 1977/M:27.

RITTER, J.A. 1989. Marine migration and natural mortality of North American Atlantic salmon (*Salmo salar* L.). Can. MS Rep. Fish. Aquat. Sci. 2041: 136 p.

SYMONS, P.E.K. 1979. Estimated escapement of Atlantic salmon (*Salmo salar*) for maximum smolt production in rivers of different productivity. J. Fish. Res. Board Can. 36: 132–140.

WARD, B.R., AND P.A. SLANEY. 1988. Life history and smolt-to-adult survival of Keogh River steelhead trout (*Salmo gairdneri*) and the relationship to smolt size. Can. J. Fish. Aquat. Sci. 45: 1110–1122.

WARD, B.R., P.A. SLANEY, A.R. FACCHIN, AND R.W. LAND. 1989. Size-biased survival in steelhead trout (*Oncorhynchus mykiss*): back-calculated lengths from adults' scales compared to migrating smolts at the Keogh River, British Columbia. Can. J. Fish. Aquat. Sci. 46: 1853–1858.

WATT, W.D. 1986. The case for liming some Nova Scotia salmon rivers. Water Air Soil Pollut. 31: 765–774.

WATT, W.D., D. SCOTT, AND W.J. WHITE. 1983. Evidence of acidification of some Nova Scotian rivers and its impact on Atlantic salmon, *Salmo salar*. Can J. Fish. Aquat. Sci. 40: 462–473.

WILKINSON, L. 1990. SYSTAT: the system for statistics. SYSTAT Inc., Evanston, Ill.

Relative Importance of Algae and Emergent Plant Litter to Freshwater Marsh Invertebrates

Suzanne Campeau[1]

Department of Renewable Resources, Macdonald College of McGill University, 21111 Lakeshore Road, Sainte-Anne-de-Bellevue, QC H9X 1C0, Canada

Henry R. Murkin

Department of Renewable Resources, Macdonald College of McGill University, 21111 Lakeshore Road, Sainte-Anne-de-Bellevue, QC H9X 1C0, Canada
and
Institute for Wetland and Waterfowl Research, c/o Ducks Unlimited Canada, Stonewall P.O. Box 1160, Oak Hammock Marsh, MB R0C 2Z0, Canada

and Rodger D. Titman

Department of Renewable Resources, Macdonald College of McGill University, 21111 Lakeshore Road, Sainte-Anne-de-Bellevue, QC H9X 1C0, Canada

Campeau, S., H.R. Murkin, and R.D. Titman. 1994. Relative importance of algae and emergent plant litter to freshwater marsh invertebrates. Can. J. Fish. Aquat. Sci. 51: 681–692.

We test the hypotheses that (1) algae are a major food source for marsh invertebrates and (2) plant litter serves mainly as cover for invertebrates and a substrate for algal growth rather than as a direct source of nutrition. Twelve enclosures (5-m diameter) were deployed in May in a nutrient-poor marsh of the Interlake region of Manitoba, six of which were fertilized to increase algal levels. The hardstem bulrush (*Scirpus lacustris glaucus*) litter present was replaced with a nonnutritive artificial substrate in half of the fertilized and unfertilized enclosures. Dominant taxa of nektonic herbivores–detritivores increased in abundance and biomass following algae manipulations but were not affected by the replacement of plant litter with a nonnutritive substrate. Epiphytic herbivores–detritivores responded to changes in both detritus and algal food sources, the importance of each factor varying among taxa. Fertilization resulted in early peaks of emergence for chironomids. In the first weeks of the study, chironomid emergence was not affected by the replacement of plant litter with a non-nutritive substrate. In August, however, more chironomids emerged in the treatments where plant litter was provided when compared with the artificial litter treatments.

Nous avons testé les hypothèses suivantes : 1) les algues constituent la principale source de nourriture pour les invertébrés des marais et 2) la litière végétale sert principalement de couvert aux invertébrés et de substrat pour la croissance des algues plutôt que comme source directe de nourriture. Douze enclos (de 5 m de diamètre) ont été mis en place en mai dans un marais pauvre en éléments nutritifs de la région d'Interlake, au Manitoba, et on a fertilisé six d'entre eux pour accroître la production algale. La litière présente, constituée de scirpe (*Scirpus lacustris glaucus*) a été remplacée par un substrat artificiel non nutritif dans la moitié des enclos fertilisés et non fertilisés. Les taxons dominants d'herbivores–détritivores nectoniques ont augmenté en abondance et en biomasse après les manipulations touchant les algues, mais n'ont pas été affectés par le remplacement de la litière par un substrat non nutritif. Les herbivores–détritivores épiphytiques ont réagi aux changements apportés à la quantité de débris et d'algues, l'importance de chaque facteur variant d'un taxon à l'autre. La fertilisation a provoqué des pics précoces d'émergence des chironomidés. Pendant les premières semaines de l'étude, l'émergence des chironomidés n'a pas été affectée par le remplacement de la litière végétale par un substrat non nutritif. En août, toutefois, on a observé l'émergence d'un plus grand nombre de chironomidés dans les enclos où le substrat était une litière végétale par comparaison avec les enclos à litière artificielle.

Received April 2, 1993
Accepted October 7, 1993
(JB872)

Reçu le 2 avril 1993
Accepté le 7 octobre 1993

Freshwater marshes provide a wide variety of resources for a broad range of vertebrate and invertebrate consumers (Mitsch and Gosselink 1986; Murkin and Batt 1987). Despite growing recognition of the importance of aquatic invertebrates to wetland values and functions, little work has dealt with invertebrate food chain support in freshwater marshes (Murkin 1989). A major hurdle to such work has been the paucity of background information on the ecology of the dominant invertebrate groups in these systems (Murkin and Batt 1987; Rosenberg and Danks 1987).

---

[1] Current address: Département de phytologie, Faculté des sciences de l'agriculture et de l'alimentation, Université Laval, Sainte-Foy, QC G1K 7P4, Canada.

Vascular plant production is high in freshwater marshes (van der Valk and Davis 1978; Brinson et al. 1981). A large portion of this material is not used directly by herbivores and enters the system as detritus (Polunin 1984; Mann 1988). It is often assumed that the processing of this litter by a variety of invertebrate consumers plays a dominant role in marsh secondary production (Mitsch and Gosselink 1986; Mann 1988; Moran et al. 1988). There is a need, however, to reevaluate the potential contribution of algae to the food chains of freshwater wetlands. Algal production represents a significant proportion of the total primary production of shallow-water systems (Allen 1971; Cattaneo and Kalff 1980), and its importance to marsh primary productivity is becoming apparent (Hooper and Robinson 1976; Hosseini 1986; Crumpton 1988). Many invertebrates are opportunistic feeders (Cummins 1973; Lamberti and Moore 1984) that may take advantage of the potential food resources represented by algae.

Algae and algal detritus are generally considered to have a high nutritive value and are readily available to consumers (Lamberti and Moore 1984; Bowen 1987). In contrast, vascular plant litter is a lower quality food source that may require processing via the microbial food web before being used by inverterbrates. Using a simulation model of a marsh community, Moran et al. (1988) suggested that microbial efficiency at transferring carbon from plant detritus to consumers is low. They concluded that although lignocellulose-derived detritus represents a dominant pool of carbon in the system they modelled, it could only support a small portion of the observed metazoan production.

Murkin (1989) suggested that algae provide a major food source for marsh invertebrates and that plant litter serves mainly as cover and habitat for invertebrates and as a substrate for algal growth rather than as a direct source of nutrition. To test these hypotheses, we monitored the response of aquatic invertebrates to varying the levels of algae and vascular plant detritus in a series of freshwater marsh enclosures. We predicted that if vascular plant detritus plays little role in invertebrate nutrition, invertebrate numbers and biomass should be similar among systems where plant litter is present or where it has been replaced by an artificial substrate with no nutritive value. Similarly, if algae are an important food resource in marshes, invertebrates should be able to take advantage of an increase in algal biomass and respond by an increase in numbers and/or biomass.

Material and Methods

Study Area

The study area was a 204-ha shallow wetland dominated by hardstem bulrush (*Scirpus lacustris* ssp. *glaucus* (Sm.) Hartm.) located in the Narcisse Wildlife Management Area in the Interlake region of south-central Manitoba, Canada (50°43′N, 97°39′W). The Interlake region is a matrix of aspen parkland, mixed grassland, and shallow wetlands. Primary production in these wetlands is nutrient limited, which in turn affects their overall secondary productivity (Neill 1990; Murkin et al. 1991).

Experimental Design

Three homogeneous bulrush stands in uniform water depths (approximately 70 cm) were selected for the study. At each of the three locations or blocks, four 5-m-diameter, 1.2-m-high watertight enclosures were established. The enclosures were modified versions of those described by Goldsborough et al. (1986). They were constructed of 1.5-mm-thick PVC sheeting with the bottom edge buried 15–20 cm into the substrate. All enclosures were placed in the marsh by 14 May 1987. Each had a 1-m-wide door which was left open until 9 June when algae standing crop manipulation began.

In mid-May 1987, all standing and fallen bulrush litter present in each enclosure was clipped and removed. In two of the four enclosures within each block, this litter was replaced by 650 pieces of bulrush litter (80 cm long) collected from the same wetland. This represented approximately 2.5 kg (dry mass) of detrital bulrush per enclosure and was similar to the amount of naturally occurring dead emergent plant biomass in the open sites. In the remaining two enclosures, 500 strands of polyurethane foam (1 × 1 × 80 cm) were installed, providing a submersed surface area similar to that in the plant litter treatment. The pieces of plant litter and artificial litter were attached at regular intervals to polypropylene ropes running across the bottom of the enclosures. Their natural buoyancy allowed them to float upright in the water column for most of the sampling season. Preliminary tests on polyurethane foam showed that this nonnutritive material was not avoided by cladocerans when tested against plant litter (Campeau 1990). This, added to the physical characteristics of the material (colour, structure resembling the inside of a dead bulrush stem), suggested that polyurethane foam was suitable to mimic detrital bulrush stems for the purpose of our study. All bulrush and artificial litter were in place by 29 May.

Beginning 9 June, water column additions of nitrogen (N) and phosphorus (P) were used to increase algal biomass in the enclosures. Within each block, one enclosure of each substrate type was fertilized weekly with ammonium nitrate and triple superphosphate. In the first week, 200 μg P/L and 4000 μg N/L were added to each fertilized enclosure. Weekly fertilizer applications decreased in concentration afterward, and from week 5 to 11 (13 July to 24 August) were generally constant at 25 μg P/L and 500 μg N/L (Campeau 1990). Fertilizers were predissolved and poured across the water surface of each enclosure. The last fertilization took place on 24 August.

Beside each block of four enclosures, an undisturbed 5-m-diameter area was delimited with five stakes. These unfertilized open sites served as controls for enclosure and disturbance effects.

Sampling

Algae

Standing crops of phytoplankton, epipelic algae, and epiphytic algae at the different sites were estimated by chlorophyll *a* determinations. Techniques used for field sampling and laboratory analysis follow Gurney and Robinson (1989).

To sample phytoplankton, one integrated water column sample was taken every second week from each enclosure and open site. Three 500-mL subsamples were used for chlorophyll *a* estimation. Samples were collected in the morning and stored in a cooler prior to filtration on Whatman GF/C filters in the afternoon or evening of the same day.

Free-standing acrylic rods (0.6-cm diameter) were used as artificial substrate for sampling epiphytic periphyton (Goldsborough et al. 1986). Rods were placed in each enclosure and open site at the end of May 1987 and sampled three at a time 4, 6, 8, and 11 wk later. The entire submersed portion of the rod was sampled for chlorophyll *a*.

To sample epipelic algae, three replicate samples of the top few centimetres of sediment were collected from each enclosure and open site every 4 wk. Samples were settled in darkened bottles and the water overlying the sediment was carefully removed the following evening (Gurney and Robinson 1989). On the following day, a lens tissue paper was placed at the surface of the sediment sample to trap the algae as they migrated to the surface at daylight (Eaton and Moss 1966; Robinson 1983). Tissue traps were sampled and replaced three times during one daylight period.

All algal samples were kept frozen until chlorophyll *a* content was determined. Extraction was done in 90% methanol in the dark over a 24-h period. Spectrophotometric readings at 665 and 750 nm before and after acidification allowed correction for the presence of chlorophyll degradation products in the sample. Chlorophyll *a* concentrations were calculated using the formulae presented in Marker et al. (1980).

Invertebrates

Two activity traps (Murkin et al. 1983) were set once a week in each enclosure and open site to monitor nektonic (free-swimming) invertebrate abundance and biomass. Activity traps consist of a 3.8-L wide-mouth glass jar with a white plastic funnel fastened in the jar opening. The traps were set horizontally in midwater column for a 24-h period. Upon retrieval, the trap contents were poured through a standard U.S. No. 35 sieve (sieve opening 0.5 mm). The animals retained by the sieve were sorted by taxon and counted.

To sample epiphytic invertebrates, two groups of three or four pieces of plant litter or artificial litter were randomly chosen from each enclosure and open site every second week. Pieces were clipped at ground level and gently transferred to a glass jar. All macroinvertebrates present (except for cladocerans, copepods, and ostracods) were removed from the surface of the substrate, sorted by taxon, and counted. Surface area of the material was also recorded.

One 0.5-m^2 surface area emergence trap (LeSage and Harrison 1979, modified by Wrubleski 1984) was set in each enclosure and open site. Insects emerging into these traps were collected in a jar of alcohol that was changed weekly, providing an integrated sample for the week.

Nektonic and epithytic invertebrate samples were generally sorted upon return from the field. If sorting had to be delayed, samples were refrigerated until they could be processed. Macroinvertebrates were identified using Merritt and Cummins (1984) and Pennak (1978). Identification was conducted to a taxonomic level sufficient to assign the animals to two broad trophic groups: herbivore–detritivore or predator–parasite. Each taxon was divided into representative size-classes. A subsample from each taxon and size-class was frozen. The mean dry mass per animal for each taxon and size-class was determined from these subsamples and used to estimate the biomass of animals present in each sample.

Emerging insects were identified to Order using Merritt and Cummins (1984), with the exception of chironomids which were identified to subfamily. Biomass was not estimated for emerging insects.

Vegetation quadrats

In mid-August 1987, two quadrats (0.5 × 0.5 m) were randomly placed in each enclosure and open site. All live plant material present in the quadrat was clipped at soil surface. Plants were divided into two groups: (1) emergent plants, mainly *Scirpus lacustris* ssp. *glaucus* and *Equisetum* spp., and (2) submersed plants, floating leaved plants, and metaphytic algae (SFA). The SFA group was largely dominated by *Utricularia* spp. Plant material was dried to constant weight and weighed to the nearest 0.01 g.

Oxygen and temperature

Once a week, dissolved O_2 levels at the water surface and at 10 cm above the bottom were recorded at approximately 07:00 and 19:00 using a YSI model 57 meter equipped with a self-stirring probe. These times corresponded with minimum and maximum daily O_2 levels (Campeau 1990). All enclosures and open sites were sampled within the same hour. Surface and bottom water temperatures were recorded at the same time. Maximum and minimum daily temperatures were recorded on three subsequent days each week using maximum–minimum thermometers set in midwater column.

Statistical Analyses

The prefertilization period data (week 0, 4–9 June) and data sets including only one measurement in time were analyzed using analysis of variance in a randomized complete block design. When sampling of a variable was repeated over a number of weeks following fetilization (weeks 1–12, 11 June – 31 August), the data were analyzed using a split-plot analysis of variance in a randomized complete block design with blocks and treatments as main-plot units and weeks of sampling as subplot units. A set of four a priori contrasts were used to locate differences between treatments. These preplanned comparisons were (1) open sites versus unfertilized plant litter treatment enclosures, (2) fertilized versus unfertilized enclosures, (3) artificial litter versus plant litter enclosures, and (4) the interaction between substrate and algal (nutrient additions) manipulations. If the interaction between weeks and treatments was significant, the contrasts tested the simple effects of treatments within each week. Otherwise, the contrasts were run on the main effects of treatments over all weeks.

When more than one sample was taken weekly from each site, the mean of these samples was considered as one observation for the purpose of the analysis of variance. Only epiphytic and nektonic invertebrate taxa where at least 40% of the observations were different from zero were considered for analysis. Chironomids were the only taxa of emerging insects analyzed.

Transformations were used for data sets that did not meet the assumption of homogeneity of variances as required by the analysis of variance procedure. For data sets where more than one sample was taken at each site for each sampling period, appropriate transformations were estimated using Taylor's power law (Downing 1979; Allan 1984). In all cases, the calculated transformation was close to either a square-root, a fourth-root, or a logarithmic transformation. Allan (1984) suggested use of $\log(x + 1)$ transformation for benthic invertebrate data sets where low means are present. This transformation proved to be effective at reducing heterogeneity of variances when invertebrate data sets

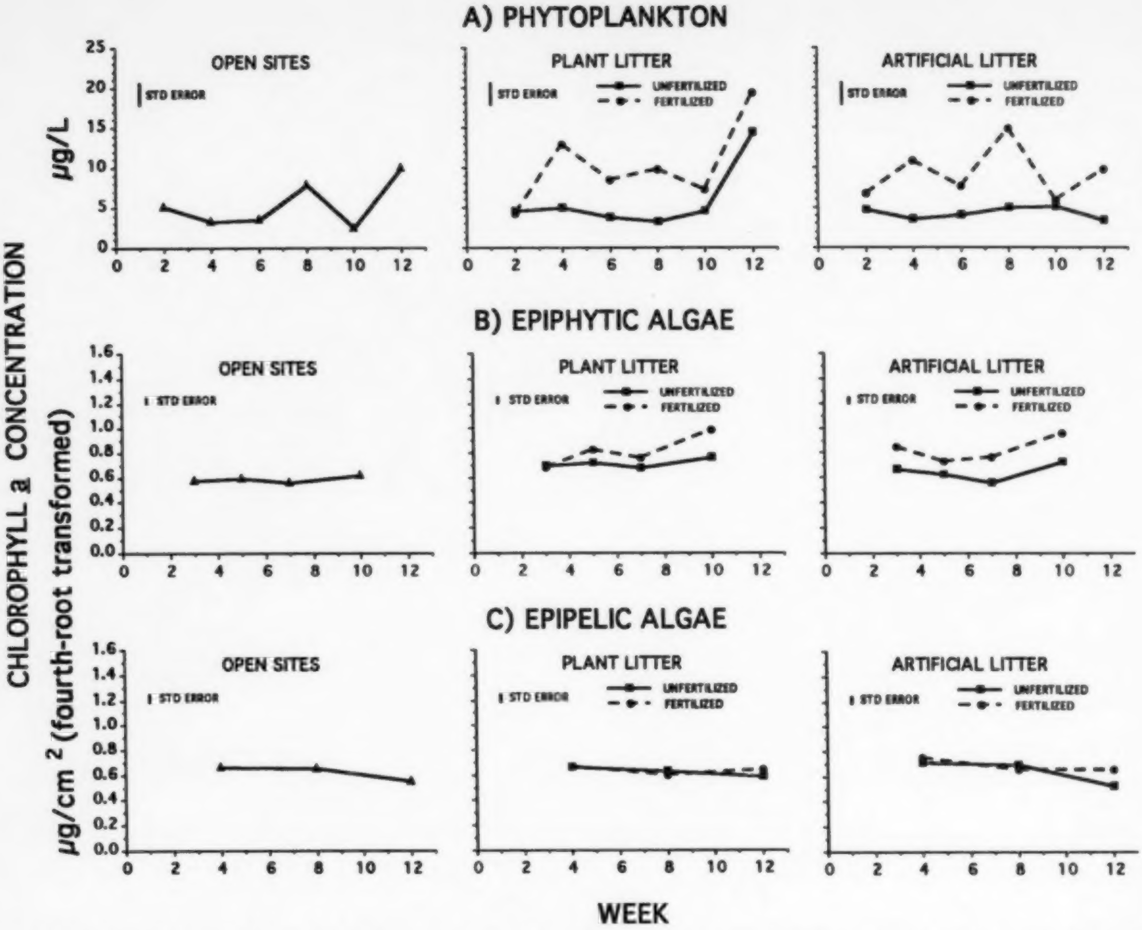

FIG. 1. Mean standing crop of algae in the treatments ($n = 3$). Standard errors of treatment means were calculated using the pooled error from each respective split-plot analysis of variance.

contained many zeros or where the range of observations was small. As no transformation could be calculated for emergence traps (only one sample per site per week), the $\log(x + 1)$ transformation was chosen based on emergence data presented in Wrubleski (1984).

All analyses of variance were performed using the GLM procedure of the Statistical Analysis System (SAS Institute Inc. 1985). The level of significance for differences between treatments was set at 0.05.

Results

Algae and Vascular Plants

In the week before nutrient addition, phytoplankton standing crops were similar among treatments ($p > 0.05$). After nutrient additions, planktonic and epiphytic algae levels in the fertilized enclosures generally exceeded the levels observed in the unfertilized enclosures ($p < 0.05$) (Fig. 1A and 1B). Of the three algal communities sampled, only the epipelon did not respond to fertilization with an increased standing crop ($p > 0.05$) (Fig. 1C). Although metaphytic algae were not sampled, we observed that metaphytic algae mats developed in all fertilized enclosures during the sampling season. Metaphytic algae occurred in only two of the six unfertilized enclosures and were never observed in the open sites. Except for epiphytic algae in weeks 5 and 10, no significant differences in algal standing crops occurred between open sites and unfertilized plant litter enclosures (Fig. 1B). In week 5, more epiphytic algae could be found in treatments where plant litter was provided in comparison with artificial litter treatments ($p < 0.05$).

Emergent and SFA plant biomass were lower in the enclosures than in the open sites due to the initial clipping ($p < 0.05$) (Fig. 2). While vegetation quadrats in the open sites were dominated by emergent plants, regrowth after clipping in both fertilized and unfertilized enclosures consisted mainly of plants of the SFA group. SFA plant biomass was higher in fertilized enclosures than in unfertilized ones ($p < 0.05$) (Fig. 2B). Emergent plant biomass in the enclosures was generally small and did not respond to nutrient additions ($p > 0.05$) (Fig. 2A).

Oxygen and Temperature

Open sites and unfertilized plant litter enclosures had comparable minimum O_2 levels ($p > 0.05$ in all weeks) that were 5 mg/L on average. Maximum daily O_2 levels were 8 mg/L on average in the open sites, which was higher than in the unfertilized plant litter enclosures, i.e., approximately 6 mg/L ($p < 0.05$ in weeks 2–8).

Fertilization and substrate manipulation significantly affected O_2 levels in our treatments. Daily minimum and maximum O_2 levels in the fertilized enclosures averaged 8 and 10 mg/L respectively, regardless of litter type. These values were higher than the average 5.5 and 6.5 mg/L levels recorded in the unfertilized enclosures ($p < 0.05$ in weeks 2–7, 9, and 12 and in all weeks, respectively). Minimum and maximum O_2 levels were lower (by approximately 2 mg/L) in the plant litter treatments than in the artificial litter treatments ($p < 0.05$ in weeks 3–7 and 12 and in weeks 3, 4, 6, 7, and 12, respectively).

Despite these differences, which can be attributed to higher standing crops of algae and vascular plants in the fertilized enclosures and to the respiration demands associated with decomposing litter, O_2 levels in the enclosures generally remained in the range recorded in the open sites. Conditions never became anoxic in any of the treatments.

Temperatures were similar between enclosed treatments ($p > 0.05$), but enclosures were generally cooler (by 0.5–1°C) than open sites ($p < 0.05$). The small difference in water temperature observed between open sites and enclosures may have been due to the increased shade provided by the PVC walls. Weekly means of water temperature varied from 15 to 24°C for minimum daily tempeatures from 18 to 28°C for maximum daily temperatures.

Nektonic Invertebrates

Numbers and biomass of herbivores–detritivores and of predators–parasites collected in activity traps prior to nutrient additions were similar for all treatments ($p > 0.05$). Fertilization increased the total number and biomass of herbivores–detritivores collected in the traps ($p < 0.05$ for number and $p < 0.05$ in weeks 5, 8, 9, 10, and 12 for biomass) (Fig. 3). The total number of herbivores–detritivores in a trap averaged 13 for unfertilized treatments and 63 for fertilized treatments (back-transformed overall mean for weeks 1–12).

The herbivore–detritivore group was dominated by cladocerans, copepods, and ostracods (Table 1). All three taxa increased significantly in number in the fertilized treatments for most or part of the season. Cladocerans responded almost immediately to changes in algal standing crop, while copepod and ostracod numbers increased respectively after 3 and 4 wk of fertilization. Caenid mayflies, the only other taxon of herbivores–detritivores that was recorded in the activity traps often enough to warrant analysis, did not respond to nutrient additions ($p > 0.05$).

Replacing natural litter with artificial litter had little or no significant impact on the abundance and biomass of herbivores–detritivores collected in activity traps for any of the groups examined (Fig. 3). Predators–parasites showed no significant response to fertilization or substrate type for either abundance or biomass.

Fewer herbivores–detritivores were collected in the activity traps in the open sites than in the unfertilized plant litter enclosures ($p < 0.05$, Fig. 3A). This response was mainly due to cladocerans. With this exception, little difference was found for activity traps between the open sites and the unfertilized plant litter enclosures.

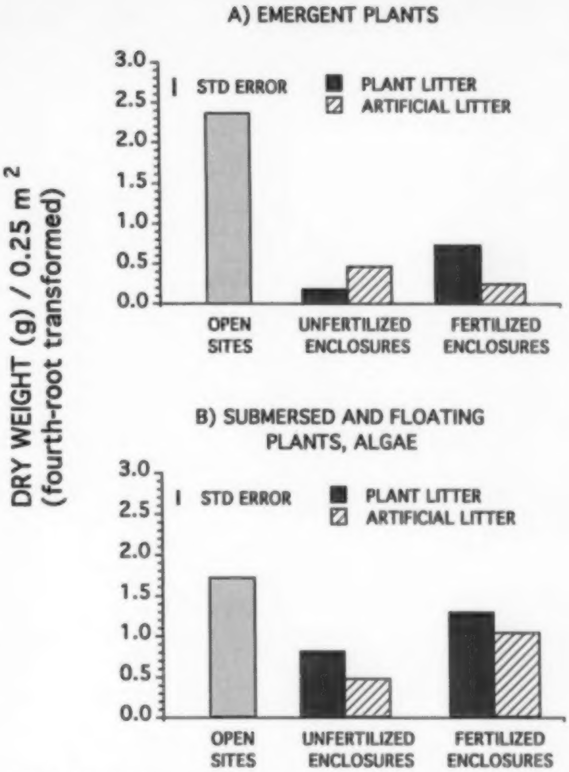

FIG. 2. Mean biomass of macrophytes in the treatments at mid-August ($n = 3$). Standard errors of treatment means were calculated using the error term from each respective one-way analysis of variance.

Epiphytic Invertebrates

The response of epiphytic invertebrates to treatments was more complex and variable than observed for nektonic invertebrates. Epithytic herbivores–detrivores as a group responded to both fertilization ($p < 0.05$ in weeks 3, 5, 9, and 11 for number and overall $p < 0.05$ for biomass) and substrate manipulation ($p < 0.05$ in weeks 1, 3, 5, and 9 for number and overall $p < 0.05$ for biomass) (Fig. 4). More epiphytic chironomid larvae were recorded in the fertilized treatments than in the unfertilized ones in the early season ($p < 0.05$ in week 3) and fewer chironomids were found on artificial litter than on plant litter ($p < 0.05$ in weeks 1, 3, 5, 7, and 9). Planorbid snails were recorded in greater numbers in the fertilized treatments than in the unfertilized enclosures in most weeks ($p < 0.05$ in weeks 3, 5, 9, and 11) and responded also to the presence of plant litter ($p < 0.05$ in weeks 5, 7, 9, and 11). Conversely, freshwater limpets (Ancylidae) did not increase significantly with fertilization and were nearly absent from the artificial litter treatments ($p < 0.05$ for differences between artificial litter and plant litter in weeks 3, 5, 7, 9, and 11)

As for nektonic invertebrates, the responses to food sources we observed for epiphytic herbivores–detrivores were not

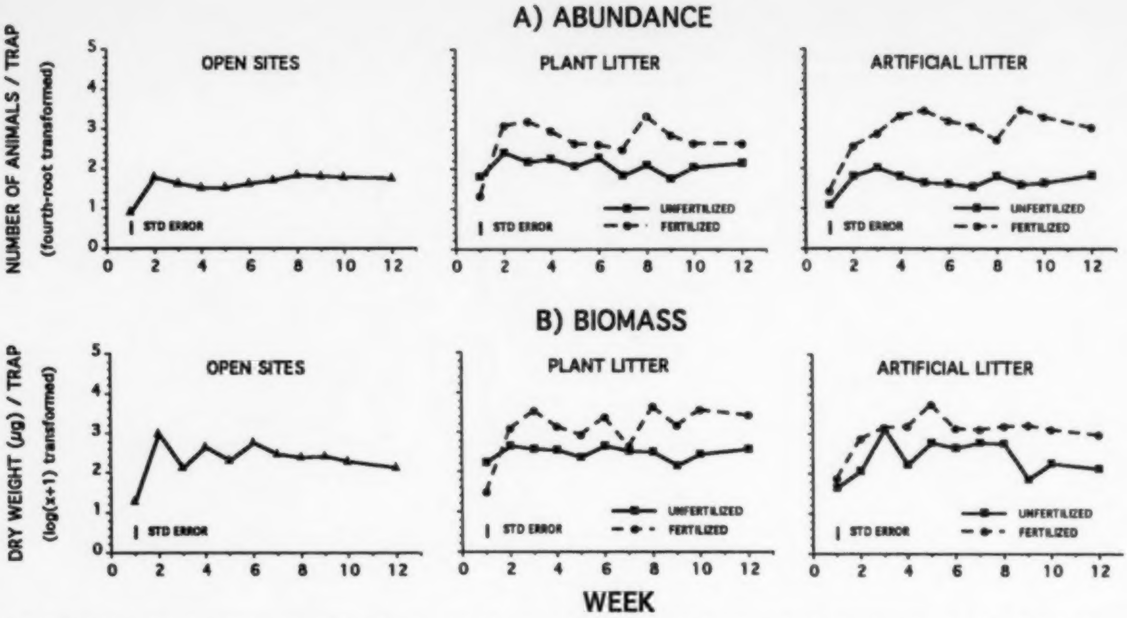

FIG. 3. Mean abundance and biomass of herbivores–detritivores collected in activity traps in the treatments ($n = 3$). Standard errors of treatment means were calculated using the pooled error from each respective split-plot analysis of variance.

carried to the predator–parasite trophic level. The only significant response of epiphytic predators–parasites to our treatments was in fact opposite to a response observed for herbivores–detrivores: number and biomass of predators–parasites were higher in the artificial litter treatments than in the plant litter treatments. This pattern reflected in good part the response of ceratopogonid larvae (Diptera) to our substrate manipulation.

More limpets ($p < 0.05$ in weeks 1, 5, 7, 9, and 11) and predators–parasites ($p < 0.05$ for number and biomass) were found in the open sites than in the unfertilized plant litter enclosures.

Emerging Insects

Chironomids were by far the numerically dominant insect group recorded in our emergence traps (Table 1). Emergence in week 0 differed between treatments for Tanypodinae and Orthocladiinae ($p < 0.05$), but not for Chironominae ($p > 0.05$). For all subfamilies, emergence in week 0 was higher in the open sites than in the enclosures, but this trend was only significant for Orthocladiinae ($p < 0.05$).

The main impact of fertilization on the dominant subfamily Chironominae (Table 1) seemed to be accelerated emergence as the number of chironomids recorded per trap peaked early in the season and then declined below the levels recorded for unfertilized treatments ($p < 0.05$ in weeks 9 and 10) (Fig. 5A). In week 5, Chironominae emergence averaged 1347 individuals per trap in the fertilized treatments and 292 in the unfertilized ones. In week 10, an average of 30 and 129 Chironominae per trap was recorded in the fertilized and unfertilized treatments, respectively. Despite these changes in the timing of emergence, the total number of Chironominae emerging over the entire sampling season remained similar between fertilized and unfertilized treatments ($p > 0.05$). Early peaks of emergence in the fertilized treatments were recorded also for Tanypodinae and Orthocladiinae ($p < 0.05$ in weeks 3–6 and in weeks 3, 4, and 6, respectively) (Fig. 5B and 5C). The patterns observed at the end of the season for these two subfamilites were, however, more complex than in the Chironominae due to the significant interaction between fertilization and substrate manipulations ($p < 0.05$ in weeks 5, 6, 7, and 9 for Tanypodinae and in weeks 6 and 10 for Orthocladiinae). For both Tanypodinae and Orthocladiinae, the total number of insects emerging over the study period was greater in fertilized treatments than in unfertilized ones ($p < 0.05$).

During the last weeks of sampling, all three subfamilies of chironomids emerged in higher numbers in plant litter enclosures than in artificial litter enclosures ($p < 0.05$ in weeks 9 and 10 for Chironominae, in weeks 8, 9, and 10 for Tanypodinae, and in week 10 for Orthocladiinae) (Fig. 5). However, only for Tanypodinae was the total emergence over the sampling season significantly higher in plant litter treatments than in artificial litter treatments ($p < 0.05$). Total emergence for both Tanypodinae and Orthocladiinae showed a significant treatment interaction: the impact of substrate type varied depending on whether the enclosures were fertilized or not. The lowest numbers of these two subfamilies emerging over the study period were observed in the unfertilized artificial litter enclosures.

Total and weekly emergence of Chironominae and Orthocladiinae were not significantly different between open sites and unfertilized plant litter enclosures. For Tanypodinae, significantly higher total emergence in the open sites was due to a species or a group of species emerging toward the end of the study ($p < 0.05$ in weeks 6–10) (Fig. 5B).

TABLE 1. Relative abundance (Ab) and biomass (Bio) of the invertebrate taxa collected at Narcisse in 1987, as a percentage of the total number or biomass of invertebrates collected during the experimental period (weeks 1–12). Only taxa where at least one of the abundance or biomass is ≥3.0% are listed.

	Enclosures		Open sites	
	Ab	Bio	Ab	Bio
Nektonic invertebrates (by trophic group)				
Herbivores–detritivores	99.1	86.3	91.2	18.9
Predators–parasites	0.9	13.6	8.0	80.7
Nektonic invertebrates (by taxa)				
Cladocera	70.2	9.1	34.6	0.7
Copepoda	22.0	5.3	31.3	1.2
Ostracoda	4.1	2.0	14.2	1.1
Gastropoda				
Planorbidae	0.5	61.0	2.0	9.1
Physidae	0.1	5.0	0.3	0.6
Hydracarina	0.5	0.5	4.6	0.5
Ephemeroptera				
Caenidae	1.5	0.7	4.7	0.5
Odonata				
Libellulidae	0.1	9.8	1.1	75.9
Epiphytic invertebrates (by trophic group)				
Herbivores–detritivores	89.2	94.9	91.8	95.3
Predators–parasites	8.0	3.7	7.1	4.3
Epiphytic invertebrates (by taxa)				
Gastropoda				
Planorbidae	23.8	58.5	3.8	9.0
Physidae	1.7	16.4	0.7	6.2
Lymnaidae	2.1	7.0	0.0	0.0
Ancylidae	10.8	7.2	58.7	67.2
Amphipoda				
Talitridae	4.2	0.7	5.8	2.7
Ephemeroptera				
Caenidae	21.8	0.7	1.1	0.1
Trichoptera				
Hydroptilidae	3.7	0.5	2.4	0.5
Diptera				
Chironomidae	22.8	4.2	20.8	9.0
Ceratopogonidae	4.1	1.0	2.3	1.1
Emerging insects (by taxa)				
Diptera–Chironomidae				
Chironominae	71.5	—	60.3	—
Tanypodinae	11.3	—	23.5	—
Orthocladiinae	12.8	—	7.6	—
Trichopetra	1.4	—	4.2	—

Discussion

Experimental Conditions

Our nutrient additions were effective in increasing algal levels except for epipelic algae. The chlorophyll *a* levels we measured in the fertilized enclosures were not abnormally high for a freshwater marsh and were in fact still low in comparison with the Delta Marsh, Manitoba, a more productive marsh approximately 75 km southwest of Narcisse (Hooper-Reid and Robinson 1978; Hosseini 1986).

In addition to increasing algae levels, fertilization increased N and P concentrations of the decomposing bulrush litter in our treatments (Campeau 1990). This change could indicate that the microbial biomass associated with the litter increased in response to nutrient additions (Triska and Sedell 1976; Polunin 1982). In addition, slightly more periphytic algae were found in treatments where plant litter was provided, possibly because decomposing bulrush releases nutrients that could be utilized by algae. These indirect effects of treatments on the algal and detrital food resources available to consumers were considered small in comparison with the large differences in the standing crops of algae and detritus that resulted from fertilization and litter replacement.

The major difference we observed between open sites and enclosures was the larger biomass of vascular plants, and, by extension, the more complex habitat offered to invertebrates in the open sites. Invertebrate density and diversity can be significantly affected by habitat characteristics (Gilinsly 1984; Gregg and Rose 1985; Hacker and Steneck 1990). Within enclosed treatments, fertilized enclosures presented greater habitat complexity than unfertilized ones, due to the enhanced growth of plants from the SFA group. Beyond

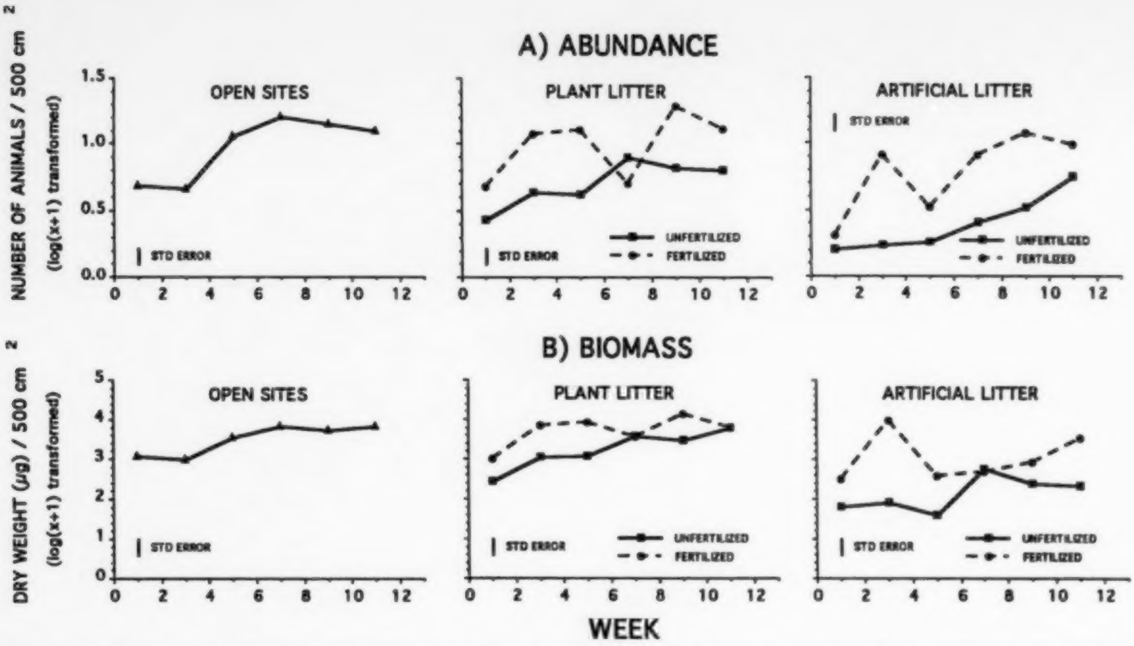

FIG. 4. Mean abundance and biomass of herbivores–detritivores collected on plant litter or on artificial litter surface in the treatments ($n = 3$). Standard errors of treatment means were calculated using the pooled error from each respective split-plot analysis of variance.

providing information on the impact of enclosed conditions, comparison between open sites and unfertilized plant litter treatments can thus indicate whether the observed invertebrate response to fertilization might be due to changes in habitat rather than changes in food resources.

Invertebrate Responses

Quantity and quality of food resources both affect aquatic invertebrate growth, development, survivorship, and/or reproduction (Danks 1978; Anderson and Cummins 1979; Ward and Cummins 1979; Söderström 1988; Urabe 1991). Invertebrates can also, under certain conditions, move to the location of a new or enhanced food resource (Mason and Bryant 1975; Rosillon 1988). Habitat requirements and life history parameters will influence the ability of each invertebrate group to respond to changes in food quality and quantity (Osenberg 1989).

Some invertebrates use detritus by feeding directly on coarse particles, while others use the fine particulate organic matter produced during the later stages of decomposition (Cummins 1973). In streams, for example, shredders utilize leaf litter that falls into the headwater zone, while downstream collectors and filter-feeders depend in part on the finer particles derived from the physical breakdown of plant litter and from the feeding activity of shredders (Anderson and Sedell 1979; Richardson and Neill 1991). Nelson and Kadlec (1984) suggested that invertebrates using freshwater marsh openings could derive a significant portion of their nutrition from the fine particles produced by the litter decomposition within adjacent stands of emergent vegetation.

Cladocerans, copepods, and ostracods feed on particles suspended in the water column and/or graze periphytic material (Monakov 1972; Pennak 1978). They have short generation times, and increasing algal levels in our enclosures resulted in a rapid numerical response that may be attributed to increased fecundity and/or survivorship. Fine particles derived from the decomposition of bulrush litter did not seem to play, in the short term, a major role in the nutrition of water column herbivores–detritivores, as no response to substrate manipulations could be detected at anytime during the study.

Many epiphytic invertebrates graze directly from the substrate and have access to both the decomposing material and associated microbes and to the epiphytic algal community (Cummins and Merritt 1984). They can also, as demonstrated for some chironomid species, use plants as a habitat while deriving most of their nutrition from the water column (Berg 1950). As they are closely associated with the substrate, specific microhabitat preferences or requirements will, in certain cases, influence their responses to resource manipulations.

The number of chironomid larvae we recorded on plant litter and artificial litter increased early after the beginning of the fertilization period. Considering the short period involved, it seems unlikely that this increase is due to reproduction. A better explanation might be that chironomid larvae in the sediments migrated to the litter surface to exploit the increased periphyton standing crop (Mason and Bryant 1975). The increase in numbers of epiphytic chironomids recorded in the fertilized treatments lasted only a short period. It coincided with, or was followed shortly after by, a peak period of chironomid emergence. As occurred for chironomids, planorbid snails responded to fertilization with an increase in the number of animals found on plant litter and natural stems. Osenberg (1989) showed that snail taxa in a Michigan lake exhibited either a positive numerical response or growth response to increased food abundance depending on the timing of fertilization relative to the snail reproduction.

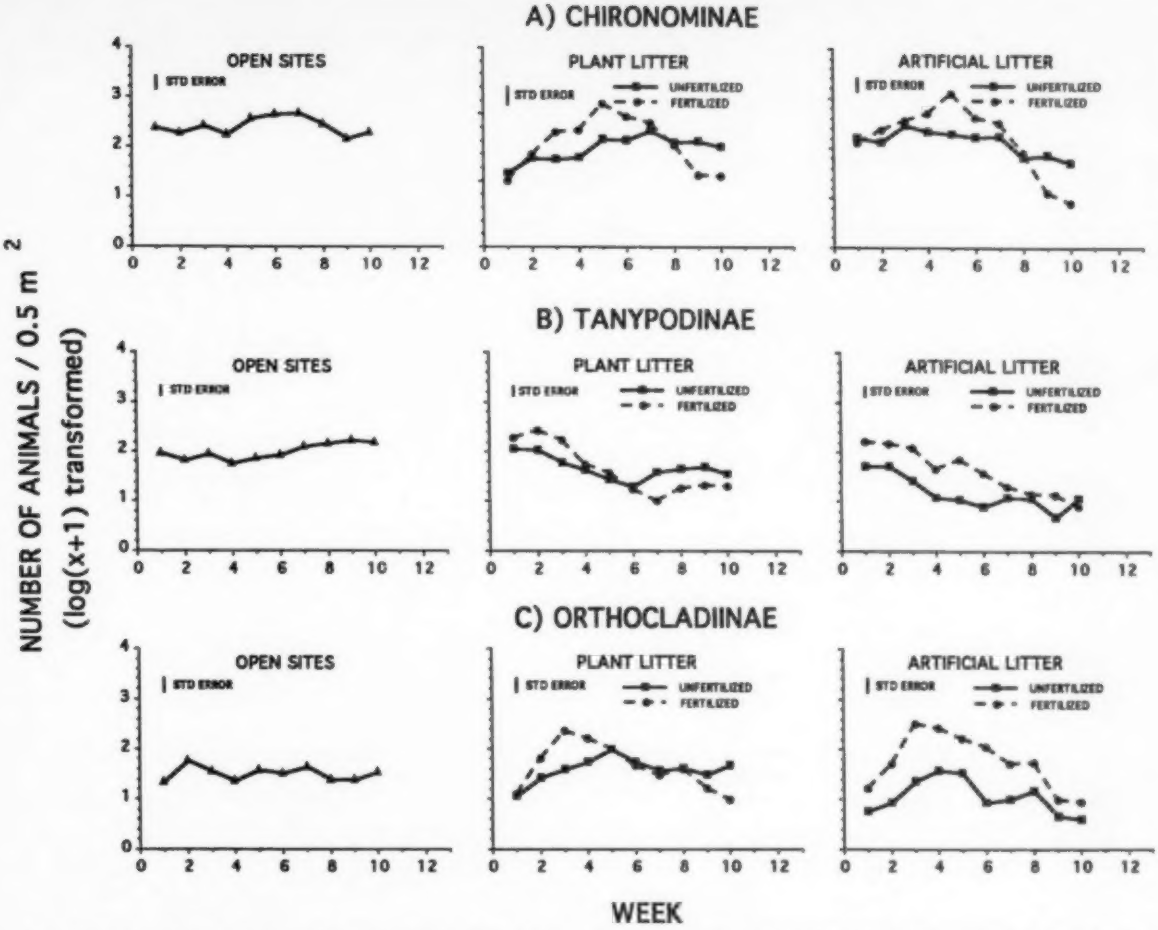

FIG. 5. Mean number of chironomids (Chironomidae) of different subfamilies emerging each week in the treatments (n = 3). Standard errors of treatment means were calculated using the pooled error from each respective split-plot analysis of variance.

Both chironomids and planorbids were found more often on detrital stems than on artificial substrate, suggesting that plant litter is more than a habitat for the two groups. Limpets were found almost solely on plant litter and did not respond to fertilization in either the plant litter or artificial litter treatments. However, part of their response to substrate may be related to differences in microhabitat between plant litter and artificial litter. Limpets may have been unable to cling to the uneven, porous structure provided by polyurethane foam.

The responses to changes in food resources that were observed for epiphytic and planktonic herbivores–detritivores were not paralleled by increases in the number of predators–parasites. Predators generally have longer life cycles than their prey, and may in general have been unable to respond to increases in prey densities in the 12 wk of our experiment.

Fewer epiphytic predators were recorded in the unfertilized plant litter enclosures than in the open sites, possibly due to the early removal of the vegetation and the resulting simpler habitat structure in the enclosures. This difference in the abundance of predators might explain the lower numbers of nektonic herbivores–detritivores in the unfertilized plant litter enclosures compared with the open sites. In contrast, both epiphytic herbivores–detritivores and emerging insects seemed to remain unaffected by the change in the number of epiphytic predators–parasites between open sites and unfertilized plant litter enclosures. This observation suggests that the impact on herbivores–detritivores of the increased abundance of epiphytic predators in the artificial litter treatments compared with the plant litter treatments would also be small, except perhaps for nektonic herbivores– detritivores, which numbers show no differences between plant litter and artificial litter treatments. The increased number of predators–parasites in the artificial litter treatments was chiefly attributable to ceratopogonids and may have been due to microhabitat preferences, as the larvae were often found in the pores of the artificial litter.

Chironomids largely dominated our emergence trap samples. A large number of chironomid species can be found in marshes and prairie ponds (Wrubleski 1987). Chironomids are often benthic, feeding off the bottom sediments or filtering material from the water column. They also live on submersed vegetation or detritus, while some are free-living predators (Oliver 1971; Coffman and Ferrrington 1984; Pinder 1986). Many chironomids are uni- or bivoltine, but three and four generations a year are not uncommon (Pinder 1986).

Despite the diversity of chironomid species likely to be found in our samples, there were some common responses to our treatments of the subfamily level. First, emergence was earlier in the fertilized treatments than in the unfertilized enclosures. This early emergence could be attributable to increased larval growth rate in response to an increase in the quantity of high-quality algal food (Ward and Cummins 1979; Sweeney 1984; Pinder 1986). The total number of Tanypodinae emerging over the season was also positively affected by fertilization, suggesting that for this group, not only growth but possibly also survival and/or emergence success were affected by changes in food resources. Previous studies of resource manipulation in insects have shown that, beyond affecting growth rate, changes in the quantity or quality of the available food can also affect the number of generations that are produced in a year (Ward and Cummins 1979). The duration and taxonomic resolution of our study precluded such observations.

A second result common to the three chironomid subfamilies was that the effect of detritus manipulations could only be detected after several weeks. Decomposing material becomes a better food source and is preferred by aquatic consumers after a period of conditioning (Bärlocher and Kendrick 1975; Smock and Harlowe 1983; Suren and Lake 1989). Our results suggest that, while plant detritus is principally a substrate for chironomids at the beginning of the season, its importance as a food source, either directly or through the release of fine particles, increases as decomposition progresses. A second possible explanation for the pattern observed is that one or more of the species present depend specifically on a detrital diet to complete their life cycle (Lawson et al. 1984). This could explain the emergence pattern observed in Tanypodinae. In the subfamily, total emergence was higher in the plant detritus treatments due to a late peak of emergence that was not observed in the artificial litter enclosures, in spite of the abundant food resource provided by algae in the fertilized artificial litter treatments. This late peak of emergence was also observed in the open sites, where plant detritus was present.

None of the differences observed between fertilized and unfertilized treatments in the nektonic, periphytic, or emerging insects groups paralleled the differences observed between open sites and unfertilized plant litter enclosures. Consequently, we assume that the differences in invertebrate numbers and biomass we observed between fertilized and unfertilized enclosed treatments were due to the increased food resources and not to changes in habitat structure.

Our substrate manipulations involved detritus of emergent plants in their first year of decomposition. A decomposition study conducted in the same marsh showed that bulrush litter lost approximately 25% of its dry mass over a 10-wk summer period (Campeau 1990). Consequently, a large portion of the bulrush material entering the water column in a given year is still present over at least the following summer. The role of older (i.e., second or third year of decomposition) emergent plant detritus in the system remains to be assessed. The importance to consumers of fast-decomposing, higher protein detritus produced by the senescence of submersed aquatic plants should also be addressed. Live and decomposing vascular plant and algae may also contribute significantly to aquatic food chains through the release of dissolved organic matter (Findlay et al. 1986; Bowen 1987; Mann 1988).

Previous studies have shown that algae account for a significant proportion of total primary production in freshwater marshes and represent a high-quality food resource for a variety of consumers. Our study showed that most invertebrate groups readily used this food resource when available. In contrast, even though plant litter represents a large proportion of the potential food resources in our system at any given time, only certain invertebrate groups seemed to depend on emergent plant litter in its early stage of decomposition.

In temperate systems, algal production is likely to vary qualitatively and quantitatively within and between seasons depending on factors such as nutrient, light, and temperature regimes. The availability of algae as a food source for invertebrates may then vary in importance throughout the year (Johannsson and Beaver 1983; Rasmussen 1984). In contrast, although plant litter input in marshes takes place mainly in the spring and early summer (Davis and van der Valk 1978), partly decomposed plant litter is present in the system on a year-round basis. Murkin (1989) suggested that the relative importance of algae and vascular plant detritus to freshwater marsh food webs would vary among consumers, among seasons, and among years. In many cases, however, it is likely that the algal contribution to marsh secondary production is significant and should be considered when discussing productivity and trophic structure in marsh systems.

Acknowledgements

This study was funded by the North American Wildlife Foundation through the Delta Waterfowl and Wetlands Research Station, by Ducks Unlimited Canada, and by the Natural Sciences and Engineering Research Council of Canada (NSERC) through an operating grant to H.R. Murkin and a postgraduate scholarship to S. Campeau. Phil Ould provided logistical support. Special thanks to Susan Holroyd, Bruce Barnett, Peter Joyce, Colleen Barber, and Bruce Pollard who assisted with the field work. Sharon Gurney and Dale Wrubleski helped us with many aspects of the algae and invertebrate sampling and analyses. The late M.H. Fanous provided statistical advice. F.G. Whoriskey and D.J. Lewis commented on an earlier version of this manuscript. This is paper No. 73 of the Marsh Ecology Research Program, a joint project of Ducks Unlimited Canada and of the Delta Waterfowl and Wetlands Research Station, and paper No. 10 of the Institute for Wetland and Waterfowl Research.

References

Allan, J.D. 1984. Hypothesis testing in ecological studies of aquatic insects. p. 484–507. *In* V.H. Resh and D.M. Rosenberg [ed.] The ecology of aquatic insects. Praeger, New York, N.Y.

Allen, H.L. 1971. Primary productivity, chemo-organotrophy, and nutritional interactions of epiphytic algae and bacteria on macrophytes in the littoral of a lake. Ecol. Monogr. 41: 97–127.

Anderson, N.H., and K.W. Cummins. 1979. Influences of diet on the life histories of aquatic insect. J. Fish. Res. Board Can. 36: 335–342.

Anderson, N.H., and J.R. Sedell. 1979. Detritus processing by macroinvertebrates in stream ecosystems. Annu. Rev. Entomol. 24: 351–377.

Bärlocher, F., and B. Kendrick. 1975. Leaf-conditioning by microorganisms. Oecologia 20: 359–362.

Berg, C.O. 1950. Biology of certain Chironomidae reared from *Potamogeton*. Ecol. Monogr. 20: 83–101.

Bowen, S.H. 1987. Composition and nutritional value of detritus. p. 192–216. *In* D.J.W. Moriarty and R.S.V. Pullin [ed.] Detritus and microbial ecology in aquaculture. ICLARM Conference Proceedings 14, International Center for Living Aquatic Resources Management, Manila Philippines.

Brisson, M.M., A.E. Lugo, and S. Brown. 1981. Primary productivity, decomposition and consumer activity in freshwater wetlands. Annu. Rev. Ecol. Syst. 12: 123–161.

Campeau, S. 1990. The relative importance of algae and vascular plant detritus to freshwater wetland food chains. M.Sc. thesis, McGill University, Montreal, Que. 187 p.

Cattaneo, A., and J. Kalff. 1980. The relative contribution of aquatic macrophytes and their epiphytes to the production of macrophyte beds. Limnol. Oceanogr. 25: 280–289.

Coffman, W.P., and L.C. Ferrington. 1984. Chironomidae. p. 551–652. *In* R.W. Merritt and K.W. Cummins [ed.] An introduction to the aquatic insects of North America. 2nd ed. Kendall/Hunt, Dubuque, Iowa.

Crumpton, W.G. 1988. Algae in northern prairie wetlands. p. 188–203. *In* A.G. van der Valk [ed.] Northern prairie wetlands. Iowa University Press, Ames, Iowa.

Cummins, K.W. 1973. Trophic relations to aquatic insects. Annu. Rev. Entomol. 18: 183–206.

Cummins, K.W., and R.W. Merritt. 1984. Ecology and distribution of aquatic insects. p. 59–65. *In* R.W. Merritt and K.W. Cummins [ed.] An introduction to the aquatic insects of North America. 2nd ed. Kendall/Hunt, Dubuque, Iowa.

Danks, H.V. 1978. Some effects of photoperiod, temperature, and food on emergence in three species of Chironomidae (Diptera). Can. Entomol. 110: 289–300.

Davis. C.B., and A.G. van der Valk. 1978. The decomposition of standing and fallen litter of *Typha glauca* and *Scirpus fluviatilis*. Can. J. Bot. 56: 662–675.

Downing, J.A. 1979. Aggregation, transformation, and the design of benthos sampling programs. J. Fish. Res. Board Can. 36: 1454–1463.

Eaton, J.W., and B. Moss. 1966. The estimation of numbers and pigment content in epipelic algal populations. Limnol. Oceanogr. 11: 584–595.

Findlay, S., L. Carlough, M.T. Crocker, H.K. Gill, J.L. Meyer, and P.J. Smith. 1986. Bacterial growth on macrophyte leachate and fate of bacterial production. Limnol. Oceanogr. 31: 1335–1341.

Gilinsky, E. 1984. The role of fish predation and spatial heterogeneity in determining benthic community structure. Ecology 65: 455–468.

Goldsborough, L.G., G.G.C. Robinson, and S.E. Gurney. 1986. An enclosure/substratum system for in situ ecological studies of periphyton. Arch. Hydrobiol. 106: 373–393.

Gregg, W.W., and F.L. Rose. 1985. Influences of aquatic macrophytes on invertebrate community structure, guild structure, and microdistribution in streams. Hydrobiologia 128: 45–56.

Gurney, S.E., and G.G.C. Robinson. 1989. Algal primary production, p. 18–22. *In* E.J. Murkin and H.R. Murkin [ed.] Marsh Ecology Research Program long-term monitoring procedures manual. Technical Bulletin 2, Delta Waterfowl and Wetlands Research Station, Portage la Prairie, Man.

Hacker, S.D., and R.S. Steneck. 1990. Habitat architecture and the abundance and body-size dependant habitat selection of a phytal amphipod. Ecology 71: 2269–2285.

Hooper, N.M., and G.G.C. Robinson. 1976. Primary production of epiphytic algae in a marsh pond. Can. J. Bot. 54: 2810–2815.

Hooper-Reid, N.M., and G.G.C. Robinson. 1978. Seasonal dynamics of epiphytic algal growth in a marsh pond: productivity, standing crop, and community composition. Can. J. Bot. 56: 2441–2448.

Hosseini, S.M. 1986. The effects of water level fluctuations on algal communities of freshwater marshes. Ph.D. thesis, Iowa State University, Ames, Iowa. 99 p.

Johannsson, O.E., and J.L. Beaver. 1983. Role of algae in the diet of *Chironomus plumosus* F. *semireductus* from the Bay of Quinte, Lake Ontario. Hydrobiologia 107: 237–247.

Lamberti, G.A., and J.W. Moore. 1984. Aquatic insects as primary consumers, p. 164–195. *In* V.H. Resh and D.M. Rosenberg [ed.] The ecology of aquatic insects. Praeger, New York, N.Y.

Lawson, D.L., M.J. Klug, and R.W. Merritt. 1984. The influence of the physical, chemical, and microbiological characteristics of decomposing leaves on the growth of the detritivore *Tipula abdominalis* (Diptera: Tipulidae). Can. J. Zool. 62: 2339–2342.

LeSage, L., and A.D. Harrison. 1979. Improved traps and techniques for the study of emerging aquatic insects. Entomol. News 90: 65–78.

Mann, K.H. 1988. Production and use of detritus in various freshwater, estuarine, and coastal marine ecosystems. Limnol. Oceanogr. 33: 910–930.

Marker, A.F.H., E.A. Nusch, H. Rai, and B. Riemann. 1980. The measurement of photosynthetic pigments in freshwaters and standardization of methods: conclusions and recommendations. Arch. Hydrobiol. Beih. Ergebn. Limnol. 14: 91–106.

Mason, C.F., and R.J. Bryant. 1975. Periphyton production and grazing by chironomids in Alderfen Broad, Norfolk. Freshwater Biol. 5: 271–277.

Merritt, R.W., and K.W. Cummins. 1984. An introduction to the aquatic insects of North America. 2nd ed. Kendall/Hunt, Dubuque, Iowa. 722 p.

Mitsch, W.J., and J.G. Gosselink. 1986. Wetlands. Van Nostrand Reinhold, New York, N.Y. 539 p.

Monakov, A.V. 1972. Review of studies on feeding of aquatic invertebrates conducted at the Institute of Biology of Inland Waters, Academy of Science, USSR. J. Fish. Res. Board Can. 29: 363–383.

Moran, M.A., T. Legovic, R. Benner, and R.E. Hodson. 1988. Carbon flow from lignocellulose: a simulation analysis of a detritus-based ecosystem. Ecology 69: 1525–1536.

Murkin, H.R. 1989.The basis for food chains in prairie wetland, p. 316–338. *In* A.G. van der Valk [ed.] Northern prairie wetlands. Iowa State University Press, Ames, Iowa.

Murkin, H.R., P.G. Abbott, and J.A. Kadlec. 1983. A comparison of activity traps and sweep nets for sampling nektonic invertebrates in wetlands. Freshwater Invertebr. Biol. 2: 99–106.

Murkin, H.R., and B.D.J. Batt. 1987. The interaction of vertebrates and invertebrates in peatlands and marshes. Mem. Entomol. Soc. Can. 140: 15–30.

Murkin, H.R., M.P. Stainton, J.A. Boughen, J.B. Pollard, and R.D. Titman. 1991. Nutrient status of wetlands in the Interlake region of Manitoba, Canada. Wetlands 10: 105–122.

Neill, C. 1990. Nutrient limitation of hardstem bulrush (*Scirpus acutus* Muhl.) in a Manitoba Interlake region marsh. Wetlands 10: 69–76.

Nelson, J.W., and J.A. Kadlec. 1984. A conceptual approach relating habitat structure and macroinvertebrate production in freshwater wetlands. Trans. N. Am. Wildl. Nat. Resour. Conf. 49: 262–270.

Oliver. D.R. 1971. Life history of the Chironomidae. Annu. Rev. Entomol. 16: 211–230.

Osenberg, C.W. 1989. Resource limitation, competition and the influence of life history in a freshwater snail community. Oecologia 19: 512–519.

Pennak, R.W. 1978. Freshwater invertebrates of the Unites States. 2nd ed. John Wiley and Sons, New York, N.Y. 803 p.

Pinder, L.C.V. 1986. Biology of freshwater Chironomidae. Annu. Rev. Entomol. 31: 1–23.

Polunin, N.V.C. 1982. Processes contributing to the decay of reed (*Phragmites australis*) litter in fresh water. Arch. Hydrobiol. 94: 182–209.

Polunin, N.V.C. 1984. The decomposition of emergent macrophytes in fresh water. Adv. Ecol. Res. 14: 115–166.

Rasmussen, J.B. 1984. The life-history, distribution, and production of *Chironomus riparius* and *Glyptotendipes paripes* in a prairie pond. Hydrobiologia 119: 65–72.

Richardson, J.S., and W.E. Neill. 1991. Indirect effect of detritus manipulations in a montane stream. Can. J. Fish. Aquat. Sci. 48: 776–783.

Robinson, G.G.C. 1983. Methodology: the key to understand periphyton, p. 245–251. *In* R.G. Wetzel [ed.] Periphyton of freshwater ecosystems. Dr. W. Junk, The Hague, The Netherlands.

Rosenberg, D.M., and H.V. Danks. 1987. Aquatic insects of peatlands and marshes in Canada: introduction. Mem. Entomol. Soc. Can. 140: 1–4.

Rosillon, D. 1988. Food preference and relative influence of temperature and food quality on life history characteristics of a grazing mayfly, *Ephemeralla ignita* (Poda). Can. J. Zool. 66: 1474–1481.

SAS Institute Inc. 1985. SAS user's guide: statistics, version 5. SAS Institute Inc., Cary, N.C. 956 p.

Smock, L.A., and K.L. Harlowe. 1983. Utilization and processing of freshwater wetland macrophytes by the detritivore *Asellus forbesi*. Ecology 64: 1556–1565.

Söderström, O. 1988. Effects of temperature and food quality on life-history parameters in *Parameletus chelifer* and *P. minor* (Ephemeroptera): a laboratory study. Freshwater Biol. 20: 295–303.

Suren, A.M., and P.S. Lake. 1989. Edibility of fresh and decomposing macrophytes to three species of freshwater invertebrate herbivores. Hydrobiologia 178: 165–178.

Sweeney, B.W. 1984. Factors influencing life-history patterns of aquatic insects, p. 56–100. *In* V.H. Resh and D.M. Rosenberg [ed.] The ecology of aquatic insects. Praeger, New York, N.Y.

Triska, F.J., and J.R. Sedell. 1976. Decomposition of four species of leaf litter in response to nitrate manipulation. Ecology 57: 783–792.

URABE, J. 1991. Effect of food concentration on growth, reproduction and survivorship of *Bosmina longirostris* (Cladocera): an experimental study. Freshwater Biol. 25: 1–8.

VAN DER VALK, A.G., AND C.B. DAVIS. 1978. Primary production of prairie glacial marshes, p. 21–37. *In* R.E. Good et al. [ed.] Freshwater wetlands: ecological processes and management potential. Academic Press, New York, N.Y.

WARD, G.W., AND K.W. CUMMINS. 1979. Effects of food quality on growth of a stream detritivore, *Paratendipes albimanus* (Meigen) (Diptera: Chironomidae). Ecology 60: 57–64.

WRUBLESKI, D.A. 1984. Species composition, emergence phenologies, and relative abundances of Chironomidae (Diptera) from the Delta Marsh, Manitoba, Canada. M.Sc. thesis, University of Manitoba, Winnipeg, Man. 115 p.

WRUBLESKI, D.A. 1987. Chironomidae (Diptera) of peatlands and marshes in Canada. Mem. Entomol. Soc. Can. 140: 141–161.

Particle-size-conversion Efficiency, Invertebrate Production, and Potential Fish Production in Lake Ontario

U. Borgmann and D.M. Whittle

Department of Fisheries and Oceans, Great Lakes Laboratory for Fisheries and Aquatic Sciences, Burlington, ON L7R 4A6, Canada

Borgmann, U., and D.M. Whittle. 1994. Particle-size-conversion efficiency, invertebrate production, and potential fish production in Lake Ontario. Can. J. Fish. Aquat. Sci. 51: 693–700.

The relationships between body size and *p,p'*-DDE and total PCB concentration in zooplankton, mysids, amphipods, slimy sculpin (*Cottus cognatus*), rainbow smelt (*Osmerus mordax*), alewife (*Alosa pseudoharengus*), and lake trout (*Salvelinus namaycush*) in Lake Ontario were determined for samples collected from 1989 to 1992. Amphipods, and to a lesser extent sculpins, had higher DDE and PCB concentrations than predicted from the contaminant concentration – body size relationship for the pelagic species. PCB, but not DDE, concentrations in zooplankton were also abnormally high. For the pelagic species, excluding PCB concentrations in zooplankton, the log contaminant concentration – log body size relationship had a slope of 0.23 (95% confidence limits = ±0.014). Combined with revised estimates of the efficiency of contaminant retention from one body size to another ($\epsilon' = 0.05–0.10$), the revised estimate of particle-size-conversion efficiency (ϵ) for Lake Ontario falls between 0.27 and 0.35. Recent estimates of invertebrate (zooplankton, mysid, and amphipod) annual production average 18 g/m^2 (dry weight) with upper and lower limit estimates of 14–27 g/m^2. Using ϵ to extrapolate from invertebrate to fish production results in estimates of mean potential fish production in Lake Ontario of 1–7 kg/ha (wet weight), as compared with previously published estimates of 6 and 14 kg/ha.

Nous avons calculé, pour des échantillons prélevés de 1989 à 1992, les relations entre la taille corporelle et la concentration de *p,p'*-DDE et des BPC totaux dans le zooplancton, les mysidacés, les amphipodes, les chaboisseaux (*Cottus cognatus*), l'éperlon (*Osmerus mordax*), le gaspareau (*Alosa pseudoharengus*), et le touladi (*Salvelinus namaycush*) du lac Ontario. Les amphipodes, et les chaboisseaux dans une moindre mesure, présentaient des concentrations de DDE et de BPC plus élevés que prévu d'après la relation concentration de contaminants – taille corporelle pour les espèces pélagiques. Les concentrations de BPC, mais non de DDE, dans le zooplancton étaient aussi anormalement élevées. Pour les espèces pélagiques, si l'on exclut les concentrations de BPC dans le zooplancton, la relation log de la concentration de contaminants – log de la taille corporelle présentait une pente de 0,23 (seuil de confiance de 95 % = ±0,014). Si on la combine à des estimations révisées de l'efficience de la rétention des contaminants d'une taille corporelle à l'autre ($\epsilon' = 0{,}05–0{,}10$), l'estimation révisée de l'efficience (ϵ) de la conversion particule-taille pour le lac Ontario tombe entre 0,27 et 0,35. Les estimations récentes de la production annuelle les invertébrés (zooplancton, mysidacés et amphipodes), est en moyenne de 18 g/m^2 (poids sec), avec des limites supérieure et inférieure estimées à 14 et 27 g/m^2. Le recours à ϵ pour extrapoler de la production d'invertébrés à la production de poisson donne des estimations de la production moyenne potentielle de poissons dans le lac Ontario de l'ordre de 1–7 kg/ha (poids humide), contre des estimations antérieures publiées de 6 et 14 kg/ha.

Received May 3, 1993
Accepted October 7, 1993
(JB910)

Reçu le 3 mai 1993
Accepté le 7 octobre 1993

In pelagic ecosystems, body size is an approximate indicator of trophic level because most predators feed on prey species smaller than themselves. This property, along with assumptions about the mean predator–prey size ratio and biomass conversion efficiencies, has been used to predict fish production and biomass from those measured at lower trophic levels (e.g., Kerr 1974; Platt and Denman 1977; Sheldon et al. 1977; see Borgmann 1987 for a discussion of different published models). To simplify computation of energy flow up the food web, Borgmann (1982) defined the term particle-size-conversion efficiency (ϵ) as the efficiency of biomass conversion from one size to another, rather than from one trophic level to another:

$$(1)\quad \epsilon = \log(C_{ij}/P_{ij})/\log(W_j/W_i) = -\log(K_1)/\log(\mathrm{PPR})$$

where C_{ij} is the biomass of species i consumed by species *j*, P_{ij} is the biomass production of species *j* resulting from this ingestion, C_{ij}/P_{ij} is the inverse of the biomass conversion efficiency (K_1), and W_j/W_i is the ratio of predator to prey body sizes (PPR). Using ϵ, total production for a mixture of predators can be calculated, even if the trophic relationships between them are not clearly understood, and potential production for any size of fish further up the food web can be estimated (Borgmann 1982). For simplicity, the subscripts *i* and *j* will be omitted from C_{ij} and P_{ij} from this point onwards.

Borgmann and Whittle (1983) demonstrated that ϵ could be estimated from the relationship between body size and the concentrations of persistent contaminants which are poorly metabolized and not readily excreted. They defined

$$(2)\quad \epsilon' = \log(C'/P')/\log(W_j/W_i) = -\log(K_1')\log(\mathrm{PPR})$$

where C' is the amount of contaminant in species i ingested by species j and P' is the amount of this contaminant retained by species j (i.e., analogous to the retention of carbon or energy as a measure of production). For simplicity and for consistency with the definition of ϵ, we define K_1' here as P'/C', the efficiency of contaminant retention. Combining equations 1 and 2 under steady-state conditions gives

$$\begin{aligned}(3)\quad \epsilon - \epsilon' &= [\log(C/P) - \log(C'/P')]/\log(W_j/W_i)\\ &= \log[(P'/P)/(C'/C)]/\log(W_j/W_i)\\ &= [\log(P'/P) - \log(C'/C)]\,[\log(W_j) - \log(W_i)]\end{aligned}$$

where P'/P and C'/C are the concentrations of contaminant in the predator and its prey, respectively. Equation 3 demonstrates that a log–log plot of contaminant concentration against body size for a predator and its prey has a slope of $\epsilon - \epsilon'$. If $\epsilon - \epsilon'$ is relatively constant from one trophic level to the next, then extending the log–log plot to include the predator of the predator, and the prey of the prey, will result in a relatively straight-line relationship across all trophic levels. The overall mean value for $\epsilon - \epsilon'$ can, therefore, be obtained by regressing the log of contaminant concentrations against the log of body size for all members of the food web. This average was 0.21 for data on PCB and DDT concentrations in biota collected from Lake Ontario between 1977 and 1979 (Borgmann and Whittle 1983). Borgmann and Whittle estimated ϵ' at 0.05, giving an estimate of ϵ of 0.26. This value of ϵ has subsequently been used to predict potential fish production in Lake Ontario, and the other Great Lakes and Lake Winnipeg (Borgmann et al. 1984, Leach et al. 1987). Production over a specified range of body sizes (P_{xy}) can be computed from

$$(4)\quad P_{xy} = d(W_y^{-\epsilon} - W_x^{-\epsilon})$$

where W_x and W_y are the lower and upper limits, respectively, of the size range and d is a constant (Borgmann 1987). If production over a given size range of invertebrates is known, the value of d can be calculated and equation 4 can be used to estimate production over other size ranges. Using this approach, and additional information on fish growth characteristics, Leach et al. (1987) predicted that past maximum yields of large fish from Lake Ontario were about 27% of the predicted maximum potential yield.

The above calculations were based on relatively limited data, both for contaminant concentrations in aquatic biota and for invertebrate production. Contaminant concentrations in invertebrates from Lake Ontario were not routinely monitored by the Department of Fisheries and Oceans after 1979 because concentrations in all biota had been decreasing with time, and many of the invertebrate measurements dropped to below the detection limits of the routine analytical techniques used at that time. The purpose of this study was to (1) reexamine the relationship between contaminant concentrations and body size in Lake Ontario, using more sensitive current analytical techniques to determine if present estimates of $\epsilon - \epsilon'$ agree with the earlier measurements, (2) re-evaluate the previous estimate of $\epsilon' = 0.05$, and (3) recompute predicted potential production for large fish in Lake Ontario using the revised estimates of $\epsilon - \epsilon'$ and more recent data on invertebrate production.

Methods

Net zooplankton, mysids (*Mysis relicta*), amphipods (*Diporeia* sp., formerly *Pontoporeia hoyi*), alewife (*Alosa pseudoharengus*), rainbow smelt (*Osmerus mordax*), slimy sculpin (*Cottus cognatus*), and lake trout (*Salvelinus namaycush*) were collected from Lake Ontario near Niagara on the Lake and Grimsby from 1989 to 1992. Some samples were also collected near Cobourg. Net zooplankton were collected using Wisconsin type nets (0.5 × 1.5 m; 153-μm mesh) towed horizontally at a depth of 1 m. Mysids and amphipods were collected with an epibenthic sled (Elster 1933) as described in detail in Whittle and Fitzsimons (1983). Lake trout were collected by Department of Fisheries and Oceans personnel using overnight bottom sets of gill nets with stretched mesh sizes ranging from 6.35 to 15.25 cm. Alewife, smelt, and sculpin samples were collected using a 20 ft modified Biloxi outboard bottom trawl with a 2 m cod end of 50 mm stretched mesh. Immediately after collection, all fish were wrapped in solvent rinsed aluminum foil, or sealed in food-grade resin plastic bags, and placed on ice or dry ice. Samples were stored as whole fish at −25°C for a maximum of 60 d before homogenization in a commercial meat grinder.

Tissue samples were extracted with dichloromethane, concentrated on rotary evaporators, cleaned up by gel permeation chromatography, fractionated on silica gel columns, and analyzed for DDE and total PCB by gas chromatography at the Ultra-trace Analytical Laboratory of the Great Lakes Laboratory for Fisheries and Aquatic Sciences, Department of Fisheries and Oceans, using a dual capillary column (60 m Rt-5 and 60 m DB-1701) gas chromatograph with electron capture detection (GC-ECD). Total PCB was computed from the ratio of the area under the PCB isomer peaks in the sample with those in a 1:1:1 mixture of Aroclor 1242, 1254, and 1260. Analyses were based on wet weight and converted to dry weight using dry to wet weight ratios of 0.25 for fish (Borgmann and Whittle 1983), 0.161 for mysids, 0.143 for amphipods (mean of three samples of 10 mysids or amphipods weighed before and after drying), and 0.138 for zooplankton (mean of eight samples).

A total of 16 samples each of zooplankton, alewife ($n = 14$ for DDE), smelt, and sculpins, 15 of mysids and amphipods, and 24 of lake trout were collected for analysis between 1989 and the spring of 1992. Duplicate analyses were performed on selected samples; the mean and standard deviation for the second/first analysis were 0.96 ± 0.09 for DDE and 0.96 ± 0.13 for PCB ($n = 18$ for each).

The slope of the contaminant concentration – body size relationship was determined by analysis of covariance using the statistical package SYSTAT (Ver. 5.0). Initially, a term for body size, a category term for year, and an interaction term (year × body size) were included to verify that the slope did not change significantly from year to year. The interaction term was then dropped from the final analysis.

Results and Discussion

Estimation of $\epsilon - \epsilon'$

There was a strong relationship between contaminant concentration and body size for both DDE and PCB (Fig. 1). Estimates of the slope of the regression ($\epsilon - \epsilon'$) were obtained for the entire data set, for the pelagic data only

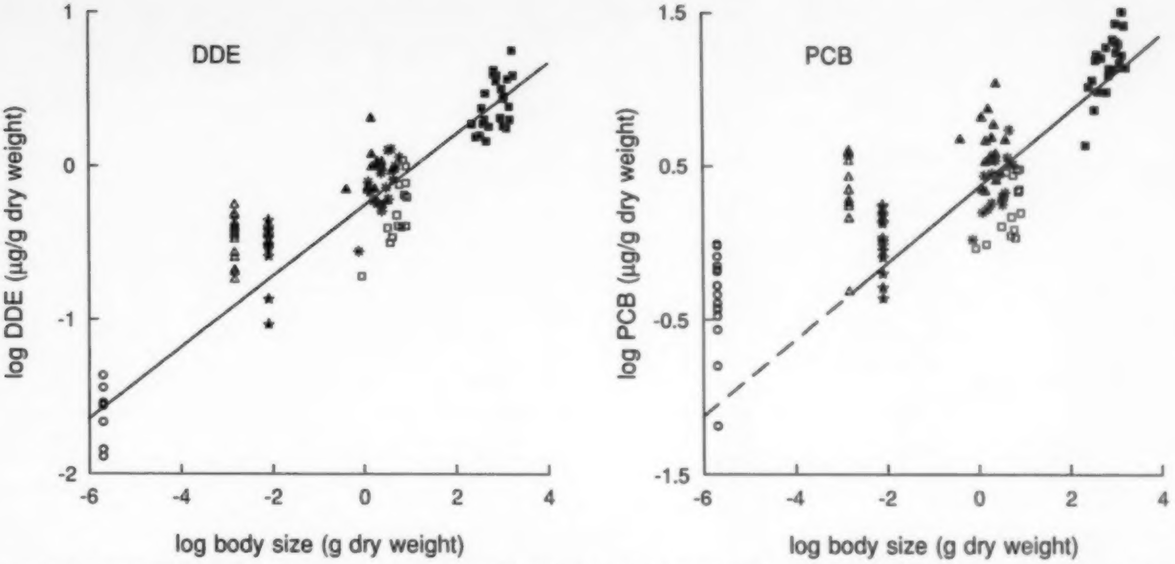

FIG. 1. Log of DDE or PCB concentration as a function of log body mass (dry weight) for zooplankton (open circles), amphipods (open triangles), mysids (stars), sculpins (solid triangles), smelt (asterisks), alewife (open squares), and lake trout (solid squares) from Lake Ontario. The straight lines were obtained by regression (see text) omitting the benthic organisms (amphipods and sculpins) for both DDE and PCBs, and also omitting zooplankton for PCBs (slope = 0.231 for DDE and 0.248 for PCB).

TABLE 1. Slope of the regression of log(DDE) or log(PCB) against log body size ($\epsilon - \epsilon'$) ± 2 SE (approximate 95% confidence limits), R^2, and number of data points (n) for the entire Lake Ontario data set, for the pelagic species only (i.e., omitting amphipods and sculpins) and for the entire and pelagic data sets omitting zooplankton. Values shown in parentheses were obtained by ignoring a statistically significant variation in slope across years.

	DDE			PCB		
	n	Slope	R^2	n	Slope	R^2
All data	116	0.218 ± 0.016	0.879	118	0.168 ± 0.018	0.742
All data less zooplankton	100	0.168 ± 0.020	0.759	102	0.177 ± 0.028	0.648
Pelagic species	85	0.231 ± 0.014	0.935	87	0.179 ± 0.018	0.819
Pelagic species less zooplankton	69	(0.201 ± 0.024)	(0.813)	71	0.248 ± 0.026	0.856

(i.e., omitting amphipods and sculpins), and for both the entire and pelagic data sets with the zooplankton data omitted (Table 1). Data were obtained from samples collected from 1989 to 1992, including samples from both the spring (April–May) and fall (October) of 1992. Visual inspection of the data revealed that PCB concentrations were unusually high in lake trout ($n = 5$) and unusually low in zooplankton ($n = 2$) in the fall of 1992. Consequently, statistical analyses of the data were performed both with and without the October 1992 data. A significant interaction term was obtained between years and body size for PCB, indicating that a common slope could not be calculated when the October 1992 data were included. Consequently, the October 1992 data were omitted from all further analyses (including the data in Table 1). Statistically significant interactions between years and body size were obtained for the DDE data ($P > 0.1$) only for the pelagic species with zooplankton omitted. Consequently, only this one of the eight regressions in Table 1 violates the homogeneity of slopes assumption needed for computing a mean slope.

Both the estimate of $\epsilon - \epsilon'$ and the R^2 for the pelagic species are higher than for the entire data set, regardless of whether zooplankton are included in the regression. This suggests that a better estimate of $\epsilon - \epsilon'$ for the pelagic zone is obtained by omitting the benthic species (Table 1). Amphipods appear to have anomalously high contaminant concentrations, relative to the pelagic species, probably because they live and feed in contaminated sediments. Consequently, eliminating the amphipods, and the associated data of their primary predator sculpin, improves the regression. Benthic organisms cannot, therefore, be included with the pelagic species to provide an overall estimate of $\epsilon - \epsilon'$.

Examination of the effect of the zooplankton data on the estimate of $\epsilon - \epsilon'$ provides insights into chemical partitioning between water and biota at the base of the food web. For very small organisms with large surface to volume ratios, direct chemical equilibria with the water are likely to play a more important role than for larger organisms. The relationship between DDE or PCB concentration and body size could, therefore, be weaker for small than for large organisms. This would result in the smallest species having contaminant concentrations higher than predicted from the regression between concentration and body size for the larger species. This appears to be the case for PCBs, but not for DDE (Fig. 1). The estimate of $\epsilon - \epsilon'$ for DDE is higher than for PCB for both the entire data set and the pelagic species alone, if the zooplankton are included. The 95% confidence limits (±2 SE) do not overlap (Table 1). Omitting the zooplankton data, however, gives similar $\epsilon - \epsilon'$ estimates for both DDE and PCB, with overlapping confidence limits. Omitting the zooplankton from the entire data set for both DDE and PCB and for the pelagic data set for DDE decreases the R^2 because a smaller size range is used in the regression. Omitting the zooplankton from the pelagic data set for DDE reduces the estimate of $\epsilon - \epsilon'$ slightly, but not significantly (confidence intervals overlap, Table 1). Omitting the zooplankton from the pelagic data set for PCB, however, increases both $\epsilon - \epsilon'$ and the R^2, with nonoverlapping confidence limits. Furthermore, the confidence limits for $\epsilon - \epsilon'$ for the pelagic data set for PCB with zooplankton omitted overlap the confidence limits for the pelagic data set for DDE, whether the zooplankton are included or excluded. Consequently, it is only the PCB data for zooplankton that do not fit on the same contaminant concentration – body size relationship for the pelagic species. This probably occurs because PCBs are a mixture of many different congeners, and the PCB congener composition for zooplankton differs from that of the higher trophic levels. Oliver and Niimi (1988) found that the relative congener composition of PCBs in mysids, smelt, and salmonids was virtually uniform, but that it differed from that found in zooplankton and water samples. Since zooplankton are small and occupy the bottom of the food chain, PCB concentrations in their tissues could be at least partially controlled by equilibrium partitioning with the water. From mysids on up, food chain biomagnification selectively concentrates those congeners with higher octanol–water partition coefficients, resulting in a more uniform congener composition mixture (Oliver and Niimi 1988). Consequently, zooplankton data (and any other data on similarly small organisms) are best omitted from regressions of total PCB versus body size.

The best estimate of $\epsilon - \epsilon'$ (0.231 ± 0.014, $R^2 = 0.935$) was obtained from the pelagic data set for DDE, including the zooplankton. Both the DDE and PCB data for the pelagic species, omitting zooplankton, are consistent with this estimate of $\epsilon - \epsilon'$, but have a poorer R^2 (both <0.86) and larger confidence limits (both ≥0.024) because a smaller range in body sizes is covered by the regression. Even inclusion of the benthic species does not significantly alter this estimate of $\epsilon - \epsilon'$ for DDE, as long as the zooplankton are not omitted, although the R^2 is reduced slightly (Table 1). This estimate of $\epsilon - \epsilon'$ also overlaps that reported for total DDT (0.206 ± 0.040) and PCB (0.203 ± 0.042) for the western basin of Lake Ontario for samples collected from 1977 to 1979 (Borgmann and Whittle 1983). Previous estimates of $\epsilon - \epsilon'$ for the eastern basin of Lake Ontario (0.222 ± 0.047 for DDT and 0.217 ± 0.050 for PCB, Borgmann and Whittle 1983), not sampled in the present study, also overlap. The more advanced analytical chemistry technology used in the current study, however, has reduced the scatter about the regression line resulting in smaller confidence limits. Consequently, 0.231 ± 0.014 is probably a fairly accurate estimate of $\epsilon - \epsilon'$ for persistent organic compounds such as DDE and PCB for which food chain biomagnification is the dominant factor controlling body concentrations in Lake Ontario. Although sampling was confined to the western half of Lake Ontario in the current study, the similarity of previous $\epsilon - \epsilon'$ estimates from the eastern basin of the lake to both previous (Borgmann and Whittle 1983) and the current estimates from the western part of the lake suggests that 0.231 should be a reasonable estimate for $\epsilon - \epsilon'$ for Lake Ontario as a whole.

The estimate of $\epsilon - \epsilon'$ and its confidence limits, as calculated above, apply only to the species (or group of species in the case of zooplankton) analyzed. This includes all the dominant components of the deepwater community in the main portion of the lake from zooplankton on up, with the exception of the various species of salmon. It should provide a reasonable estimate of $\epsilon - \epsilon'$ for the entire pelagic community of the offshore main portion of the lake as long as $\epsilon - \epsilon'$ from prey fish to salmon is similar to that from prey fish to lake trout. If a more general estimate of $\epsilon - \epsilon'$, applicable to all species, is desired, it can be argued that all the measurements made on one species represent only a single data point on the regression line. In this case the concentration and weight measurements for each species should be averaged, and only the means regressed. Regression of the logarithmic mean concentration for each species, against the logarithmic mean weight, gives a best estimate (±95% confidence limits) of $\epsilon - \epsilon'$ of 0.226 ± 0.084, based on DDE in the pelagic species ($n = 5$, $R^2 = 0.96$). A similar calculation for PCB in the pelagic species omitting zooplankton yields 0.226 ± 0.308 ($n = 4$, $R^2 = 0.83$). These estimates of $\epsilon - \epsilon'$ are almost identical to the above estimate of 0.231, but the confidence limits are much wider because of the small sample size. For future between-lake comparisons among lakes containing different species, the latter estimate of 0.23 ± 0.08 may be more appropriate.

The above estimate of $\epsilon - \epsilon'$ was obtained from samples collected annually in the spring (April–May) and fall (August–September) from 1989 to the spring of 1992. Data from October 1992 were not included. The estimates of $\epsilon - \epsilon'$ obtained from the October 1992 data are 0.36 ± 0.15 for DDE and 0.35 ± 0.16 for PCB for the pelagic species. The 95% confidence limits are much larger than those listed in Table 1 because of the small sample size ($n = 15$). It is impossible to say if this represents a real increase in $\epsilon - \epsilon'$, or just a temporary fluctuation in contaminant concentrations in zooplankton and lake trout. The similarity in the estimates of $\epsilon - \epsilon'$ shown in Table 1 and those obtained a decade earlier (Borgmann and Whittle 1983) suggests that the latter is more likely. Although a seasonal effect on contaminant concentrations cannot be discounted for the zooplankton data (the median fall 1992 sampling period was later than in previous years), the similarity among April–May and August–September samples collected previously suggests that this is unlikely. Additional survey data (unpublished) showed that there was no significant seasonal (May–December 1982) variation in lake trout DDE and PCB concentrations. Nevertheless, these data demonstrate the need for sampling on more than one occasion in order to determine that contaminant concentrations are more or less constant for at least a defined time period.

Estimation of ϵ'

Estimation of ϵ' requires estimates of the fraction of the ingested contaminant retained by pelagic predators (K_1') and the predator prey size ratio (PPR, equation 2). The body sizes of the pelagic organisms considered in this study range from 2 μg (approximate mean zooplankton size, Johannsson 1987) to 743 g dry weight (logarithmic mean of the lake trout weights in this study). This covers between two and three trophic steps (three to four trophic levels, e.g., zooplankton → alewife → lake trout or zooplankton → mysids/larval fish → smelt/alewife → lake trout). Lake Ontario zooplankton size and composition are typical of species occurring in the presence of intense alewife predation, with young alewives probably using a particulate feeding mode and adults using a filter feeding mode (Johannsson and O'Gorman 1991). Mysids, however, are also an important food of alewife in Lake Michigan (Janssen and Brandt 1980) and in Lake Ontario (Iancu 1988, as quoted in Shea and Makarewicz 1989). Mysids, in turn, feed on zooplankton, although they also consume phytoplankton (Grossnickle 1982). Lake trout feed on alewives, smelt, and, especially when young, also on sculpins (Brandt 1986; Christie et al. 1987, Elrod and O'Gorman 1991). Large smelt are piscivorous and feed on sculpins, although mysids are also consumed in Lake Ontario (Brandt and Madon 1986). Alewife may also feed on larval fish, when abundant (Brandt et al. 1987). An average of 2.5, therefore, seems like a reasonable estimate of the number of trophic steps from zooplankton to lake trout, with a lower and upper limit of two and three, respectively. This gives a mean PPR of 2700, with minimum and maximum estimates of 720–19 000. This is essentially identical to the mean PPR of 14 based on linear measurements and suggested for marine species by Sheldon et al. (1977; i.e., $14^3 = 2744$, giving a PPR of approximately 2700 based on volume).

Borgmann and Whittle (1983) estimated ϵ' to be about 0.05. For a PPR of 2700 (720–19 000), this is equivalent to a K_1' of 0.67 (0.72–0.61). More recent references on DDE and PCB uptake continue to indicate high assimilation efficiencies. Rainbow trout assimilate DDE with an efficiency of 0.67 (Niimi and Oliver 1988) and PCB with an efficiency of about 0.75 (Niimi and Oliver 1983). Invertebrate assimilation efficiencies appear to be equally high. *Mysis relicta* assimilated 53% of hexachlorobiphenyl from ingested sediment (Klump et al. 1991). Considering its low nutritional value, relative to other food sources, assimilation would be expected to be higher from zooplankton. DDT assimilation by euphausiids, another shrimp-like crustacean, was estimated at 62–76% by Cox (1971).

Overall retention of contaminants, however, is also affected by excretion following assimilation. Under steady-state conditions, contaminant retention in an organism is given by (see Appendix)

$$(5)\quad K_1' = E_o \cdot g/(g + k_e)$$

where E_o is the maximum assimilation efficiency (i.e., when the contaminant concentration is 0 in the predator, Borgmann and Whittle 1992), g is the instantaneous growth rate, and k_e is the contaminant excretion rate. Simultaneous estimates of g and k_e under conditions similar to those in the field are scarce. Borgmann and Whittle (1992), in a bioenergetics and contaminant accumulation model for lake trout in Lake Ontario, estimated g at 0.0012/d and k_e at 0.00042/d for DDE and 0.00078/d for PCB for 4-yr-old fish. This gives estimates of K_1' of 0.50 for DDE and 0.46 for PCB.

If the ratio of k_e to growth rate in other fish species is similar to that for lake trout, then 0.5 is a reasonable estimate of K_1' for the pelagic species of Lake Ontario. However, this might be an underestimate of the true annual mean K_1' (giving an overestimate of ϵ') if excretion rates for fish are much lower in winter due to reduced water temperatures. A PPR of 2700 (range 720–19 000) and K_1' of 0.5 gives an estimate of ϵ' of 0.088 (0.105–0.070). Our previous estimate of 0.05 (Borgmann and Whittle 1983) might, therefore, be a little low, while 0.10 might be on the high side. In the following analyses, we use both estimates of ϵ' and compare the results. A mean $\epsilon - \epsilon'$ of 0.231 gives estimates for ϵ ranging from 0.281 to 0.331 (0.267 to 0.345 including confidence limits of 0.014 for $\epsilon - \epsilon'$), slightly higher than our previous estimate of 0.26 (Borgmann and Whittle 1983).

Invertebrate Production in Lake Ontario

Summer epilimnetic crustacean zooplankton production estimates at four stations in Lake Ontario from 1981 to 1986 ranged from 10.4 g/m^2 in the western basin to 19.5 g/m^2 in the eastern basin, with a mean of 14.0 and standard error of 2.0 for the four stations (Johannsson and O'Gorman 1991). These stations are widely distributed throughout the lake and should provide reasonable estimates of average lakewide production. For a sample size of 4, the range (10.4–19.5) would include the true mean production with greater than 80% confidence, assuming production by station follows a normal distribution. The mean summer epilimnetic zooplankton biomass at the same sites from 1981 to 1985 was 1.54 g/m^2 (Johannsson 1987), giving a mean biomass turnover rate of 9.1/yr, lower than that initially estimated for Lake Ontario zooplankton using data collected only up to 1981 (Borgmann et al. 1984). Biomass production estimates for hypolimnetic zooplankton, or those found in the thermocline, are not available, but turnover rates would be expected to be lower than for the epilimnetic zooplankton. Total zooplankton in the upper 50 m, or from 2 m above the bottom, averaged 0.048 g/m^3 (Watson and Carpenter 1974). Seventeen of 33 stations were shallower than 50 m. Consequently, mean biomass would have been less than 2.4 g/m^2, and total zooplankton production in the upper 50 m would have been below 22 g·m^{-2}·yr^{-1}, lower than previously estimated (Leach et al. 1987) because of the lower turnover rate estimate. Since we have no direct estimates of hypolimnetic zooplankton production or turnover rates, we keep the estimate of mean zooplankton production at 14.0 g·m^{-2}·yr^{-1}, but increase the upper limit from 19.5 to 22 g·m^{-2}·yr^{-1}.

Macroinvertebrate production in Lake Ontario is lower than zooplankton production. *Mysis* production was estimated at 1.90 g/m^2 in 1984 and 2.62 g/m^2 in 1986 at a 125-m-deep station (Johannsson 1992). These estimates were considered possibly to be on the low side by 11–27% (Johannsson 1992), but they are specific to one station and not lakewide. Total mysid production in Lake Ontario in 1990, based on several lakewide cruises, divided by total lake area was 2.34 g/m^2 (O.E. Johannsson, personal communication). Estimated *Diporeia* production in Lake Ontario over the years 1964, 1972, 1977, 1981, and 1982 averaged 31.5×10^3 t (range 21.7–37.8, Johannsson et al. 1985) over an area of 17.5×10^9 m^2. This gives an estimated mean areal production of 1.8 g·m^{-2}·yr^{-1} with a range of 1.2–2.2.

TABLE 2. Predicted potential production (kg/ha) for fish between 40 and 4000 g wet weight (10–1000 g dry weight) and confidence limits (based on a mean ± 2 SE for $\epsilon - \epsilon'$ of 0.231 ± 0.014) for two estimates of ϵ' and three estimates of production (mean, minimum, and maximum) of invertebrates within the size range of 0.1 μg to 10 mg dry weight.

Invertebrate production (g dry weight/m^2)	Potential fish production	
	If $\epsilon' = 0.05$	If $\epsilon' = 0.10$
14 (minimum)	2.4 (1.9–3.0)	1.0 (0.8–1.3)
18 (mean)	3.1 (2.4–3.9)	1.3 (1.0–1.7)
27 (maximum)	4.6 (3.6–5.9)	1.9 (1.5–2.5)

Summed together, the above estimates provide a mean total crustacean invertebrate production estimate for Lake Ontario of 18 g dry weight·m^{-2}·yr^{-1}, with a range of 14–27.

Potential Fish Production in Lake Ontario

The potential fish production in Lake Ontario supportable by the invertebrate production can now be estimated using equation 4. The value of d is calculated first, using $\epsilon - \epsilon' = 0.231 \pm 0.014$, $\epsilon' = 0.05$ or 0.10, $W_x = 0.1$ μg, $W_y = 10$ mg, and minimum, mean, and maximum estimates of $P_{xy} = 14$, 18, and 27 g/m^2, respectively. Then, for each d, the value of P_{xy} is calculated using the appropriate ϵ and selected values of W_x and W_y. For example, potential fish production for 40–4000 g (wet weight) fish would be between 0.8 and 5.9 kg/ha, depending on which estimates of ϵ' and invertebrate production were used (Table 2). For a mean invertebrate production of 18 g/m^2, potential fish production would be between 2.4 and 3.9 kg/ha if $\epsilon' = 0.05$ ($\epsilon = 0.281 \pm 0.014$) and between 1.0 and 1.7 kg/ha if $\epsilon' = 0.10$ ($\epsilon = 0.331 \pm 0.014$). The average potential fish production over several years, therefore, should be in the 1–4 kg/ha range for fish between 10 and 1000 g dry weight. This represents *potential*, and not necessarily realized, production. For the potential to be realized, there must be an appropriate abundance of organisms at all trophic levels, with predators and prey spatially distributed in such a way that biomass produced within each size range is effectively consumed by larger organisms and passed on up to the largest size classes. The potential production over other size ranges could be calculated from equation 4 in a similar way.

A special case of equation 4, especially applicable to production of the largest size class, is obtained when the upper size limit (W_y) is set equal to infinity. W_y then disappears from the equation and P_{xy} refers to all production occurring at body sizes greater than W_x ($P_{>W_0}$, Leach et al. 1987). Assuming that commercially harvested fish are greater than 17 g dry weight (Leach et al. 1987), potential production of fish in the harvestable size range would be between 0.8 and 7.2 kg/ha, depending on which estimates of ϵ' and invertebrate production were used (Table 3). For a mean invertebrate production of 18 g/m^2, potential fish production would be between about 1 and 5 kg/ha.

The above estimates of potential fish production for Lake Ontario are somewhat lower than previous estimates (0.15 g dry weight/m^2 or 6 kg wet weight/ha, Borgmann and Whittle 1983; 14 kg/ha, Leach et al. 1987), partly because our estimate of ϵ (previously estimated to be 0.26) is now higher (possible values between 0.267 and 0.345) and partly because our estimates of zooplankton turnover and production are somewhat lower (mean of 14 g/m^2 instead of 18 g/m^2, Borgmann and Whittle 1983; or 43 g/m^2, Leach et al. 1987). Our current estimate of production should be more accurate than previous estimates because it is based on a much larger data set for zooplankton production (Johannsson 1987; Johannsson and O'Gorman 1991) and on more sensitive analytical methods for determination of DDE and PCB concentrations in biota.

TABLE 3. Predicted potential production (kg wet weight/ha) for fish above 17 g dry weight and confidence limits (based on a mean ± 2 SE for $\epsilon - \epsilon'$ of 0.231 ± 0.014) for two estimates of ϵ' and three estimates of production (mean, minimum, and maximum) of invertebrates within the size range of 0.1 μg to 10 mg dry weight.

Invertebrate production (g dry weight/m^2)	Potential fish production	
	If $\epsilon' = 0.05$	If $\epsilon' = 0.10$
14 (minimum)	2.8 (2.2–3.7)	1.1 (0.8–1.4)
18 (mean)	3.6 (2.8–4.8)	1.4 (1.1–1.8)
27 (maximum)	5.5 (4.2–7.2)	2.1 (1.6–2.7)

Past fish harvests in Lake Ontario have averaged 0.64 kg/ha for large fish (approximately 112–1125 g dry weight) and 0.32 kg/ha for smaller fish (17–112 g) during periods of maximum yield from 1915 to 1930 (Leach et al. 1987). In naturally reproducing fish populations, all of the production cannot be harvested if the population is to maintain itself. Assuming maximum yield represents roughly 57% of production (Leach et al. 1987), this harvest is equivalent to a total fish production of about 1.7 kg/ha. This falls within the 1–5 kg/ha range for potential fish production estimated from an invertebrate production of 18 g/m^2. It appears, therefore, that past yields, as obtained from 1915 to 1930, were close to the maximum which could have been obtained from Lake Ontario, assuming that ϵ and invertebrate production have not changed appreciably since that time. The difference between potential fish production and yield and actual harvests in the past is probably less than previously estimated (Leach et al. 1987).

Estimates of salmonine yields from Lake Ontario from 1984 to 1989 are 3.0–3.5 kg/ha, and a draft objective for yields of salmonine and coregonine fish species of 2.5 kg/ha has been recommended by the Lake Ontario Committee of the Great Lakes Fishery Commission (Kerr and LeTendre 1991). However, yields in the 1980s are above those predicted from empirical models using historical data, and it is not known if these can be sustained over the long term (Kerr and LeTendre 1991). Since almost all of the salmonid production in Lake Ontario is currently the result of stocked fish, the assumption that yield equals about 57% of production is not appropriate. All stocked fish could be harvested and there is no need for some of the fish to survive in order to reproduce. Yields of 3.0–3.5 kg/ha, therefore, may represent an estimated production of the same amount. This falls within the 1–5 kg/ha predicted from particle-size-conversion efficiency and an invertebrate production of 18 g/m^2 (Table 2). However, the predicted production includes production of all fish species, both large and small. An objective of 2.5 kg/ha might be too high if most of the yield is in larger fish, and if future yields are to be supported to a larger degree by self reproducing fish stocks. Furthermore, an objective of 2.5 kg/ha leaves little room for production by other large species (e.g., burbot (*Lota lota*), walleye (*Stizostedion vitreum*)), and includes no safety factor to allow for natural cycles in production, abnormal weather/environmental conditions, or unforseen errors in the above assumptions and calculations.

Acknowledgments

We thank GLLFAS staff Susan Huestis and Michael Leggett for conducting the DDE and PCB analyses and Dr. Ora Johannsson for providing updated estimates of mysid production in Lake Ontario. Field collections were made by M.J. Keir, W.H. Hyatt, and R.M. Kiriluk with help from the crew of the C.S.L. *Shark*, R. Gay, and A. Read.

References

BORGMANN, U. 1982. Particle-size-conversion efficiency and total animal production in pelagic ecosystems. Can. J. Fish. Aquat. Sci. 39: 668–674.

BORGMANN, U. 1987. Models on the slope of, and biomass flow up, the biomass size spectrum. Can. J. Fish. Aquat. Sci. 44(Suppl. 2): 136–140.

BORGMANN, U., H. SHEAR, AND J. MOORE. 1984. Zooplankton and potential fish production in Lake Ontario. Can. J. Fish. Aquat. Sci. 41: 1303–1309.

BORGMANN, U., AND D.M. WHITTLE. 1983. Particle-size-conversion efficiency and contaminant concentrations in Lake Ontario biota. Can. J. Fish. Aquat. Sci. 40: 328–336.

BORGMANN, U., AND D.M. WHITTLE. 1992. Bioenergetics and PCB, DDE, and mercury dynamics in Lake Ontario lake trout (*Salvelinus namaycush*): a model based on surveillance data. Can. J. Fish. Aquat. Sci. 49: 1086–1096.

BRANDT, S.B. 1986. Food of trout and salmon in Lake Ontario. J. Great Lakes Res. 12: 200–205.

BRANDT, S.B., AND S.P. MADON. 1986. Rainbow smelt (*Osmerus mordax*) predation on slimy sculpin (*Cottus cognatus*) in Lake Ontario. J. Great Lakes Res. 12: 322–325.

BRANDT, S.B., D.M. MASON, D.B. MACNEILL, T. COATES, AND J.E. GANNON. 1987. Predation by alewives on larvae of yellow perch in Lake Ontario. Trans. Am. Fish. Soc. 116: 641–645.

CHRISTIE, W.J., K.A. SCOTT, P.G. SLY, AND R.H. STRUS. 1987. Recent changes in the aquatic food web of eastern Lake Ontario. Can. J. Fish. Aquat. Sci. 44(Suppl.2): 37–52.

COX, J.L. 1971. Uptake, assimilation, and loss of DDT residues by *Euphausia pacifica*, a euphausiid shrimp. Fish. Bull. 69: 627–633.

ELROD, J.H., AND R. O'GORMAN. 1991. Diet of juvenile lake trout in southern Lake Ontario in relation to abundance and size of prey fishes, 1979–1987. Trans. Am. Fish. Soc. 120: 290–302.

ELSTER, H.J. 1933. Eine Schlitten-Dredge. Int. Rev. Gesamten Hydrobiol. Hydrogr. 29: 290–292.

GROSSNICKLE, N.E. 1982. Feeding habits of *Mysis relicta* — an overview. Hydrobiologia 93: 101–107.

JANSSEN, J., AND S.B. BRANDT. 1980. Feeding ecology and vertical migration of adult alewives (*Alosa pseudoharengus*) in Lake Michigan. Can. J. Fish. Aquat. Sci. 37: 177–184.

JOHANNSSON, O.E. 1987. Comparison of Lake Ontario zooplankton communities between 1967 and 1985: before and after implementation of salmonid stocking and phosphorus control. J. Great Lakes Res. 13: 328–339.

JOHANNSSON, O. 1992. Life history and productivity of *Mysis relicta* in Lake Ontario. J. Great Lakes Res. 18: 154–168.

JOHANNSSON, O.E., R.M. DERMOTT, R. FELDKAMP, AND J.E. MOORE. 1985. Lake Ontario long term biomonitoring program: Report for 1981 and 1982. Can. Tech. Rep. Fish. Aquat. Sci. 1414: 178 p.

JOHANNSSON, O.E., AND R. O'GORMAN. 1991. Roles of predation, food, and temperature in structuring the epilimnetic zooplankton populations in Lake Ontario, 1981–1986. Trans. Am. Fish. Soc. 120: 193–208.

KERR, S.J., AND G.C. LETENDRE. 1991. The state of the Lake Ontario fish community in 1989. Great Lakes Fish. Comm. Spec. Publ. 91-3: 38 p.

KERR, S.R. 1974. Theory of size distribution in ecological communities. J. Fish. Res. Board Can. 31: 1859–1862.

KLUMP, J.V., J.L KASTER, AND M.E. SIERSZEN. 1991. *Mysis relicta* assimilation of hexachlorobiphenyl from sediments. Can. J. Fish. Aquat. Sci. 48: 284–289.

LEACH, J.H., L.M. DICKIE, B.J. SHUTER, U. BORGMANN, J. HYMAN, AND W. LYSACK. 1987. A review of methods for prediction of potential fish production with application to the Great Lakes and Lake Winnipeg. Can. J. Fish. Aquat. Sci. 44(Suppl. 2): 471–485.

NIIMI, A.J., AND B.G. OLIVER. 1983. Biological half-lives of polychlorinated biphenyl (PCB) congeners in whole fish and muscle of rainbow trout (*Salmo gairdneri*). Can. J. Fish. Aquat. Sci. 40: 1388–1394.

NIIMI, A.J., AND B.G. OLIVER. 1988. Influence of molecular weight and molecular volume on dietary absorption efficiency of chemicals by fishes. Can. J. Fish. Aquat. Sci. 45: 222–227.

OLIVER, B.G., AND A.J. NIIMI. 1988. Trophodynamic analysis of polychlorinated biphenyl congeners and other chlorinated hydrocarbons in the Lake Ontario ecosystem. Environ. Sci. Technol. 22: 388–397.

PLATT, T., AND K. DENMAN. 1977. Organization in the pelagic ecosystem. Helgol. Wiss. Meeresunters. 30: 575–581.

SHEA, M.A., AND J.C. MAKAREWICZ. 1989. Production, biomass, and trophic interactions of *Mysis relicta* in Lake Ontario. J. Great Lakes Res. 15: 223–232.

SHELDON, R.W., W.H. SUTCLIFFE JR., AND M.A. PARANJAPE. 1977. Structure of pelagic food chain and relationship between plankton and fish production. J. Fish. Res. Board Can. 34: 2344–2353.

WATSON, N.H.F., AND G.F. CARPENTER. 1974. Seasonal abundance of crustacean zooplankton and net plankton biomass of Lakes Huron, Erie, and Ontario. J. Fish. Res. Board Can. 31: 309–317.

WHITTLE, D.M., AND J.D. FITZSIMONS. 1983. The influence of the Niagara River on contaminant burdens of Lake Ontario biota. J. Great Lakes Res. 9: 295–302.

Appendix

Parameter definitions are defined in the following table:

Symbol	Definition	Unit of Measurement
W	Predator body mass	g
P	Predator biomass production $= \int dW/dt$	g/d
P'	Contaminant accumulated and retained by predator	µg/d
C'	Contaminant ingested	µg/d
$K_1{}'$	Contaminant retention efficiency $= P'/C'$	Dimensionless
g	Instantaneous growth rate $= dW/(W \cdot dt) = dP/W$	d^{-1}
X	Contaminant concentration in predator	µg/g
B	Total contaminant burden in predator $= X \cdot W$	µg
k_e	Instantaneous contaminant elimination rate	d^{-1}
$k_e \cdot B$	Total contaminant elimination rate	µg/d
E_0	Maximum digestive absorption efficiency of contaminant	Dimensionless

E_0 is differentiated here from the net contaminant assimilation efficiency, which may be lower if some of the contaminant is excreted into the gut. This gut excretion is included in k_e. E_0 is equal to the initial assimilation efficiency when X and B are 0 (Borgmann and Whittle 1992).

Equation 5 in the text is derived below. By definition:

$$
\begin{aligned}
\text{(1A)} \quad K_1' &= P'/C' = dP'/dC' \\
&= dP'/(dP' + k_e \cdot B + \text{contaminant egested}) \\
&= E_0 \cdot dP'/(dP' + k_e \cdot B) \\
&= E_0 \cdot (dP'/B)/((dP'/B) + k_e)
\end{aligned}
$$

where E_0 is equal to $(dP' + k_e \cdot B)/(dP' + k_e \cdot B + \text{contaminant egested})$. At steady state, $B = X \cdot W$ and $P' = X \cdot P$. Consequently,

(2A) $dP'/B = d(X \cdot P)/(X \cdot W) = dP/W = g$.

Combining equations 1A and 2A gives

(3A) $K_1' = E_0 \cdot g/(g + k_e)$

which is equation 5 in the text. Note that equation 3A for contaminants is equivalent to the analogous equation for biomass:

(4A) $K_1 = E_B \cdot g/(g + m)$

where E_B is biomass assimilation efficiency $((g + m)/(g + m + \text{biomass egestion}))$ and m is the instantaneous metabolic rate expressed in units of biomass.

Spatial Autocorrelation and Assessment of Habitat–Abundance Relationships in Littoral Zone Fish

Scott G. Hinch[1]

Department of Zoology and Erindale College, University of Toronto, Mississauga, ON L5L 1C6, Canada

Keith M. Somers

Department of Zoology, University of Toronto, Toronto, ON M5S 1A1, Canada
and
Ontario Ministry of Environment, Water Resources Branch, Limnology Section, Dorset, ON P0A 1E0, Canada

and Nicholas C. Collins

Department of Zoology and Erindale College, University of Toronto, Mississauga, ON L5L 1C6, Canada

Hinch, S.G., K.M. Somers, and N.C. Collins. 1994. Spatial autocorrelation and assessment of habitat–abundance relationships in littoral zone fish. Can. J. Fish. Aquat. Sci. 51: 701–712.

Spatial autocorrelation, wherein intersite similarity is correlated with distance between sites, is a characteristic of most ecological studies spanning a large environmental range. If data are spatially autocorrelated, classical statistical techniques provide biased estimates of relationships between species attributes and environmental variables. We examined abundances of seven littoral fishes in 25 lakes that varied substantially in morphometry, chemistry, and elevation across central Ontario. Weak correlations were observed between abundances of particular species and environmental variables before correcting for spatial autocorrelation, and we hypothesized that correlations reflected species' habitat preferences. However, spatial autocorrelation existed in the abiotic and fish abundance datasets. Once large-scale geographic patterns (spatial autocorrelation) were removed using partial Mantel tests, correlations changed within and between datasets. A strong relationship emerged between abundances and lake elevation. By comparing patterns within geographically corrected data with those without correction, we identified particular species that exhibited spatially autocorrelated abundances. The geographic direction of spatial autocorrelation provided additional insights into environmental factors also correlating with species abundance. We recommend that ecologists examine both geographically corrected and noncorrected data when developing hypotheses to explain regional variation in species abundance.

L'autocorrélation spatiale, selon laquelle la similarité entre les sites est corrélée à la distance entre eux, est une caractéristique de la plupart des études écologiques qui couvrent une grande aire environnementale. Si les données sont autocorrélées sur le plan spatial, les techniques statistiques classiques donnent des estimations biaisées des relations entre les attributs spécifiques et les variables environnementales. Nous avons examiné l'abondance de sept poissons littoraux dans 25 lacs du centre de l'Ontario présentant des variations importantes sur le plan de la morphométrie, de la chimie et de l'altitude. Nous avons observé de faibles corrélations entre l'abondance d'espèces données et les variables environnementales avant d'apporter une correction pour l'autocorrélation spatiale, et nous avons posé pour hypothèse que les corrélations reflétaient les préférences des espèces en matière d'habitat. Toutefois, l'autocorrélation spatiale existait dans les séries de données sur les éléments abiotiques et l'abondance des poissons. Une fois éliminés les schémas géographiques à grande échelle (autocorrélation spatiale) à l'aide de tests de Mantel partiels, les corrélations changeaient dans les séries de données et entre elles. Une forte relation est apparue entre l'abondance et l'altitude du lac. En comparant les schémas dans les données corrigées sur le plan géographique à celles qui n'étaient pas corrigées, nous avons repéré certaines espèces qui présentaient une autocorrélation spatiale dans l'abondance. L'orientation géographique de l'autocorrélation spatiale apportait une lumière supplémentaire sur les facteurs environnementaux qui présentaient aussi une corrélation avec l'abondance spécifique. Nous recommandons que les écologistes examinent les données avec et sans correction géographique lorsqu'ils élaborent des hypothèses pour expliquer la variation régionale dans l'abondance des espèces.

Received April 30, 1993
Accepted October 7, 1993
(JB907)

Reçu le 30 avril 1993
Accepté le 7 octobre 1993

Environmental variables generally exhibit a greater range in values when they span a large spatial or geographic area than when they are examined across a small spatial range. As a result, ecologists frequently use the terms "spatial variation" and "environmental variation" synonymously. The distinction between "space" and "environment" needs to be made clear for two reasons. First, variation in geographic position (i.e., spatial variation) could be responsible for variation in particular species attributes (e.g., presence/absence, abundance, or growth rate), but geographic position is not usually considered as a response variable in ecological studies. Second, if species attributes and environmental variables are related to geographic location, then the data are spatially autocorrelated — a phenomenon that can bias results of traditional statistical techniques (Legendre and Fortin 1989; Legendre 1993). Thus, ecologists must differentiate spatial patterns from patterns caused by particular environmental variables (see Borcard et al. 1992).

---

[1] Present address: Westwater Research Centre, University of British Columbia, 1933 West Mall Annex, Vancouver, BC V6T 1Z2, Canada.

Spatial patterns can be assessed statistically by measuring and testing for spatial autocorrelation (Odland 1988). Whenever a variable exhibits a regular pattern over space in which its values at a set of locations are systematically related to values at other locations, then spatial autocorrelation exists. Spatial statistics permit the use of formal statistical procedures to quantify association among observations with respect to the spatial distribution of the samples and to test hypotheses about correlations between spatial patterns among variables.

Many climatologic and geologic phenomena (e.g., weather patterns, rainfall, bedrock composition) extend over space to occupy regions rather than single point locations (Odland 1988). Therefore, nearby sampling sites are more likely influenced by similar abiotic conditions than sites far from one another. Thus, in ecological studies, nearby sites usually have similar values for species abundance (Legendre and Fortin 1989). This positive autocorrelation can reflect a biological phenomenon if organisms from one site influence those at nearby sites. Sites that are far apart, say, at either end of a long environmental gradient, often have very different values for species abundance. Such negative autocorrelation among distant sites is common in ecological studies that span long environmental gradients (Legendre and Fortin 1989). When positive spatial autocorrelation is present among nearby sites, as is usual in ecological studies, classical statistical tests usually overestimate the significance of correlation coefficients. Thus, variables may appear correlated when in fact they are not (Legendre and Fortin 1989). This problem arises because each observation in the dataset contributes only a portion of a degree of freedom; consequently, the traditional degrees of freedom are inflated, making statistical tests too liberal and prone to Type II errors (Bivand 1980; Cliff and Ord 1981). Since the true number of degrees of freedom can only be estimated, the appropriate reference distribution for such statistical tests is not usually known.

Spatial analyses thus serve two functions. They can be used as a prerequisite to hypothesis testing for spatially distributed samples to establish whether or not autocorrelation exists. If autocorrelation is not present (i.e., there are no spatial patterns evident), traditional statistical tests can then appropriately be used to examine hypotheses. If autocorrelation is present, then spatial analyses will help define the geographic patterns that exist. Appropriate techniques can then be used to "partial-out" geographic correlations and to permit traditional hypothesis testing once spatial constraints are removed (Legendre and Troussellier 1988; Borcard et al. 1992; Legendre 1993).

Large-scale, multilake studies are commonly used to assess the possible causal relationships between environmental factors and among-lake variation in fish species distribution and abundance (Harvey 1975, 1978, 1981; Tonn and Magnuson 1982; Rahel 1984; Robinson and Tonn 1989; Dolman 1990; Bergman 1991; Hinch et al. 1991; Tonn et al. 1991; Hinch and Collins 1993). The strength of the multilake, comparative approach is that it identifies variables whose associations with fish abundance or distribution are strong enough to stand out against a background of extensive among-lake variation in other variables. Thus, the relative importance of certain variables as predictors is revealed against a background of natural variation (Duarte 1991). However, a potential limitation of the multilake approach is that spatial autocorrelation within the data may alter or disguise relationships between environmental variables and fish species composition. Previous multilake studies of freshwater fish communities employed classical statistical methods to describe relationships between fish and environmental variables (based on a list of published studies reviewed by Hinch (1991)). However, researchers have not attempted to examine how interpretation of results from their multilake studies would have been altered if spatial autocorrelation was considered.

Recently, using data collected from 25 central Ontario lakes (Hinch et al. 1991), we correlated patterns of abundance of littoral zone fishes with specific abiotic and biotic factors. We did not, however, consider spatial location as a response variable nor did we consider spatial autocorrelation when interpreting patterns of community composition. In the present study, we reexamine these data, using a different analytical approach to address three questions. (1) On a large spatial scale, are fish species abundances or environmental variables associated with geographic position (i.e., is spatial autocorrelation present)?, (2) if spatial autocorrelation does exist, (i) how do correlations between abundance and environmental variables change when geographic correlations are removed? and (ii) how are the spatial patterns interpreted biologically?, and (3) can our understanding of fish–habitat relationships be enhanced by interpreting both geographically corrected and noncorrected results?

Methods and Materials

Study Area

From 1978 to 1981 the Lake Ecosystem Working Group from the University of Toronto gathered comprehensive physical, chemical, and biological data from 37 lakes in central Ontario. Our study is based on 25 of these lakes (Fig. 1). Lakes were selected to create a diverse dataset on the basis of watershed geology, morphometry, and lake chemistry. For example, in our 25-lake dataset, watershed geology ranged from complete limestone to mixed quartzite and felsics, lake area and maximum depth ranged from 0.29 km^2 and 3.0 m to 11.42 km^2 and 57.9 m, respectively, and lake pH ranged from 4.57 to 8.27. Lake physical and chemical data are listed in Paloheimo and Zimmerman (1983) and Zimmerman et al. (1983).

Data Collection

The following is a brief description of the techniques used to sample fish and the rationale for choosing particular variables; further details can be found in Hinch et al. (1991). A variety of gear types was used to overcome problems with sampling bias. This gear included experimental gill nets, trap nets (both fine and coarse mesh), plastic traps,

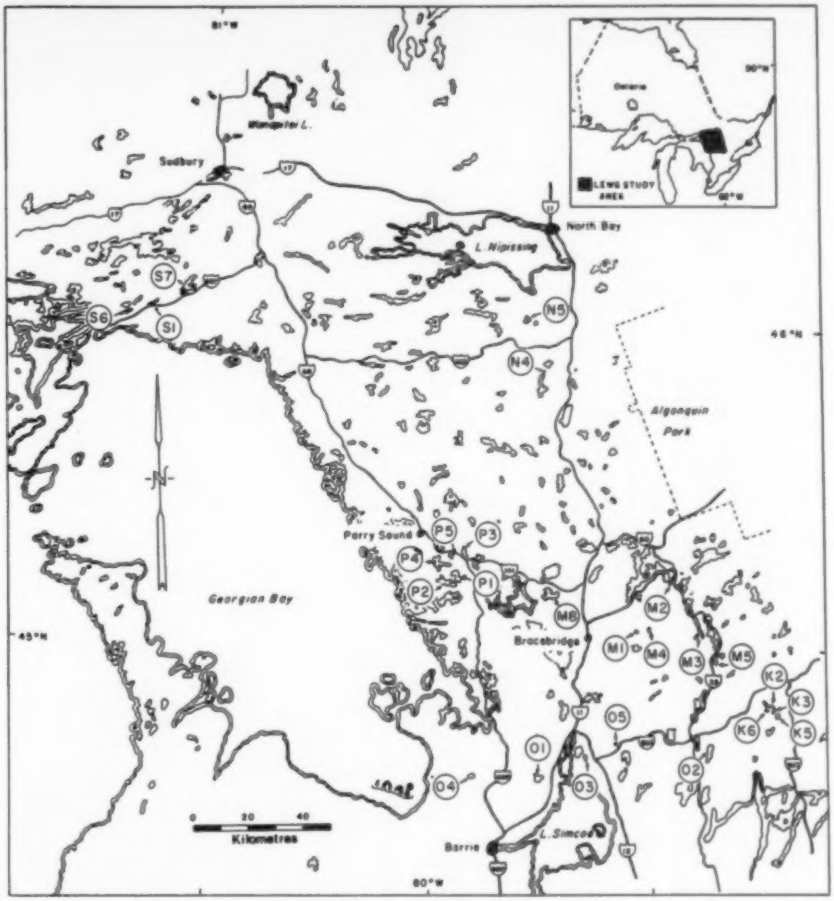

FIG. 1. Map (from Paloheimo and Zimmerman 1983, slightly modified) of the central Ontario study area showing location of lakes. Lake names that correspond with the codes on this map are given in Paloheimo and Zimmerman (1983).

and baited minnow traps (see Somers and Harvey (1984) for a detailed description of the gear). Each lake was fished for about 5 consecutive d between May and August. Effort for each 24-h period usually included 60–90 m of gill net, two trap nets, three or four plastic traps which are devices made of clear plastic resembling small trap nets, and four or five baited minnow traps. Larger lakes had more effort employed than smaller lakes. An index of species abundance for the most commonly occurring species was estimated for each lake by summing catch-per-unit-effort (CUE) data for each species over the four gear types. Because of the size- and species-specific biases involved in capturing fish with traps and nets, CUE will not likely provide a valid estimate of absolute abundance within a given lake. However, if estimates of absolute abundance are biased in a similar fashion among our study lakes, then the use of CUE is appropriate for comparing patterns of species- specific relative abundance among lakes. Abundance indices, fishing effort by gear type, and catch by species and gear type are given for each lake in Hinch (1992).

A 25-lake dataset was created by pooling abundance data collected in 1979 (17 lakes) with those collected in 1980 (eight lakes). Data from only these two years were used because sampling effort was highest in these years. Of the 38 fish species present in the 25 lakes, seven occurred in 60% or more of the lakes: yellow perch (*Perca flavescens*) 100%, pumpkinseed (*Lepomis gibbosus*) 96%, white sucker (*Catostomus commersoni*) 80%, brown bullhead (*Ameiurus nebulosus*) 76%, smallmouth bass (*Micropterus dolomieu*) 72%, rock bass (*Ambloplites rupestris*) 64%, and largemouth bass (*M. salmoides*) 60%. The remaining species occurred in less than 40% of the lakes. Because the primary goal of this study was to examine variation in the abundance of species, not their presence/absence, and because species with low frequency of occurrence have disruptive effects on multivariate analyses (Gauch 1982), only these seven commonly occurring species were used in data analyses. (Data for cyprinid species were not included in our dataset because our gear did not adequately capture individuals of these species.) Each of these seven species was caught in fairly equal numbers by the different gear types. Approximately 60% of the catch of each species was by gill nets whereas trap nets caught about 20% of each species; the remainder of the catch of each species was by plastic and minnow traps.

TABLE 1. Product–moment correlations between variables and the first PCoA axes on original and geographically corrected fish abundance, lake morphology, and lake chemistry matrices. δr is the difference, recorded as an absolute value, in the correlation coefficients for individual variables between original and corrected data. Asterisks represent significant correlations at $P \leq 0.007$, $P \leq 0.007$, and $P \leq 0.010$ which are the appropriate P-levels for multiple comparisons based on Bonferroni's correction for seven, seven, and five simultaneous tests for each respective dataset and experimentwise error rate of 0.05.

Matrix	Variable	Original PCoA axis 1	δr	Corrected PCoA axis 1
Abundance	White sucker	0.56*	0.11	0.67*
	Brown bullhead	0.73*	0.25	0.48
	Pumpkinseed	0.58*	0.33	0.25
	Rock bass	−0.64*	0.37	−0.27
	Smallmouth bass	−0.16	0.01	−0.17
	Largemouth bass	−0.18	0.17	−0.35
	Yellow perch	0.49	0.22	0.71*
	% explained variance	32.0		46.5
Morphology	Drainage area	0.82*	0.01	0.81*
	Flushing rate	−0.19	0.53	0.34
	Area	0.96*	0.05	0.91*
	Maximum depth	0.48	0.02	0.46
	Volume	0.90*	0.18	0.86*
	Perimeter	0.90*	0.02	0.88*
	Littoral area	0.65*	0.06	0.59*
	% explained variance	58.0		68.2
Chemistry	Calcium	0.97*	0.16	0.81*
	Chlorophyll *a*	0.36	0.14	0.22
	Phosphorus	0.67*	0.15	0.52*
	Conductivity	0.97*	0.14	0.83*
	pH	0.94*	0.25	0.69*
	% explained variance	77.0		58.3

Hinch et al. (1991), in an eight-lake subset of the data, found that species-specific abundance indices were correlated with electrofishing data, suggesting that combining CUE across gear types provided a reasonable assessment of among-lake species relative abundance. In addition, Hinch et al. (1991), in a 10-lake subset of the data, compared catch of the seven common species in lakes sampled in 1978 with those resampled in 1979 and 1980 and found that the proportion of fish caught by species did not change within a given lake, suggesting that among-lake patterns in fish abundance were not created by sampling in different years.

Lake water was sampled regularly from standard within-lake sites from April to August 1980; methods are outlined in Zimmerman et al. (1983). Summer averages were determined for the following water chemistry characteristics: calcium concentration, total phosphorus concentration, chlorophyll *a* concentration, pH, and conductivity. These data are listed in Zimmerman et al. (1983).

Our lake morphology dataset consisted of the following variables: perimeter length, volume, maximum depth, area, fetch, flushing rate, watershed area, and absolute littoral area. These data can be found or calculated from Paloheimo and Zimmerman (1983) and Zimmerman et al. (1983). Elevation data are given in Hinch (1992). Latitude and longitude coordinates for these lakes are listed in Paloheimo and Zimmerman (1983).

Spatial Analyses

Before statistical analyses, all raw data were transformed to values ranging from 0 to 1. Each variable was transformed by subtracting the minimum value across all lakes and dividing the result by the difference between the maximum and minimum value across all lakes. This transformation places each variable on the same relative scale but does not alter the distribution of observations within a variable like other transformations (e.g., logarithms). In a study of spatial interrelationships, it is important to minimize distortions of the multidimensional spatial arrangement of observations associated with differing units of measurement.

Because our data were multivariate in nature, we required a multivariate approach to assess the presence of spatial autocorrelation. As a result, we used Mantel tests (Mantel 1967) to compare a matrix of distances based on one set of variables (i.e., a biotic or abiotic dataset) with a matrix of geographic distances obtained from latitude and longitude coordinates. The Mantel statistic is a type of product–moment correlation that quantifies the degree of concordance between two matrices (Smouse et al. 1986). Further elaboration on the Mantel test plus a discussion of the hypotheses evaluated by this approach are given in Legendre and Fortin (1989).

Our first step in determining whether a multivariate dataset was spatially autocorrelated was to calculate an interlake Euclidean distance matrix for each dataset. A Euclidean distance matrix was also created based on kilometre distances between lakes using latitude and longitude. Next, we used a two-tailed Mantel test to compare a Euclidean distance matrix of interlake geographic distances with interlake distances based on fish abundance and abiotic datasets. Significance levels for these analyses were determined using a randomization procedure (see Jackson and Somers 1989).

For each test, 1000 permutations were conducted. Mantel tests were calculated using a program modified from Manly (1990). We checked the ability of the Mantel test to identify the presence of a gradient spatial pattern using simulated data (Hinch 1992).

We used partial Mantel tests (Smouse et al. 1986) to (i) estimate the amount of variation within each dataset that was attributable to variation in geographic location and (ii) create geographically corrected datasets. The Smouse et al. (1986) approach performs more reliably than other three-matrix permutation tests (Oden and Sokal 1992). With this technique, the upper triangular off-diagonal elements of each Euclidean distance matrix were linearly regressed against the corresponding values from a geographic distance matrix based on sampling site positions. We used the coefficient of determination (i.e., the r^2) from the linear regression of the off-diagonals of the abundance and abiotic distance matrices on the geographic distance matrix (PROC GLM; SAS Institute Inc. 1982) as an estimate of the relative amount of spatial variation in each response matrix. Geographically corrected datasets were created by placing the residuals from this regression relationship into a distance matrix. This procedure removed only simple linear spatial patterns from a given data matrix (i.e., employing the assumption that spatial patterns followed a linear gradient). More complex spatial patterns were not evaluated (e.g., see Borcard et al. 1992).

Assessing the Influence of Spatial Autocorrelation

Principal coordinates analyses (PCoA; Gower 1966) were performed on each distance matrix to reduce the dimensionality of the data and reveal the major among-lake trends. Our version of PCoA used an iterative method to resolve only positive eigenvalues (Orlóci 1978). PCoA was selected instead of other ordination methods because it operates on the same matrix of interlake distances that we used in the Mantel comparisons. Among-lake correlations between species abundances and environmental variables were inferred from the correlations between PCoA axes from different matrices (PROC CORR; SAS Institute Inc. 1982). If correlations between PCoA axes suggested relationships between particular variables, we only interpreted those correlations that were consistent with bivariate correlations between the raw (0–1 transformed) data. We used this analysis strategy because correlations between PCoA axes from different matrices may not reflect relationships among the raw data (Hinch et al. 1991). However, we did not want to rely solely on simple bivariate correlations among all variables as a way of building empirical models because this approach lacks statistical power; the comparisonwise critical alpha level to achieve statistical significance with so many simultaneous comparisons would be extremely low. Mantel tests may detect some interdataset relationships that are not detected by correlating major ordination axes because major ordination axes only account for a portion of the variation

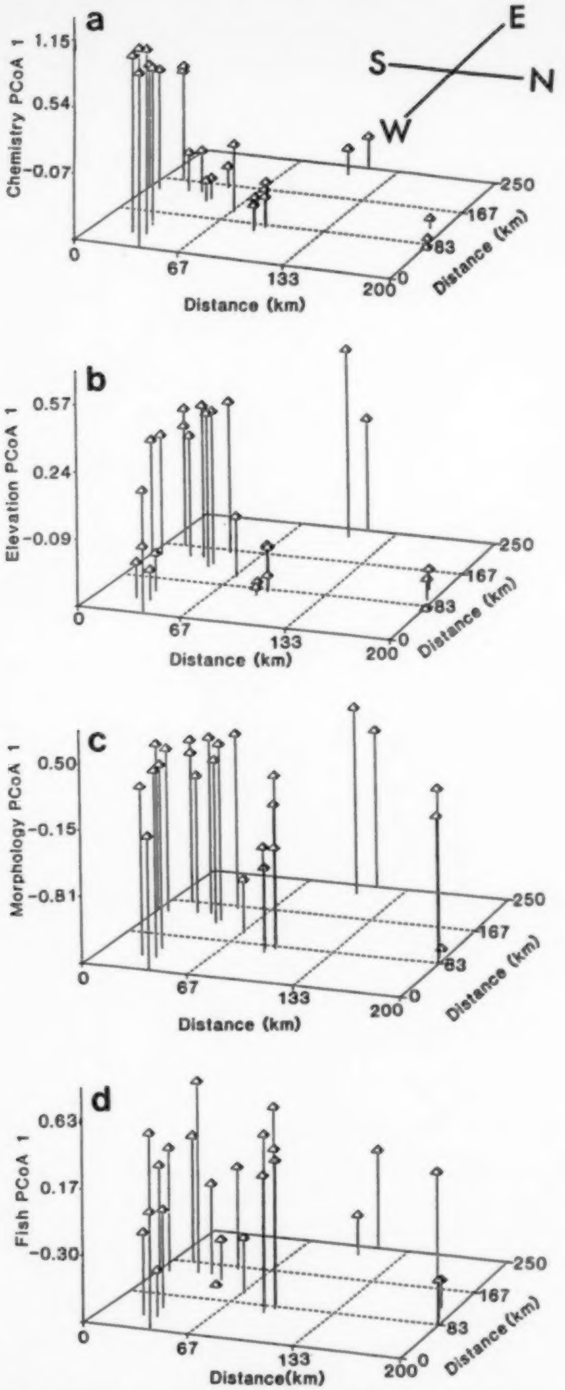

FIG. 2. Scores from the first axis of PCoA on (a) lake chemistry data, (b) lake elevation data, (c) lake morphology data, and (d) fish abundance data mapped across the study area. The map was created from a PCoA of kilometre distances between lakes using latitude and longitude coordinates from each study lake. Instead of PCoA coefficients, the relative distances between the most extreme north–south and east–west lakes are plotted on the axes to help display the relative spatial location of lakes. So that the majority of three-dimensional arrowheads (e.g., lake data points) were not hidden behind each other and obscured from view, we illustrated the north–south axis as a south–north axis on all figures. (The compass directions are identical for each figure.)

TABLE 2. Product–moment correlations between scores from the PCoA axes for geographic position and fish abundance with those for lake chemistry, morphology, and elevation datasets. Asterisks indicate significant correlations at $P \le 0.008$ which is the appropriate P-level for multiple comparisons using Bonferroni's correction for six simultaneous tests and an experimentwise error rate of 0.05.

	Geography		Abundance	
	PCoA axis 1	PCoA axis 2	PCoA axis 1	PCoA axis 2
Abundance PCoA axis 1	0.15	−0.11	1.00	0.00
Abundance PCoA axis 2	−0.17	0.16	0.00	1.00
Chemistry PCoA axis 1	0.66*	−0.42	0.03	−0.16
Morphology PCoA axis 1	0.37	0.23	−0.11	0.14
Morphology PCoA axis 2	−0.15	0.21	0.39	0.35
Elevation PCoA axis 1	0.52*	0.72*	−0.24	−0.01

within a given dataset. So Mantel tests were also used to complement the ordination correlations.

Lake location trends were established by performing a PCoA on a matrix of kilometre distances between lakes. To assess the geographic orientation of spatial patterns within the response matrices, major trends in the abundance, morphology, chemistry, and elevation datasets (i.e., PCoA axes) were correlated with the major (i.e., north–south) and minor (i.e., east–west) trends in the lake location matrix.

To estimate the influence of spatial autocorrelation, we compared the major among-lake patterns generated from PCoAs on nongeographically corrected data with the major among-lake patterns generated from PCoAs carried out on geographically corrected data. We also reevaluated the correlations between species abundances and the environmental variables (PROC CORR; SAS Institute Inc. 1982) using the major PCoA axes from geographically corrected data. In addition, Mantel tests were used as a multivariate approach to evaluate the consequences of removing spatial patterns. The technique of comparing PCoA results, before and after removing geographic influences, is demonstrated with a simulated dataset in Hinch (1992).

To illustrate how spatial autocorrelation altered relations among datasets, we ordinated the correlation matrix of Mantel statistics with PCoA using matrices before and after spatial correction. We plotted the scores of the first two PCoA axes from both analyses to exhibit the influence of spatial autocorrelation on relationships among datasets.

Results

Patterns within Datasets, Ignoring Spatial Autocorrelation

Fifty-two percent of the standardized variation in fish abundance was summarized by the first two PCoA axes. The first axis (32%) contrasted lakes with high abundances of white sucker, brown bullhead, and pumpkinseed with those having high abundance of rock bass (Table 1). The second axis (20%) ordered lakes based on the abundance of largemouth bass. Eighty-two percent of the variation in lake morphology was accounted for by the first two axes of the PCoA. The first axis (58%) described a gradient associated with lake size (Table 1), the second axis (24%) contrasted deep lakes with small littoral areas with shallow lakes with large littoral areas. Most of the variation in lake chemistry (77%) was accounted for by the first axis of PCoA which ordered lakes along a concentration gradient of most of the variables (Table 1). The second axis, which explained 16% of the variation and was not used in further analyses, summarized variation in lake productivity, since this axis was correlated with chlorophyll *a* and total phosphorus concentrations. Although it only contained one variable, the elevation dataset was ordinated using PCoA so that all response datasets were treated equally; lakes were ordered from low to high altitude along the sole PCoA axis.

A plot of lake scores from the PCoA of the geographic distance matrix recreated a map of the central Ontario study area (Fig. 2 and 3). The first axis ordered lakes along a north–south gradient and the second and final axis ordered lakes along a west–east gradient.

Relations between Datasets, Ignoring Spatial Autocorrelation

There were no significant pairwise correlations among scores from the PCoA axes of environmental factors and species abundances (Table 2), although a weak trend existed between the first fish abundance axis and the second lake morphology axis. A Mantel test revealed a significant correlation between the species abundance and lake morphology distance matrices (Table 3). Therefore, we examined correlations between species abundance and lake morphology variables that appeared to have contributed to variation along the respective PCoA axes. We thus correlated white sucker, brown bullhead, pumpkinseed, and rock bass abundances with flushing rate, maximum depth, and littoral area. Significant correlations ($P \le 0.05$) only existed between brown bullhead abundance and flushing rate ($r = 0.440$, $P = 0.028$) and between rock bass abundance and maximum depth ($r = 0.367$, $P = 0.050$). No correlation was statistically significant after using Bonferroni's correction for three simultaneous comparisons (i.e., three correlations).

In addition to the significant correlation between fish abundance and lake morphology, Mantel tests also revealed

TABLE 3. Correlations from Mantel tests (upper off-diagonal matrix) with associated probabilities (lower off-diagonal matrix) between distance matrices from geographically corrected and original (noncorrected) datasets. Asterisks represent significant correlations at $P \leq 0.005$ for multiple comparisons using Bonferroni's correction for 10 simultaneous tests and an experimentwise error rate of 0.05.

	Abundance	Elevation	Morphology	Chemistry	Geography
Original					
Abundance		0.161	0.246*	0.029	0.135
Elevation	0.010		0.072	−0.043	0.280*
Morphology	<0.001	0.216		0.182	0.099
Chemistry	0.577	0.469	0.008		0.326*
Geography	0.021	<0.001	0.108	<0.001	
Corrected					
Abundance		0.185	0.239*	−0.020	−0.007
Elevation	0.008		0.046	−0.255*	0.002
Morphology	<0.001	0.349		0.259*	−0.001
Chemistry	0.691	0.004	0.004		0.000
Geography	0.931	0.975	0.990	1.000	

a marginally significant correlation between abundance and elevation and between abundance and geographic location distance matrices (Table 3).

Spatial Patterns within Datasets

Spatial autocorrelation was indicated in the lake chemistry and elevation datasets by a significant correlation with geographic location (using Mantel tests; Table 3). Spatial autocorrelation in the species abundance matrix, after using Bonferroni's correction for 10 simultaneous tests, was nearly significant ($P = 0.021$, critical value = 0.005).

Correlations between PCoA axes for the environmental and geographic location datasets described the direction of spatial patterns. The first chemistry PCoA axis was correlated with the first geographic axis (Table 2); thus, chemistry was spatially autocorrelated in a north–south direction (Fig. 2a). This finding reflects the fact that the lakes spanned an alkalinity gradient; lakes in the south had high values for pH, conductivity, and calcium that decreased in a northerly direction. Elevation was correlated with both geographic axes (Table 2). The correlation with the first axis seemed to be driven by three low-elevation lakes located in the north (Fig. 2b). Elevation was most strongly autocorrelated in an east–west direction; high elevation lakes tended to be located in eastern portions of the study area. Lake morphology was not spatially autocorrelated in any direction (Fig. 2c; Table 3). Although a Mantel test suggested that fish abundances exhibited weak spatial autocorrelation (Table 3), a map of PCoA scores based on fish abundance did not reveal any obvious spatial pattern (Fig. 2d).

Partialling-Out Spatial Autocorrelation

Eleven percent of the variation in lake chemistry, 8% of the variation in lake elevation, and 2% of the variation in both fish abundance and lake morphology were explained by broad-scale linear patterns in geographic position (also see Table 3). Partial Mantel tests were most successful at removing spatial influences from lake chemistry and elevation datasets probably because of the linear nature of these spatial patterns (i.e., some variation in water chemistry and elevation was attributable to a north–south gradient). The first axes from ordinations on geographically corrected lake chemistry and elevation data were no longer correlated with the first geographic PCoA axis (Table 4). Thus, the north–south autocorrelation of these two datasets which was evident in Table 2 had been removed (Fig. 3a and 3b). However, the east–west autocorrelation pattern that was evident in Table 2 still existed within the elevation data (Table 4; Fig. 3b). Gradient patterns were not evident in the geographically corrected lake morphology (Table 4; Fig. 3c) or fish abundance (Table 4; Fig. 3d) data. In summary, the major geographic gradient was partialled out of the response datasets; however, spatial autocorrelation that was nonlinear (i.e., nongradient) or that was not associated with a major gradient probably still existed within our data.

Patterns within Geographically Corrected Datasets

In each case, correlations of the original variables with the PCoA axes were altered by removing geographic correlations; however, significant changes in correlations were only observed within the species abundance dataset. The first PCoA axis of geographically corrected species abundances explained 47% of the variation and ordered lakes from high to low abundances of white sucker and yellow perch (Table 1). The second axis (30%) ordered lakes according to largemouth bass abundance. The first axis on corrected abundance data differed from the first axis of the PCoA on noncorrected data where lakes with high abundances of white sucker, brown bullhead, and pumpkinseed were contrasted with those having abundant rock bass. The correlations between the first PCoA axis and abundances of brown bullhead, pumpkinseed, rock bass, and yellow perch changed the most when data were spatially corrected (i.e., the δr was the greatest for these species; Table 1). Species correlations with the second axis were similar using corrected and noncorrected data.

Spatial autocorrelation had only minor impact on the observed multivariate patterns with the lake morphology and chemistry datasets. Sixty-eight percent of the variation in geographically corrected lake morphology was explained by the first PCoA axis which described a lake size gradient (Table 1). Although the correlation between flushing rate and the first axis changed substantially after data were geographically corrected (see δr in Table 1), it remained statistically nonsignificant. The second axis (30%) con-

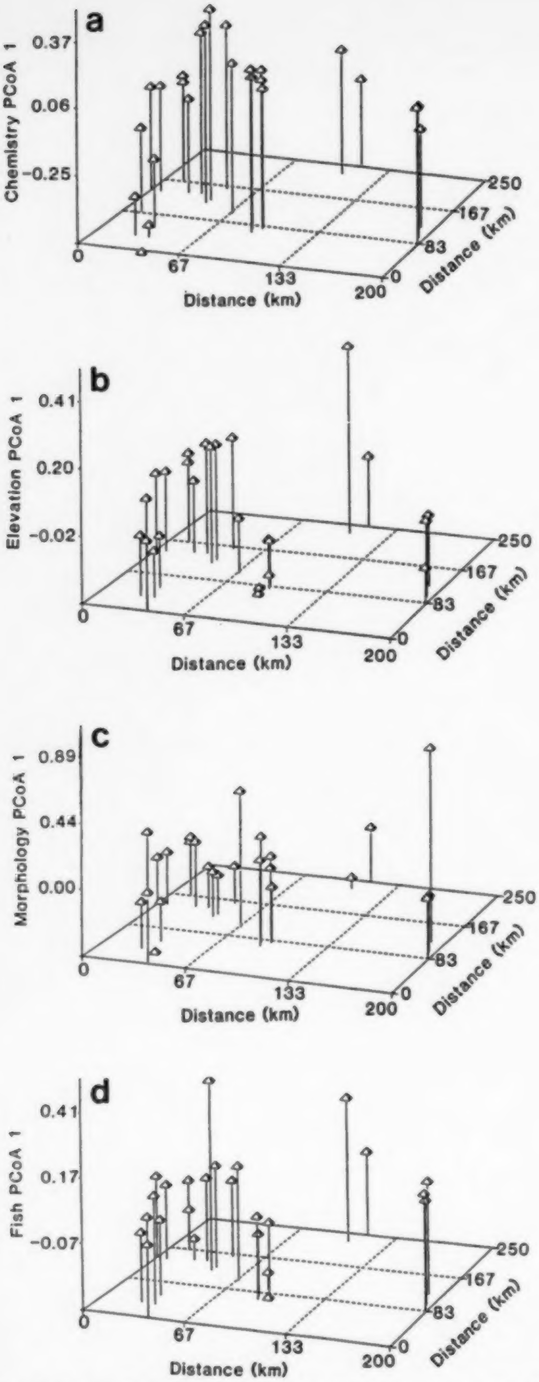

FIG. 3. Scores from the first axis of a PCoA on geographically corrected (a) lake chemistry data, (b) lake elevation data, (c) lake morphology data, and (d) fish abundance data mapped across the study area. The map and compass directions as in Fig. 1.

trasted deep lakes with those having large littoral areas and high flushing rates. Fifty-eight percent of the variation in geographically corrected lake chemistry was accounted for by the first PCoA axis which ordered lakes from high to low values of all variables with the exception of chlorophyll *a* (Table 1). The δr suggested that pH was a spatially autocorrelated variable because the correlation declined in importance once data were geographically corrected (Table 1). No single variable strongly characterized the second lake chemistry axis.

Relationships between Datasets after Geographically Correcting

The first axis from a PCoA of species abundances was correlated with the lake elevation PCoA axis (Table 4); this relationship was not observed with nongeographically corrected data (Table 2). A Mantel test confirmed that abundances became more strongly correlated with lake elevation once data were geographically corrected (Table 3). The weak correlation between the first fish abundance axis and the second lake morphology axis that appeared from analyses on noncorrected data (Table 2) was no longer evident with corrected data (Table 4). Despite geographic correction, a Mantel test still uncovered a correlation between abundance and lake morphology (Table 3).

Significant correlations between the first PCoA axis of lake geographic position (i.e., the north–south axis) and (1) the first elevation PCoA axis and (2) the first lake chemistry PCoA axis were no longer evident using corrected data (Table 4). These findings confirmed our earlier assertion that lake chemistry and elevation data were autocorrelated in a north–south direction.

A bivariate plot (Fig. 4a) of scores from a PCoA of the matrix of Mantel statistics based on the original nongeographically corrected datasets (correlation values taken from Table 3) summarized associations between the different datasets and showed that lake elevation and lake chemistry exhibited greater spatial autocorrelation (i.e., were more closely associated with geographic position) than species abundances or lake morphology. A similar plot (Fig. 4b) for the geographically corrected matrix correlations (values from Table 3) illustrated how relationships among datasets were altered by partialling-out geographic influences. Lake elevation and species abundances became more closely associated. In addition, lake chemistry became more closely related to lake morphology.

Discussion

Ignoring Spatial Autocorrelation

Overlooking the presence of spatial autocorrelation, we were first impressed by the lack of strong relationships between fish abundance and environmental variables despite the relatively strong presence of patterns as indicated by the PCoA. As a result, we were tempted to focus on the only association that was uncovered between fish abundance and environmental variables — the relationship between lake morphology and species abundance revealed by a Mantel test (Table 3). To interpret this relationship, we examined correlations among PCoA axes and found that a weak relationship existed between the second lake morphology axis and the first species abundance axis (Table 2) which suggested that pumpkinseed, white sucker, and brown bullhead were more abundant in shallow lakes with large littoral zones

TABLE 4. Product–moment correlations among scores from the PCoA axes for geographic position and fish abundance with those for lake chemistry, morphology, and elevation datasets, after partialling-out spatial autocorrelation. Asterisks represent significant correlations at $P \le 0.008$ for multiple comparisons using Bonferroni's correction for six simultaneous tests and an experimentwise error rate of 0.05. Marginally significant correlation at $P = 0.01$ is indicated by a dagger.

	Geography		Abundance	
	PCoA axis 1	PCoA axis 2	PCoA axis 1	PCoA axis 2
Abundance PCoA axis 1	−0.22	0.19	1.00	0.00
Abundance PCoA axis 2	0.36	0.15	0.00	1.00
Chemistry PCoA axis 1	−0.22	0.39	0.17	−0.26
Morphology PCoA axis 1	−0.37	−0.10	−0.12	−0.02
Morphology PCoA axis 2	0.08	0.18	−0.19	0.26
Elevation PCoA axis 1	0.20	0.62*	0.50†	0.31

and that rock bass were more abundant in deep lakes with small littoral zones. However, these relationships were not obvious from correlations among raw variables. If we were to rely solely on the correlations among PCoA axes, we would explain this weak pattern ecologically with reference to habitat preferences and requirements of each species. White sucker and brown bullhead are primarily nonvisual foragers that feed mostly in soft benthic sediments (Scott and Crossman 1973). Muddy substrates tend to be more abundant in shallow lakes with large littoral zones. Pumpkinseed feed primarily on or near macrophytes (Mittelbach 1984; Keast 1978) and, because of their relatively small size, use macrophytes as refuges from predators (Werner and Hall 1988). Thickly vegetated littoral areas, which would provide abundant food and predator protection for pumpkinseed, would be more common in shallow lakes with large littoral zones. Rock bass, as their name implies, normally feed and breed in rocky areas of lakes (Scott and Crossman 1973). This type of shoreline is common in deep lakes with steeply sloping (i.e., small) littoral areas.

Effects of Spatial Autocorrelation on Fish Abundance Patterns

Mantel tests revealed that spatial autocorrelation was evident in nearly every dataset. If we ignored the presence of spatial patterns, we might propose the habitat-related hypotheses described above. A consideration of correlations between geographically corrected datasets is necessary to evaluate how geographic variation (spatial autocorrelation) has altered our perception of the factors contributing to patterns in species composition.

Once the influence of broad-scale spatial variation was removed with partial Mantel tests, correlations changed within and between datasets. The most noticeable changes arose in the abundance dataset among correlations between the original species abundances and the new PCoA axes. The major trend in species composition was no longer correlated with variation in abundances of white sucker, brown bullhead, rock bass, and pumpkinseed. Instead, only variation in yellow perch and white sucker abundances correlated with among-lake patterns in species abundance.

If a variable exhibits patterns that are spatially autocorrelated, then either geographic position or some variable that is correlated with geographic position is responsible for these patterns. The importance of pumpkinseed and brown bullhead to the first PCoA axis for fish abundance declined once the north–south geographic influence was removed (i.e., when data were geographically corrected). This result suggests that the abundances of pumpkinseed and brown bullhead were spatially autocorrelated. To confirm this multivariate finding, we examined correlations between the raw 0–1 transformed pumpkinseed and brown bullhead abundance and scores from the first geographic PCoA axis. Raw brown bullhead abundances were weakly correlated with latitude; they tended to be more abundant in southern lakes than in northern lakes ($r = -0.363$, $P = 0.074$) whereas raw pumpkinseed abundances showed no north–south relationship ($r = -0.115$, $P = 0.586$). Therefore, taking into consideration these bivariate correlations and the preceding multivariate results, we suggest that the abundance of brown bullhead was spatially autocorrelated. Because bivariate and multivariate analyses did not provide consistent interpretations for pumpkinseed, we feel that we have limited evidence that pumpkinseed abundance was also spatially autocorrelated. Since partial Mantel tests removed a geographic gradient of north–south variation from each response dataset, latitudinal position or variables that correlate with latitudinal position, which were not considered in this study, may affect abundances of brown bullhead. Matuszek and Beggs (1988) used latitude as an index for climatic conditions, assuming that more extreme climates occurred at more northern latitudes. Latitude may also correlate, in Ontario, with isolation from postglacial colonization areas (Mandrak 1990) or lake temperature (Shuter et al. 1980). The latitude of the northernmost lakes in the present study coincides with the maximum northern distribution of brown bullhead in Ontario; their survival in more northern lakes is probably inhibited by cold climates and a limited number of degree-days (Mandrak 1990). Relatively low abundances of brown bullhead in northern lakes may thus reflect a decreased ability to grow and reproduce in colder lakes (e.g., Shuter et al. 1980). These results demonstrate how

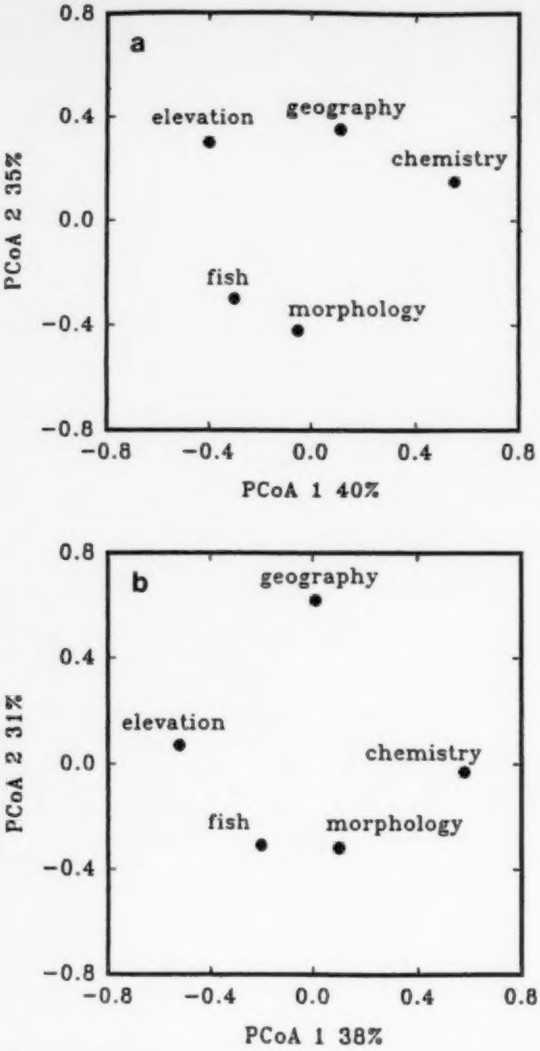

FIG. 4. Plots of the scores from the first two axes of PCoAs on (a) raw (original) matrix correlations and (b) geographically corrected matrix correlations both taken from Table 3. The percent variance that these axes account for is provided. Note that the fish abundance and lake elevation datasets become more closely associated when geographically corrected.

spatial analyses can provide additional insights into factors that may structure fish communities either because spatial autocorrelation can bias results of traditional statistical approaches or because geographic position can act as a surrogate for variables that may have been overlooked when the study was carried out or were too difficult to measure.

The contribution of variation in rock bass abundance to the first abundance PCoA axis also declined once data were geographically corrected, suggesting that rock bass abundance was spatially autocorrelated. The correlation between raw 0–1 transformed rock bass abundances and the scores from the first geography PCoA axis was weak but suggested that rock bass were more abundant in northern lakes than in southern ones ($r = -0.348$, $P = 0.090$). However, this correlation was likely based on species presence/absence because rock bass were generally absent from lakes in the southwest portion of the study area. Therefore, we have only limited evidence that rock bass abundance was spatially autocorrelated.

Other factors besides latitude may correlate with spatial variation and may contribute to spatial patterns of fish abundance. One possible factor is sampling date. Fish were trapped over a 4-mo period in the summers of 1979 and 1980 and different lakes were fished each week. However, lakes tended to be sampled in the south before those in the north. Therefore, spatial patterns in fish abundance may reflect seasonal patterns of sampling. We created an interlake Euclidean distance matrix of mean "day of the year", ignoring the year differences, for sampling periods on each lake and compared this matrix with a species abundance matrix and a geographic location matrix using a Mantel test. Geographic location and sampling date were highly correlated (Mantel statistic = 0.449, $P \leq 0.001$), and there was a weak correlation (Mantel statistic = 0.108, $P = 0.070$) between fish abundance and sampling date. Although the relation between fish abundance and geographic location (Mantel statistic = 0.135, $P = 0.021$, from Table 3) is stronger than the relation between fish abundance and sampling date, these results suggest that spatial patterns of fish abundance could be partly attributable to temporal patterns of sampling. There was no association between a geographically corrected sampling date distance matrix and a geographically corrected fish abundance distance matrix (Mantel statistic = 0.042, $P = 0.444$). Therefore, by partialling-out spatial influences, seasonal influences have also been partialled out.

Once the influence of north–south geographic variation was partialled out of each dataset, the first fish abundance PCoA axis was correlated only with an east–west lake elevation gradient. This suggests that once data were geographically corrected, high-elevation lakes had greater abundances of yellow perch and white sucker than low-elevation lakes (Table 4). Because eastern lakes are at relatively higher elevations than western lakes, and highland lakes lack native populations of the littoral zone piscivore northern pike (*Esox lucius*) (e.g., Hinch et al. 1991), predation may be responsible for the broad-scale variation we observed in white sucker and yellow perch abundance. Northern pike did not colonize high-elevation lakes in central Ontario after the Wisconsinan Glacier receded because by the time northern pike reached Ontario from their distant glacial refugia, uplift of the land had cut off immigration routes into highland areas (Mandrak 1990). In an earlier study where we used traditional statistical techniques, we observed a negative relationship between white sucker abundance and pike presence (Hinch et al. 1991), however, only with geographically corrected analyses were we able to interpret a similar relation between perch abundance and pike presence.

Piscivory by northern pike is believed to significantly alter levels of prey abundances in lakes. In a 45-yr study in a British lake, a large portion of the variation in yellow perch abundances could be explained by pike predation (Le Cren 1987). Furthermore, small-scale studies that have manipulated abundances of northern pike have consistently found that when northern pike are introduced into a lake, which sucker and yellow perch decline in abundance, and when northern pike are removed from a lake, white sucker and yellow perch increase in abundance (Colby et al. 1987, and references within; He and Wright 1992). Since northern pike are only present in low-elevation Ontario lakes, and it is these lakes that have relatively depauperate white sucker and yellow perch populations, it is reasonable to suggest that piscivory by northern pike is responsible for variation in numbers of white sucker and yellow perch caught in the present study.

In summary, we found that spatial autocorrelation altered relations within and among datasets, thereby affecting our perceptions of what factors might be responsible for variation in abundances of central Ontario fishes. Before correcting for spatial autocorrelation, only weak relationships between particular species abundances and environmental variables were evident. However, the validity of these relationships was questioned because spatial autocorrelation was evident in each dataset. We found that variation in geographically corrected species abundances was strongly related to variation in lake elevation. Highland lakes contained relatively higher abundances of yellow perch and white sucker. We hypothesized that the absence of the littoral zone predator northern pike may be responsible for relatively high abundances of yellow perch and white sucker in high-elevation lakes. A comparison of species abundance patterns using geographically corrected and noncorrected data provided additional insight into the possible factors responsible for variability in fish abundance. For instance, abundances of brown bullhead were spatially autocorrelated, brown bullhead being most abundant in southern lakes and least abundant in northern lakes. This pattern disappeared when data were geographically corrected, suggesting that latitude was an important factor influencing abundance of brown bullhead in central Ontario. Latitude may act as a surrogate for lake temperature and climate severity, variables not examined in this study. Variation in sampling dates also correlated with spatial patterns of fish abundance; therefore, spatial patterns of brown bullhead abundance may have arisen through temporal as well as spatial factors.

Recommendations for Multilake Research

In multilake ecological studies, the identification of geographic patterns (spatial autocorrelation) within and between datasets is important for several reasons. First, it makes one aware of the statistical problems that can be encountered when interpreting correlations from spatially arranged data. Correlations between autocorrelated variables based on classical statistical techniques may be biased (Cliff and Ord 1981). Thus, it can be advantageous to factor-out broad-scale geographic patterns to ensure that correlations within or between datasets are not misinterpreted, a result of autocorrelation. The identification of spatial autocorrelation is also important because it gives us the opportunity to rethink our hypotheses with respect to these geographic patterns. Patterns may be caused by some variable that correlates with geographic position that was not or cannot be measured. For instance, climate variables may be responsible for the geographic patterns of species attributes. Spatial autocorrelation may also occur as a result of a systematic sampling design such as ours. Removing the influence of spatial autocorrelation with appropriate analyses combined with a sampling strategy that does not confound temporal and spatial influences is recommended. One disadvantage of eliminating geographic correlations as a means to ensure valid statistical tests is that we are removing the influence of geographic variation from all our variables, including those variables that may contribute to patterns of species composition. Therefore, by examining only geographically corrected data, information that is needed to fully understand variation in species attributes may have been eliminated. In fact, partialling-out spatial influences may leave few relationships within and between datasets.

We recommend that ecologists examine both geographically corrected and the original noncorrected data when developing hypotheses to explain broad-scale variation in species composition. If spatial autocorrelation does not exist within datasets, then results using the original data are acceptable. If autocorrelation is present, (1) exercise caution when interpreting relations within and between datasets, (ii) examine and interpret corrected data, (iii) compare results of analyses on both types of data to determine which variables are autocorrelated, and (iv) from this comparison, develop hypotheses to explain the origin of autocorrelation patterns of specific variables.

Acknowledgements

This research has benefitted from discussions with Gary Sprules, Ann Zimmerman, Brian Shuter, and Harold Harvey. We are grateful to those involved with the Lake Ecosystem Working Group (LEWG) at the University of Toronto for collecting much of our data, in particular Cindy Lee, Edward Trippel, Jan Anderson, Jeff Hutchings, Scott Rubie, and Mary Durfey for collecting the LEWG fish abundance data. Comments provided by anonymous reviewers strengthened the manuscript. Funding for this study was provided by a Natural Sciences and Engineering Research Council of Canada (NSERC) cooperative grant to LEWG at the University of Toronto, NSERC operating grants to Nicholas Collins and Harold Harvey, and a NSERC postgraduate scholarship and a University of Toronto Open Fellowship to Scott Hinch.

References

Bergman, E. 1991. Changes in abundance of two percids, *Perca fluviatilis* and *Gymnocephalus cernuus*, along a productivity gradient: relations to feeding strategies and competitive abilities. Can. J. Fish. Aquat. Sci. 48: 536–545.

Bivand, R. 1980. A Monte Carlo study of correlation coefficient estimation with spatially autocorrelated observations. Quaest. Geogr. 6: 5–10.

Borcard, D., P. Legendre, and P. Drapeau. 1992. Partialling out the spatial component of ecological variation. Ecology 73: 1045–1055.

Cliff, A.D., and J.K. Ord. 1981. Spatial processes: models and applications. Pion Limited, London. 266 p.

Colby, P.J., P.A. Ryan, D.H. Schupp, and S.L. Serns. 1987. Interactions in north-temperate lake fish communities. Can. J. Fish. Aquat. Sci. 44(Suppl. 2): 104–128.

Dolman, W.B. 1990. Classification of Texas reservoirs in relation to limnology and fish community associations. Trans. Am. Fish. Soc. 119: 511–520.

Duarte, C.M. 1991. Variance and the description of nature, p. 301–318. *In* J.J. Cole, G.M. Lovett, and S.E.G. Findley [ed.] Comparative analyses of ecosystems: patterns, mechanisms and theories. Springer-Verlag, New York, N.Y.

Gauch, H.G. Jr. 1982. Multivariate analysis in community ecology. Cambridge University Press, Cambridge. 298 p.

Gower, J.C. 1966. Some distance properties of latent root and vector methods used in multivariate analysis. Biometrika 53: 325–338.

Harvey, H.H. 1975. Fish populations in a large group of acid-stressed lakes. Verh. Int. Ver. Limnol. 19: 2406–2417.

Harvey, H.H. 1978. Fish communities of the Manitoulin Island lakes. Verh. Int. Ver. Limnol. 19: 2031–2038.

Harvey, H.H. 1981. Fish communities of the lakes of the Bruce Peninsula. Verh. Int. Ver. Limnol. 21: 1222–1230.

HE, X., AND R.A. WRIGHT. 1992. An experimental study of piscivore–planktivore interactions: population and community responses to predation. Can. J. Fish. Aquat. Sci. 49: 1176–1183.

HINCH, S.G. 1991. Small- and large-scale studies in fisheries ecology: the need for cooperation among researchers. Fisheries 16: 22–27.

HINCH, S.G. 1992. Factors affecting abundances of common littoral fishes in central Ontario lakes. Ph.D. dissertation, University of Toronto, Toronto, Ont.

HINCH, S.G., AND N.C. COLLINS. 1993. Relationships of littoral fish abundance to water chemistry and macrophyte variables in central Ontario lakes. Can. J. Fish. Aquat. Sci. 50: 1870–1878.

HINCH, S.G., N.C. COLLINS, AND H.H. HARVEY. 1991. Relative abundance of littoral zone fishes: biotic interactions, abiotic factors, and postglacial colonization. Ecology 72: 1314–1324.

JACKSON, D.A., AND K.M. SOMERS. 1989. Are probability estimates from the permutation model of Mantel's test stable? Can. J. Zool. 67: 766–769.

KEAST, A. 1978. Feeding interrelations between age-groups of pumpkinseed (*Lepomis gibbosus*) and comparisons with bluegill (*L. macrochirus*). J. Fish. Res. Board Can. 35: 12–27.

LE CREN, E.D. 1987. Perch (*Perca fluviatilis*) and pike (*Esox lucius*) in Windermere from 1940 to 1985: studies in population dynamics. Can. J. Fish. Aquat. Sci. 44(Suppl. 2): 216–228.

LEGENDRE, P. 1993. Spatial autocorrelation: trouble or new paradigm? Ecology 74: 1659–1673.

LEGENDRE, P., AND M.J. FORTIN. 1989. Spatial pattern and ecological analysis. Vegetatio 80: 107–138.

LEGENDRE, P., AND M. TROUSSELLIER. 1988. Aquatic heterotrophic bacteria: modelling in the presence of spatial autocorrelation. Limnol. Oceanogr. 33: 1055–1067.

MANDRAK, N.E. 1990. The zoogeography of Ontario freshwater fishes. M.Sc. thesis, University of Toronto, Toronto, Ont. 193 p.

MANLY, B.F.J. 1990. Randomization and Monte Carlo methods in biology. Chapman-Hall, New York, N.Y. 281 p.

MANTEL, N. 1967. The detection of disease clustering and a generalized regression approach. Cancer Res. 27: 209–220.

MATUSZEK, J.E., AND G.L. BEGGS. 1988. Fish species richness in relation to lake area, pH, and other abiotic factors in Ontario lakes. Can. J. Fish. Aquat. Sci. 45: 1931–1941.

MITTELBACH, G.G. 1984. Predation and resource partitioning in two sunfishes (Centrarchidae). Ecology 65: 499–513.

ODEN, N.L., AND R.R. SOKAL. 1992. An investigation of three-matrix permutation tests. J. Classif. 9: 275–290.

ODLAND, J. 1988. Spatial autocorrelation. Sage Publications, London. 85 p.

ORLÓCI, L. 1978. Multivariate analysis in vegetation research. 2nd ed. Dr. W. Junk B.V. Publishers, The Hague, The Netherlands. 451 p.

PALOHEIMO, J.E., AND A.P. ZIMMERMAN. 1983. Factors influencing phosphorus–phytoplankton relationships. Can. J. Fish. Aquat. Sci. 40: 1804–1812.

RAHEL, F.J. 1984. Factors structuring fish assemblages along a bog lake successional gradient. Ecology 65: 1276–1289.

ROBINSON, C.L.K., AND W.M. TONN. 1989. Influences of environmental factors and piscivory in structuring fish assemblages of small Alberta lakes. Can. J. Fish. Aquat. Sci. 46: 81–89.

SAS INSTITUTE INC. 1982. SAS user's guide: statistics. SAS Institute Inc., Cary, N.C. 956 p.

SCOTT, W.B., AND E.J. CROSSMAN. 1973. Freshwater fishes of Canada. Bull. Fish. Res. Board Can. 184: 966 p.

SHUTER, B.J., J.A. MACLEAN, F.E.J. FRY, AND H.A. REGIER. 1980. Stochastic simulation of temperature effects on first-year survival of smallmouth bass. Trans. Am. Fish. Soc. 109: 1–34.

SMOUSE, P.E., J.C. LONG, AND R.R. SOKAL. 1986. Multiple regression and correlation extensions of the Mantel test of matrix correspondence. Syst. Zool. 35: 627–632.

SOMERS, K.M., AND H.H. HARVEY. 1984. Alteration of fish communities in lakes stressed by acid deposition and heavy metals near Wawa, Ontario. Can. J. Fish. Aquat. Sci. 41: 20–29.

TONN, W.M., AND J.J. MAGNUSON. 1982. Patterns in the species composition and richness of fish assemblages in northern Wisconsin lakes. Ecology 63: 1149–1166.

TONN, W.M., J.J. MAGNUSON, M. RASK, AND J. TOIVONEN. 1991. Intercontinental comparison of small-lake fish assemblages: the balance between local and regional processes. Am. Nat. 136: 345–375.

WERNER, E.E., AND D.J. HALL. 1988. Ontogenetic habitat shifts in bluegill: the foraging rate – predation risk trade-off. Ecology 69: 1352–1366.

ZIMMERMAN, A.P., K.M. NOBLE, M.A. GATES, AND J.E. PALOHEIMO. 1983. Physicochemical typologies of south-central Ontario lakes. Can. J. Fish. Aquat. Sci. 40: 1788–1803.

Calculation of Bayes Posterior Probability Distributions for Key Population Parameters

Carl Walters and Donald Ludwig

Fisheries Centre, University of British Columbia, Vancouver, BC V6T 1Z4, Canada

Walters, C., and D. Ludwig. 1994. Calculation of Bayes posterior probability distributions for key population parameters. Can. J. Fish. Aquat. Sci. 51: 713–722.

The Bayes posterior probability distribution is a powerful way to represent uncertainty in fisheries stock assessments, and can be calculated for key population and policy parameters of practically any population dynamics model. But the calculation is unwieldy when probabilities are to be assigned to a large grid of parameter combinations. The computational burden can be reduced substantially by analytically integrating over at least two "nuisance parameters" that occur in most assessment models: the observation error variance and the catchability coefficient. This simplification allows the analyst and manager to focus more easily on population parameters (stock size, slope of recruitment curve) that are of direct policy interest.

La distribution bayésienne de probabilité a posteriori constitue un outil puissant pour représenter les incertitudes dans les évaluations des stocks halieutiques, et peut être calculée pour des paramètres clés de la population et des politiques dans pratiquement n'importe quel modèle de la dynamique des populations. Toutefois, ce calcul est trop compliqué lorsqu'il faut attribuer des probabilités à une large grille de combinaisons de paramètres. Le fardeau du calcul peut être fortement réduit si on fait une intégration analytique d'au moins deux paramètres dérangeants qui sont présents dans la plupart des modèles d'évaluation : la variance de l'erreur d'observation et le coefficient de capturabilité. Cette simplification permet à l'analyste et au gestionnaire de s'intéresser plus directement aux paramètres sur les populations (taille du stock, pente de la courbe du recrutement) qui présentent un intérêt direct pour les politiques.

Received May 11, 1993
Accepted October 25, 1993
(JB921)

Reçu le 11 mai 1993
Accepté le 25 octobre 1993

Bayesian statistical procedures offer a way to provide information to fisheries managers about uncertainty in stock assessments. Assignments of probabilities to alternative parameter values and outcomes, rather than just best estimates and limits, is a fundamental part of recent approaches to risk assessment (Francis 1992; Restrepo et al. 1992; Hilborn et al. 1993) and adaptive management (Walters 1986; Sainsbury 1988; Hilborn and Walters 1992). By associating odds or probabilites with the many possible outcomes of each management decision option, analysts can provide decision-makers with more precise information for weighing choices about where to manage along the fundamental trade-off relationship between risk and opportunity associated with progressively more optimistic policy options. Probability calculations do not answer the social and economic question of where to operate along this trade-off, but do at least allow the choice to be made by objective and quantitative criteria.

The information is presented in the form of probability distributions for uncertain parameters such as maximum sustainable yield (MSY) and current stock size, rather than ranges or confidence limits on point estimates. Surprisingly, it often turns out to be no more difficult to calculate such probability distributions than to find single "best-fitting" point estimates and confidence limits. However, the calculation rapidly becomes intractable as the number of uncertain parameters is increased, since it must be done over a grid of parameter combinations and the number of such combinations increases geometrically with the number of parameters. This is particularly annoying when some of the parameters, such as measurement variances and catchability coefficients, represent only scaling effects in the data and are not of any direct policy interest (i.e., are "nuisance" parameters).

Here we offer suggestions for keeping the number of parameters small, and show that variance and catchability parameters can be eliminated entirely from the calculation by replacing the usual probability densities with a "marginal kernel" representing the integral of the densities over the nuisance parameters. Posterior probabilities calculated from this kernel for important population parameters represent the total probabilities for these parameters, accumulated over all possible values of the nuisance parameters. Consequently the distributions calculated from the population parameters provide a more accurate assessment of uncertainties than would be obtained by assuming particular values for the nuisance parameters.

The presentation proceeds in four steps. We first review the basic issue by presenting a general framework for Bayesian assessment of population dynamics parameters. Then we show how to simplify this framework by integrating over nuisance parameters. Next we provide simulation tests showing how the exact integration results compare with approximations that have been used in the past. Finally we provide warnings for practical users of the equations.

Overview: Bayesian Approach to Stock Assessment

Bayesian statistics begins with a fundamentally different definition and more intuitive notion of "probability" than most scientists are taught in introductory statistics courses (Box and Tiao 1973; Berger 1985; Lee 1989; Press 1989). Classical statistics uses a very restricted definition of probability based on the expected frequency of occurrence of events under random sampling of possible events from well-defined sample spaces; parameters are viewed as fixed but unknown features of such spaces. To a classical statistician, it is meaningless to speak about the "probability of a parameter value"; any particular value either is or is not the true one, and probability statements are restricted to how likely it is to see various patterns in the data or in certain statistics for a fixed parameter value. One outcome of such a restrictive definition is the cumbersome notion of a confidence limit, which is described with phrases such as "this limit represents the largest (or smallest) parameter value for which there is a 5% or higher chance of obtaining the observed parameter estimate."

Bayesian calculations begin instead with a broader definition of "probability" as a measure of credibility or degree of belief. Under this definition, it is perfectly acceptable to talk about the probability of a particular parameter value being the correct one, provided we are careful about how this probability is calculated in relation to the data. The correct procedure is provided by Bayes' Theorem about joint and conditional probabilities of events in sample spaces. Classical statisticians do not dispute this theorem, only the manner in which it is employed by Bayesians. When applied to parameters and data, the theorem can be stated in words as follows:

$$\begin{pmatrix}\text{Probability of a}\\ \text{parameter value}\\ \text{given the data}\end{pmatrix} = \frac{\begin{pmatrix}\text{Probability of the}\\ \text{data given the}\\ \text{parameter value}\end{pmatrix}\times\begin{pmatrix}\text{Prior probability of}\\ \text{the parameter value}\end{pmatrix}}{\text{Total probability of the data}}.$$

In applying this theorem, the data are regarded as fixed and the possible parameter values vary. When regarded as a function of the parameter values for fixed data, the "probability of the data given the parameter value" is called the likelihood function. The "total probability of the data" is the sum of the numerator over all parameter values. Division by the denominator can be viewed simply as a normalization to make the probabilities sum to unity; hence, this calculation can often be omitted or deferred until the last step of a series of calculations. The "probability of a parameter value given the data" is called the "Bayes posterior probability" for that value. Classical statisticians object to the specification of the "Prior probability of the parameter value", which represents a nonscientific (i.e., not based on the data) degree of credibility or judgemental weighting assigned to the parameter value. Obviously, one can generate misleading posterior probabilities by adjusting the prior probability to reflect personal beliefs and biases. Specification of the prior parameter distribution is a crucial aspect of the analysis, and it should never be done in a routine or merely conventional way. We address this issue in more detail below.

The importance of the distinction between Bayesian and classical definitions of probability is crucial when we try to answer fundamental management questions of the form "what are the odds that policy X is sustainable" for a range of possible policies (X's), given some precise definition of "sustainable". To answer such questions in the face of uncertainty about population parameters, we must examine a range of parameter values, since the total probability of sustainability is a cumulative probability summed (or integrated) over all possible parameter values. The contribution to the total probability of sustainability for any one parameter value in this sum is the probability that the value is the true one given the data, times the probability of sustainability if the parameter value is the true one. For complex models the sum may be estimated most efficiently by using Monte Carlo simulation methods (Restrepo et al. 1992). But under the classical definition of probability, we cannot even form such an obvious sum because the "probability that the value is the true one given the data" does not exist! One notion for supposedly avoiding this difficulty is the "confidence distribution" used, for example, by Francis (1992), generated by calculating the probability of obtaining the observed parameter estimates for a small neighborhood around each possible parameter value; but examination of how such distributions are calculated and renormalized reveals that they are just Bayes posterior distributions computed by a numerically cumbersome route involving sampling distributions of parameter estimates rather than direct inference from the data.

Sometimes it is appropriate to initially weight all parameter values equally, i.e., choose a uniform prior. When using a uniform prior, the Bayes posterior probability calculation reduces to the remarkably simple formula

$$\begin{pmatrix}\text{Probability of}\\ \text{a parameter value}\\ \text{given the data}\end{pmatrix} = \frac{\begin{pmatrix}\text{Likelihood of the}\\ \text{parameter value}\\ \text{given the data}\end{pmatrix}}{\begin{pmatrix}\text{Sum of likelihoods over}\\ \text{all parameter values admitted}\end{pmatrix}}.$$

Compare this approach with maximum likelihood parameter estimation: in point estimation, one must be able to calculate the probability of observing the data given any parameter value, and one must then devise a formula or search algorithm for finding the parameter value that gives the highest likelihood (that value is called the "maximum likelihood estimate" of the parameter). For most fisheries assessments, the search is done by means of a nonlinear estimation algorithm which calculates the likelihood at many different parameter values along the way.

A very important point about the Bayesian assessment of posterior probabilities is that we go directly from the data to the posterior probability using the above formula, systematically assigning probabilities to a wide range of parameter values, without ever worrying about calculating point estimates along the way (except for some nuisance parameters as discussed below). In other words, we never worry about the sampling distribution of point estimators, which the classical statistician requires in order to provide confidence limits, nor do we pretend that one can define or compute point estimates with particular properties such as being unbiased or asymptotically efficient or minimum variance or minimum risk or whatever. The posterior probability distribution is used directly to obtain estimates of the probabilities of various outcomes of interest to managers, such as stock collapse or capacity to sustain higher catches.

Notice also that the posterior probability does not depend on any constant multiplier terms that may appear in the prior or the likelihood function, and that are independent of the data and parameter values over which the sum (or integral) is taken. Below we will refer to a likelihood multiplied by the prior and stripped of such constants as the "posterior kernel". Usually this kernel is a quite simple equation involving familiar measures of goodness of fit, such as sums of squared deviations between observations and predictions.

Setting up a Bayesian estimation scheme involves three steps: (1) choice of a prior probability distribution for the parameters, (2) formulation of a likelihood function for the data used in the assessment, and (3) choice of a grid of parameter values over which the product of likelihood and prior is calculated. The following subsections discuss the first two of these steps. It is generally a simple programming or spreadsheet exercise to apply the formulae (calculate likelihood times prior) resulting from steps (1) and (2) for each parameter combination on a grid, and it is then trivial to rescale each likelihood times prior by the sum of all likelihoods times priors over the grid in order to provide the posterior probability for the parameter value at that grid point.

Selection of Prior Distribution

There has been much discussion about the best choice of prior probability distributions for Bayesian calculations. The discussion has centered on two quite distinct questions: (1) the best functional form to assume and (2) whether or not to use an "informative" prior based on expert judgement and past experience. The functional form question is mainly concerned with finding so-called "natural conjugate priors" that are analytically or computationally convenient to use; this question is not of much interest in the present context because most fisheries models make predictions that are highly nonlinear functions of the model parameters and hence always require a computationally intensive approach. Thus the main issue is whether to use an informative prior. Here we offer a few options and suggestions about potential pitfalls.

The simplest computational option is to assume a uniform prior over some specified, "reasonable" range of parameter values. This approach focusses debate on the relatively simple matter of deciding on reasonable limits, and amounts to assuming an uninformative prior provided the limits are wide enough to include most of the tails of the likelihood function. Even this simple approach involves at least two subtleties. First, if one chooses the prior to be zero outside a particular interval, say $q_1 \leq q \leq q_2$, then in effect one refuses to consider the possibility that q might lie outside this interval. If this interval is inappropriately chosen, the posterior distribution may be cut off at a point where it is substantially different from zero. The resulting inferences will be suspect in such a case. This possibility can be avoided by not making any cutoff, i.e., choosing an infinite interval on which the prior is constant. The posterior may then be restricted to an interval where the likelihood is sensibly different from zero. Second, choice of a uniform prior has different consequences, depending on the scaling or choice of variable. For instance, a catchability coefficient q cannot be negative. Therefore, a uniform prior would be nonzero on the interval $0 \leq q < \infty$ or a subset thereof. As we shall see later, sometimes $\log q$ is a more convenient variable to use than q itself. If the density of the random variable W is uniform, then

$$\Pr[w \leq W \leq w + dw] = dw.$$

But if $W = \log Q$ and $w = \log q$, then $dw = dq/q$. Hence

$$\Pr[q \leq Q \leq q + dq] = dw = dq/q.$$

Thus, if $w = \log q$ is uniform, then the density of q is dq/q. Similarly, if the density of q is uniform, the density of w is $e^w dw$. There are arguments in favor of either choice. Which is correct? We are unable to resolve this issue: a prudent procedure is to try both priors and determine whether there are substantial differences in the final inferences. If there are, this is an indication that the data are not very informative about the parameter in question. This fact should be reported as part of the analysis, so that decision-makers are not misled about the degree of risk that may be associated with one action versus another. In spite of these difficulties, we believe that an uninformative prior should be the default choice, since it eliminates the possibility that the analysis will be colored or distorted by the subjective beliefs that stock assessment scientists might carry.

A second option is to use an informative prior based on empirical distributions of parameter values reported for similar stocks. For some per-capita rate parameters that represent basic life history characteristics (such as natural mortality rate (M) and growth parameters), such distributions can be constructed from syntheses of parameter estimates in the literature, and it makes good sense to use such experience in the analysis. However, for parameters that represent abundance scaling and habitat size (carrying capacity K of logistic, unfished or natural biomass B_0), such empirical distributions are likely to be very broad and are potentially misleading (e.g., if literature values have been reported mainly for large, valuable stocks and you happen to be working on a small one).

The third option is to use an informative prior based not on empirical experience with other stocks but rather on arguments from basic biology (fecundity, longevity, maximum possible density, etc.) combined with scientific "intuition". We feel strongly that such subjective priors should be avoided whenever possible, for two reasons: (1) the track record of biologists at making intuitive predictions about ecological parameters has not been good, and we regularly are overconfident about what we "know"; and (2) it is very easy for past data and analyses of the same stock to creep into the thinking and judgement of scientists, especially about parameters that have been much debated in the past and about which some scientific concensus has been reached. Including past results of analysis in the prior causes a very dangerous type of circular reasoning or double accounting with the data.

Whatever option is chosen, care must be taken about hidden assumptions that can enter the analysis though choices of scaling for the parameters. Particularly for parameters such as the catchability coefficient that can physically take only positive values, it may be tempting to assume a uniform or flat prior distribution for the logarithm of the parameter. But this choice results in assignment of higher probabilities to larger stock sizes; below we provide an example of how large an effect such a choice can have on the assessment.

Calculation of the Likelihood Function

For most fisheries assessments, we deal with heterogeneous collection of independent observations $Y_1, \ldots, Y_n$ of quantities such as catch per unit effort (CPUE), mean fish sizes, survey biomass estimates, etc. The simplest assumption is that each observation Y_i is a random variable sampled from a normal distribution with mean U_i and variance V_i, where U_i is some function of unknown population parameters. In this case, the likelihood part of the kernel needed for the posterior distribution calculation if the V_i are assumed known is just

$$(1) \qquad L = \exp\left(-\sum \frac{(Y_i - U_i)^2}{2V_i}\right).$$

The other factors in the normal probability density cancel out when calculating the posterior probability, since the posterior is the product of L times prior for a particular parameter value divided by the sum of such products over all such values. Thus the likelihood calculation is very simple under the assumption of normal (or log-normal) measurement errors, provided there is a clear specification of how to calculate the means U_i from population parameters of interest. Here is where stock assessment population models enter the analysis. Population models are used to predict the U_i in two steps: (1) set population model parameters at particular values (i.e., a grid point) for which a likelihood is to be calculated and (2) simulate the model over time for the period for which there are data, calculating predicted values for the U_i along the way. For example, suppose Y_i is the CPUE in year 8, and one is willing (foolishly!) to assume that $Y_i = qB_8$ where q is a catchability parameter and B_8 is the stock biomass in year 8. To predict B_8, one needs (1) population model parameters for initial stock size and growth/mortality/recruitment and (2) historical removals (catches) for years 1–7. For a particular combination of values of these parameters and a particular value of q, U_i is then simply q times the model prediction of B_8.

In the presentation below, we will assume unless stated otherwise that $Y_i = qB_i$ where i is an observation counter, B_i is any predicted state variable (biomass, number, mean size, etc.), and q is an unknown scaling or proportionality parameter. Under this assumption, each element of the sum of squares is of the form $(Y_i - qB_i)^2/V_i$.

It may not be obvious just how general is this framework for calculating likelihoods. One may use literally any model that is complex enough to predict the means of the observations. When only relative abundance data (e.g., CPUE) are available, the intuitive choice would be to use simple surplus production or delay-difference models. But we can as well do the predictions with a complex age-structured model, calculating overall biomass or catch rate predictions as the simulation proceeds (e.g., Francis 1992). In fact, the model need not even do its predictions forward in time. In virtual population (VPA) or cohort analysis models and in stock reduction analysis, we specify a terminal or current stock size (usually by specifying a terminal fishing rate parameter) and then work backwards in time to reconstruct historical stock sizes by adding natural mortalities and age-specific catches back into the simulated population.

Adaptive or tuning procedures in VPA (such as ADAPT; Gavaris 1988) refer to estimation procedures where the population model is simulated backward in time, with different current (starting) stock sizes (or equivalently, terminal fishing rates), attempting to find that parameter value (current stock size) for which the backward simulation provides a best fit to some relative abundance time series. Often the tuning procedure is used to simultaneously estimate some "nuisance parameters" (partial recruitment factors or relative vulnerabilities at age) as well. Viewed in this way, the key difference between use of VPA and fitting forward simulations to relative abundance data is in the use of catch-at-age data to avoid making assumptions about the stock–recruitment relationship (some assumption is unavoidable in forward simulations whereas individual recruitments are estimated directly with VPA). However, note that in either case, a crucial assumption is that the relative abundance index is proportional to stock size. When nuisance parameters and other input data to VPA are uncertain, assessment of posterior distributions for key policy parameters might be done more efficiently using Monte Carlo procedures as described in Restrepo et al. (1992) than using the grid-based procedures discussed below. Still, care must be taken in the use of such simulation procedures; Restrepo et al. actually did not compute the posterior distribution, but instead proposed to approximate it by the sampling distribution of parameter estimates evaluated at the best-fitting parameter values (they treated the best-fitting parameter values as correct when they used these to set the expected values of sampling distributions for VPA input values). This approximation is only asymptotically valid for much longer time series than are usually available for VPA tuning; it is avoided in the confidence distribution method of Francis (1992) by computing the sampling distributions for a range of parameter values.

For forward simulations in time, in our experience it is usually worthwhile to go beyond a simple surplus production model to at least the Deriso/Schnute delay-difference biomass/numbers dynamic model (Deriso 1980; Schnute 1985), unless the data are very uninformative (Ludwig and Walters 1985). This model allows the representation of important delay effects in recruitment (especially critical in modelling population changes early in fishery development for long-lived species). It also makes predictions about changes in mean body sizes, and these changes are an important signal for detecting changes in mortality rate due to fishing (and hence estimating total population size) even if age composition data are not available or are suspect for various reasions (Hilborn and Walters 1992).

An important point is that it is impossible to say a priori what the best model structure will be. One can obviously obtain misleading results from models that are too simple, but detailed and realistic models can also fail badly (in estimation of the best fishing policy) if they require estimation of too many parameters. Luckily, it is easy to test a variety of models once one has a computational framework for the parameter grid and likelihood calculation. Thus the best strategy is just to test a sequence of increasingly realistic models, and see what each has to say about the data. It is also possible to combine both simple and complex models, as suggested by Fournier and Warburton (1989).

Choosing Parameters to Represent in the Posterior Distribution

Once we step beyond surplus production models, it is necessary to deal with the proliferation of parameters associated with population age structure (recruitment parameters, natural mortality rate, growth curves, mesh selection). The following three conventions are gaining wide use (R. Hilborn and A. Punt, University of Washington, Seattle, Wash., personal communication), and appear to be working very well.

First, it is usually necessary to treat the natural mortality rate M and growth curve parameters as known in advance, as in assessment methods like VPA. Some information about these parameters is contained in time series data on age composition and body size distribution moments of the catch, but this information is generally very weak unless the stock has been subject to strongly contrasting harvest regimes over time.

Second, it appears best to always include the initial, unfished biomass B_0 as a key parameter (or the current biomass for VPA models). There are at least three reasons for this: (1) B_0 is needed to start each simulation leading to a likelihood value, (2) B_0 is often a good, simple predictor of MSY (0.5 MB_0 type calculation), and (3) for forward simulations over time, B_0 automatically defines one recruitment parameter (the average recruitment rate at the unfished biomass level, equal to MN_0 where $N_0 = B_0/\bar{w}$ and $\bar{w}$ is average fish size in the absence of fishing). In surplus production models, B_0 is the carrying capacity (K) parameter anyway.

Third, consider including one parameter for the stock–recruitment curve slope in the Bayesian parameter grid; this slope basically measures how low the stock size can be driven before recruitment overfishing becomes evident, and hence is a key parameter in policy evaluation. For long-lived species, there will be no information about this slope parameter in the data until the fishery has been operating for at least as long as the age at recruitment. In surplus production models, the recruitment slope corresponds to the parameter for intrinsic rate of population increase (r) at low stock sizes. Notice that steps (2) and (3) result in two stock–recruitment parameters. One can then represent patterns of variation in recruitment rate between the extremes represented by the recruitment rate at unfished equilibrium and the slope at very low stock size by any functional form that seems appropriate, e.g., Beverton–Holt or Ricker.

Notice that these three steps result in a Bayesian estimation scheme that actually deals with three parameters corresponding to the K, r, and q of classical surplus production models. One difference from classical estimation methods is that it is possible to treat q as a nuisance parameter to be estimated as a conditional maximum likelihood value for each combination of K and r (B_0 and recruitment curve slope) included in the Bayes posterior distribution, or eliminate it entirely as shown in the next section.

For age-structured models, it is usually necessary to consider including further parameters such as those needed to characterize a mesh selection ogive. One may also want to look at recruitment models with more than two parameters. However, before proceeding to throw more parameters into the analysis, consider carefully the following points about parameter grids. Suppose one wants to generate a Bayes posterior distribution for p parameters. In our experience, it is necessary to represent each parameter at 40 or more discrete levels between some minimum and maximum values beyond which the posterior probabilities are vanishingly small. To get the posterior distribution, this means that it is necessary to do the likelihood calculation (run model and compute L) at 40^p combinations of parameter levels. If $p = 2$, this is not difficult with personal computers; 40^2 is just 1600 simulations, which for typical population models and 30 yr of data, an 80486-based computer can run through in about 10 s. But with a third parameter, the grid requires $1600 \times 40 = 64\,000$ simulations, which will require approximately 5–10 min. With a fourth parameter, expect to wait several hours for an answer, and it might be very difficult to visualize (or explain to a manager) a four-dimensional probability distribution. An option of course is to perform the large calculation and then add up the posterior probabilities over two or three of the parameters to provide a marginal distribution for one or two others that are of particular management interest, but in our experience this is usually not worth the trouble. Following the prescription of this section, including only B_0 and recruitment curve slope in the parameter set will generally cover about 90% of the management concerns and key uncertainties about long-term production potential.

One difficult problem is that the high probability parameter combinations often lie very close to a curved line of B_0 and r combinations (in classical terms, the joint confidence region for B_0 and r is a long, very narrow ellipse or banana-shaped region), especially if the variances V_i for the observations are relatively low or there are many years of data. What can happen in this case is that only a few scattered (or even no) grid combinations of B_0 and r happen to hit along the high probability ridge, so the calculated probability surface will look like a few peaks scattered along the line. None of these calculated peaks may even be close to the most probable parameter combination. To check for this problem, a simple trick is to artificially inflate the variances V_i to spread out the probability distribution so that the region of high probability combinations is more visible. To further ward against the problem, options are to (1) increase the number of grid points, (2) vary the parameter ranges over the grid, to "window in" on parts of the surface, and/or (3) set up a simple line search (one-dimensional nonlinear estimation) along one of the parameter dimensions. That is, for each B_0 on the grid, search for the most probable r value and plot the resulting line of high probability B_0–r combinations. This may actually take less computer time than calculating the probabilities of all r levels for each B_0.

Estimating Probability Distributions for Policy Parameters

The grid of posterior probabilities for population parameters can be used to estimate posterior probabilities for policy parameters that are derived from the population parameters. The basic procedure is to set up a grid of discrete, narrow ranges for each policy parameter and then find the total probability that the parameter lies within each of these ranges.

Suppose for example that a distribution is wanted for MSY = $rB_0/4$ predicted from a simple logistic surplus production model. To obtain this distribution, set up a series of MSY "bins", each representing a narrow range of MSY values, and set up an array to store the probability for each bin. Initially set these probability array values to zero. Then for each point in the (B_0,r) grid, calculate MSY and determine which MSY bin this falls in, and add the posterior probability assigned to (B_0,r) to the total probability for the bin. After doing this for all (B_0,r), each MSY bin should contain the total probability that MSY lies in the range represented by the bin.

One very interesting result of such calculations is that policy parameters are often much less uncertain than the original population parameters. This happens when a wide range of combinations of population parameters result in the same value of the policy parameter. In the above example, MSY = $rB_0/4$, the range is easy to see: all r–B_0 combinations such that rB_0 is the same will predict the same value of MSY. Intuitively, this just says that the same MSY can be produced either by a small, productive stock or a large, unproductive one. Early assessment methods such as Gulland's (1961) plot of catch or CPUE versus effort relied heavily on this invariance property to avoid having to estimate population parameters.

Posterior Kernels Integrated over Parameters

We show now how the product of the prior and the likelihood kernel (1) introduced above can be replaced by an alternative expression that does not depend on the nuisance parameters V and q, representing the integral or marginal probability over these parameters. We note first that the likelihood part of the kernel can be written as a product of the form

$$(2) \qquad L = L_1 L_2 \ldots L_m$$

where each of the m factors represents a collection of observations with homogeneous variance and constant scale parameter q. The prior density will be assumed to be independent of the parameter q. This assumption can be generalized to the case where the prior is proportional to power of q. Our notation will not display other parameters that may appear in the posterior. If the kth such data type has n observations, with variance V and scale parameter q and if V is assumed to be known, then

$$(3) \qquad L_k = \exp(-\mathrm{SS}_k/2)$$

where

$$(4) \qquad \mathrm{SS}_k = \frac{1}{V}[(Y_1 - qB_1)^2 + (Y_2 - qB_2)^2 + \ldots + (Y_n - qB_n)^2].$$

Here, B_i is the model prediction of the unobserved state variable (biomass, mean body size, number-at-age, etc.) to which observation Y_i is assumed to be proportional (via the constant q). In order to reduce notational clutter, we shall consider only a single term L_k and drop the subscript k. We can conveniently write SS in terms of computational sums of squares as

$$(5) \qquad \mathrm{SS} = \frac{1}{V}\left(\sum Y_i^2 - 2q\sum Y_i B_i + q^2 \sum B_i^2\right).$$

Minimization of SS with respect to q for a fixed set of population parameters leading to the predicted B_i leads to the conditional maximum likelihood estimator q^*:

$$(6) \qquad q^* = \frac{\sum Y_i B_i}{\sum B_i^2}$$

and substituting (6) into (5) leads to the familiar decomposition

$$(7) \qquad \mathrm{SS} = \frac{1}{V}[(n-1)s^2 + I(q - q^*)^2]$$

where

$$(8) \qquad s^2 = \frac{\sum (Y_i - q^* B_i)^2}{n-1} \qquad \text{and} \qquad I = \sum B_i^2.$$

The quantity $(n - 1)s^2$ is the sum of squared residuals and I is proportional to the information. The residual sum of squares is a function of the data and remaining parameters only, and hence contains no information about the dependence of the posterior on q. However, the magnitude of I determines the variance of the distribution of q.

One approximate Bayesian procedure is to replace q by q^* in (6), with the posterior kernel L^* replacing L:

$$(9) \qquad L^* = \exp\left(\frac{-(n-1)s^2}{2V}\right).$$

This procedure ignores uncertainty about q entirely, and therefore it is risky when n is small (<20).

Such simplifications are not necessary if we assume a uniform prior probability distribution for q (all values equally likely a priori). In that case, the Appendix shows that the marginal density L^q (L integrated over q) is given by

$$(10) \qquad L^q = \sqrt{\frac{V}{I}}L^*.$$

Here we use the superscript q to indicate the integration of L over q. Equation (10) can be used to eliminate the parameter q from Bayesian calculations where V is assumed known in advance, simply by substituting it for the corresponding L_k term in (2).

Elimination of the variance V from the calculation is more troublesome (e.g., see Hoenig et al. 1994). Jeffreys (1961) sugggested using prior probabilities for V proportional to $1/V$. The corresponding posterior is obtained by multiplying L^q by $1/V$ and restoring terms involving V that are not needed when L^q alone is used for numerical calculation, to form a likelihood × prior kernel. The resulting density must be integrated over V to obtain the marginal density:

$$(11) \qquad L^{qV} = \int_0^\infty \frac{L^q}{V^{(n-1)/2}}dV.$$

The superscript qV denotes integration over q and V. It is shown in the Appendix that the result of this integration is simply

$$(12) \qquad L^{qV} = (s^2)^{-m}$$

where $m = (n - 1)/2$. Note that this kernel is very similar to (9), but with the exponential function of s^2 replaced by a power function. Writing the power function as $\exp[-m \log(s^2)]$ hints that (9) and (12) will give similar shapes of posterior distributions for the population parameters that determine s^2, as sample size n increases. We show by example in the next section that this is indeed the case.

Posterior kernels similar to (10) and (12) can also be substituted for posterior components L_k that contain direct sums of squares differences between data and model predictions, without unknown scaling factors q. For these cases, simply drop the $1/\sqrt{\sum B^2}$ term from the kernel in (10) (i.e., integrate L_k times a $1/\sqrt{V}$ prior kernel, over V only; the sum of squared differences between observed and predicted values then replaces s^2).

It is often best to assume that the measurement errors are multiplicative, and that Y has a log-normal distribution (e.g., $Y = qBe^v$, where v is normal with mean 0). In this case, if we replace Y_i with $Z_i = \log(Y_i/B_i)$ and q with $q' = \log q$, then

$$(13) \qquad L_k = \frac{1}{V^{n/2}}\exp\left(-\frac{1}{2V}\sum (Z_i - q')^2\right).$$

In analogy with the preceding treatment, we can rewrite (13) for convenience in integrating over q' as

$$(14)\quad L_k = V^{-n/2}\exp\left(-\frac{1}{2V}[(n-1)s'^2 + n(q'-\hat{q}')^2]\right).$$

Here

$$(15)\quad \hat{q}' = \frac{\sum Z_i}{n}$$

and

$$(16)\quad s'^2 = \frac{\sum(Z_i - \hat{q}')^2}{n-1}.$$

Now if we assume a uniform prior for q', integration over q' results in the posterior kernel

$$(17)\quad L^{q'} = V^{-n/2}\exp\left(\frac{-(n-1)s'^2}{2V}\right)$$

within a nonessential factor. Integrating over V then results in the kernel

$$(18)\quad L^{q'V} = (s'^2)^{-m}$$

where $m = (n - 1)/2$ as before. Note that this is essentially the same kernel as (12), but with a simple change in the way the prediction errors are calculated.

It is also possible in principle to use equations similar to (9)–(18) to deal with a more general power model for the observations:

$$(19)\quad Y = q_1 B^{q_2}$$

where q_1 is a scaling parameter and the power parameter q_2 can represent both saturating ($q_2 < 1$) or accelerating ($q_2 > 1$) observation processes. This model has been suggested for example as a way to deal with saturating relationships between CPUE and stock size (Cooke and Beddington 1985).

The preceding logarithmic transformations work in this case as well: the nuisance parameters q_1, q_2, and V may be integrated out to yield a marginal kernel

$$(20)\quad L^{q_1q_2V} = (s''^2)^{-m}$$

where

$$(21)\quad s''^2 = \frac{1}{n-2}\sum_i [Z_i - (\hat{\theta}_1 + \hat{\theta}_2 W_i)]^2$$

$$(22)\quad \hat{\theta}_1 = \frac{1}{n}\sum Z_i$$

$$(23)\quad \hat{\theta}_2 = \frac{\sum Z_i W_i}{\sum W_i^2}$$

$$(24)\quad W_i = \log B_i - \frac{1}{n}\sum \log B_i$$

and $m = (n - 2)/2$. This change in m reflects the reduction in the number of degrees of freedom when two parameters are estimated. Details are given in the Appendix.

The numerical effect of using (20) can be devastating; if q_1 and q_2 truly can assume any value, then any simple time series trend in Y can be explained equally well by (i.e., you end up assigning the same posterior probability to) any population parameter values that also have a simple trend (including in the opposite direction of Y, $q_2 < 0$ case). One simple option when faced with the possibility that q_2 is less than 1.0, but almost certainly lies in some range (e.g., 0.2–1.0 for CPUE data), is to use (17) or (18) instead of (20) after replacing log B terms with q_2 log B and then integrate the resulting posterior kernel numerically over the range of q_2 values (with perhaps higher prior probabilities for some values within the range). When the Y's are relative abundances, the effect of this numerical integration will usually be to assign higher posterior probabilities to lower stock sizes (B_0).

It is not always wise to integrate over V as in (12), (18), or (20). Consider again the overall posterior function as represented in (1) for cases where more than one type of data are being used ($m > 1$, several L_k components). Retaining the variances as in (10), (17) allows tests of alternative schemes for "weighting" the data by changing V_k (high V_k means less weight on the kth type of data). Such tests are important in situations where there is fundamental uncertainty about whether or not to trust (place any weight at all upon) particular types of data such as CPUE's, especially if the $Y = qB$ assumption may have been violated by virtue of the manner in which the data were collected.

Effect of Integration on the Form of Posterior Distributions

Figure 1 shows a typical example of the differences in posterior distributions resulting from using (9)–(18). Here we generated a time series of fake relative abundance data $Y_t = qB_t$ + normal error from a logistic population model (B_t = biomass predictions only, $B_{t+1} = B_t + rB_t(1 - B_t/B_0) - C_t$, where $r = 0.2$ and $B_0 = 1.0$). The population was subject to increasing exploitation rate over time so as to generate a catch series C_t that increased at first and then declined. Then using the same dynamic model and assuming that the correct value of r known, we generated B_t time series predictions for a range of B_0 values (from 0.1 to 2.0) along with the various sums of squares defined in the previous section. For each B_0, we calculated the posterior kernels L^*, L^q, and L^{qV}. Such calculations are easy to perform using the "Table" function in a Microsoft Excel spreadsheet[1] or analogous functions in other spreadsheets. Then the posterior probability shown for each B_0 in Fig. 1 was calculated as the corresponding L value divided by the sum of L's for all B_0 values.

Two patterns are immediately obvious, and we have found essentially the same patterns for more complex models and data series. First, for high n (many years data), the three methods converge to give the same results, as shown in Fig. 1. This is a consequence of asymptotic normality of the posterior distribution. Second, for very low n, integration over q or over q and V gives similar results: higher probabilities are assigned to lower B_0 values; in contrast, using L_k^* results in a uniform posterior for B_0 when there are few observations. Recall that use of L_k^* neglects uncertainty about the value of V. Assigning higher probabilities to lower B_0 values may seem surprising considering the assumption of a uniform prior for B_0. But when there are few data points, what those data points do provide is some constraint on B_0, of the form $\bar{Y} = qB_0$, where $\bar{Y}$ is the mean of the first few observations. Thus the posterior will be concentrated around the curve given by $\bar{Y} = qB_0$. Think of the q,B_0 plane as

---

[1] The authors would be pleased to provide diskettes with sample spreadsheets to anyone who needs further assistance.

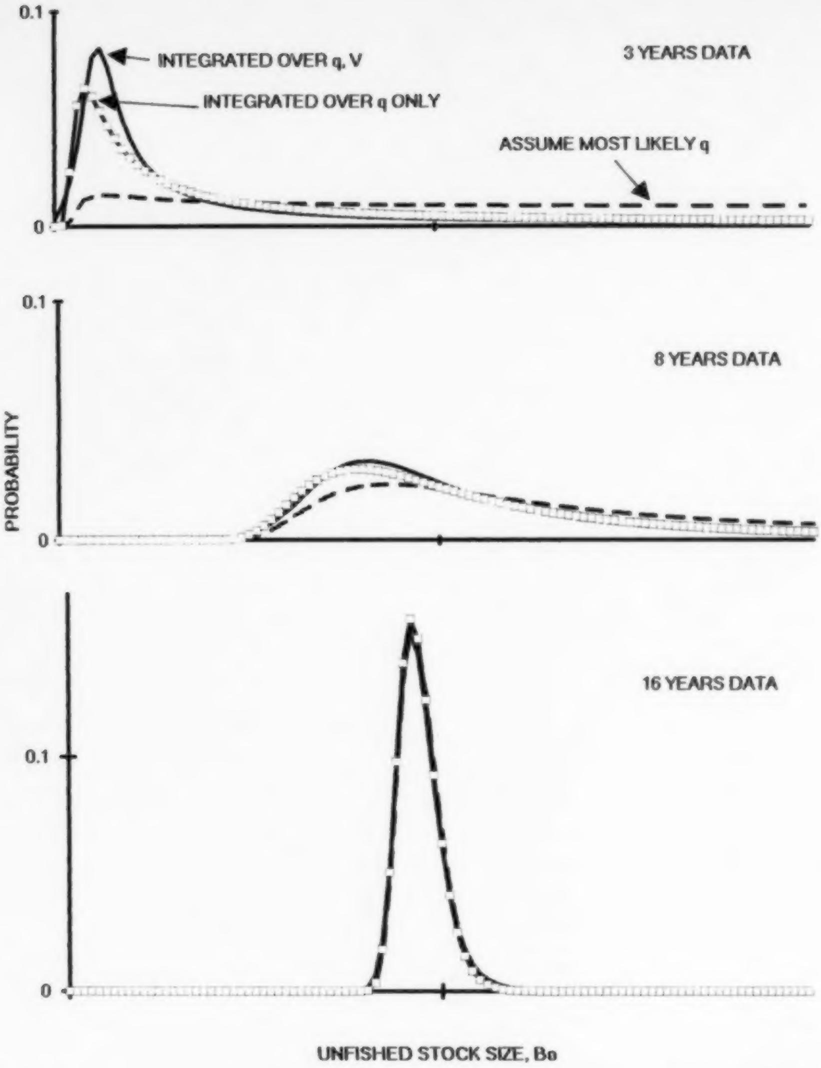

FIG. 1. Bayes posterior probability distributions for the unfished stock size parameter B_0 in a surplus production model, calculated with increasing numbers of years of data. The L^* (equation 9) calculation method ignores uncertainty in catchability q, representing each B_0 probability only for the most probable q given that B_0. The L^q and L^{qV} methods provide integral probabilities over q and the observation variance V, using the analytical expressions in equations (10) and (12).

being divided into small squares, each with an equal prior probability mass. If we integrate the posterior over q in order to obtain a marginal distribution for B_0, the total mass will be concentrated along small values of B_0, since the most of the mass of the curve lies above the small values. In other words, assigning high probabilities to low B_0 values is not a "flaw" in the analysis; rather, it is a consequence of the way the first few observations constrain the posterior distribution. Fisheries scientists who feel compelled to provide conservative assessments should actually take comfort in this result; anyone who looks at the mode of the posterior distribution (as a point estimator of B_0) will see an estimator that is biased downward, which from a conservative viewpoint is better than overestimating the stock size.

Assigning higher probabilities to low stock sizes when there are only a few relative abundance observations can be avoided either by assuming log-normality of measurement errors as in (13)–(18) or by using a prior where the logarithm of q is assumed to be uniformly distributed. In such cases the results are generally similar to the predictions of (9) in Fig. 1. The main case for using a nonconstant prior is a weakness in the argument that there are many more ways to obtain a few relative abundance values from high q, low B_0 situations than low q, high B_0 ones. In fact, we often know a priori that q cannot be high due to the way it was measured, for example as a very small swept area chosen at random from a large area over which fish are known to be distributed.

The distributions in Fig. 1 are distinctly skewed for low n, indicating that the data allow us to confidently exclude a range of parameter "hypotheses" on one side of the most likely parameter value (distribution mode), but not on the other. In the example, we can exclude very low stock size hypotheses (could not have sustained high relative abundances given the observed catch), but not the possibility that stock size is large. This asymmetry has obvious consequences for debates about how much risk to take by allowing further increase in catches during fishery development. Such consequences emphasize the importance of not using normal approximations (based on the maximum likelihood parameter estimate and its approximate covariance matrix from nonlinear estimation) to the posterior distribution, when n is small and/or the data are uninformative.

Warnings

Bayesian methods have great potential to help improve fisheries decision-making in the face of uncertainty, if for no other reason than by bringing an end to the misunderstandings and debates triggered in management settings by point estimates and confidence limits. But they can be just as misleading as classical statistical methods, and in this section we provide warnings about three mistakes that are likely to arise in practice.

The first is a relatively simple technical warning about (9)–(20). These equations apply only to elimination of measurement parameters that appear directly in the likelihood function for the data. They will not work to integrate out the effects of nuisance parameters that appear in the dynamic model that is used to make biomass predictions, such as partial recruitment (mesh selection) factors and "process error" deviations from assumed stock–recruitment relationships. At present, calculation of marginal distributions with respect to such parameters is still a matter for massive computational effort (R. Hilborn and A. Punt, University of Washington, Seattle, Wash., personal communication) although there are promising indications of radically more efficient computational methods (J. Schnute, Pacific Biological Station, Nanaimo, B.C., personal communication; Kinas 1993).

Second, and much more important, we flatly recommend that catch/effort data never be used as a direct abundance index (assumed proportional to stock size). When catch and effort data have been gathered on a fine enough spatial scale, it should be possible to develop spatially weighted catch rate indices that are indeed reflective of population changes. But in our experience, this is not the way most CPUE series are developed, and almost all can be expected to contain misleading trends due to temporal changes in gear efficiency and increasing catchability as stock size declines ($q_2 < 1$ in (19)). Bayesian probability calculations are just as vulnerable as classical assessment estimators to the biases that such changes cause (usually overestimation of stock size and production), whether you are fitting a simple production model or tuning a massive VPA. When survey and/or good spatial catch rate data are not available, we recommend instead reliance on other indices of the intensity of exploitation, such as changes in mean body size and direct measures of total mortality rate (Csirke and Caddy 1983).

Third, we caution not to use point estimators based only on the modes of posterior distributions when setting harvest policies. Fishery development where Y remains high for a longer time (slow decrease in relative abundance) slows the convergence of the three calculations shown in Fig. 1 and causes the mode of the posterior distribution from (10)–(12) to be well below the actual B_0 for a longer period. Thus, if the modal value is used as a best estimate for setting allowable catches, then the resulting low catches will further contribute to slowing development and preventing discovery of how large B_0 actually is. This potential loss of fishery value is not a result of using Bayesian assessment procedures in general, but rather of using a point estimator rather than the full probability distribution in deciding on allowable catches and acceptable levels of risk. Thus, we caution against the use of Bayesian procedures just to provide pretty pictures of uncertainty as "high-tech" substitutes for traditional confidence limits.

Acknowledgements

We thank Ray Hilborn, Jon Schnute, and Hal Geiger for advice and direction in developing the analysis. Financial support was provided by the Natural Sciences and Engineering Research Council of Canada under grants A9239 and A5869.

References

Abramowitsch, M., and I.A. Stegun. 1964. Handbook of mathematical functions. National Bureau of Standards, Washington, D.C.

Berger, J.O. 1985. Statistical decision theory and Bayesian analysis. Springer-Verlag, New York, N.Y.

Box, G.E.P., and G.C. Tiao. 1973. Bayesian inference in statistical analysis. Addison-Wesley, Reading, Mass.

Cooke, J.G., and J.R. Beddington. 1985. The relationship between catch rates and abundance in fishes. IMA J. Math. Appl. Med. Biol. 2: 1–15.

Csirke, J., and J.F. Caddy. 1983. Production modeling using mortality estimates. Can. J. Fish. Aquat. Sci. 40: 43–51.

Deriso, R.B. 1980. Harvesting strategies and parameter estimation for an age-structured model. Can. J. Fish. Aquat. Sci. 37: 268–282.

Fournier, D.A., and A. Warburton. 1989. Evaluating fisheries management models by simulated adaptive control — introducing the composite model. Can. J. Fish. Aquat. Sci. 46: 1002–1012.

Francis, R.I.C.C. 1992. Use of risk analysis to assess fishery management strategies: a case study using orange roughy (*Hoplostethus altanticus*) on the Chatham Rise, New Zealand. Can. J. Fish. Aquat. Sci. 49: 922–930.

Gavaris, S. 1988. An adaptive framework for estimation of population size. CAFSAC (Can. Atl. Fish. Sci. Adv. Comm.) Res. Doc. 88/29.

Gulland, J.A. 1961. Fishing and the stocks of fish at Iceland. U.K. Minist. Agric. Fish. Food Invest. Ser. 2, 23(4).

Guttman, I., S.S. Wilks, and J.S. Hunter. 1982. Introductory engineering statistics. 3rd ed. John Wiley & Sons, Inc., New York, N.Y.

Hilborn, R., E.K. Pikitch, and R.C. Francis. 1993. Current trends in including risk and uncertainty in stock assessment and harvest decisions. Can. J. Fish. Aquat. Sci. 50: 474–480.

Hilborn, R., and C. Walters. 1992. Quantitative fisheries stock assessment and management: choice, dynamics, and uncertainty. Chapman-Hall Publ. Co., New York, N.Y.

Hoenig, J.M., W.G. Warren, and M. Stocker. 1994. Bayesian and related approaches to fitting surplus production models. Can. J. Fish. Aquat. Sci. 51. (In press)

Jeffreys, H. 1961. Theory of probability. 3rd ed. Oxford University Press, London, U.K.

Kinas, P. 1993. Bayesian statistics for fishery stock assessment and management. Ph.D. dissertation, Faculty of Graduate Studies, Department of Statistics, University of British Columbia, Vancouver, B.C.

LEE, P.M. 1989. Bayesian statistics, an introduction. Edward Arnold, London, U.K.

LUDWIG, D., AND C. WALTERS. 1985. Are age-structured models appropriate for catch–effort data? Can. J. Fish. Aquat. Sci. 42: 1066–1072.

PRESS, S.J. 1989. Bayesian statistics, principles, models and applications. John Wiley & Sons, Inc., New York, N.Y.

RESTREPO, V.R., J.M. HOENIG, J.E. POWERS, J.W. BAIRD, AND S.C. TURNER. 1992. A simple simulation approach to risk and cost analysis, with applications to swordfish and cod fisheries. Fish. Bull. 90: 736–748.

SAINSBURY, K.J. 1988. The ecological basis of multispecies fisheries, and management of a demersal fishery in tropical Australia, p. 349–382. *In* J. Gulland [ed.] Fish population dynamics. 2nd ed. John Wiley & Sons, Ltd., Chichester, U.K.

SCHNUTE, J. 1985. A general theory for analysis of catch and effort data. Can. J. Fish. Aquat. Sci. 42: 414–429.

WALTERS, C.J. 1986. Adaptive management of renewable resources. Macmillan Publ. Co., New York, N.Y.

Appendix A

In this appendix, we provide details of some of the calculations, specifically those leading to (10), (12), (18), and (20). Similar derivations can be found in a variety of statistics texts, e.g., Guttman et al. (1982, p 201ff).

In order to derive (10), we begin with the formula (Abramowitsch and Stegun 1964, chap. 26)

$$\text{(A.1)}\quad \int_{-\infty}^{\infty} \exp(-u^2/2)\,du = \sqrt{2\pi}.$$

If we make the change of variables

$$\text{(A.2)}\quad u = \sqrt{I(q-q^*)/V}$$

the (A.1) becomes

$$\text{(A.3)}\quad \int_{-\infty}^{\infty} \exp(-(q-q^*)^2/(2V))\,dq = \sqrt{\frac{2\pi V}{I}}$$

which immediately implies (10).

Similarly, in order to derive (12), we begin with the definition of the Gamma function (Abramowitsch and Stegun 1964, p. 255):

$$\text{(A.4)}\quad \Gamma(p) = \int_0^{\infty} u^{p-1} \exp(-u)\,du.$$

If we set $p = -m$ and make the change of variables

$$\text{(A.5)}\quad u = -A/V$$

then (A.4) becomes

$$\int_0^{\infty} V^{-m-1} \exp(-A/V)\,dV = \frac{\Gamma(m)}{A^m}.$$

Finally, if we set $A = s^2$, the result is (12).

For the power model observation cases where

$$\text{(A.7)}\quad Y = q_1 B^{q_2}$$

we note that the likelihood function can be derived by considering an equivalent regression problem. Let

$$\text{(A.8)}\quad Z_i = \log Y_i$$

$$\text{(A.9)}\quad W_i \log B_i - \frac{1}{n}\sum \log B_i$$

$$\text{(A.10)}\quad \theta_2 = q_2$$

$$\text{(A.11)}\quad \theta_1 = \log q_1 + q_2 \frac{1}{n}\sum \log B_i\,.$$

In terms of these variables, we have the total sum of squares

$$\text{(A.12)}\quad \mathrm{SS} = \sum[Z_i - (\theta_1 + \theta_2 W_i)]^2 = n(\theta_1 - \hat{\theta}_1)^2 + I(\theta_2 - \hat{\theta}_2)^2 + (n-2)s''^2$$

where

$$\text{(A.13)}\quad I = \sum W_i^2$$

$$\text{(A.14)}\quad \theta_1 = \frac{1}{n}\sum Z_i$$

$$\text{(A.15)}\quad \theta_2 = \frac{\sum Z_i W_i}{\sum W_i^2}$$

$$\text{(A.16)}\quad s''^2 = \frac{1}{n-2}\sum[Z_i - (\hat{\theta}_1 + \hat{\theta}_2 W_i]^2\,.$$

In this case the likelihood L is given by

$$\text{(A.17)}\quad L = V^{-n/2} \exp\left(-\frac{1}{2V}\mathrm{SS}\right).$$

If we use flat priors on θ_1 and θ_2 (or on q_1 and q_2) and on log V, then integration by the same methods as for (10) and (12), and dropping unneeded constants, gives

$$\text{(A.18)}\quad L^{q_1 q_2 V} = (s''^2)^{-m}$$

which is the result (20).

Une méthode simple d'ajustement des clés taille/âge : application aux captures d'albacores (*Thunnus albacares*) de l'Atlantique Est

Didier Gascuel

ENSAR/ORSTOM/CRODT, département Halieutique, 65 route de Saint-Brieuc, 35042 Rennes Cedex, France

Gascuel, D. 1994. Une méthode simple d'ajustement des clés taille/âge : application aux captures d'albacores (*Thunnus albacares*) de l'Atlantique Est. Can. J. Fish. Aquat. Sci. 51 : 723–733.

Une méthode d'ajustement des clés taille/âge, qui tient compte de la variabilité interannuelle de l'abondance des cohortes, est présentée. Cette méthode s'appuie sur une modélisation de la croissance et des variations des écarts types de taille, en fonction de l'âge. Elle reprend un algorithme d'ajustement itératif. L'algorithme converge rapidement vers une solution stable, qui est identique, sous certaines conditions, à celle obtenue par le maximum de vraisemblance. Il est lui-même utilisé pour estimer les paramètres du modèle des écarts types de taille. La méthode est appliquée aux captures d'albacores (*Thunnus albacares*) de l'Atlantique Est de 1975 à 1989. Les clés mensuelles, ajustées aux captures de l'ensemble de la pêcherie, présentent une variabilité inter-annuelle importante. Elles sont utilisées pour une conversion taille/âge par métier et par carré géographique de 5° de coté. Comparativement aux estimations antérieures, réalisées par la méthode du « slicing », les captures par âge sont sensiblement corrigées; elles présentent une plus grande variabilité temporelle. Les résultats sont peu sensibles à l'estimation des paramètres du modèle des écarts types de taille. La méthode d'ajustement des clés est comparée aux méthodes classiques de décomposition polymodale par le maximum de vraisemblance. Elle s'applique particulièrement bien lorsque la croissance est connue; elle présente l'avantage d'une grande simplicité et d'une grande souplesse. Elle permet notamment la prise en compte de modèles de croissance particuliers.

An adjustment method for age–length keys is presented that incorporates yearly variability in cohort abundances. The method is based on two models (one for growth and the other for standard deviations of length versus age) and involves an iterative algorithm. The algorithm rapidly converges to stable results that yield, under some conditions, maximum likelihood estimates. It is also used to estimate parameters of the length standard deviation model. The method is applied to yellowfin tuna (*Thunnus albacares*) catches in the eastern Atlantic from 1975 to 1989. Monthly keys, adjusted to catches from the entire fishery, show a high annual variability. These keys are used for length–age conversion by gear type and 5° geographic squares. Compared with previous estimates based on the "slicing" method, catches by age are noticeably corrected; they show a greater temporal variability. The results show a low sensitivity to parameter estimates of the length standard deviation model. The adjustment method for age–length keys is compared with classical likelihood-based methods for the separation of mixtures of normal distributions; it fits particularly well under conditions of known growth, it offers the advantages of simplicity and adaptability, and importantly, it allows the use of particular growth models.

Reçu le 17 mars 1992
Accepté le 6 octobre 1993
(JB442)

Received March 17, 1992
Accepted October 6, 1993

L'estimation des captures par groupe d'âge constitue une étape préliminaire à toute approche structurale de la dynamique des stocks. Très généralement cette estimation s'appuie sur une connaissance des fréquences de taille au sein des captures, ces fréquences étant elles-mêmes estimées par échantillonnage. Parmi les méthodes de conversion des structures de tailles en structures d'âges, l'une des plus anciennes (Fridrikson 1934) et des plus courantes est l'utilisation de clés taille/âge, qui indiquent la proportion de chacun des groupes d'âge, au sein de chacune des classes de taille. Ces clés sont établies à partir d'une détermination de l'âge, soit par décomposition polymodale des fréquences de taille, soit par lecture de pièces anatomiques dures.

Les potentialités et les limites de l'utilisation des clés taille/âge sont analysées par Kimura (1977) et par Weistrheim et Ricker (1978). Ces auteurs montrent en particulier que les clés doivent théoriquement être recalculées chaque année. Bien souvent, par suite des difficultés pratiques et théoriques de la détermination de l'âge, on est cependant amené à utiliser des clés établies pour une période donnée et considérées constantes d'années en années.

Ainsi, dans le cas de l'albacore (*Thunnus albacares*) de l'Atlantique Est, la conversion des structures de taille en structures d'âge s'effectue au moyen de clés mensuelles, établies par Capisano et Fonteneau (1991). Ces auteurs s'appuient sur une décomposition des fréquences de taille des captures effectuées par les senneurs franco-sénégalais et espagnols, durant la période 1983–1988. Les clés correspondantes couvrent l'ensemble de l'Atlantique Est et traduisent une répartition estimée en moyenne inter-annuelle. En outre, il s'agit dans ce cas de « clés de découpe », qui affectent l'ensemble des captures d'une taille donnée à un âge unique, selon la méthode dite « au hachoir » ou « slicing ». Les clés de découpe constituent, en quelque sorte, des clés tailles/âge simplifiées à l'extrême.

L'application de clés considérées constantes dans le temps risque notamment de conduire à une sous-estimation des captures pour les cohortes abondantes, et, réciproquement, à une surestimation pour les cohortes de faible effectif. Le diagnostic sur l'état du stock risque ainsi d'être exagérément « moyen », c'est-à-dire trop optimiste en situation défavorable, et trop pessimiste en situation favorable. Par suite, plusieurs auteurs ont proposé des méthodes de conversion des structures de tailles en structures d'âge, tenant compte en particulier de la variabilité d'abondance des cohortes. Deux approches peuvent être distinguées.

La première, qui a une portée plus générale que la simple conversion taille/âge, s'appuie sur une hypothèse de normalité de la répartition des fréquences de taille à chaque âge. Cette hypothèse permet une décomposition polymodale des histogrammes de taille observés chaque année. On en déduit notamment une estimation des fréquences d'âge. Dans cette catégorie, la méthode statistiquement la plus satisfaisante est celle du maximum de vraisemblance (Hasselblad 1966; MacDonald et Pitcher 1979; Schnute et Fournier 1980; Fournier et al. 1990).

La seconde approche s'appuie sur la connaissance d'une clé taille/âge unique estimée une année donnée, généralement par lecture des pièces anatomiques dures. Sous certaines hypothèses, les fréquences d'âge peuvent dès lors être déduites des fréquences de taille annuelles, soit par la méthode des moindres carrés (Clark 1981; Bartoo et Parker 1983), soit par la méthode du maximum de vraisemblance (Hoenig et Heisey 1987). Kimura et Chikuni (1987) proposent une méthode d'estimation basée sur un algorithme itératif simple. Ils montrent que celui-ci est une application de l'algorithme dit « Em (expectation–maximisation) algorithm » de Dempster et al. (1977) et que les résultats obtenus sont identiques, dans certaines conditions, à ceux d'une estimation par la méthode du maximum de vraisemblance.

On propose ici une méthode qui utilise simultanément un algorithme proche de celui de Kimura et Chikuni (1987) et un modèle de répartition des tailles à chaque âge. La méthode est appliquée aux captures d'albacores réalisées dans l'Atlantique Est de 1975 à 1989. Les résultats sont comparés à ceux antérieurement obtenus par « slicing ». L'originalité et l'intérêt de la méthode sont discutés comparativement aux deux types d'approches précédemment cités.

Méthodes

La méthode d'ajustement des clés

Une clé taille/âge est ajustée chaque mois et chaque année à l'histogramme des captures réalisées pendant cette période, sur l'ensemble du stock considéré. Sous certaines hypothèses, cette clé mensuelle peut ensuite être utilisée pour une conversion taille/âge : par flottille et par zone géographique. Notons que le raisonnement, conduit ici pour une période intra-annuelle égale au mois, pourrait naturellement être utilisé de la même manière pour tout autre type de période (trimestre ou période quelconque).

Trois sources de variabilité inter-annuelle imposent théoriquement de recalculer chaque année les clés mensuelles : 1) la variabilité de l'abondance réelle ou apparente des groupes d'âge, liée notamment aux variations du recrutement et de la capturabilité, 2) les variations de sélectivité des engins de pêche et 3) la variabilité de la croissance. Cette dernière s'exprime elle-même de deux manières : par une variabilité des tailles moyennes à chaque âge, et par une variabilité des écarts types de taille à chaque âge.

Par hypothèse, seule la variabilité inter-annuelle de l'abondance des cohortes est ici prise en compte. En particulier, la croissance est considérée identique pour chacune des cohortes. À chaque groupe d'âge, peut donc être associés une taille mensuelle moyenne et un écart type de taille, constants d'année en année. La première étape de l'analyse consiste ainsi à définir un modèle de répartition des tailles à chaque âge; par hypothèse, cette répartition est indépendante de l'année considérée. La seconde étape consistera ensuite à ajuster les clés taille/âge mensuelles aux histogrammes de tailles observés chaque année.

Le modèle de répartition des tailles à chaque âge indique, pour chaque mois et chaque groupe d'âge, la proportion des poissons d'une longueur donnée, parmi ceux du groupe d'âge considéré. Ce modèle dépend du choix : d'une loi de répartition des tailles aux âges, d'un modèle de croissance linéaire, et d'un modèle de variation des écarts types de taille en fonction de l'âge. On se place ici dans le cas classique d'une répartition des tailles qui suit une loi normale. La proportion des poissons appartenant à une classe de taille indicée l, parmi ceux du groupe d'âge indicé a, est donnée par la fonction de répartition de la loi $n(L(T), \sigma(T))$ (voir la définition des notations utilisées au tableau 1). Soit :

$$(1) \quad \mathrm{PA}_l = \frac{1}{\sigma(T)\cdot\sqrt{2\pi}}\cdot\exp[-(L_l - L(T))^2 / 2\cdot\sigma(T)^2].$$

Généralement, la taille $L(T)$ est connue par l'intermédiaire d'un modèle de croissance linéaire, le modèle le plus usité étant l'équation de von Bertalanfly. L'ajustement d'un modèle décrivant les variations des écarts types de taille, en fonction de l'âge, est en revanche moins fréquent. On utilise ici un modèle comportant un terme constant, un terme proportionnel à la taille, et un terme proportionnel à l'accroissement en taille, soit :

$$(2) \quad \sigma(T) = \alpha + \beta\cdot L(T) + \gamma\cdot\Delta L(T).$$

L'estimation des paramètres de l'équation (2) est conduite par essais successifs de différentes valeurs empiriques. À chacune des valeurs des paramètres est associé un modèle de répartition des tailles par âge, qui se déduit de l'équation de croissance et des équations (1) et (2). Ce modèle de répartition permet d'ajuster, selon l'algorithme présenté au paragraphe suivant, des histogrammes théoriques aux histogrammes mensuels observés au cours d'une période pluriannuelle de référence. Ces histogrammes théoriques sont naturellement fonction des paramètres α, β et γ. Pour chaque modèle de répartition, on étudie la qualité de l'ajustement entre les histogrammes théoriques et observés; on recherche la combinaison des paramètres α, β et γ, qui permet le meilleur ajustement sur l'ensemble de la période de référence. La qualité de l'ajustement de chaque histogramme (un mois, une année) est quantifiée par une valeur de coefficient χ^2, et par une valeur D du test de Kolmokorov–Smirnov. La qualité de l'ajustement sur l'ensemble de la période est jugée par l'intermédiaire des valeurs moyennes et des écarts types des coefficients χ^2 et D.

L'ajustement des clés taille/âge mensuelles est ensuite mené par itérations, sous respect d'une double contrainte : la répartition des captures en taille, tous âges confondus, Tableau 1. Notations utilisées : symboles et définitions.

n	Nombre de groupes d'âge
a	Indice de groupe d'âge
T	Âge conventionnel (en années)
l	Indice de classe de taille
L_l	Longueur moyenne de la classe de taille l (en cm)
$L(T)$	Longueur moyenne à l'âge T
$\Delta L(T)$	Accroissement de taille à l'âge T
$\sigma(T)$	Écart type de taille à l'âge T
α,β,γ	Paramètres du modèle des écarts types de taille
PA_l	Proportion de poissons de longueur l, parmis ceux du groupe d'âge a
$F\mathrm{obs}_l$	Fréquence de longueur observée pour la classe de taille l
$P\mathrm{obs}_l$	Proportion observée des poissons de la classe de taille l, au sein de l'ensemble des captures
P_l	Proportion estimée des poissons de la classe de taille l, au sein de l'ensemble des captures
P_a	Proportion estimée des poissons du groupe d'âge a, au sein de l'ensemble des captures
$P_{a,l}$	Proportion estimée des poissons appartenant au groupe d'âge a et à la classe de taille l, au sein de l'ensemble des captures
F_l	Fréquence estimée de la classe de taille l
PL_a	Proportion estimée des poissons du groupe d'âge a, parmi ceux de la classe de taille l

est déterminée par l'histogramme observé; la répartition en taille à chaque âge est déterminée par le modèle de répartition pré-cité. L'ajustement revient en fait à rechercher les effectifs de chaque groupe d'âge, au sein de l'ensemble des captures. Ces effectifs, complétés par le modèle de répartition, permettent de déterminer un histogramme de fréquences de tailles théoriques qui est ajusté à l'histogramme observé. On utilise ici une procédure itérative voisine de celle définie par Fukuna et Chikuni (non publié) et présentée par Kimura et Chikuni (1987). Cette procédure peut être résumée de la manière suivante (voir la définition des notations au tableau 1) :

1) L'histogramme des fréquences de taille observées est exprimé en terme de proportions. La proportion des poissons de la classe de longueur l, au sein de l'ensemble des captures, est :

$$P\mathrm{obs}_l = F\mathrm{obs}_l / \Sigma_l\, F\mathrm{obs}_l.$$

2) La proportion de chacun des groupes d'âge, au sein de l'ensemble des captures, est initialisée par une valeur P_a fixée arbitrairement :

$$P_a = 1/n.$$

3) La proportion, au sein de l'ensemble des captures, des poissons appartenant au groupe d'âge a et à la classe de longueur l, est estimée d'après le modèle de répartition des tailles aux âges. Soit :

$$P_{a,l} = P_a \cdot \mathrm{PA}_l.$$

4) On en déduit une estimation de la proportion théorique des poissons de la classe de longueur l, au sein de l'ensemble des captures :

$$P_l = \Sigma_a\, P_{a,l}.$$

5) L'estimation $P_{a,l}$ est corrigée en fonction de l'écart entre les proportions de taille observées et théoriques. Soit :

$$P'_{a,l} = P_{a,l} \cdot P\mathrm{obs}_l / P_l.$$

6) La proportion de chaque âge est recalculée :

$$P_a = \Sigma_l\, P'_{a,l}.$$

7) Cette nouvelle valeur remplace la précédente estimation P_a. Les étapes trois à six sont répétées jusqu'à convergence des résultats.

8) Des estimations finales des coefficients $P'_{a,l}$, on déduit la proportion de chaque groupe d'âge, au sein de chaque classe de taille. Soit les coefficients de la clé taille/âge ajustée :

$$\mathrm{PL}_a = P_{a,l} / P\mathrm{obs}_l.$$

À l'issue de l'étape 4, on calcule la valeur du coefficient χ^2, correspondant à l'écart entre proportions observées et théoriques. La convergence des résultats est mesurée en terme de gain du χ^2, comparativement à l'itération précédente. L'histogramme des fréquences de tailles théoriques F_l se déduit des proportions P_l obtenues à l'issue de la convergence. Soit :

$$F_l = P_l \cdot \Sigma_l\, F\mathrm{obs}_l.$$

Application aux captures d'albacores de l'Atlantique Est

La croissance de l'albacore dans l'Atlantique Est présente une dynamique tout à fait particulière. D'abord extrêmement lente au début de la phase exploitée (Fonteneau 1980; Bard 1984), elle s'accélère ensuite puis présente un point d'inflexion (fig. 1). Elle peut être décrite par un modèle à cinq paramètres, qui combine une fonction linéaire et une équation de von Bertalanffy généralisée (Gascuel et al. 1992). Soit :

$$(3)\quad L(T) = 37{,}8 + 8{,}93 \cdot T + (137{,}0 - 8{,}93 \cdot T) \cdot [1 - \exp(-0{,}808 \cdot T)]^{7{,}49}.$$

Les tailles sont exprimées en longueur à la fourche (en centimètres) et les âges en âge conventionnel (en années), pour une naissance fixée au 15 janvier. Les longueurs le 15 de chaque mois sont ainsi considérées égales aux longueurs moyennes du mois correspondant. L'équation (3) est ajustée dans l'intervalle 0,25 à 6 ans, soit de 40 à 170 cm. Elle est

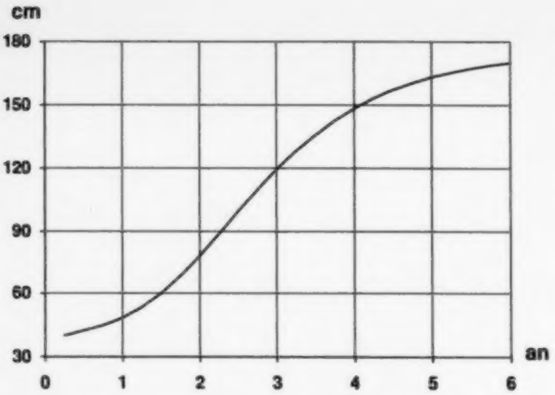

FIG. 1. Le modèle de croissance linéaire de l'albacore dans l'Atlantique Est (longueur à la fourche, en fonction d'un âge conventionnel); d'après Gascuel et al. (1992).

extrapolée entre 0 et 0,25 ans; nous verrons que cette extrapolation est sans conséquence sur l'ajustement des clés taille/âge.

L'équation (2) qui modélise les écarts types de taille en fonction de l'âge, peut être simplifiée. En effet, ni les études de décompositions polymodales des fréquences de taille (Capisano et Fonteneau 1991), ni les ajustements du modèle de croissance (Gascuel et al. 1992), ni les déterminations de l'âge de gros albacores par otholimétrie (Manooch et Hinkley 1991), ne mettent en évidence un accroissement des écarts types de taille avec l'âge. En revanche, ces écarts types semblent plus élevés en période de croissance rapide, entre approximativement 2 et 4 ans. L'équation retenue est donc de la forme :

(4) $\sigma(T) = \alpha + \gamma \cdot \Delta L(T)$.

En outre, cette équation peut être exprimée de manière à faire apparaître la demi-étendue de l'intervalle dans lequel est comprise une fraction donnée de la population. Soit, pour une fraction fixée à 0,99 (99 % des poissons d'âge T dans l'intervalle $L(T) \pm 2{,}576 \cdot \sigma(T)$) :

(5) $\sigma(T)/2{,}576 = \alpha' + \gamma' \cdot \Delta L(T)$.

Enfin, l'accroissement $\Delta L(T)$ est calculé sur une base annuelle. Soit :

(6) $\Delta L(T) = [L(T + 1) - L(T - 1)]/2$.

Les coefficients α' et γ' sont estimés en étudiant l'ajustement des histogrammes de taille théoriques aux histogrammes observés, sur une base de référence constituée par les captures des senneurs franco-ivoiro-sénagalais et espagnols, au cours de la période 1980 à 1989. C'est en effet pour ces flottilles et cette période que les statistiques de pêche et les estimations des structures de taille paraissent les plus fiables. La base de référence comporte ainsi 120 histogrammes observés (10 années et 12 mois). Ceux-ci sont établis par classes de taille de 2 cm entre 30 et 180 cm de longueur à la fourche.

À chaque couple de valeurs des coefficients $\alpha' = xx$ et $\gamma' = 0{,}yy$ est associé un modèle $S\alpha'\gamma'$ de répartition des tailles aux âges, noté par convention $Sxx \cdot yy$. L'analyse de la qualité de l'ajustement des histogrammes théoriques aux histogrammes observés, par l'intermédiaire des coefficients χ^2 et D, débouche sur le choix de paramètres α' et γ' « optimaux ». En outre, on analyse la sensibilité des résultats finaux, c'est-à-dire des captures estimées par classe d'âge, à cette estimation des paramètres du modèle de répartition.

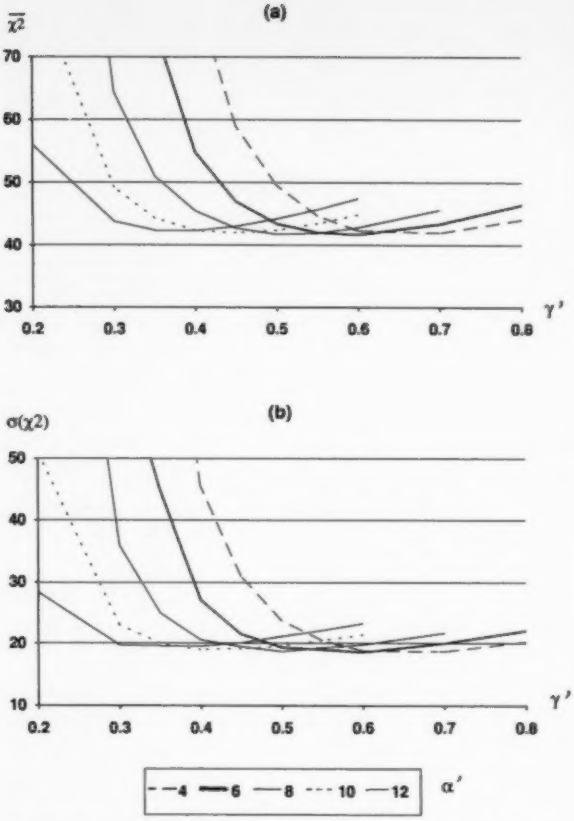

FIG. 2. Estimation des paramètres α' et γ' du modèle des écarts types de taille par âge : variations, en fonction de ces paramètres, de la qualité de l'ajustement des histogrammes théoriques aux fréquences de taille observées (base de référence : captures mensuelles des senneurs franco-ivoiro-sénégalais et espagnols de 1980 à 1989). (a) D'après les valeurs moyennes du coefficient χ^2; (b) d'après les écarts-types de ces coefficients.

Une fois le modèle de répartition déterminé, les clés taille/âge sont ajustées aux structures de taille observées au sein des captures de l'ensemble des navires opérant dans l'Atlantique Est, toutes flottilles confondues, au cours de la période 1975–1989. Deux aspects sont plus particulièrement analysés. D'une part, la convergence de l'algorithme d'ajustement est mise en évidence par l'étude des variations du coefficient χ^2 moyen (moyenne pour les 12 mois et 15 années, soit 180 histogrammes) en fonction du nombre d'itérations effectué. D'autre part, la qualité des ajustements obtenus à l'issue de la convergence est étudiée; une analyse de variance, portant sur les 180 coefficients χ^2, permet de juger de la capacité de la méthode à rendre compte des différents mois et des différentes années.

Les captures par groupe d'âge sont estimées entre 1975 et 1989. Les clés précédemment ajustées par mois et par années sont ainsi utilisées pour convertir en structures d'âge les structures de taille des captures établies selon un plan d'échantillonnage stratifié par mois, flottille, et carré géo-

TABLEAU 2. Variations de la qualité de l'ajustement des histogrammes théoriques aux fréquences de tailles observées, en fonction des paramètres α' et γ' du modèle de répartition des tailles par âge (cf. texte).

	Modèle d'écart type de taille	Coefficient du test de χ^2		Coefficient du test de Kolmogorov–Smirnov	
		χ^2 moyen	$\sigma(\chi^2)$	D moyen	$\sigma(D)$
Sensibilité au choix de α'[a]	*S*04·70	42.0	18.7	0.1315	0.0618
	*S*06·60	41.7	18.6	0.1301	0.0612
	*S*08·50	41.8	18.7	0.1285	0.0604
	*S*10·45	42.0	19.0	0.1292	0.0600
	*S*12·40	43.0	19.5	0.1299	0.0600
Sensibilité au choix de γ'[b]	*S*06·50	43.4	19.4	0.1266	0.0608
	*S*06·70	43.4	20.0	0.1339	0.0614

[a] γ' étant déterminé par minimisation du χ^2 (cf. fig. 4).

[b] Pour les valeurs de γ' entourant le modèle de référence *S*06·60.

graphique de 5° de latitude et longitude de coté (Fonteneau 1989). On présente ici les résultats cumulés par année ou par trimestre, pour l'ensemble des zones et des flottilles. Ces résultats sont comparés à ceux issus de l'estimation par « slicing ».

Trois programmes, écrits en Fortran, réalisent les différents calculs : calcul des proportions PA_l du modèle de répartition des tailles aux âges; estimation des proportions PL_a correspondant aux clés mensuelles ajustées; estimation des captures par groupe d'âge à partir des statistiques de pêche.

Résultats

Modèle de répartition des tailles à chaque âge

L'estimation du paramètre γ' de l'équation concernant les écarts types de taille se déduit du choix d'une valeur α'. À chaque valeur α' peut en effet être associée une valeur γ' unique, et donc un modèle $S\alpha'\gamma'$ qui optimise l'ajustement des clés sur la période de référence, en ce sens qu'il minimise à la fois la moyenne et l'écart type des coefficients χ^2 obtenus (fig. 2). Les structures de tailles observées déterminent le niveau moyen des écarts types de taille à chaque âge. Ainsi, les modèles $S\alpha'\gamma'$, qui se traduisent globalement par des écarts types trop faibles, ne permettent pas d'expliquer les captures observées à des tailles intermédiaires entre les valeurs modales des différents groupes d'âge. À l'inverse, des écarts types globalement trop élevés se traduisent par une proportion importante de poissons à ces tailles intermédiaires ou aux tailles extrêmes.

Le choix du paramètre α' peut quant à lui difficilement s'appuyer sur l'analyse statistique. En effet, différentes combinaisons des paramètres α' et γ' se traduisent par des qualités d'ajustement qui ne sont pas statistiquement différentes, et ceci que l'on raisonne à partir des coefficients χ^2 ou des coefficients D de Kolmokorov–Smirnov (tableau 2). Les différents modèles de répartition des tailles par âge correspondants apparaissent cependant relativement proches (fig. 3). Par convention, on retiendra comme référence le modèle *S*06·60 qui minimise le χ^2 moyen. L'écart type de taille à chaque âge varie pour ce modèle entre 4,7 et 10,5 cm. L'étendue de l'intervalle de confiance des tailles à chaque âge (à 99 % de certitude) est ainsi de 24 cm pour les groupes 0 et 5+, et de 58 cm pour le groupe 2.

Les différents modèles de répartition présentés au tableau 2 sont par ailleurs pris en compte pour analyser la sensibilité de l'estimation des captures par âge, à l'estimation des paramètres α' et γ'. Ces modèles couvrent les situations allant d'un écart type de taille variant d'un facteur 1,2 (modèle *S*12·40 : $6,2 < \sigma(T) < 7,4$ cm) à celle d'un écart type variant d'un facteur d'environ 3 (modèle *S*04·70 : $4,3 < \sigma(T) < 12,2$ cm).

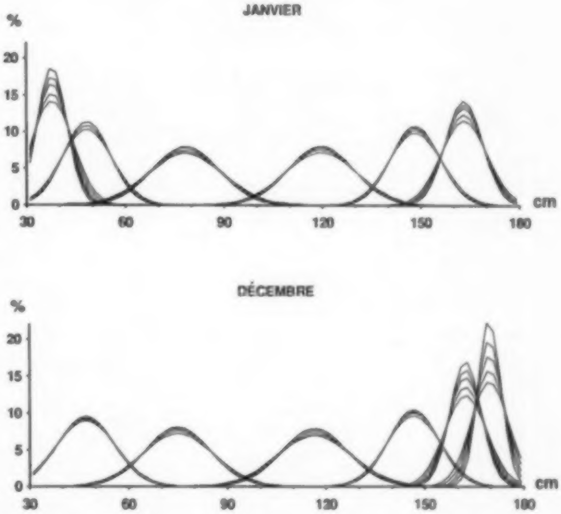

FIG. 3. Modèles de répartition des tailles à chaque âge, en janvier et décembre, en % par classe de 2 cm : modèle de référence *S*06·60 et sensiblité du modèle au choix du paramètre α' (modèles *S*04·70, *S*08·50, *S*10·45, *S*12·40; cf. texte).

Ajustement des clés taille/âge

L'algorithme d'ajustement des clés converge rapidement vers une solution stable. Au cours de l'ajustement à l'ensemble des captures de la période 1975 à 1989, le gain de χ^2 observé entre deux itérations est en moyenne inférieur à 0,02 %, à partir de la douzième itération (fig. 4). Par la suite, ce seuil a été pris comme critère d'arrêt des itérations, lors de l'ajustement de chaque histogramme.

À l'issue de la convergence ainsi définie, 12 des 180 histogrammes observés diffèrent significativement des histogrammes théoriques qui leur sont ajustés (test de χ^2 à 95 % de certitude). Les facteurs mois et année ont par

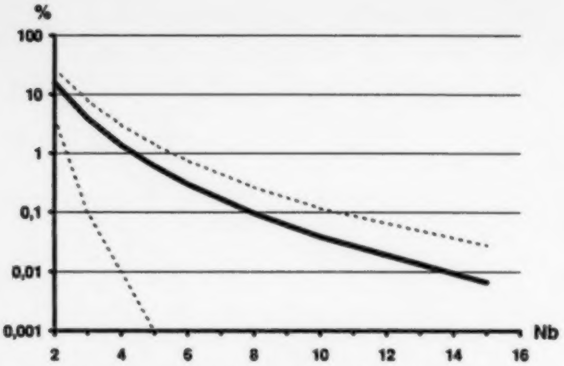

FIG. 4. Convergence de l'algorithme d'ajustement des clés : variation du gain de χ^2, d'une itération à la suivante, en fonction du nombre d'itération réalisé (en valeur moyenne et intervalle de confiance, à 95 % de certitude, pour un ajustement sur l'ensemble des captures de 1975 à 1989).

ailleurs un effet significatif sur la valeur des coefficients χ^2 (seuil de significativité de 0,0003 et 0,0316 respectivement). Globalement, aucun des mois et aucune des années ne présente cependant un χ^2 moyen supérieur au seuil critique. En outre, les autocorrélations entre χ^2 de mois successifs sont non significatives au-delà d'un délai d'un mois. Ces différentes observations tendent à montrer que la variabilité temporelle des coefficients χ^2, c'est-à-dire des qualités d'ajustement, est liée à une variabilité erratique des structures de taille observées. Les ajustements non significatifs correspondent ainsi à des structures de taille atypiques, observées sur courte période, et que pourraient expliquer notamment des variations de capturabilité par âge. La variabilité de croissance, en terme de taille moyenne et d'écart type de taille à chaque âge, apparaît quant à elle suffisamment faible pour ne pas entraîner d'écarts significatifs entre les structures de taille observées et le modèle théorique.

Les clés taille/âge obtenues à l'issue de l'ajustement mettent clairement en évidence la variabilité des proportions par âge, à chaque taille (fig. 5). Cette variabilité est naturellement liée aux fluctuations inter-annuelles des captures par taille. Dans le cas de l'albacore de l'Atlantique Est, celles-ci atteignent fréquemment un facteur 10 (fig. 5a). Globalement, les histogrammes théoriques permettent de traduire cette variabilité (fig. 5b). Au niveau des clés ajustées, la classe de taille qui sépare deux groupes d'âge voisins dans des proportions égales varie couramment de 10 cm (fig. 5c). Dans certains cas, ces variations peuvent être très supérieures. Par exemple, l'absence quasi complète de captures dans l'intervalle 60 à 100 cm, en janvier 1989, se traduit par une forte réduction des proportions affectées à l'âge 2, et par un recouvrement partiel dans les clés des groupes d'âge 1 et 3.

L'ajustement des clés permet par ailleurs de rendre compte du phénomène de recrutement. On sait que le recrutement de l'albacore dans l'Atlantique Est intervient progressivement au cours du second trimestre; le mode 0 est généralement mis en évidence au sein des captures à partir du mois de juillet (Fonteneau 1980; Bard et Capisano 1991; Capisano et Fonteneau 1991). Le modèle de répartition des tailles, adopté ici pour le groupe d'âge 1, permet effectivement de rendre compte de l'ensemble des captures d'albacores observées

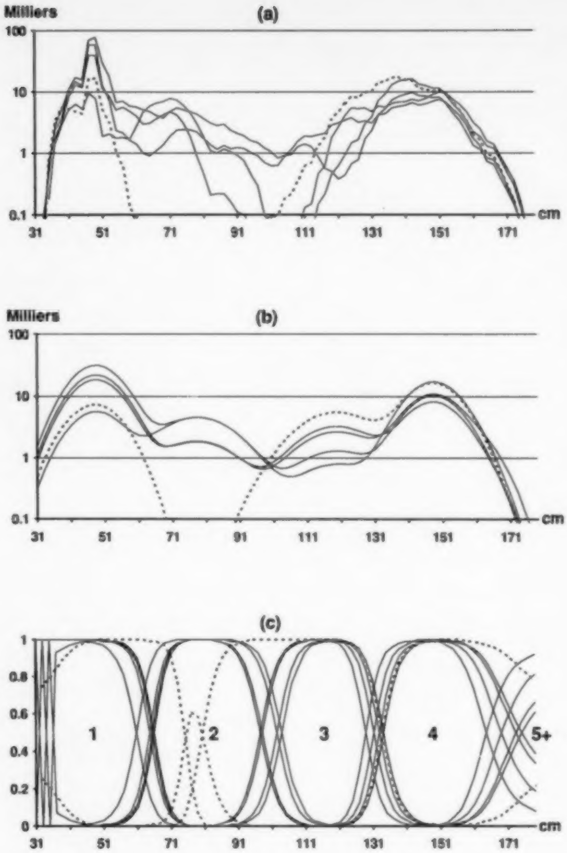

FIG. 5. Ajustement des clés taille/âge sur les captures totales d'albacores de l'Atlantique Est. À titre d'exemple, les résultats sont présentés pour le mois de janvier et les cinq années les plus récentes (1985 à 1989; année 1989 en pointillés). (a) Histogrammes des fréquences de taille observées (par classe de 2 cm); (b) histogrammes des fréquences de taille théoriques ajustées; (c) clés taille/âge ajustées (proportion des groupes d'âge par classe de taille).

au premier trimestre. Le groupe d'âge 0 est alors quasiment absent des clés taille/âge ajustées (fig. 5c) et la proportion des captures correspondantes est estimée à moins de 1 %. De mai à juillet cette proportion atteint 15 %, en même temps que le groupe 0 apparaît significativement dans les clés. Elle est, enfin, supérieure à 40 % à partir du mois d'août.

Captures estimées par groupe d'âge

Au cours de la période 1975 à 1989, l'ajustement des clés conduit à des estimations de captures par âge annuelles sensiblement différentes de celles obtenues antérieurement par « slicing » (fig. 6). Globalement, la méthode conduit à réviser à la hausse les captures des groupes d'âge 0, 3 et 4, et à la baisse celles des groupes d'âge 1, 2 et surtout 5+ (tableau 3). En valeur absolues, les écarts moyens entre les deux méthodes augmentent avec l'âge (tableau 4).

Les fluctuations temporelles des estimations sont en revanche très cohérentes entre les deux méthodes, avec des corrélations significatives (à 95 % de certitude) pour tous

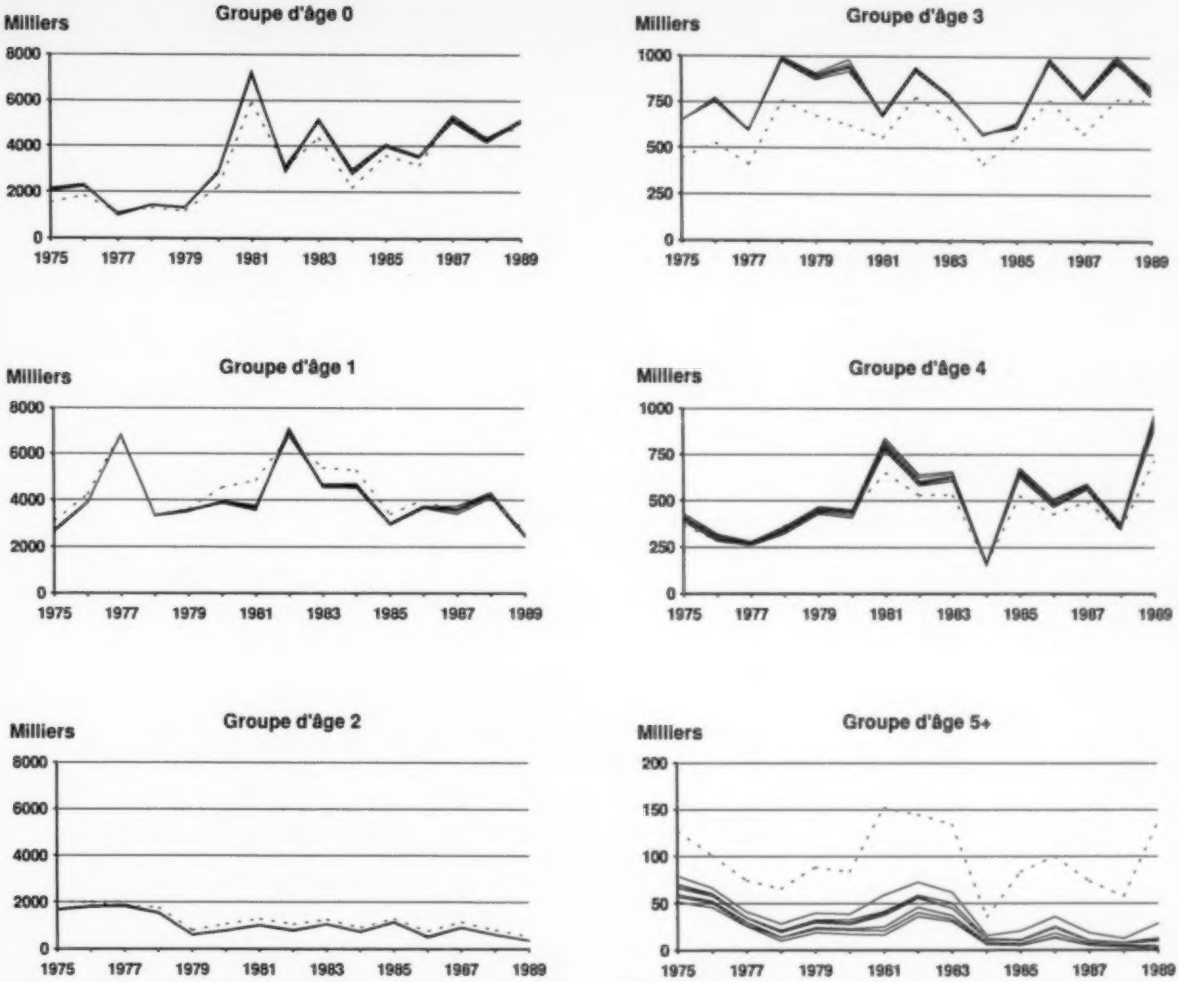

FIG. 6. Captures annuelles d'albacores dans l'Atlantique Est : estimation d'après la méthode d'ajustement des clés taille/âge (pour le modèle de référence *S*06-60; sensibilité de l'estimation, aux paramètres du modèle de répartition des tailles aux âges (pour les sept modèles $S\alpha'\gamma'$ du tableau 2); comparaison avec les estimations par la méthode du « slicing » (en pointillés).

les groupes d'âge. Comme on pouvait s'y attendre, la méthode d'ajustement des clés se traduit cependant par une plus forte variabilité des captures. Le « slicing » conduit ainsi à sous-estimer les coefficients de variation et l'étendue des variations des captures trimestrielles et annuelles par âge (tableau 3).

La sensibilité des estimations de captures, au choix des paramètres α' et γ' du modèle de répartition des tailles, apparaît faible. Pour les groupes d'âge 0 à 4 ans, les estimations issues des différents modèles de répartition présentent ainsi des écarts avec le modèle de référence (*S*06-60) qui sont en moyenne inférieurs à 3 % (tableau 4). Les courbes d'évolution des captures trimestrielles ou annuelles apparaissent ainsi quasiment confondues (fig. 6). Les estimations concernant le groupe 5+ sont, elles, plus sensibles au choix des paramètres α' et γ'. Fort logiquement, c'est pour ce dernier groupe d'âge que la conversion taille/âge est la plus délicate, par suite d'un important recouvrement des fréquences de taille entre ce groupe et le précédent. L'estimation des captures correspondantes devra ainsi être considérée comme étant de fiabilité limitée.

On notera néanmoins que les écarts liés au choix des paramètres α' et γ' sont très inférieurs à ceux découlant de l'application du « slicing ». Cette remarque est a fortiori valide pour les groupes d'âge 0 à 4. Comparativement à cette méthode, l'ajustement des clés introduit une correction dans l'estimation des captures par âge, qui est très largement indépendante de l'estimation des paramètres du modèle de répartition des tailles aux âges.

Discussion

Originalité et intérêt de la méthode d'ajustement des clés

Comparativement à la méthode très rudimentaire du « slicing », l'intérêt de la méthode d'ajustement des clés taille/âge est évident. D'abord parce que l'hypothèse d'une répartition des tailles à chaque âge suivant une loi normale

TABLEAU 3. Comparaison des méthodes d'estimation des captures par ajustement des clés taille/âge et par « slicing ». La comparaison porte sur les captures estimées (ensemble des flottilles de 1975 à 1989) et sur leur variabilité temporelle; pour chacun des paramètres, on calcule le ratio entre les valeurs obtenues par chacune des deux méthodes.

	Groupe d'âge					
	0	1	2	3	4	5+
Effectif total capturé	1.11	0.93	0.84	1.29	1.11	0.32
Étendue/moyenne des :						
captures trimestrielles	1.00	1.19	1.12	0.73	1.34	0.99
captures annuelles	0.97	1.10	1.24	0.86	1.25	1.79
Coefficient de variation des :						
captures trimestrielles	1.02	1.15	1.09	0.79	1.33	1.08
captures annuelles	1.14	1.14	1.19	0.86	1.22	1.66

TABLEAU 4. Sensibilité des estimations de captures trimestrielles (ensemble de la pêcherie de 1975 à 1989) à la méthode d'estimation et au choix du modèle $S\alpha'\gamma'$ de répartition des tailles par âge : écarts moyens aux estimations issues du modèle de référence *S*06·60 (calculés en valeur absolue et exprimés en %).

Groupe d'âge	« Slicing »	Estimation par ajustement des clés, pour les modèles :						
		*S*04·70	*S*06·60	*S*08·50	*S*10·45	*S*12·40	*S*06·50	*S*06·70
0	14.9	0.9	0	1.0	1.8	2.7	2.5	2.6
1	15.6	0.9	0	1.0	1.8	2.6	2.4	2.5
2	21.9	0.0	0	0.9	1.8	3.0	2.3	2.7
3	26.2	1.0	0	1.1	1.9	3.0	2.3	2.5
4	27.7	2.1	0	2.1	4.3	6.4	4.2	4.1
5+	214.0	5.4	0	4.8	21.9	37.6	33.7	29.0

apparaît plus réaliste que les simples clés de découpe utilisées pour le « slicing ». Dans le cas de l'albacore, cette hypothèse est validée par les résultats obtenus (cf. fig. 5a et 5b). Ensuite, et surtout, la méthode d'ajustement des clés tient compte de la variabilité d'abondance des cohortes. La forte variabilité inter-annuelle des clés taille/âge obtenues ici (fig. 5c) illustrent bien l'intérêt de cette prise en compte. Il apparaît clairement que l'utilisation d'une clé de découpe supposée constante dans le temps constitue une approximation, source d'erreurs sensibles dans les estimations (Kimura 1977; Westrheim et Ricker 1978). C'est donc essentiellement en comparaison avec les méthodes tenant également compte de cette variabilité inter-annuelle d'abondance que la méthode d'ajustement des clés doit être discutée.

De ce point de vue, la première originalité de la méthode réside dans son insertion au sein d'une procédure d'extrapolation de données statistiques obtenues par échantillonnage stratifié. En effet, tant l'algorithme décrit par Kimura et Chikuni (1987) que les méthodes classiques de décompositions polymodales utilisent un histogramme de taille unique pour estimer directement les captures par âge. La méthode d'ajustement des clés combine quant à elle différents types d'histogrammes et passe par l'estimation des proportions par âge, à chaque taille. Une clé mensuelle est ainsi ajustée sur l'histogramme de taille des captures réalisées par l'ensemble des flottilles dans toute l'aire de répartition du stock. Elle est ensuite utilisée pour une conversion taille/âge à partir des structures de taille observées pour chaque flottille et chaque carré géographique.

La procédure ainsi mise en oeuvre permet de tenir compte des différences de structure de taille des captures entre engins de pêche et carrés géographiques. En revanche, l'utilisation d'une clé mensuelle unique repose sur une hypothèse de répartition des tailles à chaque âge indépendante de l'engin de pêche et de la zone considérée. On ne tient donc compte ni de la variabilité spatiale de la croissance, ni des conséquences que pourrait avoir la sélectivité des engins de pêche sur la répartition des tailles par âge. Cette démarche appelle deux types de remarques.

En premier lieu, elle apparaît cohérente avec l'hypothèse de base de la méthode, à savoir l'absence de variations temporelles des deux grandeurs, sélectivité et croissance. Cette hypothèse de base sous-tend également toutes les méthodes de conversion taille/âge qui s'appuient sur la connaissance d'une clé établie à un moment donné (Clark 1981; Bartoo et Parker 1983; Hoenig et Heisey 1987; Kimura et Chikuni 1987). Elle peut sans aucun doute être raisonnablement faite pour un grand nombre de stocks halieutiques. En particulier, dans le cas de l'albacore, la pêcherie est essentiellement constituée de senneurs, dont l'engin de pêche apparaît peut sélectif. De même, la variabilité inter-annuelle de croissance est relativement faible (Fonteneau 1980; Gascuel et al. 1992); le modèle utilisé pour la décrire est en outre représentatif d'une croissance moyenne à l'échelle de l'ensemble de l'Atlantique Est et au cours de la dernière décennie (Gascuel et al. 1992).

En second lieu, la connaissance des captures par âge, par flottille et par zone géographique est d'un intérêt évident, tant en matière d'approche structurale de la dynamique du stock, que pour l'étude de la biologie de l'espèce. Dès lors, la seule alternative à la démarche présentée ici serait d'estimer directement les proportions par âge des captures de chaque flottille, dans chaque strate spatiale. Outre l'extrême lourdeur d'une telle approche, il est probable qu'elle serait peu efficace. Les variations erratiques des structures de taille, observées à une échelle fine, se traduiraient très vraisemblablement par un ajustement peu satisfaisant des modèles théoriques. Le recours à une clé mensuelle unique constitue ainsi une démarche pragmatique, difficilement contournable.

La seconde originalité de la méthode présentée ici réside dans l'utilisation conjointe de l'algorithme d'ajustement par itérations, et d'un modèle de répartition des tailles aux âges, qui est issu d'une équation de croissance et d'une équation relative aux écarts types de taille. Comparativement à la méthode originale de Kimura et Chikuni (1987), ceci présente deux intérêts. D'une part, on s'affranchit de la nécessité de disposer d'une clé taille/âge obtenue une année donnée, généralement par lecture directe de l'âge sur les pièces anatomiques dures. D'autre part, l'algorithme d'ajustement est lui-même utilisé pour estimer les paramètres de l'équation concernant les écarts types de taille.

Plus généralement, la méthode d'ajustement des clés conduit ici à des résultats qui peuvent être considérés identiques à ceux obtenus par la méthode du maximum de vraisemblance. Kimura et Chikuni (1987) montrent en effet que l'algorithme d'ajustement par itérations converge vers une solution stable. Ils démontrent que si toutes les proportions estimées sont différentes de zéro, alors cette solution est unique et est identique à celle obtenue par la méthode du maximum de vraisemblance. On notera que cette condition est suffisante, mais que son caractère nécessaire ne peut être démontré. Dans l'ajustement réalisé sur les données concernant l'albacore, seul le groupe d'âge 0 présente des proportions qui soient parfois nulles, généralement durant les premiers mois de l'année, en liaison avec le phénomène de recrutement. Ce résultat pourrait à l'inverse être considéré, par hypothèse, comme une contrainte d'ajustement. Pour les mois correspondants, seuls les groupes d'âge 1 à 5+ seraient ainsi pris en compte. La condition évoquée ci-dessus serait dès lors respectée.

Un autre parallèle méthodologique mérite à ce niveau discussion, dans la mesure où on travaille ici sous hypothèse de normalité de la répartition des tailles par âge. La méthode d'ajustement des clés apparaît dès lors conceptuellement très proche des méthodes de décompositions polymodales par le maximum de vraisemblance (Hasselblad 1966). MacDonald et Pitcher (1979) et Schnute et Fournier (1980) montrent qu'à partir d'un unique histogramme de fréquences de tailles, on peut ainsi estimer : les tailles moyennes, les écarts types de taille et les proportions des différents groupes d'âge sous-jacents. Ces auteurs soulignent en même temps que la recherche de solutions biologiquement acceptables rend généralement nécessaire l'introduction de contraintes sur l'un ou l'autre des paramètres estimés. Théoriquement, la méthode pourrait être utilisée, sous la contrainte de tailles moyennes à chaque âge déterminées par un modèle de croissance, ce modèle étant connu par ailleurs. L'utilisation des programmes informatiques correspondants (en particulier NORMSEP, décrit dans Abramson 1970) permettrait d'estimer, pour chaque histogramme, les écarts types de taille et les proportions par âge. Très vraisemblablement, la mise en cohérence d'une série d'histogrammes successifs conduirait ensuite à l'introduction de contraintes supplémentaires, par exemple en introduisant ici aussi une équation de variation des écarts types de taille.

Réciproquement, les estimations de proportions par âge, obtenues soit par la méthode d'ajustement des clés, soit par cette méthode de décomposition polymodale, seront identiques, si on utilise dans les deux cas les mêmes modèles de croissance et de variation des écarts types de taille. L'utilisation de programmes de décomposition polymodale, qui s'appliquent à un histogramme unique, serait cependant extrêmement lourde pour traiter des données mensuelles sur un nombre d'années conséquent. Ceci est encore plus vrai si la méthode doit être utilisée un grand nombre de fois, pour rechercher empiriquement une estimation des paramètres de l'équation caractéristique des écarts types de taille.

D'autres procédures existent, qui sont adaptées au traitement simultané de plusieurs histogrammes. La plus classique correspond au programme ELEFAN décrit par Pauly (1987). Plus récemment, Fournier et al. (1990) proposent une méthode de décomposition polymodale par le maximum de vraisemblance appliquée à plusieurs histogrammes. Ils s'appuient sur une modélisation de la croissance selon l'équation de von Bertalanffy et sur une équation dans laquelle les écarts types de taille sont proportionnels à la taille (et non, comme ici, à l'accroissement de taille). Le programme correspondant (MULTIFAN) n'est donc pas applicable dans un cas comme celui de l'albacore.

Au delà de la mauvaise adaptation de la méthode à ce cas particulier, une remarque plus générale s'impose. Les méthodes de décompositions polymodales sont potentiellement très puissantes; elles ont notamment vocation à estimer les tailles moyennes aux âges et les paramètres de croissance. Ceci n'est pas le cas de la méthode d'ajustement des clés. À l'inverse, cette dernière présente un double intérêt. D'une part, elle est d'une grande simplicité, tant en ce qui concerne la programmation (quelques dizaines de lignes) qu'en ce qui concerne sa mise en oeuvre; celle-ci ne requière aucun choix subjectif de l'utilisateur. D'autre part, elle autorise la prise en compte de n'importe quel type de loi de croissance (le programme utilise des longueurs moyennes discrètes par âge et par mois) et d'équations relative aux écarts types de taille diverses.

Modèle de répartition des tailles aux âges

Un des points centraux de la méthode d'ajustement des clés est la définition d'un modèle de variation des écarts types de taille, en fonction de l'âge. Schnute et Fournier (1980) montrent en particulier que la structure des contraintes imposées à ces écarts types a un impact déterminant sur les résultats de la décomposition polymodale par le maximum de vraisemblance. Ils présentent le modèle comportant un terme constant et un terme proportionnel à la taille comme étant celui le mieux adapté à un grand nombre d'espèces. Le premier modèle présenté ici (équation (2)) comporte également un terme proportionnel à l'accroissement de taille et est donc plus général.

D'un point de vue conceptuel, il existe un parallèle entre cette approche et la modélisation de la variabilité interindividuelle de croissance, telle qu'elle est abordée par Fonteneau (1974) dans le cas de l'albacore et plus généralement par Sainsbury (1980). Dans le cas d'un modèle de von Bertalanffy, ces auteurs expriment la variabilité interindividuelle par l'intermédiaire des trois paramètres σ_{t_0}, σ_{L_∞} et σ_K. L'interprétation biologique qui peut être donnée de ces paramètres est similaire à celle qui peut être faite pour les paramètres α, β et γ de l'équation (2). Les termes α et

σ_{t_0} peuvent ainsi être considérés comme représentatifs d'une variabilité des dates de naissance ou de recrutement, les termes β et σ_{L_∞} comme représentatifs d'une variabilité des longueurs asymptotiques, et les termes γ et σ_K comme représentatifs d'une variabilité des vitesses de croissance.

Dans la pratique, l'utilisation d'un modèle à trois paramètres rendrait l'estimation de ceux-ci relativement problématique. La procédure de recherche des valeurs optimales, par essais successifs de valeurs empiriques, serait longue; il n'est pas certain qu'elle déboucherait sur un choix univoque. La définition d'une procédure automatique serait quant à elle relativement complexe, tant au niveau de la formulation mathématique que des algorithmes et programmes correspondants.

Dans le cas de l'albacore, le problème est résolu en simplifiant le modèle général et en ne prenant en compte que les deux termes : constant et proportionnel à l'accroissement de taille. Cette simplification s'appuie sur les observations disponibles par ailleurs; elle semble particulièrement bien adaptée dans le cas présent. La courbe de croissance de l'albacore est en effet marquée par une phase de croissance juvénile lente, suivie d'une accélération très nette. Une variabilité de l'âge ou de la date de l'accélération de croissance se traduit ainsi par des écarts types de taille importants aux âges intermédiaires.

Dans le cas d'autres espèces, il est probable qu'on pourra également simplifier le modèle de variation des écarts types de taille, en revenant cette fois au modèle de Schnute et Fournier. Plus généralement, il est évidemment souhaitable, et heureusement relativement courant, de disposer d'observations qui permettent de s'orienter dans le choix du type de modèle à retenir.

En tout état de cause, l'un des résultats remarquables obtenus ici est la faible sensibilité de l'estimation des captures par âge, aux valeurs des paramètres du modèle de répartition des tailles. Entre un modèle à écarts types de taille peu variables (variations d'un facteur 1, 2), et un modèle éminemment variable (facteur 3), les estimations de captures diffèrent d'environ 5 %. Seul fait exception à cette observation le dernier groupe d'âge.

On notera d'ailleurs que pour ce dernier groupe la croissance n'est déterminée qu'avec une forte incertitude (Gascuel et al. 1992). Ceci explique sans doute, au moins pour partie, les écarts observés entre les estimations de captures par « slicing » et par ajustement des clés. Il serait ainsi préférable, dans ce cas, de considérer le groupe 4 comme un groupe +. Cette démarche se heurte cependant à l'importance tant pondérable qu'économique des gros albacores, qui représentent actuellement environ 50 % des captures en poids. Par suite, il est évidemment souhaitable d'en connaître la dynamique aussi bien que possible.

Cette difficulté, concernant les gros albacores, en rejoint d'ailleurs une autre liée aux variations du sex-ratio en fonction de la taille. Ces variations, marquées par une prédominance des mâles au-delà de 145 cm de longueur, semblent découler d'un dimorphisme sexuel de croissance (Bard et Capisano 1991; Capisano et Fonteneau 1991), qui affecterait essentiellement les âges 5 et supérieurs (Gascuel et al. 1992). Dès lors, il serait naturellement souhaitable d'établir une clé qui permette de distribuer les captures par âge et par sexe. La méthode d'ajustement des clés pourrait ainsi être combinée avec la méthode de décomposition par sexe de Garcia et Albaret (1977). En l'absence de toute donnée concernant la croissance de chaque sexe, cette approche reste cependant impossible actuellement, dans le cas de l'albacore de l'Atlantique Est.

Conclusion

La constitution de clés taille/âge, à partir d'une détermination de l'âge par lecture des pièces anatomiques dures, demeure bien évidemment souhaitable. Elle permet notamment de prendre en compte la variabilité de croissance de l'espèce considérée. Cette approche est cependant extrêmement coûteuse en temps. Elle n'est pas toujours possible, en particulier en zone intertropicale, par suite des difficultés fréquentes de la détermination de l'âge. En revanche, il est extrêmement courant, y compris dans ce dernier cas, de disposer d'un modèle de croissance, voire d'observations, éventuellement fragmentaires, concernant les écarts types de taille aux âges. La méthode d'ajustement des clés, utilisant un algorithme itératif proche de celui présenté par Kimura et Chikuni (1987), apparaît alors particulièrement bien adaptée. Elle est de toute évidence préférable à la méthode très rudimentaire du « slicing ». Elle débouche sur des résultats identiques à ceux obtenus par le maximum de vraisemblance. Elle présente, vis-à-vis des méthodes classiques de décompositions polymodales, qui ont par ailleurs une portée plus générale, l'avantage de la simplicité et de la souplesse. Tout type de croissance, décrite de manière discrète, peut ainsi être prise en compte. Les variations des écarts type de taille en fonction de l'âge peuvent suivre des modèles divers; d'autres modèles que ceux présentés peuvent être considérés sans difficultés. De même, on peut envisager de manière très simple des lois de répartition des tailles aux âges différentes de la loi normale.

Concernant les captures d'albacores dans l'Atlantique Est, l'application de la méthode d'ajustement des clés conduit, comparativement à la méthode du « slicing » antérieurement utilisée, à une révision sensible des estimations de captures par groupe d'âge. La proportion respective des différents groupes est corrigée; une plus grande variabilité inter-trimestrielle et inter-annuelle est observée. Il conviendra évidemment d'en analyser les conséquences éventuelles en matière d'étude de la dynamique du stock.

Remerciements

Je tiens à remercier ici, d'une part, A. Fonteneau pour l'aide précieuse qu'il m'a apportée dans la réalisation de ce travail, et d'autre part, l'ensemble des chercheurs et techniciens du Centre de Recherches Océanographiques de Dakar-Thiaroye qui ont contribué à l'établissement des statistiques de pêche utilisées.

Références

Abramson, N.J. 1970. Computer programs for fish stock assessment. FAO Fish. Tech. Pap. 101 : pag. var.

Bard, F.X. 1984. Croissance de l'albacore (*Thunnus albacares*) Atlantique d'après les données des marquages. Rec. Doc. Sci. ICCAT 20 : 104–116.

Bard, F.X. et C. Capisano. 1991. Actualisation des connaissances sur la reproduction de l'albacore (*Thunnus albacares*) en Océan Atlantique. Rec. Doc. Sci. ICCAT 36 : 158–181.

Bartoo, N.W. et K.R. Parker. 1983. Stochastic age–frequency estimation using the von Bertalanffy growth equation. U.S. Natl. Mar. Fish. Serv. Fish. Bull. 81 : 91–96.

Capisano, C. et A. Fonteneau. 1991. Analyse des fréquences de longueur, du sex-ratio et des zones de reproduction de l'Albacore, *Thunnus albacares*, de l'Atlantique. Rec. Doc. Sci. ICCAT 36 : 241–279.

Clark, W.G. 1981. Restricted least-squares estimates of age composition from length composition. Can. J. Fish. Aquat. Sci. 38 : 297–307.

Dempster, A.P., N.M. Laird, et D.B. Rubin. 1977. Maximum likelihood via the EM algorithm. J. Stat. Soc. Ser. B : Methodol. 39 : 1–22.

Fonteneau, A. 1974. Simulation des structures démographiques. Application aux populations d'albacores. Rec. Doc. Sci. ICCAT 3 : 174–179.

Fonteneau, A. 1980. Croissance de l'albacore (*Thunnus albacares*) de l'Atlantique Est. Rec. Doc. Sci. ICCAT 9 : 152–168.

Fonteneau, A. 1989. Note sur les problèmes d'extrapolation et de substitutions de strates pour l'albacore (*Thunnus albacares*) capturé par les senneurs FIS et espagnols. Rec. Doc. Sci. ICCAT 29 : 57–70.

Fonteneau, A. 1991. Modeling a single Atlantic yellowfin stock with a mixing model. Rec. Doc. Sci. ICCAT SCRS/91/30.

Fournier, D.A., J.R. Sibert, J. Majkowski, et J. Hampton. 1990. MULTIFAN a likelihood-based method for estimating growth parameters and age composition from multiple length frequency data sets illustrated using data for southern bluefin tuna (*Thunnus maccoyii*). Can. J. Fish. Aquat. Sci. 47 : 301–317.

Fridriksson, A. 1934. On the calculation of age distribution within a stock of cod by means of relatively few age-determinations as a key to measurements on a large scale. Rapp. P.-v. Réun. Cons. perm. Int. Explor. Mer 86 : 1–14.

Garcia, S. et J.J. Albaret. 1977. Utilisation de la relation sex-ratio/taille pour la décomposition par sexe des structures démographiques. Cah. O.R.T.O.M. sér. Océanogr. 15 : 83–87.

Gascuel, D., A. Fonteneau, et C. Capisano. 1992. Modélisation d'une croissance en deux stances chez l'albacore (*Thunnus albacares*) de l'Atlantique Est. Aquat. Liv. Ress. 5 : 155–172.

Hasselblad, V. 1966. Estimation of parameters for a mixture of normal distributions. Technometrics 8 : 431–444.

Hoenig, J.M. et D.M. Heisey. 1987. Use of a log-linear model with the EM algorithm to correct estimates of stock composition and to convert length to age. Trans. Am. Fish. Soc. 116 : 232–243.

Kimura, D. 1977. Statistical assessment of the age–length key. J. Fish. Res. Board Can. 34 : 317–324.

Kimura, D. et S. Chikuni. 1987. Mixtures of empirical distributions: an iterative application of the age–length key. Biometrics 43 : 23–35.

MacDonald, P.D.M. et T.J. Pitcher. 1979. Age groups from size frequency data: a versatile and efficient method of analyzing distribution mixtures. J. Fish. Res. Board Can. 36 : 987–1001.

Manooch, C.S. III et J.A. Hinkley. 1991. Preliminary age study of yellowfin tuna collected from the equatorial Eastern Atlantic. Rec. Doc. Sci. ICCAT 36 : 515–522.

Pauly, D. 1987. A review of the ELEFAN system for analysis of length frequency data in fish and aquatic invertebrates, p. 7–34. *Dans* D. Pauly et G.R. Morgan [ed.] Length based methods in fisheries research. ICLARM Conference Proceedings, 13,688 International Center for Living Aquatic Resource Management, Manila, Philippines, and Kuwait Institute for Scientific Research, Safet, Kuwait.

Sainsbury, K.J. 1980. Effect of individual variability on the von Bertalanffy growth equation. Can. J. Fish. Aquat. Sci. 37 : 241–247.

Schnute, J. et D. Fournier. 1980. A new approach to length frequency analysis: growth structure. Can. J. Fish. Aquat. Sci. 37 : 1337–1351.

Westrheim, S.J. et W.E. Ricker. 1978. Bias in using an age–length key to estimate age–frequency distribution. J. Fish. Res. Board Can. 35 : 184–189.

Estimation of Size Selectivity and Movement Rates from Mark–Recovery Data

Alejandro Anganuzzi,[1] Ray Hilborn, and John R. Skalski

School of Fisheries WH-10, University of Washington, Seattle, WA 98195, USA

Anganuzzi, A., R. Hilborn, and J.R. Skalski. 1994. Estimation of size selectivity and movement rates from mark–recovery data. Can. J. Fish. Aquat. Sci. 51: 734–742.

Size selectivity, movement rates among spatial strata, and size-dependent mortality rates were estimated from mark–recovery data of Pacific halibut (*Hippoglossus stenolepis*). Growth rates, area- and time-specific fishing mortality on fully vulnerable individuals, and tag return rates were assumed known from other data. We obtained similar estimates from a model that considered movement to take place immediately after tagging and a model that assumed that movement takes place once each year. The inability to distinguish between one-time and annual movement is most likely due to the fact that tagged juveniles were not recovered until 3–5 yr later when they became vulnerable to the adult fishery.

La sélectivité en fonction de la taille, le taux de déplacement entre les strates spatiales et le taux de mortalité dépendant de la taille ont été estimés à partir de données de marquage–recapture du flétan du Pacifique (*Hippoglossus stenolepis*). On a posé que le taux de croissance, la mortalité par pêche propre à un zone et à une période d'individus entièrement vulnérables et le taux de retour des étiquettes étaient connus par ailleurs. Nous avons obtenu des estimations similaires à partir d'un modèle qui tenait compte du déplacement immédiatement après le marquage et un modèle qui supposait que le déplacement avait lieu une fois par année. L'incapacité de faire la distinction entre le déplacement à un moment et le déplacement annuel est très probablement due au fait que des juvéniles marqués n'étaient récupérés que 3 ou 5 ans plus tard lorsqu'ils devenaient vulnérables à la pêche des adultes.

Received October 8, 1992
Accepted October 25, 1993
(JB649)

Reçu le 8 octobre 1992
Accepté le 25 octobre 1993

Nearly all fishing methods are size selective, with some sizes of fish more likely to be captured than others (Ricker 1975). Size selectivity may arise from the mechanics of the fishing gear, the size-specific behavior of the fish, or the interaction of the spatial distribution of the fish and the fishing effort. There are two principal approaches to estimating the size- (or age-) selectivity pattern in a fishery: experimental fishing with different gears (Hamley and Reiger 1973; Ricker 1975) or analysis of catch-at-age data using either virtual population analysis (Pope 1972) or statistical catch-at-age methods (Fournier and Archibald 1982; Deriso et al. 1985; Hilborn and Walters 1992).

To our knowledge, mark–recovery data have not been used to estimate the relationship between size and vulnerability. Mark–recovery experiments used to estimate survival or abundance usually assume size-independent probability of capture, or an assumed size–vulnerability relationship (Seber 1982).

A number of researchers (Darroch 1961; Iwao 1963; Arnason 1972, 1973; Ishii 1979; Sibert 1984; Schwarz 1988; Hilborn 1990; Deriso et al. 1991; Skalski et al. 1993) have attempted to determine movement among spatial strata from mark–recovery data. These authors have found that such estimation is possible if (1) there is marking and recoveries simultaneously in all spatial strata, (2) independent data are available on the probability of capture or, at least, relative recoveries effort, (3) the tag return rate (number of tags returned per number of tagged fish recaptured) is known, and (4) natural mortality is assumed constant in time and space. For example, Skalski et al. (1993) analyzed movements of juvenile Pacific halibut (*Hippoglosus stenolepis*) using fishing mortalities derived from the analysis of commercial catch-at-age data. Their movement model assumed that the fish moved instantly upon tagging and would remain in the destination area until they were recruited to the commercial fishery, were captured, and their tags were returned.

They found some systematic patterns in residuals, with too many tag recoveries in early years in some areas and too many tag recoveries in later years in others. They suggested that these trends in residuals might be due to a structural error in the model because the fish move continuously over their entire lives, rather than in one episode immediately after tagging. Another concern with their analysis was that the fishing mortality rates, and therefore the probabilities of recapture, of the tagged fish were determined from the analysis of commercial catch-at-age data. There is an 80-cm size limit for commercially caught halibut, but tagged halibut less than 80 cm may be retained if the tags are returned to the International Pacific Halibut Commission (IPHC). This means that the size selectivity, and therefore the fishing mortality rates, for the tagged halibut may be quite different from the size selectivity for untagged halibut.

The purpose of this study is to determine if size selectivity can be estimated from mark–recovery data simulta-

---

[1] Current address: Inter-American Tropical Tuna Commission, c/o Scripps Institution of Oceanography, 8604 La Jolla Shores Dr., La Jolla, CA 92093, USA.

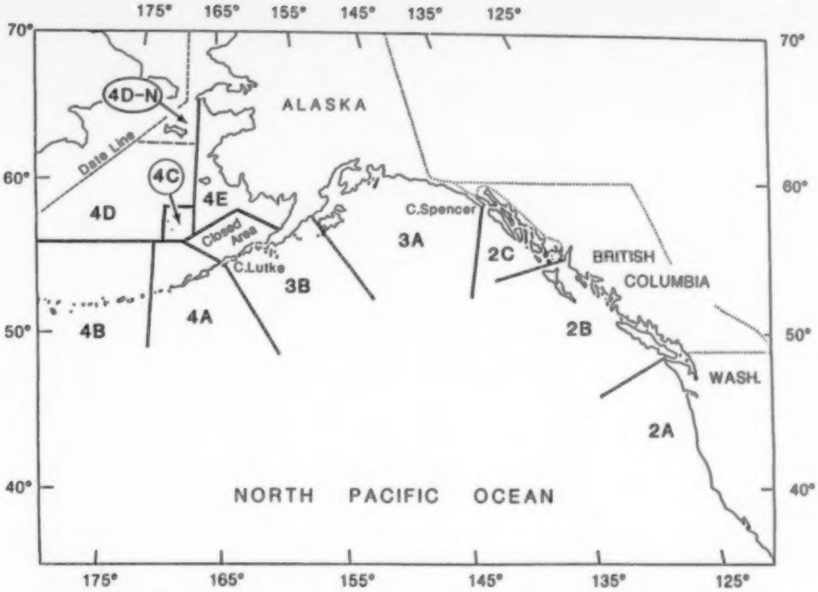

FIG. 1. Regulatory areas of the International Pacific Halibut Commission.

TABLE 1. Distribution of releases and recoverires of fish tagged in areas 3a and 3b. The percentages of recoveries from each area of release that occur in each area of recovery are given in parentheses.

	Area of release	
Area of recovery	3a	3b
2a Washington	5 (1.3%)	4 (1.8%)
2b British Columbia	100 (25.4%)	36 (16.0%)
2c Southeast Alaska	35 (8.9%)	22 (9.8%)
3a eastern area 3	249 (63.2%)	91 (40.4%)
3b western area 3	5 (1.3%)	72 (32.0%)

neously with movement rates among strata. Our model differs from that of Skalski et al. (1993) in that (1) we estimate selectivities instead of using "known" values, (2) we assume that movement takes place annually, (3) we allow for survival to be size dependent, and (4) we assume no differences in growth among areas.

Materials and Methods

In 1980, 32 620 halibut were tagged and released from two chartered trawl vessels (IPHC 1980); in 1981, 25 493 fish were tagged from chartered trawl vessels. These releases took place primarily in the Gulf of Alaska (IPHC regulatory areas 3a and 3b, Fig. 1), although there were a small number of releases off the Alaskan panhandle. Hauls of less than 15 min towing time were made, and all halibut recovered were immediately placed in a live-box on deck. Fish that appeared to be in good condition were measured and then marked with a spaghetti tag on the dark side.

Fishermen or shore workers who detect tagged fish are requested to return the tags to the IPHC with information on dates and places of capture, as well as the lengths of the fish. A reward for returning an IPHC tag is a baseball-style cap.

Analysis and Results

Most tag returns come from the longline fishery; however, there are also returns from trawl, troll, recreational, and other fisheries. For the purposes of this analysis, we use only returns from the longline fishery for fish that were released at lengths less than 65 cm. Mortality caused by fishing gears other than longline are considered natural mortality. Table 1 shows the distribution of recoveries from fish released in regulatory areas 3a and 3b. These data are aggregated for the two release years, 1980 and 1981.

Several general patterns are clear; most 3a releases are recovered in 3a, and 3b releases are recovered in slightly higher frequency in 3a than in 3b. About 25% of the 3a releases and 16% of the 3b releases were recovered in 2b. There were few recoveries in 2c despite the fact that 2c is between the northern areas (3a and 3b) and area 2b. While 2c is smaller than 2b, the paucity of recoveries in 2c seems a little surprising.

In a simple world, Table 1 could stand as the analysis of the tagging experiment, and the percentages could be estimates of movement rates between areas. This would require the assumption of equal fishing mortality, equal natural mortality, and equal tag-return rates in all areas. While we have few data on the relative magnitude of natural mortality and tag-return rates, we do know that fishing mortality is very different among areas. More specifically, we know that fishing mortality rates have generally been higher in 2a and 2b than in the more northerly areas, and, additionally, that younger and smaller fish are more vulnerable to the fishing gear in 2a and 2b than in 3a and 3b.

Each of these factors means that an individual fish that moves to 2a or 2b is more likely to be captured than a fish that remains in 3a or 3b. Therefore, movements seen in Table 1 will overestimate movements from 3a and 3b to 2a and 2b.

In order to take into account the differential probabilities of capture, a model that explicitly incorporates growth,

TABLE 2. Notation used in the model.

g	Index identifying a group of fish tagged and released over s short period of time
k	Identifies size-at-release class of fish from a given group
$t(g)$, $i(g)$	Year and area of release for group g
l_t	Length of fish at year t
a, b	Parameters of the von Bertalanffy growth equation
N^0_{gk}	Number of fish released in group g at size k
λ	Probability that a tag is lost due to tag shedding or tag-induced mortality
$\mathbf{n}_t$	Expected number of tagged fish alive just prior to movement in area i, year t, released in area g at size k
$\mathbf{n}'_t$	Expected number of tagged fish alive after movement
$\mathbf{n}''_t$	Expected number of tagged fish surviving the fishery
$\mathbf{M}_t$	Transition matrix indicating proportion of fish moving between areas in year t
$\mathbf{U}_t$	Exploited fraction of the population of tagged fish in year t
$\mathbf{C}_t$	Expected catch of tagged fish in year t
h_{it}	Instantaneous longline fishing mortality rate for fully recruited fish in area i and year t
$v_i(l_t)$	Vulnerability of fish in area i at length l_t
b_{1i}, b_{2i}	Parameters of the vulnerability function
$\mathbf{S}^f_t$	Fraction of fish surviving the fishery in year t
$\mathbf{S}^{\text{tot}}_t$	Fraction of fish surviving from recreational fishery and other causes of mortality in year t
$s^{\text{nat}}(l_t)$	Survival from natural causes for a fish of length l_t
l_s	Minimum size of fish with constant natural mortality rate
k_s	Slope parameter of the size-dependent survival function
$\mathbf{S}^{\text{spt}}_t$	Fraction of fish surviving from the recreational fishery in year t
f^{spt}_{it}	Instantaneous fishing mortality rate from the recreational fishery in area i and year t
$\mathbf{R}(t)$	Probability that a fish caught is returned to the IPHC
$\mathbf{X}_t$	Number of tagged fish recovered in year t from release group g and released at size k

fishing mortality, vulnerability to fishing gear, and natural mortality is needed. Such a model is described below.

Model Description

The following description of the model is based on the fate of a single size-at-release class. The notation is summarized in Table 2. We assume that the annual cycle of events for tagged halibut has three components: (1) movement, (2) fishing, and (3) natural mortality and growth. We also assume that fishing takes places in short periods of time so that we do not need to consider natural mortality during the fishing period.

A group of tagged fish, g, from a given size-at-release class k is released at year $t(g)$. To simplify the notation, we drop the subscripts indexing the release group g and the size-at-release k. The expected number of tagged fish alive after release is then

$$(1)\qquad N_{it} = N_{i(g)t(g)}(1 - \lambda)$$

where λ is the probability that the tag is lost or that the tagged fish died due to tag-induced mortality soon after the release. Using vector notation, if we denote the area-specific expected number of tagged fish available by $\mathbf{n}_t$, then the movement between areas following the release can be represented by

$$(2)\qquad \mathbf{n}'_t = \mathbf{M}_t\mathbf{n}_t$$

where $\mathbf{M}_t$ is a transition matrix whose elements m_{ij} represent the proportion of tagged fish that moved to area i from area j in a given time interval. According to the above definition of the elements of $\mathbf{M}_t$, the columns of the matrix are constrained to add up to 1, therefore preserving the total number of fish.

The expected number of tagged fish surviving the longline fishery is

$$(3)\qquad \mathbf{n}''_t = \mathbf{S}^f_t\mathbf{n}'_t$$

where $\mathbf{S}^f_t$ is a diagonal matrix representing the probability of survival from the longline fishery. If we define the finite mortality rate in the longline fishery as

$$(4)\qquad \mathbf{U}_t = \mathbf{I} - \mathbf{S}^f_t$$

where $\mathbf{I}$ is the identity matrix, the expected catch is then

$$(5)\qquad \mathbf{C}_t = \mathbf{U}_t\mathbf{n}'_t$$

where $\mathbf{U}_t$ is a diagonal matrix whose nonzero elements represent the finite longline fishing mortality rate, that is

$$(6)\qquad u_{ii} = 1 - e^{-h_{it}v_i(l_t)}$$

where h_{it} is the instantaneous longline fishing mortality rate for the fully recruited fish in area i and year t and $v_i(l_t)$ is the area- and size-specific vulnerability to longline gear calculated as

$$(7)\qquad v_i(l_t) = \frac{1}{(1 + e^{-b_{2i}(l_t - b_{1i})})}$$

where l_t is the length at time t of a tagged fish, and b_{1i} and b_{2i} are parameters that we assume to be potentially different for each area i.

Growth in length is modelled using a von Bertalanffy model of the form

$$(8)\qquad l_{t+1} = a + bl_t.$$

TABLE 3. Summary of estimated parameter values and discrepancies for each model. Parameters marked with an asterisk were assumed fixed at the values listed. Standard errors for the parameters are given in parentheses.

	Model 1	Model 2	Model 3	Model 4
Survival, $s^{\text{nat}}(l_t)$	0.599 (0.018)	0.586 (0.049)	0.80*	0.80*
Survival size factor, k_s	0*	0*	−0.438 (0.208)	−0.522 (0.176)
Tag loss/reporting rate, $1 - \lambda$	0*	1.365 (0.683)	0.368 (0.137)	0.249 (0.089)
Movement parameters, m_{ij}				
From 3b to 3a	0.378 (0.143)	0.111 (0.055)	0.110 (0.059)	0.144 (0.082)
From 3b to 2c	0.087 (0.080)	0.024 (0.023)	0.027 (0.028)	0.049 (0.060)
From 3b to 2b	0.099 (0.074)	0*	0*	0*
From 3b to 2a	0.021 (0.038)	0*	0*	0*
From 3a to 2c	0.095 (0.069)	0.025 (0.038)	0.026 (0.045)	0.036 (0.046)
From 3a to 2b	0.186 (0.079)	0.014 (0.035)	0.022 (0.046)	0.055 (0.054)
From 3a to 2a	0.012 (0.025)	0*	0*	0*
From 2c to 2b	0*	0.290 (0.508)	0.281 (0.598)	0.163 (0.313)
From 2c to 2a	0*	0*	0*	0*
From 2b to 2a	0*	0.043 (0.059)	0.042 (0.061)	0.036 (0.049)
Selectivity parameters				
b_{13b}	112.47*	112.47*	112.47*	77.84 (13.99)
b_{23b}	0.092*	0.092*	0.092*	0.123 (0.095)
b_{13a}	112.47*	112.47*	112.47*	87.92 (6.93)
b_{23a}	0.092*	0.092*	0.092*	0.149 (0.056)
Deviance	1050.40	998.19	1174.69	928.92
AIC	1066.40	1014.19	1190.69	952.92

After growth, the expected number of tagged fish alive prior to the next movement episode is

$$(9)\quad \mathbf{n}_{t+1} = \mathbf{S}_t^{\text{tot}}\mathbf{n}_t''$$

where the total survival, $\mathbf{S}_t^{\text{tot}}$, consists of survival from recreational fishing mortality and survival from all other mortalities (predation, incidental catch, disease, etc.):

$$(10)\quad \mathbf{S}_t^{\text{tot}} = \mathbf{S}_t^{\text{spt}} s^{\text{nat}}(l_t).$$

The elements is the diagonal of $\mathbf{S}_t^{\text{spt}}$ represent the survival from spot fishing, calculated as

$$(11)\quad s_{ii}^{\text{spt}} = e^{-f_{ii}^{\text{spt}}}$$

where f_{ii}^{spt} is the instantaneous fishing mortality rate from the recreational fishery in area i and year t.

The natural survival is allowed to be size dependent through the following relationship:

$$(12)\quad s^{\text{nat}}(l_t) = \begin{cases} s^{\text{nat}}(l_s)\left(2 - e^{\left(\frac{l_t - l_s}{l_s}\right)^{k_s}}\right), & \text{for } l_t < l_s \\ s^{\text{nat}}(l_s) & \text{for } l_t \geq l_s \end{cases}$$

where l_t is the length at time t, and l_s is a threshold size (assumed to be 80 cm). In this formulation, the natural mortality depends nonlinearly on size through the parameter k_s until a threshold size l_s (e.g., the legal size limit) is reached. From that point on, survival is assumed constant. If we were to estimate survival as size independent, we can set $k_s = 0$ and estimate s^{nat} as another parameter.

Given this model, for any parameters, and given the known number of fish released $N_{i(g)t(g)}$, we can use the above equations to predict the expected number of tags from the release group g and size-at-release class k returned after recapture in area i, year t, as

$$(13)\quad E(\mathbf{X}_t) = \mathbf{R}_t\mathbf{C}_t$$

where $\mathbf{R}_t$ is a diagonal matrix whose positive elements are the area-specific reporting rates.

Therefore, we can find the likelihood of the parameters (conditional on the observed recoveries x_{it}, the elements of the vector $\mathbf{X}_t$) for any group g, released at a size k, using a multinominal likelihood:

$$(14)\quad \mathcal{L}_{gk}(\text{parameters}|X_t) = \frac{N_{t(g)i(g)}!}{(\Pi_i \Pi_t x_{it}!)z!}\left(\prod_t \prod_i p_{it}^{x_{it}}\right)q^z$$

where

$$q = 1 - \Sigma_i \Sigma_t p_{it}$$

$$z = N_{t(g)i(g)} - \Sigma_i \Sigma_t x_{it}$$

where $N_{t(g)i(g)}$ is the number of tagged fish released in this group and size-at-release class and x_{it} is the number of tags returned from the fishery in area i at time t (for this group and size-at-release class). The ps are the probabilities that a tagged fish will be captured and returned from a space–time stratum, q is the probability that a tagged fish will never be returned, and z is the number of tags not returned. The likelihood given above is for a single tag release group and a single size-at-release class. The likelihoods of each release group and size class are multiplied to yield a total likelihood for all of the data:

$$(15)\quad \mathcal{L}_{\text{total}}(\text{parameters}|X_t) = \prod_k \prod_g \mathcal{L}_{gk}(\text{parameters}|X_t).$$

The parameters in this model may be either estimated or assumed as known from other analyses. In principle, 20 annual movement parameters can be estimated for the five areas considered in this analysis. However, there is strong evidence from independent studies that juvenile halibut migrate to the southern regions with almost negligible movement towards the northernmost area. Furthermore, in the data available for this analysis, there were virtually no recoveries of tags more than two areas away from the area of

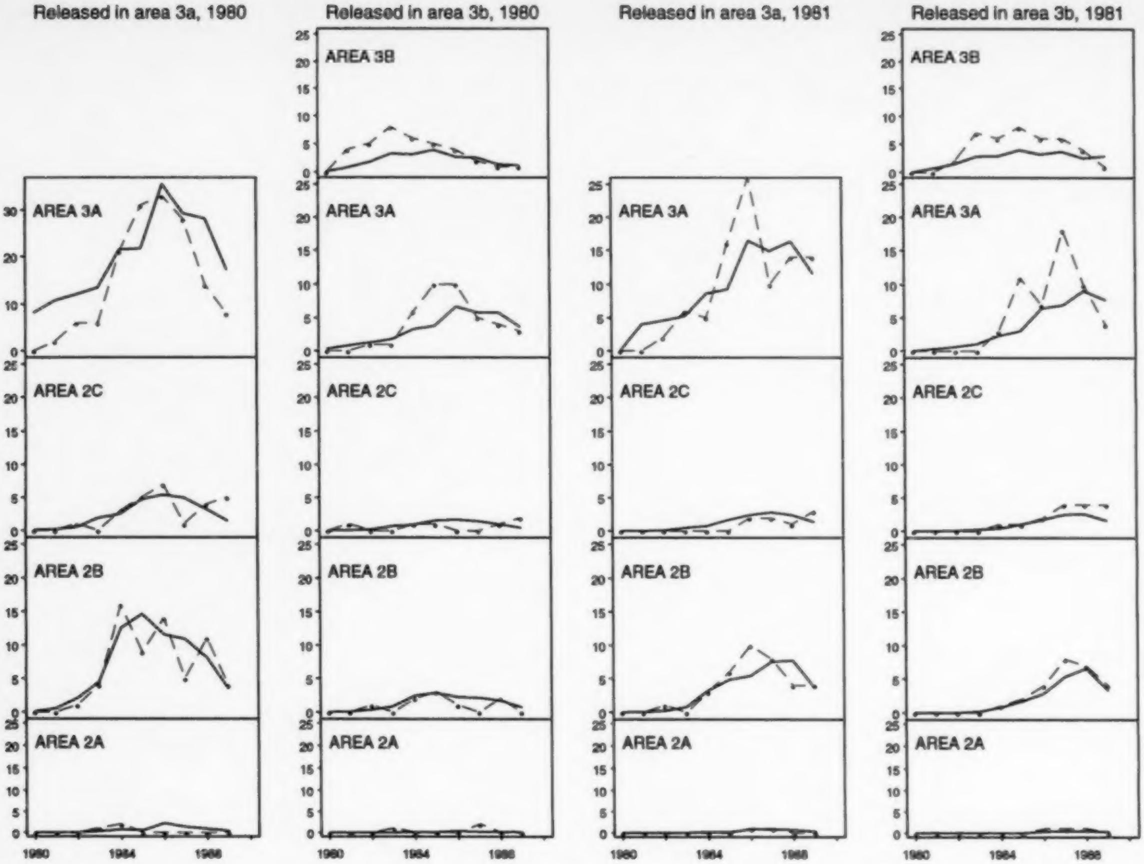

FIG. 2. Observed and predicted pattern of recoveries for Model 2. The horizotal axis represents the year of recovery; the data are grouped by year and area of release. Observed data are shown as lines with dots; solid lines represent model predictions.

release in the year of release. Therefore, we decided to limit to six the number of movement parameters to be estimated.

A different complication arises with the interpretation of the parameter λ. In the description of the model, this parameter was presented as a tag loss occurring shortly after release, loss due to tag-induced mortality, or tag shedding. However, we could also interpret $(1 - \lambda)$ as a factor multiplying the assumed reporting dates. Actually, it is not possible to discriminate between these two potential parameters, and therefore, we will interpret them as a combined effect.

The following assumptions are made for this model: (1) tagged fish are a representative sample of the population, (2) all data on marking and recovery time, area, and size are correctly recorded, (3) the tag loss and tag-induced mortality, represented by the parameter λ, occur only immediately after tagging, (4) tagging does not affect the movements, growth, or vulnerability of the fish, and (5) the fate of each tagged animal is independent of the fate of other tagged animals.

In an earlier analysis (Skalski et al. 1993), we assumed that movement took place once, instantaneously just after tagging. Because we wish to compare the results of the model considered here with those of a one-time movement model, we can modify the current model to be a one-time movement model simply by setting $m_{ij} = 0$ for all years except the year of tagging.

Results

We compare four variants of the model. Model 1 is one-time movement with selectivities fixed, using values obtained from catch-at-age/length analysis (this is the model described in Skalski et al. 1993). Model 2 is annual movement with selectivities fixed. Model 3 incorporates size dependency in the survival from sources of mortality other than the longline fishery. Model 4 incorporates the estimation of the selectivities in areas 3a and 3b. Table 3 summarizes the different models and their results.

To compare the different models, we use a measure of the discrepancy between the model and the data, known as Akaike's Information Criterion (AIC). The AIC is defined as (Akaike 1972):

$$(16) \quad \mathrm{AIC} = D + 2p$$

where p is the number of estimated parameters and D is the deviance, defined as (McCullagh and Nelder 1983)

$$(17) \quad \text{Deviance} = -2(\log \mathcal{L}(\text{parameters}|\text{data}) - \log \mathcal{L}(\text{data}|\text{data})).$$

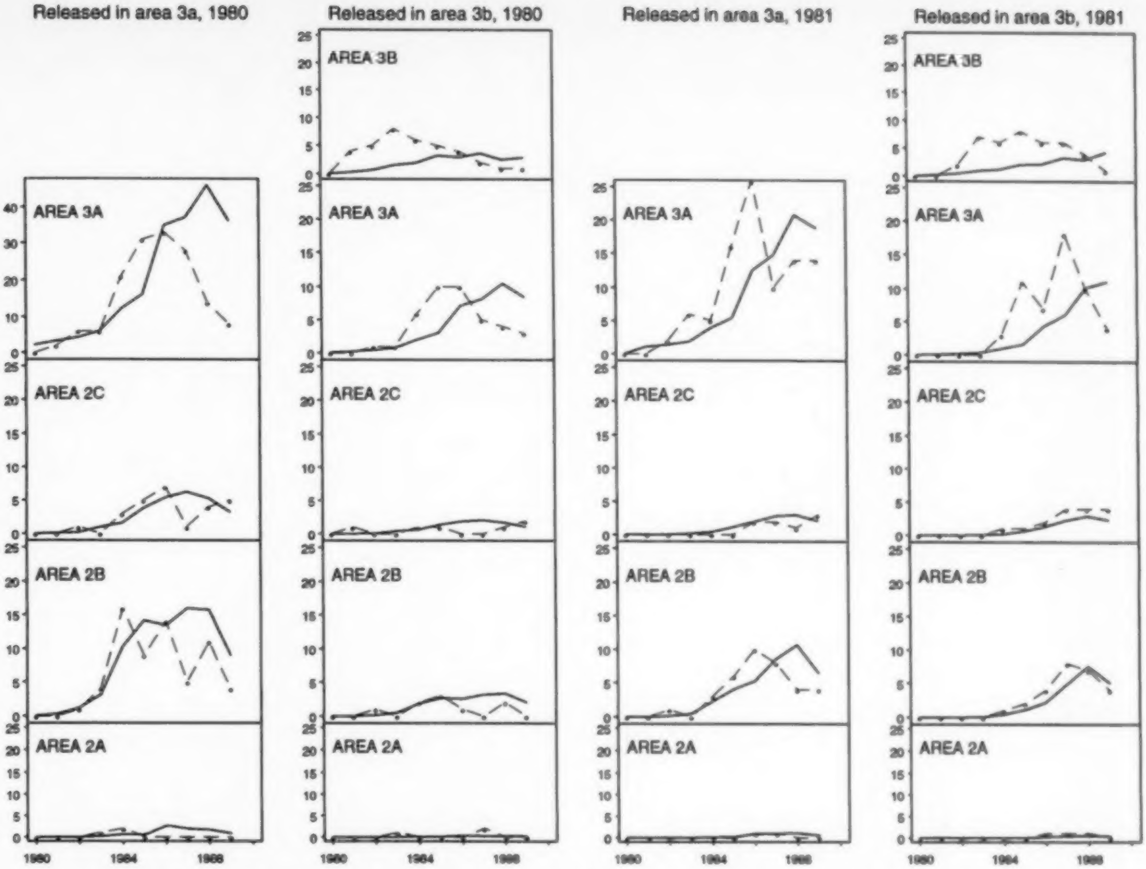

FIG. 3. Observed and predicted patterns of recoveries for Model 3. See caption to Fig. 1 for further explanation.

The second term in the above equation, $\log \mathcal{L}(\text{data}|\text{data})$, represents the log-likelihood of the "full" model (a model with as many parameters as observations), computed by setting the expected recoveries equal to the observed recoveries. The asymptotic distributional properties of the deviance can be used to build a model selection strategy based on hypothesis testing when the competing models are nested. The models that we present are not nested, and therefore, we based our model comparisons on the AIC statistic, a strategy that does not require the models to belong to the same hierarchy. For a review of the application of the AIC statistic to model selection in mark–recovery experiments, see Lebreton et al. (1992).

We can see in Table 3 that the continuous-movement model (Model 2) provides a better fit to the data than the one-time movement model. Figure 2 presents the observed and predicted recoveries for Model 2; the line with the dots represents the observed recoveries, and the solid line the predicted values. The x-axis in each case is the year of recovery, and the data are shown for the four groups of tagged fish considered, those released in 3a in 1980, 3b in 1980, 3a in 1980, and 3b in 1981. Note the systematic bias in recoveries, particularly in 3a and 3b, where more tags were recovered in earlier years than the model predicts.

There is a high correlation (−0.929) between the reporting rate/tag loss parameter and the natural survival parameter which suggests that these parameters are not well determined. This is not unexpected because they operate in the model in a way analogous to the slope and intercept parameter in a linear regression. There is also another problem with the estimation of the natural survival parameter: the catch-at-age analyses that provided the estimates of fishing mortality are based on the assumption that the natural survival is 0.80 for recruited fish (larger than 80 cm). Therefore, for consistency and try to obtain a better definition of the parameters, in Model 3 we model survival as defined in equation 12, setting the threshold size l_s to 80 cm and estimating the parameter k_s from the data. The results from this model indicate that these changes cause the performance of the model to deteriorate (Table 3; Fig. 3) and that other alternative structures should be explored. We do this in Model 4 by estimating the selectivity parameters for the two northern areas, 3a and 3b. In principle, we could have attempted to estimate the selectivities for other areas as well, but due to the small number of recoveries in those areas, it is unlikely that the parameter estimates would have been well defined. The results from Model 4 show a significant improvement, both in terms of deviance and in the pattern of the residuals.

Figure 4 shows the observed and predicted recoveries for Model 4. Note that the systematic pattern of residuals has dis-

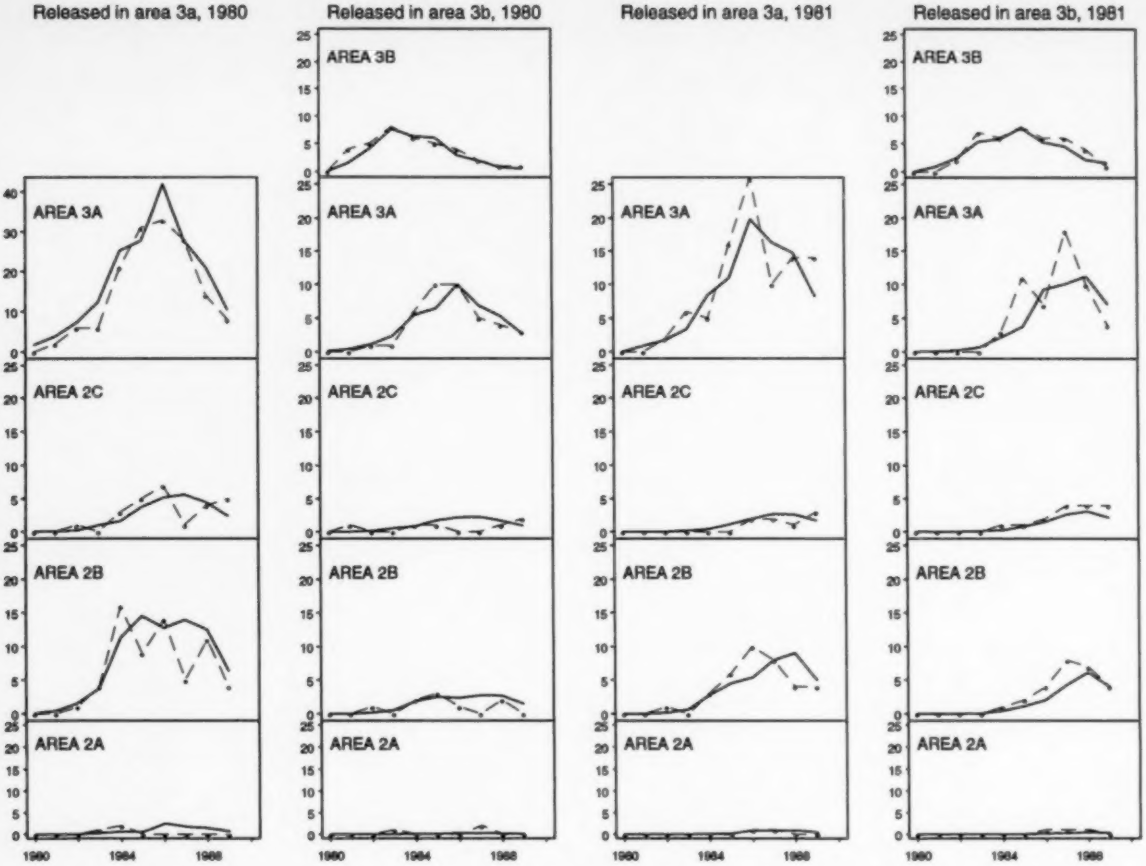

FIG. 4. Observed and predicted patterns of recoveries for Model 4. See caption to Fig. 1 for further explanation.

appeared and the fits appear very good. The reason the fit has improved is that the mark–recovery data indicate a far different selectivity pattern than that determined from catch-at-age analysis and length data from commercial data.

Figure 5 shows the selectivity patterns in 3a and 3b estimated from catch-at-age/length data and from Model 4. Note that Model 4 predicts that the fish become vulnerable much sooner, and therefore, it is able to "fit" the large number of early recoveries in 3a and 3b that the other models were unable to fit .

The differences in selectivity between the estimated rates and those derived from the catch-at-age/length analysis have a significant impact on the estimated movements rates between areas. In order to compare the one-time movement model with the annual movement models and the raw observed data, we have applied the annual movement rates five times to obtain the distribution of individuals 5 yr after release. Most fish were tagged at ages 3 and 4, and most recoveries were at ages 8 and 9, so we use 5 yr as a rough guide for how many years elapsed between tagging and recovery.

Table 4 shows the distribution of tagged fish after 5 yr of movement from Model 2, Model 4, and the raw data in Table 1. Note the great differences between Models 2 and 4; Model 2 needed to keep most fish in 3a and 3b to try to fit the observed recovery pattern. Because Model 2 showed such low vulnerability at the smaller sizes, there had to be many recaptures in 3a and 3b to fit the observed recoveries. Interestingly, the observed recovery pattern is quite similar to that estimated from Model 4. Finally, the movements from the one-time model and the annual model (Models 1 and 2) are quite similar.

One of the key questions in fitting complex nonlinear models is the confounding of model parameters. Table 5 shows the parameter correlation matrix for Model 4. The largest values correspond to confounding between the mortality rate and tag loss/recovery, which occurs in any tagging analysis. There is also some confounding between movement rates between the more southerly areas. This is expected because there were no releases in 2c, 2b, or 2a, and releases in those areas would be required to determine the exact migratory path between them. This table is derived from the variance–covariance matrix which can be used to provide estimates of the variance of the parameters. A word of caution is necessary about the interpretation of the correlation between parameter estimates. This correlation measures the linear relationship between the parameters, and if the parameters are nonlinearly related (as is often the case with constrained parameters), these correlations might be underestimating the degree of confounding. A more ade-

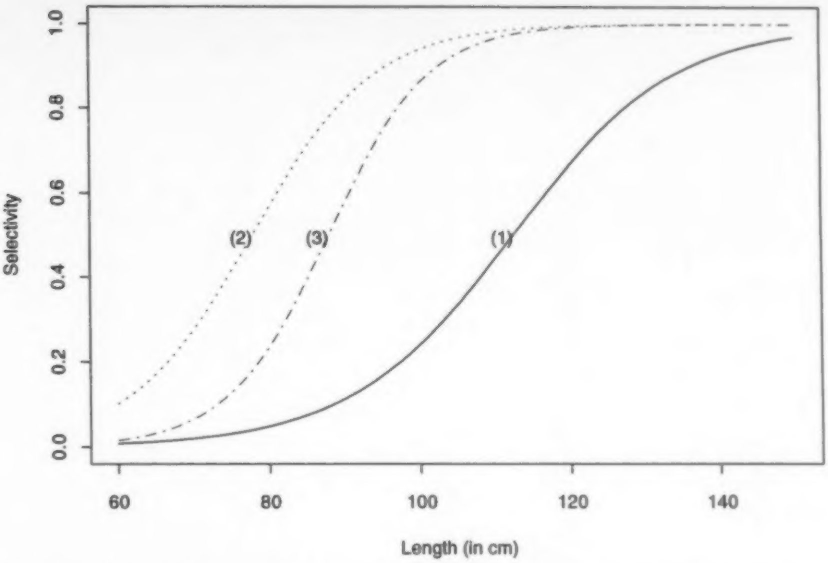

FIG. 5. Size-selectivity pattern estimated from Model 4, and curves drawn from assumed values: (1) selectivity curve derived from catch-at-age/length analyses and assumed for areas 3a and 3b in Models 1, 2, and 3, (2) selectivity curve estimated in Model 4 for area 3a, and (3) selectivity curve estimated in Model 4 for area 3b.

TABLE 4. Estimated distribution of individuals from areas 3a and 3b after 5 yr of movement using annual movement rates from Models 2 and 4. All numbers are percentages of fish still alive afer 5 yr. Raw recovery data and one-time movement rates from Model 1 are also shown.

	From area							
	Model 2		Model 4		Raw data (Table 1)		Model 1	
To area	3b	3a	3b	3a	3b	3a	3b	3a
3b	42		27		32		42	
3a	43	79	41	56	40	63	37	71
2c	7	7	15	11	10	9	9	10
2b	8	13	16	30	16	25	10	18
2a	1	1	1	3	2	1	2	1

quate way to assess the confounding between the parameters (but expensive in terms of computing time) would be to apply a bootstrap procedure and do pairwise plots of the bootstrap parameter estimates, or carry out a profiling of the parameters.

Discussion

We have demonstrated that mark–recovery data can be used to estimate size selectivity and movement rates simultaneously. In particular, estimation of selectivity parameters from tagging data is appealing because we know the initial length distribution of the fish. Therefore, if we have a significant number of recoveries by the commercial fishery shortly after the tagging experiment, the selectivity parameters mith be well defined. The general approach of nonlinear minimization of a likelihood has been called "tuned simulation" and provides a powerful framework for extending mark–recovery models beyond what can be developed analytically. Our model is fundamentally the logical extension of the work of Ishii (1979), Sibert (1984), and Hilborn (1990).

One must remember, however, that we were using assumed values for growth, fishing mortality on fully vulnerable individuals, and area-specific probability of tag return. It may be possible to estimate some of these parameters from the data as well. In particular, there were many tag returns that included the length of the fish; therefore, it is possible that growth rates could be estimated simultaneously. The estimates of movement rate are strongly affected by tag return rates, and we expect it would be most difficult to design a mark–recovery experiment that estimated tag return rates. It is also likely to be difficult to estimate fishing mortality and selectivity simultaneously (Schwarz 1988; Dorazio and Rago 1991). It may be possible to estimate both fishing

Table 5. Parameter correlation matrix for Model 4.

	m_{3a3b}	m_{2c3b}	m_{2c3a}	m_{2b3a}	m_{2b2c}	m_{2a2b}	k_s	b_{13b}	b_{23b}	b_{13a}	b_{23a}	$1 - \lambda$
m_{3a3b}	1.000											
m_{2c3b}	−0.464	1.000										
m_{2c3a}	−0.269	0.274	1.000									
m_{2b3a}	0.342	−0.422	−0.799	1.000								
m_{2b2c}	−0.386	0.423	0.814	−0.839	1.000							
m_{2a2b}	−0.056	0.060	0.145	−0.149	0.150	1.000						
k_s	0.016	−0.009	−0.027	0.005	−0.028	0.003	1.000					
b_{13b}	−0.344	−0.096	0.059	−0.037	0.071	0.015	−0.000	1.000				
b_{23b}	0.207	0.055	−0.037	0.023	−0.044	−0.008	−0.020	−0.745	1.000			
b_{13a}	0.157	−0.064	−0.096	−0.098	−0.004	0.020	0.101	0.009	0.014	1.000		
b_{23a}	−0.085	0.032	0.060	0.089	−0.013	−0.015	−0.124	−0.009	−0.005	−0.779	1.000	
$1 - \lambda$	−0.008	0.000	−0.025	−0.003	−0.024	−0.010	0.823	−0.097	0.016	−0.131	0.017	1.000

mortality and selectivity if there are releases every year. It would likely be more fruitful to explore this avenue without the complicating effect of spatial strata and movement.

Naturally, our results are conditioned upon the data and the parameter values we used. In particular, it is quite possible that the selectivity pattern estimated is determined by the estimated tag return rates and fishing mortality rates.

The model presented in this paper differs from the earlier analysis of halibut in Skalski et al. (1993) in three ways: (1) growth is assumed deterministic and the same in all areas, (2) movement takes place each year, rather than in a single episode immediately after tagging, and (3) we estimate size selectivity in areas 3a and 3b from the tagging data, rather than assuming that it is known. There are a number of other additions to the model such as using area- and time-specific tag-return rates and the inclusion of sport-fishing mortality, but it appears that none of these makes a major difference in our results.

Skalski et al. (1993) found that a stochastic growth model provided movement rate estimates similar to those obtained with a deterministic growth model. Because stochastic growth is computationally burdensome, particularly in the continuous-movement model, we have assumed deterministic growth. In the earlier analysis, we were using different growth rates in different areas, but if we were to allow for different growth in each area, the computations would become even more difficult.

However, even with this change in growth assumption, we found that the results of our continuous-movement model provide substantially the same estimates of net movement rates as those obtained by Skalski et al. (1993) with the one-time movement model.

Acknowledgments

This research was made possible by the International Pacific Halibut Commission through access to its data, experience, and generous financial support. We especially thank Donald McCaughran, Pat Sullivan, Ana Parma, and Bill Clark. Rich Deriso, formerly with IPHC, provided very useful advice during this study. We would also like to thank Bob Dorazio and an anonymous reviewer for providing valuable comments and suggestions.

References

Akaike, H. 1972. Information theory and an extension of the maximum likelihood principle. In Proc. 2nd Int. Symp. Inf. Theor. Suppl. Probl. Control Inc. Theor. 267–281.

Arnason, A.N. 1972. Parameter estimation from mark–recapture experiments subject to migration and death. Res. Popul. Ecol. 12: 97–113.

Arnason, A.N. 1973. The estimation of population size, migration rates, and survival in a stratified population. Res. Popul. Ecol. 13: 1–8.

Darroch, J.N. 1961. The two-sample capture–recapture census when tagging and sampling are stratified. Biometrika 48: 241–260.

Deriso, R.B., R.G. Punsly, and W.H. Bayliff. 1991. A Markov movement model of yellowfin tuna in the eastern Pacific Ocean and some analyses for international management. Fish. Res. 11: 375–395.

Deriso, R.B., T.J. Quinn II, and P.R.Neal. 1985. Catch-at-age analysis with auxiliary information. Can. J. Fish. Aquat. Sci. 42: 815–824.

Dorazio, R.M., and P.G. Rago. 1991. Evaluation of a mark–recapture method for estimating mortality and migration rates of stratified populations. Can. J. Fish. Aquat. Sci. 48: 254–260.

Fournier, D.A., and C. Archibald. 1982. A general theory for analyzing catch at age data. Can. J. Fish. Aquat. Sci. 39: 1195–1207.

Hamley, J.M., and H.A. Regier. 1973. Direct estimates of gillnet selectivity to walleye (*Stizostendion vitreum*). J. Fish. Res. Board Can. 30: 817–830.

Hilborn, R. 1980. Determination of fish movement patterns from tag recoveries using maximum likelihood estimators. Can. J. Fish. Aquat. Sci. 47: 635–643.

Hilborn, R., and C.J. Walters. 1992. Quantitative fisheries stock assessment: choice, dynamics and uncertainty. Chapman and Hall, New York, N.Y. 570 p.

International Pacific Halibut Commission. 1980. Annual Report, Seattle, Wash. 49 p.

Ishii, T. 1979. Attempt to estimate migration of fish population with survival parameters from tagging experiment data by the simulation method. Invest. Pesq. 43: 301–317.

Iwao, S. 1963. One method for estimating the rate of population interchange between two areas. Res. Popul. Ecol. 5: 44–50.

Lebreton, J.D., K.P. Burnham, J. Clobert, and D.R. Anderson. 1992. Modeling survival and testing biological hypotheses using marked animals: a unified approach with case studies. Ecol. Monogr. 62: 67–118.

McCullagh, P., and J.A. Nelder. 1983. Generalized linear models. Monographs on statistics and applied probability. Chapman and Hall, New York, N.Y. 261 p.

Pope, J.G. 1972. An investigation of the accuracy of virtual population analysis using cohort analysis. Int. Comm. Northwest Atl. Fish. Res. Bull. 9: 65–74.

Ricker, W.E. 1975. Computation and interpretation of biological statistics of fish populations. Bull. Fish. Res. Board. Can. 191: 382 p.

Schwarz, C.J. 1988. Post-release stratification and migration models in band–recovery and capture–recapture models. Ph.D. dissertation, University of Manitoba, Winnipeg, Man. 384 p.

Seber, G.A.F. 1982. The estimation of animal abundance. MacMillan Pub., New York, N.Y. 654 p.

Sibert, J.R. 1984. A two-fishery tag attrition model for the analysis of mortality, recruitment and fishery interaction. Tech. Rep. 13. Tuna and Billfish Assessment Programme, South Pacific Commission, Noumea, New Caledonia. 27 p.

Skalski, J.R., R. Hilborn, A. Hoffman, and A. Anganuzzi. 1993. Estimation of movement rates of juvenile halibut. Ecology. (In press)

Remote Sensing in Fisheries: A Tool for Better Management in the Utilization of a Renewable Resource

James J. Simpson

Digital Image Analysis Laboratory, Scripps Institution of Oceanography, La Jolla, CA 92093, USA

Simpson, J.J. 1994. Remote sensing in fisheries: a tool for better management in the utilization of a renewable resource. Can. J. Fish. Aquat. Sci. 51: 743–771.

A framework is developed for the interactions among the diverse groups involved in operational fisheries oceanography: fishing industry, basic and operational researchers, and tactical and strategic stock assessment managers. The basis for these interactions is the need for accurate and timely information, information so complex and diverse that no single sector of the community can efficiently and economically satisfy its own information requirements. Some presently available remotely-sensed data and analysis methods that have potential for providing part of the required information are presented. Projections of future capabilities in this area also are made. The increased use of Geographical Information Systems (GIS) and near-real-time communication networks among the various sectors of the community also is discussed.

Nous élaborons un cadre représentant les interactions entre les divers groupes engagés dans l'océanographie opérationnelle des pêches : industrie de la pêche, recherche fondamentale et opérationnelle et enfin gestionnaires s'occupant des évaluations tactiques et stratégiques des stocks. La base de ces interactions est la nécessité d'obtenir une information exacte dans les meilleurs délais; l'information est si complexe et diverse qu'aucun secteur de la communauté ne peut efficacement et économiquement satisfaire à ses propres besoins d'information. Nous présentons certaines données de télédétection et des méthodes d'analyse qui sont utilisables actuellement et ont le potentiel de fournir une partie de l'information nécessaire. Nous faisons aussi des projections sur les moyens qui seront disponibles dans ce domaine. Le recours accru aux systèmes d'information géographique (SIG) et aux réseaux de communication en temps presque réel entre les divers secteurs de la communauté fait aussi l'objet d'une analyse.

Received August 10, 1993
Accepted October 27, 1993
(JC045)

Reçu le 10 août 1993
Accepté le 27 octobre 1993

Since about 1979, remote sensing has played an ever-increasing role in both the management and utilization of marine fisheries. Remote-sensing products have been used to (1) assist commercial and sports fishermen in harvesting fish from the sea (e.g., Svejkovsky 1988a, 1988b), (2) provide marine resource managers with information useful for assessing the survival of fish eggs and larvae to the juvenile stage within a given year class (e.g., Peláez and McGowan 1986; Simpson 1987), and (3) provide indications of the onset of major interannual events (e.g., ENSO and associated midlatitutde warming events) which can have a potentially devastating effect on a local fishery (e.g., Fiedler 1984). There also has been an increased awareness of the importance of both remotely-sensed and in situ environmental data for understanding the scientific basis of marine fisheries (e.g., Lasker 1975; Parrish et al. 1981; Leggett 1984; Simpson 1987), as well as for the intelligent management (e.g., Tillman 1968; Jakobsen 1978; Ushakov and Ozhigin 1987) and utilization (e.g., Hogan and Clark 1989; Laevastu and Bax 1989) of the marine fisheries resource. Moreover, recent advances in data acquisition, mass storage, and communications technologies, coupled with more powerful analysis methods, indicate that the role of satellites and environmental oceanography will expand considerably in the future. This is especially likely in terms of both near-real-time support of actual fishing activity and the retrospective analysis of historical data to determine long-term trends and variations in a fishery.

This paper discusses some of the potential benefits to be gained from increased use of remote sensing and geographical information systems in operational fisheries oceanography. It is divided into nine sections, including the present introduction. In the second section, the diverse composition and needs of the operational fisheries oceanography community are identified and some possible modes of interaction are developed. In the third section, present and anticipated types of remotely-sensed data of use to the community are discussed. Some analysis methods especially useful in operational fisheries oceanography are presented in the fourth section. In the fifth section, the representativeness of satellite data of interior ocean structure and processes is evaluated. The combined use of remote sensing/geographical information system technology to overcome the limitations of satellite data alone is discussed in the sixth section. Examples of remotely-sensed products useful to the community are provided in the seventh section. Some possible future direc-

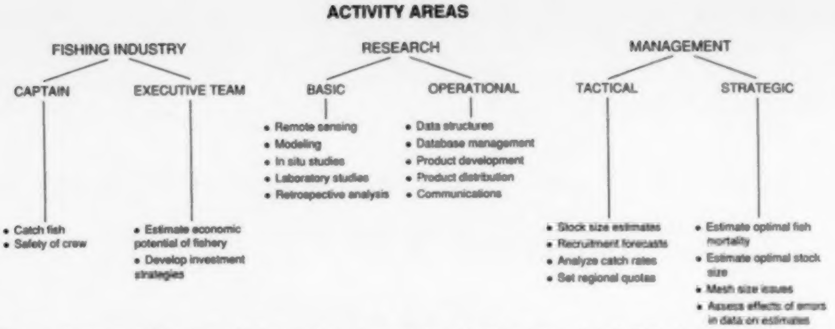
ACTIVITY AREAS
FISHING INDUSTRY
RESEARCH
MANAGEMENT
CAPTAIN
EXECUTIVE TEAM
BASIC
OPERATIONAL
TACTICAL
STRATEGIC
• Remote sensing
• Modeling
• In situ studies
• Laboratory studies
• Retrospective analysis
• Data structures
• Database management
• Product development
• Product distribution
• Communications
• Catch fish
• Safety of crew
• Estimate economic potential of fishery
• Develop investment strategies
• Stock size estimates
• Recruitment forecasts
• Analyze catch rates
• Set regional quotas
• Estimate optimal fish mortality
• Estimate optimal stock size
• Mesh size issues
• Assess effects of errors in data on estimates

FIG. 1. Conceptualization of the various sectors involved in operational fisheries oceanography and some of the functions performed by each.

tions are discussed in the last section. Finally, this paper should not be viewed as an exhaustive treatment of remote-sensing/geographical information systems in operational fisheries oceanography. Rather, it illustrates some of the potential benefits to be gained by cooperative incorporation of these technologies into the field.

An Interaction Matrix

In this section, an attempt is made to describe some activities of the various sectors of the operational fisheries oceanography community (i.e., fishing industry, tactical and strategic stock assessment managers, and basic and operational fisheries researchers) and to identify common needs and linkages between them.

Fishing Industry

The fishing industry's primary concern should be to harvest economically a given resource from the sea in such a way as to insure its continued, long-term use. Thus, the fishing industry should constantly try to optimize catch per unit of effort without jeopardizing the fecundity of the stock. Unfortunately, this has not always been the case; in some circumstances (e.g., the California sardine fishery) the desire for short-term economic gain, coupled with inadequate resource management and an inability to properly observe and recognize early, major, interannual, environmental changes in the fishery (e.g., the 1940–41 ENSO mid-latitude warming event), has contributed to the collapse of a fishery.

Most offshore fishing can be profitable only on aggregations such as shoals, or where the density of fish per unit area is high (Laevastu and Bax 1989). Fish aggregations may be associated with spawning, feeding, or migration. Major environmental factors that tend to produce aggregation are temperature, coastal and bathymetric boundaries, currents, and salinity. Thus, fish often aggregate near oceanic fronts; that is, at boundaries between water types and currents. Satellite data and modern methods of digital image analysis make it possible to accurately detect the near-surface expression of these boundaries, follow their evolution in space and time, and determine the velocity and current shears associated with them. Advances in communications technology make such information available in near-real time to help optimize fishing operations. Remotely-sensed data also can be used to monitor storms and, in polar regions, to identify sea ice – ocean boundaries. These latter two analyses can lead to a safer fishing environment.

Most captains of fishing vessels do not have the time or training to obtain and analyze satellite and/or in situ oceanographic data. Moreover, the economics of fishing, of which the need for prorated capitalization (e.g., vessel, processing plant costs) is only one factor, should motivate commitment to conservation on the part of the fishing industry (Fig. 1). This commitment to conservation can be effective even if it is better expressed as a desire on the part of the fishing industry for good counsel (i.e., technically sound and informed) from stock assessment managers. Ultimately, the quality of such counsel is critically dependent upon the availability of reliable, near-real-time data on catch: data that can come only from the fishing industry. Thus, the exchange of accurate information between the fishing industry and stock assessment managers represents the only practical way to insure a long-term, economically viable fishery. Efforts must be made to educate the fishing industry of the benefits to be obtained from such an exchange of information.

Fisheries Managers

Fisheries management often consists of groups of fisheries biologists and stock assessment personnel who are required to monitor or predict fish stocks and recommend total allowable catch (TAC) on a species-by-species basis (Fig. 1). The basis for management of a given fishery usually involves an estimate or prediction of mortality and/or recruitment. The ratio of the importance of the two measures (mortality versus recruitment) is species dependent with relative importance being determined largely by how long the fish lives. For squid, which live for only 1 yr, recruitment is the key to management success; for rockfish, which live to 70 yr and hence have many year classes in the fishery, recruitment data are tactically less important than mortality data for good management of the stock.

Accurate estimates of either mortality or recruitment are difficult to make because data are limited and the scientific basis for the tactical estimate is uncertain. For example, observationally based estimates of mortality are often determined empirically (e.g., Reed et al. 1989), depend upon assumed or measured patch size (McGurk 1986), and may have regional dependencies. Such estimates describe only observed change and do not distinguish between contributions from physical processes (e.g., advection, temperature) and mortality; thus, a decrease in concentration can serve as an estimate of mortality only if one assumes no significant physical change (Reed et al. 1989). In general, however, such an assumption is not likely to be valid. For example, advection affects both mortality and recruitment because it can carry eggs and larvae into areas poor in food, rich in predators, or both. Conversely, water movement can carry eggs and larvae into areas rich in food, poor in predators, or both. The precise effects of water motion on a biological population depend upon the detailed phase relation (where and when) between the space–time history of the population and the environmental factors that form its habitat (Simpson 1987). English sole off Oregon (Kruse and Tyler 1989) and the cod fishery of Hecate Strait, British Columbia (Tyler and Westrheim 1986; Tyler and Crawford 1991), illustrate the importance of transport.

Spawner–recruitment models also have been used to estimate fish mortality between spawning and recruitment (e.g., Rothschild 1986). Wooster and Bailey (1989) pointed out that the most common models are those of Ricker (1954) and Beverton and Holt (1957); both models contain density-dependent and density-independent terms. The density-dependent term, through compensatory mortality, has the effect of reducing recruitment with increasing stock size. Although compensatory mortality acts on new recruits in both models, the mechanism of interaction is interpreted differently. The Ricker model emphasizes the role of predation (e.g., predators and cannibalism) whereas the Beverton and Holt model emphasizes starvation (i.e., prerecruits increase with increasing spawner abundance but the amount of available food per fish decreases). The underlying assumptions of such models, however, are far from universally accepted. Jones and Henderson (1985) concluded that, in general, little evidence exists for a significant relation between spawners and recruits in fish species. Other studies (e.g., Hollowed and Bailey 1989; MacCall 1990) find some density-dependent spawner–recruit relations but have difficulty separating these relations from density-independent effects. Thus the job of stock assessment managers to establish, on a species-by-species basis, realistic and profitable TACs to ensure resource fecundity is an unenviable task limited by both insufficient near-real-time observations and an inadequately developed scientific basis for management. Present and planned remote sensing instrumentation, improved methods of digital image analysis, and the development of meaningful environmental/biological indices using both satellite and in situ data (i.e., those that relate directly to stock assessment) provide a possible means of mitigating one of these handicaps, namely the lack of adequate, near-real-time observations. Moreover, retrospective analyses of long-term data sets provide an opportunity to improve our scientific understanding of an operational fishery.

Mortality and recruitment data, however, are not solely related to the conservation side of stock management. In fact, accurate estimates of both mortality and recruitment can help ensure more efficient harvesting of a given stock through improved estimates of abundance (e.g., Wooster and Bailey 1989). Stock assessment managers should use this latter relation to educate and encourage the fishing industry (i.e., it is in their own best interests) to provide accurate catch statistics for management use.

Finally, a distinction should be made between tactical and strategic management of a given fisheries resource (Fig. 1). Tactical management (e.g., Anthony 1990; Megrey and Wespestad 1990; Stocker and Leaman 1990) estimates stock size for the current year, forecasts recruitment, and analyses catch rates and events in the fishery. This information is used to decide on quotas, establish allowable fishing areas, and determine the opening and closing times of the fishery. Strategic management (e.g., Cook and Copes 1987; Murphy et al. 1990; Zhang and Gunderson 1990) is concerned with mesh size, optimal fishing mortality given growth and natural mortality, optimal stock size for maximal recruitment, and how to handle errors in measured data and derived fishing indices. Clearly, a well-managed fishery is guided by closely coordinated tactical and strategic stock assessment decisions.

Fisheries Research

Research activity broadly can be divided into basic and operations research. Both require environmental information and catch statistics that, in part, must be supplied by the fishing industry (Fig. 1).

Basic research addresses questions that can provide a better scientific basis for operational fisheries oceanography. Clearly, improved understanding of the environmental and biological processes that influence both recruitment and mortality is a central concern that relates directly to both the tactical and strategic needs of stock assessment (Fig. 1). For example, basic research must develop a theoretically sound means for determining the temporally and spatially varying relative importance of advection (e.g., Parrish et al. 1981; Simpson 1987) versus starvation (e.g., Hjort 1914; Lasker 1975) versus predation (e.g., Hunter 1981; Parsons et al. 1984) in the recruitment process of a given fishery. Also, methods need to be developed for separating the effects of density-dependent versus density-independent factors in spawner–recruitment models used to estimate mortality. Basic research advances in these two areas alone will directly improve the ability of stock assessment personnel to develop better strategies and improved tactical indices for monitoring and managing a given fish stock.

The examples cited above are only two of the many fundamental environmental–biological questions that need to be studied if the complex interactions between fish and environment are to be clearly understood. Basic questions such as these, however, require a broad spectrum of research activity for proper resolution: (1) process-oriented experiments (e.g., Checkley et al. 1988; Rose and Leggett 1988), (2) laboratory studies (e.g., Theilacker 1986), (3) numerical models (e.g., Murdie and Hassell 1973; MacCall 1980), and (4) biogeographic and population dynamics studies (e.g., MacCall 1990). Remote sensing analyses can provide real-time guidance for process-oriented experiments, some of the initial and boundary conditions needed by numerical models, data for validating the prognostic capabilities of such models, and data useful in biogeographical and population dynamics studies of marine fishes.

Operations research is concerned with the design of data structures that can provide an efficient and compact representation for environmental and biological data used in operational fisheries oceanography (Fig. 1). Such data structures are required to meet the ever-growing near-real-time support needs of a typical operational fishery, especially given the constraints and costs of present-day ship-to-shore communication networks. These data structures, in turn, are needed to build data bases for the development and validation of operational products useful to the community and

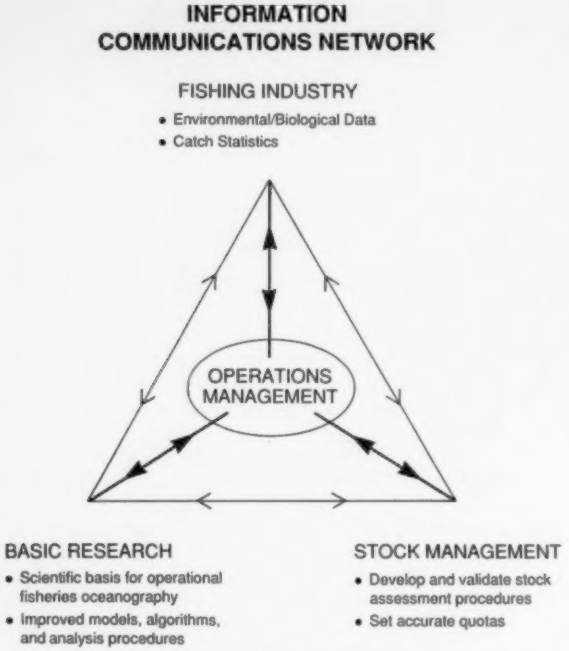
INFORMATION COMMUNICATIONS NETWORK
FISHING INDUSTRY
• Environmental/Biological Data
• Catch Statistics
OPERATIONS MANAGEMENT
BASIC RESEARCH
• Scientific basis for operational fisheries oceanography
• Improved models, algorithms, and analysis procedures
STOCK MANAGEMENT
• Develop and validate stock assessment procedures
• Set accurate quotas

FIG. 2. Conceptualization of the major types of information and communication linkages needed for a successful regional operational fisheries oceanography program. Bold lines indicate primary communications links via an operations research center. Secondary communications links are shown with lighter lines.

for use in the retrospective analyses of long-term trends and changes in a fishery.

Operations research encompasses many activities. This diversity is largely determined by the near-real-time needs for data (e.g., catch statistics) of both the fishing industry and marine resource managers or for operational products derived from data (e.g., sea-surface temperature charts) or models (e.g., wind-field analysis, marginal ice-zone analysis, fish mortality and recruitment analysis). Thus, operations research activity includes, but is not limited to, real-time data acquisition (e.g., satellite data), archiving and distribution (including near-real time and ship-to-shore) of processed data sets to support fishing activity, and the design and implementation of computer-assisted decision-making tools to help prevent information overload to bridge personnel. Operations research also can provide the focal point (Fig. 2) for the collection of information from the fishing fleet (e.g., length of fish, gonad statistics, infestation data) and the subsequent distribution of this information to other sectors of the fisheries community (e.g., stock assessment personnel). Moreover, this information provides the basis for both the validation and refinement of operational products supplied to the fishing fleet and for the development and refinement of basic research concepts through the analysis of both process-oriented experimental data and the retrospective analysis of long-term historical data.

Community Interactions

The basis for interactions among the various sectors of the operational fisheries oceanography community is a need for accurate and timely information. The information is so diverse and complex that no single sector of the community can effectively and economically gather all of the information it needs; thus, the various sectors must hang together (i.e., communicate and share data) or hang separately (not meet their respective objectives). The vehicle for interaction is a communications network. Operations research, by virtue of its functions (Fig. 1) and its position within the framework of the entire community (Fig. 2), is the logical sector to develop and maintain the communications network. These are the premises under which the following matrix of interactions for an operational fishery was developed.

The fishing industry uses information at two primary levels: (1) the executive team and (2) the captain, or skipper-group (Hogan and Clarke 1989). The executive team (Fig. 1) uses information to formulate strategies, policies, capital investments, and other corporate decisions that affect the socioeconomic life of a fishing region. These corporate decisions and actions are made within the framework of estimating the opportunities deemed to exist in the resource (i.e., the regional fish stocks) and the environmental factors governing their exploitation. Thus, the fishing industry is critically dependent upon the stock assessment sector of the community to properly set TACs. A TAC that is set too low can result in an underutilized stock and probably economic hardship for the fishing region. Likewise, a TAC that is too high can result in an overutilized resource with potential long-term ecological and economic damage to the regional fishery. The captain, or skipper-group (Fig. 1), needs near-real-time information to make decisions and implement actions that affect the safety of crews and the efficiency of the fishing effort.

Traditionally, the fishing industry has been perceived as the "consumer" of information. The industry's potentially important role as a data source for the rest of the community, however, largely has been ignored (Fig. 2). A fishing vessel, which is at sea for well over 200 d a year, is virtually a floating information-collection platform (Hogan and Clarke 1989). At the least, estimates of catch per unit of effort can be made from fishing industry data. But the prospects for additional information are more exciting. Consider a fishery in which the catch normally is eviscerated at sea. Evisceration makes it possible to collect gonad statistics and to estimate predator–prey relations from gut contents, and fish preying on the catch are hauled in with the target species and can be counted. Infestation data, discards of other biota, sightings of cetaceans, the activity of foreign vessels in the regional fishery, and environmental data are additional types of information that other sectors of the fisheries oceanography community can glean from the fishing industry.

Both the strategic and tactical aspects of fisheries management need environmental and biological information. Strategic management issues (e.g., mesh size, estimation of optimal stock size, optimal fishing mortality, adult behavioral studies, recruitment research) directly involve some aspect of operational fisheries oceanography. Tactical management issues (e.g., gathering indices of recruitment and mortality including ocean model predictions, survey design and covariates analysis, interpretation of events (varying catch rates) in the fishery caused by environmental factors (e.g., El Niño – Southern Oscillation (ENSO) activity in the Northeast Pacific or severe winters in the Northwest Atlantic)) also require large amounts of high-quality environmental and biological data.

At present, the strategic side of fisheries management uses significantly more data than the tactical side. The tactical side of fisheries management, however, can reduce risk and uncertainty in a given fishery by more aggressively incorporating various oceanographic indices (developed in cooperation with basic fisheries research efforts) into assessment analyses. Remote sensing products provide a basic source of information for such indices; instrumentation planned for the 1990s (e.g., Sea-viewing Wide Field of View Sensor (SeaWiFS), Moderate-Resolution Imaging Spectrometer (MODIS)) will expand this capability. Of special interest are sensors that can image through the clouds (e.g., the SSM/I sensor on the DMSP satellite). The potentially diverse sets of fishing industry and historical data, collected and distributed via a community-wide communications network, provide another source of data for developing and evaluating tactical fishing indices.

Two primary goals of basic fisheries oceanography research are to (1) provide a better scientific basis for both the use and management of an operational fishery and (2) develop improved algorithms and analyses for efficiently representing the state of a fishery from the large, diverse, and complex data sets needed to understand that fishery. Thus, the need for high-quality environmental and biological data is clear. Ultimately, the objective should be to translate advances in basic fisheries research into operational products that can improve both the use and management of the resource. Such products normally would be developed, evaluated, distributed, and maintained by operations researchers working in close collaboration with the fishing industry and stock assessment managers.

The communications network, complete with products, historical data bases, current data bases, satellite data, and geographical reference data, provides feedback mechanisms for the entire operational fisheries oceanography community (Fig. 2). Operations research centers, funded jointly by government and industry, may be one way to develop and maintain the required data bases, operational products, and communications network. Ultimately, lively debate within the community will determine the best implementation scenario(s) to meet the information imperative.

Remotely-Sensed Data and Operational Fisheries Oceanography

In this section, the types of remotely-sensed data of most interest to operational fisheries oceanography are identified. Data are divided into three groups: currently available operational data, experimental data, and future instrumentation. Only the three most relevant types of currently available operational data are discussed in this paper. Experimental satellite data, future remote sensing platforms (e.g., Earth Observing System (EOS)), and the use of aircraft data within an operational fisheries oceanography context are discussed in Simpson (1992b).

Advanced Very High Resolution Radiometer (AVHRR) Data

The remotely-sensed data most routinely used today in an operational fishery are taken with the Advanced Very High Resolution Radiometer (AVHRR) on the NOAA series of weather satellites (NOAA-6 to NOAA-12). The five-channel AVHRR instrument measures radiances in the following bands: 0.58–0.68, 0.725–1.1, 3.55–3.93, 10.5–11.5, and 11.5–12.5 μm. The first two channels are in the visible region of the spectrum and can provide information on cloud cover and solar radiation during daytime periods. The last three channels are in the near-infrared and the infrared regions of the electromagnetic spectrum. They provide information on cloud cover during nighttime periods and either single-channel or multiple-channel estimates of sea-surface temperature (SST). Cloud cover and SST from AVHRR data provide the basis for most presently available operational fisheries oceanography products.

The AVHRR provides data for transmission in both Automatic Picture Transmission (APT) and High Resolution Picture Transmission (HRPT) formats. HRPT data are transmitted at full resolution (1.1. km at nadir) whereas APT data have reduced resolution, typically by a factor of 4 compared with HRPT data. A further restriction in the APT format is that only two of the five available AVHRR channels are transmitted in the APT format. Overall, HRPT data are superior to APT data for almost all operational fisheries oceanography applications.

The Data Collection and Location System (DCLS), often referred to as the ARGOS Data Collection and Location System, also is operational on the NOAA series of weather satellites. ARGOS provides a means for locating the position of fixed or moving platforms (e.g., buoys and icebergs) and for obtaining environmental data from them (e.g., temperature, pressure, etc.). This system can be used, for example, to monitor the location of drifting icebergs which "calf" yearly off glaciers on the west coast of Greenland and migrate southward into the rich fishing areas of the Grand Banks. Such information can help provide additional safety to North Atlantic fishermen.

The TIROS Operational Vertical Sounder (TOVS) refers to a collection of three instruments that also fly on the TIROS-N series of NOAA polar orbiting satellites. The instruments in the TOVS package are the High Resolution Infrared Radiation Sounder (HIRS/2), the Microwave Sounding Unit (MSU), and the Stratospheric Sounding Unit (SSU). Of these, the HIRS/2 and the MSU instruments have the most immediate application to an operational fishery. With proper processing, vertical profiles of air temperature, dewpoint temperature, geopotential height, geostrophic wind as well as individual point values of precipitable water vapor, total outgoing long-wave radiation, cloud top temperature, and cloud top pressure can be computed. Some of these environmental variables can be used directly in operation fisheries oceanography whereas others are needed indirectly to more accurately estimate other variables of interest such as photosynthetic available radiation (PAR), net short-wave and net long-wave radiation at the sea surface which, in turn, can be related to phytoplankton abundance in the well-mixed layer (e.g., Frouin et al. 1989). It is likely that this less-well-known form of satellite data will become more readily available and used by the operational fisheries oceanography community in the future.

Geostationary Operational Environmental Satellite (GOES)

The Geostationary Operational Environmental Satellite (GOES) provides frequent visible (VIS) and infrared (IR) images to monitor routine as well as cataclysmic weather events such as hurricanes and other severe storms, relay meteorological data from surface collection points to a processing center, and broadcast processed graphic and image weather data (WEFAX) to field stations (Clark 1983). Historically, the primary direct application of GOES data to operational fisheries oceanography has been storm monitoring to help insure the safety of fishing vessels at sea. Data from GOES are also proving to be of increasing scientific value for snow mapping (e.g., Carroll 1987), relative cloud cover, and incident solar radiation estimation (e.g., Gautier et al. 1980; Frouin et al. 1989). TOVS data from the NOAA polar orbiting satellites also can be combined with GOES and AVHRR data for improved estimates of solar radiation, net long-wave flux, and PAR. Current efforts to improve the quality of GOES data, as part of the GOES Pathfinder Project, should make GOES data more valuable for scientific research in support of the operational fisheries community (e.g., Simpson et al. 1994b).

Defense Meteorological Satellite Program (DMSP)

Because the DMSP is a classified program, relatively little use of DMSP data (compared with either NOAA polar orbiter or GOES data) has occurred in either civilian or educational applications. Moreover, many of the basic features of DMSP data are not well-known to the unclassified community. This section provides a concise overview of DMSP capabilities with specific emphasis on the Operational Linescan System (OLS) and the Special Sensor Microwave Imager (SSM/I). As DMSP data become more available, they will play a more significant role in future environmental studies.

Two spectral channels are used in the OLS. One channel responds to reflected solar or lunar radiation in the 0.4–1.1 μm range, chosen to provide maximum contrast between earth, sea, and cloud elements of the image field, and is termed the visible light or L-band (e.g., Dickinson et al. 1974; Nichols 1975). Two different detectors are used for collection of L-band data; one is a silicon diode detector for collection of fine-resolution (0.3 nautical mile) data (LF) during daytime, and the other is a photomultiplier tube (PMT) for collection of low-resolution (1.5 nautical mile) data (LS) under quarter moonlight or brighter nighttime conditions. Originally, the other channel of the OLS responded to emitted Earth, atmosphere, and cloud radiation in the 8.0–13.0 μm range. This choice was made to minimize ozone and water vapor absorption while still maintaining an acceptable signal-to-noise ratio. This data is called the thermal infrared or T-band. On the F-4 and subsequent DMSP satellites, the infrared channel was narrowed to 10.8–12.5 μm.

The SSM/I was launched in 1987 as part of the DMSP program. The SSM/I is a seven-channel, four-frequency, linearly polarized, passive microwave radiometer (Hollinger et al. 1987). A summary of its sensor characteristics is given in Neale et al. (1990). The SSM/I data have proven especially useful for estimating surface wind speed and rainfall over the ocean (e.g., Sharma et al. 1991; Chang et al. 1993; Chiu et al. 1993; Claud et al. 1993) and for land surface classification studies of vegetation, snow cover and snow water equivalents, surface moisture, and precipitation (e.g., Neale et al. 1990 and references contained therein). Because the SSM/I sensor can image through the clouds, it will be especially useful in polar and/or high cloud cover areas. The SSM/I sensor has coarser spatial resolution than the AVHRR sensor because it senses in the microwave region of the electromagnetic spectrum. Therefore, a hybrid SST product consisting of high spatial resolution AVHRR data for cloud-free regions and coarser spatial resolution SSM/I data for cloud-contaminated regions may prove to be an effective product for many global fisheries analyses.

Analysis Methods

In this section, a few of the more important quantitative analyses that relate directly to operational fisheries oceanography are presented. Accurate, automated quantitative analyses are critically important if remote sensing products are to be used optimally. Herein, the methods are applied only to the most commonly used data, that taken by the AVHRR. These methods also can be applied to LandSat TM data, retrospectively to Coastal Zone Color Scanner (CZCS) data, and DMSP data, and in the future to data taken by the SeaWiFS. In fact, the spatial resolution of LandSat TM data (10–30 m) makes it particularly well-suited to nearshore and estuarine applications. It is important to emphasize, however, that the ultimate usefulness of remotely-sensed products is critically dependent upon proper preprocessing and subsequent rigorous analysis of the raw satellite data.

Preliminary Processing

The AVHRR, like most other Earth-observing instruments, measures radiation at several wavelengths and transmits this information in sequential form to ground-based receiving stations. The raw telemetry bit stream archived for later use at these ground stations has little resemblance to the SST maps routinely used in operational fisheries oceanography. Several preliminary processing steps are required to produce these SST maps which then serve as the basis for all other AVHRR-derived operational products.

For the preliminary processing, a subset of data centered over the chosen operational area is first extracted from the archived telemetry bit stream (e.g., Lauritson et al. 1979), converted from a band interleaved to a band sequential representation, and then stored as a two-dimensional data structure. Next, data from each band (i.e., separate region of the electromagnetic spectrum measured by the sensor) are calibrated (e.g., Lauritson et al. 1979 and updates) from brightness counts to geophysical units (i.e., percent albedo for AVHRR bands 1 and 2 and temperature (degrees Celsius or kelvins) for AVHRR channels 3, 4, and 5). Then, a geometric correction procedure (e.g., Legeckis and Pritchard 1976) is applied to each pixel in the image to (1) minimize distortion from oblique viewing over a wide range of satellite viewing angles and (2) map the geometrically corrected pixels onto a given map projection (e.g., Mercator) by identifying the correct latitude and longitude for each pixel in the image. Next, image segmentation is performed; that is, land, ice, water, and cloud pixels are identified and separated from each other. Often, bit masks are used to keep track of this segmentation information. Cloud screening (e.g., Simpson and Humphrey 1990; Gallaudet and Simpson 1991) is especially important for operational fisheries applications because even a few cirrus clouds can seriously contaminate SST maps and any higher level products (e.g., SST gradient maps) derived from them (Simpson 1990). Moreover, land masking (e.g., Simpson 1992a) can significantly improve the available dynamic range of the final operational product used by the community. Finally, either a single-channel SST map or a multichannel (MCSST) map is produced which is the basis for all other derived products.

AVHRR channel 3 data often can be contaminated by highly variable, sensor/satellite-dependent noise. If uncorrected, this noise generally will compromise an analysis (e.g., Gallaudet and Simpson 1991). To circumvent this problem, a Wiener filter model (Simpson and Yhann 1994) can be used to minimize the noise in channel 3 prior to further analysis. Their results show that (1) the Wiener-filtered channel 3 data have a significantly improved signal-to-noise ratio compared with the original data, (2) the Wiener filter model introduces minimum spatial distortion, and (3) use of the filtered data significantly improves the quality of image segmentation analyses (e.g., cloud detection). They also tested alternative models of noise reduction (e.g., constrained least squares filter, Conditional Markov filter, vertical 5 averaging filter, notch filter) and compared these results with those of the Wiener filter model. The Wiener filter model proved superior for all images tested. For these reasons, it should be used to signal precondition the AVHRR channel 3 data prior to use in fisheries applications.

Atmospheric water vapor attenuates the AVHRR channel 4 and 5 signals (Lauritson et al. 1979 and updates). Because atmospheric water vapor concentration can vary greatly in a given region (e.g., between ENSO and non-ENSO periods, Quiroz 1983), it also is necessary to correct the channel 4 and 5 data for atmospheric water vapor attenuation prior to analysis. The atmosphere correction of Harris and Mason (1992) is recommended for this purpose. A MCSST which incorporates this correction can be computed using

$$(1)\quad \mathrm{MCSST} = 1.0095\,T_4 + \frac{1.6692\,T_4}{R_{12}} - \frac{1.6682\,T_5}{R_{12}} - 2.64$$

where R_{12} is estimated on a pixel-by-pixel basis as $R_{12} = \Delta T_5/\Delta T_4$ where ΔT_i is the temperature difference between adjacent pixels in channels 4 and 5, respectively. This model assumes that the atmospheric variation in water vapor changes slowly over the spatial scales of local SST gradient. Use of this assumption allows an additional nonlinear atmospheric transmittance correction to be computed from the local brightness temperature changes and to be incorporated into the MCSST estimate of (1). This split-window MCSST is very different from that given by McClain et al. (1985):

$$(2)\quad \mathrm{MCSTT} = 1.0346T_4 + 2.5779(T_4 - T_5) - 283.21.$$

Our results show that eq. (1) is more robust than eq. (2) for estimating an atmospherically corrected, split-window MCSST.

Maximum information is contained in the Wiener filtered channel 3 and the MCSST data (eq. (1)) because these data are correlated less than channel 4 and channel 5 data (Simpson 1994). Use of channel 3 data is especially important in nighttime applications (e.g., Gallaudet and Simpson 1991) and for ice detection. A more detailed discussion of AVHRR telemetry is given in the NOAA polar orbiter data users guide (NOAA/NESDIS 1991). An extensive discussion of proper preprocessing steps for AVHRR data is given in Simpson (1992b) who also gave detailed examples of the impact of improper preprocessing of satellite data on operational fisheries analyses and products.

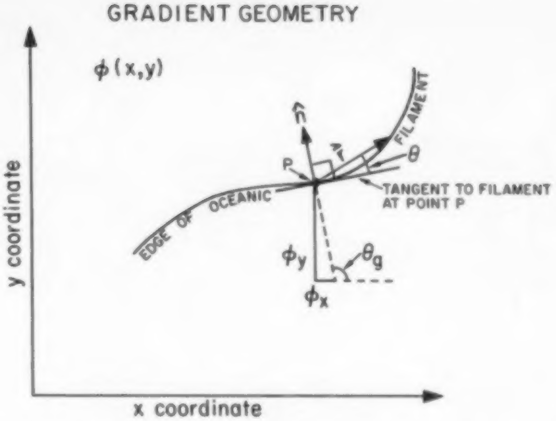

FIG. 3. Gradient of $\phi(x,y)$ along the r direction and its geometric relation to the x and y components of the gradient of $\phi(x,y)$.

Ocean Frontal Analysis

General comments

Edge detection is a problem of fundamental importance in digital image analysis because edges characterize object boundaries in visual scenes. In the image domain, edges are pixel locations at which there is an abrupt change in gray scale or intensity. Edge detection serves to simplify the analysis of images by significantly reducing the amount of data processed while at the same time preserving useful structural information about object boundaries (Canny 1986). Regardless of application, there are a few common criteria relevant to the performance measure of all edge detectors. First, the error rate must be low. That is, edges that occur in the image should be identified, while no spurious edges should be detected. The second general criterion is that the edge points should be well localized. That is, the distance between the points marked by the detector and the "center" of the true edge should be minimized. An alternative interpretation of the localization constraint is that contributions to each point in the filtered image should arise from a smoothed average of nearby points, rather than any kind of average of widely scattered points (Marr and Hildreth 1980). These general criteria provide the basis for objectively evaluating the performance of any edge detection algorithm.

The visual primitive of importance for edge detection applications in oceanography is the brightness temperature gradient which can be computed three different ways using gradient operators, edge detectors, and edge enhancers. Gradient operators are used when the actual values of the temperature gradient are needed. Initialization and updating of numerical models of geophysical variability with satellite data require such information. Edge detectors are used when only an accurate determination of the location of the frontal boundary is needed. Computation of the normal component of near-surface oceanic velocity and some commercial and/or sportsfishing applications often need accurate edge detectors. Edge enhancements are used to increase the signal-to-noise ratio of a feature which is only weakly visible in a parent image. Each of these analyses can be useful in operational fisheries oceanography.

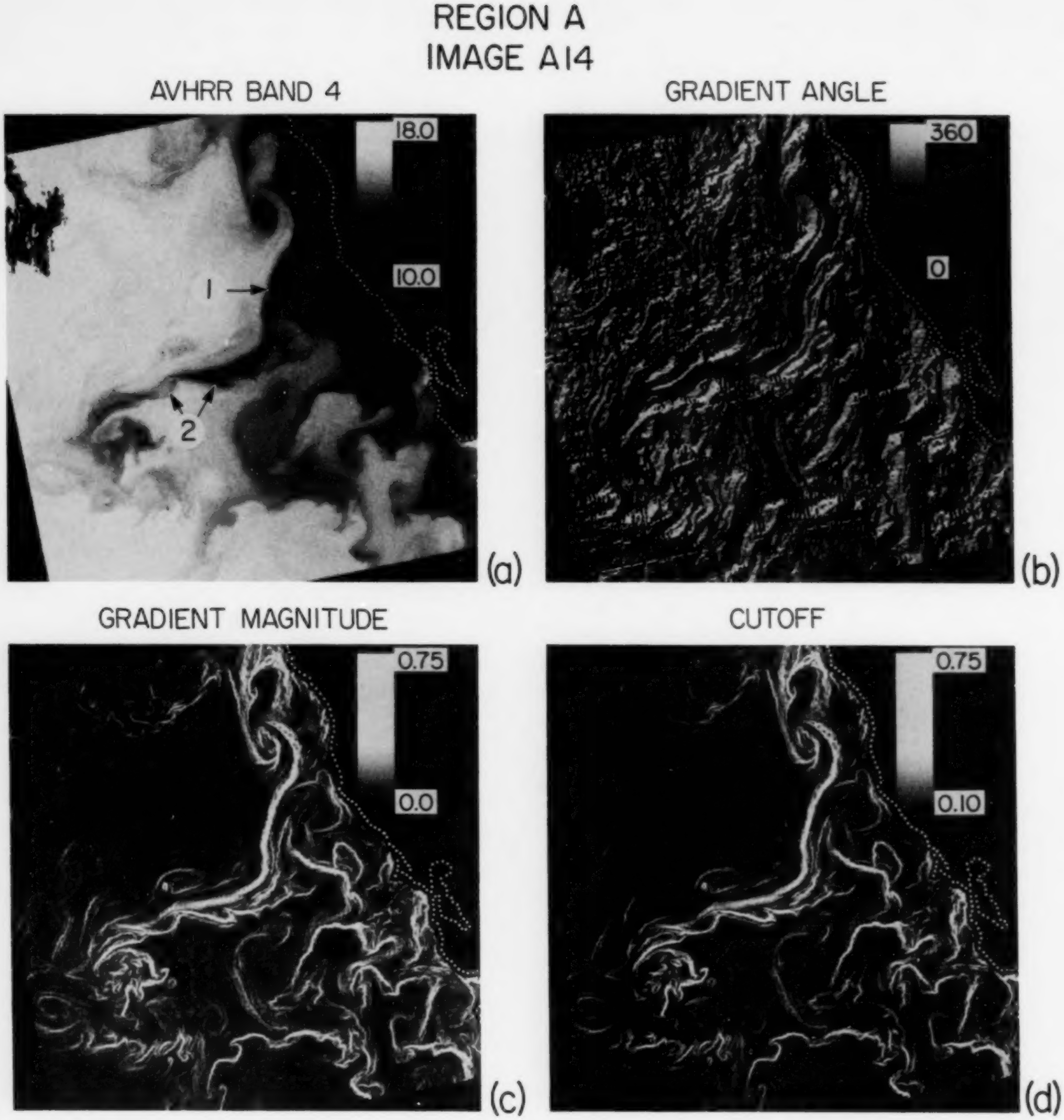

FIG. 4. (a) AVHRR band 4 SST (°C) image off northern California; (b) image of gradient angle (degrees of the compass) computed using eq. (4); (c) image of gradient magnitude (°C/km) computed using the isotropic gradient operator and; (d) thresholded version of Fig. 4c with all values below the cutoff value of 0.1°C/km removed.

Gradient operators

The two-dimensional temperature gradient is defined as

$$(3) \quad \bar{\nabla}\phi = \frac{\partial\phi}{\partial x}\hat{i} + \frac{\partial\phi}{\partial y}\hat{j}$$

where $\phi(x,y)$ is the temperature distribution of the image. $\bar{\nabla}\phi$ measures a local maximum of the temperature distribution in the direction of an edge (i.e., locally perpendicular to the tangent to the edge at an arbitrary point P; Fig. 3). The direction of the edge is determined by the relation

$$(4) \quad \theta = \operatorname{atan}\left[\frac{\partial\phi / \partial y}{\partial\phi / \partial x}\right].$$

In the two-dimensional image domain, two orthogonal filters are needed to properly and efficiently compute the gradient ($\nabla\phi$) in both the x and y directions (e.g., Jain 1989).

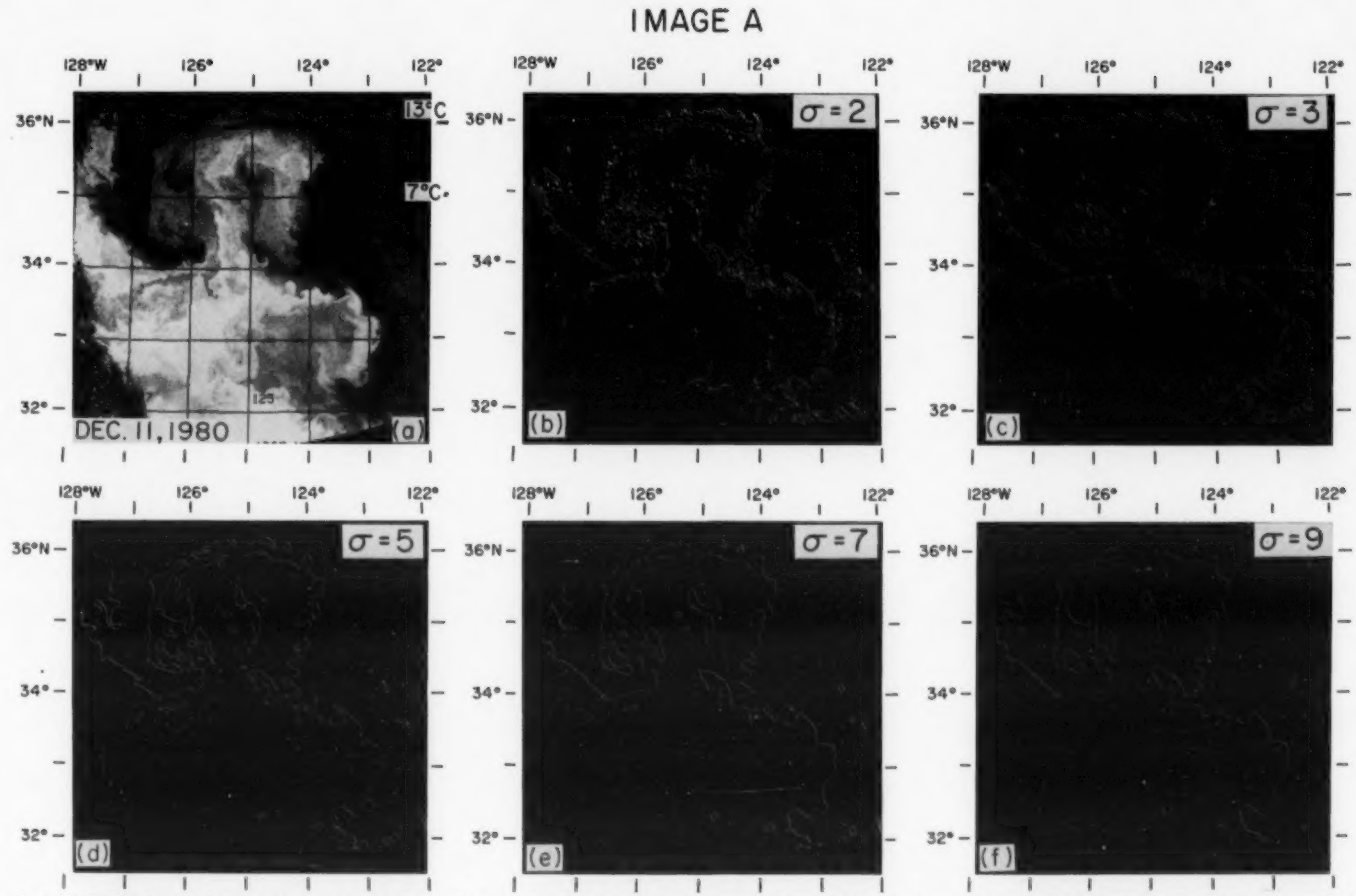
IMAGE A
128°W
126°
124°
122°
36°N
34°
32°
13°C
7°C
DEC. 11, 1980
(a)
σ = 2
(b)
σ = 3
(c)
σ = 5
(d)
σ = 7
(e)
σ = 9
(f)

FIG. 5. (a) AVHRR image showing the surface signature of two oceanic eddies; (b–f) edges of these eddies as detected by the LOG operator for values of $\sigma = 2, 3, 5, 7$, and 9 (from Simpson 1990).

Only the smoothed or isotropic operator should be used to compute gradients from AVHRR data for operational fisheries applications (Simpson 1990). Moreover, because cloud contamination is the largest source of noise in AVHRR-derived distributions of SST (Robinson 1985), it is also recommended that careful attention be paid to proper cloud removal (e.g., Simpson and Humphrey 1990; Gallaudet and Simpson 1991), land removal (Simpson 1992a), and exclusion of pixels near cloud–ocean and/or land–ocean boundaries (e.g., Simpson 1990) prior to gradient analysis. Because differentiation also enhances the noise in the image, additional steps must be taken to counteract this effect. For example, the cumulative histogram of the $\bar{\nabla}\phi$ distribution can be used to determine an appropriate gradient threshold for eliminating high-frequency noise introduced by the differentiation. A more detailed discussion of the computation of gradients from remotely-sensed data is given in Simpson (1990).

Application of the gradient computations described above is shown in Fig. 4. For all panels in this figure, clouds, land, and data not in the grid are masked in black (pixels equal to zero); coastlines are shown with dotted white lines. Figure 4a is a calibrated SST map constructed from AVHRR band 4. Very dark or grey shades represent cold, inshore coastal water; lighter shades represent warmer offshore California Current water. Wedge units are in degrees Celsius. Figure 4b is a map of gradient angle computed using eq. (4) with the directional conventions as defined by Randerson and Simpson (1993). Wedge units are given in degrees of the compass. Figure 4c shows the magnitude of the SST gradient computed using a 3 × 3 isotropic gradient operator. The wedge has units of degrees Celsius per kilometre. Figure 4d shows the thresholded magnitude of the SST gradient (i.e., all temperature gradients <0.1°C/km were deleted from the data to eliminate high-frequency noise (e.g., Simpson 1990)). These data clearly show the location, geometry, thermal gradient strength, and direction of a major filament between Point Arena and Point Reyes, California. The arrow labeled 1 (Fig. 4a) shows the location of the broad, diffuse northern boundary of this filament and the areas labeled 2 (Fig. 4a) show the sharper southern boundary of the filament. This characteristic structure of filaments found off the west coast of North America is discussed further in Randerson and Simpson (1993 and references contained therein).

Edge detectors

A major problem with natural images is that features within these images occur over a wide range of scales (e.g., Marr 1976). Marr and Hildreth (1980) showed that there are two physical considerations that combine to produce the optimal smoothing filter for digital edge detection. First, the image is filtered to reduce the range of scales over which the intensity (or temperature for AVHRR) changes take place. Thus, the filter's spectrum should be smooth and roughly band limited in the frequency domain. Second, the filter should satisfy a spatial localization constraint in the spatial domain. These two constraints, however, are mutually exclusive and hence are related by an uncertainty principle, $\Delta X \cdot \Delta k \geq \pi/4$ (Bracewell 1965). Note that k refers to the spatial frequency under consideration. Marr and Hildreth (1980) determined that the Laplacian of the Gaussian (LOG) operator was the ideal edge detector because (1) the Gaussian distribution is the only distribution that optimizes the relation between spatial localization and band width and (2) the problem of finding intensity changes reduces to that of finding the zero crossings of the second derivative of intensity (or temperature) in an appropriate direction (i.e., the LOG operator gives the zero crossings and the edges are simply the zero contours of the LOG convolved image).

The LOG operator is defined by

$$(5)\quad \mathrm{LOG} = \nabla^2 G = k\left\{1 - \frac{x^2 + y^2}{2\sigma^2}\right\}\exp\left\{-\frac{x^2 + y^2}{2\sigma^2}\right\}$$

where x and y are the number of lines and samples from the function center, σ is the Gaussian width parameter, and k is a normalization constant. The LOG operator is often referred to as the "sombrero" filter because it has a central positive-valued lobe and two negative side lobes. The maximum width of the central lobe is $2\sqrt{2}\sigma$, and thus the parameter σ determines the spatial scales of detectable edges by varying the width of its central excitatory response (Marr and Ullman 1981). The LOG operator must also include the negative slide-lobe widths, so the dimensions of the filter typically are set at $4\sigma \times 4\sigma$ because about 95% of the LOG function is included in this area. The ability to choose σ in relation to the physical scales of the process under study makes the LOG operator especially well suited to operational fisheries applications. Details about the use of the LOG operator are given by Simpson (1990).

Figure 5a shows the surface signature of two offshore mesoscale eddies. Spatial variation in thermal structure near the centers of the two eddies is small compared with that about 50 km from the eddies' centers. The locations of the thermal boundaries for this image were detected using the LOG operator with values of σ = 2, 3, 5, 7, and 9, respectively (Fig. 5b–5f). For $\sigma = 2$, the result is a very noisy pattern of small-scale edges. As the value of σ increases, the smaller-scale edges gradually disappear and only the largest-scale thermal gradient remains when $\sigma = 9$. It is these latter well-localized thermal boundaries that are of interest to an operational fishery.

The edge detection methods discussed above are more sophisticated (and computationally more demanding) than simple finite differencing; the latter method, however, often has appeared in the literature. The methods presented herein are recommended for use in operational fisheries oceanography over often-used simpler methods for several reasons: (1) generally the dynamic range of the data in a typical satellite image is such that ocean fronts cannot be easily and reliably detected visually and the approaches cited above are extremely useful for accurately determining front boundaries in such images, (2) in general, it is better to transmit analyzed images (e.g., frontal analyses are presented as binarized black and white images) to a fishing vessel than full gray-scale images because the reception equipment on most fishing vessels generally degrades the gray-scale image to such a degree that it cannot easily be interpreted, and (3) most fishing captains prefer clearly analyzed products to the satellite data itself (i.e., captains are often too busy to do their own analysis and interpretation of the image).

Edge enhancement

Edge enhancement can be accomplished by superimposing the gradients of an image onto the parent image. Compass operators often are used to "illuminate" the image with respect to the differing angular location of a Lambertian lightsource. Of the eight commonly used compass opera-

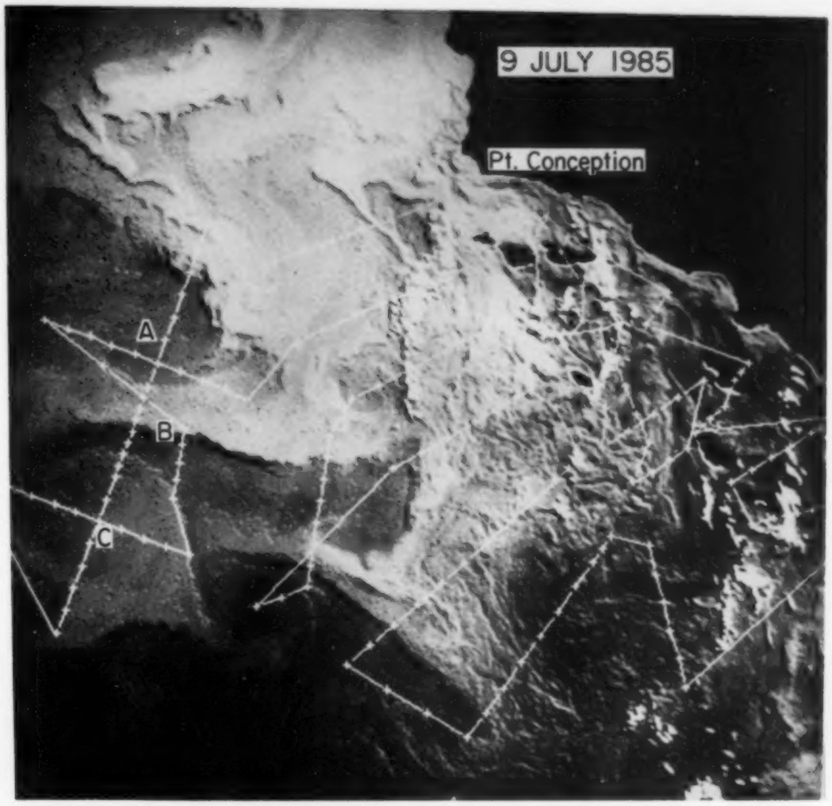

FIG. 6. Edge enhancement of an AVHRR image of a mesoscale eddy dipole; the anticyclonic eddy (A), the cyclonic eddy (C), and a sharp frontal zone (B) are indicated. The ship track of RV *David Starr Jordan* is overlain. Stations are marked with crosses.

tors, only four are linearly independent. These 3 × 3 matrix operators provide angular resolution to within 45°. Angular resolution can be improved by increasing the size of the matrix. Because compass operators determine the directional gradient relative to the local normal of an edge, only one filter (as opposed to two filters to compute gradient magnitude) is needed to produce the desired image (e.g., Simpson 1990).

Compass operators produce a three-dimensional shaded visualization. For example, if a north compass operator is used to create a gradient for superposition on the original image, then the shaded image will appear to have uplifted ridges where the gradient is positive and valleys where the gradient is negative. In some applications, the input image can have low dynamic range. Then, the gradient will be small and when superimposed on the parent image will show little or no enhanced visualization. Under these conditions, the gradient can be multiplied by a gain factor prior to superposition. Typically, a gain of 10 is sufficient.

In some applications, a three-dimensional shaded visualization of the image is desirable. Such enhancements, for example, can be useful in real-time support of oceanographic cruises when facsimile copies of images sometimes must be sent to a ship that has onboard equipment with limited gray-scale resolution. An example of such an application with a ship's track overlain is shown in Fig. 6. Note that the overall effect obtained with compass operators is critically dependent upon the direction of illumination chosen.

Velocity Estimates from Image Sequences

The estimation of near-surface velocity from sequences of image data (e.g., AVHRR, CZCS, or LandSat TM data) is important to all aspects of operational fisheries oceanography because aggregation, mortality, and recruitment are strongly affected by the structure and variability of ocean currents (e.g., Parrish et al. 1981; Tyler and Westrheim 1986; Simpson 1987; Kruse and Tyler 1989; Tyler and Crawford 1991). LandSat TM data may be especially useful in estuarine environments because of its higher spatial resolution compared with either AVHRR or CZCS data. The same methods can be combined with cloud-screening procedures (e.g., Simpson and Humphrey 1990; Gallaudet and Simpson 1991) to compute ice motion from imagery over polar regions. Also, because along isopycral transport often is larger than cross-isopycral transport, careful distinctions are made among the total, normal, and tangential flow fields in this section.

General comments

All methods of motion estimation based upon image sequence analysis depend in some way upon the detection of image brightness gradients. These gradients (Fig. 3 and 4) are

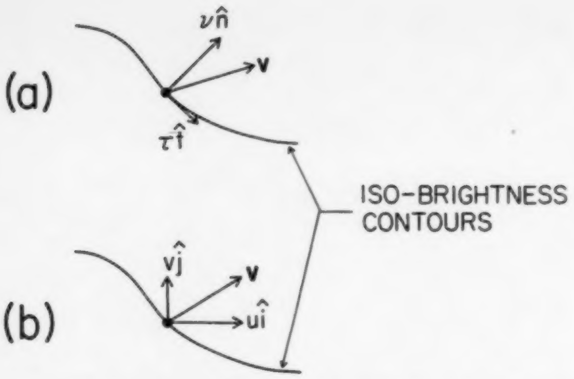

FIG. 7. Vector decomposition of the total velocity $\vec{v}$ along a contour of constant brightness into (a) normal and tangential components and (b) Cartesian coordinates.

defined as normal in direction to contours of constant brightness (or SST for the case of AVHRR data). The total velocity, **v**, at any point on a contour can be written as

$$(6)\quad \vec{v} = \nu\hat{n} + \tau\hat{t}$$

where ν and τ are the magnitudes of the normal and tangential velocity components, respectively, and $\hat{n}$ and $\hat{t}$ are the unit vectors in the directions normal and tangential to the contour, respectively (Fig. 7a). The total velocity vector also can be decomposed into ordinary Cartesian coordinates

$$(7)\quad \vec{v} = u\hat{i} + v\hat{j}$$

where u and v are the magnitudes of the x and y velocity components, respectively, and $\hat{i}$ and $\hat{j}$ are the unit vectors in the x and y directions, respectively (Fig. 7b). Below, an overview of some objective methods for computing the total, normal, and tangential components of near-surface oceanic flow from sequences of AVHRR data is presented. Atmospheric motions can be computed from sequences of either AVHRR (band 1 or 2) or GOES data using these same methods. An example of motion inferred from sequences of CZCS data is given in Garcia and Robinson (1989).

Total velocity

The maximum cross-correlation (MCC) method has been used to objectively estimate the total advective velocity of features common to a sequence of satellite images that have been registered to the same grid and properly cloud-screened (e.g., Lesse et al. 1971; Emery et al. 1986; Garcia and Robinson 1989; Tokmakian et al. 1990; Wahl and Simpson 1990, 1991; Kelly and Strub 1992). The MCC method, however, often can introduce considerable uncertainty in both the magnitude and direction of the resulting velocity vectors. Simpson and Gobat (1994) have developed a method that overcomes these traditional limitations of the MCC method and also allows for computation of stream functions and simulated Lagrangian drifter tracks. Each of these areas is discussed briefly below.

Maximum cross-correlation (MCC) method — Let P and $S(k,l)$ be two-dimensional random variables that correspond to a pattern tile and a search footprint (Fig. 8) that is located at a two-dimensional spatial lag (k,l) from the pattern tile. The dimensions of the pattern and search tiles are constrained by the spatial and temporal scales of the physical process being tracked. Thus, these tile sizes should be selected on an application-by-application basis in conjunction with available in situ velocity calibration data (see Simpson and Gobat 1994). The cross-covariance between the pattern tile and the search footprint, $C_{PS}(P, S(k,l))$, and the standard deviation of the pattern tile, σ_P, and of the search footprint, $\sigma_{S(k,l)}$, can be computed in terms of expectation values of the pattern tile and the search footprint. Thus, the correlation between the pattern tile P and a search footprint $S(k,l)$ is simply

$$(8)\quad r_{PS}(k,l) = \frac{C_{PS}(P,S(k,l)}{\sigma_P \sigma_{S(k,l)}}.$$

In the limit that the correlation approaches 1, the pattern tile and search footprint are identical. This procedure is computed for all search footprints within a given search tile (Fig. 8), and the pair that maximizes the value of the cross-correlation is determined. The MCC method may also be implemented in the wavenumber domain using the discrete Fourier transform. If the number of nonzero terms in the pattern tile is less than 132, however, it is more efficient to compute the correlation function in the spatial domain (eq. (8)) than in the Fourier domain (Campbell 1969). Details of the computational procedure are given in the references cited above.

Improved velocity computation — Figures 9a and 9b show two coregistered 330 × 390 image subsections from a 1024 × 1024 image centered at 38°N and 125°W. The two images were taken by the NOAA-9 and NOAA-11 polar orbiters, respectively, and are separated in time by 4 h and 53 min. Figure 9c shows the velocity field computed using the MCC method described above. For these calculations, pattern and search tile sizes of 14 × 14 and 30 × 30 pixels were used, respectively. These choices were made on the basis of in situ drifter data for this filament (Ramp et al. 1991). The vectors in this panel clearly illustrate both directional ambiguity and large-magnitude variation. In fact, the computed pattern of flow (Fig. 9c) often deviates substantially

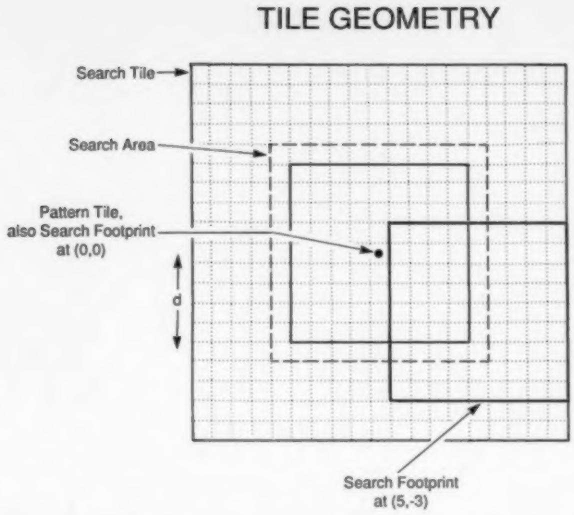

FIG. 8. Diagram showing the relation between pattern tile, search tile, active search area, and search footprint used in the MCC method of velocity estimation.

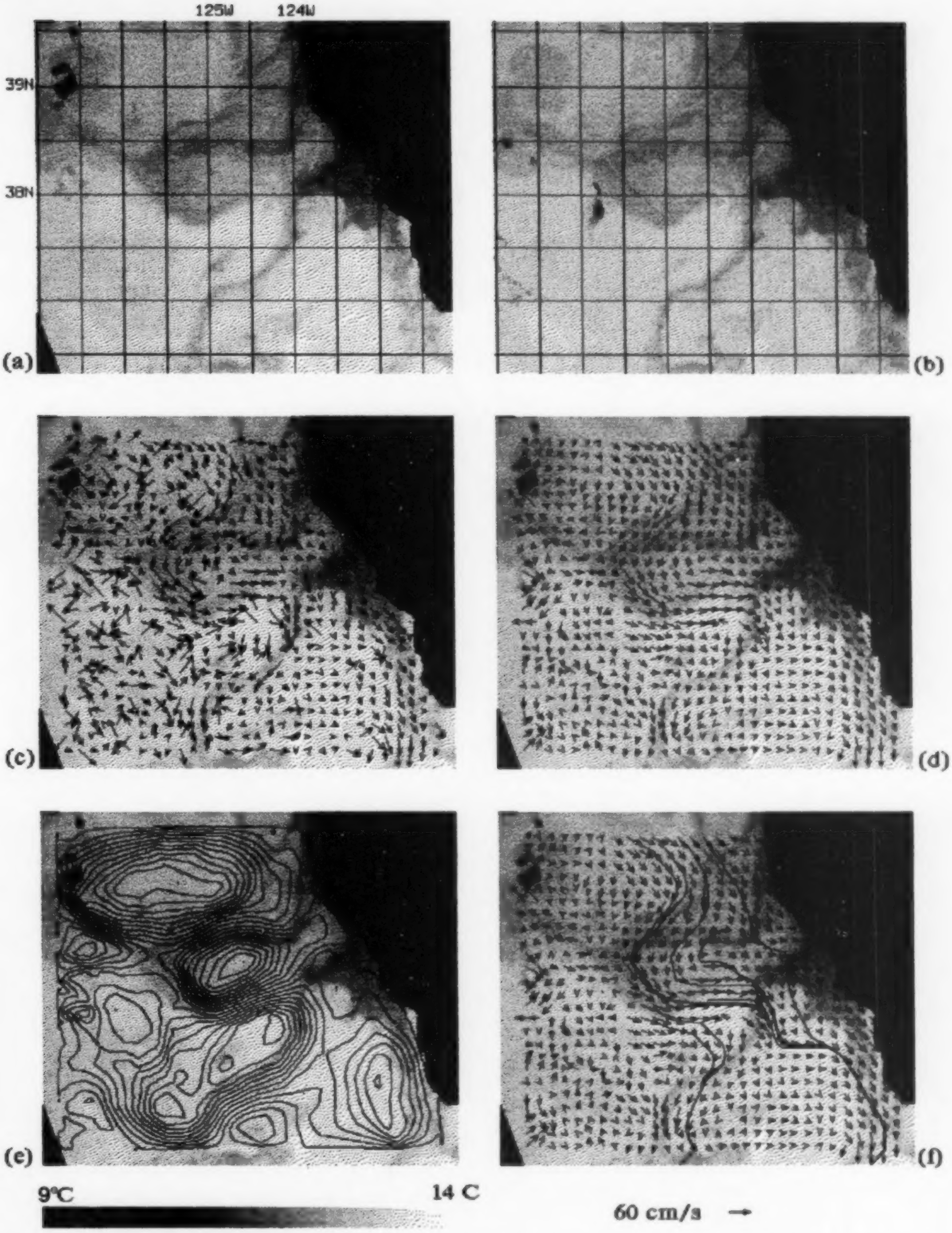

FIG. 9. (a and b) Coregistered images of a filament off northern California (the images are separated in time by 4 h and 53 min); (c) near-surface velocity field derived from these two images using the MCC method; (d) vector median filtered near-surface velocities for the same filament based on the procedure developed by Simpson and Gobat (1994); (e) computed stream function for the filament; (f) simulated Lagrangian drifters (solid lines) for the filament computed using the method of Simpson and Gobat (1994).

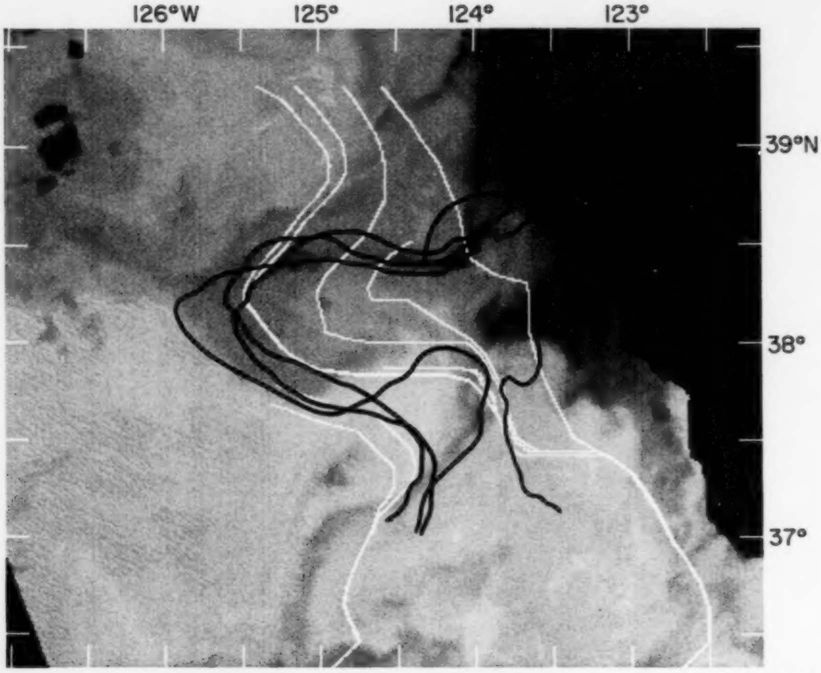

FIG. 10. Simulated Lagrangian drifters (white) and in situ drifter observation (black) for this filament as reported by Ramp et al. (1991). There is overall good agreement between the satellite-derived drifter tracks and the in situ observations. See the text for details of the difference in release points of the simulated and in situ Lagrangian drifters.

from the expected flow pattern inferred visually from the two filament realizations (Fig. 9a and 9b). This directional ambiguity and magnitude uncertainty occur because the two-dimensional cross-correlation functions used in the MCC method often contain saddle points which can give rise to uncertainties of the types shown in Fig. 9c (Simpson and Gobat 1994).

Simpson and Gobat (1994) have developed a mathematical procedure to minimize these negative aspects of the MCC method. The primary steps necessary to numerically compute accurate estimates of near-surface oceanic velocities from sequences of satellite data are (1) compute the velocity at every possible pixel in the image using the MCC method and (2) vector median filter the resultant velocity field to remove the MCC-induced ambiguity. Velocity calculation at every point is computationally demanding, but is increasingly feasible with modern workstations. The smoothness that the vector median filter imposes on this dense grid (compare Fig. 9c and 9d) then allows for stable, low-order-error numerical computations useful in fisheries oceanography (e.g., stream functions, simulated Lagrangian drifters).

Once a vector median filtered velocity field (Fig. 9d) has been produced, the stream function (Fig. 9e) can be computed as follows: (1) extract the boundary of the velocity field, (2) compute the vorticity and divergence of the field using finite differences, (3) compute the normal (V_n) and tangential (V_s) velocities around the boundary, (4) adjust V_s and V_n to satisfy two-dimensional integral constraints on both the divergence and vorticity of the vector median filtered velocity field, (5) solve for the velocity potential associated with the two-dimensional divergence equation (i.e., $\nabla^2\chi = \vec{\nabla}\cdot\vec{u} = D$) assuming a zero boundary condition, (6) compute the normal derivatives of χ around the boundary, (7) substitute these derivatives into a Neuman boundary condition for the normal component of velocity V_n and integrate to compute the stream function ψ around the boundary, (8) solve the two-dimensional form of the vorticity equation (e.g., $\nabla^2\psi = \zeta$) with the new boundary condition computed from step 7, (9) compute the normal derivative of ψ around the boundary, (10) substitute these derivatives into the Neuman boundary condition for the tangential velocity (V_s) and integrate to get χ around the boundary, (11) solve for χ with this new boundary condition, and (12) repeat steps 6–11 until convergence. The resultant stream function for the filament (Fig. 9e) matches well the flow of the filament as inferred visually by comparing Fig. 9a and 9e.

Because the velocity fields derived using the method of Simpson and Gobat (1994) are numerically stable, simulated Lagrangian drifters also can be computed from the velocity data using fourth-order Runge–Kutta update equations. Ramsden and Holloway (1991) have shown that this procedure is superior to other methods of Lagrangian particle tracking for oceanic applications. Simpson and Gobat (1994, their Fig. 5) showed good correspondence between their simulated Lagrangian drifters and in situ drifters deployed by Swenson et al. (1992) during the CTZ experiment. Figure 10 shows a comparison between simulated Lagrangian drifters (white) and another set of in situ drifter observations (black) for the filament in Fig. 9. In situ data are from Ramp et al. (1991). The in situ drifters (Fig. 10) were released close to shore. Because of the fixed-grid numerical procedure used to compute the simulated Lagrangian drifters, the simulated

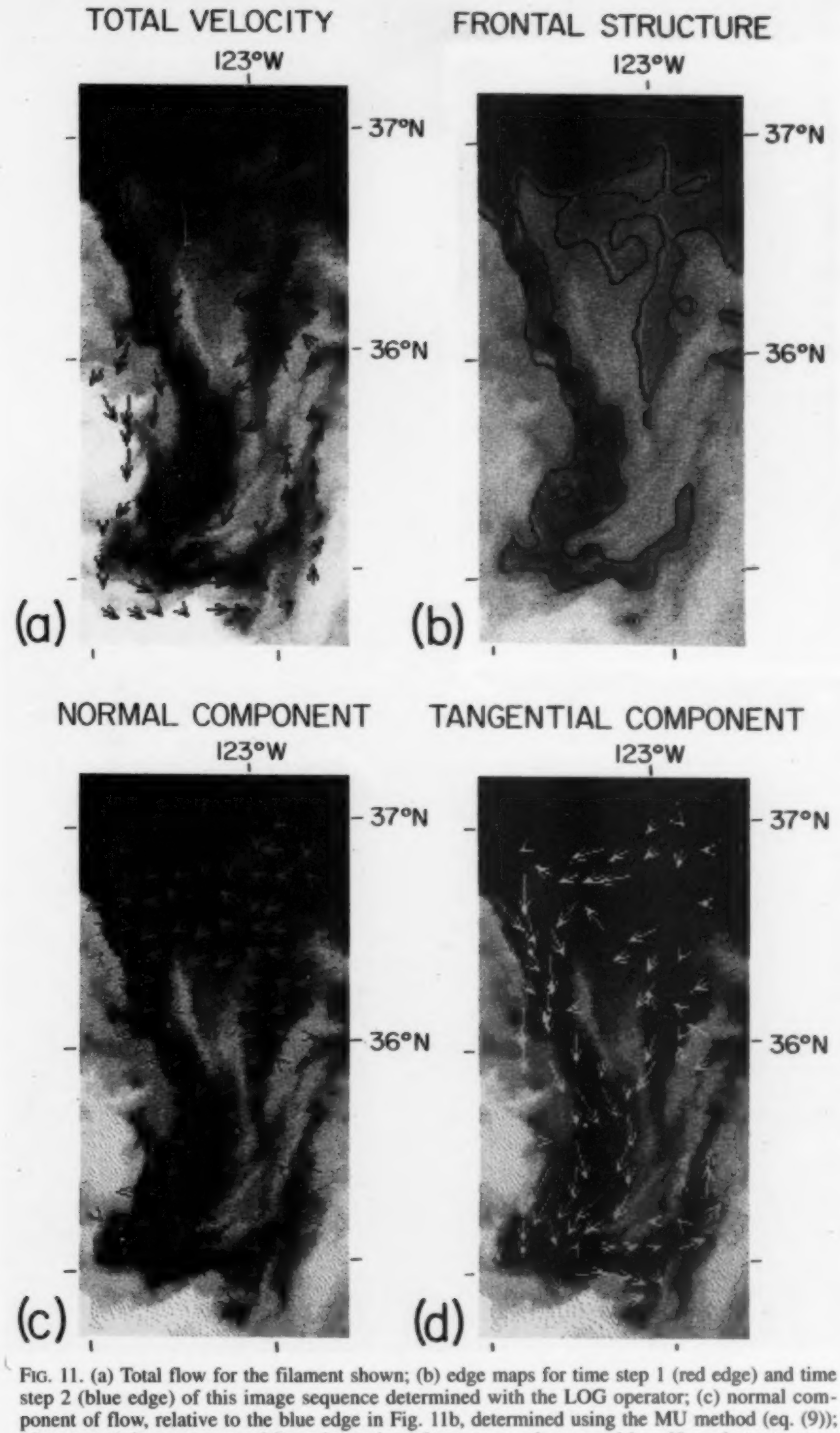
TOTAL VELOCITY
FRONTAL STRUCTURE
NORMAL COMPONENT
TANGENTIAL COMPONENT
123°W
37°N
36°N
(a)
(b)
(c)
(d)

FIG. 11. (a) Total flow for the filament shown; (b) edge maps for time step 1 (red edge) and time step 2 (blue edge) of this image sequence determined with the LOG operator; (c) normal component of flow, relative to the blue edge in Fig. 11b, determined using the MU method (eq. (9)); (d) tangential component of flow determined from vector decomposition. Note that a tangential component will be computed only if both valid total and normal velocities have been computed previously.

drifters must be "released" further offshore than the in situ drifters. Nonetheless, once the simulated Lagrangian drifters enter the main flow of the filament, they show good correspondence with the in situ observations.

In order to improve the numerical solution of the advective–diffusive equation and make the solution more robust near irregular coastal boundaries, finite elements methods presently are being implemented for these computations. This will allow use of an adaptive size grid and deployment of the simulated drifters very near the coast. When combined with higher spatial resolution LandSat TM data (10–30 m), the technique should prove very useful, for example, to estimate the transport of eggs/larvae into or out of spawning areas. Moreover, such studies could be performed at reduced cost because only a limited number of in situ drifters are needed to calibrate the remotely-sensed velocities.

Limitations of total velocity computational methods — The basic assumption of these methods is shape invariance of the pattern under translation. Rotational motion of the pattern, however, can also occur. Pattern matching techniques that detect rotational motion and/or combined translational–rotational motion of the pattern have been developed (e.g., Kamachi 1989). These methods are computationally very expensive but will perform well in the presence of curvature in the motion field of the pattern. Only translational techniques were used herein because they were (and generally are) sufficient to determine the general flow pattern in most sequences of satellite images. Moreover, results from the MCC method are critically dependent upon pattern and search tile sizes (e.g., Tokmakian et al. 1990; Wahl and Simpson 1991; Kelley and Strub 1992). Therefore, limited amounts of in situ velocity measurements are especially helpful for determining tile geometries. Thus, it is recommended that a given field program deploy a minimum number of drifters if best-quality satellite-derived velocity estimates are desired.

Normal component of flow

The idea of directionally sensitive units that can establish the direction of movement of an edge detected by the LOG operator was introduced by Marr and Ullman (1981) (hereafter referred to as MU) to determine the motion of visual elements. If I is a demeaned image, then locations of zero crossings of the convolution of the LOG operator with I will correspond to locations of intensity changes (i.e., gradients). Let this be denoted $\nabla^2 G ** I = I'$. Note that the units of I and I' are the same (for AVHRR data, degrees Celsius). Given an approximation to the time derivative of I' and the spatial rate of change of I', the direction of motion of a zero crossing in either the line or sample direction can be determined. The locations of zero crossings in the first and second convolved images of a different filament sequence as determined by a zero crossing operator are shown in Fig. 11b, (red edge and blue edge, respectively). Then, at each zero crossing pixel, the normal component of flow can be estimated using the equation

$$(9) \quad v = \frac{-I'_t}{|\bar{\nabla} I|}$$

where the subscript represents differentiation with respect to time, and the unit normal vector $\hat{n}$ is in the direction of the gradient $\bar{\nabla} I'$. Eq. (9) is the conservation of heat equation ($DT/dt = 0$) for the convolved image I'. If the magnitude of the gradient is negative and I'_t is positive, then the motion of the edge is in the positive x direction. If I'_t is negative, motion is in the negative x direction. The opposite is true if the magnitude of the gradient is positive. Thus, the negative sign in eq. (9) gives the correct direction of the normal component of flow. It can be seen that a directionally sensitive unit is represented by a transition in the sign of I'_t combined with the sign of the gradient.

Methods used to compute the normal component of flow employ small neighborhoods, typically 4 × 4 pixels or less in size. The total velocity is computed over a much larger neighborhood. Typically, pattern tile sizes vary between 16 × 16 and 32 × 32 pixels. Thus, estimates of the total velocity using the MCC method represent the mean motion of the centroid of the pattern as measured by the displacement of the two-dimensional maximum cross-correlation (eq. (8)). The normal velocities, however, provide local estimates of the displacement of small spatial-scale gradient. This basic difference in spatial scales further constrains the computation of the tangential component of the total flow. Computation of the normal component of velocity is discussed further in Wahl and Simpson (1991).

Tangential component of flow

In the previous section, only the component of flow normal to iso-brightness contours was discussed because the tangential component of flow cannot be calculated *directly*. The difficulty arises from what is known as the aperture problem and manifests itself in different ways for different motion estimation algorithms. In the MU case, the problem occurs when the motion of an oriented edge is detected by a directionally sensitive unit that is small compared with the moving edge. Then, the only information that can be extracted is the component of motion perpendicular to the local orientation of the edge. Hence, the component of motion oriented along the edge is invisible. An alternative interpretation of the aperture problem occurs if a point of brightness along an iso-brightness contour moves along that contour from time t_1 to time t_2; this motion cannot be detected because all points on an iso-brightness contour have *identical* properties. These considerations show that a direct method for computing the tangential component of flow is not possible. Vector decomposition of the known total velocity field, given a known normal component of flow, however, can yield an estimate of the tangential component of flow. These considerations are consistent with a proof given by Verri and Poggio (1989).

Given the total flow field computed on a rectangular grid as discussed by Wahl and Simpson (1991) and median filtered to remove ambiguity in velocity estimates (Simpson and Gobat 1994), one can take the normal component of flow and perform a vector subtraction to obtain the tangential component. The MU normal velocities are computed only at the points of zero crossings of edges. These vectors must be spatially aligned on the same grid as that of the total velocity prior to the decomposition. To estimate the normal components of velocity at the locations of the total flow, the MU normal components were subsectioned into the same size tiles as the total flow. The normal velocities that fell within the region of the pattern tile area of the first image were then averaged to produce an overall average normal velocity for a given tile. This procedure is consistent with the assumption that the total velocity vector produced by the pattern matching technique represents the average velocity of the feature in a pattern tile. The mean normal component of flow was then decomposed into its Cartesian components (Fig. 8), which were used in the final vector decomposition to compute the tangential component of flow. A more detailed discussion of the computation is given in Wahl and Simpson (1991).

Example

A sequence of two cloud-free AVHRR images for a region off the central California coast was coregistered to a latitude–longitude grid and calibrated to SST. This sequence is characterized by a cold-water filament extending southward from the top of the sampled region. The total velocity (Fig. 11a) was computed as described by Wahl and Simpson (1991). The thermal structure edge maps for time step 1 (Fig. 11b, red) and for time step 2 (Fig. 11b, blue) of the image sequence were computed using the LOG operator with a value of $\sigma = 5$. The displacement of the blue edge from the red edge indicates the motion of the filament during the 3.5-h interval between the images. Motion inferred from these edge maps agrees well with estimates of the total flow field computed using the pattern matching method (compare Fig. 11a and 11b).

These edge maps were then used to compute the normal component of velocity of the thermal structure over time using Eq. (9) at the zero crossing points. A centered finite difference scheme was used to compute the spatial gradient of I', and a single time-centered difference was used to approximate the temporal derivative of I'. It is important to emphasize that the MU method only yields an estimate of the normal component of velocity near a well-defined edge (e.g., Fig. 11b). The normal component of flow so obtained (Fig. 11c) accurately represents motion inferred from the edge maps (examine the displacements shown in Fig. 11b). Note especially the north–south-oriented feature in the center right region of Fig. 11b. The tangential component of flow (Fig. 11d) again shows good correspondence with motion inferred from the edge maps.

Ideally, the estimated normal and tangential components of flow should be orthogonal. The need for spatial averaging of the normal components, however, may introduce directional errors in the approximation of the tangential component. Wahl and Simpson (1991) have shown that typically the angles between the normal and tangential components of flow are between 75 and 80°. Thus, this method generally will not produce an exact tangential solution. It does, however, produce an approximate tangential solution which can be useful in many oceanographic applications (e.g., computation of the offshore transport of nutrients and/or eggs and larvae associated with coastal upwelling). It should be reemphasized that there is no direct method for computing the tangential component of motion from sequences of image data.

Representativeness of Satellite Data of Subsurface Ocean Structure

The ocean is nearly electromagnetically opaque. Hence, most satellite observations only measure the sea-surface signatures (e.g., AVHRR measures infrared SST in the thermomolecular boundary layer at the air–sea interface which typically is 1–2 μm thick (Paulson and Simpson 1981)) or near-surface signatures (e.g., CZCS measures over a depth between 1 and 2 optical attenuation lengths depending upon the optical water type (Jerlov 1976)) of interior ocean processes. Thus, a practical question of considerable importance to operational fisheries oceanography is: How representative are satellite data of interior ocean processes and how does this limitation potentially affect an operational fishery?

The majority of evidence clearly indicates that satellite data generally are quite revealing of subsurface conditions both on the continental shelf and even in deep water. For example, satellite data proved very helpful in identifying the locations of and subsequently designing oceanographic cruises to map filaments (Flament et al. 1985; Ramp et al. 1991; Strub et al. 1991) and mesoscale eddies in the California Current (Koblinsky et al. 1984). In fact, vertical decorrelation scales, computed between satellite data (AVHRR and CZCS) and in situ CTD and optical/fluorometric data, show that satellite data can be representative of deep (>600 m) ocean structure (e.g., Simpson et al. 1986). Moreover, bathymetric effects often can be observed in satellite data. Figure 6 shows the surface signature (with ship track overlay) of a confirmed mesoscale eddy dipole which probably developed as a result of a bathymetrically induced baroclinic instability of the California Undercurrent near the Santa Rosa – Cortes Ridge in water between 300 and 400 m deep (Simpson and Lynn 1990). This study also provided evidence that such a mechanism might be responsible for many of the mesoscale eddies found in the offshore waters between Punta Eugenia, Baja California, and Sitka, Alaska.

Complicated baroclinic effects are not always represented either completely or correctly in satellite data. For example, Simpson et al. (1984) made detailed in situ observations of the horizontal and vertical structure beneath one of the recurrent, semistationary mesoscale eddy surface signatures generally found off Pt. Conception, California, in AVHRR data. The CTD data revealed the presence of a highly symmetric three-layered system. A subsurface warm-core eddy, which extended from about 250 to 1200 m, was the dominant dynamical feature. A warm surface layer, which extended to a depth of 75 m, laid over the eddy. Between the warm surface layer and the subsurface warm-core eddy, there was a cold-core region that extended to a depth of about 200 m. Because the satellite detected the quasi-geostrophic readjustment of the near-surface layer to the dominant subsurface warm-core eddy (i.e., the dynamic height anomaly of the warm-core eddy was larger than that of the cold-core region), the satellite provided no evidence of the existence of the intermediate cold-core region. Other observational studies (e.g., Voorhis et al. 1976) and numerical models (e.g., Nelepo et al. 1978) provide evidence for the expected effects of subsurface eddies on satellite-derived SST distribution; these other studies and that of Simpson et al. (1984) are consistent. Finally, it should be noted that as the degree of baroclinic complexity increases, the representativeness of satellite surface signatures to the details of interior ocean structure should be expected to decrease. Emery et al. (1980) provided further insight into this question. Their results, however, may be partially compromised by the fact that the multiship XBT survey data available to them was not sampled on as fine a spatial scale as preferred for mesoscale eddy detection.

From the point of view of an operational pelagic fishery, surface and near-surface signatures from space generally

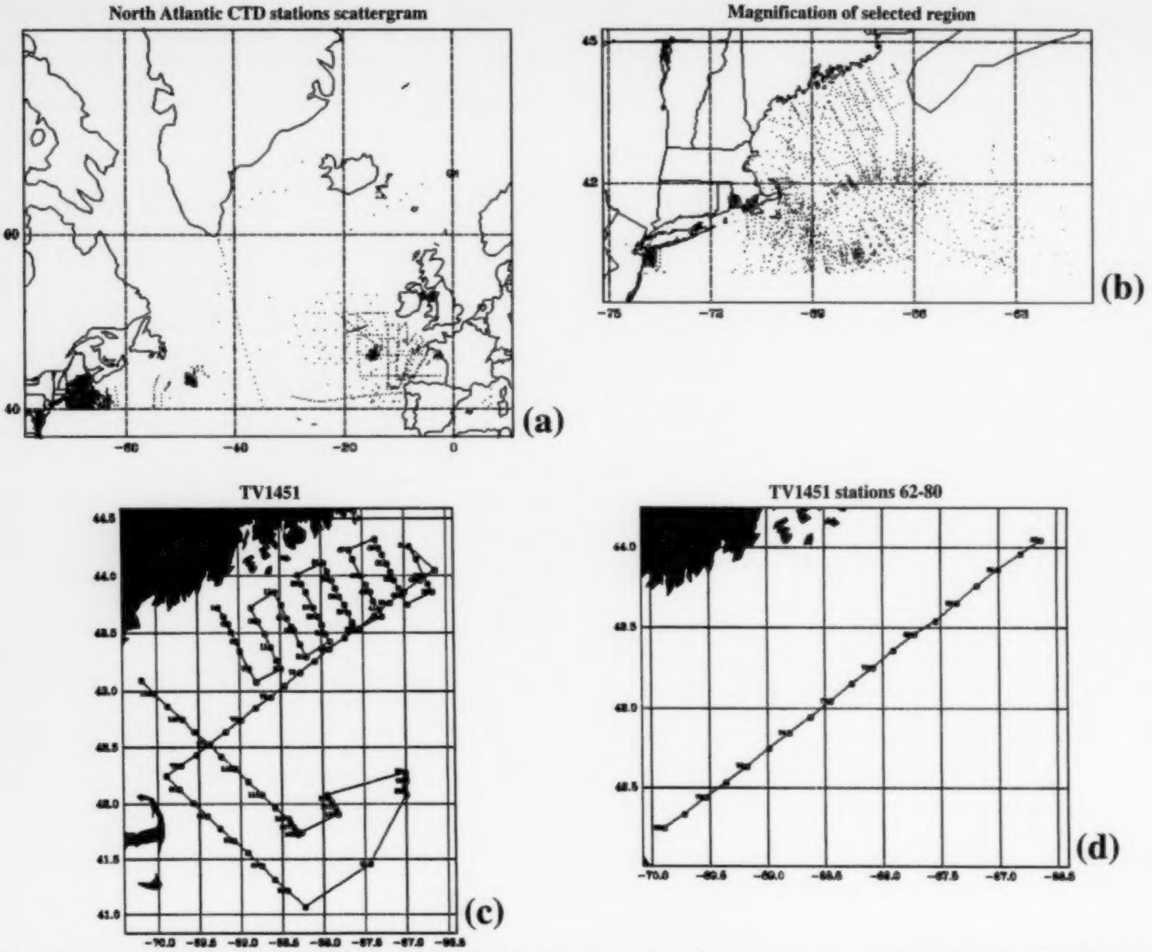
North Atlantic CTD stations scattergram

Magnification of selected region

TV1451

TV1451 stations 62-80

FIG. 12. Use of the selective search capabilities of CORAL (Simpson et al. 1994a) to isolate progressively smaller and smaller subsets of the global database for analysis. (a) Region of the North Atlantic; (b) region off the New England and Canadian Maritime coasts; (c) specific cruise within the region selected by Fig. 12b; (d) line of stations from the cruise identified in Fig. 12c.

will prove adequate to support the fishery. The biggest operational problem associated with satellite data for a pelagic fishery is the absence of satellite data because of cloud cover. Under these circumstances, historical data bases may provide the only operational insight. A combined remote sensing/geographical information system (RS/GIS) provides the only practical solution for support of a pelagic fishery often overcast with clouds (Simpson 1992b).

For an operational mid- or deepwater fishery, satellite data can prove quite useful but must be supplemented by historical and contemporaneous interior ocean data (e.g., temperature, salinity, catch statistics) and bathymetric data. A combined RS/GIS technology may be most appropriate for these types of fisheries (e.g., dover sole (*Microstomus pacificus*)). The advantages of RS/GIS technology in support of both pelagic and mid- and deepwater operational fisheries are discussed below.

Geographical Information Systems

Historically, geographical information systems (GIS) have not been used extensively in fisheries oceanography. They have the potential, however, to assist the community in at least three areas: (1) provide information on a pelagic fishery when satellite coverage is precluded by cloud cover, (2) provide information to support mid- and deepwater fisheries when and where satellite data may be unrepresentative of environmental conditions, and (3) provide capabilities for the retrospective analyses of large data sets to determine long-term, large-scale trends and variations in the fishery.

Species-specific behavior and preferred environmental conditions provide the basis for integration of GIS technology into an operational fishery. For example, 98% of the spawning biomass of Dover sole in Central California waters live in a region of the continental slope between 640 and 1006 m depth, which is characterized by low oxygen concentration (0.27–0.31 mL/L) and cold temperature (3.2–5.9°C) (Hunter et al. 1990). Dover sole settle on the continental shelf and gradually move down the continental slope over their lifetime, reaching the oxygen minimum as they attain sexual maturity. This ontogenetic movement down the slope

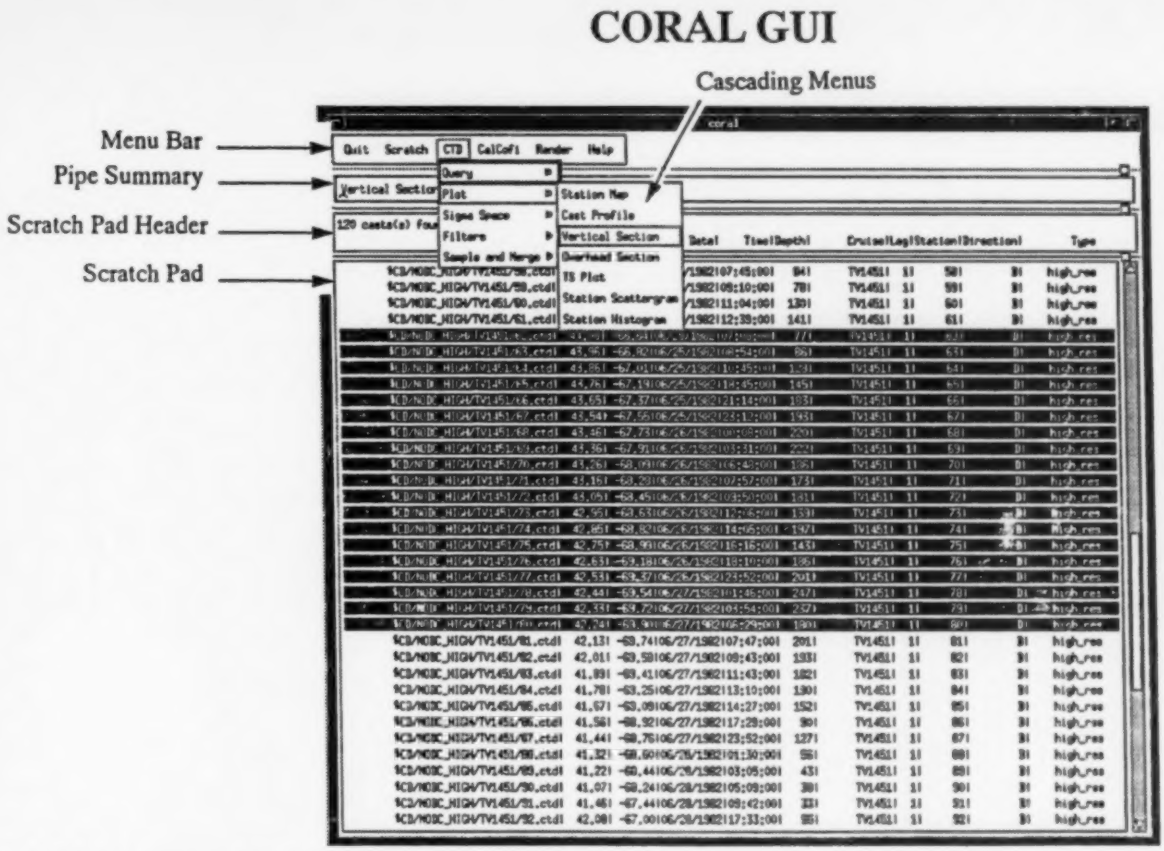

```
120 casts(s) fou                                  Date|   Time|Depth|     Cruise|Leg|Station|Direction|     Type
     $CD/NODC_HIGH/TV1451/58.ctd|                /1982|07:45:00|  84|     TV1451| 1|  58|      D|  high_res
     $CD/NODC_HIGH/TV1451/59.ctd|                /1982|09:10:00|  78|     TV1451| 1|  59|      D|  high_res
     $CD/NODC_HIGH/TV1451/60.ctd|                /1982|11:04:00| 130|     TV1451| 1|  60|      D|  high_res
     $CD/NODC_HIGH/TV1451/61.ctd|                /1982|12:39:00| 141|     TV1451| 1|  61|      D|  high_res
     $CD/NODC_HIGH/TV1451/62.ctd| [illegible]                       77|     TV1451| 1|  62|      D|  high_res
     $CD/NODC_HIGH/TV1451/63.ctd| 43.95| -66.82|06/25/1982|08:54:00|  86|     TV1451| 1|  63|      D|  high_res
     $CD/NODC_HIGH/TV1451/64.ctd| 43.86| -67.01|06/25/1982|10:45:00| 131|     TV1451| 1|  64|      D|  high_res
     $CD/NODC_HIGH/TV1451/65.ctd| 43.76| -67.19|06/25/1982|18:45:00| 145|     TV1451| 1|  65|      D|  high_res
     $CD/NODC_HIGH/TV1451/66.ctd| 43.65| -67.37|06/25/1982|21:14:00| 183|     TV1451| 1|  66|      D|  high_res
     $CD/NODC_HIGH/TV1451/67.ctd| 43.54| -67.55|06/25/1982|23:12:00| 193|     TV1451| 1|  67|      D|  high_res
     $CD/NODC_HIGH/TV1451/68.ctd| 43.46| -67.73|06/26/1982|00:08:00| 220|     TV1451| 1|  68|      D|  high_res
     $CD/NODC_HIGH/TV1451/69.ctd| 43.36| -67.91|06/26/1982|03:31:00| 222|     TV1451| 1|  69|      D|  high_res
     $CD/NODC_HIGH/TV1451/70.ctd| 43.26| -68.09|06/26/1982|06:43:00| 136|     TV1451| 1|  70|      D|  high_res
     $CD/NODC_HIGH/TV1451/71.ctd| 43.16| -68.28|06/26/1982|07:57:00| 173|     TV1451| 1|  71|      D|  high_res
     $CD/NODC_HIGH/TV1451/72.ctd| 43.05| -68.45|06/26/1982|09:50:00| 181|     TV1451| 1|  72|      D|  high_res
     $CD/NODC_HIGH/TV1451/73.ctd| 42.95| -68.63|06/26/1982|12:06:00| 159|     TV1451| 1|  73|      D|  high_res
     $CD/NODC_HIGH/TV1451/74.ctd| 42.85| -68.82|06/26/1982|14:05:00| 197|     TV1451| 1|  74|      D|  high_res
     $CD/NODC_HIGH/TV1451/75.ctd| 42.75| -68.99|06/26/1982|16:16:00| 143|     TV1451| 1|  75|      D|  high_res
     $CD/NODC_HIGH/TV1451/76.ctd| 42.63| -69.18|06/26/1982|18:10:00| 186|     TV1451| 1|  76|      D|  high_res
     $CD/NODC_HIGH/TV1451/77.ctd| 42.53| -69.37|06/26/1982|23:52:00| 201|     TV1451| 1|  77|      D|  high_res
     $CD/NODC_HIGH/TV1451/78.ctd| 42.44| -69.54|06/27/1982|01:46:00| 247|     TV1451| 1|  78|      D|  high_res
     $CD/NODC_HIGH/TV1451/79.ctd| 42.33| -69.72|06/27/1982|03:54:00| 237|     TV1451| 1|  79|      D|  high_res
     $CD/NODC_HIGH/TV1451/80.ctd| 42.24| -69.90|06/27/1982|06:29:00| 180|     TV1451| 1|  80|      D|  high_res
     $CD/NODC_HIGH/TV1451/81.ctd| 42.13| -69.74|06/27/1982|07:47:00| 201|     TV1451| 1|  81|      D|  high_res
     $CD/NODC_HIGH/TV1451/82.ctd| 42.01| -69.59|06/27/1982|09:43:00| 193|     TV1451| 1|  82|      D|  high_res
     $CD/NODC_HIGH/TV1451/83.ctd| 41.89| -69.41|06/27/1982|11:43:00| 182|     TV1451| 1|  83|      D|  high_res
     $CD/NODC_HIGH/TV1451/84.ctd| 41.78| -69.25|06/27/1982|13:10:00| 130|     TV1451| 1|  84|      D|  high_res
     $CD/NODC_HIGH/TV1451/85.ctd| 41.67| -69.09|06/27/1982|14:27:00| 152|     TV1451| 1|  85|      D|  high_res
     $CD/NODC_HIGH/TV1451/86.ctd| 41.56| -68.92|06/27/1982|17:29:00|  90|     TV1451| 1|  86|      D|  high_res
     $CD/NODC_HIGH/TV1451/87.ctd| 41.44| -68.76|06/27/1982|23:52:00| 127|     TV1451| 1|  87|      D|  high_res
     $CD/NODC_HIGH/TV1451/88.ctd| 41.32| -68.60|06/28/1982|01:30:00|  56|     TV1451| 1|  88|      D|  high_res
     $CD/NODC_HIGH/TV1451/89.ctd| 41.22| -68.44|06/28/1982|03:05:00|  43|     TV1451| 1|  89|      D|  high_res
     $CD/NODC_HIGH/TV1451/90.ctd| 41.07| -68.24|06/28/1982|05:09:00|  38|     TV1451| 1|  90|      D|  high_res
     $CD/NODC_HIGH/TV1451/91.ctd| 41.46| -67.44|06/28/1982|09:42:00|  33|     TV1451| 1|  91|      D|  high_res
     $CD/NODC_HIGH/TV1451/92.ctd| 42.08| -67.00|06/28/1982|17:33:00|  55|     TV1451| 1|  92|      D|  high_res
```

FIG. 13. Main elements of the CORAL GUI. A scratch pad also is shown. It contains the results (metadata) from a query to the global CTD database. Highlighted entries in the scratch pad were selected by the user for analysis.

continues after sexual maturity and is accompanied by a significant increase in the water content of the body and a subsequent decrease in caloric density per gram net weight (Hunter et al. 1990). These facts, coupled with robust GIS technology and updated in situ data bases, provide a means for optimizing catch per unit of effort for Dover sole. Moreover, they provide a basis for targeting the subpopulation of Dover sole that is commercially most profitable (i.e., that with the maximum caloric density per gram).

GIS technology has especially important implications for fisheries research and fisheries management. Consider the North Atlantic rim cod. Serval null hypotheses can be formulated relating comparisons between various cod stocks throughout the rim: (1) no temporal coherence in cod recruitment (year-class strength) or zooplankton production exists across the North Atlantic, (2) neither cod nor zooplankton populations correlate similarly with temperature (other physical variables) either between western and eastern North Atlantic cod or within both western and eastern North Atlantic stocks, (3) differences in the growth, respiration, fecundity, and maturity between cod stocks can be accounted for by differences in temperature, food availability, and fishing and predation pressure rather than by inherent differences in the stocks, and (4) cod abundance, production, recruitment, and spatial distribution respond differently to zooplankton population abundance and distribution either between western and eastern North Atlantic Stocks or within both western and eastern North Atlantic Stocks.

Clearly, to provide the wherewithal to address these and related hypotheses, one must have sufficient data on environmental conditions and prey, cod, and predator stocks. These data generally would consist of spatially and temporally georeferenced biological and physical data sets. Available biological data include trawl surveys, Continuous Plankton Recorder transects from ships of opportunity, ICNAF plankton surveys, and MARMAP plankton surveys. These examples are based on Northwest Atlantic data sources, a summary and preliminary analysis of which have been compiled by Meyers (1993) for 22 North Atlantic rim stocks. Environmental data include AVHRR satellite SST (1982–present), the NODC Global High Resolution CTD data base and global bathymetry and coastline data bases, climate data, and ships of opportunity ocean monitoring data on the New York Bight and Gulf of Maine routes (from 1978) and Southern New England (1974–84). Additional time series from NOAA data buoys, NOS tide stations, coastal weather stations, and stream flow are available for long time periods. The data archive and retrieval capabilities of a GIS system make the use of such diverse and complex data sets tractable.

For most effective and efficient use of a GIS system, the

Spiciness vs. Pressure Vertical Section

GUI Interface

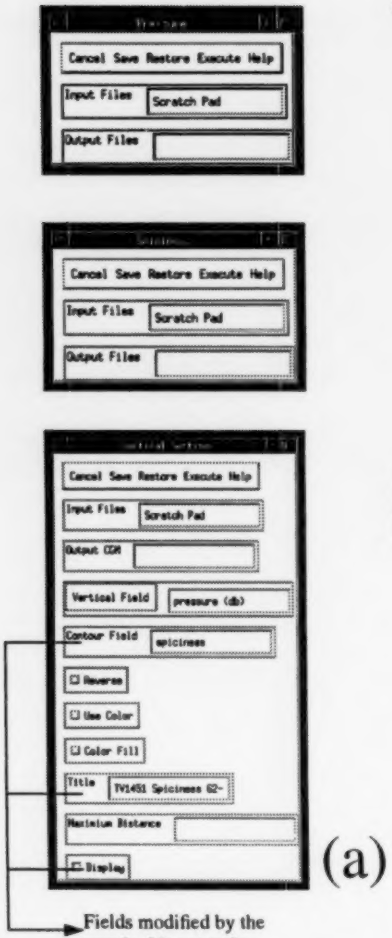

Input Files: Scratch Pad

Input Files: Scratch Pad

Input Files: Scratch Pad

Vertical Field: pressure (db)

Contour Field: spiciness

Title: TV1451 Spiciness 62-

☑ Display

Fields modified by the user in this example

Command Line

```
ctd_pressure -in
        $CD/NODC_HIGH/TV1451/62.ctd
        $CD/NODC_HIGH/TV1451/63.ctd
        $CD/NODC_HIGH/TV1451/64.ctd
        $CD/NODC_HIGH/TV1451/65.ctd
        $CD/NODC_HIGH/TV1451/66.ctd
        $CD/NODC_HIGH/TV1451/67.ctd
        $CD/NODC_HIGH/TV1451/68.ctd
        $CD/NODC_HIGH/TV1451/69.ctd
        $CD/NODC_HIGH/TV1451/70.ctd
        $CD/NODC_HIGH/TV1451/71.ctd
        $CD/NODC_HIGH/TV1451/72.ctd
        $CD/NODC_HIGH/TV1451/73.ctd
        $CD/NODC_HIGH/TV1451/74.ctd
        $CD/NODC_HIGH/TV1451/75.ctd
        $CD/NODC_HIGH/TV1451/76.ctd
        $CD/NODC_HIGH/TV1451/77.ctd
        $CD/NODC_HIGH/TV1451/78.ctd
        $CD/NODC_HIGH/TV1451/79.ctd
        $CD/NODC_HIGH/TV1451/80.ctd
|ctd_potemp
|ctd_spice
|ctd_vertical -vertical pressure -channel spiciness
        -label "TV1451 Spiciness 62-80" -display
```

(b)

FIG. 14. GUI for the vertical section function. (a) Text entries made by the user to produce a vertical section of spiciness versus pressure for the color display on an X-Window terminal; (b) corresponding UNIX command line created by CORAL to produce the vertical section (Fig. 15). The command instructed CORAL to pick the appropriate stations (highlighted) from the CORAL scratch pad (Fig. 13), compute spiciness and potential temperature, and then produce and label a color-rendered vertical section of spiciness for display on the terminal.

user should first define the desired hypothesis to test (as above) or alternatively the analysis to perform. This will determine which regional subsets of appropriate data are needed and will provide the basis for choosing query criteria and map projection/display formats. Then, the user would login to the GIS system. A map of the entire Atlantic rim (on the appropriate map projection), for example, might appear on the screen (e.g., Fig. 12a) along with the data base query menus.

Queries could be by SPATIO-TEMPORAL-STOCK and by VARIABLE. The user also should be able to zoom into a subarea (e.g., via a mouse-delineated bounding box) and choose specific areas by STOCK or by REGION (e.g., Fig. 12b). GIS technology, customized for an operational fishery, would make it possible to search variables by Trophic Level, Temperature, Hydrology, and Bathymetry. Each Variable category will have a submenu. For example, Trophic Level might give Zooplankton, Phytoplankton, and Fish (cod). Under Fish would be Data Type including Population, Age Class, Recruitment, and Stomach Contents. Metadata associated with all data sets chosen would appear in the appropriate scratch pads (a separate scratch pad for each basic type of data, e.g., Fig. 13). Subsets of the data could be selected with even finer precision based upon data attributes returned to the scratch graphical user interface (GUI) pad(s) via the guided query (Fig. 12c and 12d).

The CORAL system (Simpson et al. 1994a) can be used to show how a user would enter the exploratory phase of a GIS browser. Mapped displays of the locations of data points could be made (Fig. 12d) and exploratory analysis performed. GUI-based commands could be used to perform the chosen analysis (Fig. 14). Spiciness, for example, could be computed and used to tag water masses (Fig. 15). Secondary displays of chosen individual variables could be made by contour plot, raster image plot, or overlays of time series at the location where the data are collected (or at the center of a region for regionally averaged data), and distribution histograms, boxplots, or time series of individual variables could be drawn on the map or on separate windows. Scatterplots of chosen variables also could be drawn.

Because so many of the possible hypotheses relate to comparisons of time series of variables between regions or stocks, the GIS analysis capabilities should include tests comparing two or more time series. Time series methods such as multivariate autoregression or the fast Fourier transform might be used to look at coherence between the spectra for the different variables, or the cross covariance might help in comparing different variables across regions. Another approach is to use nonparametric regression to model cod abundance with a stock effect, a year effect, a region effect, or a temperature effect, etc. Generalized additive models (GAM) could help uncover relations between variables when the functional form of the relation is unknown and where the underlying distribution is not normal. Multivariate analysis of variance might be used when significance of a factor, but not the underlying form of the relation, is to be tested for. Other multivariate methods, such as interval testing or hierarchical clustering, might be useful when the user desires to identify stocks that have similar temporal patterns.

The above discussion shows that considerable emphasis must be placed on three specific design components of a fisheries-oriented GIS system: (1) the GUI, (2) analysis and display methods, and (3) computer-aided decision making. The GUI is essential because most members of the operational fisheries oceanography community have had little formal training in computer science. The GUI also must shield the community from the drudgery of computer applications programming and/or command line execution while simultaneously making available all capabilities of the underlying system. Analysis procedures must be incorporated into the basic design of the GIS to insure that large amounts of data can be reduced to manageable amounts of high-quality information. Computer-aided decision making also is essential because the volume of data that often needs to be processed in near-real time (e.g., Pacific Northwest Salmon Fishery) virtually precludes direct human involvement with all aspects of the analysis. Thus, the GIS system envisioned here is considerably different from those typically used in geographical applications. These latter GIS systems usually emphasize graphical overlay capabilities and human visual analysis.

Fisheries Application

Management

ENSO events and their contemporaneous midlatitude warming events can drastically reduce fish stocks in eastern boundary currents (e.g., anchovy fishery off Peru, tuna fishery off California). Monitoring these large-scale phenomena with updated sequences of AVHRR data could provide early indications of the onset of ENSO events and help prevent overfishing during these events when the fish stock is particularly vulnerable to overfishing.

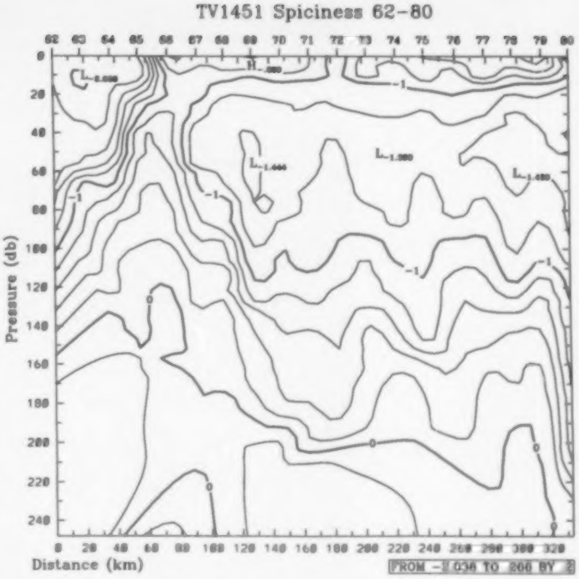

FIG. 15. Vertical section of spiciness versus pressure along the line selected (Fig. 12d) produced by CORAL from user-specified information (Fig. 14a).

Three large-scale composite maps of SST are shown in Fig. 16. These composite maps were prepared by Richard Legeckis of NOAA/NESDIS from AVHRR data taken aboard NOAA-7 and have a spatial resolution of 100 km. Figure 16b is the SST distribution in the Pacific for 20 January 1984. Warmest water is found in the western Pacific (1), and a tongue of relatively cool water (2) extends along the equator westward from South America. The source of this cool water is twofold: (1) upwelling off the Peruvian and Chilean coast and (2) upwelling along the equator associated with strong easterly Trade Winds. Figure 16c is for 20 January 1983 and shows the anomalous warm SST patterns associated with the 1982–83 ENSO event. Note that the cool waters associated with coastal and equatorial upwelling are absent from this image (compare Fig. 16b and 16c). The difference between the SST distributions for 1983 and 1984 is shown in Fig. 16d. Note that along the equator in the eastern Pacific (3), upwelling had ceased and temperatures were 2–6°C warmer in 1983 than in 1984, while large regions of the western tropical Pacific (4) where 1–3°C colder than 1984. These conditions persisted for many months.

Analogous patterns developed in the major midlatitude eastern boundary currents of the world where some of the most productive global fisheries are found (e.g., California Current). SST distributions for 29 January 1982 (Fig. 17a) and 10 January 1983 (Fig. 17b) show that the operational fishing area off southern California (Fig. 16a) experienced changes in ocean thermal structure (and implicitly circulation) similar to those observed in the tropics and off Peru.

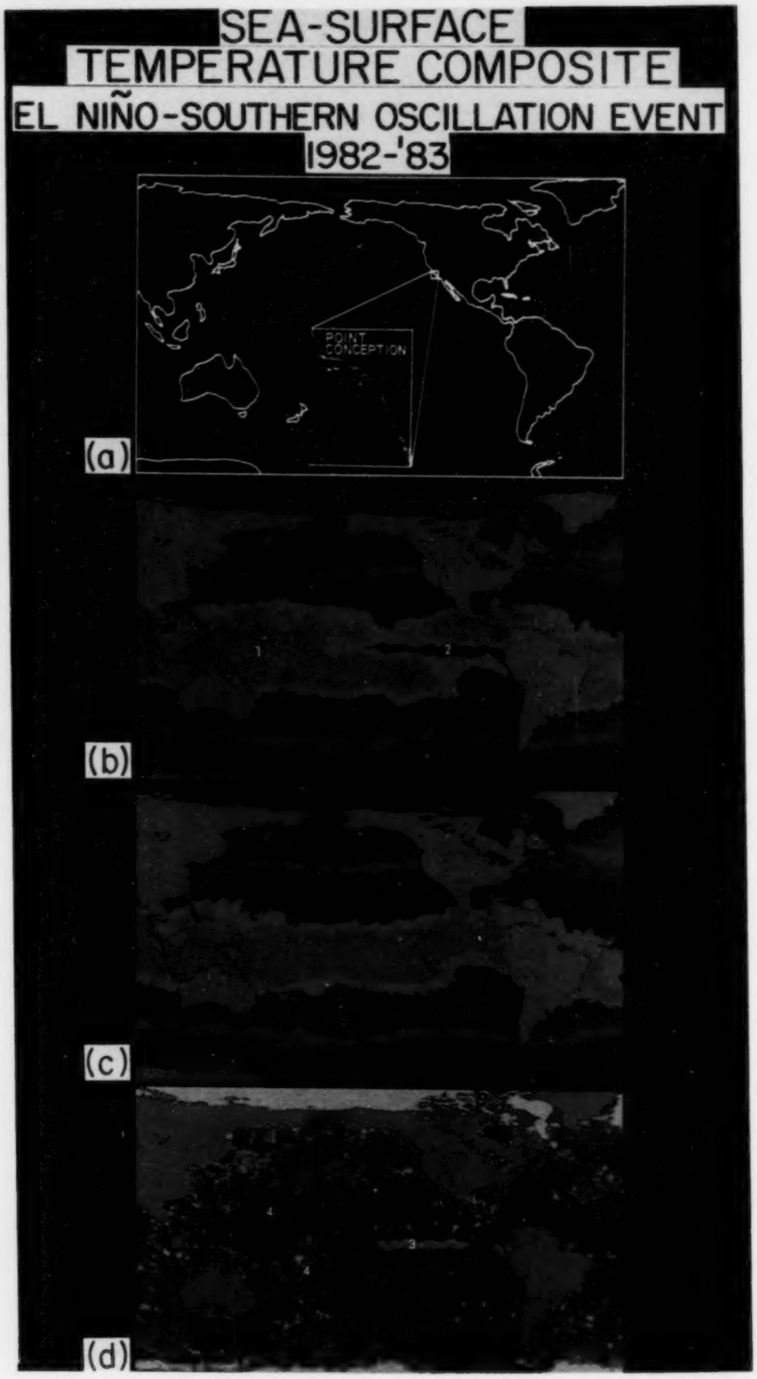
SEA-SURFACE
TEMPERATURE COMPOSITE
EL NIÑO-SOUTHERN OSCILLATION EVENT
1982-'83
POINT CONCEPTION
(a)
1
2
(b)
(c)
4
3
4
(d)

FIG. 16. (a) Map of the Pacific with detail of an active fishery area off southern California; (b) SST map for 1984; (c) SST map for 1983; (d) difference between the 1983 and 1984 maps. Maps were prepared by Richard Legeckis of NOAA/NESDIS from AVHRR data taken with the NOAA-7 satellite and have a spatial resolution of 100 km. Blue indicates cool water (0–12°C), green intermediate water (13–24°C), and yellow–red–magenta warm water (25–30°C). Features are described in the text. Maps were provided by NASA.

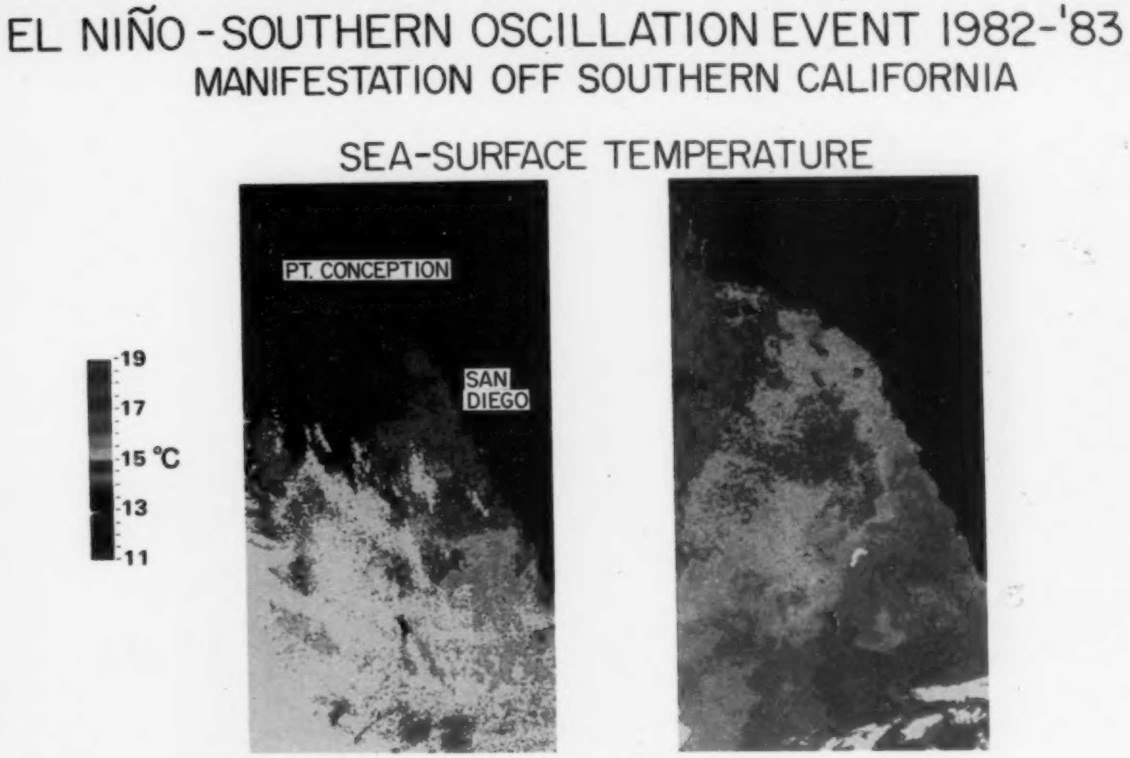
EL NIÑO - SOUTHERN OSCILLATION EVENT 1982-'83
MANIFESTATION OFF SOUTHERN CALIFORNIA
SEA-SURFACE TEMPERATURE
PT. CONCEPTION
SAN DIEGO
19
17
15 °C
13
11

(a) 29 January 1982 (b) 10 January 1983

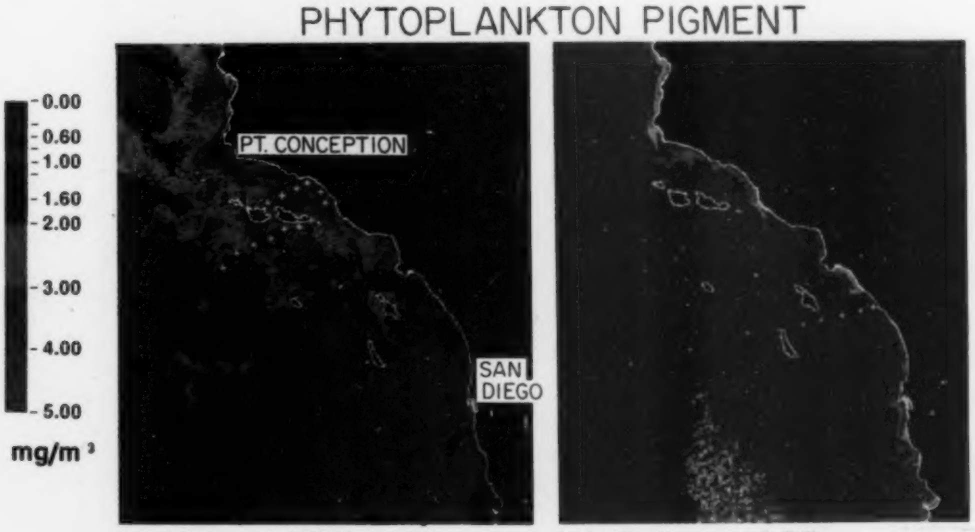
PHYTOPLANKTON PIGMENT
PT. CONCEPTION
SAN DIEGO
0.00
0.60
1.00
1.60
2.00
3.00
4.00
5.00
mg/m³

(c) 19 April 1982 (d) 15 March 1983

FIG. 17. Manifestation of the 1982–83 ENSO event in a southern California operational fishery (Fig. 16a). SST maps for (a) 29 January 1982 and (b) 10 January 1983. CZCS-derived phytoplankton pigment maps for (c) 19 April 1982 and (d) 15 March 1983. Closest available dates were chosen for comparison. Data were generously supplied by P. Fiedler and are from Fiedler (1984). CalCOFI line 90 (shown as crosses in Fig. 17d) was sampled monthly throughout 1983.

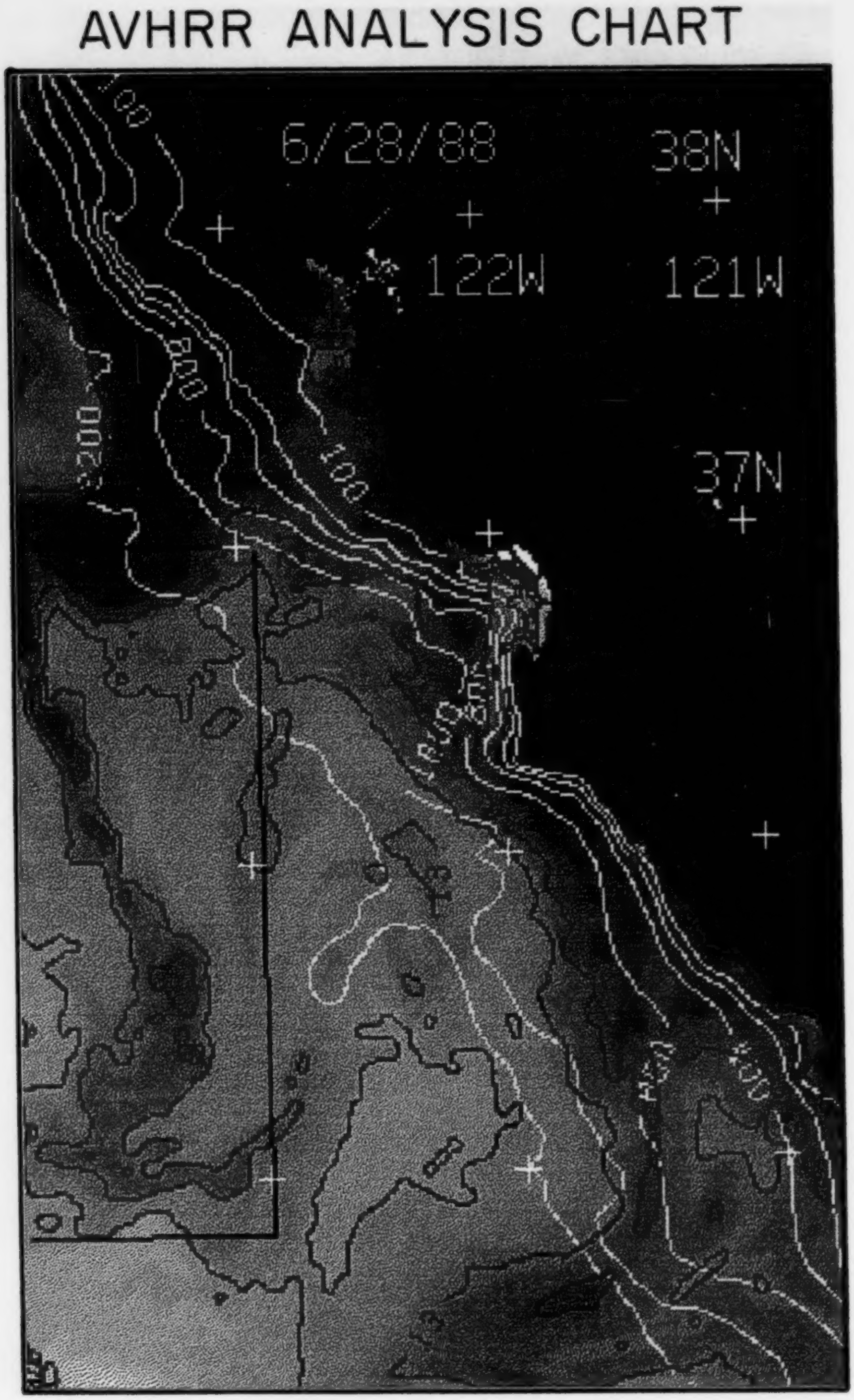

FIG. 18. Proposed near-real-time satellite analysis for a hypothetical fishing vessel operating in the region outlined by the blue box. Thermal structure is shown with dark gray scales (cold) and light gray scales (warm). Coastline (green), bathymetry (yellow), and dominant thermal boundaries (red) are overlain. A near-surface current analysis, based upon satellite data and the methods discussed in the text, is given in Fig. 11. Using modern graphical data structures and state-of-the-art communications equipment, an operations center could send similar analyses to a fishing vessel's bridge within a few minutes of the analysis. Estimated time from capture of satellite data to receipt of product on the fishing vessel is less than 1 h.

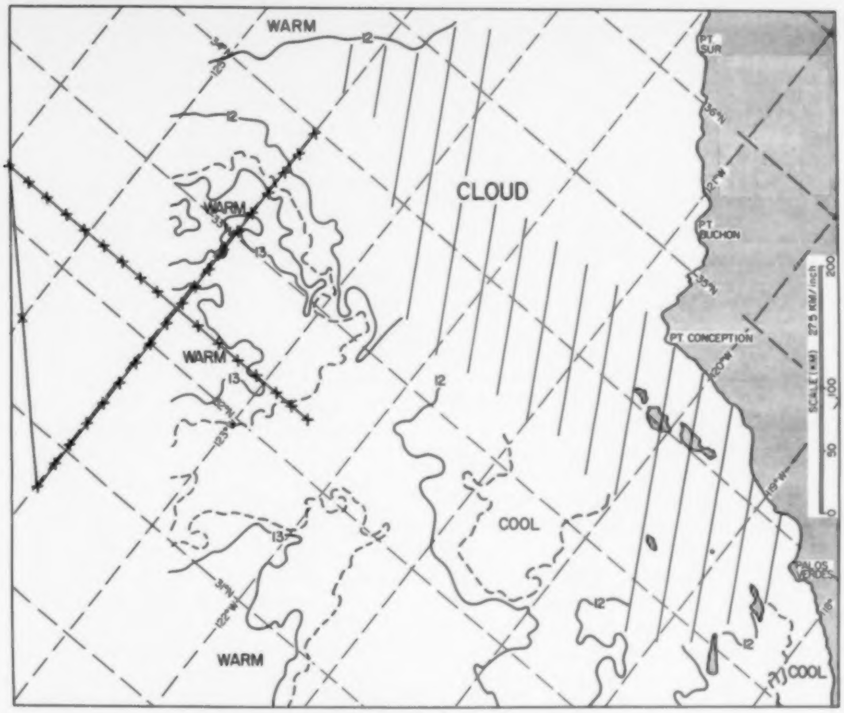

FIG. 19. Gradient analysis used in actual near-real-time support of research cruise activities. The station plan (marked with crosses) sampled two vertical sections through a subsurface warm-core eddy. Note the intense frontal structure sampled along the boundary of the northeast quadrant of this eddy. Cruise track was prepared on the basis of available AVHRR data.

CZCS-derived plant pigment distributions for 19 April 1982 (Fig. 17c) and 15 March 1983 (Fig. 17d) clearly show the impact of this event on phytoplankton standing stock in this southern California operational area.

The reduction in phytoplankton abundance (Fig. 17d) was accompanied by a significant reduction in fish catch (FAO 1987). FAO Fishing Region 77 is located in the eastern Pacific, covers from 5°S to 40°N and from 80°W to 175°W, and includes the rich coastal fisheries from the Peru–Ecuador border to Oregon, U.S.A. In 1980 and 1981, about 2.5 million metric tons of fish were caught in Region 77. During the 1982–83 ENSO event (with contemporaneous midlatitude coastal warming), only about 1.5 million metric tons of fish were caught. This represents about a 40% reduction in catch. (Note that the majority of this decrease was associated with coastal species such as sardine and anchovy (P. Smith, NOAA Southwest Fisheries Center, personal communication).) After the ENSO event (i.e., 1985–86), fish catch again increased or exceeded 2.5 million metric tons. Routine monitoring of operational fisheries areas, such as Region 77, with satellite data could help detect the onset of ENSO activity, thereby providing stock assessment managers the time and opportunity to help prevent the potential loss of a valuable fishery. This information also could be used by the fishing industry to redirect fishing efforts to alternative fisheries.

Relatively cloud-free CZCS data were not available for the operational area (Fig. 16a) during the same spring months of 1982 and 1983. Hence, the temporally nearest available CZCS images (Fig. 17c and 17d) were used to make the phytoplankton abundance comparison cited above. This comparison would have been compromised if the normal pattern of seasonal upwelling and spring bloom (see Simpson 1987, his fig. 4) had occurred during 1983. CalCOFI Line 90 (shown in Fig. 17d as white crosses) was occupied every month during 1983. These data showed temporally increasing departures from normal in situ chlorophyll distributions; the chlorophyll maximum layer deepened along with a deepening thermocline, and vertically integrated chlorophyll values declined to one quarter of the normal value from March 1983 to August 1983 (Fiedler 1984; McGowan 1984). The effects of this unusual decrease in phytoplankton abundance also were observed in zooplankton abundances and distributions (McGowan 1985). El Niño-induced onshore transport in the California Current during 1982–83 (Simpson 1984a, 1992c) significantly arrested the normal seasonal upwelling/spring bloom cycle. Evidence for this also appears in observed vertical sections of dissolved oxygen and inorganic nitrate (Simpson 1984a). Thus, the difference in dates between the two CZCS images (Fig. 17c and 17d) used in the above comparison had little or no effect on the significance of the results.

Fishing Industry

Most offshore fishing can be profitable only on fishing aggregations and, as discussed earlier, environmental factors that tend to produce aggregation include, but are not limited to, temperature, coastal and bathymetric boundaries, and ocean currents. Consider the case of a fishing group operating in the region defined by the blue box shown in Fig. 18. A useful analysis for this group might include a properly cloud-screened, geometrically corrected and earth-located SST map (Fig. 18, dark gray scales are cold and lighter scales are warm) with coastline (green), bathymetry (yellow), and major frontal boundaries (red) overlain. The frontal boundaries were detected using the LOG operator (eq. (5)). Temperatures and the catch statistics could easily be annotated to the chart if requested by the captain. A detailed ocean current analysis for the operational area (Fig. 11) also could be provided. Information outside the operational area provides the captain with insight into the larger-scale environmental conditions that might be affecting the operational area. Note that the left-hand side of the image was excluded from analysis (and transmission to the ship, thus reducing operational costs) because clouds were properly detected by robust cloud-screening algorithms. A regional operations center, equipped with modern image displays (e.g., XWINDOWS-based) and communications technologies, could send these actual charts (i.e., Fig. 11 and 18) to the fishing vessel's bridge for near-real-time display within a few minutes of completion of the analysis. This proposed approach would provide the captain with more and better-quality information than is generally available at present; the majority of ships are currently being supported by facsimile transmission. In fact, ship-to-shore communications tests show that analyses such as those shown in Fig. 11 and 18 can be received and displayed at sea within 1 min of transmission from shore.

Research

Process-oriented experiments designed to provide insight into the complex interactions between fish and environment (e.g., Checkley et al. 1988; Rose and Leggett 1988) also can benefit from the use of near-real-time satellite data to develop and modify their sampling strategies. In this regard, the needs of researchers are closely akin to those of fishermen. A warm-core eddy and associated frontal structure was identified in satellite imagery (Fig. 19); this imagery was used to develop the station sampling plan shown in the figure (Simpson et al. 1984). Analysis of chemical distributions (Simpson 1984b) and biological populations (Haury 1984) showed that the eddy had entrained waters of coastal origin (and coastal species of zooplankton) several hundred kilometres offshore. In fact, phytoplankton abundance was extremely high; it and optical water clarity varied significantly across the northeast boundary of this eddy system (Simpson et al. 1986). Zooplankton distributions also deviated substantially from those expected for offshore California Current water (Haury et al. 1986). The temperature, plant pigment, optical, and zooplankton distributions across frontal zones, such as the one described above, appear to provide preferential feeding areas (and hence, preferred operational fishing areas) for tuna (e.g., Laurs et al. 1986).

Historically, most researchers in fisheries oceanography have used remotely-sensed data to help plan a shipboard study (e.g., Fig. 19). Remotely-sensed data, however, also can be used alone and/or with historical in situ observations to address basic and applied research questions in fisheries oceanography. Randerson and Simpson (1993), for example, retrospectively analyzed 10 yr of AVHRR data off northern, central, and Baja California to determine differences and similarities in the structure of filaments found in these regions. Their statistical analyses showed that two distinct types of filament geometries constitute most of the filaments found off the west coast of the United States and that filaments in the central California region were statistically different from those found off northern and Baja California. Their analyses also imply that the results of an acoustic survey of a fisheries population may be strongly influenced by the direction of sound propagation from detector to fish shoal relative to the geometry of an intervening filament. Moreover, difference in filament structure and associated transport for the three regions (i.e., northern and Baja California versus central California) may partially explain the biogeographical distribution of some species found in the California Current system (e.g., the northern anchovy (*Engraulis mordax*)). Numerical simulations of egg/larvae advection and dispersion by Simpson and Gobat (1994) lend additional support to the findings of Randerson and Simpson (1993).

Time–space series of remotely-sensed data also can be used to establish large- and mesoscale patterns of transport in oceanic regions where ship and/or buoy observations are relatively sparse. Gallaudet and Simpson (1994) performed such an analysis for a particularly poorly sampled region of the California Current (i.e., in a $500 \times 500\ \text{km}^2$ region centered near Punta Eugenia, Baja California). Their analysis of the remotely-sensed data provided evidence that this region of the California Current system behaves dynamically and thermodynamically like the southern and central regions of the California Current system, at least on large- and mesoscale space and time scales.

Other Recommendations

Most analyses useful in operational fisheries oceanography require high spatial resolution (i.e., Local Area Coverage (LAC)) data. The area of such coverage for a given tracking station is limited, typically 3000–4000 × 2048 km (the width of an AVHRR high spatial resolution pass). Thus, a given ground receiving station cannot directly acquire satellite data for an entire fishing region (e.g., FAO Region 77). Multiple (and suitably distributed) tracking stations coupled with high band width data networks, however, provide a way to circumvent this difficulty. For example, the United States National Weather Service recently completed installation of three satellite tracking stations at Anchorage, Alaska, Honolulu, Hawaii, and Monterey, California. Data from these three stations provide coverage of the entire eastern tropical Pacific from the equator to Alaska. Moreover, efforts by the NOAA/NASA-sponsored Global 1 km Land Project and by the United Nations have led to the installation of satellite tracking equipment in traditionally uncovered areas of the world (e.g., South America). Installation of high-speed data networks among such ground receiving stations ultimately may provide some of the needed space–time coverage for both prudent management and proper utilization of marine fisheries resources on regional and global scales.

Regional operational centers are needed if operational fisheries oceanography is to make maximum use of potentially available remotely-sensed products derived from distributed collection points such as those cited above. Archiving, storage, data base management, and data distribution are other important operational issues that probably are best handled on a regional basis (Fig. 1). Software systems (e.g., Simpson and Harkins 1993; Simpson et al. 1994a) are beginning to emerge that will help serve as prototypes of future computer architectures to be used by such regional centers. Regional fisheries also may require specialized analyses. Again, these are best implemented in a regional operational center which has direct access to regional fisheries scientists working with that particular fish stock (Fig. 2). Regional operational centers also can provide a focal point for operational research in support of fisheries oceanography by supporting the community with a communications network which can be used to assemble, process, retrospectively analyze, and distribute data among the various sectors of the community (Fig. 2). Development of computer-assisted decision-making tools to help the fishing captain determine the best strategy to maximize his catch per unit effort is another example of the operations research that could be conducted in such centers. Other examples include the incorporation of GIS and modern networking/communications technologies into fishing fleet operations.

Ultimately, the community will have to determine the need for and best method of implementing such facilities. The author believes that such operational centers should not be located at universities because the necessary infrastructure to support such activities generally is lacking. Moreover, universities often view applied/operational activities as inappropriate for an academic environment. It is possible that some emerging programs (EOS Distributed Active Archive Centers (DAACs), NOAA's Coast Watch Program) may provide the infrastructure to support the needs of regional fisheries. Alternatively, the fishing industry itself may elect to support entirely (or jointly with government) such activities. It is unlikely that a unique plan will emerge that is suitable for all situations. Thus, flexibility in the design and implementation of regional infrastructures to support the data collection, archive, integration, analysis, and distribution needs of a given operational fishery is recommended.

Acknowledgments

This work was sponsored by the Marine Life Research Group of the Scripps Institution of Oceanography, by a grant from the National Aeronautics and Space Administration (NASA), and by the National SeaGrant College Program, National Oceanic and Atmospheric Administration, U.S. Department of Commerce, under grant No. NOAA NA89AA-D-SG138, project No. 14-F-N, and project No. A/S-3 through the California SeaGrant College, and in part by the California State Resources Agency. The views expressed herein are those of the author and do not necessarily reflect the views of NOAA or any of its subagencies. All work was done in J.J.S.'s Image Analysis Laboratory. Satellite data for Fig. 4, 5, 6, 9, 10, 11, 18, 15, and 19 were supplied by the Scripps Satellite Oceanography Center. Satellite data in Fig. 16 were provided by NASA and data in Fig. 17 by Dr. Paul Fiedler. All image analysis was done in J.J.S.'s Image Analysis Laboratory. Darren Atkinson, Lance Al-Rawi, Jason Gobat, and Darren Wahl assisted with computer programming. Sharon McBride and Mary Wilke typed the manuscript. Guy Tapper assisted with final figure preparation. Comments from Scott Akenhead are gratefully acknowledged. Discussions with Dr. Gordon Swartzman helped formulate a prototype strategy for incorporation of GIS technology into an operational fisheries oceanography environment. Finally, special thanks are due to the late Reuben Lasker, who initially introduced the author to operational fisheries oceanography and to an anonymous reviewer whose comments helped the author to more carefully focus the manuscript.

References

Anthony, V.C. 1990. The New England groundfish fishery after 10 years under the Magnuson Fishery Conservation and Management Act. N. Am. J. Fish. Manage. 10: 175–184.

Beverton, R.J.H., and S.J. Holt. 1957. On the dynamics of exploited fish populations. U.K. Minis. Agric. Fish. Fish. Invest. Ser. 2: 533 p.

Bracewell, R. 1965. The Fourier transform and its applications. McGraw-Hill, New York, N.Y.

Campbell, J.D. 1969. Edge structure and the representation of pictures. Ph.D. dissertation, Department of Electrical Engineering, University of Missouri, Columbia, Mo.

Canny, J. 1986. A computational approach to edge detection. IEEE Trans. Pattern Anal. Mach. Intell. 6: 679–698.

Carroll, T.R. 1987. Operational airborne measurements of snow water equivalents and soil moisture using terrestrial gamma radiation in the United States. *In* Large Scale Effects of Seasonal Snow Cover (Proceedings of the Vancouver Symposium, August 1987). IAHS Publ. No. 166: 213–223.

Chang, A.T., L.S. Chou, and T.T. Wilheit, 1993: Random errors of oceanic monthly rainfall derived from SSM/I using probability distribution functions. Mon. Weather Rev. 121: 2351–2354.

Checkley, D.M. Jr., S. Raman, G.L. Maillet, and K.M. Mason. 1988. Winter storm effects on the spawning and larval drift of a pelagic fish. Nature (Lond.) 335: 346–348.

Chiu, L.S., A.T. Change, and J. Janowiak. 1993: Comparison of monthly rain rates derived from GPI and SSM/I using probability distribution functions. J. Appl. Meteorol. 32: 323–334.

Clark, J.D. 1983. The GOES user's guide. U.S. Department of Commerce, National Oceanic and Atmospheric Administration, National Environmental Satellite, Data, and Information Service, Washington, D.C.

Claud, C., N.M. Mognard, K.B. Katsaros, A. Chedin, and N.A. Scott. 1993. Satellite observations of a polar low over the Norwegian Sea by Special Sensor Microwave Imagery, GEOSAT, and TIROS-N operational vertical sounder. *J. Geophys. Res.* 98: 14487–14506.

Cook, B.A., and P. Copes. 1987. Optimal levels for Canada's Pacific halibut fishery. Mar. Resour. Econ. 5: 71–77.

Dickinson, L.G., S.L. Boselly III, and W.S. Bergmann. 1974. Defense Meteorological Satellite Program (DMSP) user's guide. AWS-TR-74-250, Air Weather Service, United States Air Force, Scott Air Force Base. 109 p.

Emery, W.J., C.C. Ebbesmeyer, and J.P. Dugan. 1980. The fraction of vertical isotherm deflection associated with eddies: an estimate from multiship XBT surveys. J. Phys. Oceanogr. 10: 885–899.

Emery, W.J., A.C. Thomas, and M.J. Collins. 1986. An objective method for computing advective surface velocities from sequential infrared satellite images. J. Geophys. Res. 91: 12865–12878.

FAO. 1987. Food and Agricultural Organization (FAO) of the United Nations Yearbook of Fisheries Statistics and Commodities. Vol. 65. FAO, Rome. 369 p.

Fiedler, P.C. 1984. Satellite observations of the 1982–1983 El Niño along the U.S. Pacific coast. Science (Wash., D.C.) 224: 1251–1254.

Flament, P., L. Armi, and L. Washburn. 1985. The evolving structure of an upwelling filament. J. Geophys. Res. 90: 11765–11778.

Frouin, R., D. Lingner, C. Gautier, K.S. Baker, and R.C. Smith. 1989. A simple analytical formula to compute clear sky total and photosynthetically available solar irradiance at the ocean surface. J. Geophys. Res. 94: 9731–9740.

Gallaudet, T.C., and J.J. Simpson. 1991. Automated cloud screening of AVHRR imagery using split-and-merge clustering. Remote Sens. Environ. 38: 77–121.

Gallaudet, T.C., and J.J. Simpson. 1994. Empirical orthogonal function analysis: application to satellite derived image data and the sea surface temperature variability off Punta Eugenia. Remote Sens. Environ. 47: 375–389.

Garcia, C.A.E., and I.S. Robinson. 1989. Sea surface velocities in shallow sea extracted from sequential Coastal Zone Color Scanner satellite data. J. Geophys. Res. 94: 12681–12691.

Gautier, G., G. Diak, and S. Masse. 1980. A simple physical model to estimate incident solar radiation at the surface from GOES satellite data. J. Appl. Meteorol. 19: 1008–1012.

Harris, A.R., and I.M. Mason, 1992: An extension to the Split-Window technique giving improved atmospheric correction and total water vapour. Int. J. Remote Sens. 3: 881–892.

Haury, L.R. 1984. An offshore eddy in the California Current System. Part IV. Plankton distributions. Prog. Oceanogr. 13: 95–111.

Haury, L.R., J.J. Simpson, J. Peláez, C.J. Koblinsky, and D. Wiesenhahn. 1986. Biological consequences of a recurrent eddy off Point Conception, California. J. Geophys. Res. 91: 12937–12956.

Hjort, J. 1914. Fluctuations in the great fisheries of northern Europe viewed in light of biological research. Rapp. P.-v. Reun. Cons. Perm. int. Explor. Mer 19: 3–228.

Hogan, M., and H.M. Clarke. 1989. An ocean information network a view from the commercial fisheries. International Symposium on Operational Fisheries Oceanography, St. Johns, Nfld.

Hollinger, J., R. Lo, G. Poe, R. Savage, and J. Pierce, 1987: *Special Sensor Microwave/Imager users' guide*. Naval Research Laboratory, Washington, D.C.

Hollowed, A.B., and K.M. Bailey. 1989. New perspectives on the relationship between recruitment of Pacific hake (*Merluccius productus*) and the ocean environment, p. 207–220. *In* R.J. Beamish and G.A. McFarlane [ed.] Effects of ocean variability on recruitment and an evaluation of parameters used in stock assessment models. Can. Spec. Publ. Fish. Aquat. Sci. 108.

Hunter, J.R. 1981. Feeding ecology and predation of marine fish larvae, p. 34–77. *In* R. Lasker [ed.] Marine fish larvae morphology, ecology and relation to fisheries. University of Washington Press, Seattle, Wash.

Hunter, R.J., J.L. Butler, C. Kimbell, and E.A. Lynn. 1990. Bathymetric patterns in size, age, and sexual maturity, water content and caloric density of dover sole. CalCOFI Rep. 31: 132–144.

Jain, A.K. 1989. Fundamentals of digital image processing. Prentice-Hall, Englewood Cliffs, N.J. 569 p.

Jakobsen, J. 1978. The North Icelandic herring fishery and environmental conditions 1960–1968. Paper 30, ICES Symposium, Biological Basis of Pelagic Fish Stock Management. (Mimeo.)

Jerlov, N.G. 1976. Marine optics. Elsevier, New York, N.Y.

Jones, R., and E.W. Henderson. 1985. Population regulation and implications for the recruitment process in fish. Int. Counc. Explor. Sea Demersal Fish Comm. CM 1985/G:21.

Kamachi, M. 1989. Advective surface velocities derived from sequential images for rational flow field: limitations and applications of maximum cross-correlation method with rotation registration. J. Geophys. Res. 94: 18227–18223.

Kelly, K.A., and P.T. Strub. 1992. Comparison of velocity estimates from advanced very high resolution radiometer in the Coastal Transition Zone. J. Geophys. Res. 97: 9653–9668.

Koblinsky, C.J., J.J. Simpson, and T.D. Dickey. 1984. An offshore eddy in the California Current System. Part II: Surface manifestation. Prog. Oceanogr. 13: 51–69.

Kruse, G.H., and A.V. Tyler. 1989. Exploratory simulation of English sole recruitment mechanisms. Trans. Am. Fish. Soc. 118: 101–118.

Laevastu, T., and N. Bax. 1989. Environment fish behavior interactions, numerical simulations and operational use (review of a dynamic system). International Symposium on Operational Fisheries Oceanography, St. Johns, Nfld.

Lasker, R. 1975. Field criteria for survival of anchovy larvae: the relation between inshore chlorophyll maximum layers and successful first feeding. Fish. Bull. U.S. 73: 453–462.

Lauritson, L., G.G. Nelson, and R.W. Porto. 1979 (and updates). Data extraction and calibration of TIROS-N/NOAA A-G radiometers. NOAA Tech. Memo. NESS 107, U.S. Department of Commerce, Washington, D.C.

Laurs, R.M., K.S. Bliss, and J.A. Wetherall. 1986. Preliminary results from R/V *Townsend Cromwell* South Pacific Albacore Research Survey. Admin. Rep. JL-86-13, NOAA/National Marine Fisheries Service, Southwest Fisheries Center, La Jolla, Calif.

Lesse, J.A., C.S. Novak, and B.B. Clarke. 1971. An automated technique for obtaining cloud motion from geosynchronous satellites using cross correlation. J. Appl. Meteorol. 10: 118–132.

Legeckis, R., and J. Pritchard. 1976. Algorithms for correcting VHRR imagery for geometric distortion due to earth curvature, earth rotation, and spacecraft roll altitude. NOAA Tech. Memo NESS 77, U.S. Department of Commerce, Washington, D.C.

Leggett, W.C. 1984. Fish migrations in coastal and estuarine environments: a call for new approaches to the study of an old problem, p. 159–178. *In* J.D. McCleave, G.P. Arnold, J.J. Dodson, and W.H. Neill [ed.] Mechanisms of migration in fishes. Plenum Press, New York, N.Y.

MacCall, A.D. 1980. Population models for the northern anchovy (*Engraulis mordax*). Rapp. P.-v. Reun. Cons. int. Explor. Mer 177: 292–306.

MacCall, A.D. 1980. Dynamic geography of marine fish populations. Books in Recruitment Fisheries Oceanography, University of Washington Press, Seattle, Wash.

Marr, D. 1976. Analyzing natural images: a computational theory of texture vision. Cold Spring Harbor Symp. Quant. Biol. 40: 647–662.

Marr, D., and E.C. Hildreth. 1980. Theory of edge detection. Proc. R. Soc. Lond. B 207: 187–217.

Marr, D., and S. Ullman. 1981. Directional sensitivity and its use in early visual processing. Proc. R. Soc. Lond. B 211: 151–180.

McClain, E.P., W.G. Pichel, and C.C. Walton. 1985. Comparative performance of AVHRR-based multichannel sea surface temperature. *J. Geophys. Res.* 90: 11587–11601.

McGowan, J.A. 1984. The California El Niño, 1983. Oceanus 27: 48–51.

McGowan, J.A. 1985. El Niño 1983 in the Southern California Bight, p. 166–184. *In* W.S. Wooster and D.L. Fluharty [ed.] El Niño North: Niño effects in the eastern subarctic Pacific Ocean. University of Washington Press, Seattle, Wash.

McGurk, M.D. 1986. Natural mortality of marine pelagic eggs and larvae: role of spatial patchiness. Mar. Ecol. Prog. Ser. 34: 227–242.

Megrey, B.A., and V.G. Wespestad. 1990. Alaskan groundfish resources: 10 years of management under the Magnuson Fishery Conservation and Management Act. N. Am. J. Fish. Manage. 10: 125–143.

Meyers, R.A.M. 1993. Summary of stock and recruitment data. Can. Tech. Rep. Fish. Aquat. Sci. (In press)

Murdie, B., and M.P. Hassell. 1973. Food distribution, searching success, and predator–prey models, p. 87–101. *In* M.S. Bartlett and R.W. Hiorns [ed.] The mathematical theory of the dynamics of biological populations. Academic Press, London and New York.

Murphy, B.R., M.L. Brown, and T.A. Springer. 1990. Evaluation of the relative weight (W_r) index, with new applications to walleye. N. Am. J. Fish. Manage. 10: 85–97.

Neale, C.M.U., M.J. Marshall, and K. Chang, 1990: Land-surface-type classification using microwave brightness temperatures from the Special Sensor Microwave Imager. *IEEE Trans. Geosci. Remote Sens.* 28: 829–838.

Nelepo, B.A., Y.M. Kuftarkov, and V.K. Kosnyrev. 1978. Effects of mesoscale eddies on sea surface temperature. Izv. Atmos. Oceanic Phys. 14: 545–550.

Nichols, D.A. 1975: Block 5D Compendium. Headquarters, Space and Missile Systems Organization, Air Force Systems Command, United States Air Force. 106 p.

NOAA/NESDIS. 1991. NOAA polar orbiter data users guide. Washington, D.C. p. 206 and appendices.

Parrish, R.H., C.S. Nelson, and A. Bakun. 1981. Transport mechanisms and reproductive success of fishes in the California Current. Biol. Oceanogr. 1: 175–203.

Parsons, T.R., M. Takahashi, and B. Hargrave. 1984. Biological oceanographic processes. 3rd ed. Pergamon Press, Oxford, England.

Paulson, C.A., and J.J. Simpson. 1981. The temperature difference across the cool skin of the ocean. J. Geophys. Res. 86: 11044–11054.

Peláez, J., and J.A. McGowan. 1986. Phytoplankton pigment patterns in the California Current as determined by satellite. Limnol. Oceanogr. 31: 927–950.

Quiroz, R.S. 1983. The climate of the "El Niño" winter of 1982–83: a season of extraordinary climatic anomalies. *Mon. Weather Rev.* 111: 1695–1706.

Ramp, S.R., P.F. Jessen, K.H. Brink, P.P. Niiler, F.L. Dagget, and J.S. Best. 1991. The physical structure of cold filaments near Point Arena, California, during June 1987. J. Geophys. Res. 96: 14859–14883.

Ramsden, D., and G. Holloway. 1991. Time-stepping Lagrangian particles in two dimensional Eulerian flow fields. J. Comput. Phys. 95: 101–116.

Randerson, J.T., and J.J. Simpson. 1993. Recurrent patterns in the surface frontal structure associated with cold filaments along the west coast of North America. Remote Sens. Environ. 46: 146–163.

Reed, R.K., L.S. Incze, and J.D. Schumaker. 1989. Estimation of the effects of flow on dispersion of larval Pollock, *Theragra chalcogramma*, in Shelikof Strait, Alaska, p. 239–246. *In* R.J. Beamish and G.A. McFarlane [ed.] Effects of ocean variability on recruitment and an evaluation of parameters used in stock assessment models. Can. Spec. Publ. Fish. Aquat. Sci. 108.

Ricker, W.E. 1954. Stock and recruitment. J. Fish. Res. Board Can. 11: 559–623.

Robinson, I.S. 1985. Satellite oceanography: an introduction for oceanographers and remote-sensing scientists. Ellis Horwood Limited, Chichester, England. 455 p.

Rose, G.A., and W.C. Leggett. 1988. Atmosphere–ocean coupling and Atlantic cod migrations: effects of wind-forced variations in sea temperatures and currents on nearshore distributions and catch rates of *Gadus morhua*. Can. J. Fish. Aquat. Sci. 45: 1234–1243.

Rothschild, B.J. 1986. Dynamics of marine fish populations. Harvard University Press, Cambridge, Mass. 277 p.

Sharma, A.K., A.T. Chang, and T.T. Wilheit. 1991. Estimation of the diurnal cycle of oceanic precipitation from SSM/I data. *Mon Weather Rev.* 114: 2168–2175.

Simpson, J.J. 1984a. El Niño-induced onshore transport in the California Current during 1982–83. Geophys. Res. Lett. 11: 233-236.

Simpson, J.J. 1984b. An offshore eddy in the California Current System. Part III. Chemical structure. Prog. Oceanogr. 13: 71–93.

Simpson, J.J. 1987. Transport processes affecting the survival of pelagic fish stock in the California Current. Am. Fish. Soc. Symp. 2: 39–60.

Simpson, J.J. 1990. On the accurate detection and enhancement of oceanic features observed in satellite data. Remote Sens. Environ. 33: 17–33.

Simpson, J.J. 1992a. Image masking using polygon fill and morphological operations. Remote Sens. Environ. 40: 161–183.

Simpson, J.J. 1992b. Remote sensing and geographical information systems: their past, present and future use in global marine fisheries. Fish. Oceanogr. 1: 238–280.

Simpson, J.J. 1992c. Variability of the Southern California Current System during mid-latitude North Pacific coastal warming events of 1982–83 and 1940–41. Fish. Oceanogr. 1: 57–79.

Simpson, J.J. 1994. Accurate change detection during ENSO events using the multivariate change detection transformation. Remote Sens. Environ. (In press)

Simpson, J.J., J. Bloom, and M.A. Botta. 1994a. The CTD Ocean Rendering and Analysis Laboratory (CORAL). J. Atmos. Oceanic Technol. (In press)

Simpson, J.J., T.D. Dickey, and C.J. Koblinsky. 1984. An offshore eddy in the California Current System. Part I: Interior dynamics. Prog. Oceanogr. 13: 5–49.

Simpson, J.J., and J. Gobat. 1994. Robust velocity estimates, streamfunctions and simulated Lagrangian drifters from sequential spacecraft data. IEEE Trans. Geosci. Remote Sens. (In press)

Simpson, J.J., J.I. Gobat, and R. Frouin. 1994b. Improved destriping of GOES images using frequency domain filters. Remote Sens. Environ. (In press)

Simpson, J.J., and D.N. Harkins. 1993. The SSABLE system: automated archive, catalog, browse, and distribution of satellite data in near-real time. IEEE Trans. Geosci. Remote Sens. 31: 515–525.

Simpson, J.J., and C. Humphrey. 1990. An automated cloud screening algorithm for daytime AVHRR imagery. J. Geophys. Res. 95: 13459–13481.

Simpson, J.J., C.J. Koblinsky, J. Peláez, L.R. Haury, and D. Wiesenhahn. 1986. Temperature plant pigment optical relations in a recurrent offshore eddy near Point Conception, California. J. Geophys. Res. 91: 12919–12936.

Simpson, J.J., and R.J. Lynn. 1990. A mesoscale eddy dipole in the offshore California Current. J. Geophys. Res. 95: 13009–13022.

Simpson, J.J., and S. Yhann. 1994. Noise reduction in AVHRR channel 3 using Wiener filtering methods. *IEEE Trans. Geosci. Remote Sens.* (In press)

Stocker, M., and B.M. Leaman. 1990. Effects of extended jurisdiction on management and conservation of Canada's Pacific coast fisheries. N. Am. J. Fish. Manage. 10: 144–153.

Strub, P.T., P.M. Kosro, and A. Huyer. 1991. The nature of the cold filaments in the California Current System. J. Geophys. Res. 96: 14743–14768.

Svejkovsky, J. 1988a. Sea surface flow estimation from Advanced Very High Resolution Radiometer and Coastal Zone Color Scanner satellite imagery. A verification study J. Geophys. Res. 93: 6735–6743.

Svejkovsky, J. 1988b. Fishfinding from space. Saltwater Sportsman 50: 96–97f, 178–179.

Swenson, M.S., P.P. Niiler, K.H. Brink, and M.R. Abbott. 1992. Drifter observations of a cold filament off Point Arena, California, in July 1988. J. Geophys. Res. 97: 3593–3610.

Theilacker, G.H. 1986. Starvation-induced mortality of young sea-caught jack mackerel, *Trachurus symmetricus*, determined with historical and morphological methods. Fish. Bull. U.S. 84: 1–17.

Tillman, M.F. 1968. Tentative recommendations for management of the coastal fishery of Pacific hake, based on a simulation study of the effects of fishing upon a virgin population. M.S. thesis, University of Washington, Seattle, Wash.

Tokmakian, R., P.T. Strub, and J. McClean-Padman. 1990. Evaluation of the maximum cross-correlation method for estimating sea surface velocities from sequential satellite images. J. Atmos. Oceanic Technol. 7: 852–865.

Tyler, A.V., and W.R. Crawford. 1991. Modeling recruitment patterns for Pacific cod in Hecate Strait, British Columbia. Can. J. Fish. Aquat. Sci. 48: 2240–2249.

Tyler, A.V., and S.J. Westrheim. 1986. Effects of transport, temperature, and stock size on recruitment of Pacific cod (*Gadus macrosephalus*). Int. North Pac. Fish. Comm. Bull. 47: 175–190.

Ushakov, N.G., and V.K. Ozhigin. 1987. The abundance of year classes of the Barents Sea capelin and peculiarities of the distribution of the young in relation to hydrographic conditions, p. 159–167. *In* H. Loeng [ed.] The effects of oceanographic conditions on distribution and population dynamics of commercial fish stocks in the Barents Sea. Institute of Marine Research, Bergen, Norway.

Verri, A., and T. Poggio. 1989. Motion field and optical flow: qualitative properties. IEEE Trans. PAMI 11: 490–498.

Voorhis, A.D., E.H. Schroeder, and A. Leetmaa. 1976. The influence of deep mesoscale eddies on sea surface temperature in the North Atlantic subtropical convergence. J. Phys. Oceanogr. 6: 953–961.

Wahl, D.D., and J.J. Simpson. 1990. Physical processes affecting the objective determination of near-surface velocity from satellite data. J. Geophys. Res. 95: 13511–13528.

Wahl, D.D., and J.J. Simpson. 1991. Satellite derived estimates of the normal and tangential components of near-surface flow. Int. J. Remote Sens. 12: 2529–2571.

Wooster, W.S., and K.M. Bailey. 1989. Recruitment of marine fisheries revisited, p. 153–159. *In* R.J. Beamish and G.A. McFarlane [ed.] Effects of ocean variability on recruitment and an evaluation of parameters used in stock assessment models. Can. Spec. Publ. Fish. Aquat. Sci. 108.

Zhang, C.I., and D.R. Gunderson. 1990. Yield per recruit and management recommendations for Alaska plaice in the Eastern Bering Sea. N. Am. J. Fish. Manage 10: 1–9.

Aquaculture International

JOURNAL OF THE EUROPEAN AQUACULTURE SOCIETY

Editor in Chief:
Michael G. Poxton

Aquaculture International is the journal of the European Aquaculture Society. It publishes original research papers, short communications, technical notes and review papers on topics which include:

- The biology, physiology, pathology and genetics of cultured fish, crustaceans, molluscs and plants - especially new species.
- The water quality of supply systems, fluctuations of water quality within farms, and the environmental impacts of aquacultural operations.
- Nutrition, feeding and stocking practices, especially as they affect the health, behavior, appetite, growth rate and conversion efficiency of cultured species.
- The development of economically sound and sustainable production techniques.
- Bioengineering studies, focusing on important aspects of the design and management of both off-shore and land-based systems, as well as the integration and application of improved scientific and engineering technologies.
- The improvement of quality and marketing of farmed products

Each article, where appropriate, includes a clear statement of the practical significance and implications of the results obtained from original research conducted or literature synthesized in a way that can readily be appreciated by commercial farmers. Recommendations are made whenever possible.

Order Form - Aquaculture International

Please enter my subscription to Volume 2, 1994 (4 issues).

Personal Rate: ☐ European Community £50, ☐ North America $85, ☐ Rest of World £50
☐ Please send me a FREE sample copy ☐ Send me a FREE sample copy of ***Reviews in Fish Biology and Fisheries***

☐ Please bill me ☐ I enclose a cheque made payable to Chapman & Hall ☐ Please charge my credit card:
☐ Mastercard ☐ Visa ☐ American Express

Card No____________________ Expires__________

Name____________________ Signature__________

Address____________________

____________________ Date__________

If paying by credit card, please use billing address. Canadian Customers please add 7% GST.

CHAPMAN & HALL

Borgmann, U., and D.M. Whittle. Particle-size-conversion efficiency, invertebrate production, and potential fish production in Lake Ontario **693–700**
Hinch, S.G., K.M. Somers, and N.C. Collins. Spatial autocorrelation and assessment of habitat–abundance relationships in littoral zone fish **701–712**
Walters, C., and D. Ludwig. Calculation of Bayes posterior probability distributions for key population parameters **713–722**
Gascuel, D. Une méthode simple d'ajustement des clés taille/âge : application aux captures d'albacores (*Thunnus albacares*) de l'Atlantique Est **723–733**
Anganuzzi, A., R. Hilborn, and J.R. Skalski. Estimation of size selectivity and movement rates from mark–recovery data **734–742**

Perspectives

Simpson, J.J. Remote sensing in fisheries: a tool for better management in the utilization of a renewable resource **743–771**

National Research Council Canada
Ottawa, Canada
K1A 0R6

Conseil national de recherches Canada
Ottawa, Canada
K1A 0R6

Postage paid at Ottawa
Publications mail
Registration pending

Port payé à Ottawa
Poste-publication
Enregistrement en cours

Canadian Journal of Fisheries and Aquatic Sciences

Journal canadien des sciences halieutiques et aquatiques

Volume 51, No. 3, March 1994

Volume 51, n° 3, mars 1994

Danylchuk, A.J., and M.G. Fox. Seasonal reproductive patterns of pumpkinseed (*Lepomis gibbosus*) populations with varying body size characteristics **490–500**

Ogura, M., and S. Ito. Change in the known ocean distribution of Japanese chum salmon, *Oncorhynchus keta*, in relation to the progress of stock enhancement **501–505**

Panfili, J., M.-C. Ximénès, and A.J. Crivelli. Sources of variation in growth of the European eel (*Anguilla anguilla*) estimated from otoliths **506–515**

Mooij, W.M., E.H.R.R. Lammens, and W.L.T. Van Densen. Growth rate of 0+ fish in relation to temperature, body size, and food in shallow eutrophic Lake Tjeukemeer **516–526**

Wilson, R.W., H.L. Bergman, and C.M. Wood. Metabolic costs and physiological consequences of acclimation to aluminum in juvenile rainbow trout (*Oncorhynchus mykiss*). 1: Acclimation specificity, resting physiology, feeding, and growth **527–535**

Wilson, R.W., H.L. Bergman, and C.M. Wood. Metabolic costs and physiological consequences of acclimation to aluminum in juvenile rainbow trout (*Oncorhynchus mykiss*). 2: Gill morphology, swimming performance, and aerobic scope **536–544**

Gauldie, R.W., K. Xi, and S.K. Sharma. Developing a Raman spectral method for measuring the strontium and calcium concentrations of fish otoliths **545–551**

Labelle, M. A likelihood method for estimating Pacific salmon escapement based on fence counts and mark–recapture data **552–566**

Plisetskaya, E.M., T.W. Moon, D.A. Larsen, G.D. Foster, and W.W. Dickhoff. Liver glycogen, enzyme activities, and pancreatic hormones in juvenile Atlantic salmon (*Salmo salar*) during their first summer in seawater **567–576**

Tallman, R.F., and M.C. Healey. Homing, straying, and gene flow among seasonally separated populations of chum salmon (*Oncorhynchus keta*) **577–588**

Perry, R.I., and S.J. Smith. Identifying habitat associations of marine fishes using survey data: an application to the northwest Atlantic **589–602**

Forbes, L.S., and R.M. Peterman. Simple size-structured models of recruitment and harvest in Pacific salmon (*Oncorhynchus* spp.) **603–616**

de Lafontaine, Y. Zooplankton biomass in the southern Gulf of St. Lawrence: spatial patterns and the influence of freshwater runoff **617–635**

Bosakowski, T., and E.J. Wagner. Assessment of fin erosion by comparison of relative fin length in hatchery and wild trout in Utah **636–641**

Shackell, N.L., P.A. Shelton, J.M. Hoenig, and J.E. Carscadden. Age- and sex-specific survival of northern Grand Bank capelin (*Mallotus villosus*) **642–649**

Brylinsky, M., J. Gibson, and D.C. Gordon Jr. Impacts of flounder trawls on the intertidal habitat and community of the Minas Basin, Bay of Fundy **650–661**

Korman, J., D.R. Marmorek, G.L. Lacroix, P.G. Amiro, J.A. Ritter, W.D. Watt, R.E. Cutting, and D.C.E. Robinson. Development and evaluation of a biological model to assess regional-scale effects of acidification on Atlantic salmon (*Salmo salar*) **662–680**

Campeau, S., H.R. Murkin, and R.D. Titman. Relative importance of algae and emergent plant litter to freshwater marsh invertebrates **681–692**

(Continued inside back)

CJFSDX51(3)489–771 (1994)
ISSN 0706-652X

Canada

Printed in Canada by / Imprimé au Canada par
University of Toronto Press, Inc.
Typesetting by / Typographie par
Aubut & Nadeau Services Inc.

0706-652X(199403)51:3;1-K